VOL. 535 NOS. 1 + 2 DECEMBE
COMPLETE IN ONE ISSUE

14th International Symposium
on Column Liquid Chromatography
Boston, MA, May 20–25, 1990
Part I

NAL OF

HROMATOGRAPHY

UDING ELECTROPHORESIS AND OTHER SEPARATION METHOD

SYMPOSIUM VOLUMES

ELSEVIER

JOURNAL OF CHROMATOGRAPHY

Scope. The *Journal of Chromatography* publishes papers on all aspects of chromatography, electrophoresis and related methods. Contributions consist mainly of research papers dealing with chromatographic theory, instrumental development and their applications. The section *Biomedical Applications*, which is under separate editorship, deals with the following aspects: developments in and applications of chromatographic and electrophoretic techniques related to clinical diagnosis or alterations during medical treatment; screening and profiling of body fluids or tissues with special reference to metabolic disorders; results from basic medical research with direct consequences in clinical practice; drug level monitoring and pharmacokinetic studies; clinical toxicology; analytical studies in occupational medicine.

Submission of Papers. Manuscripts (in English; *four* copies are required) should be submitted to: Editorial Office of *Journal of Chromatography*, P.O. Box 681, 1000 AR Amsterdam, The Netherlands, Telefax (+31-20) 5862 304, or to: The Editor of *Journal of Chromatography, Biomedical Applications*, P.O. Box 681, 1000 AR Amsterdam, The Netherlands. Review articles are invited or proposed by letter to the Editors. An outline of the proposed review should first be forwarded to the Editors for preliminary discussion prior to preparation. Submission of an article is understood to imply that the article is original and unpublished and is not being considered for publication elsewhere. For copyright regulations, see below.

Subscription Orders. Subscription orders should be sent to: Elsevier Science Publishers B.V., P.O. Box 211, 1000 AE Amsterdam, The Netherlands, Tel. (+31-20) 5803 911, Telex 18582 ESPA NL, Telefax (+31-20) 5803 598. The *Journal of Chromatography* and the *Biomedical Applications* section can be subscribed to separately.

Publication. The *Journal of Chromatography* (incl. *Biomedical Applications*) has 38 volumes in 1991. The subscription prices for 1991 are:

J. Chromatogr. (incl. *Cum. Indexes, Vols. 501–550*) + *Biomed. Appl.* (Vols. 535–572):
Dfl. 7220.00 plus Dfl. 1140.00 (p.p.h.) (total *ca.* US$ 4696.50)

J. Chromatogr. (incl. *Cum. Indexes, Vols. 501–550*) only (Vols. 535–561):
Dfl. 5859.00 plus Dfl. 810.00 (p.p.h.) (total *ca.* US$ 3746.50)

Biomed. Appl. only (Vols. 562–572):
Dfl. 2387.00 plus Dfl. 330.00 (p.p.h.) (total *ca.* US$ 1526.50).

Our p.p.h. (postage, package and handling) charge includes surface delivery of all issues, except to subscribers in Argentina, Australia, Brasil, Canada, China, Hong Kong, India, Israel, Malaysia, Mexico, New Zealand, Pakistan, Singapore, South Africa, South Korea, Taiwan, Thailand and the U.S.A. who receive all issues by air delivery (S.A.L. — Surface Air Lifted) at no extra cost. For Japan, air delivery requires 50% additional charge; for all other countries airmail and S.A.L. charges are available upon request. Back volumes of the *Journal of Chromatography* (Vols. 1–497) are available at Dfl. 195.00 (plus postage). Claims for missing issues will be honoured, free of charge, within three months after publication of the issue. Customers in the U.S.A. and Canada wishing information on this and other Elsevier journals, please contact Journal Information Center, Elsevier Science Publishing Co. Inc., 655 Avenue of the Americas, New York, NY 10010, U.S.A., Tel. (+1-212) 633 3750, Telefax (+1-212) 633 3990.

Abstracts/Contents Lists published in Analytical Abstracts, Biochemical Abstracts, Biological Abstracts, Chemical Abstracts, Chemical Titles, Chromatography Abstracts, Clinical Chemistry Lookout, Current Contents/Life Sciences, Current Contents/Physical, Chemical & Earth Sciences, Deep-Sea Research/Part B: Oceanographic Literature Review, Excerpta Medica, Index Medicus, Mass Spectrometry Bulletin, PASCAL-CNRS, Pharmaceutical Abstracts, Referativnyi Zhurnal, Research Alert, Science Citation Index and Trends in Biotechnology.

See inside back cover for Publication Schedule, Information for Authors and information on Advertisements.

0021-9673/90/$03.50

Printed in The Netherlands

NEW DEXTRAN STANDARDS

Pharmacosmos introduces a complete series of 10 Dextran Standards with close to Gaussian molecular weight distribution.

Together, the Standards cover a broad molecular weight range.

Pharmacosmos' 10 Dextran Standards make molecular weight calibration much easier, much faster and much better in comparison with traditional Dextran Standards.

Like the Pullulan Standards, Pharmacosmos Dextran Standards are also very useful for universal calibration.

Pharmacosmos Dextran Standards are characterized by Low Angle Laser Light Scattering (LALLS), Gel Permeation Chromatography (GPC), Reducing End Group Titration (EGT) and Viscosity Measurements (VISC).

NEW CONCEPT FOR MOLECULAR WEIGHT CALIBRATION

Pharmacosmos has the pleasure of introducing a new concept for molecular weight calibration using the Peak Average Molecular Weight, $\bar{M}_p$. When applying the Peak Average Molecular Weight for general GPC calibration and for universal calibration it is easy to construct the correct calibration curve as described in "Pharmacosmos Dextran Standards".

Data Sheet - Pharmacosmos' 10 Dextran Standards

	GPC	GPC	LALLS	GPC	EGT	VISC
	$\bar{M}_p$	$\bar{M}_w$	$\bar{M}_w$	$\bar{M}_n$	$\bar{M}_n$	$[\eta]$ ml/g
Dextran 1	1080	1270	-	1010	1034	4.4
Dextran 5	4440	5220	5700	3260	3326	7.8
Dextran 12	9890	11600	11700	8110	8000	11.2
Dextran 25	21400	23800	22700	18300	17944	16.9
Dextran 50	43500	48600	50800	35600	36654	23.0
Dextran 80	66700	80900	79800	55500	55632	31.5
Dextran 150	123600	147600	143000	100300	98559	39.4
Dextran 270	196300	273000	262000	164200	167500	49.4
Dextran 410	276500	409800	403000	236300	239903	55.4
Dextran 670	401300	667800	676000	332800	349303	70.8

Differential Distribution - Pharmacosmos' 10 Dextran Standards

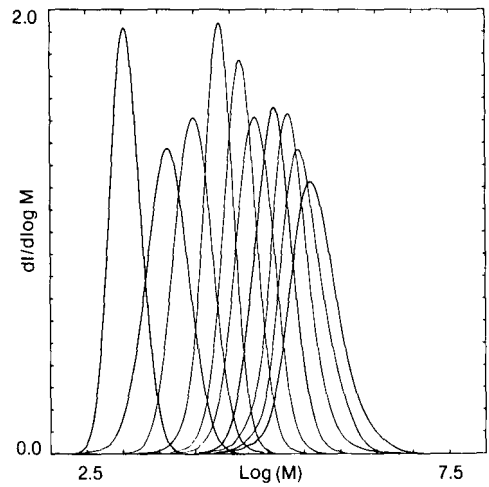

Pharmacosmos' 10 Dextran Standards are available in a 10-Kit containing 0.8 g of each Standard, at a price of DKK 4,200,-. Alternatively, each Standard is supplied separately in 5 g vials, at a price of DKK 3,000,-.
The Standards are supplied together with "Pharmacosmos Dextran Standards", which contains the complete data sheets for all Standards and instructions for molecular weight calibration.

Dextran 1, $\bar{M}_p$ = 1080
Dextran 5, $\bar{M}_p$ = 4440
Dextran 12, $\bar{M}_p$ = 9890
Dextran 25, $\bar{M}_p$ = 21400
Dextran 50, $\bar{M}_p$ = 43500
Dextran 80, $\bar{M}_p$ = 66700
Dextran 150, $\bar{M}_p$ = 123600
Dextran 270, $\bar{M}_p$ = 196300
Dextran 410, $\bar{M}_p$ = 276500
Dextran 670, $\bar{M}_p$ = 401300

PHARMACOSMOS

P.O.B. 29, DK-4130 Viby Sj., Denmark
Tel.: +45 2 39 33 62, Fax: +45 2 39 34 28, Telex: 43178 cosmos dk

PHARMACOSMOS is a large-scale producer of Dextrans and Iron Dextrans.
Pharmacosmos' production is based on methods developed from research by its own laboratories.

Scientific Computing and Automation (Europe) 1990

Proceedings of the Scientific Computing and Automation (Europe) Conference, 12-15 June, 1990, Maastricht, The Netherlands

edited by **E.J. Karjalainen,** *Helsinki, Finland*

(Data Handling in Science and Technology, 6)

This book comprises the majority of papers presented at the second **European Scientific Computing and Automation (SCA 90)** meeting which was held in June 1990 in Maastricht, The Netherlands. The increasing use of computers in data acquisition, processing, interpretation and storage makes integration of these activities possible. SCA concentrates on computer-based tools which can be applied in several disciplines.

Laboratory Information Management Systems (LIMS) are covered in depth, including LIMS design, acquisition and standards for data transfer between instruments, between LIMS and instruments and between different LIMS. Finally, scientific results are displayed as images and computer-based animations in several examples with colour illustrations.

The book should be of interest to those managing R&D projects, doing research in laboratories, acquiring or planning LIMS, designing instruments and laboratory automation systems and those involved in data analysis of scientific results.

Contents: I. Scientific Visualization and Supercomputers *(6 Papers).* II. Statistics *(6 Papers).* III. Data Analysis and Chemometrics *(8 Papers).* IV. Laboratory Robotics *(4 Papers).* V. LIMS and Validation of Computer Systems *(7 Papers).* VI. Standards Activities *(3 Papers).* VII. Databases and Documentation *(4 Papers).* VIII. Tools for Spectroscopy *(4 Papers).* Author Index. Subject Index.

1990 514 pages

Price: US$ 220.00 / Dfl. 385.00

ISBN 0-444-88949-3

Elsevier Science Publishers

P.O. Box 211, 1000 AE Amsterdam, The Netherlands
P.O. Box 882, Madison Square Station, New York, NY 10159, USA

Ion Chromatography

Principles and Applications

by **P.R. Haddad,** *University of New South Wales, Kensington, N.S.W., Australia and* **P.E. Jackson,** *Waters Chromatography Division, Milford, MA, USA*

(Journal of Chromatography Library, 46)

Ion chromatography (IC) was first introduced in 1975 for the determination of inorganic anions and cations and water soluble organic acids and bases. Since then, the technique has grown in usage at a phenomenal rate. The growth of IC has been accompanied by a blurring of the original definition of the technique, so that it now embraces a very wide range of separation and detection methods, many of which bear little resemblance to the initial concept of ion-exchange separation coupled with conductivity detection.

Ion Chromatography is the first book to provide a comprehensive treatise on all aspects of ion chromatography. Ion-exchange, ion-interaction, ion-exclusion and other pertinent separation modes are included, whilst the detection methods discussed include conductivity, amperometry, potentiometry, spectroscopic methods (both molecular and atomic) and post-column reactions. The theoretical background and operating principles of each separation and detection mode are discussed in detail. A unique extensive compilation of practical applications of IC (1250 literature citations) is presented in tabular form. All relevant details of each application are given to accommodate reproduction of the method in the laboratory without access to the original publication.

This truly comprehensive text on ion chromatography should prove to be the standard reference work for researchers and those involved in the use of the subject in practical situations.

1990 798 pages
Price: US$ 191.50 / Dfl. 335.00
ISBN 0-444-88232-4

Elsevier Science Publishers
P.O. Box 211, 1000 AE Amsterdam, The Netherlands
P.O. Box 882, Madison Square Station, New York, NY 10159, USA

Energy Dispersive X-Ray Fluorescence Analysis

by **B. Dziunikowski,** *Institute of Physics and Nuclear Techniques, Academy of Mining and Metallurgy, Warsaw, Poland*

(Wilson & Wilson's Comprehensive Analytical Chemistry Vol. XXIV)

G. Svehla (Series editor)

In Volume IIC of the series, G.L. Macdonald contributed a chapter on X-Ray Spectrometry in which the principles of X-ray fluorescence analysis were presented with great clarity. Since that contribution appeared in 1971 tremendous developments have taken place with one of the most important new features being the appearance of energy-dispersive methods.

This new volume gives a detailed and up-to-date account of this important technique. It covers the various physical and technical problems associated with this analytical method, with emphasis on explaining the interferences due to matrix and particle size effects. Methods for overcoming these interferences are described and other sources of errors and the processing of measurement data are discussed. Also described are numerous applications of EDXRF analysis in a variety of fields including geological prospecting and mining, trace element analysis, biology, medicine, environmental pollution control, archaeology, forensic sciences, and others.

Contents: **1. Fundamentals.** Energy quantization. Distribution of electrons in an atom. Atom excitation. Atom deexcitation. Photon scattering. Attenuation of X-ray beam. Mean and effective atomic number. **2. Sources of Primary (Exciting) Radiation.** Properties of radioisotope sources. Production of radioisotope sources. Isotope X-ray sources. Influence of measuring conditions on the shape of X-ray spectrum. Low-power X-ray tubes. **3. Secondary Radiation of Sample.** Intensity of fluorescence radiation. Intensity of scattered radiation. **4. Detection of X-Rays.** Proportional counter. Scintillation counter. Solid-state detector. Detection efficiency. Energy resolution. Gas proportional-scintillation counters. **5. X-Ray Spectrometry.** Electronic methods (pulse-height selection). Filter methods. Radiator methods. **6. Selection of Optimum Conditions for Analysis.** Calibration. Sensitivity of analysis. Factors influencing sensitivity. **7. Disturbing Effects.** Interelement radiation. Matrix effects. Particle-size effects. Mineralogical effects. Surface effects. **8. Methods for Eliminating Matrix Effects.** Analysis of three-component materials. Analysis of multicomponent materials. Calculation correction methods. Methods requiring special preparation of samples. **9. Other Sources of Errors.** Errors due to statistical fluctuations. Equipment effects. Background interference. Effects due to the physical state of the sample. **10. Processing of Measurement Data.** Statistical distributions and their parameters. Precision. Accuracy. Rejecting an outlier. Decision limit, detection limit, and determination limit. **11. Applications of Energy-Dispersive X-Ray Fluorescence Analysis in Geological Prospecting and Mining.** Field prospecting analyses. Analysis of drill cores and drillings. Analyses in boreholes (X-ray fluorescence logging). Laboratory analyses of geological materials. Analyses of lunar and Martian surfaces. **12. On-Stream Analyses.** Introduction. Mineral processing control. Calciferous sludge analysis. Analysis of loose materials. **13. Trace Analysis.** Introduction. Preconcentration methods. Analysis of water and effluent-waste pollutants. Analysis of air pollutants. X-ray fluorescence analysis in medical applications. **14. Miscellaneous Applications.** Alloy analysis. Analysis of solutions. Analysis of gases. Analysis of petroleum products. Analysis of paints and lacquers. EDXRF analysis in archaeology. Coating thickness measurements. Other applications of EDXRF. **References. Subject Index.**

1989 xx + 432 pages
Price: US$ 215.50 / Dfl. 420.00
Subscr. Price: US$ 194.75 / Dfl. 380.00
ISBN 0-444-98897-1

Elsevier Science Publishers

P.O. Box 211, 1000 AE Amsterdam, The Netherlands

P.O. Box 882, Madison Square Station, New York, NY 10159, USA

JOURNAL OF CHROMATOGRAPHY

VOL. 535 (1990)

JOURNAL *of* CHROMATOGRAPHY

INTERNATIONAL JOURNAL ON CHROMATOGRAPHY,
ELECTROPHORESIS AND RELATED METHODS

SYMPOSIUM VOLUMES

ELSEVIER
AMSTERDAM — OXFORD — NEW YORK — TOKYO

J. Chromatogr., Vol. 535 (1990)

0021-9673/90/$03.50

Printed in The Netherlands

SYMPOSIUM VOLUME

FOURTEENTH INTERNATIONAL SYMPOSIUM ON COLUMN LIQUID CHROMATOGRAPHY

PART I

Boston, MA (U.S.A.), May 20–25, 1990

Guest Editor

B. L. KARGER

(Boston, MA)

The proceedings of the *Fourteenth International Symposium on Column Liquid Chromatography, Boston, MA, May 20–25, 1990*, are published in two consecutive volumes of the *Journal of Chromatography*: Vols. 535 (1990) and 536 (1991). The Foreword to the proceedings and information on the Science Advisory and Organizing Committees only appear in Vol. 535. A combined Author Index to both Vols. 535 and 536 only appears in Vol. 536.

VOL. 535, NOS. 1+2 JOURNAL OF CHROMATOGRAPHY DECEMBER 28, 1990

CONTENTS

14TH INTERNATIONAL SYMPOSIUM ON COLUMN LIQUID CHROMATOGRAPHY, BOSTON, MA, MAY 20–25, 1990, PART I

In articles with more than one author, the name of the author to whom correspondence should be addressed is indicated in the article heading by a 6-pointed asterisk (*)

Journal of Chromatography, 535 (1990) 1
Elsevier Science Publishers B.V., Amsterdam

FOREWORD

The *Fourteenth International Symposium on Column Liquid Chromatography* was held in Boston, MA, U.S.A. on May 20–25, 1990. The meeting maintained the excitement and interest in the development of this most important separation field. Attendance was again well over 1000, with over 100 oral lectures and 300 poster presentations. The instrument exhibition included almost all of the major vendors of high performance liquid chromatography (HPLC) equipment and supplies.

Some major trends, seen in other meetings, continued. The increasing interest in biological applications, particularly separations of biopolymers, was evident. This was especially seen in the new designs of packing materials for analytical and preparative-scale separations and purifications. The increased focus of the pharmaceutical industry on optically pure materials was also evident in a large number of papers and spirited discussions. New techniques, such as high performance capillary electrophoresis were broadly discussed and inevitably compared to HPLC. In the instrumentation area, lasers continue to achieve lower detection limits through direct and indirect fluorescence detection. Undoubtedly, with continued miniaturization, laser-based detection will finally reach commercialization.

The opening plenary session brought together leading experts —Fred Regnier, Jack Kirkland, Dieter Hoehn and Michael Widmer— to talk about critical issues facing the separation sciences of the 1990s. There was remarkable agreement among the panel. Future directions in instrumentation and column design will include miniaturization, high-speed separations, automation and expert systems. The thrust of the analytical field into bioengineering and the biological sciences was noted. Finally, great concern was voiced on the decline in the number of students in science and analytical chemistry, in particular, in light of the critical need for researchers in biotechnology and molecular biology. The session evoked a great deal of discussion.

A special effort was made to support the travel of students to this meeting. Special thanks are due to the Bay Area Chromatography Colloquium and the Barnett Institute for their support of this effort. The following instrument companies are also thanked for their assistance in making the meeting so successful: Hewlett-Packard, Perkin-Elmer, Bio-Rad and Beckman.

A meeting of this size cannot be successful without a great deal of help from a number of people. Special thanks goes to Tom Gilbert, Vice Chairman, without whose mighty efforts the meeting would not have been possible. Grateful appreciation is given to Shirley Schlessinger for her organizational skills and assistance with the instrument exhibition and hotel accommodations. Erich Heftmann again did an excellent job in editing the symposium volumes in a timely fashion. The Permanent Scientific Committee, the Science Advisory Committee and the Organizing Committee are all thanked for their counsel and assistance in making the meeting so successful.

International meetings are often remembered many years after they have passed, because of the stimulating scientific discussions in both formal and informal settings. Most attendees left the meeting with a feeling that HPLC is alive and well. We can look forward to a number of years of exciting developments, as the premier separation technique continues to advance.

Boston, MA (U.S.A.) BARRY L. KARGER

Journal of Chromatography, 535 (1990) 3–12
Elsevier Science Publishers B.V., Amsterdam

CHROMSYMP. 1991

Key moments in the evolution of liquid chromatography

LESLIE S. ETTRE
Advanced Analytical Technology Group, The Perkin-Elmer Corporation, Norwalk, CT 06859-0284 (U.S.A.)

ABSTRACT

The paper is focusing on the work and activities of a few key scientists, from the very beginning to the mid-1940s, who had a key role in the evolution of liquid chromatography, and who laid the foundation on which present-day high-performance liquid chromatography could be developed.

INTRODUCTION

Today, with all the excitements related to the new developments, it is worthwhile to stop for a second and recall the work and activities of the pioneers in our discipline. Obviously, I would not have time to discuss the evolution of liquid chromatography from its inception to this symposium. Rather, I want to deal with the activities of a few people. In their selection I try to follow the principle used by Stephan Zweig (1881–1942), an Austrian writer famous mainly for his biographies. In one of his books entitled *Die Sternstunden der Menschheit*[a] [1] he tried to deal with the "star moments" of the human race: with key situations when, for a moment, the decision of a single person had a major influence on future events. Such a case was for example near Waterloo, on that faithful morning of June 18, 1815, when the French General Grouchy, whose orders were to find the army of the Prussian General Blücher, heard that a battle is under way, just a few miles from his troops. However, instead of turning around and joining Napoleon —which would undoubtly have tilted the balance in his favor— he continued to march to nowhere. He missed Blücher's troops who reached Waterloo at the decisive moment and were aiding Wellington in the final defeat of Napoleon.

In this paper, I am also dealing with such *Sternstunden,* key moments. I will discuss the activities of five people or groups who, at a certain moment during their professional life, were faced with a decision to select the proper method for the solution of their problem, and their decision influenced the future of chomatography.

[a] This is an almost untranslatable title. The English edition published in 1940 translated it as *The Tide of Fortune*. However, in my opinion, this translation of the original German title does not reproduce its real meaning.

0021-9673/90/$03.50

D. T. DAY AND THE "FILTRATION THEORY"

Let us start with David Talbot Day (1859–1925). He was a graduate of The Johns Hopkins University and has served between 1886 and 1914 as one of the principal scientists of the United States Geological Survey. This is the early period in the evolution of the American petroleum industry when the major petroleum fields were in Pennsylvania and Ohio. At that time a theory had been developed according to which there existed a "primary petroleum" which then migrated through the earth. During this migration the higher-boiling compounds were retained by the limestones and shales. Thus, some of the petroleum wells, located closer to the source of the primary petroleum will contain more high-boiling components than the petroleum of other wells further down from the original source, which are enriched in the lower-boiling components. This was called as the "filtration theory" and Day was one of its proponents. In 1897 in a paper entitled "A suggestion as to the origin of Pennsylvania petroleum" [2] he even suggested that the validity of this theory could be easily demonstrated by some experiments, which, of course, we would call today as frontal chromatography:

> *"... by experimental work it may be easily demonstrated that if we saturate a limestone such as the Trenton limestone with the oils characteristic of that rock and exert slight pressure upon it, so that it may flow upward through finely divided clay, it is easy to change it in its color to oils similar in appearance to the Pennsylvania oils, the oil which filters through being the lighest in color and the following oils growing darker."*

In the next years Day evidently carried out some experiments, with partial success; encouraged by these results, he presented a paper at the *First World Petroleum Congres* held in Paris, August 16–28, 1900, in conjunction with the International Exposition (where he was in charge of the petroleum exhibits of the U.S.A.). Day's paper was entitled "The variation in the characters of the crude oils of Pennsylvania and Ohio" and it was published in 1902, in the proceedings of the congress [3]; it is a relatively short paper, less than four printed pages long, written in a highly personal, first-singular mode and in a very eloquent French. Contrary to some reports[a] the "filtration experiments" are described only in general terms stating that

> *"the practical value of the process lies in the promise which inspired us to develop a scientific process for the separation of the various oils with which we now deal",*

without giving any information on the system he may have used, or on any results. The key statement in Day's paper is that

> *"the filtration method offers good hope; I wish to communicate to the world of scientists as the voice of the Congress, and I believe that before the next winter, I will be able to accomplish complete separations."*

---

[a] For example, Weil [4] refers to this paper as one which supposed to have shown partial separation of petroleum fractions. However, his English translation of the quoted key sentence significantly differs from the original French text.

In the decade after the congress Day and his associates and colleagues published a few papers [5–8] showing that if crude oil is passed through a column (they used tubes about 5.5 ft. long, with 1.25 in. I.D.) packed with Fuller's earth or clay, then there will be some differences in the physical properties (specific gravity and boiling range) of the fractions present at different distances along the column. However, there is no mentioning in these papers on any "complete separation" of various petroleum constituents; and even Day himself, in an 1911-paper summarizing his activities in the last 15 years [9], does not mention at all that real separation would have achieved.

Obviously Day was very close to "chromatography" and even the system used by him is not much different than the one used by Tswett about the same time (although Tswett's columns were shorter and generally had a smaller internal diameter). Tswett also relied on the separated fractions remaining on the column; we are still about 30 years away of collected fractions. The major differences were that Tswett carried out elution chromatography, with a finite sample dissolved in a solvent, and used a mobile phase for elution, while Day and his colleagues simply sucked the whole oil through the column; and that, by the skillfull selection of the adsorbent and the solvents, Tswett could separate pure compounds while Day only achieved some distribution of the petroleum's components along the column. Here is our key moment: Day was at the treshhold of inventing a new separation method. As correctly stated by Zechmeister [10] —himself a pioneer in chromatography— Day and his colleagues "might well under favorable circumstances developed (the filtration experiments) into systematic chromatography." However, this did not happen and thus, chromatography was invented by another scientist, M. S. Tswett, a contemporary of Day.

M. S. TSWETT AND THE DISCOVERY OF THE CHROMATOGRAPHIC SEPARATION TECHNIQUE

We now arrived at M. S. Tswett (1872–1919), the true inventor of liquid chromatography. Tswett's life and activities have been the subject of many papers and even books (see, *e.g.*, refs. 11–17); what I want to discuss here is the important moment in his life which represented the difference between playing in his laboratory or becoming the esteemed inventor of a new technique.

By his job description. Tswet was a botanist (this is what he was teaching between 1902 and 1916 in Warsaw) although I would rather consider him a physicochemist. He was interested in plant pigments and he tried to isolate them from the plants; but he also realized that there are many compounds present simultaneously and thus, not only isolation of a single compound is needed but also separation of the compounds present together. Being a botanist by training, he was also interested in the natural systems represented by the plants in which these pigments are present. He considered adsorption as one of the natural forces fixing the chloropast pigments in plants and thus, his interest turned to this process and to the behavior of the various adsorbents. He postulated that the reason why polar solvents can extract the pigments from plant material while non-polar solvents cannot is that the former can break down the original adsorption complex while non-polar solvents do not have this ability. He even carried out some model experiments showing how pigment mixtures became adsorbed to various materials; as the next step he tried to utilize controlled adsorption to separate pigments extracted from plants.

Evidently Tswett started to utilize the technique we now call chromatography around 1902. We have the text of a lecture he presented in March 1903, at a meeting of the Biological Section of the Warsaw Society of Natural Sciences, entitled "On a new category of adsorption phenomena and their application to biochemical analysis" [18]. He used inulin as the adsorbent, packed in a small column. A ligroin solution of a plant extract was added onto the column and washed down with the solvent, creating well-defined and separated green and yellow rings. Obviously this has already been chromatography, although in the paper, Tswett did not use this name as yet.

It is interesting to note that although Tswett had a number of publications in western (German and French) journals in this period, he did not describe the new technique in them. It is difficult to explain the reason for this: either he did not feel it ready for publication, or considered it just a routine laboratory technique, not important enough for publication. Let me repeat: Tswett was a botanist, dealing with plant pigments, and not with separation methods, and most of his western publications were in botanical journals.

He finally changed his attitude in 1905. In September of that year Tswett published a paper [19] in which he criticized a report [20] on the pigments of brown algae written by Hans Molisch (1856–1937), an important and highly respected botanist in the Austro-Hungarian Monarchy who, at that time, was professor at the University of Prague and head of the Institute of Plant Physiology. In this paper Tswett mentioned that his more correct data were obtained with help of a "new, reliable method" he developed during the past few years. A controversy evolved in which everybody important in this field ridiculed Tswett's comments; after all, he did not give any details. In his reply [21] Tswett rejected the arguments of his opponents and promised that he will now really publish a report on his method; and indeed, within a month, in June 1906, he submitted two papers to the Bulletins of the German Botanical Society which represent the fundamental description of the chromatographic separation method. Due to their importance we should list here the titles of these two papers: "Physical-chemical studies on the chlorophyll. The adsorptions" [22], and "Adsorption analysis and the chromatographic method. Application to the chemistry of chlorophyll" [23].

This was the moment when Tswett had to make a decision: keep his method for himself or disclose it to the international scientific community. He selected the latter and, of course, the rest is history: chromatography was born.

L. S. PALMER: CHROMATOGRAHY EXPLAINING WHY THE BUTTER IS YELLOW

In the next 25 years, Tswett had only a few followers from whom I mention three, two in Europe and one here in the United States. The two Europeans are Charles Dhéré (1876–1955) at the University of Fribourg, in Switzerland, and Theodor Lippmaa (1829–1944) at the University of Tartu, in Estonia. For both Dhéré and Lippmaa chromatography was simple a tool for separation, they did not even describe the technique in their publications; therefore, from the point of the evolution of chromatography, their activities are only secondary. There was, however, one American scientist in this period who had a key role both as an original researcher expanding the utilization of chromatography and as the transmission between Tswett and the next generation. He is Leroy Sheldon Palmer (1887–1944).

Leroy Sheldon Palmer graduated in 1910 as a chemical engineer at the University of Missouri, in Columbia; however, in graduate school he switched to agricultural chemistry. After receiving his Ph.D., in 1913, Palmer joined the faculty of the College of Agriculture at the University of Missouri; in 1919, he moved to the University of Minnesota where he became Professor of Agricultural Biochemistry and later the head of that Division. During his long and distinguished career Palmer became one of the most important scientists of his time in the field of dairy chemistry and nutrition.

Palmer started to work on his Ph.D. thesis in 1910, finishing it in 1913. The work dealt with the carotenoid pigments in milk and milk products and their relationship to the pigments present in the food intake of the animal. He started these investigations at the time when the information available was very little; let us not forget that, *e.g.*, even the elementary composition of "carotin" and "xanthophyll" were established only in 1907 by Willstätter and Mieg [24] as $C_{40}H_{56}$ and $C_{40}H_{56}O_2$ respectively. At that time no structural information was available except that "carotin" is a hydrocarbon and "xanthophyll" has hydroxy groups. Even the fact that we are faced with a group of similar compounds was not a generally accepted fact. The name "carotenoids" was proposed in 1911 by Tswett [25] to indicate their apparent close relationship to the most important member of the group, but the final nomenclature of these compounds was not established until the late 1930s.

It is simply amazing to recognize how quickly Palmer adopted Tswett's method, chromatography, for his own research. He started his graduate research only four years after Tswett's publications and he fully utilized it for the separation of the various pigments present in milk and milk products. In this thesis [26] which was also published in four parts in the *Journal of Biological Chemistry* [27], coauthored with C. H. Eckles (1875–1933), the head of the Department of Dairy Husbandry at Columbia, he described in detail the technique and showed a number of practical applications.

Palmer's graduate work represents without any question the first systematic investigation to show that there is a definite relationship between the yellow pigment present in the plants and in the animals' fat. In fact he made it clear that the plant pigments are directly transferred into the animals' fat: in other words, the animals do not produce them. In connection with this work, I should mention an interesting finding. Recently, in a storage room of the University of Missouri, in Columbia, we have found a large poster, obviously prepared by Palmer in the 1913–1919 period [28]. It had the title "why the butter is yellow" and explained in a popularizing way that the grass the cows are eating contain among others yellow pigments which are transferred into the milk and milk products, causing the yellow color of the butter. Most likely this poster was prepared as part of the exhibition of the University's School of Agriculture or of the Missouri Agricultural Experient Station at various county fairs.

Another interesting point in Palmer's work was that —similarly to Tswett— he used ultraviolet spectroscopic measurements for the identification of the pigments present in the individual fractions of various samples. If two fractions occurring in different samples had the same absorption maxima, he considered them being chemically identical. In this, again, he was ahead of his time: UV identification of the chromatographic fractions was systematically used only over 20 years later, in the laboratory of Richard Kuhn, in Heidelberg.

In the years following his graduation Palmer continued to be engaged in

investigations relating the pigments present in the animal feed to the pigments present in milk and milk products, and further refining the methodology used for the separation of these pigments. This work finally culminated in a book on carotenoids [29] in which he again gave a detailed description of the chromatographic technique. This book is particularly important because, as we shall see below, Edgar Lederer learned chromatography from it.

As explained in the Introduction, our criterion for inclusion in this discussion was whether, at one point during his activities, a person had a key moment, facing the need for a decision which, in turn, significantly influenced the evolution of chromatography. This was certainly the case with Palmer: when he started his investigations on the pigments present in plants and in milk and milk products, chromatography, a very new and yet unproven technique, was certainly not the obvious choice: he could have utilized the techniques used at that time by Willstätter and others studying these pigments, which were based on selective extraction and crystallization. In this respect it is worthwhile to quote from a paper by Schertz of the U.S. Department of Agriculture (*i.e.*, another agricultural chemist), published in 1929 [30]:

> *"While Tswett's methods have been shown to be unreliable in identifying and distinguishing carotin and xanthophyll, the methods of Willstätter have been shown to be more reliable for this purpose."*

Even 20 years after Palmer's investigations, the reliability of chromatography was questioned!

To be fully objective, I must also mention that Palmer has another *Sternstunde*, key moment, in his later professional life, but there, he apparently did not recognize the opportunity. This refers to his nutrition studies: for a long time Palmer refused to accept the physiological and chemical relationship between the carotenoids and vitamin A, and he did not believe that vitamin A can be produced in the animal's body from carotene. This discovery was done in the late 1920s and early 1930s by Hans Euler-Chelpin (Stockholm University), Thomas Moore (Dunn Nutrition Laboratory, Cambridge, U.K.) and Paul Karrer (University of Zürich, Switzerland). Palmer had years earlier many data indicating this, but he did not consider them conclusive.

EDGAR LEDERER AND THE REBIRTH OF CHROMATOGRAPHY

By the late 1920s, chromatography was almost forgotten in Europe. Its "rebirth" can be accredited to Edgar Lederer, in the laboratory of Richard Kuhn, in Heidelberg, and we have here again a *Sternstunde* in the evolution of chromatography. The story had been told a number of times (see, *e.g.*, refs. 31–33); therefore, just a brief summary is given here.

Edgar Lederer (1908–1988) was born and studied at Vienna, Austria. After receiving his Ph.D., he joined in September 1930 the Institute of Chemistry of the Kaiser Wilhelm Institute for Medical Research at Heidelberg, Germany, headed by Professor Richard Kuhn, a pupil of Willstätter. There, Lederer's first job was to investigate whether the yellow pigment in egg yolk is not a mixture of some pigments found in plant material. As usual with young postdocs, Lederer carefully checked the literature the most important of which was Palmer's carotenoid book [29], and in it, he

found reference to Tswett, description of his chromatograhic separation method and illustrations for its possible use. Continuing his search, he also found a personal copy of the German translation of Tswett's 1910 book [34] (prepared specially for Willstätter). Based on all this information, Lederer decided —and this is that fateful moment— to try out chromatography, a technique which up to then was not used by anybody at Heidelberg.

In December 1930, he prepared a small (15 cm × 1 cm I.D.) column containing powdered calcium carbonate, and added the solution of a pigment mixture in carbon disulfide. By adding additional solvent to the top of the column, four well-separated rings were obtained. This experiment was then followed by others, separating the xanthophylls of egg yolk. The results were summarized first in a single-page report [35] followed by two detailed papers [36, 37], representing the rebirth of chromatography. From here on, the evolution of our technique is uninterrupted and straightforward.

THE MANHATTAN PROJECT AND THE PREPARATIVE SEPARATION OF RARE EARTHS BY ION-EXCHANGE CHROMATOGRAPHY

As the last example for a key development in he evolution of chromatography a little known application of the technique is mentioned which was the first application of chromatography for preparative (or, probably, more correctly, for production) purposes.[a] Here, again, we have a case where a problem evolved and the scientists involved in it had to make a decision how to solve it. Chromatography was not the obvious solution, but nevertheless it was a right decision.

We have to go back 50 years, to the start of the Manhattan project. Obviously this project consisted not only of the direct development of the atomic bomb, but there were also many parallel investigations on various theoretical and practical aspects. One of these had to do with the need to identify the fission products of uranium which in turn led to the project dealing with the separation of rare earth elements. This work started in 1942 at the Metallurgical Laboratory of the University of Chicago, but within a year moved to Clinton National Laboratories at Oak Ridge, Tennessee (the present-day Oak Ridge National Laboratories). From the many possibilities they decided to try the new synthetic ion-exchange resins which were commercially available just about that time (see *e.g.*, the work of Samuelson [38, 39]). The project was very difficult and also had to deal with basic investigations on ion exchange. They advanced rapidly and by December 1944, a second group at the Institute for Atomic Research at Iowa State College, at Ames, Iowa (the present-day Iowa State University), headed by F. H. Spedding, started to use ion-exchange chromatography on the preparative scale.

Obviously, because of the confidential nature of the work, nothing could be published during the war: they received the green light for this only after the war. Their first report was at a special Symposium on Ion-Echange Separations held during the Fall 1947 National Meeting of the American Chemical Society, in New York City, followed by the publication of 13 articles as a single issue of the *Journal of the American*

[a] Both Tswett and Lederer had already used chromatography for the preparation of pure fractions. However, their work involved only relatively small (up to maybe a few grams) quantities.

TABLE I

PURE RARE EARTHS PREPARED AT THE INSTITUTE FOR ATOMIC RESEARCH, IOWA STATE COLLEGE- AMES, IOWA, AS PART OF THE MANHATTAN PROJECT

After Spedding *et al.* [40,43].

Element		Quantity prepared (g)	Purity[a]
No.	Name		
59	Praseodymium	35	99%
		160	90%
60	Neodymium	800	99.9%
		770	98%
62	Samarium	160	>99.9%
		600	99%
69	Thulium	15	"Very rich"
70	Ytterbium	300	"Pure"
71	Lutetium	15	"Spectroscopically pure"

[a] Purity expressed as percent rare earth oxide.

Chemical Society in November 1947 of which one paper [40], by Spedding's group, discussed the "pilot-plant scale separations" of rare earths.

The "chromatographic plants" at Ames, Iowa, consisted of 24 columns, each 10 ft. long, with 4 in. diameter, and as one sample, 100 g of crude rare earth salts were introduced into each column. For one such sample over thousand liters of mobile phase (a 0.5% aqueous citrate solution, with a velocity of 0.5 cm/min) were used. The individual fractions were collected and then the halids of the rare earths were recovered and transformed into the rare earth metals by thermal reduction with calcium. In order to have some idea of the extent of these activities, in Table I, I list the amounts of the pure rare earths prepared during the project.

One of the most important chromatographic meetings ever happened was organized in September 1949, in England, by the Faraday Society [41]. At this meeting 43 papers were presented; from these two were given by members of the Manhattan Project team; the first, presented by Tompkins of Oak Ridge, dealt with the theoretical aspects and the use of ion-exchange chromatography for the separation of rare earth salts in very low concentrations [42], while the paper by Spedding reported on the large-scale separation of rare-earth salts and the preparation of the pure metals [43]. The highlight of the meeting was when Spedding opened his briefcase and took out rods of pure rare earth metals, showing them to the audience.

EPILOGUE

With this, we arrived close to our time. I could continue by pointing out additional key moments in the evolution of liquid chromatography such as, *e.g.*, the fundamental work by Martin and Synge published in 1941 and first describing liquid–liquid partition chromatography [44] for which they received the 1952 Nobel Prize in Chemistry; the development of paper chromatography in 1944 by Consden, Gordon and Martin [45]; or the first description of reversed-phase chromatography, in

1950, by Howard and Martin [46] and of gradient elution by Tiselius' group, in 1952 [47]. I could also deal with the pioneering work done in the mid-1960s by J. F. K. Huber [48] and Csaba Horváth [49] leading to HPLC [50]. But these are much too recent developments, and I leave their discussion to the next chronicler.

REFERENCES

1 S. Zweig, *Die Sternstunden der Menschheit*. First published in 1928 by Insel Verlag (Leipzig); current edition: Fischer Taschenbuch Verlag, Frankfurt, 1964. English translation: *The Tide of Fortune*, The Viking Press, New York, 1940.
2 D. T Day, *Proc. Am. Phil. Soc.*, 36 (1897) 112–115.
3 D. T. Day, *Congrès International du Pétrole, Paris, 1900; J. Pét.*, (1902) 53–56.
4 H. Weil, *Petroleum (London)*, 14, No. 1 (1951) 5–12, 16.
5 D. T. Day, paper presented at the *143rd Meeting of the Geological Society of Washington, D.C.*; see W. C. Mendenhall, *Science (Washington, D.C.)*, 17 (1903) 1007–1008.
6 D. T. Day and J. E. Gilpin, *Ind. Eng. Chem.*, 1 (1909) 449–455.
7 J. E. Gilpin and M. P. Cram, *Am. Chem. J.*, 40 (1908) 495.
8 J. E. Gilpin and D. E. Bransky, *Am. Chem. J.*, 44 (1910) 251–303.
9 D. T. Day, *Trans. Am. Inst. Mining (Metal) Eng.*, 44 (1911) 219–224.
10 L. Zechmeister, paper presented at the *Conference on Chromatography organized by the New York Academy of Sciences, New York, November 29–30, 1946; Ann. N.Y. Acad. Sci.*, 49 (1948) 145–160.
11 Ch. Dhéré, *Candollea (Génève)*, 10 (1943) 23–73.
12 T. Robinson, *Chymia*, 6 (1960) 146–160.
13 K. I. Sakodynskii, *Chromatographia*, 3 (1970) 92–94.
14 K. I. Sakodynskii, *J. Chromatogr.*, 49 (1970) 2–17.
15 K. I. Sakodynskii, *J. Chromatogr.*, 72 (1972) 303–360.
16 E. M. Senchenkova, *Mikhail Semenovich Tsvet*, Nauka, Moscow, 1973 (in Russian).
17 K. I. Sakodynskii, *Mikhail Tswett —His Life and Work*, Carlo Erba, Milan, 1982.
18 The Russian text of this paper was published in *Tr. Varshavskogo Obshch. Estestvoispytatelei Otd. Biologii*, Vol. 14 (1903; actually published in 1905). The English translation of the paper was included in G. Hesse and H. Weil, *Michael Tswett's First Paper on Chromatography*, Woelm, Eschwege, 1954.
19 M. S. Tswett, *Botan. Z.*, 63 (1905) (II) 273–278.
20 H. Molisch, *Botan. Z.*, 63 (1905) (I) 131–162.
21 M. S. Tswett, *Ber. Dtsch. Botan. Ges.*, 24 (1906) 235–244.
22 M. S. Tswett, *Ber. Dtsch. Botan. Ges.*, 24 (1906) 316–323.
23 M. S. Tswett, *Ber. Dtsch. Botan. Ges.*, 24 (1906) 384–393.
24 R. Willstätter and W. Mieg, *Ann. Chem.*, 355 (1907) 1–28.
25 M. S. Tswett, *Ber. Dtsch. Botan. Ges.*, 29 (1911) 630–636.
26 L. S. Palmer, *Carotin: the Principal Natural Yellow Pigment of Milk Fat. Chemical and Physiological Relations of Pigments of Milk Fat of the Carotin and Xanthophylls of Green Plants*. Ph.D. Thesis, University of Missouri, Columbia, MO, 1913.
27 L. S. Palmer and C. H. Eckles, *J. Biol. Chem.*, 17 (1914) 191–221, 223–236, 237–243, 245–249.
28 L. S. Ettre and R. L. Wixom, *Leroy Sheldon Palmer and the Beginnings of Chromatography in the United States of America*. Manuscript deposited at the Library of the University of Missouri, Columbia, MO, 1989.
29 L. S. Palmer, *Carotinoids and Related Pigments. The Chromolipoids*, Chemical Catalog Co., New York, 1922.
30 F. M. Schertz, *Plant Physiol.*, 4 (1929) 337–348.
31 E. Lederer, *J. Chromatogr.*, 73 (1972) 261–266.
32 E. Lederer, in L. S. Ettre and A. Zlatkis (Editor), *75 Years of Chromatography —a Historical Dialogue*, Elsevier, Amsterdam, 1979; pp. 247–254.
33 L. S. Ettre, *J. High Resolut. Chromatogr. Chromatogr. Commun.*, 2 (1979) 500–506.
34 M. S. Tswett, *Khromofilly v Rastitel'nom i Zhivotnom Mire* (*Chromophylls in the Plant and Animal World*), Izd. Karbasnikov, Warsaw, 1910. The book was partially reprinted in 1946 by the Publishing House of the Academy of Sciences of the U.S.S.R., Moscow; the reprint was edited by A. A. Rikhter and T. A. Krasnosel'skaya.

35 R. Kuhn and E. Lederer, *Naturwiss.*, 19 (1931) 306 only.
36 R. Kuhn, A. Winterstein and E. Lederer, *Z. Physiol. Chem.*, 197 (1931) 141–160.
37 R. Kuhn and E. Lederer, *Ber.*, 64 (1931) 1349–1357.
38 O. Samuelson, *Z. Anal. Chem.*, 116 (1939) 328.
39 O. Samuelson, *Svensk. Kem. Tidskr.*, 51 (1939) 195–206. The original (German) text of the paper and its English translation was included in: H. F. Walton (Editor), *Ion-Exchange Chromatography* (*Benchmark Papers in Analytical Chemistry*, No. 1), Dowden, Hutchinson & Ross, Stroudsburg, PA, 1976; pp. 10–24.
40 F. H. Spedding, E. I. Fulmer, T. A. Butler, E. M. Gladrow, M. Gobush, P. E. Porter, J. E. Powell and J. M. Wright, *J. Am. Chem. Soc.*, 69 (1947) 2812–2818.
41 *General Discussion on Chromatographic Analysis, Organized by the Faraday Society, Reading University; September 22–24, 1949.* The proceedings of the meeting were published as No. 7 of the *Discussions of the Faraday Society*.
42 E. R. Tompkins, *Disc. Faraday Soc.*, No. 7 (1949) 232–237.
43 F. H. Spedding, *Disc. Faraday Soc.*, No. 7 (1949) 214–231.
44 A. J. P. Martin and R. L. M. Synge, *Biochem. J.*, 35 (1941) 1358–1368.
45 R. Consden, A. H. Gordon and A. J. P. Martin, *Biochem. J.*, 38 (1944) 224–232.
46 G. A. Howard and A. J. P. Martin, *Biochem. J.*, 46 (1950) 532–538.
47 R. S. Alm, R. J. P. Williams and A. Tiselius, *Acta Chem. Scand.*, 6 (1952) 826–836.
48 See J. F. K. Huber, in L. S. Ettre and A. Zlatkis (Editors), *75 Years of Chromatography —A Historical Dialogue*, Elsevier, Amsterdam, 1979, pp. 159–166.
49 See Cs. Horváth, in L. S. Ettre and A. Zlatkis (Editors), *75 Years of Chromatography —A Historical Dialogue*, Elsevier, Amsterdam, 1979, pp. 151–158.
50 For a brief summary of the start of HPLC, see L. S. Ettre, *LC Mag.*, 1 (1983) 408–410, 413.

Journal of Chromatography, 535 (1990) 13–31
Elsevier Science Publishers B.V., Amsterdam

CHROMSYMP. 2041

Performance of wide-pore silica- and polymer-based packing materials in polypeptide separation: effect of pore size and alkyl chain length

NOBUO TANAKA*, KAZUHIRO KIMATA, YASUHIRO MIKAWA, KEN HOSOYA and TAKEO ARAKI
Kyoto Institute of Technology, Matsugasaki, Sakyo-ku, Kyoto 606 (Japan)
YUTAKA OHTSU and YOSHIHIRO SHIOJIMA
Shiseido Research Centre, Yokohama 223 (Japan)
RIYOU TSUBOI
Nacalai Tesque, Muko, Kyoto 617 (Japan)
and
HAJIME TSUCHIYA
Nitto Technical Information Centre, Ibaraki 567 (Japan)

ABSTRACT

The effects of pore size and alkyl chain length of silica- and polymer-based packing materials in the elution of polypeptides with an acetonitrile gradient in the presence of trifluoroacetic acid were studied. Considerable differences were found in the performance of alkylsilylated phases prepared from various wide-pore silica particles assumed to have 30–50-nm pores. The pore size of such silica gels was found to be the critical factor in determining the efficiency for high-molecular-weight polypeptides. Silica C_{18} phases having small pore volumes below 20 nm pore diameter showed comparable performances to C_4 and C_8 phases for polypeptides with molecular weights of up to 80 000, and were more stable. Polymer-based packing materials with adequate pore size provided excellent column efficiencies and recoveries for polypeptides with higher chemical stabilities than silica-based materials.

INTRODUCTION

Silica-based packing materials for reversed-phase liquid chromatography (RPLC) have been extensively studied with respect to silica surface and bonding chemistry in order to produce current high-performance materials. These silica-based packing materials, however, are not totally satisfactory. Relatively low chemical stability in acidic and basic mobile phases and an inadequate performance for high-molecular-weight polypeptides are potential problems with these materials. Although the pore sizes were taken into account when chemically bonded silica gels were applied to the separation of high-molecular-weight solutes [1–10], current wide-pore packing materials have not yet been critically evaluated in this respect. The advantage of wide-pore over small-pore materials in polypeptide separations has been

0021-9673/90/$03.50

well recognized. However, different wide-pore silica gels have rarely been compared with each other.

Polymer gels for RPLC possessing higher chemical stability have been introduced recently. Although their performances with small molecules are generally believed to be lower than those of silica-based materials, they have been employed for the separation of small molecules and polypeptides with adequate performance, especially under severe elution conditions [11].

Silica- and polymer-based packings are frequently compared with each other, and they should complement each other in the separation of small molecules, because silica-based packings are not as chemically stable as polymer gels and polymer gels are generally less efficient, particularly in highly aqueous mobile phases.

One area of RPLC where silica- and polymer-based packings can be in serious competition is the separation of polypeptides under an acetonitrile gradient in the presence of trifluoroacetic acid (TFA). Although a high performance of some polymer gels has been reported [10,12–14], silica-based materials are still mainly used in these applications [10,15]. The most commonly employed packing materials are prepared from wide-pore silica gels having a pore size of *ca.* 30 nm bonded with short alkyl groups such as C_3–C_6 [10,15,16]. These materials however, possess a serious problem with regard to chemical stability [17,18], in spite of their better performance than longer alkyl-chain stationary phases in terms of protein recovery and column efficiency. On the other hand, Szczerba *et al.* [19] reported that a wide-pore C_{18} stationary phase showed a high column efficiency for high-molecular-weight polypeptides.

Users should be better informed about the choice of wide-pore packing materials, whether short-chain alkyl-bonded silica phases are really required, or whether more stable stationary phases can also be used. The effect of chain length should be examined with wide-pore silica gels with sufficiently large pores, as pointed out by Cooke *et al.* [4]. We report here that silica C_{18} and polymer-based packing materials with adequate pore sizes can give high efficiencies for polypeptide separations and higher chemical stabilities than silica C_4 phases. Polymer-based packing materials having C_4 or C_8 alkyl groups provide both high efficiency and high recoveries for high-molecular-weight or hydrophobic polypeptides.

EXPERIMENTAL

Equipment

Two types of liquid chromatograph were used. One consisted of two Model 880 pumps and a Model 875 UV detector (JASCO, Tokyo, Japan) with a Model C-R3A data processor (Shimadzu, Kyoto, Japan), and the other two Model LC-6A pumps, a Model SPD-6A UV detector and a Model C-R3A data processor (all from Shimadzu).

Materials

The silica gels and polymer gels listed in Table I were examined. In addition to the commercially obtained materials, some experimental silica gels, Hypersil 300E, Shiseido 300E and Kromasil 200E, were also examined (according to the manufacturer of Hypersil, the current commercial materials possess the characteristics of Hypersil

300E used in this work). All the silica particles were derivatized to C_4 and C_{18} phases with maximum surface coverage by using alkyldimethylchlorosilanes as reported previously [20]. A C_{18} phase (C_{18}T) was also prepared from LiChrospher Si 500 by using octadecyltrichlorosilane instead of monochlorosilane.

Prepacked columns were used for Asahipak (150 mm × 4.6 mm I.D.) and Shodex (150 mm × 6 mm I.D.) materials, and PLRP-S 300, TSK C_{18}-4PW and all the silica-based materials were packed into stainless-steel columns (100 mm × 4.6 mm I.D.) in the laboratory.

Protein standards were obtained from Sigma (St. Louis, MO, U.S.A.). TFA and HPLC-grade solvents, acetonitrile and water were obtained from Nacalai Tesque (Kyoto, Japan).

Characterization of packing materials

Transmission electron microscopy (TEM) was carried out at the Nitto Technical Information Centre. Ultrathin sections of the particles were prepared as reported previously [21].

Nitrogen adsorption measurements were carried out at the Shiseido Research Centre by using Autosorb I (Quantachrome, Syosset, NY, U.S.A.). The pore-size distribution of the polymer gels was also determined by inverse size-exclusion

TABLE I

PORE PARAMETERS OF WIDE-PORE SILICA AND POLYMER GELS

Manufacturer's specifications (with values found experimentally by nitrogen adsorption in parentheses).

Packing material	Surface area (m^2/g)	Pore size (nm)[a]	Pore volume (ml/g)	Particle size (μm)	Manufacturer
LiChrospher Si 500	50(69)	50(40)	0.8(0.90)	10	Merck
Spherisorb 300	190(209)	30(35)	1.5(1.62)	5	Phase Separations
Nucleosil 300	100(109)	30(15,70)	0.8(0.81)	5	Machery, Nagel & Co.
Vydac TP	80(93)	30(26)	0.6(0.69)	10	Separations Group
Hypersil 300(I)	60(58)	30(20)	0.6(0.53)	5	Shandon
Hypersil 300(II)	(47)	(20)	(0.56)	5	
Hypersil 300E	(71)	(35)	(0.73)	5	
Shiseido 300E	(180)	(26)	(1.47)	5	Shiseido
Kromasil 200E	(174)	20(18)	(0.86)	10	Eka Nobel
Kromasil 100	350	10	0.9	10	
Cosmosil 100	330(300)	11(12)	(1.08)	5	Nacalai Tesque
PLRP-S 300	(380)	30(60)	(1.26)	8	Polymer Labs.
TSK C_{18}-4PW	(64)	(50)	(0.64)	10	Tosoh
Asahipak ODP	(108)	(26)	(0.57)	6	Asahi Chem.
Asahipak C8P	(260)	(26)	(0.81)	6	Ind.
Asahipak C4P	(374)	(26)	(0.95)	6	
Shodex D18-613	(56)	–	(0.42)	6	Showa Denko
Shodex D8-613	(98)	–	(0.53)	6	
Shodex D4-613	(100)	–	(0.54)	6	
Shodex DE-613	(354)	(5)	(0.41)	6	

[a] Experimentally obtained values indicate the pore diameter that corresponds to the maximum in the pore volume–pore radius plot.

chromatography using polystyrene standards in tetrahydrofuran as reported by Knox and Scott [22].

The metal contents of the silica particles were examined by inductively coupled plasma atomic emission spectrometry (Jobin-Yvon, Longjumeau, France).

The chemical stabilities of the packing materials, Shodex D4-613, LiChrospher C_4 and C_{18} and also $C_{18}T$, were tested by keeping the materials in columns in 0.1% TFA at 60°C. The columns were flushed with 20 ml of tetrahydrofuran at intervals at room temperature, and the retention of alkylbenzenes was measured in 60% methanol at 30°C.

Chromatographic measurements

Two types of linear acetonitrile gradient were used: (I) from 20% acetonitrile (0.1% TFA) to 60% acetonitrile (0.1% TFA) in 20 min, and (II) from 0.1% TFA in water to 60% acetonitrile (0.1% TFA) in 30 min. Type I was used for the evaluation of packing materials with the three polypeptides, cytochrome *c*, lysozyme and bovine serum albumin (BSA), and type II for the elution of a wider range of peptides (molecular weight in parentheses), glycyltyrosine (238), α-endorphin ($1.7 \cdot 10^3$), Leu-enkephalin (556), insulin (6000), cytochrome *c* ($12 \cdot 10^3$), transferrin ($80 \cdot 10^3$), BSA ($66 \cdot 10^3$), β-lactoglobulin ($18 \cdot 10^3$) and γ-globulin ($160 \cdot 10^3$).

Protein recovery was examined with a type I gradient by observing the peak areas of cytochrome *c*, lysozyme, BSA, β-lactoglobulin and ovalbumin in the gradient elution and two subsequent runs without sample injection. The ratio of the peak area in the first gradient run to the total peak areas of the three runs obtained with the C_4 phase was taken as the recovery of proteins. The recoveries on the other phases were calculated by normalizing the peak area by using BSA as a standard.

RESULTS AND DISCUSSION

Silica-based packing materials

Several wide-pore silica gels, shown in Table I, including the commercially obtained materials and the experimental batches (Hypersil-300E, Shiseido 300E and Kromasil 200E) and also small-pore materials (Kromasil 100 and Cosmosil 100) were examined. Average pore sizes determined by nitrogen adsorption agreed well with the specifications of the commercial material, either 30 or 50 nm for wide-pore silica gels, although considerable variations were found in the pore-size distributions. The pore size corresponding to maximum pore volume of each packing material is given in Table I. Nucleosil 300, showing a bimodal pore-size distribution in Fig. 1b, is a blended material as previously observed by TEM [21].

As shown in Fig. 1, LiChrospher Si 500 and Spherisorb 300 possess small pore volumes below 20 nm pore diameter, whereas Hypersil 300 (I and II), Vydac TP and Nucleosil 300 showed the presence of considerable pore volumes in the pore-size range 10–20 nm. The two experimental batches of silica gel, Hypersil 300E and Shiseido 300E, showed relatively sharp pore-size distributions with small pore volumes below 20 nm. The pore sizes of Kromasil 200E, Kromasil 100 and Cosmosil 100 were *ca.* 18, 10 and 12 nm, respectively. A considerable overlap was seen in the pore-size distributions of Kromasil 200E and Hypersil 300.

All the silica gels were derivatized to C_4 and C_{18} phases and tested in the gradient

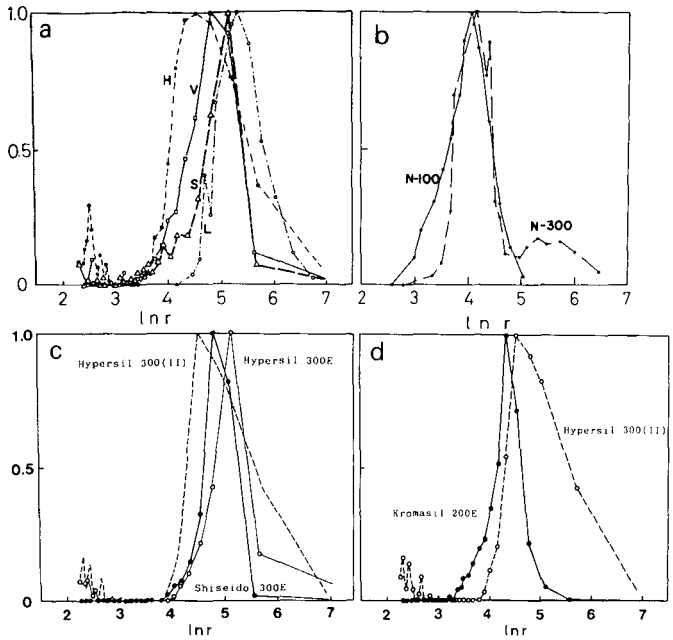

Fig. 1. Pore-size distributions of silica particles determined by nitrogen adsorption. The vertical axis corresponds to the fraction of pore volume; r = pore radius. (a) L = LiChrospher Si 500; S = Spherisorb 300; V = Vydac TP; H = Hypersil 300(I). (b) N-300 = Nucleosil 300; N-100 = Nucleosil 100. (c) Hypersil 300E, Hypersil 300(II) and Shiseido 300E. (d) Kromasil 200E and Hypersil 300(II).

elution of polypeptides. The interaction of the stationary phases with basic substances was minimized by washing the silica particles with acids prior to the bonding reaction with alkyldimethylchlorosilanes to achieve maximum surface coverages. For small molecules, differences in the preparation methods and in the silica particles resulted in a variety of commercial C_{18} phases, providing different selectivities which can be chromatographically characterized by using several sets of solutes [23]. In this study, a variety of packing materials with C_4–C_{18} alkyl groups prepared from various wide-pore silica gels were subjected to examination with polypeptides.

Although silica-based short-chain alkyl-bonded phases have been extensively employed in polypeptide separations [15], the use of C_{18} phases would be preferable if chemical stabilities are to be considered. As shown in Fig. 2, the C_{18} phases of LiChrospher Si 500 and Spherisorb 300 showed excellent performance for all the polypeptides with molecular weight up to 80 000, including BSA and transferrin.

In contrast, the C_{18} phase from 10-nm pore silica gel and those from the three wide-pore silica gels, Nucleosil 300, Vydac TP and Hypersil 300(I), having relatively small pores, showed peak broadening and tailing for BSA, as shown in Fig. 2. The peaks of BSA and transferrin with Nucleosil 300-C_{18} are reasonably sharp, but they are tailed and much broader than the other peaks. The results indicate that the peak broadening and tailing seen with materials containing relatively small pores are caused by the high molecular weight of the polypeptides, not by the high hydrophobicities,

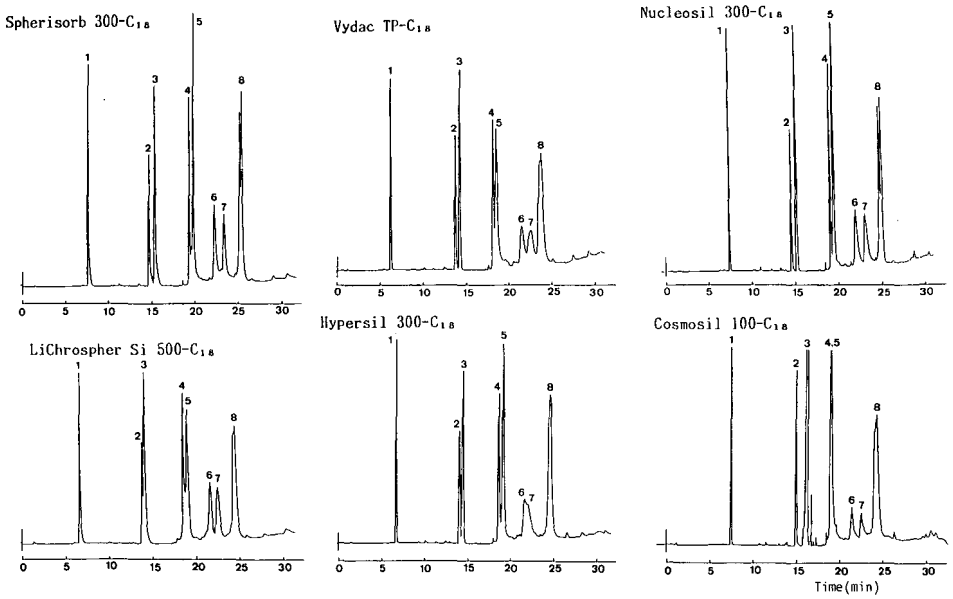

Fig. 2. Elution of peptides [(1) glycyltyrosine; (2) α-endorphin; (3) Leu-enkephalin; (4) insulin; (5) cytochrome *c*; (6) transferrin; (7) BSA; and (8) β-lactoglobulin] on C_{18} phases prepared from wide-pore silica gels. Gradient type II (see Experimental) was used.

because the late-eluting β-lactoglobulin was eluted with high efficiency. We therefore included BSA to test other packing materials in the following study.

Fig. 3 shows the effect of alkyl chain length on LiChrospher Si 500 and Spherisorb 300. In the examination of packing materials with polypeptides, including cytochrome *c*, lysozyme and BSA, 1-naphthylmethanol was also included so that poor column packing with some stationary phases can be taken into account. When the small molecule shows peak tailing, as with Spherisorb C_4, the peak tailing with polypeptides can be discounted.

All the stationary phases from Spherisorb 300 and LiChrospher Si 500, regardless of the alkyl chain length, showed satisfactory performance for the polypeptides. The peak shape on the C_{18} phase was comparable to that on C_4 or C_8 phases. The results indicate that a C_{18} phase instead of C_4 can be selected for polypeptide separation if desired separations can be achieved with acceptable recovery. There seems to be little difference in peak capacity among these phases.

The C_{18} phases from Hypersil 300E and Shiseido 300E also showed excellent performance for the three polypeptides, as shown in Fig. 4. Although BSA was separated into two sharp peaks appearing as a shoulder with Hypersil 300E, the peak tailing on the C_{18} phases prepared from commercial Hypersil 300 (I and II) disappeared. It should be noted that a small pore volume was found below 20 nm with these experimental silica gels of 30 nm pore size, as shown in Fig. 1c. Hypersil 300E showed considerable improvements in the extent of tailing compared with the older type commercial products. The results shown in Figs. 2–4 indicate that the alkyl chain length of the stationary phase is not a critical factor in determining the column efficiency for the polypeptides under the present conditions [1,5,19].

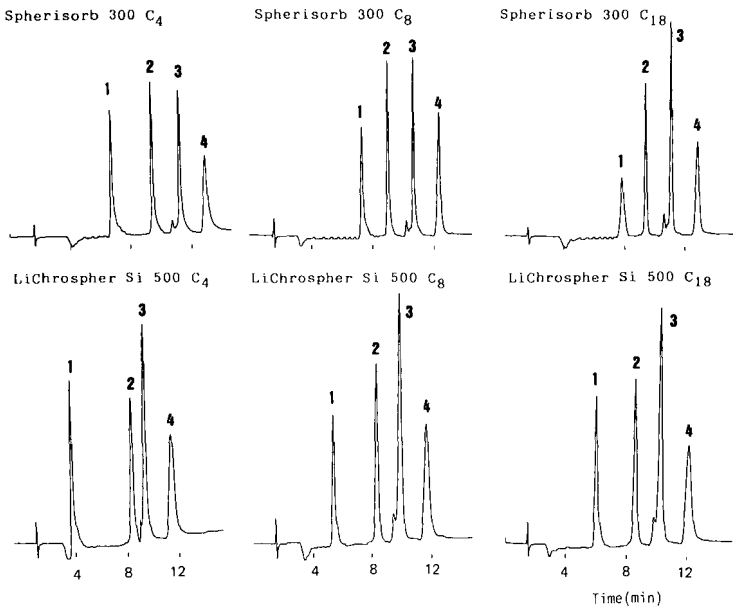

Fig. 3. Effect of alkyl chain length on the elution of (1) 1-naphthylmethanol, (2) cytochrome *c*, (3) lysozyme and (4) BSA using gradient elution type I with alkyl-bonded phase prepared from Spherisorb 300 and LiChrospher Si 500.

However, the C_4 and C_{18} phases prepared from Kromasil 100 and 200E and the commercial batch of Hypersil 300(II) showed instances where one could obtain a better performance with a C_4 bonded phase than a C_{18} phase as suggested generally. As shown in Fig. 5, both C_4 and C_{18} phases from 10-nm pore silica gels showed poor performances for the peptides, especially BSA. With an increase in pore size from 10 to about 20 nm, an improved performance was seen with the C_4 phase, whereas not much improvement was seen with the C_{18} phases for BSA.

Considerable differences between C_4 and C_{18} phases in performance for BSA can be seen for silica particles having pore sizes in the range *ca.* 15–20 nm. Some earlier

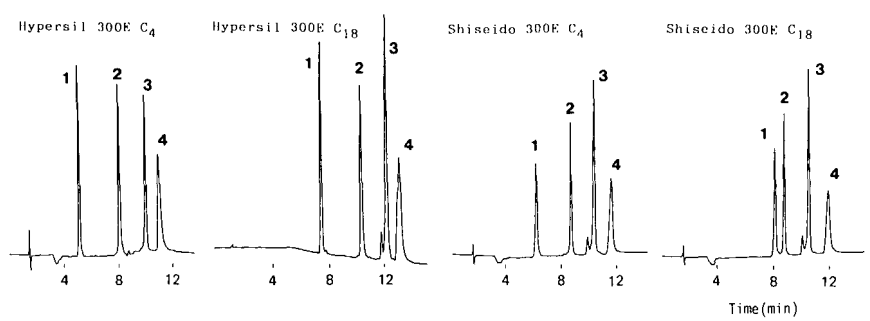

Fig. 4. Performance of C_4 and C_{18} phases prepared from Hypersil 300E and Shiseido 300E experimental wide-pore silica gels. Conditions and peaks as in Fig. 3.

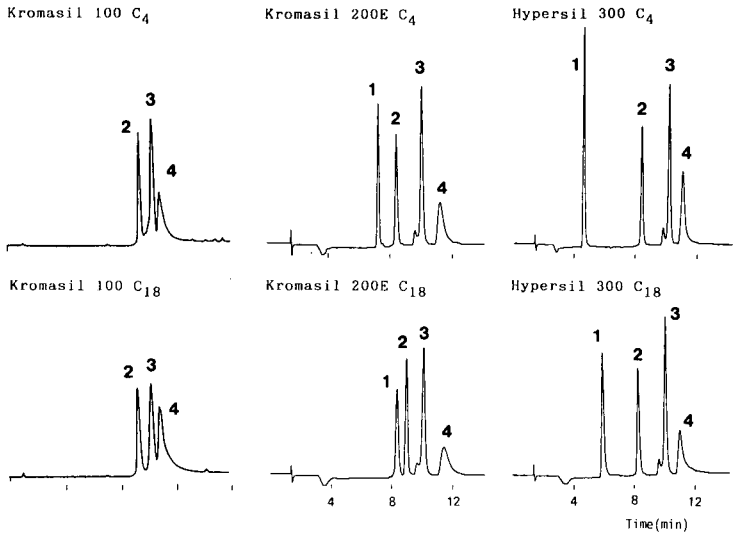

Fig. 5. Performance of C_4 and C_{18} phases prepared from Kromasil 100, Kromasil 200E and Hypersil 300(II). Conditions and peaks as in Fig. 3.

workers might have concluded from such results that the short-chain alkyl stationary phases can give better performances than a C_{18} phase for high-molecular-weight polypeptides. The present results, however, indicate that the effect of alkyl chain length on efficiency is much smaller with packing materials having an adequate pore size or too small a pore size. The effect of alkyl chain length on protein recovery will be discussed later.

In Figs. 2–4, the tailing of the BSA peak was generally accompanied by a narrower band spacing between lysozyme and BSA, indicating the partial steric exclusion for the high-molecular-weight polypeptide from small pores. This indicates

TABLE II

METAL CONTENTS OF WIDE-PORE SILICA GELS

Silica gel	Metal content (ppm)							
	Al	Ca	Fe	Na	Ti	K	Mg	Zr
Hypersil 300[a]	191	11	134	896	58	31	14	122
Hypersil 300E	152	17	46	669	79	15	7	29
Nucleosil 300	22	38	14	405	36	5	27	7
LiChrospher Si 500	1	5	12	315	<1	0	2	0
Spherisorb 300	9	6	8	9	1	0	1	<1
Shiseido 300E	<1	1	<1	7	<1	0	<1	0
Kromasil 100	<1	<1	<1	25	2	<1	<1	<1

[a] A different batch of a commercial product.

the presence of pores that barely permit the permeation of the polypeptide, leading to a more limited performance of C_{18} phases. This effect might be related to the limited surface area available with small-pore materials [6]. The presence of such pores that allow solute permeation but do not allow fast equilibration should be minimized.

The presence of metal impurities was shown to be less important. Spherisorb 300, Shiseido 300E and LiChrospher Si 500 were found to be relatively pure silica particles, while Hypersil 300E contained considerable amounts of metal impurities, as shown in Table II, yet all of these materials showed excellent performance for the polypeptides. The results indicate that the presence of the metal impurity itself is not the source of peak tailing, although there is a possibility that the effect of alkyl chain length is enhanced by the presence of metal impurities.

The TEM photographs provide a common observation for the wide-pore silica gels which gave high efficiencies for high-molecular-weight polypeptides. Spherisorb 300 and Shiseido 300E showed very similar appearances with a thin skeleton and a highly porous structure, as shown in Fig. 6. In contrast, Hypersil 300(I) and Vydac TP showed the presence of a thick skeleton, or large primary spheres in a particle, and a much denser structure with fewer pores.

The size of the primary structures of Hypersil 300E is larger than those in Spherisorb 300 and in Shiseido 300E, but smaller than those in commercially obtained Hypersil 300(I). Fig. 6f shows the internal structures of one of the two types of particles having the smaller pore size found in LiChrospher Si 500 [21]. This material also possesses a highly porous structure with a variety of sizes of primary spheres. The pores in the particles having smaller porosity are assumed to be more winding. Details of the pore structure study of wide-pore silica and polymer gels will be presented elsewhere [24], The difference in the pore structure is probably related to the method of preparation of these particles.

The present study indicates that the major factor determining the column efficiency of silica-based packing materials for high-molecular-weight polypeptides seems to be the porosity and the pore size, not the average pore size of 30 nm, but the absence of pores below 20 nm. These wide-pore silica gels, possessing a satisfactory pore size distribution and a low metal content, can be regarded as truly high-performance wide-pore packing materials. One aspect to be noted is that the large-pore materials with higher porosity are usually more fragile than those with smaller pores, and care should be taken with column packing.

The present results will be of help in selecting wide-pore silica packing materials depending on the molecular weight of the solutes. Although a C_4 phase might be better for the separation of polypeptides with higher molecular weights or more hydrophobic polypeptides [5,8,10], C_{18} phases prepared from 30-nm pore silica gels can give high efficiencies for polypeptides with molecular weight up to 80 000. The C_{18} phases are much more stable than C_4 phases in TFA solution, as shown below.

Polymer-based packing materials

Various types of polymer-based packing materials have become available recently for RPLC. They include polystyrene gel (PLRP-S 300), esterified poly(vinyl alcohol) gels (Asahipak C4P, C8P and ODP), alkyl ethers of poly(hydroxyalkyl methacrylate) gels (Shodex D4-613, D8-613 and D18-613) and a poly(alkyl methacrylate) gel having short alkyl groups (Shodex DE-613). The polymer gels are stable

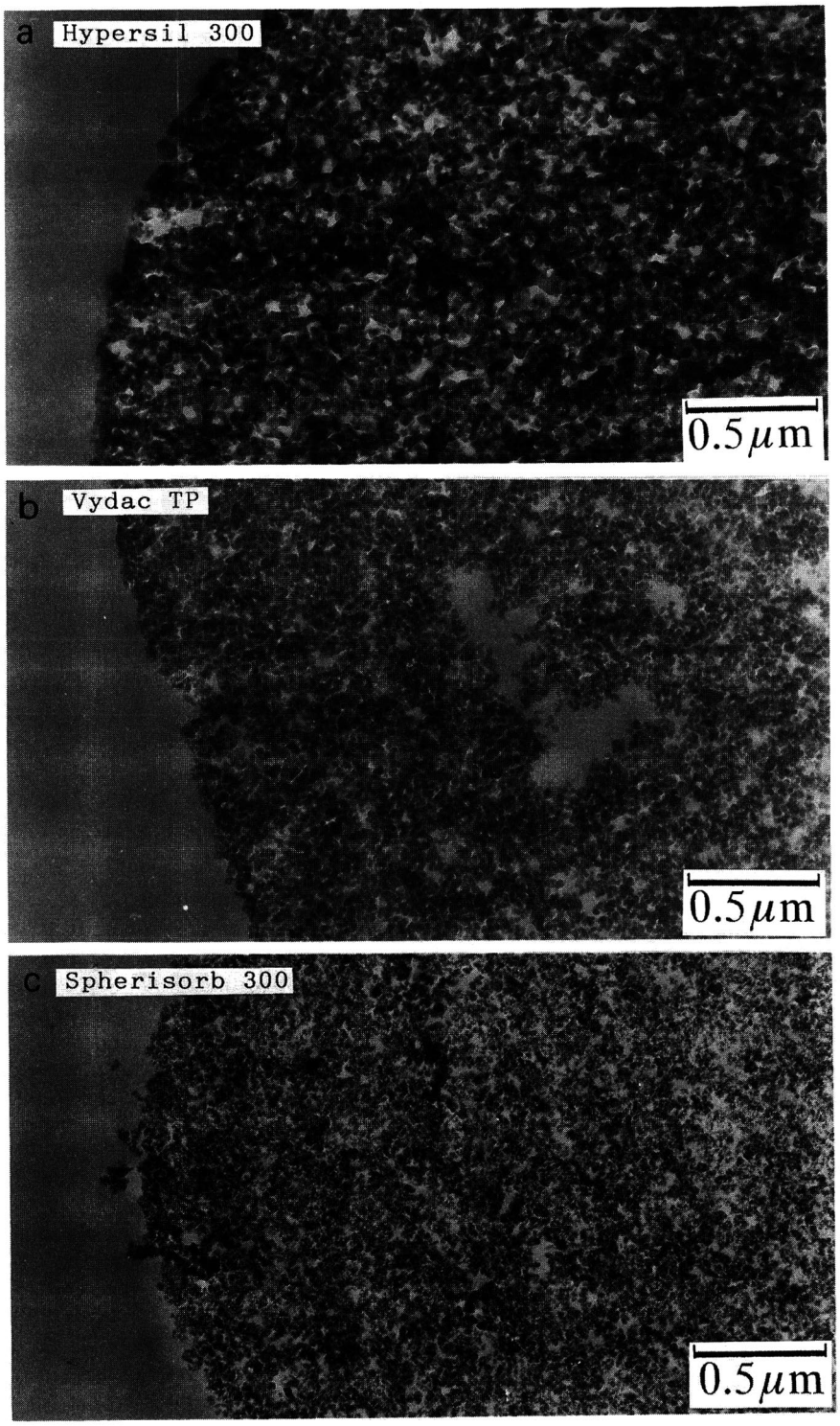

Fig. 6.

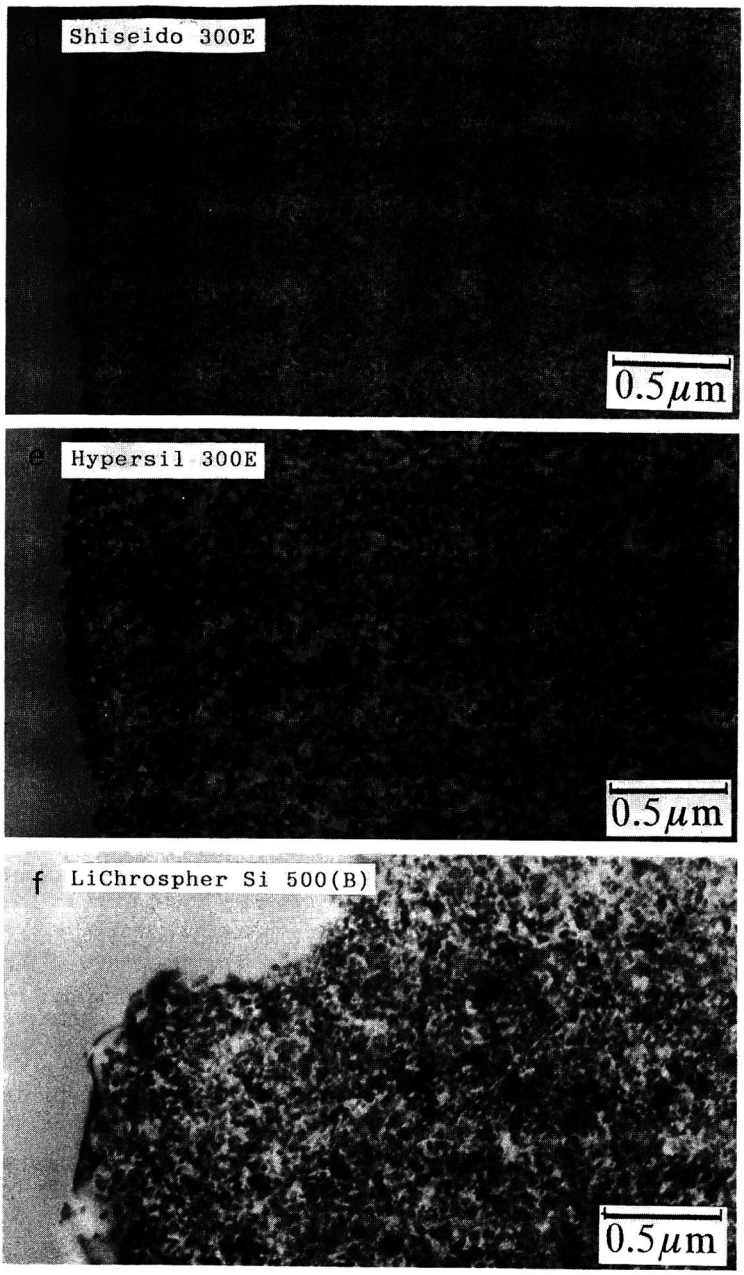

Fig. 6. TEM photographs of wide-pore silica gels.

between pH 2 and 12, and some of them are intended to be used for polypeptide separation [12–14,25,26].

The polymer gels possess a bimodal pore-size distribution when they are macroporous, as shown in Fig. 7. Although the results of nitrogen adsorption

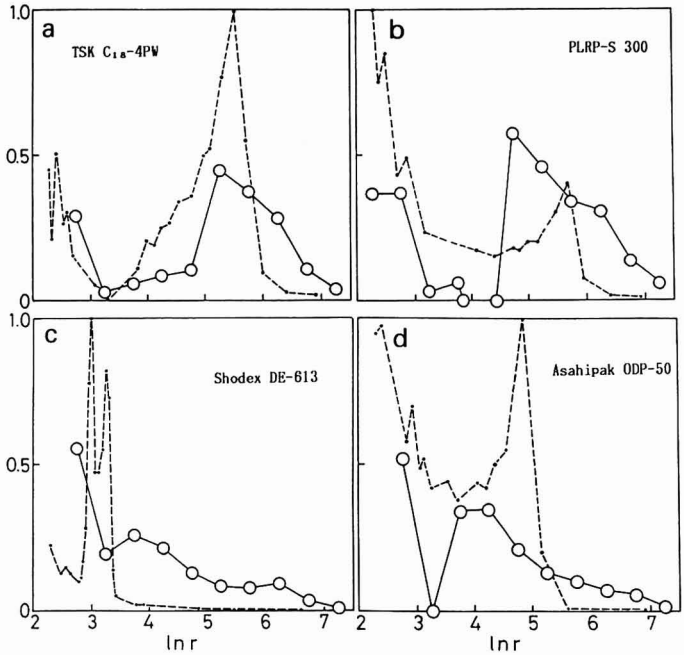

Fig. 7. Pore-size distributions of polymer gels measured by nitrogen adsorption (dashed lines) and size-exclusion chromatography (solid lines). The vertical axis corresponds to the fraction of pore volume, normalized in the case of inverse SEC; r = pore radius.

measurements are thought to be of less significance for polymer gels, the results with PLRP-S 300 were not affected by the use of tetrahydrofuran prior to drying or by the drying temperature between room temperature and 100°C. The micropores of the polymer gels are assumed to be provided by dense network structures, which give selective binding of rigid compact solutes [27,28]. One of the characteristics of the pore-size distribution of these polymer gels is the small pore volume for pore sizes in the range between 5 and 20 nm. This seems to be advantageous for polypeptide separations, considering the results obtained with silica particles.

In Fig. 8, the TEM photographs of TSK C_{18}-4PW, PLRP-S 300 and Asahipak show the presence of macropores throughout the particle. TSK C_{18}-4PW has the appearance of a network structure. Shodex DE-613 and D4-613 from the same manufacturer showed a clear difference in internal structure: whereas D4-613 showed the presence of macropores throughout the particle, DE-613 showed the presence of macropores only at the periphery of the particle. Some steric exclusion effects can be expected for large peptides with DE-613 packing material.

Wide-pore TSK C_{18}-4PW and PLRP-S 300 and also ODP-50 showed an excellent performance for the three polypeptides, as shown in Fig. 9. Shodex DE-613 eluted BSA together with lysozyme, presumably owing to steric exclusion. The retention of a small molecule, 1-naphthylmethanol, indicates how micropores are participating in the retention of small solutes [28]. The greatest contribution of the micropores was seen with Shodex DE-613.

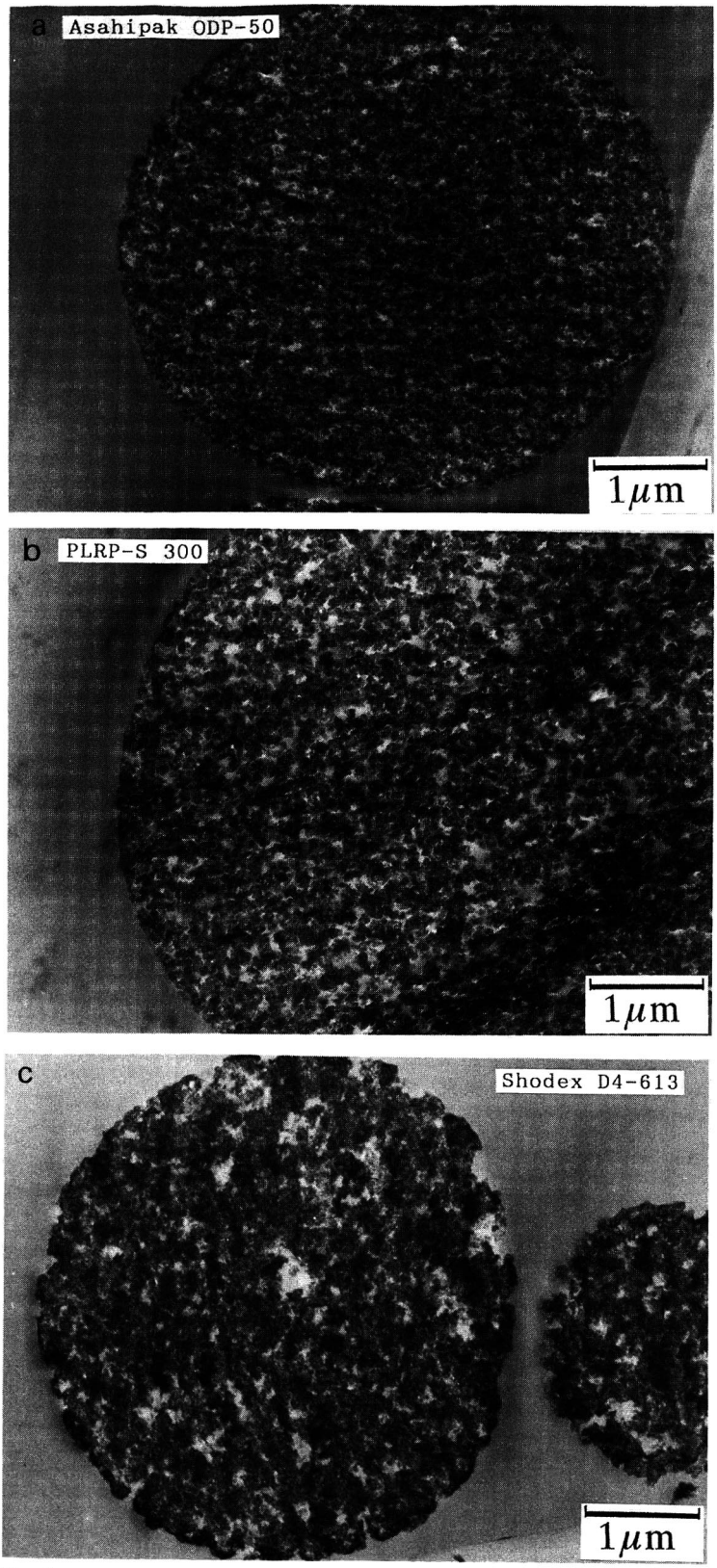

Fig. 8.

(Continued on p. 26)

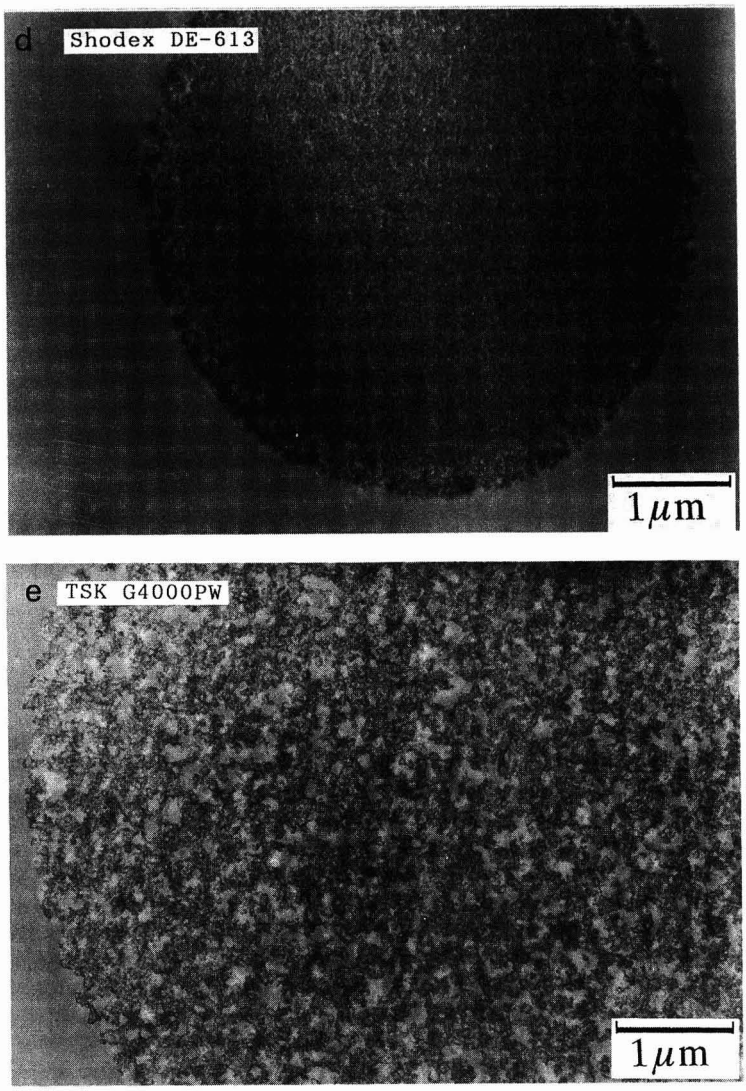

Fig. 8. TEM photographs of polymer gels.

The chromatograms in Fig. 10 show the performance of polymer gels having C_4 to C_{18} alkyl chains. Shodex D4-613 and D8-613 and Asahipak C4P and C8P gave high efficiencies for the peptides. Although tailing was seen for BSA with the C_{18} phases, there is no need to use a C_{18} phase in these cases, because polymer-based C_4 materials are much more stable than silica C_{18} phases. The tailing found with the C_{18} phase could be caused by the smaller pore size, as seen with some silica particles.

Although the packing materials were tested with only the three polypeptides, the elution of a wider range of polypeptides supported the results. Fig. 11 shows that TSK-C_{18}-4PW and PLRP-S 300 can give an even better efficiency than silica-based

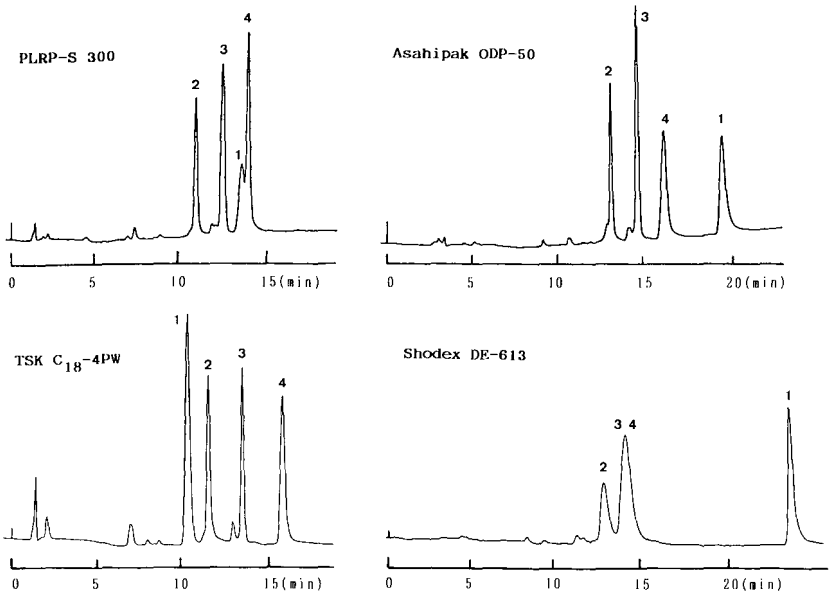

Fig. 9. Elution of polypeptides with polymer gels in gradient type I. Conditions and peaks as in Fig. 3.

materials. Polymer gels having C_4 or C_8 alkyl groups also showed a similar high efficiency. The performance and chemical stability of polymer-based packing materials may make them more attractive than silica-based materials for polypeptide separations, as reported by Burton *et al.* [10] and Welinder [29].

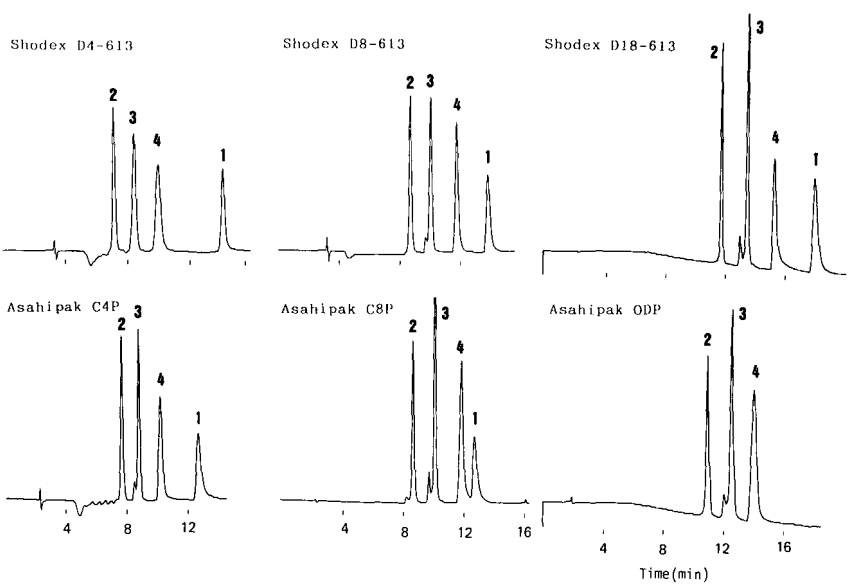

Fig. 10. Performance of polymer gels having C_4, C_8 and C_{18} carbon chains with gradient elution (type I) of polypeptides.

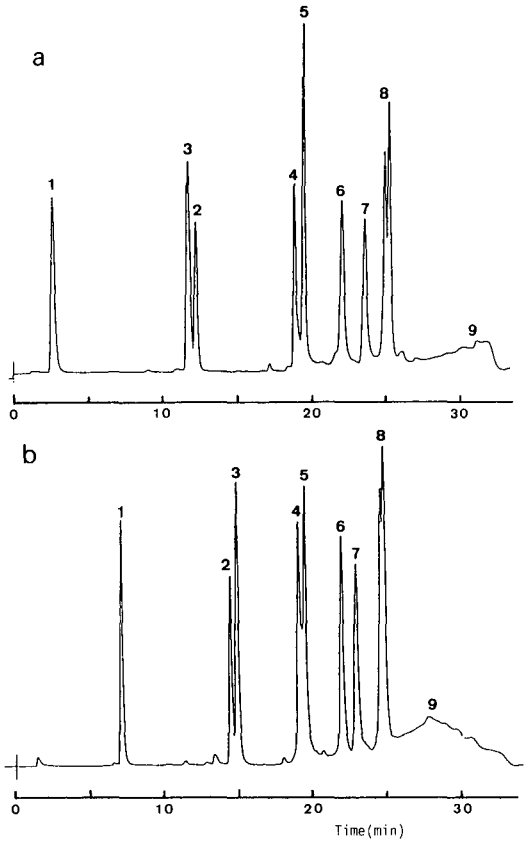

Fig. 11. Elution of polypeptides from polymer-based packing materials with gradient elution (type II). (a) TSK C_{18}-4PW; (b) PLRP-S 300. Peak 9: γ-globulin. Other conditions as in Fig. 2.

Protein recovery

By using the same gradient conditions (type I), consistent peak areas were obtained for cytochrome *c*, lysozyme, BSA and β-lactoglobulin without any indication of carryover (elution of a polypeptide in subsequent gradient runs without sample injection) with all the wide-pore packing materials. A small carryover was seen for BSA with Kromasil 200E-C_{18} and Cosmosil 100 C_{18}, and considerable carryover for ovalbumin with all the packing materials.

As shown in Table III, the recovery of ovalbumin with the first gradient was about 80–90% with C_4 phases. The total peak areas in the three gradient runs on C_{18} phases (one run with sample injection followed by two runs without sample) were 30–50% of those on the C_4 phase, although 60–80% of the total peak areas were obtained with the first gradient. The better recovery of polypeptides, especially ovalbumin, and the better resolution for high-molecular-weight polypeptides were the major reasons for the recommendation of short-chain alkyl-bonded silica phases [2,3,4,16]. The results obtained here are consistent with the reported results. However, the present results also showed that wide-pore materials, including polymer gels and

TABLE III

RECOVERY OF POLYPEPTIDES

Stationary phase	Polypeptide recovery (%)	
	BSA[a]	Ovalbumin[b]
LiChrospher Si 500		
C_4	100	87
C_8	100	88 (92)[c]
C_{18}	100	48 (76)[c]
Spherisorb 300		
C_4	100	87
C_8	100	70 (85)[c]
C_{18}	100	35 (76)[c]
Hypersil 300(II)		
C_4	100	88
C_{18}	100	28 (71)[c]
Kromasil 200E		
C_4	99.6	93
C_{18}	99.4	78 (90)[c]
Cosmosil 100-C_{18}[d]	97	– (76)[c]
Asahipak		
C4P	100	90
C8P	100	92 (84)[c]
Shodex		
D4-613	100	95
D8-613	100	84 (94)[c]

[a] Peak area of BSA in the first gradient was taken as 100% when no carryover was observed and used to normalize the recovery of ovalbumin.

[b] The recovery of ovalbumin on the first gradient run is shown. The total recovery of ovalbumin in three successive gradient runs on C_4 phase was taken as 100%, and used to calculate the recovery of ovalbumin on the other packing materials from the same support.

[c] The ratio of the recovery in the first gradient run to the total recovery in the three runs.

[d] Cytochrome *c* (*ca.* 2%), lysozyme (*ca.* 0.3%) and β-lactoglobulin.

silica C_{18} phases, can give high efficiencies and high recoveries of polypeptides including BSA and β-lactoglobulin, eluting later than BSA. Essentially no carryover was observed with any of the polypeptides except ovalbumin with all the stationary phases based on wide-pore materials, whereas a small carryover was seen for BSA on small-pore materials.

The better polypeptide recovery with short-chain alkyl-bonded silica phases would not justify their use except for polypeptide separations that would be accompanied by poor resolution or very low recoveries with longer chain alkyl-bonded phases. Even in these instances, polymer-based packing materials can provide comparable efficiencies and recoveries with much higher chemical stability. Optimization of the mobile phase and gradient profile may lead to even better recoveries of hydrophobic polypeptides on the more stable polymer gels and on silica C_{18} stationary phases [30]. Further studies of the effect of the structure of silica- and polymer-based packing materials on the recovery of a wide range of proteins are in progress.

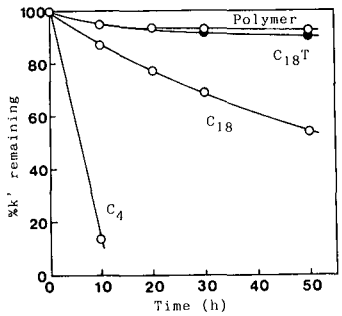

Fig. 12. Stability of packing materials under acidic conditions. The k' values for alkylbenzenes (toluene for LiChrospher C_{18}, $C_{18}T$ and Shodex D4-613 and amylbenzene for LiChrospher C_4) were measured in 60% methanol following tetrahydrofuran flushing at intervals while keeping the packing materials in 0.1% TFA solution at 60°C. The initial retention was taken as 100% for each packing material.

Stability of packing materials in TFA solution

Fig. 12 shows the decrease in the retention of alkylbenzenes in 60% methanol observed after keeping the packing materials in 0.1% aqueous TFA solution at 60°C. Whereas polymer-based Shodex D4-613 and LiChrospher Si 500-$C_{18}T$ bonded with trichlorosilane showed relatively high chemical stabilities, the silica-based phases bonded with monochlorosilane, especially the C_4 phase, showed low stabilities. The results obtained under the severe degradation conditions showed fairly good agreement with those reported by Kirkland *et al.* [18] and by Sagliano *et al.* [17]. Asahipak C4P materials have also been shown to be stable under similar conditions [14]. Polypeptides were eluted with considerably broader peaks with extensively decomposed packing materials.

The present results suggest the use of polymer-based packing materials or C_{18} packing materials prepared by reacting trifunctional silanes with wide-pore silica gels having adequate pore size, with regard to both column efficiency and chemical stability, if acceptable recoveries can be obtained.

CONCLUSION

The effect of the alkyl chain length of packing materials was shown to be related to the pore size of wide-pore silica gels when examined with high-molecular-weight polypeptides.

A wide-pore silica gel should contain few pores smaller than 20 nm in order to be a good packing material, then the C_{18} phase can be as efficient as the short-chain alkyl-bonded phases. Such a stationary phase would give a good column efficiency and recoveries for many polypeptides with molecular weights up to 80 000 with much higher stability than C_4 phases. The efficiency and recovery with polymer-based phases are comparable to those with optimized silica-based materials. Polymer-based packing materials having a higher chemical stability may be more efficient than silica-based packing materials in these applications.

The results also showed that the pore structure is of prime importance in wide-pore packing materials, and TEM may help in their characterization and optimization.

ACKNOWLEDGEMENTS

We are grateful to Dr. Y. Kato of Tosoh, Dr. I. Kaiho of Showa Denko, Dr. K. Noguchi of Asahi Chemical Industry, Ms. L. Lloyd of Polymer Labs. Dr. D. Sanchez of Eka Nobel and Dr. D. Woodward of Shandon for gifts of packing materials.

REFERENCES

1 J. D. Pearson, W. C. Mahoney, M. A. Hermodson and F. E. Regnier, *J. Chromatogr.*, 207 (1981) 325.
2 J. D. Pearson, N. T. Lin and F. E. Regnier, *Anal. Biochem.*, 124 (1982) 217.
3 J. D. Pearson and F. E. Regnier, *J. Liq. Chromatogr.*, 6 (1983) 497.
4 N. H. C. Cooke, B. G. Archer, M. J. O'Hare, E. C. Nice and M. Capp, *J. Chromatogr.*, 255 (1983) 115.
5 M. T. W. Hearn and B. Grego, *J. Chromatogr.*, 282 (1983) 541.
6 K. K. Unger, J. N. Kinkel, B. Anspach and H. Giesche, *J. Chromatogr.*, 296 (1984) 3.
7 M. T. W. Hearn and B. Grego, *J. Chromatogr.*, 296 (1984) 61.
8 M. A. Stadalius, H. S. Gold and L. R. Snyder, *J. Chromatogr.*, 327 (1985) 27.
9 B. W. Sands, Y. S. Kim and J. L. Bass, *J. Chromatogr.*, 360 (1986) 353.
10 W. G. Burton, K. D. Nugent, T. K. Slattery, B. R. Summers and L. R. Snyder, *J. Chromatogr.*, 443 (1988) 363.
11 N. Tanaka and M. Araki, *Adv. Chromatogr.*, 30 (1989) 81.
12 K. A. Tweeten and T. N. Tweeten, *J. Chromatogr.*, 359 (1986) 111.
13 L. L. Lloyd, Z. Dryzek, D. B. Harrison and F. P. Warner, paper presented at the 10th International Symposium on Column Liquid Chromatography, San Francisco, May 1986.
14 T. Ohtani, Y. Tamura, M. Kasai, T. Uchida, Y. Yanagihara and K. Noguchi, *J. Chromatogr.*, 515 (1990) 175.
15 J. Frenz, W. S. Hancock, W. J. Henzel and C. Horvath, in K. M. Gooding and F. E. Regnier (Editors), *HPLC of Biological Macromolecules*, Marcel Dekker, New York, 1990, Ch. 6.
16 E. C. Nice, M. W. Capp, N. H. C. Cooke and M. J. O'Hare, *J. Chromatogr.*, 218 (1981) 569.
17 N. Sagliano, Jr., T. R. Floyd, R. A. Hartwick, J. M. Dibussolo and N. T. Miller, *J. Chromatogr.*, 443 (1988) 155.
18 J. J. Kirkland, J. L. Glajch and R. D. Farlee, *Anal. Chem.*, 61 (1989) 2.
19 T. J. Szczerba, D. N. Baehr, L. J. Glunz, J. A. Perry and M. J. Holdoway, *J. Chromatogr.*, 458 (1988) 281.
20 K. Jinno, S. Shimura, N. Tanaka, K. Kimata, J. C. Fetzer and W. R. Biggs, *Chromatographia*, 27 (1989) 285.
21 N. Tanaka, K. Hashizume, M. Araki, H. Tsuchiya, A. Okuno, K. Iwaguchi, S. Onishi and N. Takai, *J. Chromatogr.*, 448 (1988) 95.
22 J. H. Knox and H. P. Scott, *J. Chromatogr.*, 316 (1984) 311.
23 K. Kimata, K. Iwaguchi, S. Onishi, K. Jinno, R. Eksteen, K. Hosoya, M. Araki and N. Tanaka, *J. Chromatogr. Sci.*, 27 (1989) 721.
24 N. Tanaka, K. Kimata, T. Araki, H. Tsuchiya and K. Hashizume, *J. Chromatogr.*, in press.
25 Y. Yamasaki, T. Kitamura, S. Nakatani and Y. Kato, *J. Chromatogr.*, 481 (1989) 391.
26 Y. Kato, S. Nakatani, T. Kitamura, Y. Yamasaki and T. Hashimoto, *J. Chromatogr.*, 502 (1990) 416.
27 N. Tanaka, K. Hashizume and M. Araki, *J. Chromatogr.*, 400 (1987) 33.
28 N. Tanaka, T. Ebata, K. Hashizume, K. Hosoya and M. Araki, *J. Chromatogr.*, 475 (1989) 195.
29 B. S. Welinder, paper presented at *the 14th International Symposium on Column Liquid Chromatography, Boston, May 1990*, paper No. P642.
30 K. D. Nugent, W. G. Burton, T. K. Slattery, B. F. Johnson and L. R. Snyder, *J. Chromatogr.*, 443 (1988) 381.

Journal of Chromatography, 535 (1990) 33–39
Elsevier Science Publishers B.V., Amsterdam

CHROMSYMP. 2070

Post-column continuous-flow analysis combined with reversed-phase liquid chromatography and computer-aided detection for the characterisation of peptides

A. F. FELL* and J. B. CASTLEDINE
Department of Pharmaceutical Chemistry, School of Pharmacy, University of Bradford, Bradford (U.K.)
B. SELLBERG and R. MODIN
Pharmacia Leo Therapeutics AB, S-751 82 Uppsala (Sweden)
and
R. WEINBERGER
Applied Biosystems (ABI), Ramsey, NJ 07446 (U.S.A.)

ABSTRACT

Peptide mapping is a key technique for structural identification of new proteins or the products of recombinant gene technology. The recognition of oligopeptides, separated by reversed-phase liquid chromatography, is limited by the conventional reliance on the correlation of retention times with standards, supported by dual-wavelength chromatograms. It has been reported that the recognition of phenolic compounds can be achieved by a novel technique, based on computer-aided photodiode-array detection of the pH-shifted solutes after post-column continuous-flow analysis. This work describes how the generation of the pH-shifted difference spectra for dipeptides, containing a tyrosyl residue, may be used to enhance peak recognition, when used in conjunction with absorbance ratios.

INTRODUCTION

Combination of liquid chromatography photodiode-array detection (PDAD) with flow-injection analysis (FIA) as a post-column reaction system offers several possibilities for enhanced detection capability. Recognition of phenolic compounds can be achieved by a novel technique, based on computer-aided PDAD of the pH-shifted solutes after post-column continuous-flow analysis [1,2]. It is proposed that this technique may be used in the characterisation of peptides, such as those generated from tryptic digests. Although phenylalanine (Phe), tyrosine (Tyr), and tryptophan (Trp) display characteristic chromophores above 230 nm, which allow characterisation by PDAD [3], the extensive band overlap leads to complex composite profiles in peptide mixtures. Moreover, in samples of biological origin, additional absorbing constituents often contribute spectral interference. A common problem arises from the closely overlapping chromophores of Tyr and Trp between 270 and 280 nm. Although Trp, being rather more absorptive than Tyr, tends to dominate the spectrum, the labile phenolic group of Tyr permits its spectrum to be shifted to higher wavelength (*ca.* 293

0021-9673/90/$03.50

nm) by raising the solution pH. Since the Trp chromophore is less pH-sensitive, this feature may form the basis for resolving peptides containing varying proportions of these amino acids. The use of pH shifting as a peak recognition technique, for various dipeptides containing a tyrosyl residue, has been investigated and is reported below.

EXPERIMENTAL

Reagents

Methanol [high-performance liquid chromatographic (HPLC) grade, Rathburn, Walkerburn, U.K.] was used as received. The 5-m*M* potassium dihydrogenphosphate solution (AnalaR, BDH, Poole, U.K.) and 0.1 *M* potassium hydroxide solution (Convol, BDH, Poole U.K.) were prepared with glass-distilled water and filtered through 0.45-μm filters (Millipore Waters, Middlesex, U.K.), using all-glass equipment. All eluents and FIA carrier streams were degassed for 10 min in an ultrasonic bath under reduced pressure. L-tyrosine (Tyr), L-tyrosyl-L-tyrosine (Tyr–Tyr), L-tyrosylglycine (Tyr–Gly), glycyl-L-tyrosine (Gly–Tyr), L-tyrosyl-L-phenylalanine (Tyr–Phe), L-phenylalanyl-L-tyrosine (Phe–Tyr), tryptophyl-tyrosine (Trp–Tyr) and L-phenylalanyl-glycine (Phe–Gly) were obtained from (Sigma, St. Louis, MO, U.S.A.). Solutions of the dipeptides and tyrosine (all *ca.* 250 μM) were prepared in distilled water.

Apparatus

The apparatus was configured as shown in Fig. 1 [3]. The chromatographic system used consisted of a Kratos SF-400 pump (Kratos Analytical, Warrington, U.K.) with a rheodyne injection valve (Model 7125) provided with a 20-μl loop, together with an ABI 1000S diode-array detector (Applied Biosystems (ABI) Ramsey, NJ, U.S.A.) and a BD-40 chart recorder (Kipp & Zonen, Delft, The Netherlands). The ABI 1000S was interfaced, via a RS-232C link, to an IBM-compatible personal computer (Elonex, Bradford, U.K.) with a Panasonic KX-P1081 printer (supplied by ABI) and a HP-ColorPro plotter (Hewlett-Packard, Cheadle Heath, Stockport, U.K.). The data acquisition and manipulation was performed using Lab. Calc. software (Galactic Industries, Salem, NH, U.S.A.). Spectra acquired, in the range 230–350 nm, during chromatography were normalised with reference to maximal absorbance at the λ_{max}, using the Lab. Calc. facility to apply the appropriate scale multiplier. This

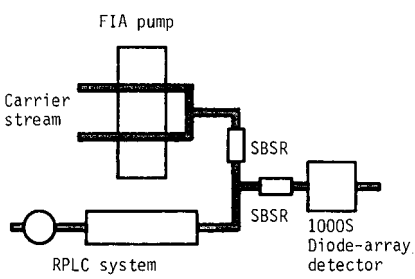

Fig. 1. Experimental system combining liquid chromatography with post-column continuous-flow analysis and photodiode-array detection.

enabled the difference spectrum to be obtained in such a way that any changes in the intrinsic profile of the spectrum can be obtained in a standardised format.

The post-column reaction system consisted of a Gilson Minipuls-3 peristaltic pump (Anachem, Luton, U.K.), together with Elkay accu-rated tubing (Laboratory Products, Basingstoke, U.K.) and two single-bead string reactors (SBSRs) (100 cm × 0.8 mm I.D. and 50 cm × 0.8 mm I.D.) to promote mixing. All connections were made with 0.5 mm I.D. PTFE tubing. The FIA carrier stream was combined with the post-column eluent stream by a suitable T-piece (Anachem). The two FIA carrier streams were combined through a suitable Y-piece (Anachem).

LC–FIA conditions

A stainless-steel column (250 mm × 4.6 mm I.D.) packed with Techsphere 5 μm ODS (HPLC Technology, Macclesfield, U.K.) was used. The mobile phase, pumped at 1.0 ml/min, consisted of, for Tyr, Gly–Tyr and Tyr–Gly, methanol–5 m*M* KH_2PO_4 (pH 4) buffer (10:90, v/v) and for Tyr–Phe, Phe–Tyr, Phe–Gly, Tyr–Tyr and Trp–Tyr, methanol–5 m*M* KH_2PO_4 (pH 4) buffer (15:85, v/v). Detection was effected using the diode-array at 272 nm. The FIA system consisted of 0.03 ml/m tubing, the pump speed was set to deliver 0.05 ml/min from each of the two FIA carrier streams. 0.1 *M* KOH was used to effect the post-column pH-shift.

RESULTS AND DISCUSSION

The pH-shifted difference spectrum was obtained for each dipeptide by subtracting the normalised spectrum under alkaline conditions (apparent pH of the methanolic mobile phase, pH* 12.4) from the spectrum obtained under the reversed-phase liquid chromatography (RPLC) conditions (pH* 4.4) as illustrated with Gly–Tyr in Fig. 2. As previously reported, the mobile phase and potassium hydroxide solution concentrations used were such that they had similar spectra [4]. Data from wavelengths below 230 nm were not used because solvent effects, due to absorption by alkali, were observed even in the spectrum of Phe–Gly. A comparison of the difference between the spectra of the normalised dipeptides and the normalised pH-shifted difference spectra of the dipeptides is shown in Fig. 3. Visual examination of these data reveals no obvious advantages in the use of pH-shifted difference spectra to enhance recognition.

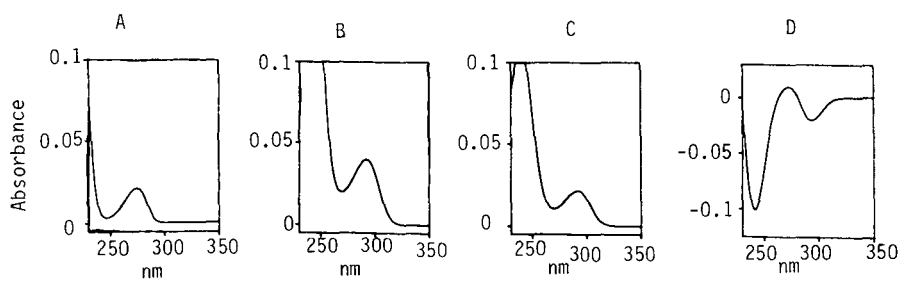

Fig. 2. Spectral manipulation to obtain the pH-shifted difference spectrum. (A) Gly–Tyr, pH* 4.4; (B) Gly–Tyr, pH* 12.4; (C) Gly–Tyr, pH* 12.4, normalised; (D) Gly–Tyr, difference spctrum.

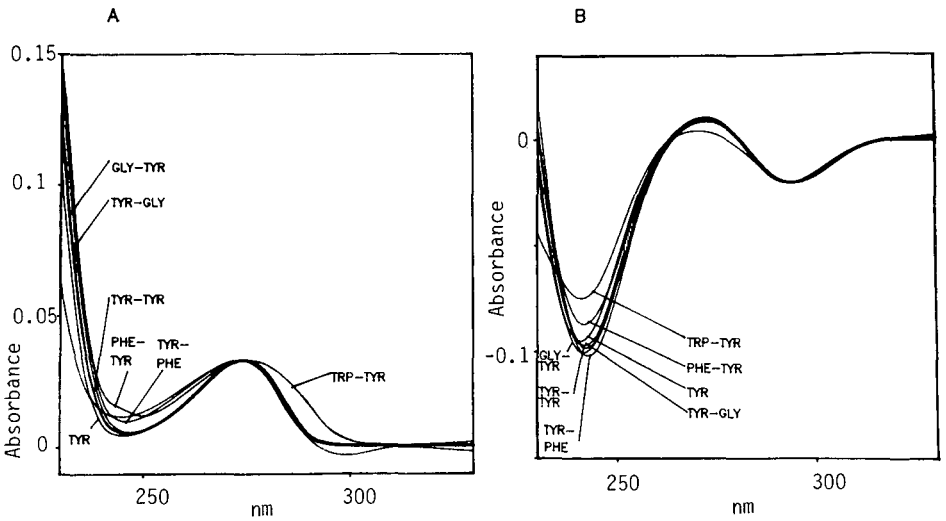

Fig. 3. A comparison of the difference between the normalised spectra (A) and the normalised pH-shifted difference spectra (B) of the dipeptides.

The use of absorbance ratios has been reported as a powerful technique for solute identification and sample discrimination [5]. This technique was investigated for the recognition of the dipeptides by both spectral and pH-shifted difference spectral data. To determine the wavelengths of choice for good discrimination between the peptides, the difference spectrum between normalised difference spectra of the two

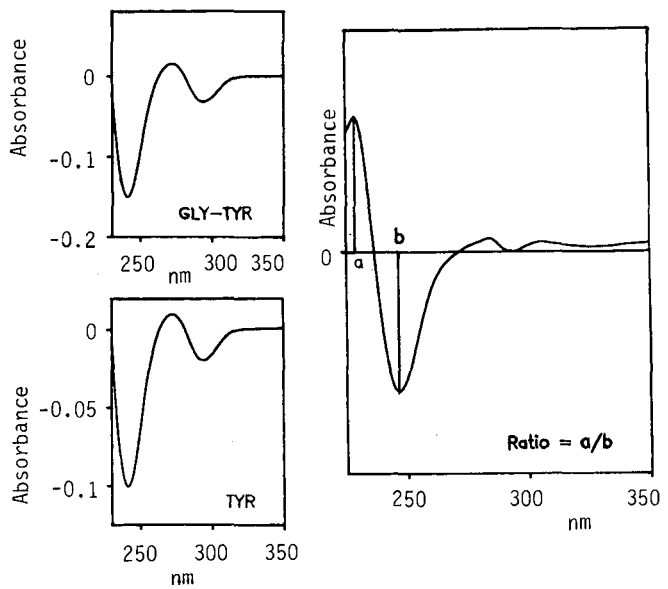

Fig. 4. Determination of the wavelength for the absorbance ratio of choice, for good discrimination between the peptides. Right: the difference spectrum between normalised difference spectra of Gly–Tyr and Tyr.

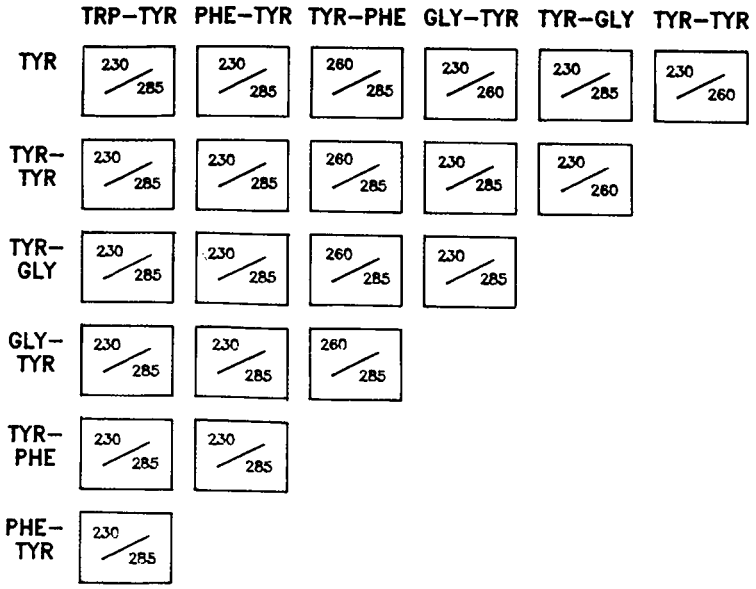

Fig. 5. The modified absorbance ratio wavelengths of choice for discrimination between dipeptides containing a Tyr residue: unshifted spectra.

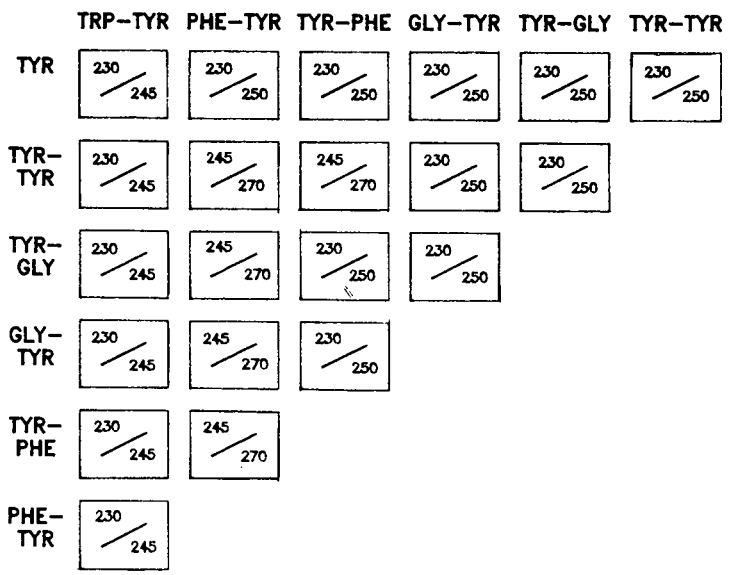

Fig. 6. The modified absorbance ratio wavelengths of choice for discrimination between dipeptides containing a Tyr residue: pH-shifted difference spectra.

peptides was computed. The wavelengths of maximum positive and negative Δ absorbance (above 230 nm for difference spectra) were recorded. This is illustrated by Fig. 4.

To facilitate automation of this technique, the number of wavelengths for the absorbance ratios was reduced, to establish six ratios for use with both the unshifted and pH-shifted difference spectra. In most cases, this necessitated a change of less than 3 nm from the wavelength determined above, and in all cases a significant difference was observed between the two normalised spectra at the chosen wavelengths. Figs. 5 and 6 show the simplified absorbance ratios.

The absorbance ratios calculated from the data determined above are shown in Tables I and II.

It can be observed, by comparing Figs. 1 and 2 with the results obtained (Tables I and II) that the method used for determination of the wavelengths of choice for the absorbance ratios did not always give the greatest numerical difference between the dipeptides in question, hence further work is being undertaken to improve the method

TABLE I

ABSORBANCE RATIOS FOR PEAK RECOGNITION OF UNSHIFTED SPECTRA

x = mean, R.S.D. = % relative standard deviation, n = 9.

Ratio	x (R.S.D.)		
	285/230 nm	260/230 nm	285/260 nm
Tyr	0.138 (0.43)	0.156 (0.23)	0.882 (0.27)
Tyr–Tyr	0.112 (0.69)	0.119 (0.33)	0.944 (0.38)
Tyr–Gly	0.109 (0.54)	0.134 (1.59)	0.815 (0.93)
Gly–Tyr	0.134 (1.09)	0.134 (1.54)	1.00 (0.47)
Tyr–Phe	0.091 (6.64)	0.147 (4.85)	0.620 (2.32)
Phe–Tyr	0.106 (2.08)	0.138 (2.70)	0.766 (0.78)
Trp–Tyr	0.405 (0.08)	0.367 (0.17)	1.10 (0.15)

TABLE II

ABSORBANCE RATIOS FOR PEAK RECOGNITION OF pH-SHIFTED DIFFERENCE SPECTRA

x = mean, R.S.D. = % relative standard deviation, n = 9.

Ratio	x (R.S.D.)		
	230/250 nm	270/245 nm	230/245 nm
Tyr	0.223 (0.67)	−0.108 (0.30)	0.152 (0.72)
Tyr–Tyr	−0.088 (10.7)	−0.088 (2.52)	−0.064 (10.9)
Tyr–Gly	−0.081 (27.0)	−0.101 (2.86)	−0.059 (27.1)
Gly–Tyr	0.080 (6.43)	−0.097 (0.31)	0.056 (6.39)
Tyr–Phe	−0.260 (14.0)	−0.099 (4.64)	−0.193 (13.7)
Phe–Tyr	−0.128 (12.5)	−0.093 (5.81)	−0.093 (12.2)
Trp–Tyr	0.909 (1.71)	−0.058 (4.56)	0.641 (1.65)

for determining absorbance ratios so that sensitivity may be improved. In this respect, the method of multiple absorbance ratio correlation as proposed by Marr *et al.* [6] has potentially interesting applications for peptide recognition.

Examination of the absorbance ratios for the characterisation of the unshifted spectra shows that, with the exception of Trp–Tyr, the dipeptides have similar ratios. Comparison of the ratios generated from the pH-shifted difference spectra reveals that, in general, greater differences are observed between the dipeptides. This is partly a result of both positive and negative ratios being generated from the difference spectra. The greater relative standard deviations observed for the pH-shifted difference spectra may be attributed to the increased background noise created by this technique. Despite this increased variation, the ratios generated are sufficiently different, for the dipeptides, for this technique to be a useful addition to the tools available in peptide recognition.

It has previously been reported that the relative standard deviation for absorbance ratios is dependent on the absorbance at the wavelengths of interest, in addition to background noise [5]. Hence, it is unlikely that the technique as proposed could be used in the characterisation of sub-nanogram quantities of dipeptides, on column.

CONCLUSIONS

The generation of the pH-shifted difference spectra for dipeptides containing a tyrosyl residue, may be used to enhance peak recognition, when used in conjunction with absorbance ratios. It is proposed that this low cost technique may be used to enhance the characterisation of oligopeptides generated by tryptic mapping. The use of absorbance ratios common to various peptides will allow automation of the technique for the analyst.

ACKNOWLEDGEMENTS

The authors thank the British Council and the Spanish Government for supporting part of this work under the Acciones Integradas Programme. Valuable discussions with Professor M. Valcarcel and M.D. Luque De Castro are acknowledged with thanks. One of the authors (J.B.C.) would like to thank Pharmacia Leo Therapeutics AB for providing the studentship for this research.

REFERENCES

1 A. F. Fell, T. Z. Woldemariam, P. A. Linley, J. Ge, M. D. Luque De Castro and M. Valcarcel, *Anal. Chim. Acta*, 234 (1990) 89–95.
2 K. Hostettmann, B. Domon, D. Schaufelberger and M. Hostettmann, *J. Chromatogr.*, 283 (1984) 137–147.
3 A. F. Fell, B. J. Clark and H. P. Scott, *J. Chromatogr.*, 297 (1984) 203–214.
4 J. B. Castledine, A. F. Fell, B. Sellberg, R. Modin, M. D. Luque De Castro and M. Varcarcel, *J. Pharm. Biomed. Anal.*, 8 (1990) 1079–1082.
5 P. C. White and T. Catterick, *J. Chromatogr.*, 402 (1987) 135–147.
6 J. G. D. Marr, G. G. R. Seaton, B. J. Clark nd A. F. Fell, *J. Chromatogr.*, 506 (1990) 289–301.

Journal of Chromatography, 535 (1990) 41–53
Elsevier Science Publishers B.V., Amsterdam

CHROMSYMP. 2073

Post-column reaction detection and flow injection analysis

H. ENGELHARDT*, R. KLINKNER and G. SCHÖNDORF
Angewandte Physikalische Chemie, Universität des Saarlandes, D-6600 Saarbrücken (F.R.G.)

ABSTRACT

Post-column derivatization with chemical reaction detection (CRD) and flow injection analysis (FIA) use the same principle, *viz.* reaction in a flow system. For CRD, dispersion must be minimized so as to maintain the separation achieved. In FIA, dispersion is required to mix the reagent and solute. It has been demonstrated that by using low-dispersion knitted capillaries and various modifications of the FIA principle (forced mixing in a branched system; inverse FIA; plug injection of solute and reagent in an inert carrier), the detection limit can be improved. In plug injection, one can also use coloured reagents and solutes to reduce reagent consumption.

INTRODUCTION

Continuous-flow analysis in open tubes is of increasing interest for process monitoring and control and for the colorimetric identification of solutes. Starting from identical fundamentals, two very similar analytical systems have been developed in parallel, varying only in their purpose:

(1) Chemical reaction detection (CRD) [1] for the derivatization of chromatographically separated solutes is intended to improve detection selectivity, specifity and sensitivity while preserving the chromatographic separation achieved. The axial dispersion (mixing), which causes additional peak broadening (impairing the separation) and hence a reduction in peak height (detection sensitivity), must be minimized during derivatization in the reaction coil.

(2) In flow injection analysis (FIA) [2], the sample is injected into a stream of reagent. A certain dispersion (axial mixing, band broadening) is required to mix sample and reagent so as to start the derivatization reaction.

Although the two methods have been developed separately and independent of each other, the basic principle of both methods is the same, namely the use of open tubes holding the sample and reagent during derivatization. The main difference is that in CRD axial dispersion is undesirable, whereas it is required in FIA. In both instances, quantitative reaction is unnecessary, because the reaction time is determined by both the flow-rate and the length of the reaction tubes. The aim of this paper is to compare the principles of CRD and FIA and to point out synergistic possibilities for both methods.

0021-9673/90/$03.50

CHEMICAL REACTION DETECTOR

CRD is applied in high-performance liquid chromatography (HPLC) for the selective and sensitive detection of solutes in complex matrices or for the sensitive detection of solutes without a chromophore or fluorophore, such as sugars and amino acids. The advantage of this method, especially for multi-functional solutes, where complete and quantitative precolumn derivatization is difficult to achieve, is that they can be separated as such.

In a typical experimental set-up for post-column detection, the reagent is added continuously to the effluent from the chromatographic column. An additional pump is required, which should be able to deliver the sometimes very corrosive reagents continuously and free from pulsations with great precision. The use of a cyclone-type mixer [3,4] with an extremely small dead volume (10 nl) is advantageous. Cyclone mixers have the additional advantage that a relatively small reagent flow (as little as 1/25th of the eluent flow) can be applied, in contrast to the 1:1 flow-rate required with conventional mixers with T- or Y-connections. This helps to improve the detection sensitivity, because the inherent dilution of the solute peak with reagent is minimized.

The most important part of the experimental set-up is the reactor, where the effluent and reagent must be held for the time required for the reaction to proceed. Principally three different types of reactors have been applied: (a) open tubes with large diameters (>1 mm) and segmentation of the flow, either by air or by an immiscible liquid; (b) packed columns; and (c) narrow, open tubes (<0.4 mm), geometrically deformed [3].

The advantages and disadvantages of these three types of reactors have been discussed in detail [5], so only a brief summary will be given here. With increasing column efficiency the peak volumes in HPLC have been drastically reduced (10–100 μl). Consequently, reactors with flow segmentation cannot be used in HPLC without vitiating the separation achieved in the column. Only for extremely long reaction times (>5 min) may their application have some advantage.

Packed reactors are inert chromatographic columns. The efficiency of both should be identical. Consequently, the reactors must be packed with particles of a diameter similar to that of the chromatographic column. The additional back-pressure may also be a limitation and particulate matter precipitating from the reagent may plug the reactor. The use of packed-bed reactors for heterogeneous catalysis is advantageous.

When open tubes are used, the formation of a parabolic stream profile, causing peak broadening, must be prevented. This can be achieved by segmentation, but more efficiently by deforming the capillaries geometrically either by coiling, knitting or stitching. With straight, open tubes, the peak broadening, measured as the H value, increases linearely with linear eluent velocity. This curve can be described by the Aris–Taylor equation [6,7], correlating effective dispersion in open tubes with tube diameter and flow velocity. By coiling the tube, the effective dispersion becomes smaller the tighter the tube is coiled. The most efficient reduction of dispersion is obtained with "knitted" tubes [3–5]. Here, tight coiling and a change of flow direction after each half circle introduces artificial radial mixing, thus preventing the formation of a parabolic flow profile. The induced secondary radial flow increases the back-pressure with a knitted tube by a factor of 2–3, compared with the theoretical value for

straight tubes, calculated via the Hagen–Poisseuille equation. Of course, if turbulent flow were reached here, a much higher pressure would have to be applied.

Comparison of the efficiency of packed reactors and knitted open tubes (KOT) showed that a packed-bed reactor with 5–10-μm particles gives the same peak broadening (measured as volume variance per unit reactor volume) as a KOT with 0.34 mm I.D. [5]. Both reactors could be coupled to a 5-μm column without noticeable destroying the separation, as can be seen by comparing the chromatograms in Fig. 1.

KOT reactors of I.D. 0.25–0.35 mm and standard length of 10 m permit reaction times of up to 90 s at the usual chromatographic flow-rates of 0.5–1 ml/min, and are compatible with the efficiency achievable with chromatographic columns packed with 5–10-μm particles. KOT reactors are also good heat exchangers. Short (less than 50

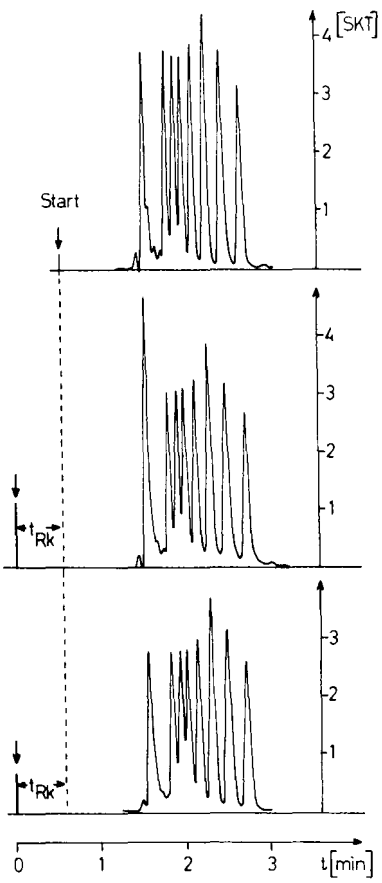

Fig. 1. Demonstration of the effect of various reactors on separation efficiency. Top chromatogram: 120 × 4 mm I.D. column packed with LiChrospher Si 60 RP-8; d_p, 4 μm; eluent, 95% aqueous methanol; flow-rate, 1 ml/min; pressure, 87 bar. Samples: inert = nitromethane; phenylalkanes (C_1–C_6) (k' range 0–1.2). Middle chromatogram: identical conditions, plus a packed reactor (100 × 4 mm I.D., d_p 5 μm). Reaction time, 35 s; additional pressure, 35 bar. Bottom chromatogram: identical conditions, but with KOT reactor (1070 × 0.33 mm I.D.). Reaction time, 40 s; additional pressure, 9 bar.

cm) pieces are sufficient to cool the liquid to the detector temperature necessary for optimum fluorescence detection.

Applications of CRD in chromatography are manifold, starting with the classical amino acid analysis by Spackman *et al.* [9] involving ninhydrin reaction detection. By applying HPLC technology, it was possible to improve the detection sensitivity drastically. The relatively slow ninhydrin reaction was replaced with *o*-phthalaldehyde (OPA) derivatization and fluorescence detection. Nowadays, amino acid analysis in the picogram range is possible [4]. As it is not our purpose here to review the literature on CRD, only two examples will be given to demonstrate the two main advantages: the selective detection of solutes in complex matrices and the sensitive detection of solutes without chromophores.

The determination of carbamate pesticides in vegetables and water is of increasing importance. They can be detected sensitively and selectively by gas chromatography with a nitrogen-specific detector. However, sample pretreatment and carbamate extraction are tedious and time consuming and constitute inherent sources of errors. For HPLC with the CRD, sample pretreatment can be reduced to an extraction with dichloromethane, solvent evaporation and redissolution in methanol. For selective detection, two-step CRD is required [8], hydrolysis with sodium hydroxide and detection of the methylamine, the common structural group of all carbamates, which is produced, with OPA.

Sugars cannot be detected sensitively by photometry. However, they can be detected with pulsed amperometric detectors. Although matrix solutes may block the electrode surface, reducing sugars can be detected by CRD, whereas non-reducing sugars and sugar acids can only be detected with reagents such as thymol and concentrated sulphuric acid. It has been shown [10] that sensitive detection of trace amounts of sugars and sugar acids in wine can thus be achieved.

FLOW INJECTION ANALYSIS

With FIA, solute derivatization also takes place in a stream of reagent. The instrumentation resembles that for CRD. Typically, peristaltic pumps are used in FIA. Because the pressure drop is more limited, wider capillaries must be used, usually of 1 mm I.D. The solute is injected into the streaming reagent. In contrast to stationary colorimetric reactions, but common to CRD, the reaction does not have to go to completion. Because the solute is injected as a plug into the reagent, mixing must occur during transport through the tube. Consequently, the reaction does not start immediately with the whole sample. The laminar flow in the capillary leads to the parabolic Hagen–Poiseuille profile. Mixing of reagent and sample is caused by concentration differences at the front and rear ends of the solute plug. This axial dispersion is essential in FIA to start the derivatization reaction. Mixing of sample and solute occurs in the capillary. Consequently, there is a limitation to the applicable sample volume. With large sample volumes in the middle of the solute plug no reaction may occur. This is demonstrated in Fig. 2, where various solute volumes were injected. Only up to solute volumes of 20 μl was a strict linearity of peak height and peak area observed. At sample volumes of 50 μl and above mixing is incomplete. This leads to peak splitting at sample volumes above 100 μl. Here, reaction takes place only at the two ends of the solute plug.

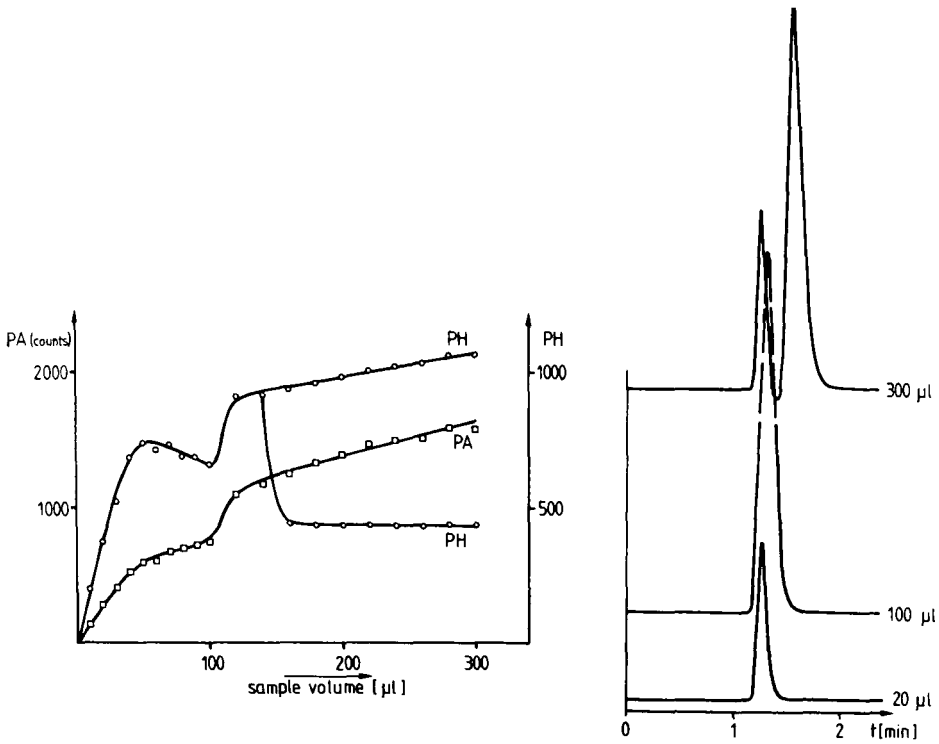

Fig. 2. Effect of sample volume on quantification by conventional FIA. Determination of formaldehyde with acetylacetone and ammonia forming dihydrolutidine [12]. PA = peak area; PH = peak height.

RESULTS AND DISCUSSION

Impact of CRD on FIA

The problems discussed here can be prevented if a FIA system identical with a CRD system is used. The solute is introduced into a carrier stream (in the simplest case, pure water) and the reagent is added by a mixing device. The principle of this set-up is compared in Fig. 3 with a classical FIA system. With this branched FIA system (BFIA), complete reaction with the whole sample volume can be achieved even if it is large, and a linear calibration graph of peak area could be obtained, as shown in Fig. 4. It should be mentioned that much larger areas have been measured for sample volumes above 50 µl than with the classical FIA set-up. With this system, low-dispersion capillaries, such as KOT, with smaller diameters can be used, because dispersion is no longer required to mix the solute and reagent. Hence better detection sensitivity can be achieved.

Another advantage of BFIA is the possibility of displacing the inevitable refractive index peak caused by the injection pulse from the signal, which usually causes problems in quantification at low detection levels. With the set-up shown in Fig. 3, the injection pulse is separated from the sample peak by the short capillary between

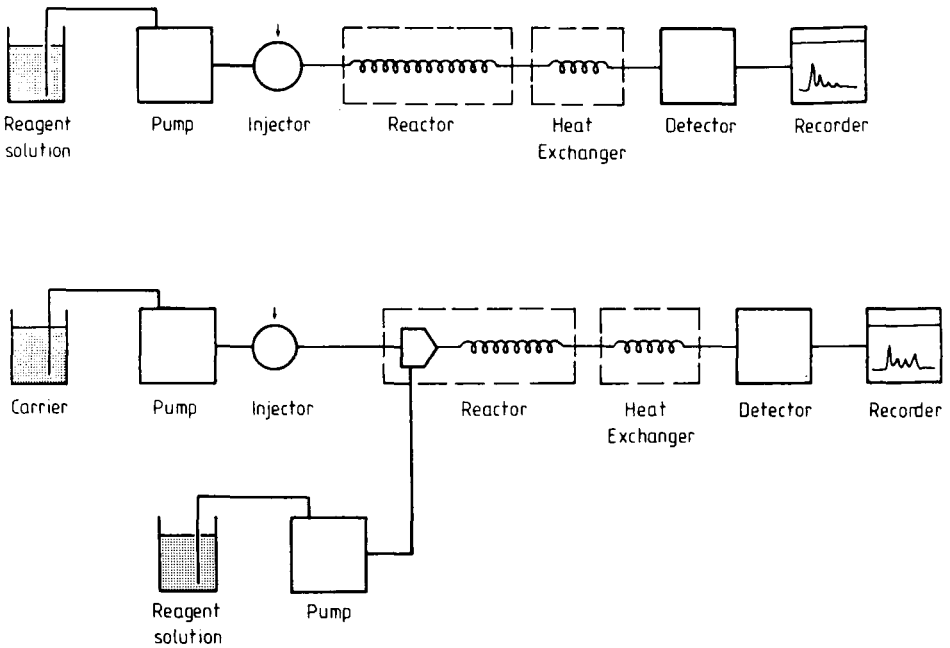

Fig. 3. Schematic diagram of the set-up for FIA. Top, conventional FIA; bottom, branched FIA.

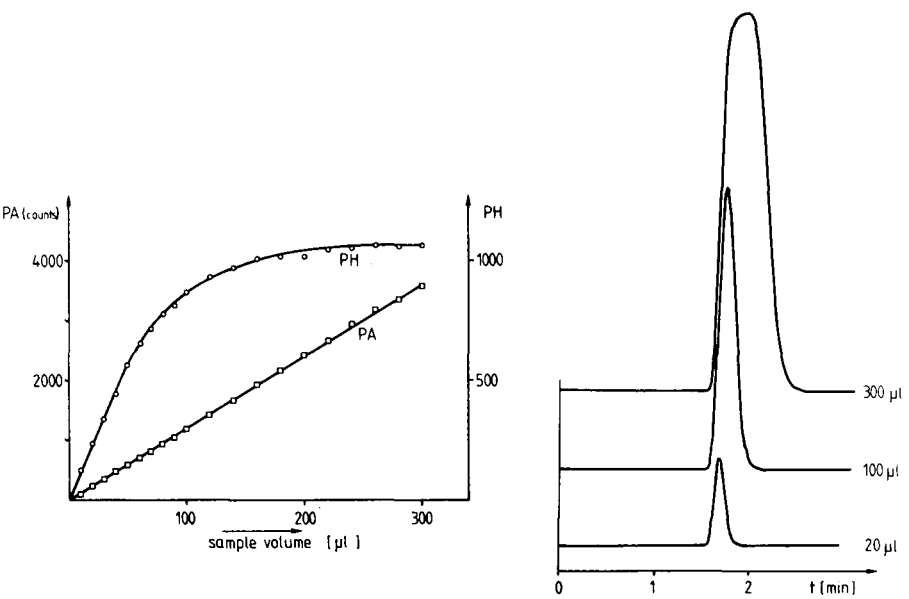

Fig. 4. Effect of sample volume on quantification with branched FIA. Conditions as in Fig. 2.

the injector and mixer. The improvement in detection sensitivity which is thus achievable has been demonstrated earlier [11].

It should be added that the use of low-dispersion capillaries common to CRD, such as KOT, and effective mixers will be most advantageous only with branched systems. High-speed analysis without limitations on solute volume can be attained without a reduction in detection sensitivity caused by inefficient mixing of solute and reagent.

Table I shows the advantages of BFIA with and without a spacer capillary. The introduction of KOT instead of conventional coiled FIA capillaries (in both instances the tube diameter was identical) into a normal FIA system improves the detection sensitivity of the determination of formaldehyde [12] by a factor of 4 and increases the number of determinations from 100 to 430. The use of a BFIA set-up improves the detection sensitivity again by a factor of 4. Compared with standard FIA, the improvement is 16-fold. The spacer capillary reduces the influence of the refractive index peak, and a slight improvement in detection sensitivity can be obtained. An additional advantage of BFIA is that reagent absorption does not cause any problems.

Inverse- and switched-flow injection analysis

FIA offers the possibility of performing many quantitative determinations of the same kind per unit time. More than 200 analyses per hour have been reported. Such fast analysis cycles are not often required. Because in FIA the reagents are pumped continuously, they are wasted when no analysis is performed. With the standard set-up, changes in the determination reaction by changing the reagents is time consuming. In this instance, two different approaches can be used to save reagents and to perform different determinations without completely changing the equipment.

In the simplest case, when several different determinations must be carried out in a continuous stream, the system can simply be inverted. In inversed flow injection analysis (IFIA) the sample is pumped continuously and the reagent is injected. Consequently, IFIA can advantageously be applied in process control or in the determination of various components in waste water. The use of automatic HPLC injectors, where the different reagents can be stored, permits the direct and automatic determination of many solutes in the system. The required change in detection

TABLE I

COMPARISON OF FIA AND BFIA IN FORMALDEHYDE DETERMINATION

Parameter	FIA	BFIA		
	Standard tubes	KOT	KOT	KOT and spacer
Peak volumes (flow-rate = 1.1 ml/min; tube, 0.3 mm I.D.) (μl)	430	100	150	>150[a]
Samples per hour	100	430	430	<430[a]
Detection limit (ppb)	80	20	5	3
Problems with RI switching peaks	No	No	Yes	No
Influence of absorption of reagent	Yes	Yes	No	No

[a] Depending on length of spacer capilary.

wavelength can be initialized by the automatic sample injector. The second generation of HPLC injectors can be programmed to take samples from various vials and to inject them in one step. In HPLC, this has already been used for automatic precolumn derivatizations. The advantage of this type of injector in IFIA is that reagents can also be used which have only limited stability when all the components are mixed together. This simplest approach is demonstrated in Fig. 5 for the determination of cyanide in waste water. Pump I feeds waste water continuously into the system. In the mixing device one part of the reagent (barbituric acid in pyridine) is mixed with the waste water. For the determination of cyanide, a plug of chloramine T in a buffer solution is added to this mixture ahead of the mixer. Only when this plug is present in the water will the reaction take place. The detection limit for cyanide with this set-up is 2 ppb. Surprisingly, in the classical set-up, where both reagent components are pumped and water is injected, the detection limit is inferior by a factor of 10 [12]. The calibration graph for cyanide determinations with normal FIA and IFIA is presented in Fig. 6. With the same set-up it was also possible to determine nitrite in water with a detection limit of 1 ppb by diazotization of sulphanilamide and coupling with N-(1-naphthyl)-ethylenediamine to an azo dye.

Table II summarizes the results of the determination of various anions and of zinc. The reagent compositions are also given. Again, with IFIA the detection limit is always better by a factor of at least 5. Nitrate is reduced to nitrite in an additionally installed solid-phase reactor, packed with cadmium beads, prior to the addition of the reagents. Only with rhodanide could no difference be observed between both types of set-up. The reason for this may be the small molar absorption coefficient of the iron–rhodanide complex.

Some of the reagents used in the determination of inorganic ions are extremely aggressive and can ruin pumps and other metal parts owing to complexation reactions. Also, at least one reagent component must be pumped continuously with the set-up shown in Fig. 5. Therefore, a different set-up has been developed where an inert carrier stream, in most instances pure water, can be used. The reagent components and/or the sample are introduced simultaneously in the form of plugs into the carrier and mixed, and the reaction products are detected photometrically. The equipment used for this type of FIA with reagent switching (SFIA) is shown in Fig. 7.

The inert carrier is displaced by the two pumps, P_1 and P_2. The use of two pumps is superior to that of one pump and a splitting device. With a single-pump system and reagent solutions differing in viscosity, the flow through the two branches will differ.

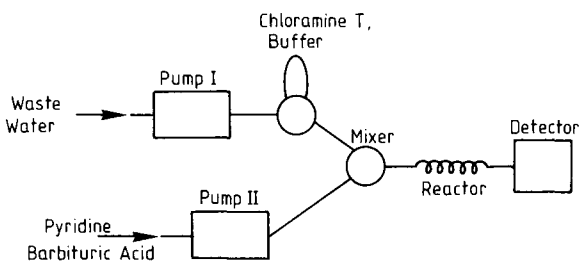

Fig. 5. Schematic diagram of the set-up for inverse FIA. Determination of cyanide in waste water. For experimental conditions, see Appendix.

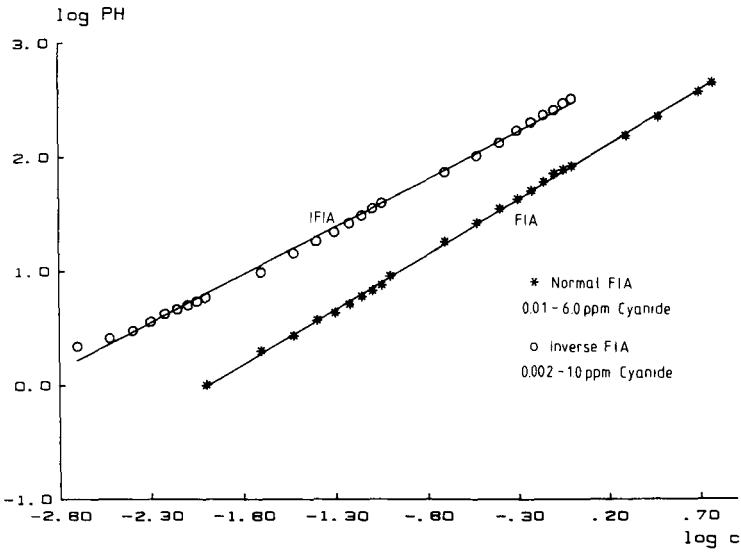

Fig. 6. Calibration graphs for cyanide determination in waste water. For experimental conditions, see Appendix. (×) Normal FIA (0.01–6.0 ppm cyanide); (○) inverse FIA (0.002–1.0 ppm cyanide).

When the reagents or reagent and sample are injected with the two valves (S_1 and S_2), both plugs are mixed and, after reaction in the knitted tube, the reaction products can be determined photometrically. The volume in both branches between sampling device and mixer must be identical. Relatively large sample volumes (300–600 μl) must be injected to ensure overlap. This approach also permits the use of coloured reagents and samples where the absorption is in the same region as where the reaction products are determined. In this instance, it is advantageous to delay one partner for a certain time. This is demonstrated schematically in Fig. 8. With this set-up it is possible to determine first the absorption of the solute or of reagent I (A1 in Fig. 8). When both plugs overlap, it is possible to determine the absorption of the reaction product together with that of the reagent and solute (A2). In the last part it is possible to determine the absorption of the second injected component (A3), and the absorption of the reaction product can be obtained by subtracting the absorption values of the two components

TABLE II

DETECTION LIMITS FOR INORGANIC IONS

Ion	RC I	RC II	FIA	IFIA
CN^-	Chloramine T	Pyridine-barbituric acid	10 ppb	2 ppb
SCN^-	$Fe(NH_4)(SO_4)_2$	–	1 ppm	1 ppm
NO_2^-	Sulphanilamide	N-(1-Naphthyl)ethylenediamine	50 ppb	1 ppb
NO_3^-	Cd-sulphanilamide	N-(1-Naphthyl)ethylendiamine	100 ppb	10 ppb
$[Fe(CN)_6]^{4-}$	$FeCl_3$	4,7-Diphenyl-1,10-phenanthroline	1 ppm	–
Zn^{2+}	Xylenol orange	–	1 ppm	0.1 ppm

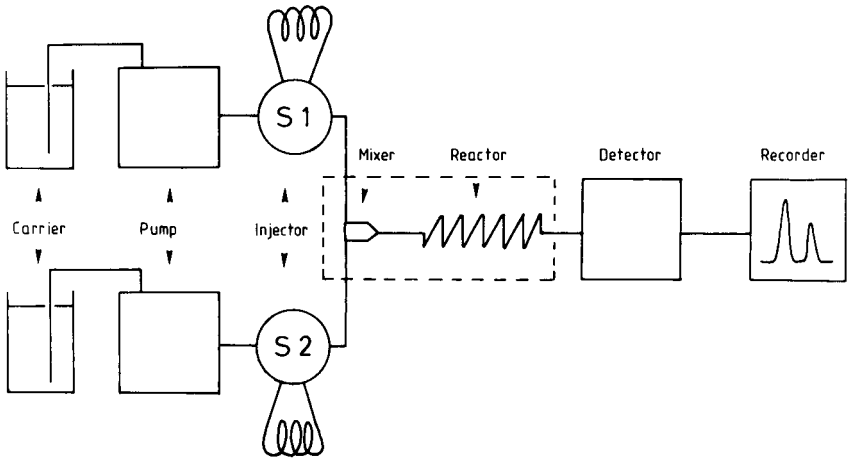

Fig. 7. Schematic diagram of the set-up for switched FIA.

(A2–A1–A3). The applicability of this set-up is demonstrated in Fig. 9 for the determination of formaldehyde in a yellow shampoo. The usual reagent [12] was additionally dyed with riboflavin. The experimental curves show, first, the signal obtained for the reagent and the injected shampoo solution. In a second step, the blank reagent was injected. The UV detector used permitted directly the subtraction of this reagent blank from the absorption peak. The peak thus obtained after the reagent absorption has been subtracted is also shown. The absorption caused by the colour of

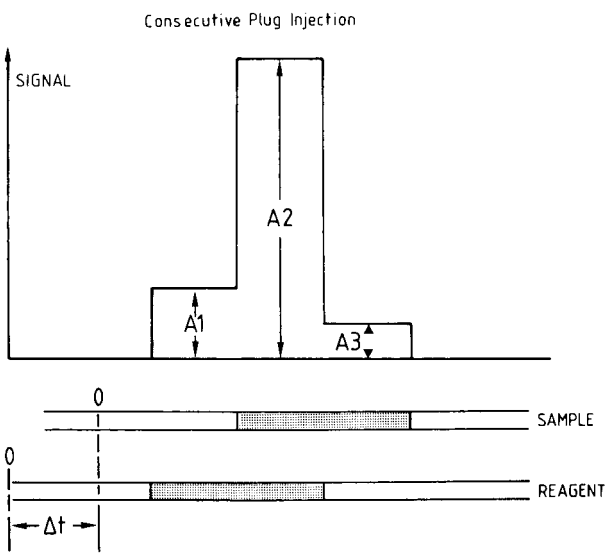

Fig. 8. Schematic presentation of plug injection with switched FIA for reactions with coloured samples and reagents.

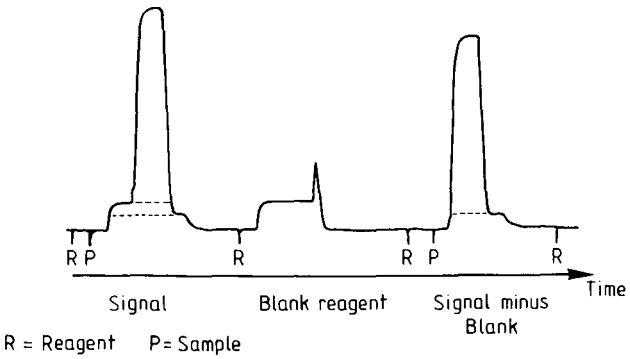

Fig. 9. Determination of formaldehyde in a coloured shampoo. Experimental conditions as published [12]. R = reagent; P = sample.

the shampoo is below the dashed line and can easily be subtracted from the main absorption.

For these measurements, the plug volumes are chosen to be large enough to reach a plateau and to make the plugs overlap at least for 50% of their width. Consequently, additional precautions must be taken to minimize zone dispersion in the sample loops and to reduce the so-called "log bottle" effect when the sample loop is

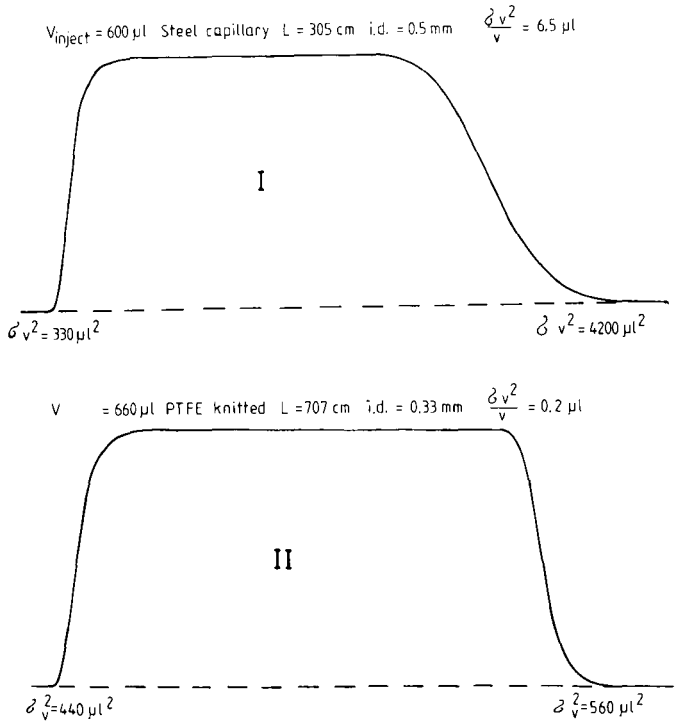

Fig. 10. Plug forms with large sample loops. For explanations, see text.

flushed with carrier. Here, the use of knitted Teflon capillaries in the sample loops is also advantageous. Fig. 10 shows the plug profile obtained when a 600-μl sample loop (coiled stainless-steel capillary, 305 × 0.5 mm I.D.) is emptied (I). The broadening of the tailing part of the plug is unacceptibly large. The volume variance of this part is 4200 μl^2, compared with 330 μl^2 for the leading part of the plug. The volume variance per unit volume ($\sigma_v^2 v^{-1}$), corresponding to the H value ($\sigma_L^2 L^{-1}$) of this loop, is 6.5 μl. The plug form with a knitted Teflon capillary (707 cm × 0.33 mm I.D.) as the sample loop is shown as curve II in Fig. 10. The variance of the tail end is only 560 μl^2 and that of the leading portion is 400 μl^2. The volume variance per unit volume is in this instance only 0.2 μl. This shows clearly that geometrically deformed open tubes are also advantageous as sample loops when large sample volumes must be injected. In preparative chromatography this is the case, when dilute sample solutions must be applied, owing to limitations in sample solubility.

CONCLUCIONS

The synergistic effects of using both CRD and FIA have been demonstrated. By applying forced sample reagent mixing and hence low-dispersive reaction capillaries, the limitations of FIA in sample volume can be obviated. The low dispersion in KOT improves the detection sensitivity by a factor of at least 10–50. Continuous determination of products in process control is possible when the reagent is injected into the sample stream. Various forms of switching techniques permit the use of aggressive reagents, even at an absorption wavelength where the reaction product is measured. An additional advantage is that in this instance the amount of reagents required can be reduced drastically.

ACKNOWLEDGEMENTS

Financial assistance by the Deutsche Forschungsgemeinschaft (R.K.) and the Bundesministerium für Forschung und Technologie (Projekt "Ausarbeitung von Analysenverfahren zur simultanen Bestimmung anorganischer und organischer Verbindungen in Kokereiwässern und zur Untersuchung cyanidhaltiger Altlasten") (G.S.) is gratefully appreciated.

APPENDIX

Experimental conditions for the carbamate and formaldehyde determination have been described elsewhere [8,12]. For the equipment set-up, various HPLC components were used: pumps (Waters Assoc. M6000, 590; LKB or Dionex); detectors (Waters Assoc. 490; Milton Roy); Teflon tubing (0.3 mm I.D.) was knitted as described in Ref. 7.

Reagent compositions for anion determinations in Table II were as follows:
Cyanide: Solution I:

(1) CN^-:

RC I: 1 g of chloramine T in 100 ml of water.

RC II: 15 g of barbituric acid, 75 ml of pyridine and 15 ml of concentrated HCl, diluted with water to 250 ml.

(2) SCN^-:

RC I: 0.25 g of $Fe(NH_4)(SO_4)_2 \cdot 12\ H_2O$ in 100 ml of 0.5 *M* HNO_3.

(3) NO_2^-, NO_3^-:

RC I: 2.5 g of sulphanilamide in 13 ml of concentrated HCl, diluted with water to 250 ml.

RC II: 0.25 g of N-(1-naphthyl)ethylendiamine in 250 ml of water.

(4) $Fe(CN)_6^{4-}$:

RC I: 0.0033 *M* iron(III) chloride in 0.1 *M* acetic acid.

RC II: 10 mg of 4,7-diphenyl-1,10-phenanthrolinedisulphonic acid in 30 ml of water.

(5) Zn^{2+}:

RC I: 0.012 g of xylenol orange in 100 ml of water.

REFERENCES

1 I. Krull (Editor), *Post Column Derivatization in HPLC*, Marcel Dekker, New York, 1986.
2 J. Růžička and E. H. Hansen, *Flow Injection Analysis*, Wiley, New York, 1981.
3 H. Engelhardt and U. D. Neue, *Chromatographia*, 15 (1982) 403.
4 H. Engelhardt and B. Lillig, *J. High Resolut. Chromatogr. Chromatogr. Commun.*, 8 (1985) 531.
5 H. Engelhardt and B. Lillig, in I. Krull (Editor), *Post Column Derivatization in HPLC*, Marcel Dekker, New York, 1986, pp. 1–61.
6 G. Taylor, *Proc. R. Soc. London, Ser. A*, 219 (1953) 186.
7 R. Aris, *Proc. R. Soc. London, Ser. A*, 235 (1956) 67.
8 H. Engelhardt and B. Lillig, *Chromatographia*, 21 (1986) 136.
9 D. H. Spackman, W. H Stein and S. Moore, *Anal. Chem.*, 30 (1958) 1190.
10 H. Engelhardt and P. Ohs, *Chromatographia*, 23 (1987) 657.
11 H. Engelhardt and R. Klinkner, *Fresenius', Z. Anal. Chem.*, 319 (1984) 277.
12 H. Engelhardt and R. Klinkner, *Chromatographia*, 20 (1985) 559.
13 G. Schöndorf and H. Engelhardt, *Fresenius', Z. Anal. Chem.*, 333 (1989) 719.

Journal of Chromatography, 535 (1990) 55–74
Elsevier Science Publishers B.V., Amsterdam

CHROMSYMP. 2029

High-performance liquid chromatographic computer simulation based on a restricted multi-parameter approach

I. Theory and verification

J. W. DOLAN, D. C. LOMMEN and L. R. SNYDER*
LC Resources Inc., 3182C Old Tunnel Road, Lafayette, CA 94549 (U.S.A.)

ABSTRACT

A computer program (DryLab MP®) is described for the simulation of HPLC separations where two or more variables (*e.g.*, temperature and pH) are changed simultaneously. It is assumed that preliminary method development has resulted in a mobile phase of appropriate strength, such that $1 < k' < 20$ for all bands in the chromatogram. If it is desired to simulate separation as a function of changes in the values of n variables, then one or two additional runs are carried out for each variable —changing only that variable. Retention times for each of the latter runs are entered into the computer, and predictions of separation as a function of all conditions are now possible. Because simultaneous changes in two or more variables can lead to significant interaction effects and less accurate predictions, the software evaluates each simulation for possible errors. Allowed conditions must be capable of predicting values of α with an accuracy better than ± 2% (1 S.D.).The present computer program has a number of possible applications during and following method development, as discussed in the following paper (Part II).

INTRODUCTION

Users of high-performance liquid chromatography (HPLC) are faced with various problems during method development and the routine application of a final procedure. For samples of any complexity, the selection of experimental conditions that can provide an adequate separation can be a considerable challenge [1]. Once a suitable method is developed, other laboratories may experience difficulty in obtaining the same separation; *i.e.*, the method is not sufficiently rugged. When a replacement column is required, it may be found that columns from different batches do not yield the same separation [2] —requiring modification of the original procedure. Finally, other problems can arise as a result of errors in formulating the mobile phase (including errors in the measurement of pH), setting the proper flow-rate, etc. [2].

Procedures for HPLC method development vary widely among different laboratories. Many chromatographers adopt a trial-and-error approach, although this is often inefficient. Several method development schemes have been described which utilize a defined number of experimental runs to predict (and optimize) separation for

0021-9673/90/$03.50

a wide range of conditions [1,3–5]. These latter procedures can be divided into two groups, depending on whether one or several separation parameters are varied. When only one parameter is varied, two or three initial experimental runs usually suffice for computer-assisted mapping of retention and separation. When two or more separation variables are to be mapped, the number of initial experimental runs increases rapidly. Multi-variable mapping is more likely to uncover a near-optimum separation, but the amount of work required can be prohibitive.

In this paper we describe a somewhat different approach to HPLC method development, based on "restricted" multi-parameter mapping of retention and resolution. This procedure can be used from the beginning of method development, or it can complement procedures based on the optimization of a smaller number of experimental parameters. The software we will describe for multi-parameter mapping can also be applied to the various problems noted above: lack of method ruggedness, variations in retention from column to column, etc.

THEORY

The dependence of HPLC retention (values of k') on different separation variables has been studied rather thoroughly, and various equations have been reported which describe these results. When only one separation parameter is varied at a time, these theoretical or empirical relationships are often of rather simple form and are reasonably accurate. They are thus ideally suited to single-parameter mapping of separation —including both interpolation and extrapolation of initial experimental data. When two or more parameters are varied simultaneously, the resulting equations are usually much more complex —and also less reliable. As a result, multi-parameter mapping usually employs general-purpose (empirical) fitting equations which require a larger number of data points (initial runs).

In the present treatment we have tried to combine the best features of single- and multi-parameter mapping, by determining under what conditions the simple relationships for the single-parameter case can be extended to multi-parameter mapping. In the limiting case where the variation of all parameters is sufficiently restricted, it can be assumed that there will be no interaction among the different variables, so that retention for a change in one or more variables i is given as

$$k' = k_R \prod^{i} (k_i/k_R) \tag{1}$$

Here k_R refers to a value of k' for a given band in the reference (starting) run, and k_i is the value of k' for a run where only variable i is changed. Thus the dependence of k' on i is determined with other variables unchanged (same values as in reference run), so that k_i/k_R can be calculated for any value of each variable i.

For small enough variations in the different variables i, eqn. 1 can be written in an equivalent form

$$k' = k_R + \sum^{i} (k_i - k_R) \tag{2}$$

However the following treatment is based on eqn. 1 rather than eqn. 2.

TABLE I

VARIABLES THAT AFFECT RETENTION IN REVERSED-PHASE AND ION-PAIR CHROMATOGRAPHY

Group	Non-ionizable solutes	Ionizable solutes
I[a]	Organic solvent (mixtures of methanol, acetonitrile, THF)	pH, ion-pair-reagent concentration
II	%B, column type	%B, temperature, column type, additive[b] concentration
III	Temperature	Ion-pair-reagent type

[a] Variables from group I are most likely to be useful for controlling values of α and band spacing; group III variables are least promising [1].

[b] Buffer, amines, salt, etc.

Retention relationships (single parameter)

Those experimental conditions which have been used to control retention in HPLC are summarized in Table I (see discussion in ref. 1, Ch. 4 and 5). They are grouped (I–III) according to their relative potential for use in controlling band spacing (values of α). While changes in the parameters listed in group I of Table I are more likely to create large changes in α, it is our premise that any or all of the remaining variables can be of potential value for a given sample—especially samples which prove more difficult to separate. The present treatment will emphasize changes in mobile phase composition and temperature.

Solvent strength (%B). Numerous studies [6,7] have established that retention in reversed-phase and ion-pair chromatography is usually well approximated by the empirical relationship

$$\log k' = \log k_w - S\,\varphi \tag{3}$$

Here k' is the capacity factor of the solute in a mobile phase A/B, φ is the volume fraction of the organic solvent B, k_w is the (extrapolated) value of k' for water (solvent A) as mobile phase, and S is a constant whose value depends on the solute and (to a lesser extent) experimental conditions.

The value of α for two solutes i and j is then given by

$$\log \alpha = \log (k_{wj}/k_{wi}) + (S_i - S_j)\,\varphi$$

$$= (\text{constant}) + \Delta S\,\varphi \tag{4}$$

Here subscripts i and j refer to the respective solutes. The value of ΔS for two solutes thus determines the effect of a change in φ (or %B) on band spacing and α.

Small deviations of experimental data from eqn. 3 are often observed, but these usually have little effect on the accuracy of this relationship over a range in values of φ corresponding to $1 < k' < 20$ for all sample components [8].

Temperature (T). In chromatography (as for other chemical or physical

processes) the enthalpy and entropy of retention can usually be assumed constant over some range in temperature, leading to a dependence of retention on temperature of the form

$$\log k' = A + \bar{B}/T \tag{5}$$

where A and $\bar{B}$ are constants for a given system, and T is the absolute temperature (K). Numerous examples of the applicability of eqn. 5 for HPLC systems have been reported [9–11].

The value of α for two solutes i and j is given by

$$\begin{aligned} \log \alpha &= (A_j - A_i) + (\bar{B}_j - \bar{B}_i)\,(1/T) \\ &= (\text{constant}) + \Delta\bar{B}\,(1/T) \end{aligned} \tag{6}$$

The value of $\Delta\bar{B}$ for the two solutes thus determines the effect of a change in temperature on band spacing and α.

pH. The effect of pH on sample retention has been described in detail by several workers [12–16]. The ionization of the solute is defined by its K_a value, and the observed k' value is equal to the sum of k' values for the ionized and non-ionized forms of the solute:

$$k' = k^\circ\,(1 - F^\pm) + k^\pm\,F^\pm \tag{7a}$$

Here $k^\pm$ and k° refer to the values of k' for the solute in the ionized and non-ionized forms, respectively; $F^\pm$ is the fraction of solute molecules that are ionized; *i.e.*,

$$\text{acids} \qquad F^- = 1/\{1 + ([H^+]/K_a)\} \tag{7b}$$

$$\text{bases} \qquad F^+ = 1/\{1 + (K_a/[H^+])\} \tag{7c}$$

Eqns. 7a–c have been shown to provide accurate predictions of the retention of acids and bases as a function of pH.

Values of K_a, $k^\pm$ and k° can, in principle, be derived from measurements of k' at three values of pH. In practice, this is complicated by small errors in the measurements of (a) the mobile phase pH and (b) individual values of k'. Optimally, the mobile phase pH values will bracket the pK_a value of the solute and be spaced over a 1–2 unit pH range.

Concentrations of buffer, ion-pair reagent, salt, amine modifiers, etc. The effect on sample retention of these mobile phase additives is usually complex, as discussed by several authors [13,14,16]. Over a small range in concentrations, retention can often be described [17,18] by an equation of the form

$$\log k' \approx C + D \log [X] \tag{8}$$

Here, C and D are constants for a given solute and HPLC system, and [X] refers to the concentration of the mobile phase additive. The approximate nature of eqn. 8 must be

stressed; it is unsuitable for extrapolation beyond the range of values of [X] used to determine C and D.

Mixtures of organic solvents. Retention is often mapped for ternary-solvent mobile phases during method development [1,4,5]. In some cases, the concentration ratio of two organic solvents is varied while holding %B constant (B refers to the sum of the two solvents). In other cases, two binary solvents A/B and A/C having different values of φ are blended. In either case, the resulting dependence of k' on mobile phase composition is complex, and no theoretical equations have been demonstrated to be generally reliable. The use of quadratic equations with interaction terms appears to give a reasonable fit in most cases [19].

Retention relationships (multi-parameter)

These are necessarily based on some model of solute retention, and there is still a general lack of agreement on these retention models for different systems (*cf., e.g.*, the discussion of Horváth in ref. 16 concerning reversed-phase ion-pair systems). Even where physically reasonable models can be derived, the many fitting parameters require a corresponding (large) number of initial experiments, and the reliability of these models over a significant range in values of different variables is often poor. This is particularly true when the objective is the accurate mapping of resolution as a function of separation conditions, since then values of α must be accurate within (at most) a few percent.

Interaction effects. The effects of %B, T, pH and other variables X on the retention of a given solute are given by the parameters S, $\bar{B}$, (K_a, k°, k^+), and D, respectively (eqns. 3, 5, 7a–c). By "interaction effects" we refer to the dependence of these solute parameters on other variables; *e.g.*,

$$S = \mathrm{f}(T, \mathrm{pH}, [\mathrm{X}_1], [\mathrm{X}_2], \ldots) \tag{9a}$$

$$\bar{B} = \mathrm{f}(\%\mathrm{B}, \mathrm{pH}, [\mathrm{X}_1], [\mathrm{X}_2], \ldots) \tag{9b}$$

$$D_1 = \mathrm{f}(\%\mathrm{B}, T, \mathrm{pH}, [\mathrm{X}_2], \ldots) \tag{9c}$$

$$D_2 = \mathrm{f}(\%\mathrm{B}, T, \mathrm{pH}\ [\mathrm{X}_1], \ldots) \tag{9d}$$

$$K_a = \mathrm{f}(\%\mathrm{B}, T, [\mathrm{X}_1], [\mathrm{X}_2], \ldots) \tag{9e}$$

$[\mathrm{X}_1]$, $[\mathrm{X}_2]$, ... refer to the concentrations of different mobile phase additives.

Since the dependence of retention on pH involves three separate parameters (K_a, k°, $k^\pm$), it will prove convenient to ignore changes in these parameters with %B, T, X, etc. by means of the following convention. In every case we begin with a reference set of experimental conditions and a corresponding chromatogram. The problem is then to predict how retention will change as these conditions are varied. If pH is one of the variables, it will be assumed that a change in pH is carried out *first*, so that the effect of pH on retention can be described in terms of the values of K_a, k°, $k^\pm$ for the reference run. Subsequent changes in retention as a result of a change in other parameters (%B, T, X, ...) can then be described in terms of eqn. 9a–e.

Consider next the case where two variables are changed simultaneously; *e.g.*,

%B and temperature. Eqn. 9a–e provide a generalized description of the resulting changes in retention. Thus, a change in %B and T can be described as a two-step process, involving a change in T (for which the reference value of $\bar{B}$ applies), followed by change in the %B (note eqn. 1). It is assumed that values of S and $\bar{B}$ for the reference run have been determined by one-at-a-time changes in %B and T. Retention for the new values of %B and T is thus determinable from the reference value of $\bar{B}$ and a value of S at the new temperature T (S_T). The question is then: how much does S vary with temperature (eqn. 9a)? Alternatively, if S does not vary with temperature, it means that eqn. 1 is applicable for the prediction of retention at the new values of %B and T (*i.e.*, interaction effects are negligible).

Example of variation of S with temperature. A detailed study of retention as a function of temperature and %B has been published for some (predominantly) non-ionic compounds [20]. We will use these data to illustrate our approach to determining the error in predictions based on eqn. 1 (ignoring interaction effects). Values of S for nine solutes at different temperatures can be determined from the data in ref. 19, as summarized in Table II; values of S are shown for 30°C, and the change in S (δS) is shown between 30°C and other temperatures. If values of δS were zero for all solutes and temperatures, this would correspond to no error in the application of eqns. 1, 3 or 5 for changes in %B of up to 20% and changes in temperature of up to 30°C.

The actual values of δS are seen to vary systematically with temperature, reflecting the significance of eqn. 9a. If all solutes exhibited the same value of δS at a given temperature, this would mean that all values of k' are changed by the same ratio (eqn. 3). Consequently there would be no change in values of α, and no error in

TABLE II

VARIATION OF S WITH TEMPERATURE

Conditions: 15 × 0.46 cm I.D. C_8 column; 50 and 70% methanol–water mobile phases used to calculate values of S (eqn. 3); 1 ml/min flow-rate; temperatures as indicated; data calculated from ref. 19.

Solute	S	δS		
	30°C	41–30°C	51–30°C	59.5–30°C
p-Nitrophenol	2.73	(+0.04)[a]	−0.37	−0.47
Phenol	2.57	−0.27	−0.34	−0.48
Acetophenone	2.93	−0.27	−0.42	−0.55
Methyl benzoate	3.28	−0.21	−0.43	−0.45
Anisole	2.97	−0.23	−0.37	(−0.19)[a]
Benzene	2.88	−0.25	−0.33	−0.45
Phenetole	3.39	−0.21	−0.36	−0.42
Toluene	3.35	−0.26	−0.37	−0.37
Ethylbenzene	3.80	−0.21	−0.34	−0.50
Av. δS[b]		−0.24±0.02	−0.37±0.03	−0.46±0.06
Error in k'		−12±1%	−19±1%	−24±3%
Error in α		±1.4%	±2.0%	±4.0%

[a] Out-of-line value, not included in calculations of error.

[b] Average values of δS for a given temperature change (*e.g.*, 30 to 41°C) with S.D. values (see discussion of text and Fig. 1); the errors in k' and α correspond to average errors in these quantities as predicted from eqn. 1 and 30°C as reference temperature.

predicted values of α. The latter hypothesis comes close to approximating the data of Table II, as seen in the average values of δS listed for each temperature (deviations from this value expressed as 1 S.D.).

Thus for a change in %B from 50 to 70% the average decrease in S by 0.24 units at 41 *vs.* 30°C (Table II) corresponds to an average change in log k' of (change in S) (change in φ) = $(-0.24) \times (-0.2) = -0.048$; *i.e.*, eqn. 3. This is equivalent to a 12% increase in the actual value of k' at 41°C and 70% B. This increase in k' due to the interaction of temperature and %B (eqn. 9a) is relative to the value of k' calculated from eqn. 1, so that the resulting error in eqn. 1 is −12% for this case.

The corresponding error in values of α determined from eqn. 1 is given by the deviation of values of S from the average; *e.g.*, ±0.02 units at 41 *vs.* 30°C (see Table II). That is, values of S at 41°C are not all exactly 0.24 units lower than values at 30°C; otherwise, there would be no error in values of α from eqn. 1. The average error of ±0.02 units in S for each solute leads to an error in the difference of S-values (eqn. 4) of $2^{0.5} \times 0.02 = 0.03$ units, which, multiplied by 0.2 (eqn. 4, change in %B from 70 to 50%), leads to an error in predicted values of α = 1.4%[a].

If our goal is to maintain the accuracy of calculations of α by eqn. 1 better than ±2%, it is seen that the system in Table II can be varied by 20% B and 21°C[b]. There is no reason to believe that other HPLC separations which involve non-ionized solutes will be much different in this respect, suggesting that eqn. 1 should be valid (for predictions of α) over a rather wide range in %B and T. Because mixtures of ionizable acids and bases involve an additional temperature-dependent process (the change of K_a with T), we can anticipate that eqn. 1 will be less reliable for such samples. This will prove to be the case.

The prediction of values of k' by means of eqn. 1 is illustrated for the data of Table II in Table III (DryLab MP calculations). Here the reference conditions are selected as 50% B and 30°C, and values of S and B were determined from runs at 60% B and 41.5°C, respectively. Because the change in %B is only 10% in Table III *vs.* 20% in Table II, the errors in k' and α are predicted to be half as great in the comparisons of Table III *vs.* those of Table II for 41°C (−12% in retention, ±1.4% in α); *i.e.* predicted errors of −6% in k' and ±0.7% in α[c].

EXPERIMENTAL

Equipment and materials

Separations reported here were carried out on a Beckman/Altex System Gold HPLC system (Beckman, San Ramon, CA, U.S.A.). A 25 × 0.46 cm I.D. Zorbax™ C_8 column was used with various methanol–water mobile phases, buffered with acetic

---

[a] These estimated errors in values of α from eqn. 1 are actually *maximum* values, since they include random errors in the measurement of the values of S in Table II.

[b] The prediction of retention times from eqn. 1 will be in error by −24%, however (Table II).

[c] The larger error in α in Table III (±1.7% *vs.* 0.7% predicted from Table II) reflects a greater contribution of experimental error in these calculated values of α. That is, the errors in α of Table II are due primarily to changes in S with T, whereas the α values of Table III reflect additional random experimental error in the measurements of the three experimental k' values used to calculate α (k' values for 50% B/30°C, 50% B/41.5°C and 60% B/30°C runs), as well as error in the measurement of k' values for the 60% B/41.5°C run.

TABLE III

PREDICTIONS OF RETENTION (EQN. 1) FOR SYSTEM IN TABLE II

T = 41.5°C, 60% methanol.

Solute	k'		α	
	expt.	calc.	expt.	calc.
p-Nitrophenol	0.42	0.42	1.00	(0.94)[a]
Phenol	0.42	0.40	1.64	1.63
Acetophenone	0.69	0.65	1.80	1.84
Methylbenzoate	1.24	1.20	0.99	0.96
Anisole	1.23	1.15	1.08	1.11
Benzene	1.33	1.28	1.50	1.52
Phenetole	2.00	1.93	1.16	1.15
Toluene	2.31	2.22	1.66	1.66
Ethylbenzene	3.84	3.69		
Error		$-4 \pm 3\%$		$\pm 1.7\%$

[a] Out-of-line value, not included in error calculation.

acid–sodium acetate (column dead-time t_0 = 2.56 min). Solvents and reagents were of HPLC grade. Water was purified with a Milli-Q system (Millipore, Milford, MA, U.S.A.). The various solutes (see Table IV) were obtained from Aldrich (Milwaukee, WI, U.S.A.).

Software

Computer simulations were carried out by means of DryLab MP software (LC Resources, Lafayette, CA, U.S.A.), using an IBM-compatible personal computer (IBM-AT) with a math-coprocessor.

RESULTS AND DISCUSSION

The present approach to multi-parameter mapping of resolution for application to HPLC method development (and related problems in the routine laboratory) is illustrated in Fig. 1. An initial gradient elution separation (Fig. 1A) is carried out in order to determine an approximately optimum %B for an isocratic separation (see discussion in pp. 239–244 of ref. 1). This latter run (Fig. 1B) then becomes the reference run for further method development (Fig. 1C) via multi-parameter computer simulation. The example of Fig. 1 assumes that %B, temperature and pH will be varied. Therefore additional runs as indicated in Fig. 1C are carried out (dark circles, changing %B by 10%, T by 10°C and pH by ± 0.6 units).

As a result of interaction effects, it is not possible to vary two or more separation conditions simultaneously for every value of these parameters —and achieve accurate predictions. This is illustrated schematically in Fig. 2, which indicates the various combinations of two variables which are allowed; *i.e.*, which provide an accuracy in predictions of α of better than $\pm 2\%$ (1 S.D.). The simultaneous variation of all three of these parameters is also possible, within limits that will shortly be defined. The example

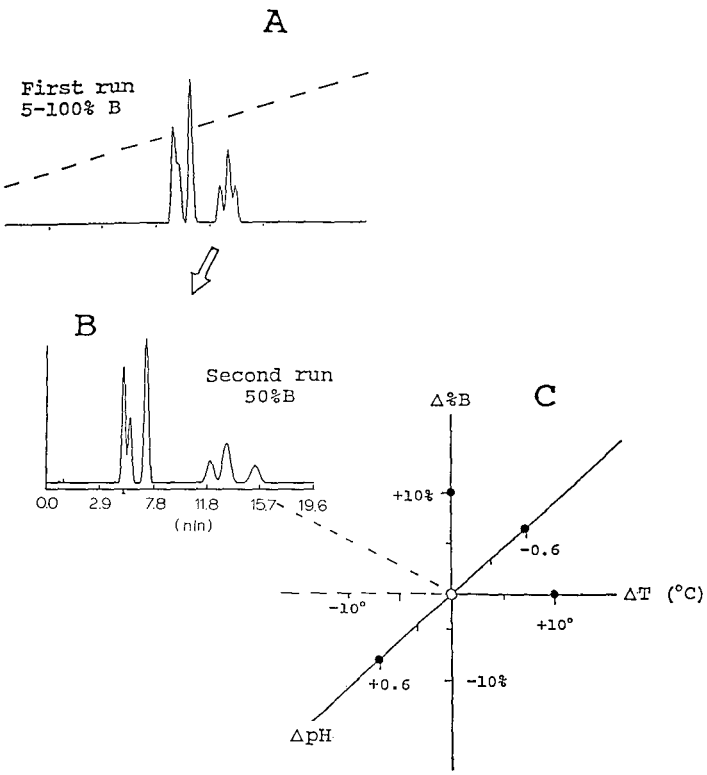

Fig. 1. Hypothetical representation of simplified multi-parameter mapping (interaction effects ignored). (A) Initial gradient elution run; (B) isocratic run predicted from run A; (C) multi-parameter mapping using run B (open circle at center of diagram) as reference run. Closed circles correspond to runs 3–6 (change in %B, T or pH *vs.* reference run).

of Figs. 1 and 2 can be extended to any number n of separation parameters. In the present study, we have examined the simultaneous variation of %B, temperature, pH and buffer concentration for the separation of a mixture of substituted benzoic acids.

Single-parameter relationships

Figs. 3–6 show representative plots of sample retention *vs.* each of the four variables examined in this study: %B, T, pH and buffer concentration. In each case, the solid curves through the data points represent predictions of the appropriate fitting equations (eqns. 3, 5, and 7a–c). Apart from the excellent fit observed in each case, it can be seen that a change in each of these parameters can markedly affect the separation of one or more band-pairs in the sample. That is, whenever two k' plots intersect it signifies that a change in that variable can result in band reversals and marked changes in resolution.

Interaction effects and resulting limits on multi-parameter mapping

The main question in the use of the present resolution-mapping procedure concerns the limits that must be placed on various values of the separation variables

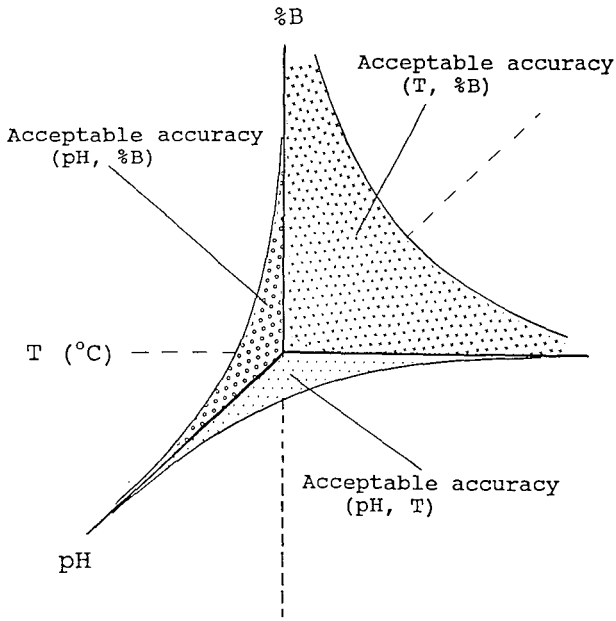

Fig. 2. Illustration of applicability of simplified multi-parameter mapping for prediction of separation when two variables are changed simultaneously (for accuracy in predicted values of α better than $\pm 2\%$).

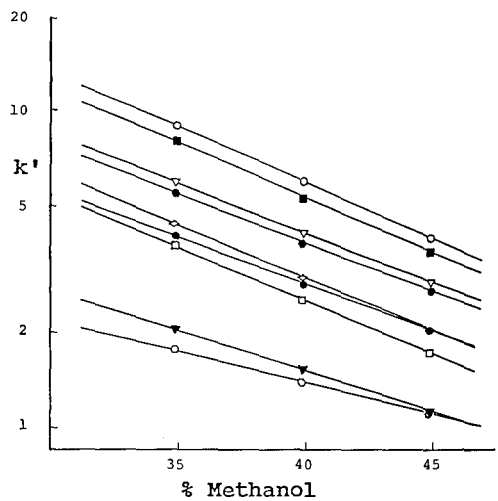

Fig. 3. Dependence of retention of substituted benzoic acid sample on methanol concentration. Conditions: pH 2.9, 35°C, 25 m*M* buffer concentration. Solid curves are from eqn. 3; solutes are in the order of Table IV with 2-nitrobenzoic acid at the bottom and 2,6-dimethylbenzoic acid at the top.

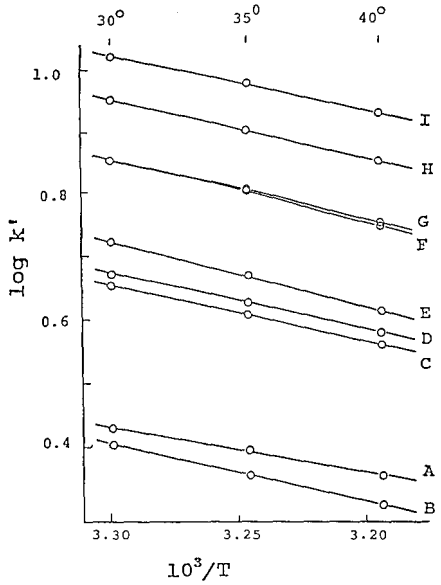

Fig. 4. Dependence of retention of substituted benzoic acid sample on temperature. Conditions: pH 2.6, 35% B, 25 m*M* buffer concentration. Solid curves are from eqn. 5; solutes identified in Table IV.

during computer simulations, so as to maintain the required accuracy in predicted values of α (as illustrated in Fig. 2). One approach to determining such limits was illustrated in the Theory section (discussion of Tables II and III), for a sample of (mainly) non-ionized compounds reported by Gant *et al.* [20]. Here we wish to extend these findings to a sample whose components are partially ionized under the conditions of separation, and to include certain other variables (pH, buffer concentration).

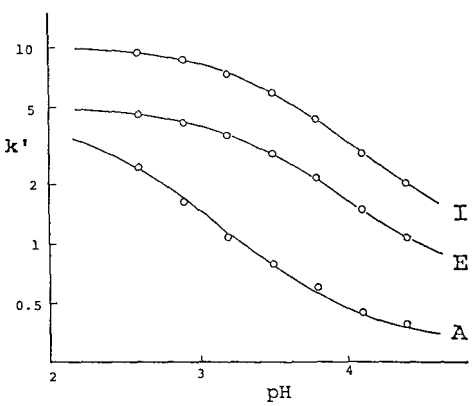

Fig. 5. Dependence of retention of representative benzoic acids on pH. Conditions: 35% B, 35°C, 25 m*M* buffer concentration. Solid curves are from eqns. 7a–c; solutes are (A) 2-nitrobenzoic acid, (E) 3-cyanobenzoic acid and (I) 2,6-dimethylbenzoic acid.

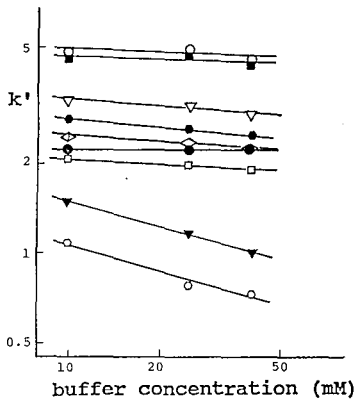

Fig. 6. Dependence of retention of representative benzoic acids on buffer concentration. Conditions: pH 3.2, 40% B and 35°C. Solid curves are from eqn. 8; solutes are in the order of Table IV, with 2-nitrobenzoic acid at the bottom and 2,6-dimethylbenzoic acid at the top.

TABLE IV

RETENTION DATA FOR SUBSTITUTED BENZOIC ACIDS AS A FUNCTION OF EXPERIMENTAL CONDITIONS

See Experimental section for other conditions.

Exptl. conditions				Retention times (min)[a]								
pH	%B	*T*	Buffer	A	B	C	D	E	F	G	H	I
2.6	35	30	25	9.43	9.05	14.11	14.61	16.04	20.87	20.87	25.51	29.40
		35	10	10.22	10.22	12.83	12.90	14.40	18.91	18.91	22.15	26.00
			25	8.91	8.42	12.97	13.44	14.51	18.86	18.86	23.04	26.80
			40	8.14	7.47	12.18	12.78	13.64	17.66	17.66	21.80	25.16
		40	25	8.39	7.81	11.89	12.35	13.11	17.10	16.99	20.78	24.32
	40	30	25	7.94	7.43	10.11	10.86	11.60	15.14	15.14	17.96	20.27
		35	10	8.72	8.72	9.46	9.99	10.70	14.03	14.03	15.85	18.26
			25	7.53	7.00	9.43	10.10	10.65	13.84	13.84	16.39	18.59
			40	6.88	6.25	8.96	9.70	10.12	13.10	13.10	15.68	17.66
		40	25	7.10	6.53	8.75	9.38	9.73	12.56	12.56	14.88	16.99
	45	30	25	6.82	6.30	7.65	8.35	8.76	11.35	11.35	12.95	14.38
		35	10	7.73	7.46	7.73	8.08	8.55	11.12	11.12	12.15	13.82
			25	6.47	5.96	7.19	7.84	8.12	10.43	10.43	11.92	13.28
			40	5.99	5.42	7.04	7.80	7.94	10.14	10.14	11.78	13.04
		40	25	6.11	5.61	6.72	7.48	7.48	9.53	9.53	10.88	12.16
2.9	35	30	25	7.16	8.05	12.83	13.55	14.77	17.51	18.88	24.35	26.87
		35	10	8.08	9.26	12.04	12.50	13.64	16.58	17.64	21.59	24.45
			25	6.88	7.56	11.91	12.58	13.49	16.30	17.23	22.18	24.75
			40	6.34	6.80	11.33	12.08	12.82	15.49	16.29	21.24	23.55
		40	10	7.16	8.28	10.85	11.32	12.12	14.58	15.52	19.33	21.81
			25	6.16	6.84	10.72	11.36	11.96	14.29	15.11	19.76	21.99
			40	5.73	6.23	10.28	10.99	11.46	13.70	14.41	19.10	21.14
	40	30	25	6.20	6.64	9.39	10.20	10.80	12.99	13.85	17.23	18.78
		35	10	7.03	7.69	8.99	9.57	10.19	12.52	13.18	15.50	17.35
			25	5.98	6.30	8.85	9.60	10.03	1..21	12.81	15.90	17.49
			40	5.52	5.70	8.44	9.23	9.55	11.59	12.11	15.24	16.63

TABLE IV *(continued)*

Exptl. conditions				Retention times (min)[a]								
pH	%B	T	Buffer	A	B	C	D	E	F	G	H	I
		40	10	6.28	6.93	8.24	8.78	9.19	11.16	11.73	14.03	15.66
			25	5.40	5.75	8.07	8.80	8.99	10.83	11.34	14.31	15.71
			40	5.04	5.27	7.76	8.64	8.64	10.38	10.84	13.83	15.08
	45	30	25	5.47	5.64	7.19	7.91	8.20	9.86	10.43	12.44	13.44
		35	10	6.30	6.67	7.25	7.80	8.17	10.01	10.47	11.89	13.22
			25	5.29	5.29	6.86	7.60	7.72	9.35	9.75	11.63	12.65
			40	4.95	4.95	6.72	7.56	7.56	9.12	9.50	11.52	12.44
		40	10	5.67	6.05	6.70	7.22	7.44	9.01	9.39	10.83	11.98
			25	4.83	4.98	6.37	7.04	7.04	8.45	8.79	10.62	11.53
			40	4.55	4.55	6.24	6.89	6.89	8.24	8.54	10.50	11.33
3.2	35	30	25	5.26	6.80	10.44	11.32	12.29	12.29	15.15	21.78	21.78
		35	10	5.78	7.46	9.87	10.47	11.30	12.04	14.08	19.01	19.92
			25	5.07	6.36	9.75	10.54	11.20	11.76	13.76	19.63	20.16
			40	4.76	5.82	9.26	10.10	10.59	11.18	12.97	19.00	19.13
		40	25	4.93	6.01	9.22	9.92	10.36	11.15	12.69	18.01	18.88
	40	30	25	4.72	5.71	7.98	8.81	9.22	9.78	11.39	15.78	15.78
		35	10	5.15	6.22	7.61	8.22	8.59	9.45	10.69	13.79	14.51
			25	4.45	5.38	7.51	8.26	8.49	9.20	10.43	14.24	14.68
			40	4.31	4.97	7.18	8.11	8.11	8.80	9.92	13.68	14.01
		40	25	4.43	5.10	7.14	7.93	7.93	8.76	9.69	13.17	13.78
	45	30	25	4.29	4.90	6.32	7.10	7.16	7.77	8.78	11.50	11.69
		35	10	4.73	5.46	6.34	6.88	7.07	7.87	8.72	10.80	11.41
			25	4.16	4.66	6.01	6.67	6.67	7.37	8.13	10.54	10.90
			40	3.98	4.34	5.90	6.56	6.56	7.22	7.95	10.48	10.76
		40	25	4.05	4.46	5.76	6.32	6.32	7.05	7.63	9.86	10.31
2.9	35	35	25	6.71	7.48	11.82	12.49	13.38	16.00	17.03	22.15	24.65
3.2				5.36	6.61	10.27	11.06	11.77	12.67	14.56	20.43	21.37
3.5				4.59	5.97	8.64	9.38	9.98	9.98	12.04	18.07	17.70
3.8				4.09	5.45	7.05	7.60	8.17	7.60	9.62	14.93	13.79
4.1				3.72	4.96	5.58	5.84	6.41	5.84	7.42	10.97	10.01
4.4				3.53	4.60	4.76	4.76	5.38	4.97	6.19	8.18	7.81
3.8	30			4.43	6.29	8.61	9.07	9.07	10.23	11.99	19.23	17.44
	35		10	4.56	6.19	7.47	7.93	8.65	8.25	10.33	15.10	14.44
			40	3.95	5.19	6.88	7.42	7.97	7.42	9.34	14.73	13.52
	40		25	3.74	4.65	5.70	6.26	6.40	6.26	7.52	11.08	10.49
5.2	30		25	3.48	3.86	4.33	3.86	4.83	4.45	5.56	6.28	5.75
	35		10	3.13	3.34	3.61	3.34	3.90	3.76	4.39	4.94	4.50

[a] A = 2-Nitrobenzoic acid; B = phthalic acid; C = impurity; D = 2-fluorobenzoic acid; E = 3-cyanobenzoic acid; F = 2-chlorobenzoic acid; G = 3-nitrobenzoic acid; H = 3-fluorobenzoic acid; I = 2,6-dimethylbenzoic acid.

Variation of S, $\bar{B}$ and D (eqns. a–d). Table IV summarizes the experimental data used in the present investigation. Four separation parameters (%B, T, pH and buffer concentration) were varied singly and in combination, so as to allow the study of interaction effects as given by eqns. 9a–c. These data allow the determination of values of S, $\bar{B}$ and D as a function of the other variables, in the same general way as outlined in Table II. The resulting data are summarized in Table V.

As in our example of Table II, the parameters S, $\bar{B}$ and D show both (a) an average variation due to change in the various conditions (T, pH, buffer concen-

TABLE V

SUMMARY OF THE VARIATION OF THE CHROMATOGRAPHIC PARAMETERS S, $\bar{B}$ AND D AS A FUNCTION OF CHANGE IN DIFFERENT EXPERIMENTAL CONDITIONS

Separation parameter	Expt. condition		Variation in parameter	Error in α[a]	
	Variable	Change		Calc.	Measured
S	T	+10°C	-0.05 ± 0.07	±0.6%	±0.4%
	pH	+0.6	-0.21 ± 0.19	±1.6%	±2.9%
	buffer	+30 mM	$+0.22 \pm 0.08$	±0.7%	±0.6%
$\bar{B}$	pH	+0.6	-126 ± 118	±1.0%	±2.1%
	buffer	+30 mM	$+49 \pm 19$	±0.2%	±1.2%
D	pH	+0.6	$+0.010 \pm 0.033$	±1.6%	±2.7%

[a] "Calculated" values determined as in Table II (assumes changes of ±5% in B, ±5°C on T, ±0.3 units in pH and ±15 mM in buffer); "measured" values determined as in Table III or VII.

tration) and (b) scatter. This scatter leads to errors in the prediction of values of α from eqn. 1. The reference run assumed in Tables IV and V is for 40% B, 35°C, pH = 2.9 and a 25 mM buffer concentration. We have used data for ±5% B, ±5°C, ±0.3 units in pH and ±15 mM buffer concentration to determine values of (k_i/k_R) in eqn. 1; the calculated errors in α reported in Table V correspond to changes in each variable by the latter amount (±5% B, etc.).

Because of the roughly linear change in δS and the other parameters of Table V with the concentration of the second experimental condition ("variable"), it is possible to derive some relationships that predict the total error in a value of α from eqn. 1; these are summarized in Table VI. If the error in α is defined as $\delta\alpha$, then for simultaneous change in three or more variables we have

$$\delta\alpha^2 = \sum^{i} \delta\alpha_i^2 \tag{10}$$

TABLE VI

ERROR IN PREDICTIONS OF α FROM EQN. 1 DUE TO INTERACTION EFFECTS

Expt. variables	Error in α	Maximum change[a]	
%B, T	0.00016 (Δ%B) (Δ°C)	11 %B	11°C
%B, pH	0.014 (Δ%B) (ΔpH)	0.3 pH	5°C
%B, buffer	0.004 (Δ%B) (Δlog [X])[b]	10 %B	3×[c]
T, pH	0.014 (ΔpH) (Δ°C)	0.3 pH	5°C
T, buffer	0.008 (Δlog [X]).(Δ°C)	8°C	2×[c]
buffer, pH	0.30 (ΔpH) (Δlog [X])	0.25 pH	1.8×[c]

[a] *e.g.*, a simultaneous change of 11 %B and 11°C is allowed, as is a change of 5.5% B and 22°C, etc.

[b] [X] is the buffer concentration.

[c] Indicated change in [X] that is allowed; *i.e.*, 1.8 to 3-fold.

TABLE VII

ERRORS IN α AS A RESULT OF INTERACTION EFFECTS

Comparison of experimental data in Table IV with values from eqn. 1. Errors for Bands C-I only; Bands A and B gave larger, more erratic errors, for reasons which we do not fully understand at present.

Run conditions				Error in α ($\delta\alpha$)	
pH	%B	T	Buffer	Found	Eqn. 10[a]
2.6	35	30	25	0.023	0.029
		35	10	0.030	0.036
			25	0.018	0.021
			40	0.030	0.036
		40	25	0.026	0.029
	40	30	25	0.025	0.021
	40	35	10	0.029	0.027
			40	0.034	0.027
		40	25	0.023	0.021
	45	30	25	0.025	0.029
		35	10	0.036	0.036
			25	0.026	0.021
			40	0.044	0.036
		40	25	0.033	0.029
		average difference		$\pm$0.004	
2.9	35	30	25	0.005	0.004
		40	25	0.003	0.004
		35	10	0.006	0.006
		40	10	0.015	0.016
		35	40	0.004	0.006
		40	40	0.009	0.015
	40	40	10	0.009	0.012
		40	40	0.019	0.012
	45	30	25	0.004	0.004
		40	25	0.003	0.004
		35	10	0.009	0.006
		40	10	0.014	0.015
		35	40	0.010	0.006
		40	40	0.017	0.015
3.2	35	30	25	0.054	0.029
		35	10	0.031	0.036
			25	0.024	0.021
			40	0.050	0.036
	40	30	25	0.032	0.021
	45	30	25	0.024	0.029

[a] Best fit to eqn. 10.

where $\delta\alpha_i$ is the error from one of the combinations of Table VI. The limits defined in Table VI (for an error in α from eqn. 1 $< \pm 2\%$) are incorporated into the DryLab MP software. These limits are in the process of further refinement and extension to other separation conditions (see Table I).

Direct measurement of errors in α from eqn. 1. We have also compared experimental values of α with values predicted from eqn. 1 for the various runs in Table

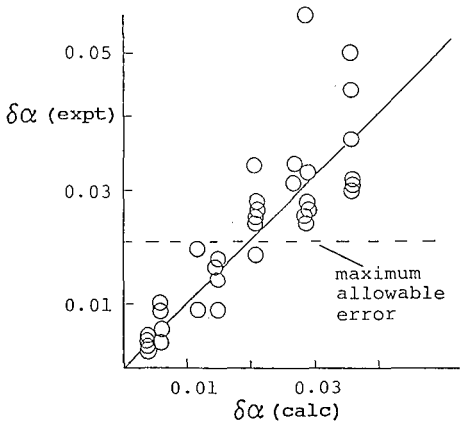

Fig. 7. Comparison of experimental changes in α ($\delta\alpha$) due to interaction effects (simultaneous change of two or more separation conditions) with values predicted from Table VI and eqn. 10.

IV. The resulting average "errors"[a] $\delta\alpha$ are summarized in Table VII. Before analyzing these data, the repeatability of experimental values of α must be addressed. Several replicate runs were carried out for our reference conditions, with the conclusion that values of α were repeatable within about $\pm 0.8\%$ (1 S.D.). About half of this variation appears to be due to small errors in the pH of the mobile phase, which is difficult to reproduce to better than ± 0.02 units. In order to minimize the accumulation of errors from the reference run and the other runs required in the application of eqn. 1 (equivalent to the determination of S, $\bar{B}$, D, etc.), average values of k' were determined from three replicates of the reference run. Similarly, multiple data points and an extended range in each variable were employed in order to maximize the accuracy of values of S, $\bar{B}$, D, etc. In this way the effect of experimental repeatability (error) was minimized, so that resulting determinations of error in eqn. 1 could be directly related to interaction effects. That is, our treatment in Table V was designed to minimize random error contributions —and provide good estimates of $\delta\alpha$ due to interaction effects alone.

Returning to the data in Table VII, these values of $\delta\alpha$ were used to determine the interaction effects as defined in Table V. Table V (last column) summarizes these "measured" values, which are a best fit to the data in Table VII. The corresponding "calculated errors in α" in Table V (next to last column) were determined as described in Table II; these "calculated" and "measured" values should be similar —but not identical. Thus the "measured" values refer to errors in α for the present sample; they therefore depend on the elution order (and values of α) of these compounds. The "calculated" errors in α do not depend on elution order and are therefore less sample specific; they are also less subject to errors in experimental values of retention time.

The "measured" errors in α of Table V, which form the basis of the limit equations of Table VI, were then used to recalculate values of $\delta\alpha$ in Table VII— as a test of (a) the internal consistency of these data and (b) the reliability of eqn. 10. Good

[a] These "errors" in α (expt. *vs.* eqn. 1) are due to interaction effects.

TABLE VIII

VALUES OF S FOR SOME ALKYL PHTHALATES AS A FUNCTION OF TEMPERATURE AND COLUMN

Data calculated from study of ref. 21.

Solute[a]	Values of S[b]		
	Column A[c]		Column B[c]
	35°	60°	35°
C_1	2.24	2.12	2.21
C_2	2.56	2.49	2.55
C_3	2.95	2.78	2.90
C_4	3.50	3.48	3.40
C_5	3.96	3.94	3.86
Average δS[d]	-0.08 ± 0.06		-0.06 ± 0.03

[a] Refers to alkyl chainlength; *e.g.*, C_1 is dimethyl phthalate.

[b] Calculated for 60 and 75% acetonitrile–water for indicated columns (A, B) and temperatures (35 and 60°C).

[c] Both columns are C_8 for reversed-phase; column A has a pore diameter of 6 nm and column B has a pore diameter of 15 nm; the surface area of column B is therefore smaller.

[d] Calculated as in Table II ("error in S") relative to column A at 35°C.

overall agreement is seen, as summarized in Fig. 7. Here values of $\delta\alpha$ (expt) are the "found" values of Table VII, while $\delta\alpha$ (calc) are values of $\delta\alpha$ obtained from eqn. 10 and the "measured" errors in α from Table V.

Data for dialkyl phthalates

Data dealing with the dependence of S on temperature are reviewed in Tables II and III for a non-ionized sample taken from the literature [20]. Similar data have been reported for a series of dialkyl phthalates [21], separated at different temperatures on different columns. These data are summarized in Table VIII.

It is interesting to compare the values of δS for the three cases examined here, normalized to a change in T of 25°C: substituted benzenes (Table II), -0.41 ± 0.05, benzoic acids (Table V), -0.12 ± 0.17 and alkyl phthalates (Table VIII), -0.08 ± 0.06. The phthalates show less effect of temperature on the average value of δS, but the variability of δS (which determines errors in α from eqn. 1) is comparable to the substituted benzenes. This suggests that other non-ionized solutes will exhibit a similar dependence of S on temperature. The limits of Table VI (derived for the benzoic acids in Table IV) are thus overly conservative when applied to non-ionic solutes.

Values of S (at 35°C) are seen to be similar for the two columns (A and B) of Table VIII, implying that values of S (and $\bar{B}$, D, etc.) determined for one column will be applicable to another column. This observation has important implications, which are considered further in the following paper [22].

pH mapping and the determination of values of K_a, k° and k^+

We have noted that the accurate prediction of retention as a function of pH

(based on the measurement of values of K_a, k° and $k^\pm$) requires care in the selection of three runs (including the reference run) with varying pH. We have found it difficult to make up mobile phases within better than ± 0.02 units of the desired pH, and other errors in the determination of values of k' are unavoidable. As a consequence, the application of eqns. 7a–c for the purposes of measuring values of K_a, k° and $k^\pm$ requires that the difference in pH values be fairly large; *i.e.*, a pH range of ≈ 1 unit or greater, corresponding to pH values of *e.g.*, 4, 4.5 and 5 in the three runs. The required range in pH values must be even greater, when the range selected does not bracket the pK_a values of the sample.

However, the use of differences in pH >0.5 units between adjacent runs can create other problems. Changes in band spacing and relative band areas as pH is varied are well documented, making peak tracking (required in all retention mapping procedures) more difficult. This problem becomes more serious, as the sample becomes more complex, and as the change in pH between runs is increased. Ideally, it would be preferable to use smaller differences in pH; *e.g.*, <0.3 units. Thus, some compromise between peak tracking and the accurate determination of K_a, k° and $k^\pm$ for each solute is necessary. We will address this issue elsewhere, in conjunction with a new approach to peak tracking which is underway in our laboratory [23].

CONCLUSIONS

A new procedure for developing and optimizing HPLC separations has been described, based on limited-range multi-parameter mapping. Any number of experimental parameters can be varied simultaneously, and only a few experimental runs are required for computer simulations of separation as a function of these experimental conditions. Only the primary effects of each experimental variable on separation are considered, but errors due to interaction effects are predictable. This allows the restriction of multi-parameter mapping to combinations of conditions that yield acceptable errors ($<\pm 2\%$) in predicted values of α. Errors in retention time will generally be larger ($<25\%$), but this will have little effect on predicted values of resolution (which is of primary importance in method development).

In the present study, we examined the effects of changing %B, temperature, pH and buffer concentration, for the separation of a 9-component substituted benzoic acid sample. In addition, more limited data for other samples from the literature were included. Based on the present study it appears that this approach can provide accurate predictions of separation (especially values of α and resolution) over a fairly wide range of conditions, while requiring only a small number of experimental runs. This, in turn, leads to a number of practical applications of the related software that we have developed (DryLab MP)— as described in the following paper.

SYMBOLS (PARTS I AND II)

Reference to equations in the papers in this series is identified by use of I- or II-, *e.g.*, eqn. I-1 refers to eqn. 1 in Part I.

A	constant in eqn. I-5;
A	weaker solvent in a mobile phase A/B

A_i, A_j	values of A (eqn. I-5) for solutes i and j
B	strong solvent in a mobile phase A/B
$\bar{B}$	coefficient measuring dependence of retention on temperature for a given solute (eqn. I-5)
$\bar{B}_i, \bar{B}_j$	values of $\bar{B}$ for solutes i and j
C, D	constants in eqn. I-8 for a given solute
D_1, D_2	values of D in eqn. I-8 for different mobile phase additives and a given solute
F	mobile phase flow-rate
F^-	fraction of an acidic compound which is ionized under the conditions of separation
F^+	fraction of a basic compound which is ionized under the conditions of separation
$F^\pm$	fraction of an acidic or basic compound which is ionized under the conditions of separation
$[H^+]$	concentration of hydrogen ion in the mobile phase
k'	solute capacity factor
k_i	value of k' for some change in the separation parameter i, other conditions remaining the same as for the reference run (eqn. I-1)
k_R	value of k' for reference conditions
k_w	value of k' for water as mobile phase (eqn. I-3)
k_{wi}, k_{wj}	values of k_w for solutes i and j
k°	value of k' for an acidic or basic solute in the non-ionized form
$k^\pm$	value of k' for an acidic or basic solute in the ionized form
K_a	acid dissociation constant; equal to 10^{-pK_a}
MP	multi-parameter
N	column plate number
N_0	value of N for large k'
R_s	resolution of two adjacent bands
S	solute parameter, equal to $-\mathrm{d}(\log k')/\mathrm{d}\varphi$
S_i, S_j	values of S for solutes i and j
t_R	solute retention time (min)
T	temperature (K)
W	bandwidth (eqn. II-2, min)
W_{ec}	contribution to W from extra-column effects and the dependence of N on k' (eqn. II-2, min)
W_0	bandwidth due to the column alone (eqn. II-1, min)
X	a mobile phase additive (buffer, ion-pair reagent, amine modifier, etc.)
$[X_1], [X_2], \ldots$	concentrations of different mobile phase additives 1, 2, ...
[X]	concentration of X in the mobile phase separation factor, equal to ratio of values of k' for two adjacent bands
δS	a change in S due to change in some other variable(s)
α	separation factor for two solutes
$\delta\alpha$	an error in a predicted value of α due to the neglect of interaction effects
$\delta\alpha_i$	a contribution to $\delta\alpha$ from a specific interaction effect (eqn. I-10)
$\Delta\bar{B}$	difference in $\bar{B}$ values for adjacent solute bands i and j; equal to $\bar{B}_i - \bar{B}_j$
ΔS	difference in S values for two adjacent solutes i and j; equal to $S_i - S_j$
φ	volume fraction of strong solvent B in mobile phase A/B, equal %B/100

REFERENCES

1 L. R. Snyder, J. L. Glajch and J. J. Kirkland, *Practical HPLC Method Development*, Wiley-Interscience, New York, 1988.
2 J W. Dolan and L. R. Snyder, *Troubleshooting LC Systems*, Humana Press, Clifton, NJ, 1989.
3 J. C. Berridge, *Techniques for the Automated Optimization of HPLC Separations*, Wiley, New York, 1985.
4 P. J. Schoenmakers, *Optimization of Chromatographic Selectivity*, Elsevier, Amsterdam, 1986.
5 J. L. Glajch and L. R. Snyder (Editors), *Computer-assisted Method Development for High-performance Liquid Chromatography*, Elsevier, Amsterdam, 1990.
6 W. R. Melander and Cs. Horváth, in Cs. Horváth (Editor), *High-performance Liquid Chromatography —Advances and Perspectives*, Vol. 2, Academic Press, New York, 1980, p. 114.
7 P. Jandera and J. Churacek, *Gradient Elution in Column Liquid Chromatography*, Elsevier, Amsterdam, 1985, p. 19.
8 L. R. Snyder and M. A. Quarry, *J. Liq. Chromatogr.*, 10 (1987) 1789.
9 J. Chmielowiec and H. Sawatzky, *J. Chromatogr. Sci.*, 17 (1979) 245.
10 N. Lammers, J. Zeeman and G. J. deJong, *J. High Resolut. Chromatogr. Chromatogr. Commun.*, 4 (1981) 444.
11 D. E. Henderson and D. J. O'Connor, *Adv. Chromatogr. (N.Y.)*, 23 (1985) Ch. 2.
12 Cs. Horváth, W. Melander and I. Molnar, *Anal. Chem.*, 49 (1977) 142.
13 J. L. M. van de Venne, J. L. H. M. Hendrikx and R. S. Deelder, *J. Chromatogr.*, 167 (1978) 1.
14 B. L. Karger, J. N. LePage and N. Tanaka, in Cs. Horváth (Editor), *High-performance Liquid Chromatography —Advances and Perspectives*, Vol. 1, Academic Press, New York, 1980, p. 113.
15 M. Otto and W. Wegscheider, *J. Chromatogr.*, 258 (1983) 11.
16 M. T. W. Hearn (Editor), *Ion-pair Chromatography*, Marcel Dekker, New York, 1985.
17 S. O. Jansson and S. Johansson, *J. Chromatogr.*, 242 (1982) 41.
18 A. Bartha, G. Vigh and J. Stahlberg, *J. Chromatogr.*, 506 (1990) 85.
19 J. L. Glajch, J. J. Kirkland, K. M. Squire and J. M. Minor, *J. Chromatogr.*, 199 (1980) 57.
20 J. R. Gant, J. W. Dolan and L. R. Snyder, *J. Chromatogr.*, 185 (1979) 153.
21 M. A. Quarry, R. L. Grob and L. R. Snyder, *J. Chromatogr.*, 285 (1984) 19.
22 L. R. Snyder, J. W. Dolan and D. C. Lommen, *J. Chromatogr.*, part II.
23 J. W. Dolan and L. R. Snyder, presented at *the 14th International Symposium on Column Liquid Chromatography, Boston, MA, May 20–25, 1990.*

Journal of Chromatography, 535 (1990) 75–92
Elsevier Science Publishers B.V., Amsterdam

CHROMSYMP. 2030

High-performance liquid chromatographic computer simulation based on a restricted multi-parameter approach

II. Applications

L. R. SNYDER*, J. W. DOLAN and D. C. LOMMEN
LC Resources Inc., 3182 C Old Tunnel Road, Lafayette, CA 94549 (U.S.A.)

ABSTRACT

A computer program (DryLab® MP) is described that allows restricted multi-parameter mapping for any number (or kind) of separation variables, based on only a few experiments. Multi-parameter computer simulation can be used to develop an high-performance liquid chromatographic method from the beginning, or it can be used to enhance a method developed by other means; *e.g.*, by trial-and-error, single-parameter mapping, etc. The software can also be used to evaluate (and improve) method ruggedness. Finally, various problems (column-to-column variability, change of retention with ambient temperature fluctuations, experimental errors, etc.) that are commonly encountered during routine operation can be handled in the same general way. Examples of these various applications are given.

INTRODUCTION

The preceding paper [1] describes a new approach for high-performance liquid chromatographic (HPLC) computer simulation: restricted multi-parameter mapping of separation and resolution. Software based on this procedure (DryLab MP, for use with an IBM-compatible personal computer) has been developed as an aid in (a) HPLC method development and (b) related problems that can arise in the routine use of a final method. For method development, two initial experimental runs are carried out in order to define a mobile phase composition (%B) that provides a satisfactory k' range for all sample components. Next, one or two additional separations are made for each variable that is to be varied or mapped (see Fig. 1 of Ref. 1). Finally it is possible to predict separation as a function of change in the different separation variables.

Alternatively, a method that has already been developed can be used as the starting point for similar computer simulations directed toward other goals: improvement of separation, determination (and improvement) of method ruggedness, anticipation and solution of various problems that can arise during routine use of the method. The present paper provides examples of these and other possibilities, based on restricted multi-parameter mapping.

0021-9673/90/$03.50

THEORY

Column plate number

In the preceding paper [1], the prediction of retention via multi-parameter mapping has been emphasized. However, the column plate number N also plays an important role in determining sample resolution. Previous examples of computer simulation have often assumed that N is constant for all bands in the chromatogram (for a specific set of separation conditions). Thus, a value of N obtained for any well-resolved band can be used for other bands as well. This is often not true in practice, however. The reason is that there is a general tendency for N to increase with k', and extra-column effects (which work in the same direction) are also often significant in a given HPLC system.

We have previously observed [2] (for capillary gas chromatographic separation) that this (total) increase in values of N with increasing retention can be described quantitatively in terms of a "pseudo" extra-column correction. A similar increase in N with k' was observed in the present study for the reversed-phase HPLC separation of a sample of substituted benzoic acids. Table I summarizes this effect for a given set of conditions. The approach in ref. 2 (for gas chromatography) is as follows. The "limiting" plate number N_0 for a large value of k' is defined, and this yields a corresponding bandwidth W_0 for all solutes in the chromatogram

$$W_0 = (4\, N_0^{-0.5})\, t_R \tag{1}$$

Here, t_R is the band retention time. The actual bandwidth W is then given as

$$W^2 = W_0^2 + W_{ec}^2 \tag{2}$$

TABLE I

VARIATION OF PLATE NUMBER N WITH SAMPLE RETENTION

Substituted benzoic acid sample (see Table IV in ref. 1 for band identification); pH = 2.9, 35% B, 30°C, 25 mM buffer.

Band	Plate number N		
	Experimental	Calculated[a]	Error (%)
A	11 100	9 630	−13
B	9 500	10 800	+13
C	15 000	15 600	+4
D	15 500	16 100	+4
E	17 000	16 900	0
F	17 400	18 100	+4
G	14 100	18 500	(+31)[b]
H	19 300	19 800	+3
I	23 000	20 200	−13
Average error			±6

[a] From Eqns. 1 and 2 with W_{ec} = 0.22 min, N_0 = 22 000.
[b] Out-of-line value, not included in average error.

where W_{ec} is a "pseudo extra-column" contribution to bandwidth that reflects both the dependence of N on k' and actual extra-column effects. DryLab MP requests bandwidths and retention times for an early and late band in the reference chromatogram, from which values of N_0 and W_{ec} are derived. The latter are then used to estimate N for any band as a function of its retention time.

The calculated plate numbers in Table I show an average error of only $\pm 6\%$, corresponding to a 3% error in resolution. This is negligible compared to the effect of expected errors in predicted values of α; see the discussion in ref. 1.

Change in temperature. If temperature is selected as one of the variables, the plate number N (therefore values of N_0 and W_{ec}) is expected to change somewhat. However, for changes in temperature less than 10–20°C, the effect on N is predicted to be minor. One study [3] has found little change in N with temperature for a typical reversed-phase system. The present program (DryLab MP) ignores any change in N with temperature.

Column variability

A common, potentially serious problem in routine HPLC analysis is a change in sample retention when a new column (from a different lot) is used. Several studies [6–8] have noted striking differences in retention for a given sample on different columns. It would be a great convenience, if these changes in column retention (and separation) could be easily corrected by an appropriate change in one or more separation conditions. This can be done using computer simulation, if the effects of each variable on the retention of different solutes remain approximately the same from column to column. This is equivalent to requiring that the chromatographic parameters S, $\bar{B}$, K_a, k°, $k^\pm$, and D (see the preceding paper [1]) be largely independent of the column.

There is some evidence that these latter chromatographic parameters tend to remain roughly the same from column to column. We will consider this question for each parameter.

Effect of %B: values of S. The origin of solute S values has been discussed by various workers. One hypothesis [9] is that these S values represent the ratio of molecular sizes of the solute (A_s) and strong solvent B (A_b): $S = A_s/A_b$[a]. If this is true, then the column would appear to be of little importance in determining values of S. This is confirmed by several reversed-phase HPLC studies in the literature, which are discussed below.

Thus, for the separation of various ribosomal proteins on four C_3 or C_4 columns (three different suppliers) , it was found [12] that retention varied considerably for these compounds, but values of S were quite similar. The average variation of S from column to column was only ± 3.6 units, for $31 < S < 66$. For an even larger change in column composition, another study [13] reported S values for several digitalis derivatives on a C_{18} *vs.* a cyano column. Values of S for the cyano column equalled $79 \pm 6\%$ of the value for the C_{18} column. In still another study [14] it was

[a] More accurately, S is believed to reflect the number of solvent molecules B displaced by a solute molecule upon retention in reversed-phase, ion-exchange or normal-phase [10] HPLC. Constancy in S (for different columns) would also be expected if the mobile phase (solution activity coefficients) dominates the separation [11].

found for C_1–C_{18}, cyano, phenyl and fluoroalkyl columns that relative values of S were also similar. Finally, the preceding paper [1] has reported S values for various alkyl phthalates on two different C_8 columns (Table VIII of ref. 1) and found approximately equal values for a given solute and each column.

It can be concluded on the basis of these findings that values of S should be similar for different columns, particularly those of the same type (*e.g.*, C_8 and C_{18}).

Effect of temperature: values of $\bar{B}$. Similar studies of values of $\bar{B}$ for various solutes on different columns have not been reported. However the factors that contribute to the enthalpy of retention (and $\bar{B}$) are expected to be the same for different reversed-phase columns of the same type. This should in turn lead to similar relative values of $\bar{B}$ for the same solute on different columns.

Effect of pH; values of K_a, k° *and* $k^\pm$. The value of K_a is a property of the solute and mobile phase, and should be the same for different columns. The ratio of values of $k^\circ/k^\pm$ tends to be similar for different systems, and in any case $k^\pm$ is usually small. On this basis, it can be argued that the effect of a change in pH should be similar for different columns of the same general type (*e.g.*, reversed phase).

EXPERIMENTAL

Equipment and materials

See the preceding paper [1].

Software

All computer simulations described in this paper (except where noted otherwise) were carried out with a prototype version of software that is still under development (DryLab MP, LC Resources).

RESULTS AND DISCUSSION

A nine-component sample of substituted benzoic acids (see Part I [1]) was used in most of the following examples. Two initial exploratory separations were carried out to define conditions for a reasonable k' range for the sample. These starting conditions ("reference" conditions) were: pH = 2.9, 40% methanol, 35°C, 25 mM acetate buffer. The resulting separation is shown in Fig. 1A and compared with the corresponding computer simulation (DryLab MP) in Fig. 1B[a]. The range of k' values is $1.3 < k' < 5.8$.

Restricted multi-parameter mapping requires one or two additional experimental runs for each variable to be studied. In the present case, pH, %B, temperature and buffer concentration were selected. The conditions for these additional five runs are given in Table II. The bandwidth data in Table I were also used in further computer simulations. The resulting retention times for each experimental run are summarized in Table IV of ref. 1.

---

[a] The chromatogram of Fig. 1B is based on the experimental run of Fig. 1A as input; therefore, the retention times in these two chromatograms should be (and are) exactly the same. The chromatogram of Fig. 1B does provide a test of the ability of DryLab MP to predict column plate number and bandwidth as a function of k', however.

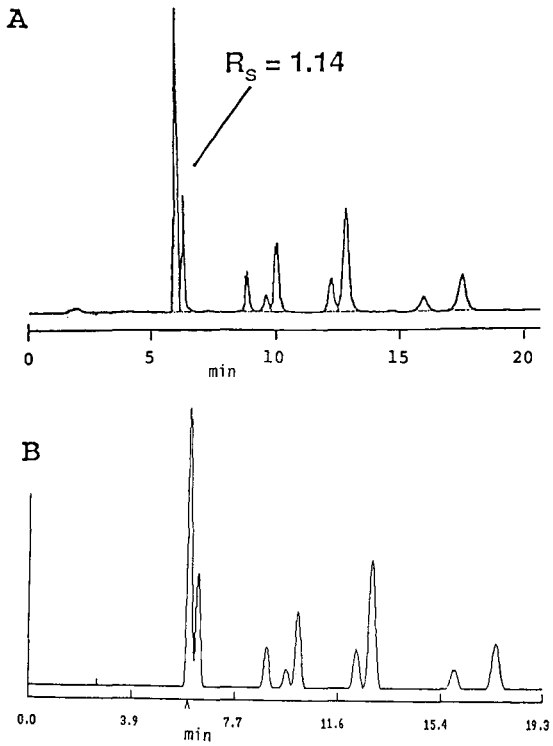

Fig. 1. Chromatograms for reference conditions in Table II. (A) Experimental; (B) computer simulation.

Method development

Beginning with the separation in Fig. 1 (the reference run), a good approach in multi-parameter mapping is to examine resolution maps for each variable (single-parameter mapping). Resolution maps for the four variables of Table II are shown in Fig. 2. The pH map in Fig. 2A exhibits a maximum resolution of 1.2 for a pH of 2.91, which is essentially the same resolution as is exhibited by the reference run (pH 2.90). Therefore, a change in pH does not appear useful as a means of improving resolution. The %B map (Fig. 2B) indicates that resolution can be improved significantly by lowering %B from 40% (reference run) to a value of about 36%; R_s = 1.8 *vs.* 1.2 for the reference run. Similar, but smaller, increases in resolution are possible by varying temperature (Fig. 2C) or buffer concentration (Fig. 2D). Our first choice is therefore to optimize solvent strength (%B).

The resolution map in Fig. 2B shows a flattening for mobile phases of < 38%B, meaning that further increase in resolution for lower %B values is more costly in terms of increase in run time (which increases as %B decreases). This suggests an optimum mobile phase composition of about 37%B[a]. With this initial choice of

[a] The choice of 37%B *vs.* 36 or 38%B is somewhat arbitrary, and is in any case not an important distinction.

TABLE II

EXPERIMENTAL SEPARATIONS CARRIED OUT PRIOR TO MULTI-PARAMETER MAPPING

Substituted benzoic acid sample; see Table IV in ref. 1 for retention times for each run.

Run	pH	%B	T (°C)	Buffer (mM)
Reference	2.9	40	35	25
Vary pH	2.6	40	35	25
	3.2	40	35	25
Vary %B	2.9	35	35	25
Vary T	2.9	40	30	25
Vary buffer	2.9	40	35	10

37%B (other reference conditions remaining the same), we can now examine the advantage of changes in other variables. Since a change in either temperature or buffer concentration seems equally likely, resolution maps are requested for each

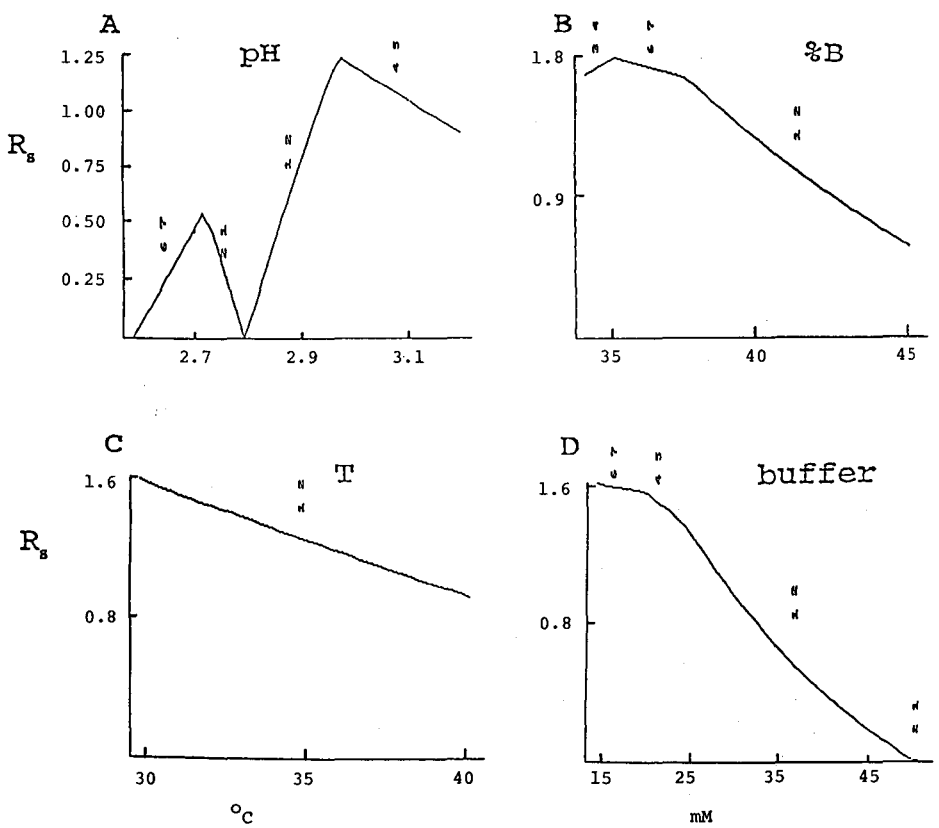

Fig. 2. Resolution maps for different variables (single-parameter changes beginning with reference conditions in Table I). (A) pH; (B) %B; (C) temperature (°C); (D) buffer concentration (mM).

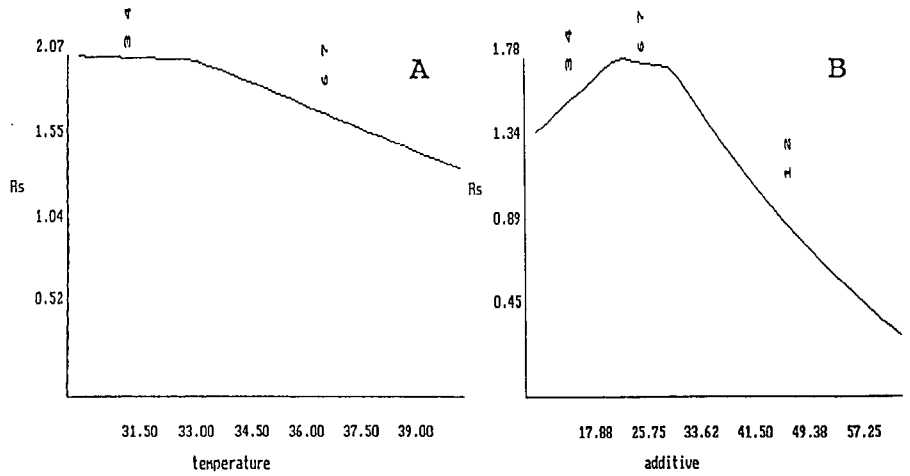

Fig. 3. Resolution maps for (A) temperature (°C) and (B) buffer concentration (m*M*) [single-parameter changes beginning with (A) 37% B, pH 2.90, 25 m*M* buffer or (B) 35°C, pH 2.90, 25 m*M*].

variable (37%B, other conditions as for the reference run). These maps are shown in Fig. 3.

Fig. 3B (buffer map) shows little advantage in varying buffer concentration; 25 m*M* (the reference value) is very close to the optimum value. A change in temperature (Fig. 3A), on the other hand, is clearly beneficial. A temperature of 32°C (*vs.* 35°C in the reference run) yields an increase in sample resolution to R_s = 2.06. The experimental and predicted chromatograms for these conditions (pH 2.9, 37% B, 32°C, 25 m*M*) are shown in Fig. 4A and B, respectively. There is close agreement between the two chromatograms in terms of both retention time (± 1.3 %) and resolution (± 5%), as summarized in Table III.

Further variation in conditions is possible, but resolution maps for pH and buffer concentration (for 37% B and 32°C) show no significant further improvement in resolution. Our final separation (Fig. 4A) is clearly much better than the starting in Fig. 1; resolution is almost doubled, with an increase in run time of only 20%. If desired, the run time can be reduced to the starting value (18 min) by an increase in flow-rate, as shown in the simulation of Fig. 4C (flow-rate = 1.3 ml/min, R_s = 1.91).

Developing an assay for selected bands. In many cases, the separation of the entire sample is not of interest; instead, the assay of only one or a few bands in the chromatogram is required. We will use the mixture of substituted benzenes (Table II of ref. 1) as an example, inasmuch as data have been reported [15] which allow us to map %B and temperature for this sample. Fig. 5 shows reconstructed chromatograms (from the data of ref. 6) for this sample[a] (25 × 0.46 cm I.D., 5-μm column, 1 ml/min) for reference conditions (Fig. 5A; 50% methanol, 30°C), and for runs where

[a] Anisole has been omitted from this sample for better illustration; the revised sample contains eight components.

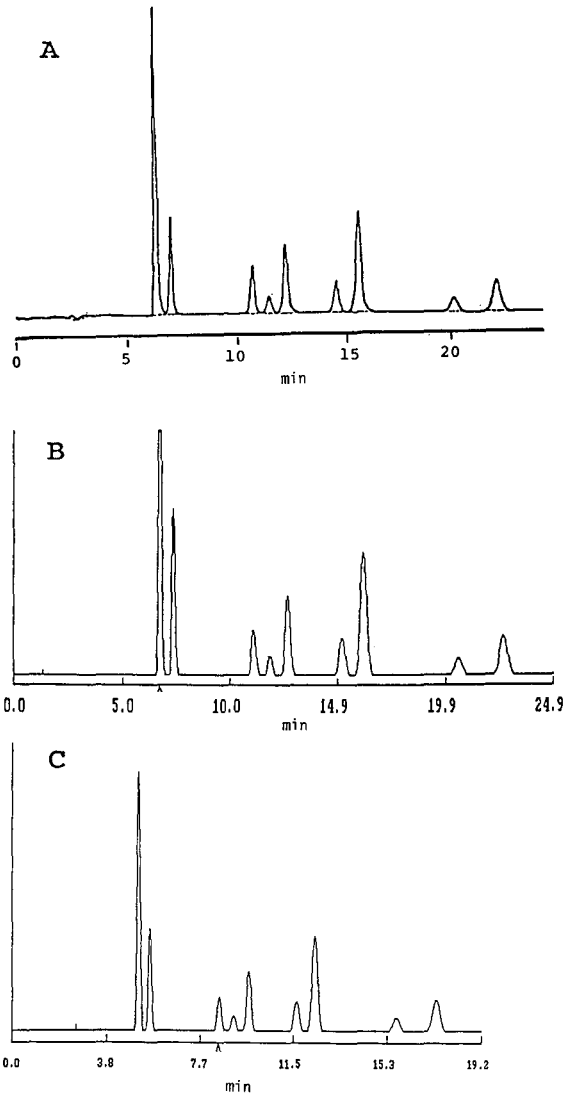

Fig. 4. Separation of substituted benzoic acids for optimized conditions; pH 2.90, 37% methanol, 32°C, 25 m*M* buffer. (A) Experimental chromatogram, 1 ml/min; (B) predicted chromatogram, 1 ml/min; (C) predicted chromatogram, 1.3 ml/min.

%B (Fig. 5B; 60% B, 30°C) and temperature (Fig. 5C; 50% B, 41°C) are varied. These data allow us to carry out multi-parameter mapping using DryLab MP.

The resolution maps for the entire sample (as a function of %B and T) are shown in Fig. 6A and B. These suggest marginal separation, although $R_s = 1.7$ is possible for a temperature of about 20°C). However, this involves a long run time, and temperature control will be a problem (resolution is seen to vary markedly with temperature, and most temperature controllers cannot be used near room temper-

TABLE III

COMPARISON OF EXPERIMENTAL *VS.* PREDICTED SEPARATION OF SUBSTITUTED BENZOIC ACIDS FOR OPTIMIZED CONDITIONS

pH 2.9, 37% methanol, 32°C, 25 m*M* buffer.

Band	Retention times (min)		Resolution R_s	
	Experimental	Calculated	Experimental	Calculated
A	6.4	6.6	2.4	2.1
B	7.1	7.2	11.3	11.3
C	10.8	10.9	2.1	2.0
D	11.6	11.7	2.0	2.1
E	12.3	12.5	6.5	6.0
F	14.7	15.1	2.0	2.1
G	15.8	16.0	8.6	8.2
H	20.3	20.4	3.3	3.5
I	22.3	22.5	3.3	3.5
Average error	±0.2 (1.3%)		±0.2 (5%)	

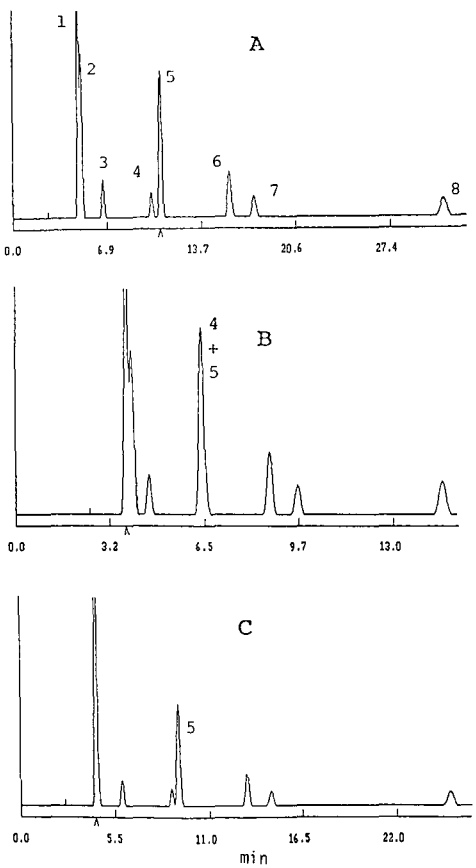

Fig. 5. Reconstructed chromatograms for the separation of the substituted-benzene sample in ref. 6 (anisole band excluded). (A) Reference run: 50% methanol, 30°C, 25 × 0.46 cm I.D., 5-μm C_8 column; (B) same as A, except 60% B; (C) same as A, except 41°C.

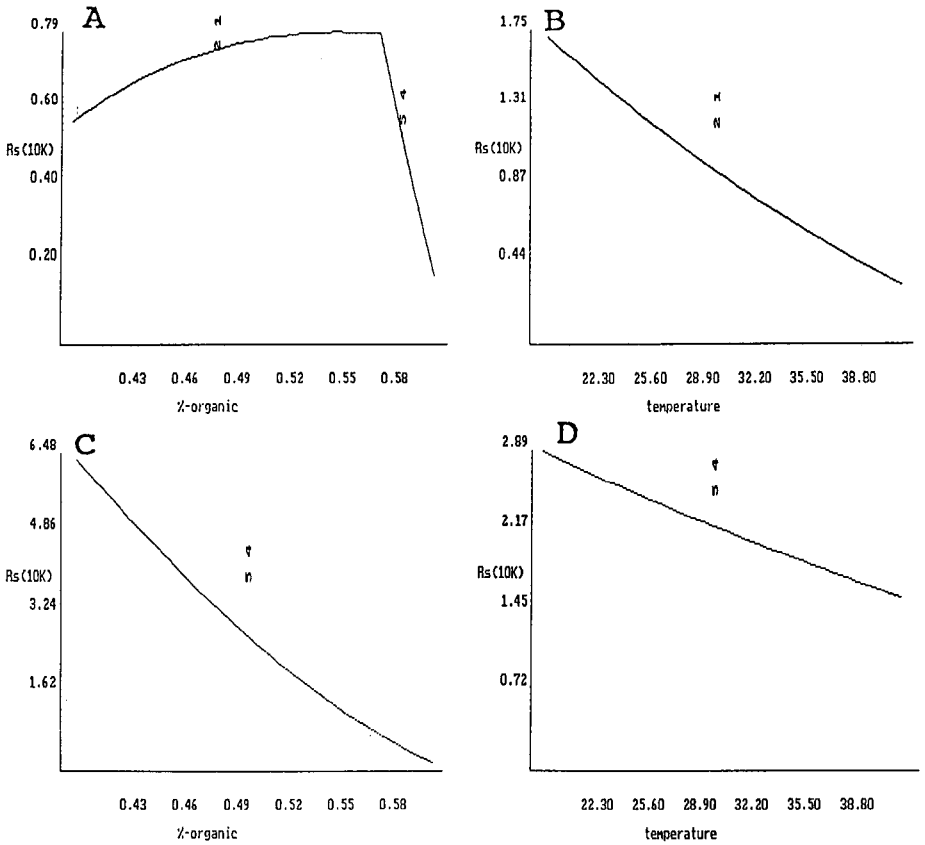

Fig. 6. Resolution maps for separations of Fig. 5. (A) Map for all bands, varying %B (T = 30°C); (B) map for all bands, varying T (50%B); (C) map for Band 5 only, varying %B (T = 30°C); (D) map for band 5 only, varying T (50% B). Temperature in °C.

ature). Let us assume, however, that only band 5 is of interest. In this case we can request *partial resolution maps* (*vs.* %B and T) for Band 5[a], ignoring the separation of other bands in the sample. Fig. 6C and D show the corresponding maps for this situation, which are more encouraging. For a temperature of 30°C, $R_s > 2$ for < 50%B. A mobile phase of 42% B provides a resolution of $R_s = 5.5$ with $k' = 22$ for the last band. This separation is shown in Fig. 7A. The run time is too long (60 min), but the excess resolution of band 5 ($R_s = 5.5$) can be traded for a shorter run time through the use of increased flow-rate and/or a shorter column. The predicted chromatogram (using computer simulation with DryLab I [4]) for a 5-cm column and 2 ml/min flow-rate is shown in Fig. 7B. The resulting run time is only 6 min, with a resolution of band 5 equal to 2.1.

[a] In a partial resolution map for Band (Fig. 6C, D), the resolution of the most poorly resolved band pair *which includes band 5* is plotted *vs.* the separation condition being varied.

Method ruggedness

Once a reasonable separation has been achieved (as in Fig. 4 or 7), the proposed method should be evaluated for ruggedness. That is, sample resolution should remain acceptable for likely variations in run conditions. Thus, a method that has been developed for ambient conditions should be able to tolerate variations in temperature of ± 5°C, since these are likely to be encountered in some laboratories. Similarly, errors in mobile phase composition of $\pm 2\%$ B are not unlikely, and a change in %B of this magnitude should not compromise the separation. Possible errors in mobile phase pH are often of most concern, for two reasons. First, separations which are pH-dependent often exhibit marked changes in resolution for rather small changes in pH. Second, the control of mobile phase pH in the average laboratory is unlikely to be much better than ± 0.05 unit, and occasional errors of ± 0.10 unit should be anticipated.

The "optimized" separation of the substituted benzoic acid sample (Fig. 4) will provide an example of the potential use of multi-parameter mapping for avoiding problems that can arise from a lack of method ruggedness. If computer simulation is used initially to develop an HPLC method (as in the present case), testing for method ruggedness can be carried out (using computer simulation) without the need for further experiments. Alternatively, for methods developed in some other way, it is

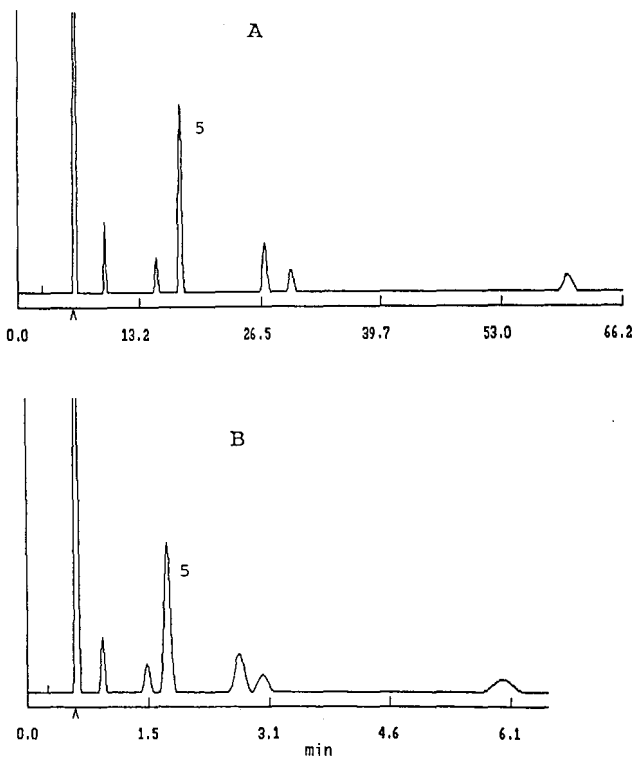

Fig. 7. Predicted separation of sample in Fig. 5 for optimized conditions (42% B, 30°C); other conditions as in Fig. 5. (A) 25-cm column, 1 ml/min (DryLab MP); (B) 5-cm column, 2 ml/min (DryLab I).

necessary to enter in run conditions and retention times for (a) the routine method and (b) additional runs where one experimental parameter is changed at a time.

In the present case, we will first evaluate the method of Fig. 4 (pH 2.9) for its sensitivity to inadvertent changes in pH; *e.g.*, ±0.1 unit. This is easily done by examining chromatograms for pH 2.8 and 3.0, as seen in Fig. 8 and summarized in Table IV. It is seen that an error in mobile phase pH of −0.10 unit (pH = 2.8) results in an unacceptable decrease in resolution (R_s = 1.16 *vs.* 2.05 expected). This result could have been anticipated from the resolution map in Fig. 2A, which shows a sharp drop in R_s for a decrease in pH below 2.9. The map in Fig. 2A also shows that the sensitivity of resolution to pH is less when pH > 2.9, suggesting that an increase in pH of the routine method might serve to diminish the sensitivity of R_s to a change in pH. This is confirmed by the data in Table IV for a target mobile-phase pH of 2.95 (designated by[b]). Now, a change of ±0.10 unit in pH does not reduce resolution below R_s = 1.66 (*vs.* 1.16 for pH 2.90).

We can further improve the latter method (pH 2.95, other conditions remaining the same as in Fig. 4) by noting that the critical band-pairs are 1/2 and 4/5. It is useful in cases such as this to request information on the response of these band pairs to a change in each of the separation variables: %B, T, pH and buffer concentration. Fig. 9 shows the resulting computer display.

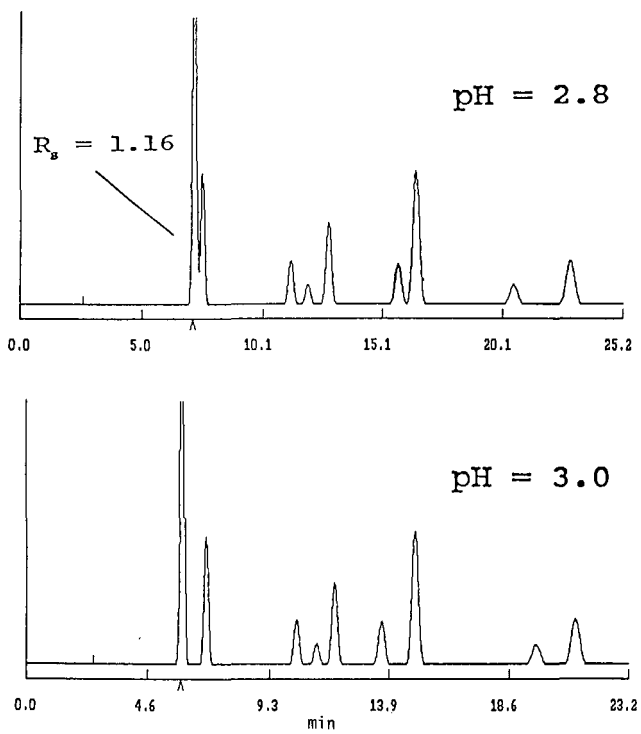

Fig. 8. Simulated chromatograms for the effect of a change in pH (by ±0.10 unit) on the "optimized" separation of Fig. 4.

TABLE IV

CHANGE OF SEPARATION WITH INADVERTENT CHANGE IN pH

"Optimized" separations of substituted benzoic acids.

Conditions	pH	Resolution	
		R_s	Bands[a]
37% B, 32°C, 25 m*M*	2.80	1.16	1/2
	2.90[b]	2.05	4/5
	3.00	1.89	4/5
Same	2.85	1.66	1/2
	2.95[b]	2.00	4/5
	3.05	1.77	4/5
36% B, 32°C, 25 m*M*[c]	2.85	1.84	3/4
	2.95[b]	1.99	3/4
	3.05	1.97	4/5

[a] Critical band pair.
[b] Optimized pH.
[c] Chromatograms in Fig. 10

What is desired is a change in one (or more) of these variables so as to improve the resolution of both critical band pairs (1/2, 4/5). Thus, it is seen that an increase in pH favors the separation of bands 1/2, but worsens the separation of bands 4/5. Likewise a change in temperature or buffer concentration has little effect on the separation of bands 4/5. A decrease in %B, on the other hand, leads to improved resolution for both band pairs. Thus the computer display in Fig. 9 suggests that the value of %B should be decreased.

Trial-and-error changes in %B were carried out by computer simulation, with examination of the effect of a ± 0.10 unit change in pH for each 1% decrease in %B. On this basis, it was found that 36% B gave a significant improvement in method ruggedness with regard to pH. These results are summarized in Table IV and Fig. 10. Now a change in pH of ± 0.10 unit has only a minor effect on separation: $1.84 < R_s < 1.99$. Note also that the resolution for the correct pH mobile phase ($R_s = 1.9$, pH 2.95) is little different from the original method (37% B, pH 2.90, $R_s = 2.06$), which was optimized for resolution alone (ruggedness ignored).

Computer simulations, such as those in Figs. 8-10 are able to both measure and improve method ruggedness for each experimental condition that can affect the separation. In some cases, it will not be possible to achieve really rugged separations for all experimental variables. Even in these cases, however, the sensitivity of the method to one or more conditions can be noted in the method procedure. That is, if the method is unduly sensitive to changes in %B, the user can be warned that greater care must be given to the formulation of the mobile phase; *e.g.*, a requirement for $\pm 1\%$ accuracy in %B.

Column variability

The problem of column variability was discussed in the Theory section. Once

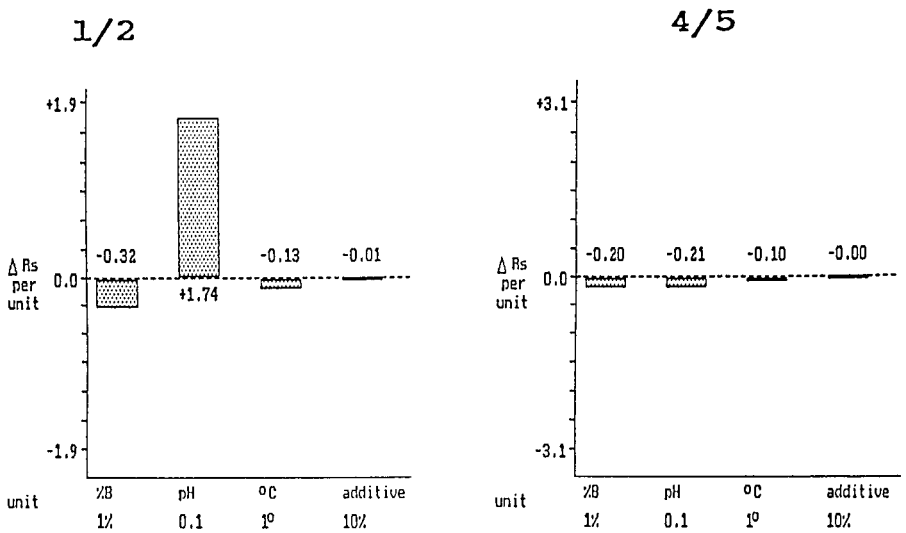

Fig. 9. DryLab MP screens, showing the effect of a change in different variables on the resolution of critical band pairs 1/2 and 4/5.

the effects of a change in different variables have been stored in DryLab MP (for the original column, as discussed above), it is possible to enter data for the separation of the same sample on a different column —presumably one that does not give the same relative retention or separation. The effect of a change in experimental conditions on the separation with the new column can then be predicted. Chromatograms or tabulated data can be used in this connection, but resolution charts as in Fig. 9 are particularly useful. Thus, if the separation in Fig. 4 or 10 were carried out on a new column, and bands 1/2 were found to merge ($R_s \approx 0$), Fig. 9 indicates that the most promising approach is to increase pH; an increase in pH of 0.1 unit should lead to an increase in the resolution of bands 1/2 by 1.74 units.

The use of computer simulation and data as in Fig. 9 in this way assumes that the dependence of sample retention on experimental conditions (values of S, B, etc.) is similar for different columns. This may not always be true, but this approach is a good way to start. Alternatively, any method can be modified for use on a new column by carrying out a few additional runs; *i.e.*, one or two runs for each experimental variable (multi-parameter mapping).

An example of correcting for differences between columns is provided by data from ref. 16, for the separation of a six-component steroid mixture on two different C_8 columns from the same supplier. In this case, it was found that the second column gave a poorer separation, as illustrated in the reconstructed chromatograms in Fig. 11. In the original paper, the mobile phase composition (%B) was modified by trial-and-error to improve the separation on the second column. We will illustrate how this same process can be facilitated with the use of computer simulation.

Fig. 11A shows the separation of this sample on the old column; bands 1/2 are the critical pair, with $R_s = 1.23$. Resolution is marginal, but this is the method that

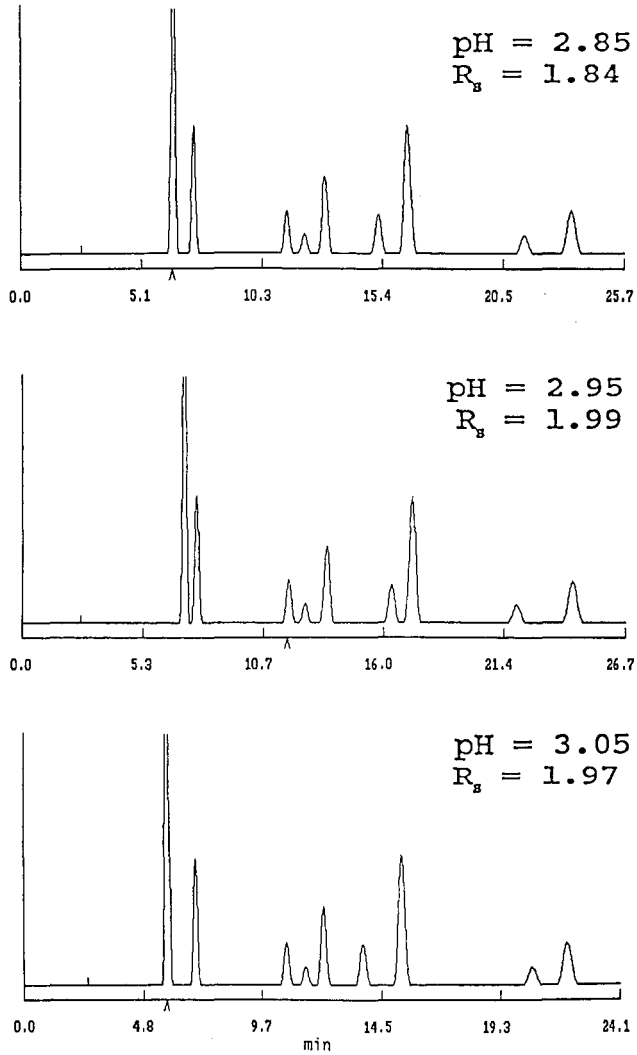

Fig. 10. Improvement in ruggedness in method of Fig. 4 (with respect to pH) for slightly different conditions: pH (intended) 2.95, 36% B, 32°C, 25 m*M* buffer.

was originally developed (49% methanol). Separation on the new column (Fig. 11B) is even worse, and the resolution of bands 4/5 (R_s = 0.89) is unacceptable for reliable quantitation. Retention times for the latter run were entered into DryLab MP, and separation was studied as a function of %B (using values of S for the old column). It was predicted that a resolution of R_s = 1.2 could be obtained for 54%B (Fig. 11C).

The actual separation on the new column with 54% methanol is shown in Fig. 11D, and it is seen to differ somewhat from that predicted in Fig. 11C, due to small differences in sample *S* values on the two columns. However, now the data for the runs of Fig. 11B and D can be entered into the computer for more accurate sim-

ulations of separation on the new column, and the separation of Fig. 11E (51% methanol) represents the highest resolution that can be achieved with the new column. R_s = 1.19; *i.e.*, close to the original value of R_s = 1.23 (bands 1/2) for Fig. 11A.

Troubleshooting HPLC Problems. Changes in separation may also be observed from day to day on the same column, possibly due to errors in mobile phase composition or flow-rate settings, changes in ambient temperature, loss in column efficiency, etc. These various possibilities can be quickly checked via computer simulation. For example, if all bands leave the column with shorter retention times, it might be logical to suspect a flow-rate error or pump malfunction. This can be easily verified via computer simulation, simply by examining separation *vs.* flow-rate. If the questionable chromatogram can be reproduced with a change in flow-rate, the origin of the separation problem is then confirmed.

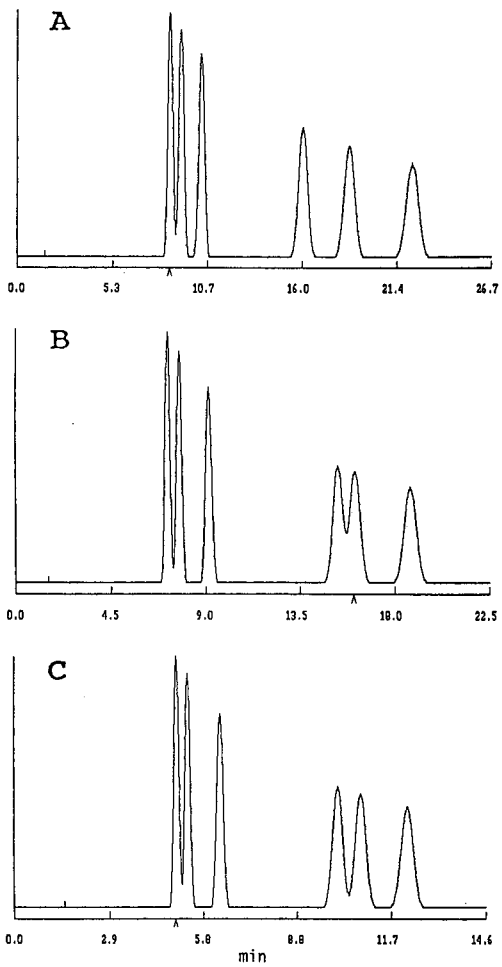

Fig. 11.

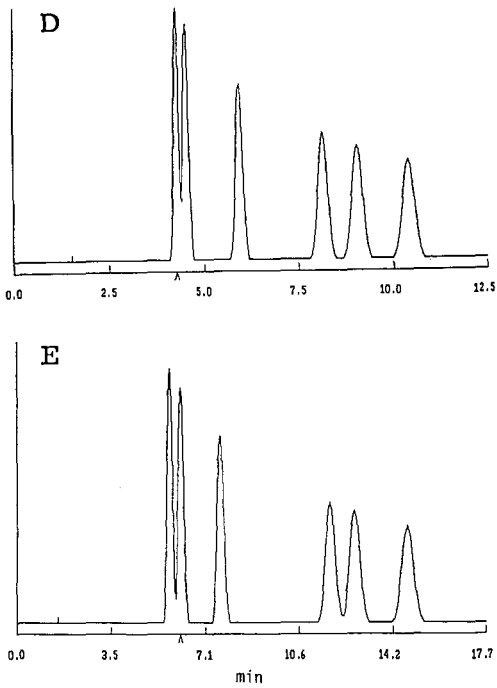

Fig. 11. Separation of six-component steroid sample in ref. 16. Conditions: 15 × 0.46 cm I.D., 5-μm Zorbax C_8 column, 1 ml/min. (A), original method and column [methanol-water (49:51)]; (B), same on new column; (C), simulated separation on new column with 54% B as mobile phase (using S values for old column); (D), actual separation on new column with 54% B; (E), separation on new column with 51% B.

A change in retention due to changes in ambient temperature can be checked in similar fashion by computer simulation, by trying different temperatures until a match with the faulty separation is achieved. Errors in the mobile phase composition (%B, pH, etc.) can be detected in the same way. This approach is especially helpful in the case of data that have already been collected, where there is no way of retrospectively checking for various errors of this kind.

CONCLUSIONS

Computer simulation based on restricted multi-parameter mapping represents a potentially powerful approach to HPLC method development and the improvement of existing methods. This procedure can also facilitate testing for method ruggedness and improving methods that are sensitive to small changes in experimental conditions. Finally, the same software can help deal with the problem of poor column-to-column reproducibility, as well as assist in the diagnosis of various errors or artifacts that cause poor separation. Only a few experimental runs (one or two per variable used in computer simulation) allow the use of computer simulation for all of these goals.

Examples that illustrate some of these capabilities are reported for several different samples: mixtures of substituted benzenes, substituted benzoic acids and steroids.

REFERENCES

1 J. W. Dolan, D. C. Lommen and L. R. Snyder, *J. Chromatogr.*, 535 (1990) in press.
2 D. E. Bautz, J. W. Dolan, W. D. Raddatz and L. R. Snyder, *Anal. Chem.*, 62 (1990) 1561.
3 F. V. Warren, Jr. and B. A. Bidlingmeyer, *Anal. Chem.*, 60 (1988) 2821.
4 L. R. Snyder, J. W. Dolan and D. C. Lommen, *J. Chromatogr.*, 485 (1989) 65.
5 J. W. Dolan, D. C. Lommen and L. R. Snyder, *J. Chromatogr.*, 485 (1989) 91.
6 A. P. Goldberg, *Anal. Chem.*, 54 (1982) 342.
7 L. R. Snyder, J. L. Glajch and J. J. Kirkland, *Practical HPLC Method Development*, Wiley-Interscience, 1988, Ch. 3.
8 L. C. Sander and S. A. Wise, *LC · GC*, 8 (1990) 378.
9 X. Geng and F. E. Regnier, *J. Chromatogr.*, 332 (1985) 147.
10 L. R. Snyder, *Principles of Adsorption Chromatography*, Marcel Dekker, New York, 1968, Ch. 8.
11 W. J. Cheong and P. W. Carr, *J. Chromatogr.*, 499 (1990) 373.
12 B. F. D. Ghrist, *Ph.D. Thesis*, University of Pennsylvania, Philadelphia, PA, 1988, Table 51.
13 B. Pekić, S. M. Petrović and B. Slavica, *J. Chromatogr.*, 268 (1983) 237.
14 P. E. Antle, A. P. Goldberg and L. R. Snyder, *J. Chromatogr.*, 3211 (985) 1.
15 J. R. Gant, J. W. Dolan and L. R. Snyder, *J. Chromatogr.*, 185 (1979) 153.
16 J. W. Dolan, L. R. Snyder and M. A. Quarry, *Am. Lab.*, August (1987) 43.

Journal of Chromatography, 535 (1990) 93–110
Elsevier Science Publishers B.V., Amsterdam

CHROMSYMP. 2042

Studies on system peaks in ion-pair adsorption chromatography

IV. Optimization of peak compression

T. FORNSTEDT and D. WESTERLUND*
Department of Analytical Pharmaceutical Chemistry, Biomedical Centre, Uppsala University, P.O. Box 574, S-751 23 Uppsala (Sweden)
and
A. SOKOLOWSKI
Pharmacia LKB Biotechnology, Chemical Production, 751 82 Uppsala (Sweden)

ABSTRACT

Optimization of a chromatographic system in order to obtain extremely narrow analyte peaks was investigated. The system consisted of silanized silica as a solid phase and an acidic eluent containing an UV-detectable hydrophobic amine (the probe). Large probe deficiency peaks (system peaks) were generated by injecting high concentrations of an organic anion together with the analyte. In the rear part of the large system peaks the probe concentration increased steeply. Strong peak compression effects were obtained when small amounts of cationic analytes were eluted together with this co-ion gradient. Variation of the probe concentration in the eluent was an efficient way of obtaining peak matching. Peak deformations developed at high analyte concentrations and/or when the analyte was eluted in other parts of the system peak. Guidelines for increasing the peak compression effect and to avoid the deformations are presented.

INTRODUCTION

Possibilities of obtaining narrow chromatographic peaks are of special interest owing to the accompanying improvement of the detection limit. In gradient elution this can be achieved by a continuous increase in the eluent component with the greatest eluting strength [1]. This gives a larger increase in the migration speed of the rear part of the analyte zone, resulting in narrower peaks than in corresponding isocratic runs.

In reversed-phase ion-pair adsorption chromatography, gradients of organic ionic components can be utilized in order to obtain extremely narrow peaks. This was achieved for cationic analytes by a stepwise increase in the eluent concentration of an organic co-ion (an ion with the same charge as the analyte) [2–4]. The drawback of the technique is the long re-equilibration times required. A technique offering extremely strong peak compression effects of cationic analytes with relatively short run times involves the utilization of large system peaks of an organic co-ion present in the eluent [5–7].

0021-9673/90/$03.50

System peaks, in which the eluent components have concentration deviations from the bulk, are generated by the injection of a sample deviating in composition from the eluent [8]. If the system is equilibrated with an organic cation in the eluent, large negative system peaks containing a deficiency of the eluent cation can be induced by the injection of high concentrations of a hydrophobic organic anion. Large peak compression effects were then obtained when the simultaneously injected cationic analyte was eluted together with the steeply increasing co-ion (cation) concentration in the rear part of the system peak [5–7]. When the analyte was eluted in other positions within the system peak, peak deformations were developed [5,9]. Deformations could also be developed when the analyte was eluted in the position normally giving peak compression [5], provided that high analyte concentrations were injected and/or that the simultaneously injected organic anion was eluted close to the analyte. Distorted peak performances, such as peak deformation or even peak splitting [9–15], have been reported in many instances when eluents including an ionic organic component were used. In most explanations for these effects, system peak interactions with the analytes were, however, not considered [11–16].

The peak compression and deformation effects and the parameters governing the retention volume of the co-ion gradient and the analyte have been investigated earlier [5,7,17]. Rough matching of gradient and analyte retention volumes, in order to achieve co-elution, was obtained by varying the co-ion eluent concentration [7]. Fine matching could be made by changing the anion concentration in the injected solution [5].

The aims of this optimization study were twofold: to increase the degree of the peak compression effect and to avoid the risk of peak deformation occurring when designing the system for peak compression. In addition, some aspects of the selectivity of the technique are discussed below.

EXPERIMENTAL

Apparatus, chromatographic technique and preparation of the eluent

These were as described previously [17,18].

Eluents with four different protriptyline (PT) concentrations were equilibrated with the solid phase Nucleosil C_{18}, 5 μm [7]. The ionic strength ($I = 0.05$) and pH (2.0) were kept constant. For all injections a 100-μl loop was used.

Chemicals

These were the same as used previously [7].

Detection technique

For eluents lacking the probe (PT), the analyte signal was measured at 235 nm. The organic anion was then registered with a Beckman 156 refractive index (RI) detector.

When the eluent contained the probe, the photodiode-array UV detector used allowed parallel signal recording of the analyte and the probe. For a sample including tricyclic amines, a compensating detection technique was utilized to register the analyte signal [5,7,17,18]. This technique could not be used at high probe concentrations owing to baseline interferences in the analyte signals due to incomplete

compensation. Under these conditions the sample only contained benzamides. The analyte signal was then registered at 350 nm, where the probe had no absorbance. The probe signal was measured at 323 nm at the two lowest probe concentrations, whereas longer wavelengths were chosen for higher probe concentrations [7], except in the experiments presented in Figs. 7 and 8b.

Separation terms

A zone is defined as a region in the column where the composition of the mobile phase deviates from the eluent. The injection zone or starting zone is then the initial part of the column in which the component to be separated will be located, before the migration along the column. A peak is the portion of the chromatogram which corresponds to the eluted and detected zone. An exception is the very large deficiency zones of the probe, which lacked a sharp region of minimum concentration. These zones were named "zones" also when they appeared on the chromatogram (see Fig. 1).

The analyte peak retention volume is measured at the peak maximum (Fig. 1). The peak width, w_b (ml), is measured as the distance between the inflection points of the two peak tangents and the baseline. The depth, ΔC, of the negative system zone or peak is measured as the distance between the baseline and the zone minimum, given in concentration units (M). The width of the probe gradient in the rear part of the zone, ΔV, is determined according to Fig. 1 and given in volume units (ml). The gradient steepness, obtained by taking the ratio $\Delta C/\Delta V$, is then given as molarity per millilitre (M/ml). The gradient retention volume, $V_{R,G}$, is measured at half the upslope of the probe gradient.

RESULTS AND DISCUSSION

Solid phases such as silanized silica have often been found to contain more than one kind of adsorption site [17–20]. A previous adsorption study of PT as the phosphate ion-pair to Nucleosil C_{18} indicated a two-site adsorption behaviour of the

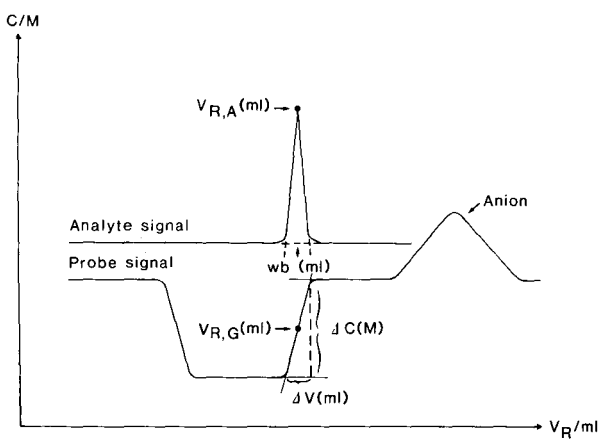

Fig. 1. Schematic presentation of the peak compression situation. The large probe system zone is induced by injection of an anion with a larger retention than the probe. The simultaneously injected analyte was eluted together with the probe gradient.

Langmuir type [17]. It was assumed that the adsorption isotherm is non-linear when more than 10% coverage of the adsorption capacity is reached [17–21]. In this series of studies, the primary variable was the eluent concentration of the probe, PT. The two highest probe concentrations corresponded to the non-linear part of the adsorption isotherm. At the highest probe concentration, the strong site was covered to the extent of 78%. The cationic analytes were substituted benzamides [17] and desipramine, imipramine and nortriptyline [19].

The retention equations used are based on the stoichiometric ion-pair adsorption model [7,8,17–20]. Eqn. 1 describes the net retention volume of a cationic analyte, HA^+, in the presence of an organic cationic eluent component, the co-ion Q^+; X^- is a buffer component. To simplify the equation, the expression for a homogeneous surface is used.

$$V_{N,HA} = \frac{W_s K_0 K_{HAX}[X^-]_m}{1 + K_{QX}[Q^+]_m[X^-]_m} \quad (1)$$

The total adsorption capacity of the solid phase is given by K_0, and K_{HAX} and K_{QX} are the adsorption constants. This equation assumes symmetrical peaks, whereas for high analyte concentrations no quantitative equation is yet available. Similar equations are valid for the net retention volumes of the organic anion injected and for the system peak [7,8,17–20].

At high sample concentrations there are interactions between all zones at the column inlet (the starting zones), and certainly also between unresolved zones during the migration along the column before the separation. When injecting cations and anions simultaneously, this will lead to retention changes in comparison with single-component injections, even though the components are well separated at the column outlet. In the retention equation discussed, these interactions are not taken into consideration.

Retention regulation

The retention regulation of the system has been described earlier [5,7,17]. In line with eqn. 1, the retention volume of the cationic analyte decreased with increasing PT (co-ion) concentration. If the cationic analyte was injected together with a large amount of organic anion, the analyte retention volume increased [5], an effect which was more pronounced when the analyte and the anion had similar retention volumes. The retention volume of the organic anion increased with increasing PT (counter ion) concentration.

As a consequense of the non-linear adsorption behaviour, the probe system peak retention volume decreased with increasing probe concentration. In order to obtain negative probe system peaks, the organic anion injected must have a larger retention volume than the probe; consequently, less hydrophobic anions could be used with higher probe concentrations [7] to achieve this.

Peak compression

Conditions necessary to obtain peak compression have been described earlier [5,7]. Large negative system peaks are generated by the injection of high concentrations

of alkylsulphonate or -sulphate with higher retention volumes than the probe. The probe concentration in such a probe zone is very low, whereas the rear part of the zone consists of a steeply increasing probe gradient (Fig. 1). An estimate of the degree of probe equilibrium disturbance is the ratio between the zone depth and the bulk concentration of the probe, $\Delta C/C_b$ [7]. This ratio is close to 1.0 at very large equilibrium disturbances. As described earlier, peak compression is achieved when the simultaneously injected cationic analyte is eluted together with the increasing co-ion gradient in the rear part of the zone (*cf.*, Fig. 1). The degree of the peak compression effect was measured as the decrease in peak width (w_b) compared with the isocratic experiment. Optimum matching of the analyte peak and co-ion gradient is obtained when they overlap perfectly, *i.e.*, when the ratio between analyte retention volume and gradient retention volume, $V_{R,A}/V_{R,G}$, is 1.00 (*cf.*, Fig. 1).

Anion effects in eluent without probe

In a previous study, it was found that the simultaneously injected anion had significant effects on the analyte retention volume even when it was well separated from the analyte on elution [5]. It was also observed that the peak compression effect was disturbed when the anion was eluted to close to the analyte. In this instance the cationic probe was present in the eluent. To determine the importance of the anion itself on the analyte retention volume and peak shape without any effect of the probe, an investigation was made with eluents lacking the probe.

Three cationic analytes were injected together with 5.0 m*M* decanesulphonate (Fig. 2a). The anion, detected by an RI detector, was eluted with a much longer

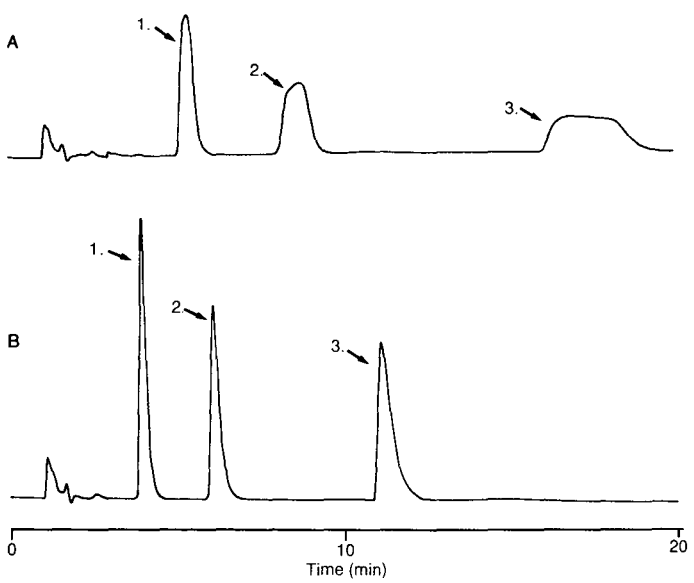

Fig. 2. Effects on analytes when injected simultaneously with a large amount of anion in a system lacking probe in the eluent. (A) Sample, $1.0 \cdot 10^{-5}$ *M* analytes and 5.0 m*M* decanesulphonate in eluent; eluent, phosphate buffer (pH 2.0)–acetonitrile (3:1). (B) As A, but without decanesulphonate in the sample. Analytes: 1 = FLA 731; 2 = FLA 913; 3 = FLA 797.

retention time than the analytes, in this instance about 25 min. The eluted analyte peaks were greatly deformed and the retention times and peak widths were significantly larger than in the isocratic experiment (*i.e.*, injection without organic anions in the sample); see Fig. 2b. The degree of deformation seems to be larger the closer the analyte peaks were eluted to the anion. However, even the weakly retarded analyte FLA 731, which had a five times lower retention time than the anion, was seriously affected. Its retention time increased from 4.0 to 5.4 min and its peak width from 0.40 to 0.72 min, compared with the isocratic experiment.

The effect on the amine analyte retention times of injected organic anions can be explained as ion-pairing effects in the starting zones and also in co-migrating zones in the column. In reversed-phase ion-pair chromatography, similar effects were utilized to determine if a solute is negatively or positively charged [22,23]. One or several injections of extremely high counter ion or co-ion concentrations were then made just before the sample injection. Solute–solute interactions discussed in the literature usually describe the situation in preparative chromatography, when the eluted components more or less overlap with each other [24,25].

Anion effects in eluent with probe

The analyte was injected together with the anion at different probe concentrations in the eluent. The analyte eluted just after the probe gradient induced by the anion, but before the anion (Table I). $\Delta V_{R,A}$ is the difference in the analyte retention volumes between the injections with and without anions. At low probe concentrations, the increases in analyte retention volume and peak width were significant. The effects decreased with increasing probe concentration and were negligible at the highest probe concentration. The increased probe concentration was accompanied by an improved anion separation from the analyte. At the highest probe concentration, a less hydrophobic anion was injected, as otherwise the retention volume of the anion would be unsuitably large [7].

TABLE I

INFLUENCE ON ANALYTE RETENTION AND PEAK WIDTH OF THE SIMULTANEOUSLY INJECTED ORGANIC ANION AT DIFFERENT PROBE ELUENT CONCENTRATIONS

The analyte was eluted between the system peak and the anion peak. Sample: $1.0 \cdot 10^{-5}$ *M* analyte with or without 5.0 m*M* anion in phosphate buffer (pH 2.0). Eluent: protriptyline (PT) in phosphate buffer (pH 2.0)–acetonitrile (3:1). $\Delta V_{R,A}$ = Analyte retention volume difference: injection with anion minus the isocratic experiment (without anion). $w_b/w_{b,iso}$ = Relative analyte peak width: injection with anion relative to the isocratic experiment.

PT (*M*)	Analyte and anion	$\Delta V_{R,A}$ (ml)	$\frac{w_b}{w_{b,iso}}$	$\frac{V_{R,anion}}{V_{R,analyte}}$
$7.6 \cdot 10^{-6}$	Imipramine and decanesulphonate	4.5	1.6	1.1
$3.8 \cdot 10^{-5}$	As above	3.5	1.4	1.3
$1.9 \cdot 10^{-4}$	As above	1.6	1.2	2.3
$9.5 \cdot 10^{-4}$	FLA 659 and octanesulphonate	0.0	1.0	2.1

The results show that the effects on the analyte caused by the anion in the starting and migrating zones were efficiently counteracted by the increased probe concentration. The reason is mainly increased competition due to the probe, especially the competition between the probe and the analyte for the organic anion. The interactions were also decreased by an increasing anion separation from the analyte.

Influence on analyte retention in the gradient

Peak compressions were obtained when the analyte was eluted together with the rear part of the negative system zone. The retention volume of the analyte was then greater than that in the isocratic experiment, owing to the low probe (co-ion) concentration in the negative zone. In addition, the initial ion-pair distribution with the organic anion will increase the retention volume.

The contributions from the two effects were determined qualitatively at different probe concentrations (Table II). $\Delta V_{R,A}$ is the analyte retention volume of the compressed analyte peak minus the value in the isocratic experiment. $\Delta V^*_{R,A}$ is the difference in isocratic analyte retention volumes in eluents lacking and containing the probe, respectively. The latter value is an estimate of the largest increase in analyte retention volume that could possibly be achieved owing to migration in a minimum probe concentration in the system zone. This value was only 0.4 ml at the lowest probe concentration, whereas the increase in the analyte retention volume under the peak compression conditions was 3.9 ml. This indicated a very large contribution from the hydrophobic anion, decanesulphonate. With increasing probe concentration, the influence of the low probe concentration in the system zone on the analyte retention volume increased. On the other hand, the contribution from the anion to the analyte retention volume decreased with increasing probe concentration (*cf.*, Table I). In the peak compression situation it may therefore be assumed that the contribution from the anion was very low at the probe concentrations corresponding to the non-linear part of the adsorption isotherm. The largest increase in retention volume (Table II) was

TABLE II

INFLUENCE OF DIFFERENT PROBE CONCENTRATIONS ON THE RETENTION OF COMPRESSED ANALYTES

Sample: $1.0 \cdot 10^{-5}$ *M* analyte with or without 5.0 m*M* anion in phosphate buffer (pH 2.0). Eluent: phosphate buffer (pH 2.0)–acetonitrile (3:1) with or without protriptyline (PT). $\Delta V_{R,A}$ = Compressed analyte retention volume minus isocratic retention volume (eluent containing probe). $\Delta V^*_{R,A}$ = Isocratic analyte retention volume in eluent lacking probe minus isocratic retention volume in eluent containing probe.

PT (*M*)	Analyte and anion	$\Delta V_{R,A}$ (ml)	$\Delta V^*_{R,A}$ (ml)	$\frac{V_{R,anion}}{V_{R,analyte}}$
$7.6 \cdot 10^{-6}$	Desipramine and decanesulphonate	3.9	0.4	1.2
$3.8 \cdot 10^{-5}$	Desipramine and nonylsulphate	4.6	1.6	1.5
$1.9 \cdot 10^{-4}$	FLA 659 and decanesulphonate	2.2	4.8	2.6
$9.5 \cdot 10^{-4}$	FLA 870 and octanesulphonate	2.3	5.9	2.5

obtained at a probe concentration of $3.8 \cdot 10^{-5}$ M (strong site covered to 12%). This is probably due to a combination of a considerable contribution from the anion injected together with the effect due to the low probe concentration in the system zone. At the two highest probe concentrations the $\Delta C/C_b$ values were 0.7, indicating that the analyte retention volume could be further increased by an additional lowering of the probe concentration in the gradient.

This is in line with previous results which indicated that the ion-pair distribution with the anion substantially influenced the retention volume of the gradient at low probe concentrations [7]. It is obvious that eqn. 1 is not qualitatively valid when the cationic analyte is eluted together with the gradient at low probe concentrations in the eluent. According to the significant initial ion-pair distribution with the organic anion, the equation may be modified to the expression below for a qualitative description. In this equation, the competing effect from the probe is assumed to be negligible.

$$V_{N,HA} \approx W_s K_0 (K_{HAX}[X^-]_m + K_{HAZ}[Z^-]_m) \quad (2)$$

where X^- is a buffer component in the eluent and Z^- is the simultaneously injected organic anion. It is important to note that the term corresponding to the organic anion is only significant in the injection zone and during migration of unresolved analyte and anion zones. Further, the concentrations of both X^- and Z^- will vary during the migration of the analyte zone together with the anion and system zones. The equation can therefore, only be used to indicate the different parameters that are of importance for the analyte retention. At increasing probe eluent concentrations, the retention gradually becomes governed by the unmodified eqn. 1.

Matching

In order to obtain the conditions such that the analyte and the gradient are eluted together, an appropriate choice of the eluent amine is necessary. Rough matching of the analyte and gradient retention volumes can then be made by a careful variation of the probe concentration [7]. If the analyte is eluted close to the gradient, fine matching can be performed by changing the concentration of the anion, injected together with the analyte [5]. An alternative for fine matching is to change the nature of the injected anion, as demonstrated below.

Fine matching. As illustrated above, both the analyte retention volume and the gradient retention volume are influenced by the ion-pair distribution with the organic anion at low probe concentrations in the eluent [7]. The analyte desipramine was injected together with anions of different hydrophobicities at a low probe concentration in the eluent, *i.e.*, $3.8 \cdot 10^{-5}$ *M*. When the analyte was injected with decanesulphonate, a small part of the analyte front was eluted before the gradient (see Fig. 3). Changing the anion to nonylsulphate resulted in both increased gradient and analyte retention volumes. However, the increase in analyte retention volume was larger, resulting in an improved matching and therefore a narrower analyte peak. The analyte peak width decreased from 0.55 to 0.45 ml. When the even more hydrophobic anion decylsulphate was used, the gradient retention volume increased more than the analyte retention volume and the peak compression effect was lost, resulting in an increased peak width, *i.e.*, 0.85 ml. In this instance, the lower peak compression effect was also due to a lower gradient steepness (see below).

At high probe concentrations, both analyte and gradient retention volumes were determined by the non-linear adsorption behaviour of the probe [7]. When the depth of the system peak or zone was constant despite increasing concentrations of the anion injected, the matching giving peak compression could be maintained when the anion concentration was increased up to fivefold (*cf.*, Fig. 10b and c). In addition, at higher probe concentrations it was possible to compress analytes with more varying isocratic retention volumes compared with the case with low probe concentrations.

The results indicate that fine matching is important at both low and high probe concentrations. However, at high probe concentrations the analyte peak is more easily captured in the gradient. This effect can be described in the light of eqn. 1 by the term in the denominator containing the probe concentration. When the analyte zone migrates within the low co-ion concentration in the system zone, it will have a lower migration speed than the system zone. When the analyte zone reaches the high co-ion concentration in the rear part of the system zone (the gradient), the rapidly increasing competition for adsorption sites results in a faster migration speed of the analyte zone. The analyte is caught in the gradient and a compressed peak results.

Dependence of gradient steepness on peak compression

The gradient steepness, $\Delta C/\Delta V$, an important parameter for peak compression, is dependent on both zone depth and gradient width (*cf.*, Fig. 1). Maximum steepness at a certain probe concentration is achieved when the probe concentration in the negative system zone approaches zero, *i.e.*, $\Delta C/C_b = 1.0$ [5]. The rear gradient steepnesses of the system zone or peak, obtained by the injection of 5.0 m*M* decanesulphonate at different probe concentrations, are shown in Table III. With increasing probe concentration, the depth of the system zone or peak increased and the gradient width decreased, resulting in a larger gradient steepness. The magnitude of the equilibrium disturbances decreased with increasing probe concentration [7], indicating possibilities of increasing the gradient steepness further. The narrower gradient width at higher probe concentrations is a result of the non-linear adsorption behaviour [26].

When decylsulphate was used instead of decanesulphonate at the lowest probe concentration in Table III, the gradient width was larger, which resulted in a lower gradient steepness (*cf.*, Fig. 3).

Peak compression effects obtained at different probe eluent concentrations are illustrated in Fig. 4. The compressed analyte peak width and the corresponding gradient width are plotted *versus* the probe concentration in the eluent. The analyte

TABLE III

DEPENDENCE OF GRADIENT STEEPNESS ON PROBE ELUENT CONCENTRATION

Sample: 5.0 m*M* decanesulphonate in phosphate buffer (pH 2.0). Eluent: Protriptyline (PT) in phosphate buffer (pH 2.0)–acetonitrile (3:1).

Bulk concentration of PT (*M*)	Depth, ΔC (*M*)	Gradient width, ΔV (ml)	Gradient steepness, $\Delta C/\Delta V$ (*M*/ml)
$3.8 \cdot 10^{-5}$	$3.8 \cdot 10^{-5}$	0.35	$1.1 \cdot 10^{-4}$
$1.9 \cdot 10^{-4}$	$1.3 \cdot 10^{-4}$	0.16	$8.1 \cdot 10^{-4}$
$9.5 \cdot 10^{-4}$	$3.5 \cdot 10^{-4}$	0.13	$2.7 \cdot 10^{-3}$

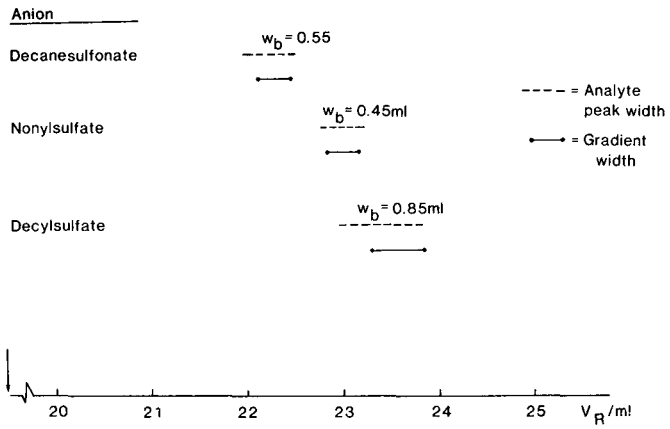

Fig. 3. Fine matching of analyte and gradient retention volumes. The character of the simultaneously injected anion was changed. Sample, $1.0 \cdot 10^{-5}$ *M* desipramine and 5.0 m*M* anion in phosphate buffer (pH 2.0); eluent, $3.8 \cdot 10^{-5}$ *M* protriptyline in phosphate buffer (pH 2.0)–acetonitrile (3:1).

peaks were more strongly compressed at higher probe concentrations (larger gradient steepness). At the two highest probe concentrations the peak heights increased several times and the peak widths decreased 4–5-fold (compared with the isocratic experiments).

In each peak compression situation in Fig. 4 the degree of matching was optimum according to the definition $V_{R,A}/V_{R,G} = 1.00$. However, perfect overlapping

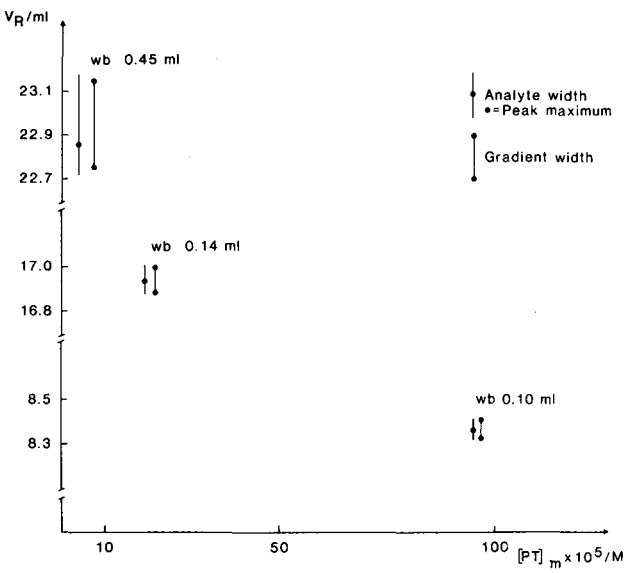

Fig. 4. Dependence of peak compression on probe eluent concentration. Sample, $1.0 \cdot 10^{-5}$ *M* analyte and 5.0 m*M* anion in phosphate buffer (pH 2.0); eluent, protriptyline in phosphate buffer (pH 2.0)–acetonitrile (3:1). The analyte–anion pair used at the respective PT concentration are given in Table II.

of compressed analyte peak widths with the respective gradient widths were obtained only at the two highest probe concentrations. This indicates that the gradient width is a key parameter in order to obtain efficient peak compression effects. The gradient width is expected to decrease with increasing column efficiency [27], which is probably another important parameter for optimum peak compressions, which, however, has not yet been studied systematically.

Analyte peak deformations in the gradient

When the analyte peak was eluted together with the front part of the negative system peak, an analyte peak deformation developed [5]. The analyte peak then eluted in a decreasing probe gradient, resulting in broadening of the peak (*cf.*, Fig. 11). However, if the analyte is eluted closer to the rear gradient, this will result in an improved peak shape. When the analyte is eluted very close to the rear gradient, peak deformation seems to be avoided. An example is shown in Fig. 5, where the shape and width of the eluted analyte peak are comparable to those in the isocratic experiment.

Even with analytes in the position normally giving peak compression, deformations may appear, *e.g.*, when the co-injected anion was eluted too close after the gradient and/or when high analyte concentrations were injected [5]. The conditions responsible for peak deformation in this position were investigated carefully, in order to find guidelines for avoiding their appearance in the design of separations where peak compression is desired.

Deformation at low analyte concentration. In Table I it was demonstrated that the tendency for the anion to affect the analyte peak shape, *i.e.*, increase in peak width, decreased with increasing probe concentration. When the analyte was eluted together with the gradient, the tendency of the anion to increase the analyte peak width was further counteracted by the compression effect. At the lowest probe concentration at which peak compression was demonstrated in Fig. 4, *i.e.*, $3.8 \cdot 10^{-5}$ *M*, the retention volume of the compressed peak was largely affected by the ion-pair distribution with the anion (*cf.*, Table II). Despite this, the peak shape seemed to be unaffected and an adequate peak compression effect was obtained. The ratio between the anion and the

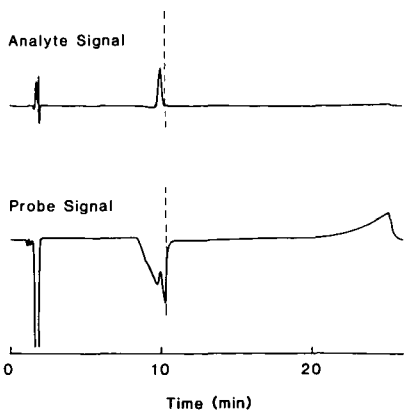

Fig. 5. Effects on the analyte peak shape when it was eluted together with the front part but very close to the rear part gradient of the system peak. Sample, $1.0 \cdot 10^{-5}$ *M* FLA 870 and 3.0 m*M* octanesulphonate in phosphate buffer (pH 2.0); eluent, $9.1 \cdot 10^{-4}$ *M* protriptyline in phosphate buffer (pH 2.0)–acetonitrile (3:1).

analyte retention volumes was 1.5. When the probe concentration was further decreased, giving the above ratio of 1.2, the analyte peak showed significant tailing caused by the closely eluting anion (see Fig. 6). At this low probe concentration, where the peak compression effect was also low, the analyte peak deformations due to the more retained anion (cf., Fig. 2a) will be more pronounced.

The anion front is often broad and deformed owing to its initial migration together with the gradient [7]. At increasing probe concentration, the tendency of the gradient to deform the later eluted anion peak increased and ultimately resulted in a deformed gradient. When the analyte peak was eluted in such a deformed probe gradient, a tailed and deformed analyte peak resulted instead of a compressed one (Fig. 7). In this instance, the analyte signal was registered at 343 instead of 350 nm (see Experimental). Therefore, the disturbance of the analyte signal due to the high probe absorbance was pronounced and contributed to the deformed shape of the analyte peak.

In conclusion, it is essential to have an adequate selectivity between the large anion peak and the gradient, irrespective of whether the probe eluent concentration is low or high.

Deformation at high analyte concentration. When the analyte concentration was increased tenfold, *i.e.*, from $1.0 \cdot 10^{-5}$ to $1.0 \cdot 10^{-4}$ *M*, the peak compression effect disappeared and instead analyte peak deformation and splitting developed [5]. This deformation occurred when the analyte was still eluted in the probe gradient, which was expected to result in peak compression. The probe signal was also deformed at the corresponding retention volume (the gradient). Fig. 8a shows that this kind of deformation arose when $1.0 \cdot 10^{-4}$ *M* of the analyte was injected and the probe concentration was $3.8 \cdot 10^{-5}$ *M*. When the probe concentration was increased fivefold, the analyte peak was compressed and the degree of deformation of both the analyte peak and the gradient was less significant (Fig. 8b). When the analyte concentration

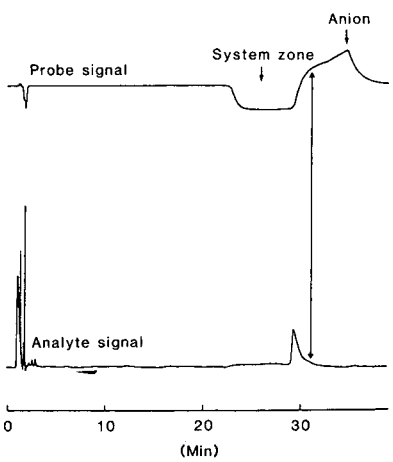

Fig. 6. Tailing effects on the compressed analyte peak by the closely eluted anion. Sample, $1.0 \cdot 10^{-5}$ *M* desipramine and 5.0 m*M* decanesulphonate in phosphate buffer (pH 2.0); eluent, $7.6 \cdot 10^{-6}$ *M* protriptyline in phosphate buffer (pH 2.0)–acetonitrile (3:1).

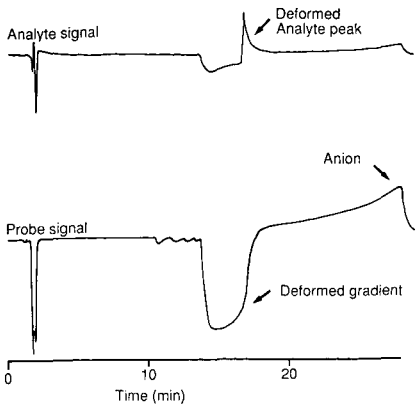

Fig. 7. Effects on the analyte peak when eluted in a deformed gradient. Sample, $1.0 \cdot 10^{-5}$ *M* FLA 965 and 5.0 m*M* nonanesulphonate in phosphate buffer (pH 2.0); eluent, $1.9 \cdot 10^{-4}$ *M* protriptyline in phosphate buffer (pH 2.0)–acetonitrile (3:1). An unsatisfactory compensation of the analyte signal can be seen.

was increased further, using the same high probe concentration, a deformed peak again developed.

Similar effects arose also in eluents without the probe. The analytes injected in the run shown in Fig. 2a were injected at a tenfold higher concentration, *i.e.*, $1.0 \cdot 10^{-4}$ *M*, together with 5.0 m*M* decanesulphonate into a system where the eluent consisted of only a buffer–acetonitrile mixture (Fig. 9). The anion retention time was 25.5 min. The analyte peaks were extremely broad and deformed, despite the relative large separation from the anion. The greater deformation compared with the experiment where lower

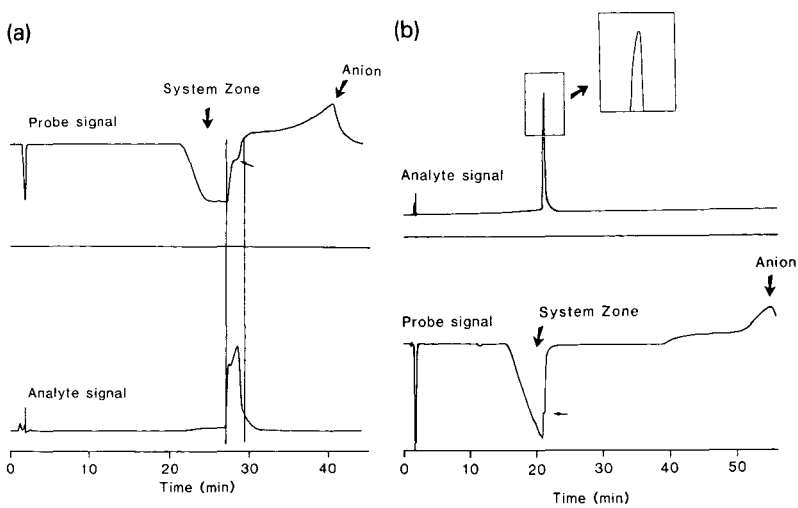

Fig. 8. Deformations when high analyte concentrations were eluted together with the gradient. Sample, $1.0 \cdot 10^{-4}$ *M* analyte and 5.0 m*M* decanesulphonate in phosphate buffer (pH 2.0); eluent, protriptyline in phosphate buffer (pH 2.0)–acetonitrile (3:1). (a) $C_{PT} = 3.8 \cdot 10^{-5}$ *M*, analyte desipramine; (b) $C_{PT} = 1.9 \cdot 10^{-4}$ *M*, analyte FLA 659.

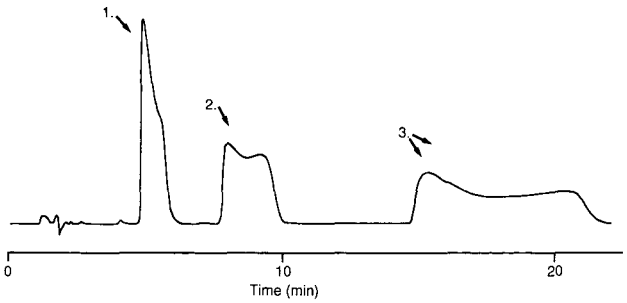

Fig. 9. Anion effects at high analyte concentrations with eluent lacking probe. Sample and eluent as in Fig. 2a except that the concentrations of the analytes were $1.0 \cdot 10^{-4}$ *M*.

analyte concentrations were injected (*cf.*, Fig. 2a) was due to an increased interaction between the starting and unresolved analyte and anion zones. On the other hand, even when peak compression was induced by means other than the injection of an organic anion, deformation developed at higher analyte concentrations injected [28].

The principal factors which cause peak deformation when high analyte concentrations are eluted in the gradient are of at least two types: more extensive analyte–anion interactions and a lower ability of the probe to displace the analyte. The contributions from both of these factors are counteracted by increasing the eluent probe concentration. It should be noted that the contribution from the anion on deformation of both low and high analyte concentrations was not properly taken into consideration in a previous paper [5].

Aspects of selectivity

Several analytes, the benzamides FLA 870, FLA 965 and FLA 659, desipramine, imipramine and nortriptyline (in order of increasing retention volumes), were injected together with 5.0 m*M* nonylsulphate (Fig. 10a). The column was equilibrated with a low probe concentration of $3.8 \cdot 10^{-5}$ *M*. FLA 870 and FLA 965 were eluted in the front and the plateau of the system zone, respectively, and were both deformed. The simultaneously injected anion may also be partly responsible for this deformation (*cf.*, Fig. 2a). FLA 659 and desipramine (isocratic separation factor = 1.02) were both eluted in the gradient and appeared as a single compressed peak. The analytes which were eluted after the gradient were deformed owing to overlap with the anion front. In a second experiment, the substituted benzamides were injected together with octanesulphonate when the eluent contained a high probe concentration of $9.5 \cdot 10^{-4}$ *M* (Fig. 10b). In this instance the analytes FLA 870 and FLA 965, with an isocratic separation factor of 1.29, were eluted with the same retention volumes and appeared as a single compressed peak. The retention volume and peak shape of FLA 659, which was eluted after the gradient, were identical with those in the isocratic experiment. Separation between FLA 870 and FLA 965 could be achieved when a fivefold higher anion concentration was used, *i.e.*, 25 m*M* (Fig. 10c). At this high anion concentration, the gradient retention volume was decreased [7], accompanied by FLA 870, which was still compressed. The retention volumes of FLA 965 and FLA 659 were increased owing to an increased ion-pair distribution with the anion. In this run and also in the run in Fig. 10b, the retention time of the later eluted anion peak was about 25 min.

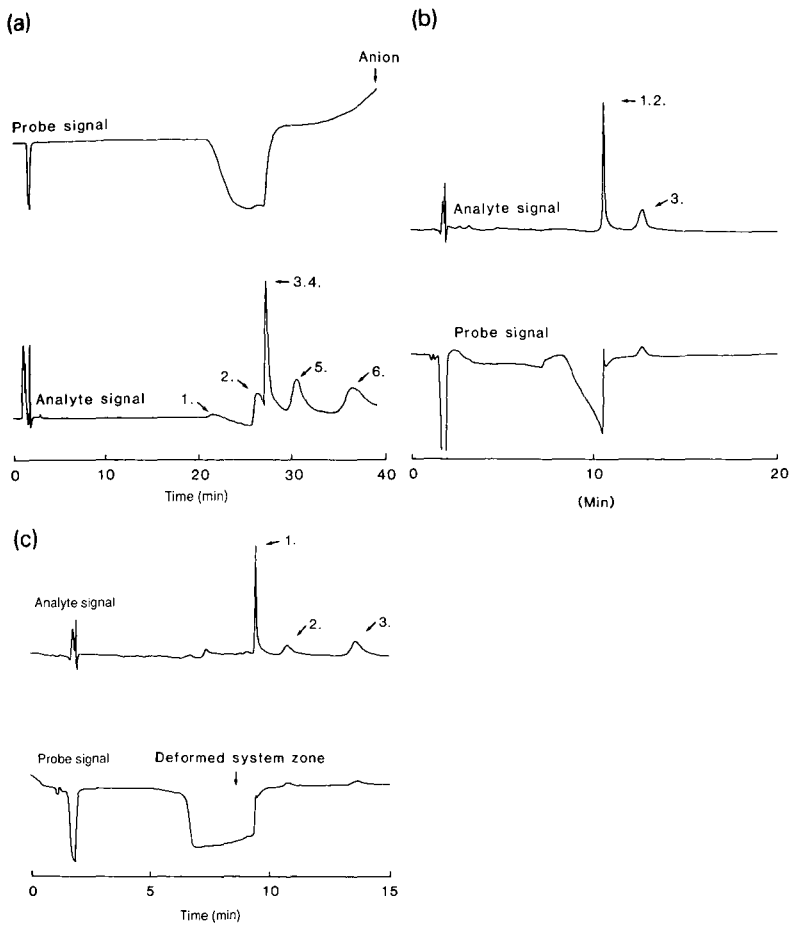

Fig. 10. Selectivity of peak compression, induced at different probe eluent concentrations. Sample, $1.0 \cdot 10^{-5}$ *M* analytes and anion in phosphate buffer (pH 2.0); eluent, protriptyline in phosphate buffer (pH 2.0)–acetonitrile (3:1). (a) Analytes: 1 = FLA 870; 2 = FLA 965; 3 = FLA 659; 4 = desipramine; 5 = imipramine; 6 = nortriptyline. Anion: 5.0 m*M* nonylsulphate. $C_{PT} = 3.8 \cdot 10^{-5}$ *M*. (b) Analytes: 1–3 as in (a). Anion: 5.0 m*M* octanesulphonate. $C_{PT} = 9.5 \cdot 10^{-4}$ *M*. (c) Conditions as in (b), except 25.0 m*M* octanesulphonate.

This series of results indicate that high probe concentrations in the eluent give low selectivity between the amine analytes. However, there are possibilities of achieving the desired selectivity between the analytes by adjustments of the anion concentration. It is further obvious that by this peak compression technique only one component at a time can be compressed. An important advantage of the use of high probe concentrations is the improved separation between the gradient and the anion, which is necessary to avoid deformations of analytes being eluted after the gradient.

Other ways to induce system peaks

In the experiments described above, the analytes and anions were dissolved in

phosphate buffer. The injection of pure phosphate buffer containing no organic ions results in positive system peaks [17]. The injection of eluent without a probe, *i.e.*, phosphate buffer–acetonitrile (3:1), into the system equilibrated with the probe resulted in a negative system peak, because in the injection zone some of the PT molecules adsorbed to the solid phase will diffuse into the injected solvent. This leaves a deficiency of the probe (PT) in the injection zone to be eluted as a negative system peak.

By use of this technique, the analytes FLA 870, FLA 965 and FLA 659 were injected (Fig. 11). The probe concentration was $9.5 \cdot 10^{-4}$ *M*. None of the analytes were clearly eluted within the rear gradient of the system peak, but the peak width of FLA 965 decreased from the isocratic value of 0.52 ml to 0.34 ml. This was due to its elution very close after the gradient. The poorly retarded FLA 870 was partly eluted with the front part of the system peak and was therefore strongly deformed, whereas the analyte FLA 659, which was eluted well separated after the rear gradient, was unaffected.

This demonstrates the importance of careful control of the injection conditions in order to avoid disturbances in ion-pair chromatographic systems. The results also indicate that it is possible to achieve peak compressions without the simultaneous injection of an organic anion [28].

Reproducibility of peak compression

Limited studies on the reproducibility of the technique were made by a comparison of single injections made several weeks apart (Table IV). The retention volume of the compressed analyte peak and also the matching of analyte and gradient retention volumes remained almost constant after more than 7 weeks of running the system. With desipramine, the analyte retention volume increased very slightly from 22.86 to 23.05 ml, while the matching was still optimum. Tendencies towards higher retentions

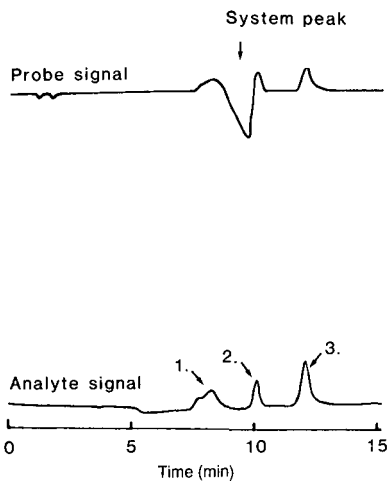

Fig. 11. System peak effects on analytes induced by injecting small amounts of analytes dissolved in eluent lacking probe. Sample, $1.0 \cdot 10^{-5}$ *M* analytes 1–3 as in Fig. 10 in eluent without probe; eluent, $9.5 \cdot 10^{-4}$ *M* protriptyline in phosphate buffer (pH 2.0)–acetonitrile (3:1).

TABLE IV

REPRODUCIBILITY OF PEAK COMPRESSION: COMPARISON OF SINGLE INJECTIONS MADE SEVERAL WEEKS APART

Sample: $1.0 \cdot 10^{-5}$ *M* analyte with 5.0 m*M* anion in phosphate buffer (pH 2.0). Eluent: protriptyline in phosphate buffer (pH 2.0)–acetonitrile (3:1). Systems: (A) analyte FLA 870, anion octanesulphonate, $C_{PT} = 9.5 \cdot 10^{-4}$ *M*; (B) analyte desipramine, anion nonylsulphate, $C_{PT} = 3.8 \cdot 10^{-5}$ *M*.

System	$V_{R.A}$ (ml)	$V_{R.A}/V_{R.G}$	w_b (ml)
A	8.37 } same day	1.00	0.09
	8.38 }	1.00	0.10
	8.41 (7 weeks later)	1.00	0.13
B	22.86	1.00	0.45
	23.05 (3 weeks later)	1.00	0.20[a]

[a] A small amount of new solid phase was added on the top of the column.

in similar systems have been observed before [18]. The slight changes in the retention volume of the compressed analyte peaks followed the changes in gradient retention volume, maintaining the good matching of the peaks. The differences in the compressed peak widths obtained was probably a result of similar changes in the gradient widths (gradient steepness). Further studies on reproducibilities in order to adapt the technique for quantitative determinations are in progress.

CONCLUSIONS

Peak compression is optimum at high probe concentrations (non-linear distribution behaviour), giving large gradient steepnesses at low analyte concentrations and when an adequate separation between the system peak and the anion peak is obtained. Peak deformation was obtained in the position normally giving peak compression when the anion peak eluted close after the system peak and interfered with the analyte. Such interferences were efficiently suppressed by increased probe concentrations and improved anion separations.

The analyte desired for peak compression was more easily captured in the gradient at high probe concentrations. A single compressed peak may then appear when two analytes are eluted simultaneously together with the gradient, but the components can be separated by suitable adjustments of the injected anion concentration.

ACKNOWLEDGEMENTS

The authors thank the Swedish Natural Science Research Council (NFR) and Pharmacia LEO Therapeutics for financial support of this project. We also thank the Swedish Academy of Pharmaceutical Sciences (T.F.) and the I.F. Foundation of Pharmaceutical Research (T.F. and A.S.) for travel grants and Astra Research Centre for supplying the substituted benzamides.

REFERENCES

1 P. Jandera and J. Churacek, *Gradient Elution in Column Liquid Chromatography (Journal of Chromatography Library*, Vol. 31), Elsevier, Amsterdam, 1985.
2 A. Sokolowski, *Chromatographia*, 22 (1986) 177.
3 A. Sokolowski, *J. Chromatogr.*, 384 (1987) 1.
4 A. Sokolowski, *J. Chromatogr.*, 384 (1987) 13.
5 T. Fornstedt, D. Westerlund and A. Sokolowski, *J. Liq. Chromatogr.*, 11 (1988) 2645.
6 L. B. Nilsson and D. Westerlund, *Anal. Chem.*, 57 (1985) 1835.
7 T. Fornstedt, D. Westerlund and A. Sokolowski, *J. Chromatogr.*, 506 (1990) 61.
8 G. Schill and E. Arvidsson, *J. Chromatogr.*, 492 (1989) 299.
9 T. Arvidsson, *J. Chromatogr.*, 407 (1987) 49.
10 S. O. Jansson and M. L. Johansson, *J. Chromatogr.*, 395 (1987) 495.
11 W. S. Hancock, C. A. Bishop, J. E. Battersby and D. R. K. Harding, *J. Chromatogr.*, 168 (1979) 377.
12 H. U. Ehmcke, H. Kelker, K. H. König and H. Ollner, *Fresenius' Z. Anal. Chem.*, 294 (1979) 251.
13 G. K. C. Low, A. M. Duffield and P. R. Haddad, *Chromatographia*, 15 (1982) 289.
14 J. Kirschbaum, S. Perlman and R. B. Poet, *J. Chromatogr. Sci.*, 20 (1982) 336.
15 T.-L. Ng and S. Ng, *J. Chromatogr.*, 329 (1985) 13.
16 G. K. C. Low and P. R. Haddad, *J. Chromatogr.*, 336 (1984) 15.
17 A. Sokolowski, T. Fornstedt and D. Westerlund, *J. Liq. Chromatogr.*, 10 (1987) 1629.
18 A. Sokolowski, *Chromatographia*, 22 (1986) 168.
19 A. Sokolowski and K.-G. Wahlund, *J. Chromatogr.*, 189 (1980) 299.
20 A. Tilly-Melin, M. Ljungcrantz and G. Schill, *J. Chromatogr.*, 185 (1979) 225.
21 L. R. Snyder, *Anal. Chem.*, 39 (1967) 698.
22 V. V. Berry and R. E. Shansky, *J. Chromatogr.*, 284 (1984) 303.
23 G. K. C. Low, *J. Chromatogr.*, 478 (1989) 21.
24 F. Eisenbeiss, S. Ehlerding, A. Wehrli and J. F. K. Huber, *Chromatographia*, 20 (1985) 657.
25 A. Katti and G. Guiochon, *Anal. Chem.*, 61 (1989) 982.
26 J. R. Conder and C. L. Young, *Physicochemical Measurement by Gas Chromatography*, Wiley, New York, 1979.
27 C. N. Reilley, G. P. Hildebrand and J. W. Ashley, *Anal. Chem.*, 34 (1962) 1198.
28 T. Fornstedt, A. Sokolowski and D. Westerlund, presented at the *13th International Symposium on Column Liquid Chromatography, Stockholm, June 25–30, 1989.*

Journal of Chromatography, 535 (1990) 111–125
Elsevier Science Publishers B.V., Amsterdam

CHROMSYMP. 2059

Porous zirconia and titania as packing materials for high-performance liquid chromatography

U. TRÜDINGER, G. MÜLLER and K. K. UNGER*
Institut für Anorganische und Analytische Chemie, Johannes Gutenberg Universität, P.O. Box 3980, D-6500 Mainz 1 (F.R.G.)

ABSTRACT

Porous amorphous zirconia (ZrO_2) and titania (TiO_2) packings were synthesized as rigid microparticulate beads by means of a sol–gel process. Sufficient rigidity and desired mesoporosity of the ZrO_2 and TiO_2 particles were achieved only by a gel hardening process, followed by heat treatment. The mean pore diameter, $\bar{p}_d$, the specific surface area, a_s, and the specific pore volume, v_p, were controlled by the heat treatment. Typical values were $\bar{p}_d$ = 8 nm, a_s = 80 m^2/g and v_p = 0.23 ml/g. ZrO_2- and TiO_2-based revesed-phase packings were prepared by subjecting the native materials to a specific surface activation process and reaction with octadecyltrimethoxysilane. Native ZrO_2 and TiO_2 of graduated polarity, tested under normal-phase conditions, yielded a solvent strength series similar to those observed with silica and alumina. Retention of lipophilic analytes in *n*-heptane and dichloromethane was scarcely affected by the relative water content of the mobile phase. Native ZrO_2 and TiO_2 were found to be suitable for the separation of structural isomers. From calcined ZrO_2 and TiO_2 amines were eluted with totally symmetrical peaks when water-modified dichloromethane was used as the mobile phase. The retention and selectivity of *n*-octadecyl-bonded ZrO_2 and TiO_2 packings were identical with those of silica-based materials, except for showing a pronounced pH stability up to pH 12 in aqueous–organic mobile phases.

INTRODUCTION

The development of high-performance liquid chromatography (HPLC) as an efficient separation technique was always dependent on the synthesis of suitable packing materials. Silica and its bonded derivatives still maintain a leading position as packings in HPLC. However, polymer packings have improved remarkably and are now being increasingly applied.

Many attempts have been undertaken to improve the quality of silica packings with regard to chemical stability and residual adsorptivity towards basic analytes. The limited chemical and pH stability of silica and its bonded derivatives in HPLC has led to extensive research activity to overcome these undesirable properties. Stabilized silicas have been prepared by drastically reducing inorganic impurities [1], by subjecting it to hydrothermal and acid treatment [2,3] or by coating it with alkali-resistant oxides [4]. These stabilized silicas were either made to react with protective silanes [5] or coated with polymeric phases [6] to yield stable reversed-phase

0021-9673/90/$03.50

packings. In spite of all efforts to increase the pH stability, silica persists in being soluble in strong alkaline solution.

Porous aluminas are used as packing materials to a lesser extent. The potential of porous alumina has been re-investigated by De Galan and co-workers [7,8]. Recently, a polybutadiene-coated alumina has become commercially available [9].

A few attempts have been made to utilize titania and zirconia ceramics as packing materials, in HPLC [10,11]. A polybutadiene-coated microporous zirconia was prepared by Rigney *et al.* [12] which showed excellent chemical and thermal stability. Mesoporous crystalline zirconia beads have been studied by the same group, in particular their ion-exchange properties [13].

Both titania and zirconia are basic oxides and are therefore insoluble in alkaline media. Moreover, they are stable in acidic media, down to pH 1. Compared with conventional packing materials, titania and zirconia exhibit completely different chemical surfaces. As the interaction of analytes with the surface of the stationary phase determines the chromatographic selectivity, divergent selectivities could be expected when titania or zirconia is used as packing material.

We found all commercially available zirconia and titania products to be unsuitable for HPLC use. They were either highly crystalline and non-porous, with almost no chromatographic retentivity, or amorphous and microporous, showing poor chromatographic performance.

The objective of this work was to develop a method for preparing amorphous titania and zirconia particles, based on a sol–gel process, which permits the combination of oxide synthesis and control of their physical properties with the shaping of the final products [14]. The main problems were to obtain particles with a rigid texture, an adjustable particle size, a sufficient porosity and mesopores of mean pore diameter between 2 and 50 nm.

EXPERIMENTAL

Preparation of starting materials

Highly concentrated titania and zirconia sols were used as starting materials for oxide synthesis. They were obtained either by partial hydrolysis of the corresponding tetravalent metal chlorides [15] or, in the case of zirconia, by dissolving zirconyl chloride in water. Titania sol was prepared by hydrolysing 1 l of titanium tetrachloride (Merck, Darmstadt, F.R.G.) in portions of *ca.* 50 ml in 300 g of ice. Precautions were taken to collect the hydrogen chloride fumes evolved. The foam-like precipitates were dissolved in cold water.

Zirconia sol was supplied ready for use by Goldmann (Bielefeld, F.R.G.). The elemental analyses and physical properties of the sols are given in Table I.

Preparation of reactive sols and gelation reaction

To initiate the gel reaction, the acid-stabilized sols were made to react with an appropriate amount of a weak base, such as hexamethylenetetramine (HMTA) and urea [16]. Sufficient hydroxyl ions were released owing to hydrolysis (Fig. 1). It is essential to set the conditions of the gelation reaction properly in order to obtain homogeneous rigid titania and zirconia gels.

For the preparation of the titania sol reactive to gelling, 340 g of titania sol were

TABLE I

ELEMENTAL ANALYSIS AND PHYSICAL PROPERTIES OF TITANIA AND ZIRCONIA SOLS

Concentrations given in mol dm^{-3}.

Sol	[M(IV)][a]	$[H^+]$[b]	$[Cl^-]$[b]	δ/kg dm^{-3}[c]	η/cSt[d]
TiO_2	6.8–7.2[e]	10.7–11.8[e]	11.1–12.4[e]	1.565–1.601[e]	67–78[e]
ZrO_2	2.35	4.80	4.86	1.385	3.5

[a] Gravimetric analysis.
[b] Titrimetric analysis.
[c] Pycnometry.
[d] Viscosimetry.
[e] Tolerance range of different sol batches.

mixed with 380 g of HMTA (3.5 *M*) and 60 g of urea (8 *M*). For zirconia, 560 g of zirconia sol, 380 g of HMTA (3.5 *M*) and 65 g of urea (8 *M*) were used. The sols were converted to transparent monolithic hydrogels at elevated temperatures (40–45°C) within 8 min. The sol–gel transition occurred within a few seconds.

Emulsification

Prior to gelation, sols (so-called w phase) were emulsified in a water-immiscible liquid (so called o phase), containing various non-ionic surfactants to stabilize the liquid–liquid dispersion. Emulsion stability was optimized by utilizing the hydrophilic lipophilic balance (HLB) system with respect to a low coalescence rate to prevent the dispersion from breaking, creaming or sedimenting [17].

Finely divided w/o emulsions were achieved by making use of a high-shear rotor stator dispersion unit, generating small droplets within the organic phase [18]. The

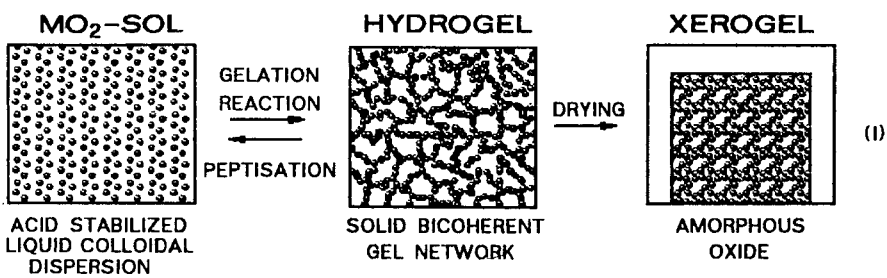

Fig. 1. Scheme for the sol–hydrogel–xerogel conversion (I) due to hydrolyis of hexamethylenetetramine (II) and urea (III).

organic phase was prepared by adding a multi-emulsifier complex ($HLB_{mixture} = 4.9$), containing 49 g of Span 85, 15 g of Tween 85 and 11 g of Brij 30 (Serva, Heidelberg, F.R.G.), to 2.5 kg of light petroleum (b.p. 100–140°C) (Merck).

The sols were dispersed in the organic phase by means of an Ultra-Turrax T45/4G dispersion unit (Janke & Kunkel, Staufen, F.R.G.) at 6500 rpm for 30 s to prepare 2–25-μm particles and at 8500 rpm for 60 s to prepare 2–7-μm beads. After the gelation reaction had been accomplished, the former emulsified liquid sol droplets were converted to solid, transparent hydrogel particles.

Particle processing and characterization

To remove adherent light petroleum, surfactants and residual substances, such as hydrochloric acid, and unreacted base, the microparticulate, swollen hydrogel particles were subjected to a multi-stage washing procedure (Table II).

Drying was carried out either by conventional methods or by applying a gel-hardening process [19]. For gel hardening, 2 kg of hydrogel particles were suspended into 3.5 l of isoamyl acetate (Merck) in order to remove enclosed water by azeotropic distillation (b.p. 122–130°C).

Sizing of the xerogel spheres was achieved by means of a laboratory air classifier (Alpine, Augsburg, F.R.G.). The particle-size distribution was determined by laser diffraction (Mastersizer, Malvern, U.K.). Morphological studies of particles were performed by scanning electron microscopy (Philips PSEM 500).

Residual organic matter, enclosed in native products, was removed by controlled pyrolysis to obtain carbon-free calcined products. The calcination was carried out in a preheated oven (N3 R; Naber, Flörsheim, F.R.G.) with a constant height of the solid bed (15 mm) in flat-bottomed porcelain crucibles. As the thermal treatment diminished the number of surface hydroxyl groups, the calcined products were rehydroxylated at different pH values following a procedure described elsewhere [20].

The physical properties of the final products were determined by means of thermogravimetric and differential thermal analysis (Model 84; Linseis, Selb, F.R.G.), X-ray powder diffraction (Philips APD) and nitrogen adsorption measurements (4102 and 4433 microbalances; Sartorius, Göttingen, F.R.G.; Omicron 100; Omicron Techn., Berkeley Heights, NJ, U.S.A.). Particular emphasis was placed on the reproducibility and standardization of sample pretreatment. As is well known, the

TABLE II

HYDROGEL WASHING PROCEDURE

Chemicals: technical grade, Merck, Darmstadt, F.R.G.

Washing liquid	Amount (l)	Cycles	Washing time (h per cycle)
Light petroleum (b.p. 40–80°C)	1.5	1	0.5
Acetone	1.5	1	0.5
Ethanol	2	3	1
Water	2	3	0.5
Ammonia (2.5%)	1	1	12
Water	until neutral reaction of supernatant		

determination of the specific surface area and pore volume of metal oxides depends strongly on the sample history [21].

Preparation of reversed-phase packings, column filling procedures

Calcined titania and zirconia xerogels were activated and converted to reversed-phase packings by making the oxide spheres react with *n*-octadecyltrimethoxysilane (Wacker, Burghausen, F.R.G.), as described by Engelhardt and Orth [20]. The carbon content of modifying ligands was determined by elemental analysis. Stainless-steel columns (Hyperchrome, 125 × 4 mm I.D.; Bischoff, Leonberg, F.R.G.) were filled with the packing materials by conventional slurry packing techniques. Column filling was carried out with a home-made packing unit, provided with a 100-ml reservoir and a membrane pump (Model S 80; Orlita, Giessen, F.R.G.). For native zirconia and titania packings, ethanol served as the dispersant. Toluene–dioxane–cyclohexanol (4:4:1, v/v/v) was employed to suspend zirconia- and titania-bonded packings. The final filling pressure was kept below 45 MPa to avoid particle cracking.

Chromatographic tests

Chromatographic tests were carried out with standard HPLC equipment [pump, Kontron 420 (Kontron, Munich, F.R.G.); UV detector, LKB 2158 (wavelength 254 nm) (Pharmacia–LKB, Freiburg, F.R.G.); injection system (sample loop, 20 μl), Rheodyne 6125 (Bischoff); integrator, Shimadzu C-R3A (Shimadzu, Kyoto, Japan)].

Native and calcined titania and zirconia packings were tested under normal-phase conditions to assess the solvent strength sequence and the influence of water-containing eluents on retention. Capacity factors of solutes with different polarities were determined in order to evaluate the chromatographic selectivity of these packings, with chloroform as a t_0 marker.

N-Octadecyl-modified titania and zirconia packings were tested under reversed-phase conditions employing aqueous acetonitrile as the mobile phase.

The pH stability of reversed-phase packings based on titania and zirconia was monitored under dynamic conditions. The columns were flushed with buffers of increasing pH. The pH of the buffer was adjusted in steps of 0.5 unit. In each cycle the columns were operated for 24 h at a flow-rate of 1 ml/min before they were equilibrated to a 60% (v/v) aqueous acetonitrile eluent. A test mixture was then injected to monitor changes in capacity factors and peak width of test solutes due to a pH increase.

RESULTS AND DISCUSSION

Gel formation

The gelation reaction was found to be very sensitive to the reaction conditions with respect to the initial sol pH, the sol-to-base ratio, the concentration of urea and the reaction temperature. Among these the sol-to-base ratio turned out to be the most critical factor in gel synthesis. At a high ratio of sol to base, hydrous oxides precipitated owing to complete and rapid neutralization (Fig. 2a), whereas no gelation occurred at low sol-to-base ratios (Fig. 2c). However, rigid monolithic transparent hydrogels were exclusively obtained when the gel pH (Fig. 2d) was approached at the proper rate (Fig. 2b). Beyond that, urea was found to act as an additional factor controlling the rate of

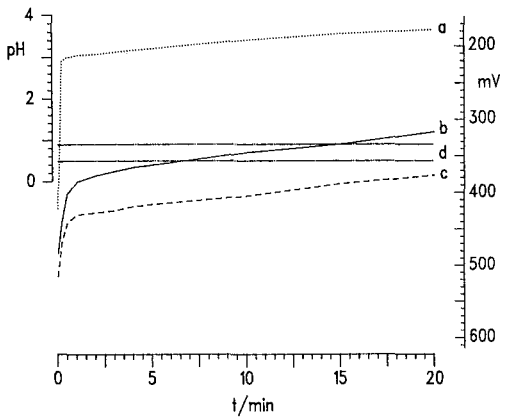

Fig. 2. Change in pH during titania sol–gel reaction at different sol-to-base ratios. (a) [Ti(IV)]/[HMTA] = 0.58, precipitation of hydrous oxides; (b) [Ti(IV)]/[HMTA] = 0.90, monolithic transparent gels; (c) [Ti(IV)]/[HMTA] = 1.25, viscous liquid sol (no gelation); (d) pH threshold of gel formation.

hydrolysis of the initial sols. This turned out to be useful for the preparation of large batches.

Physical properties of packings

Conventional drying procedures caused particle shrinkage, aggregation of particles, compaction of microstructure and hence a decrease in porosity, generation

TABLE III

COMPARISON OF PHYSICAL PROPERTIES OF CONVENTIONALLY AND AZEOTROPICALLY DRIED XEROGELS

a_s = Specific surface area; v_p = specific pore volume; $\bar{d}_p$ = mean pore diameter.

Conventional drying					
	H_2O (%)[a]	a_s (m^2g^{-1})	v_p (ml g^{-1})	$\bar{d}_p$ (nm)	Pore size
TiO_2	31	470	0.105	<2	Microporous
ZrO_2	48	420	0.094	<2	Microporous
Azeotropic drying					
	H_2O (%)[a]	a_s (m^2 g^{-1})	v_p (ml g^{-1})	$\bar{d}_p$ (nm)	Pore size
TiO_2	31	343	0.251	2.9	Mesoporous
	65	309	0.337	4.2	Mesoporous
	85	327	0.472	5.8	Mesoporous
ZrO_2	48	335	0.152	1.4	Microporous
	65	319	0.161	2.2	Mesoporous
	85	327	0.274	3.3	Mesoporous

[a] Initial water content of sol.

of a large specific surface area and microporosity. These properties are very disadvantageous for the use of these packings in HPLC. A comparison of the physical characteristics of xerogels which had been subjected to different dryring procedures is given in Table III. The physical data of conventionally dried gels indicated that microporous products were mainly formed. Azeotropically dried gels, however, exhibited larger pore volumes with a pronounced mesoporous structure. In addition, the porosity could be regulated by varying the initial water content of the sol.

Subjecing the hydrogels to azeotropic drying obviously prevented the pore structure from collapsing and led to mesoporous products, providing much faster mass transfer throughout the chromatographic process than conventionally dried products. In addition, azeotropic drying yielded free-flowing, fluffy powders, facilitating further particle processing. Scanning electron micrographs of the xerogels showed non-aggregated spherical partices without lumps, cracks or protrusions, and particle fragments (Fig. 3). By passing them through an air classifier, the starting polydisperse products were separated into narrow particle-size fractions (Fig. 4). This narrow particle-size distribution provided the necessary homogeneity of column packings at reasonable column back-pressures.

The xerogels contained up to 10% of residual organic matter, which had to be removed by pyrolysis to yield pure zirconia and titania materials. Therefore, the determination of the thermal properties of xerogels by means of thermogravimetric and differential thermal analyses was essential. The xerogels reached a constant weight

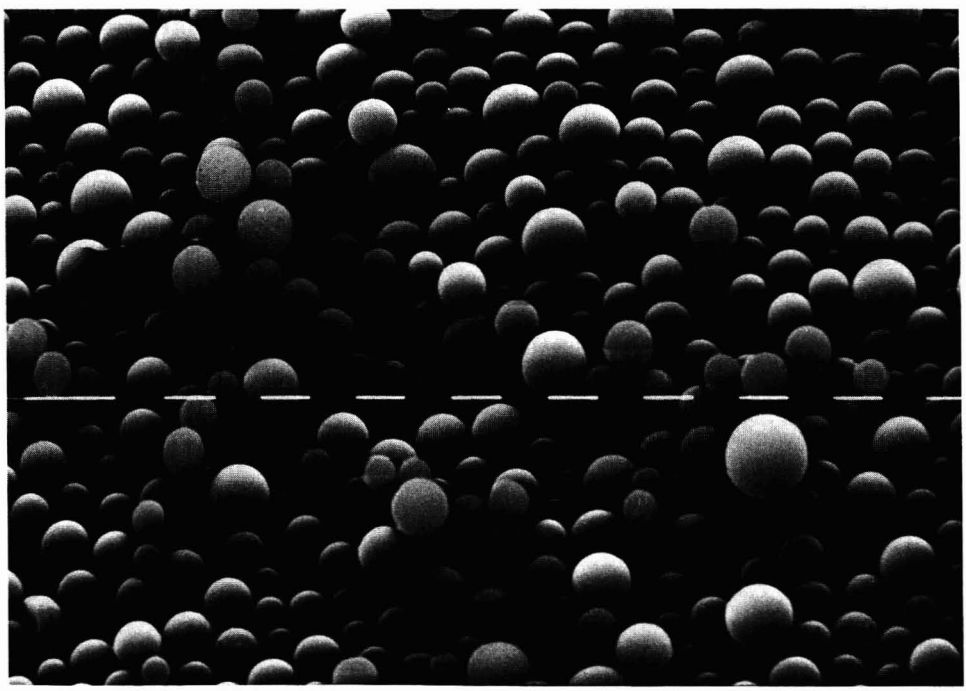

Fig. 3. Scanning electron micrograph of a zirconia xerogel, prepared according to the sol–gel process. White scale bars represent 10 μm.

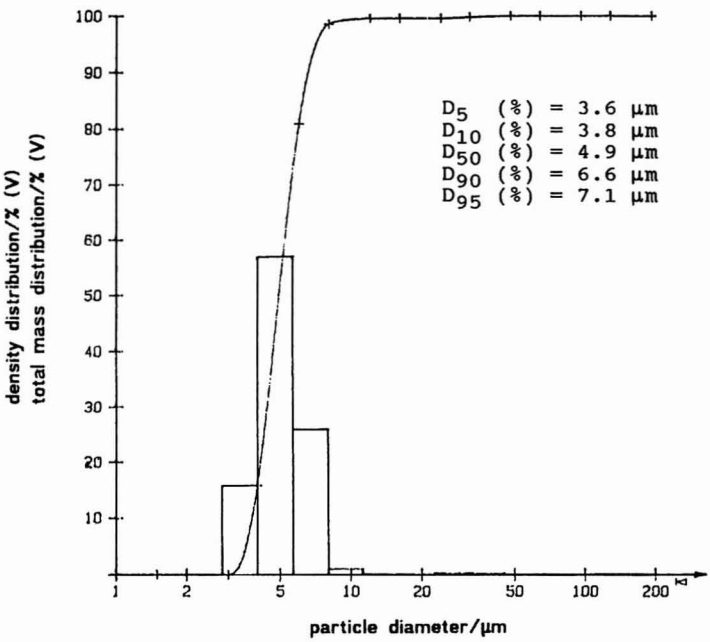

Fig. 4. Particle size distribution of a titania packing material ($\bar{p}_d$ = 5 μm).

at about 400°C, losing *ca.* 30–40% of their initial weight (Fig. 5). Up to 300°C a broad endothermic peak was observed, due to the release of water and coking of the organics. At about 400°C, a sharp exothermic peak indicated the beginning of the crystallization of amorphous oxides. This process is known as the glow phenomenon [22]. This behaviour indicated that the thermal properties of sol–gel-derived oxides were similar to those of precipitated products [23].

As crystallization is always accompanied by a drastic decrease in specific surface area and porosity [24], the conditions of the heat treatment had to be carefully

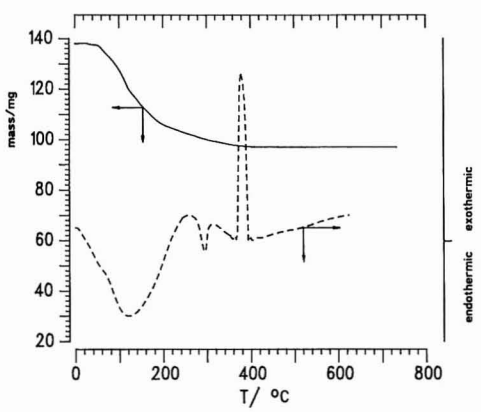

Fig. 5. Thermogravimetric (solid line) and differential thermal analysis (dashed line) of a titania xerogel.

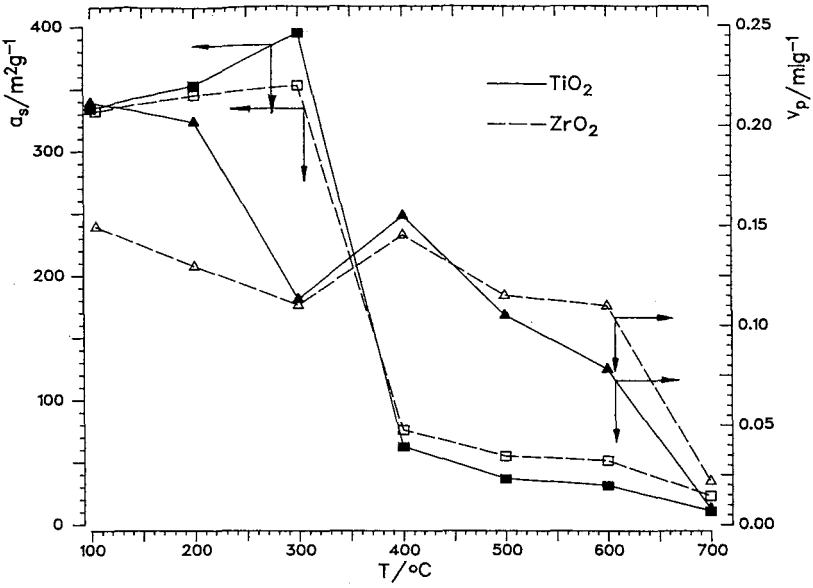

Fig. 6. Change in specific surface area (a_s) and specific pore volume (v_p) of titania (solid lines) and zirconia (dashed lines), xerogels as a function of calcination temperature (T).

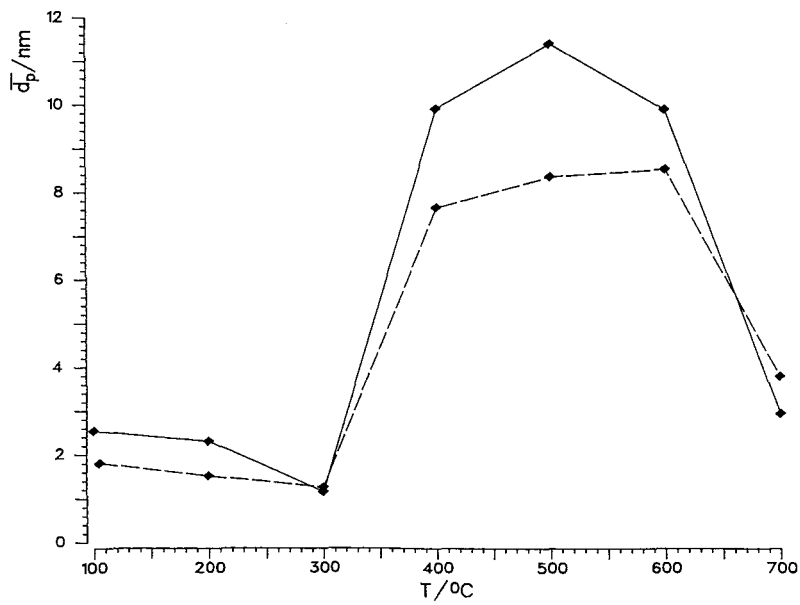

Fig. 7. Change in mean pore diameter ($\bar{d}_p$) of titania (solid line) and zirconia (dashed line) xerogels as a function of calcination temperature (T).

TABLE IV

PHYSICAL PROPERTIES OF TITANIA AND ZIRCONIA PACKING MATERIALS

a_s = Specific surface area; v_p = specific pore volume; $\bar{d}_p$ = mean pore diameter.

	a_s ($m^2\ g^{-1}$)	v_p (ml g^{-1})	$\bar{d}_p$ (nm)	Pore size
Native TiO_2	330	0.26	3	Micro-/mesoporous
Calcined TiO_2	78	0.23	8	Mesoporous
Native ZrO_2	308	0.18	2	Micro-/mesoporous
Calcined ZrO_2	104	0.15	6	Mesoporous

adjusted. Whereas the microporous structure of conventionally dried gels was insensitive to calcination, azeotropially dried gels showed a completely different behaviour (Fig. 6). On calcining these xerogels at different temperatures, a considerable decrease of *ca.* 70% in surface area was observed at about 400°C, whereas a_s remained almost constant on further temperature increase. The specific pore volume also decreased with increasing calcination temperature, but at a much slower rate.

Both a_s and v_p affected the development of pore size as a function of the calcination temperature. As Fig. 7 indicates, the mean pore diameter of products initially in the lower mesopore range could be enlarged to 10 nm by increasing the calcination temperature. The physical properties of titania and zirconia packings, subjected to chromatographic tests, are summarized in Table IV. X-Ray powder diffraction patterns indicated that neither native nor calcined xerogels were crystalline.

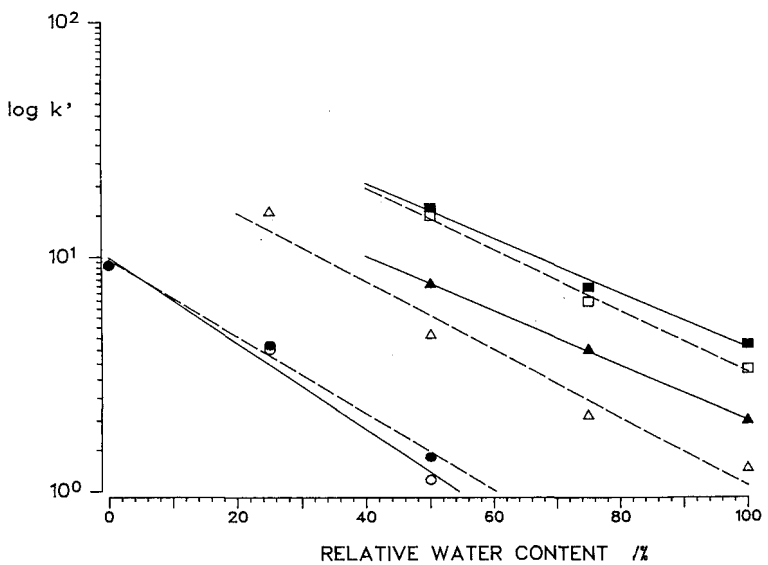

Fig. 8. Capacity factors of test solutes as a function of the relative water content of dichloromethane as the mobile phase, with calcined titania xerogel as packing material. $\bar{p}_d$ = 5 μm; injection volume, 20 μl; flow-rate, 1 ml/min. ■ = Diazepam; ▲ = pyridine; ● = *o*-toluidine; □ = *p*-toluidine; △ = aniline; ○ = N-methylaniline.

Normal-phase chromatography

The zirconia and titania particles prepared withstood a packing pressure up to 50 MPa without cracking.

Chromatographic tests under normal-phase conditions demonstrated that there was no major difference in the solvent strength sequence found for silica or alumina. Increasing the relative water content of the eluent affected the capacity factor of solutes, as shown for dichloromethane as eluent in Fig. 8. In normal-phase chromatography of silica and alumina packings, conditioning and reconditioning of columns has always been a time-consuming procedure [25]. Up to *ca.* 100 column volumes are required to equilibrate the silica and alumina with a non-polar mobile phase and water as modifier. In contrast, calcined zirconia and titania packings required only 5–10 column volumes for equilibration.

Native titania and zirconia exerted a strong retention towards hydrophobic solutes, such as polycyclic aromatic hydrocarbons. The latter were eluted only with

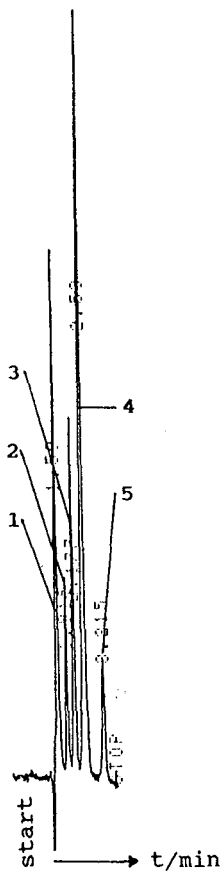

Fig. 9. Isocratic separation of lipophilic test solutes using native titania as packing material and a mobile phase of high solvent strength. $\bar{P}_d$, 10 μm; injection volume, 20 μl; eluent, dry methanol; flow-rate, 1 ml/min. Peaks: 1 = benzene (10.8 μg); 2 = naphthalene (3.2 μg); 3 = fluorene (2.5 μg); 4 = phenanthrene (4.3 μg); 5 = pyrene (2.2 μg).

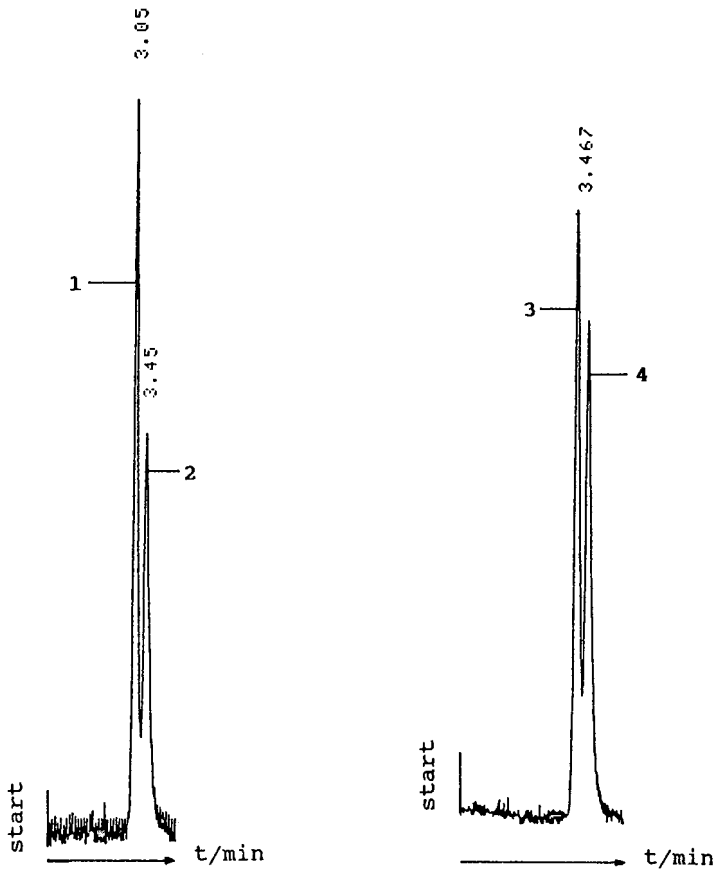

Fig. 10. Isocratic separation of isomers with native titania as packing material. $\bar{p}_d$, 10 μm; injection volume, 20 μl; eluent, *n*-heptane; flow-rate, 1 ml/min. Peaks: 1 = *p*-xylene (11.3 μg); 2 = *o*-xylene (6.2 μg); 3 = *o*-xylene (9.2 μg); 4 = *m*-xylene (7.7 μg).

eluents of high solvent strength, such as methanol, indicating a high solute surface interaction (Fig. 9). However, the same solutes were eluted from the calcined packings with *n*-heptane as mobile phase. These results demonstrate that the polarity of the adsorbents could be controlled by the conditions of heat treatment. As a result, the highly polar, native ZrO_2 and TiO_2 packings were well suited for the separation of isomers, as demonstrated in Fig. 10. However, on silica or alumina columns, this separation could not be performed under identical conditions.

It is well known that the acidic properties of silica are responsible for the strong retention of basic analytes, which is often accompanied by severe tailing. Basic compounds with pK_B values up to 11 were separated on calcined titania and zirconia packings with water-containing dichloromethane as eluent (Fig. 11). The basic analytes showed a high peak symmetry.

This chromatographic retention behaviour is due to the surface chemistry of titania and zirconia being different from that of silica and alumina. Amorphous

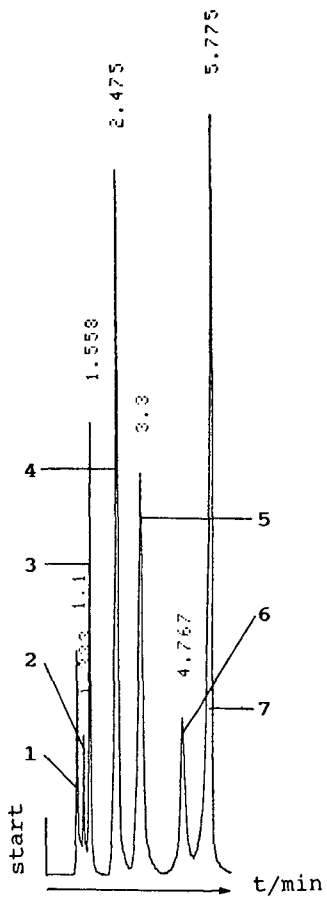

Fig. 11. Isocratic separation of basic analytes with calcined titania as packing material. $\bar{p}_d$, 5 μm; injection volume, 20 μl; eluent, dichloromethane (relative water content 100%); flow-rate, 1 ml/min. Peaks: 1 = N,N-dimethylaniline (10.8 μg); 2 = N-methylaniline (3.2 μg); 3 = *o*-toluidine (5.4 μg); 4 = aniline (15.4 μg); 5 = *p*-toluidine (5.4 μg); 6 = pyridine (3.4 μg); 7 = diazepam (1.9 μg).

titania, and also zirconia, represent more or less ionic compounds, carrying highly polar tetravalent metal cations. Hydroxyl groups attached to the surface metal ions neutralize the surface charge. It is known that titania and zirconia carry two different kinds of surface hydroxyl groups [26]. One type is singly bonded, acting as a base, whereas hydroxyl groups bridging two neighbouring metal ions are acidic in behaviour. The number and strength of these distinct hydroxyl groups are almost balanced. Therefore, the isoelectric point and the point of zero charge for pure tiania and zirconia are both at *ca.* pH 7.

Reversed-phase chromatography

The zirconia- and titania-based reversed-phase packings were C_{18}-modified with a surface concentration of 1.2–1.4 μmol/m^2. The packings exhibited typical

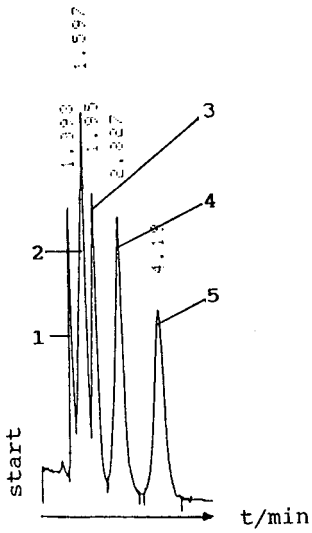

Fig. 12. Isocratic separation of polycyclic aromatic hydrocarbons with *n*-octadecyl-modified zirconia as packing material. $\bar{p}_d$, 10 μm; injection volume, 20 μl; eluent, 60% aqueous acetonitrile; flow-rate, 1 ml/min. Peaks: 1 = benzene (10.0 μg); 2 = naphthalene (4.2 μg); 3 = fluorene (2.9 μg); 4 = phenanthrene (4.6 μg); 5 = pyrene (2.2 μg).

features of reversed-phase packing such as lipophilic behaviour and an exponential increase in the capacity factors of solutes with increasing water content of the acetonitrile eluent. An example is the separation of a standard test mixture under reversed-phase conditions shown in Fig. 12.

The most useful feature of these reversed-phase packings is their pH stability. It was found that titania-based C_{18} packings are stable up to pH 11 and zirconia up to pH 12 without any noticeable effect on the capacity factor or peak width of test solutes. Even after a period of 500 h at pH 12, zirconia-based reversed-phase packings still maintained their performance level. From these results, we conclude that the porous oxide networks of titania and zirconia were neither altered nor attacked by strongly alkaline solutions. Even the heterogeneous metal siloxane binding system is, to a large extent, stable towards alkali. This reflects well that the sequence of hydrolytic stability of silanized oxides obeys the order given in Fig. 13, which has been established for binary siloxane compounds [27].

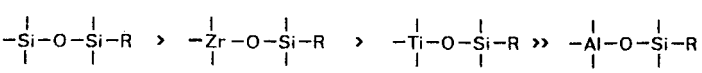

Fig. 13. Hydrolytic stability of binary siloxane compounds [27].

CONCLUSIONS

By means of a sol–gel process and special particle processing procedures, the synthesis of spherical mesoporous titania and zirconia particles was achieved. They satisfy the physical requirements for application as packing materials in HPLC. As the polarity of titania and zirconia packings can be varied to a large extent by heat treatment, their chromatographic retention and selectivity can be adapted to a range of separation problems. Thus, titania and zirconia xerogels appear to be well suited for normal-phase chromatographic separations of isomers in addition to basic analytes. Owing to the chemical nature of the amorphous oxide and the metal–siloxane bonds, stable reversed-phase titania and zirconia packings were obtained, which proved to be superior to other silanized inorganic oxides with respect to their hydrolytic stability towards alkaline eluents.

REFERENCES

1 M. Nyström, W. Herrmann, D. Sanchez and P. Möller, *Kromasil, a New High Performance Silica for Liquid Chromatography*, Eka Nobel, Surte, 1990.
2 K. K. Unger (Editor), *Packings and Stationary Phases in Chromatographic Techniques (Chromatographic Sciences Series*, Vol. 47), Marcel Dekker, New York, 1990, p. 363.
3 J. Köhler and J. J. Kirkland, *J. Chromatogr.*, 385 (1987) 125.
4 R. W. Stout and J. J. DeStefano, *J. Chromatogr.*, 326 (1985) 63.
5 A. L. Glajek and J. J. Kirkland, *LC · GC Int.*, 3 (1990) 50.
6 H. Figge, A. Deege, J. Köhler and G. Schomburg, *J. Chromatogr.*, 351 (1986) 393.
7 C. Laurent, H. A. H. Billiet and L. de Galan, *Chromatographia*, 17 (1983) 253.
8 H. Billiet, C. Laurent and L. de Galan, *Trends Anal. Chem.*, 4 (1985) 100.
9 *Unisphere Alumina*, Biotage, Charlotteville, VA, 1990.
10 M. Kawahara, H. Nakamura and T. Nakajima, *Anal. Sci.*, 5 (1989) 485.
11 M. Kawahara, H. Nakamura and T. Nakajima, *Anal. Sci.*, 5 (1989) 763.
12 M. P. Rigney, T. P. Weber and P. W. Carr, *J. Chromatogr.*, 484 (1989) 273.
13 M. P. Rigney, E. F. Funkenbusch, P. W. Carr, *J. Chromatogr.*, 499 (1990) 291.
14 B. E. Yoldas, *J. Mater. Sci.*, 12 (1977) 1203.
15 R. Caletka, University of Ulm, Ulm, personal communication.
16 V. Baran, R. Caletka, M. Tympl and V. Urbanek, *J. Radioanal. Chem.*, 39 (1977) 353.
17 H. Benett, J. L. Bishop and M. F. Wulfinghoff, *Practical Emulsions*, Chemical Publishing, New York, 1968.
18 R. Zimmermann, *GIT Fachz. Lab.*, 7 (1985) 720.
19 J. A. Pierce and C. N. Kimberlin, *U.S. Pat.*, 2 454 941 (1970).
20 H. Engelhardt and P. Orth, *J. Liq. Chromatogr.*, 10 (1987) 1999.
21 J. Rouquerol, F. Rouquerol, Y. Grillet and M. J. Torralvo, *Fundam. Adsorpt., Proc. Eng. Found. Conf.*, (1983) 501.
22 J. Böhm, *Z. Anorg. Chem.*, 149 (1925) 217.
23 Y. D. Dolmatov, V. A. Tyustin, R. F. Dobrovol'skii and R. F. Arbuzina, *J. Appl. Chem. USSR*, 48 (1975) 2465.
24 R. C. Asher and S. J. Gregg, *J. Chem. Soc.*, (1960) 5057.
25 H. Engelhardt and H. Elgass, in C. Horvath (Editor), *HPLC: Advances and Perspectives*, Vol. 2, Academic Press, London, 1980, pp. 57–108.
26 H. P. Boehm, *Chem.-Ing.-Tech.*, 46 (1974) 716.
27 F. Schneider and H. Schmidbauer, *Angew. Chem.*, 79 (1967) 697.

Journal of Chromatography, 535 (1990) 127–145
Elsevier Science Publishers B.V., Amsterdam

CHROMSYMP. 2052

New family of high-resolution ion exchangers for protein and nucleic acid purifications from laboratory to process scales

DONNA M. DION*, KEVIN O'CONNOR, DOROTHY PHILLIPS, GEORGE J. VELLA and WILLIAM WARREN

Waters Chromatography, Division of Millipore Corporation, 34 Maple Street, Milford, MA 01757 (U.S.A.)

ABSTRACT

A new family of polymer-based ion exchangers was tested for the purification of acidic and basic proteins on both the analytical and preparative scales. Protein-Pak™ HR series packings are available as strong cation (SP) and weak anion (DEAE) exchangers, allowing the development of a purification method regardless of the isoelectric point of protein. Three particle sizes, 8, 15 and 40 μm, are offered in scalable Advanced Purification (AP) glass columns or as bulk packings. The lower back pressures of the 15- and 40-μm packings compared to that of the 8-μm material allow rapid throughput of large volumes without exceeding the pressure limitations of the resin or the column. The capacity of the API (100 mm × 10 mm) glass columns, containing these ion-exchange packings, is comparable to other ion-exchange columns. The resolution of mouse serum, plasmids, and a standard protein mixture was demonstrated and compared with the results obtained with other resin-based ion exchangers of similar particle size. Proteins were purified without significant loss of biological activity or mass.

INTRODUCTION

High-performance ion-exchange chromatography is one of the most popular separation techniques in biochemistry. Proteins can usually be separated based on the electrostatic interactions between the zwitterionic protein surface and the charged stationary phase [1,2]. Nucleic acids with negatively charged backbones can also be separated by ion-exchange chromatography. High resolution is possible with this technique, because it is capable of separating such molecules with only small differences in charge on either the surface or the backbone.

Ion-exchange chromatography has been used extensively for protein purification for a long time. The first hydrophilic ion exchangers for proteins were developed in the 1950's and were based on cellulose [3]. These soft gel materials, diethylaminoethyl (DEAE) and carboxymethyl (CM) derivatives of cellulose are still used today; the softness and shrinking or swelling properties of these gels do not allow the optimum separation to be obtained. Porath *et al.* [4] in 1971 attempted to solve this problem with hard hydrophilic ion exchangers by developing cross-linked agarose ion-exchange gels. Other groups developed hydrophilic vinyl polymer ion-exchange gels [5]. In order to improve the resolution by the ion exchangers, packing materials with small particle

0021-9673/90/$03.50

sizes became available in both silica gels and hydrophilic polymer gels [6,7]. Most polymeric packings today occur as either analytical or preparative, but do not offer the particle size range that allows one to scale-up their separation from test tube to process with the same resin.

The new packing material discussed in this report, the Protein-Pak™ HR series, is similar to the currently available high-performance ion-exchange packings; they give a high separation efficiency and a high speed of separation. In addition, one chemistry is available for both preparative and analytical chromatography since three particle sizes are available (8, 15 and 40 μm).

Protein-Pak DEAE HR and SP HR materials are made from a rigid, spherical, porous, hydrophilic, polymeric, methacrylate gel. The 1000-Å pore size particles permit proteins with up to 10^6 molecular weight to penetrate the pores and interact with the functional groups. The packing materials have covalently bonded functionalities of diethylaminoethyl (DEAE) and propylsulfonic acid (SP), respectively. Here, we report the characteristics, performance and applications of the new family of packings and compare it with other commercial ion exchangers.

EXPERIMENTAL

Three tests were performed on the Protein-Pak HR materials and, for comparison, with Protein-Pak 5PW packings: the separation of a standard protein mixture, mass recovery and protein binding capacity. The protein binding capacity was determined at several different pH values. The system used for these assays was a Waters 840 chromatography data station with a Waters 600E solvent delivery system, Model 490 detector, 712 WISP autoinjector and a Wescan conductivity meter. The Protein-Pak HR materials were packed in the Waters Advanced Purification (API) 100 mm × 10 mm glass columns, while the Protein-Pak 5PW glass column dimensions were 75 mm × 8 mm. All proteins and buffer salts were purchased from

TABLE I

PROTEINS USED TO EVALUATE THE PERFORMANCE OF ION-EXCHANGE COLUMNS

Protein	Molecular weight	Isoelectric point	Concentration (%)
Protein-Pak DEAE HR series protein mixture			
Adenosine	267	–	0.3
Carbonic anhydrase	28 000	7.3	12.5
Human transferrin	77 000	6.0–6.5	31.1
Ovalbumin	44 500	4.7	25.0
Soybean trypsin inhibitor	21 500	4.5	31.1
Protein-Pak SP HR series protein mixture			
Myoglobin	17 500	7.0	8.0
Ribonuclease A	13 500	8.8	33.0
Chymotrypsinogen A	25 000	9.0	17.0
Cytochrome *c*	12 400	9.4	25.0
Lysozyme	14 400	11.0	17.0

Sigma (St. Louis, MO, U.S.A.), unless otherwise noted. Assay Kit 345-B from Sigma was used to measure biological activity of glucose-6-phosphate dehydrogenase and Coomassie protein assay reagent (Pierce) was used to determine protein concentrations. The column efficiencies were measured with acetone as the marker.

Protein-Pak DEAE HR packing in 8-, 15- and 40-μm particle sizes and Protein-Pak DEAE-5PW (nominally 10 μm) were evaluated with 20 m*M* Tris–HCl (pH 8.2) (eluent A), and with 20 m*M* Tris–HCl (pH 8.2) with 1 *M* sodium chloride (eluent B) for all three assays. The proteins in the standard protein mixture were carbonic anhydrase, human transferrin, ovalbumin and soybean trypsin inhibitor with adenosine (molecular weight 267) as the void-volume marker. These proteins were chosen because they cover a wide range of molecular weights and isoelectric points and represent a variety of protein characteristics. The molecular weights and isoelectric points are given in Table I. The DEAE HR series columns were eluted with a gradient of 0 to 25% eluent B over 38 min at a flow-rate of 1.56 ml/min. The gradient for the DEAE-5PW packing was 0 to 25% eluent B over 30 min at a flow-rate of 1.0 ml/min; the flow-rate and gradient duration were adjusted for differences in the column dimensions (see Appendix 1 for scale-up equations). The sample injection volume was 100 μl, containing 0.5 mg protein.

Protein-Pak SP HR in 8-, 15- and 40-μm particle sizes and the Protein-Pak SP-5PW (nominally 10 μm) packings were evaluated by gradient elution with 20 m*M* sodium phosphate (pH 7.0) (eluent A), and 20 m*M* sodium phosphate (pH 7.0) with 1 *M* sodium chloride (eluent B) in all three assays. The molecular weights and isoelectric points of the proteins in the standard protein mixture are given in Table I. The injection volume was 100 μl, containing 0.35 mg protein. The gradient for the SP HR series packings was from 0 to 50% eluent B over 74 min at a flow-rate of 1.56 ml/min. The gradient of the SP-5PW packing was 0 to 50% eluent B over 60 min at a flow-rate of 1.0 ml/min. Flow-rate and gradient duration were adjusted to account for differences in column dimensions and gave equivalent linear velocities.

The ten proteins used for mass recovery experiments with the DEAE 8HR and 5PW columns, are given in Table II. The mass recoveries of these proteins at 100-μg loads (20 μl) were determined from the ratio of peak areas with and without the column in-line.

A similar mass recovery study was performed with 100-μg loads of ten proteins on the Protein-Pak SP 8HR and SP-5PW columns (Table III).

The protein binding capacities of the weak anion exchangers (DEAE) were determined on-line by pumping a bovine serum albumin solution (4 mg/ml) into the column until breakthrough occurred. The column was then flushed with eluent A until the absorbance at 280 nm decreased to less than 0.02 units. The bound protein was then removed with eluent B and quantitated (extinction coefficient equal to 0.65 absorbance units per mg/ml). The binding buffer for this study was 20 m*M* Tris–HCl (eluents A and B), except at pH 10, where the buffer was 20 m*M* 2-(N-cyclohexylamino)-ethanesulphonic acid (CHES).

The protein binding capacities of the strong cation exchangers (SP) were measured with cytochrome *c* (4 mg/ml) at 280 nm (extinction coefficient equal to 1.9 absorbance units per mg/ml). The binding buffers were 20 m*M* sodium acetate and 20 m*M* MES 2-(N-morpholino)ethanesulphonic acid (MES) for pH 5.0, and 20 m*M* sodium phosphate for pH 6.5, 7.0 and 7.5.

TABLE II

MASS RECOVERY OF 100 μg OF VARIOUS PROTEINS USING PROTEIN-PAK DEAE 8HR COMPARED TO DEAE-5PW

Conditions: eluent A: 20 m*M* Tris–HCl, pH 8.2; eluent B: eluent A + 1 *M* sodium chloride; injection volume: 20 μl in eluent A (100 μg); flow-rate: 1 ml/min; gradient: isocratic in 100% eluent B.

Proteins, 100 μg (0.03% of capacity)	Molecular weight	Isoelectric point	Recovery (%)	
			DEAE 8HR	DEAE-5PW
Bovine serum albumin	67 500	4.9	100	95
Carbonic anhydrase	28 000	7.3	100	99
Conalbumin	76 600	6.8	98	97
Cytochrome *c*	12 400	9.5	98	77
Human transferrin	77 000	6.0–6.5	98	100
β-Lactoglobulin	35 000	5.1	99	90
Ovalbumin	44 500	4.7	100	100
Rabbit immunoglobulin G	155 000	6.0–7.0	100	90
Rat immunoglobulin G	155 000	6.0–7.0	100	95
Soybean trypsin inhibitor	21 500	4.5	80	86

The recovery of biological activity was detemined on both types of the Protein-Pak HR material. A Waters 650 Advanced Protein Purification System with a non-metallic 484 detector, 712 WISP, FOXY fraction collector and a Wescan conductivity meter (Santa Claire, CA, U.S.A.) were used for this study.

The recovery of applied biological activity of pure glucose-6-phosphate dehydrogenase, from yeast, was determined on the Protein-Pak DEAE 15HR glass column. The buffers used were 20 m*M* Tris–acetate (pH 8.0) as eluent A and eluent B

TABLE III

MASS RECOVERY OF 100 μg OF VARIOUS PROTEINS USING PROTEIN-PAK SP 8HR COMPARED TO SP-5PW

Conditions: eluent A: 20 m*M* sodium phosphate, pH 7.0; eluent B: eluent A + 1 *M* sodium chloride; injection volume: 20 μl in eluent A (100 μg); flow-rate: 1 ml/min; gradient: isocratic in 100% eluent B.

Proteins, 100 μg (0.03% of capacity)	Molecular weight	Isoelectric point	Recovery (%)	
			SP 8HR	SP-5PW
Chymotrypsin	21 600	8.8	100	96
Chymotrypsinogen A	25 000	9.0	92	96
Cytochrome *c*	12 400	9.4	98	90
Hemoglobin	64 500	7.0	84	65
β-Lactoglobulin	35 000	5.1	90	90
Lysozyme	14 400	11.0	98	95
Myoglobin	17 500	7.0	90	86
Ovalbumin	44 500	4.7	95	90
Ribonuclease A	13 500	8.8	100	95
Soybean trypsin inhibitor	21 500	4.5	93	91

was 20 m*M* Tris–acetate (pH 8.0) plus 0.5 *M* sodium acetate. Glucose-6-phosphate dehydrogenase (100 μg) was injected and eluted over 44 min with a gradient from 0 to 100% eluent B at a flow-rate of 1.25 ml/min. The fractions were collected at 1-min intervals. The glucose-6-phosphate dehydrogenase activity of each fraction was measured by monitoring the reduction of NADP at 340 nm.

The purification of lysozyme from egg white was used to determine recovery of biological activity from a crude preparation on a Protein-Pak SP 8HR glass column. The rate of lysis of *Micrococcus lysodeikticus* was monitored spectrophotometrically at 450 nm [8,9]. The buffers were 20 m*M* sodium phosphate (pH 7.0) (eluent A) and 20 m*M* sodium phosphate (pH 7.0) plus 1 *M* sodium chloride (eluent B). The proteins in egg white (50 mg load) were separated by a linear gradient from 0 to 50% eluent B over 84 min at a flow-rate of 1.56 ml/min. Fractions were collected at 1-min intervals.

APPLICATIONS

Scale-up studies

Sample load was scaled up on a Protein-Pak DEAE 8HR AP1 glass column under the conditions outlined above for the DEAE HR standard protein mixture. The protein resolution assay load of 0.5 mg in 100 μl, which is about 0.2% of the dynamic column capacity, was scaled up to 22 mg protein in 4.4 ml, a 44-fold increase, which is equivalent to 6.2% of the dynamic column capacity.

A second study demonstrated a large-scale preparative purification which involved scale-up from an AP1 (100 mm × 10 mm) to an AP5 (100 mm × 50 mm) glass column. The protein mixture was injected in 110 ml of eluent A containing 550 mg. The same conditions were used as described above for the AP1 glass column, except the flow-rate was 39 ml/min (to maintain a constant linear velocity) and the initial isocratic hold in the gradient was for 25 min (to allow time for sample load onto the column).

Mouse serum

The proteins in mouse serum were separated using identical conditions to those used for the standard protein mixture of the DEAE HR packings. The sample load was 4 mg in 75 μl eluent A.

Plasmid purification

Another application was the separation of pRSVcat plasmid from an RNase-treated and alkaline-lysed preparation on the Waters Protein-Pak DEAE 8HR glass column. Eluent A was 25 m*M* Tris–HCl (pH 8.0) with 1 m*M* EDTA and eluent B was 25 m*M* Tris–HCl (pH 8.0) with 1 m*M* EDTA plus 1 *M* sodium chloride. The preparation (20.8 mg total mass) was loaded at 40% eluent B, pumped isocratically for 40 min, and then increased linearly to 60% eluent B over 40 min at a flow-rate of 1.5 ml/min. This separation was carried out at room temperature.

RESULTS AND DISCUSSION

The average efficiency of the AP1 column, with acetone as the marker, was 2000 theoretical plates for both the 8HR and 15HR packing materials.

The chromatograms for the standard protein mixture for the Protein-Pak DEAE

8HR, 15HR and 40HR are shown in Figs. 1–3 and demonstrate the high resolution capabilities of the 8HR and 15HR using the standard protein mixture. The resolution of a seven-protein mixture at 100 μg load by 8 and 15HR did reflect the two-fold difference in particle size. In addition, the 40HR column gave significantly broader peaks, as expected. The protein resolution was greater on the DEAE-8HR and 15HR column than on the DEAE-5PW column; the DEAE-5PW chromatogram is in Fig. 4. The resolution (R_s) values were measured for the ovalbumin and soybean trypsin inhibitor separation; DEAE 8HR was 24, DEAE 15HR was 20 and DEAE-5PW was 17. The DEAE 15HR column gave better resolution than the DEAE-5PW which has a smaller particle size, 15 *versus* 10 μm, respectively. The separation factors (α) also reflected the improved resolution of the HR materials over the DEAE-5PW column.

The chromatography for the standard protein mix on the SP-8HR, 15HR and 40HR materials are shown in Figs. 5–7. Again, the resolution between the 8HR and 15HR materials was similar and the 40HR had broader peaks. The Protein-Pak SP 8HR and 15HR columns had better resolution of cytochrome *c* and lysozyme than the SP-5PW column, R_s of 33 and 31 *versus* 20, respectively; the chromatogram for the SP-5PW is in Fig. 8.

The figures for the standard protein mixtures show that the proteins are not eluted on the anion exchangers and cation exchangers based on their isoelectric points, p*I*. The ion-exchange process is determined primarily by electrostatic interactions, but

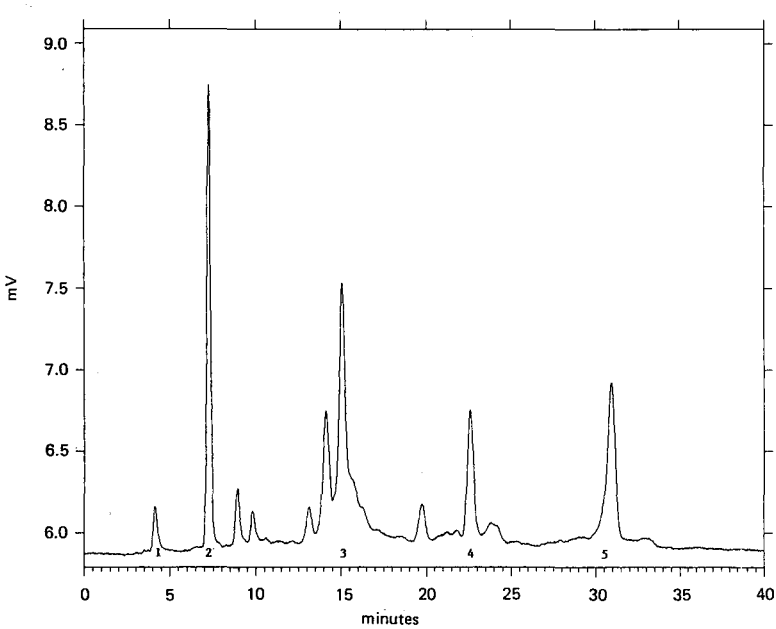

Fig. 1. Protein resolution on Protein-Pak DEAE 8HR anion-exchange column. Column: API (100 mm × 10 mm) glass column; eluent A: 20 m*M* Tris–HCl at pH 8.2; eluent B: eluent A + 1 *M* sodium chloride; flow-rate: 1.56 ml/min; detector: 280 nm; gradient: 0 to 25% eluent B over 38 min; sample load: 0.5 mg protein. Peaks: 1 = adenosine; 2 = carbonic anhydrase; 3 = human transferrin; 4 = ovalbumin; 5 = soybean trypsin inhibitor.

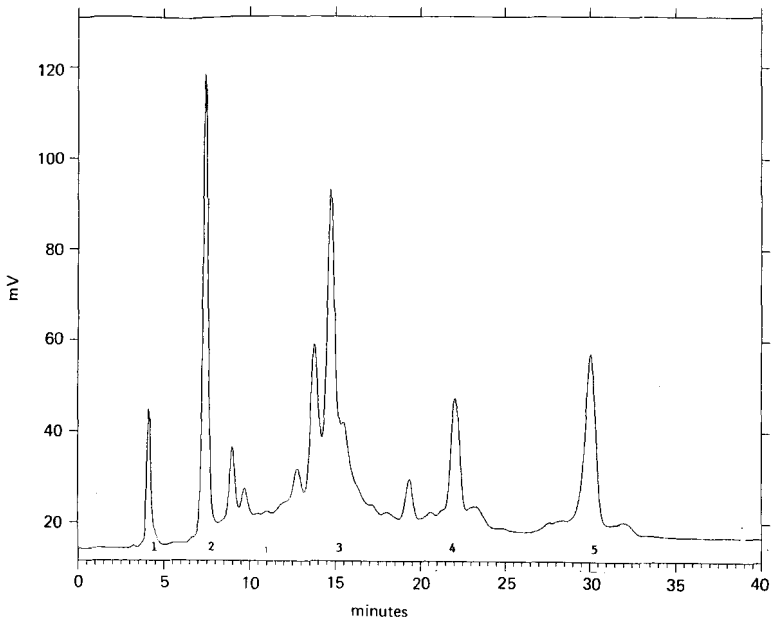

Fig. 2. Protein resolution on Protein-Pak DEAE 15HR anion-exchange column. Conditions and peaks as in Fig. 1.

protein retention is the result of the interaction between the surface charge (not the net charge) of the proteins (Z-value) and that of the stationary phase [10]. Therefore, the elution order of the proteins in the standard mixtures for the SP and DEAE columns (Figs. 1–8) did not follow the order of the pI values.

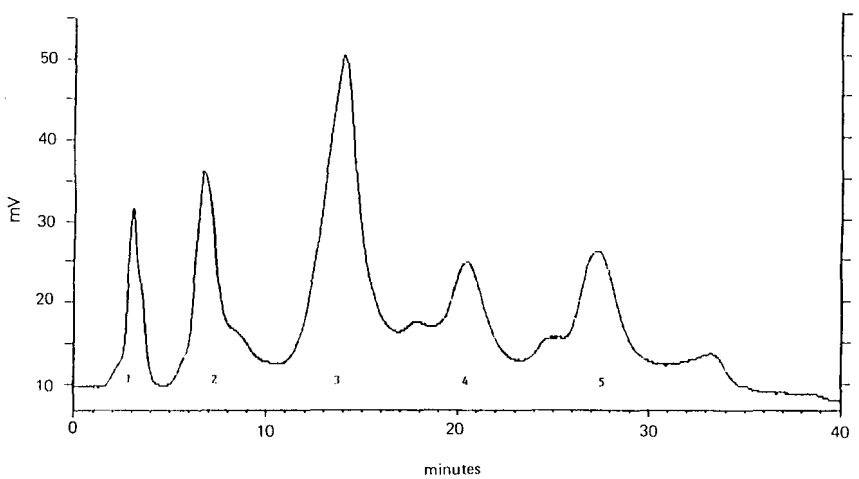

Fig. 3. Protein resolution on Protein-Pak DEAE 40HR anion-exchange column. Conditions and peaks as in Fig. 1.

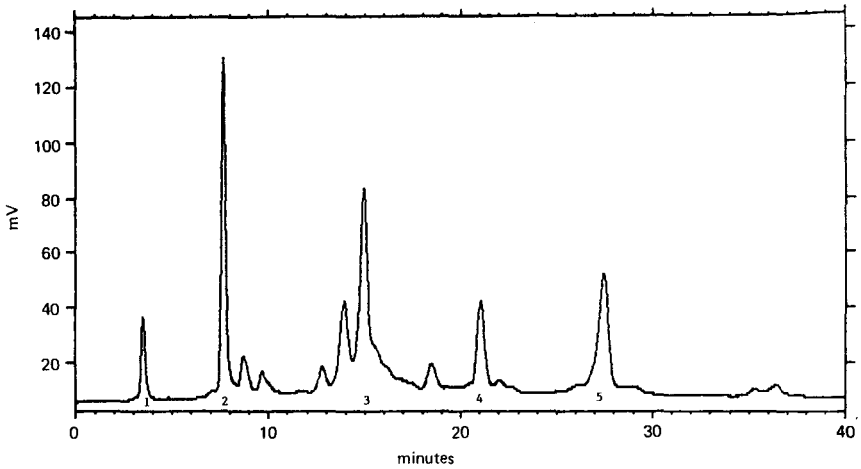

Fig. 4. Protein resolution on Protein-Pak DEAE-5PW anion-exchange column. Column: 75 mm × 8 mm glass column; eluent A: 20 m*M* Tris–HCl at pH 8.2; eluent B: eluent A + 1 *M* sodium chloride; flow-rate: 1 ml/min; detector: 280 nm; gradient: 0 to 25% eluent B over 30 min; sample load: 0.5 mg protein. Peaks: 1 = adenosine; 2 = carbonic anhydrase; 3 = human transferrin; 4 = ovalbumin; 5 = soybean trypsin inhibitor.

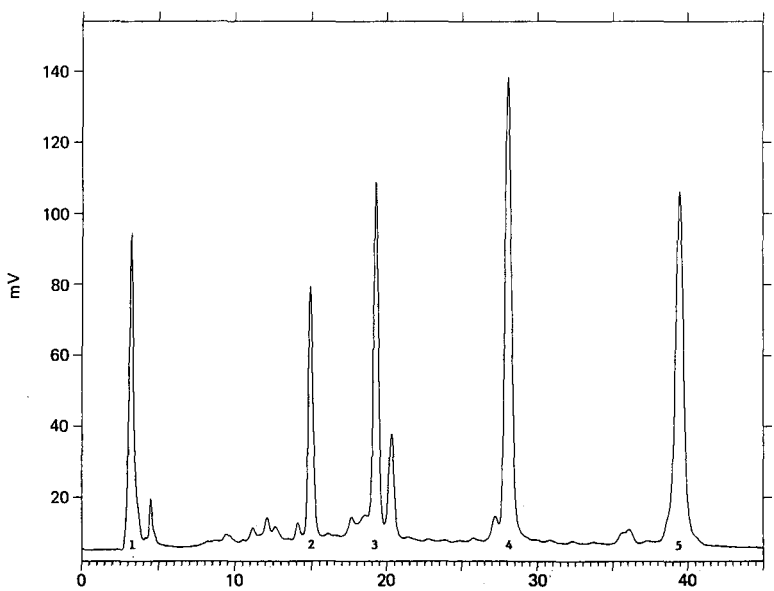

Fig. 5. Protein resolution on Protein-Pak SP 8HR cation-exchange column. Column: API (100 mm × 10 mm) glass column; eluent A: 20 m*M* sodium phosphate at pH 7.0; eluent B: eluent A + 1 *M* sodium chloride; flow-rate: 1.56 ml/min; detector: 280 nm; gradient: 0 to 50% eluent B over 74 min; sample load: 0.35 mg protein. Peaks: 1 = myoglobin; 2 = ribonuclease A; 3 = chymotrypsinogen A; 4 = cytochrome *c*; 5 = lysozyme.

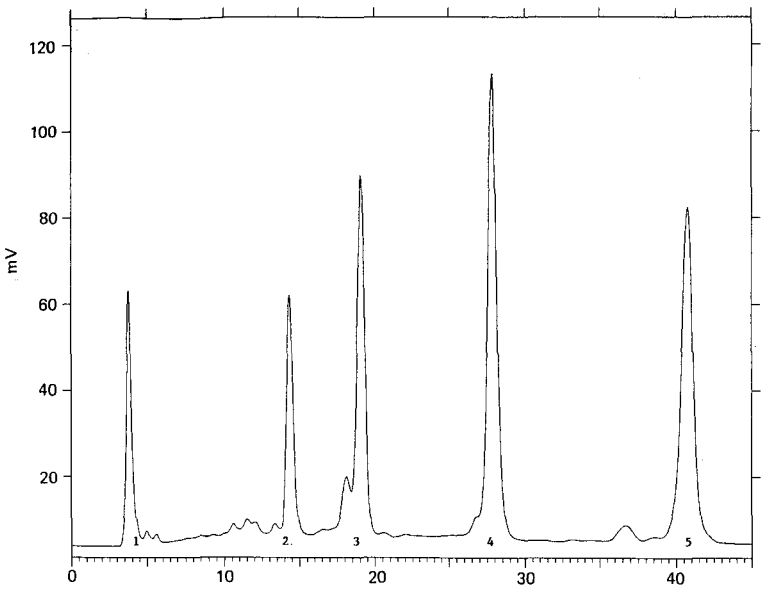

Fig. 6. Protein resolution on Protein-Pak SP 15HR cation-exchange column. Conditions and peaks as in Fig. 5.

The hydrophilic nature of the polymer surface resulted in high recovery of basic and acidic proteins regardless of the charge of the packing; the 1000-Å pore size led to excellent recovery for a full range of molecular weights. The mass recovery data for the Protein-Pak DEAE 8HR and DEAE-5PW columns are summarized in Table II. All of the recoveries on the DEAE 8HR were 98% or greater except for the soybean trypsin

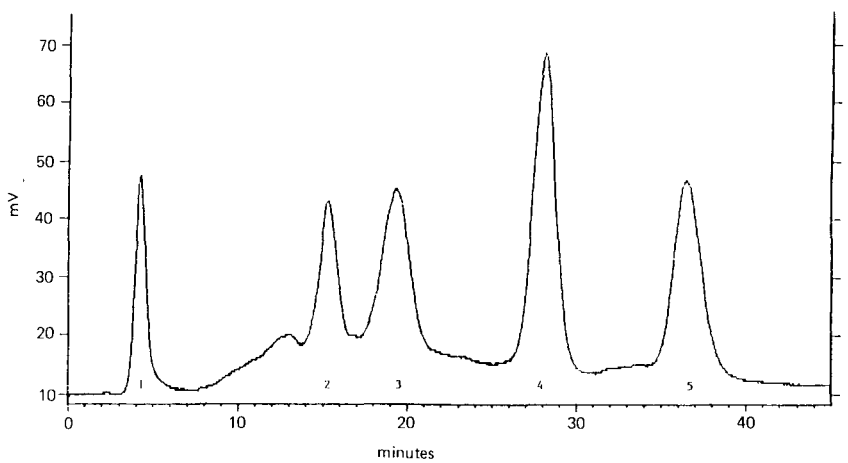

Fig. 7. Protein resolution on Protein-Pak SP 40HR cation-exchange column. Conditions and peaks as in Fig. 5.

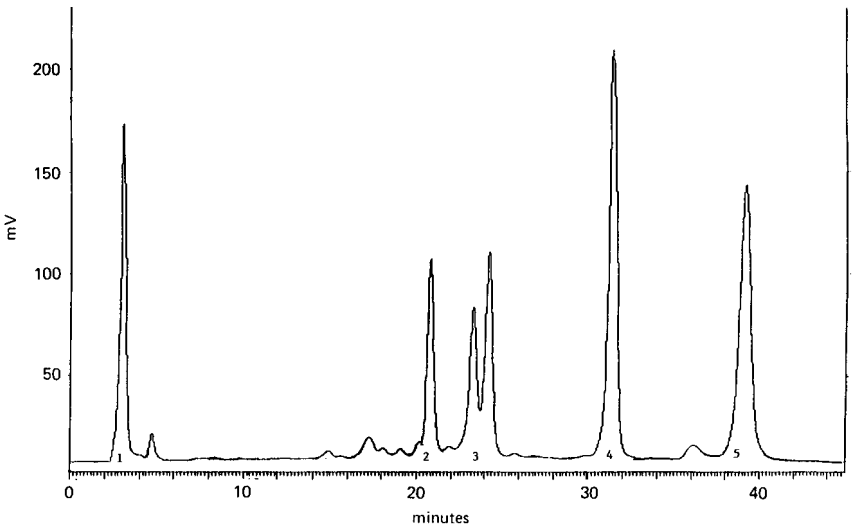

Fig. 8. Protein resolution on Protein-Pak SP-5PW cation-exchange column. Column: 75 mm × 8 mm glass column; eluent A: 20 m*M* sodium phosphate at pH 7.0; eluent B: eluent A + 1 *M* sodium chloride; flow-rate: 1 ml/min; detector: 280 nm; gradient: 0 to 50% eluent B over 60 min; sample load: 0.35 mg protein. Peaks: 1 = myoglobin; 2 = ribonuclease A; 3 = chymotrypsinogen A; 4 = cytochrome *c*; 5 = lysozyme.

inhibitor which had an 80% recovery. The packing has low non-specific binding using cytochrome *c*, and the more hydrophobic proteins, such as ovalbumin, did not interact with the polymer at pH 8.0. The recovery of cytochrome *c* was 77% on the DEAE-5PW column. Despite its high isoelectric point of 9.5, cytochrome *c* was partially retained on the DEAE-5PW as expected; 43% of the recovered protein was in a retained peak. The difference in behavior of cytochrome *c* on the two DEAE packings suggests that there may be some residual carboxyl groups on the DEAE-5PW polymer backbone; the presence of negative charges is further supported by the fact that the retained cytochrome *c* was recovered with high salt. The mass recoveries of the remaining proteins on the DEAE-5PW were greater than 90%, except for soybean trypsin inhibitor which was 86%.

The protein mass recoveries for the Protein-Pak SP HR and the SP-5PW are summarized in Table III. The recoveries on the SP HR packings were 90% or greater except for that of hemoglobin which had an 84% recovery. The recoveries on the Protein-Pak SP-5PW column were all 86% or greater, except for hemoglobin which had only 65% recovery. The SP-5PW was reported to give only 73% recovery of hemoglobin at pH 6.0 and that the recovery of hemoglobin is dependent on the gradient steepness and the pH. Hemoglobin is comprised of four subunits and is difficult to recover as an intact protein, resulting in possible mass loss on the ion-exchange surface. Alternatively, if the conformational changes in hemoglobin during chromatography affect the extinction coefficient at 280 nm, then the resulting error in the spectrophotometric analysis could result in low percent recoveries.

The degrees of substitution of ion exchangers as determined by titration (total

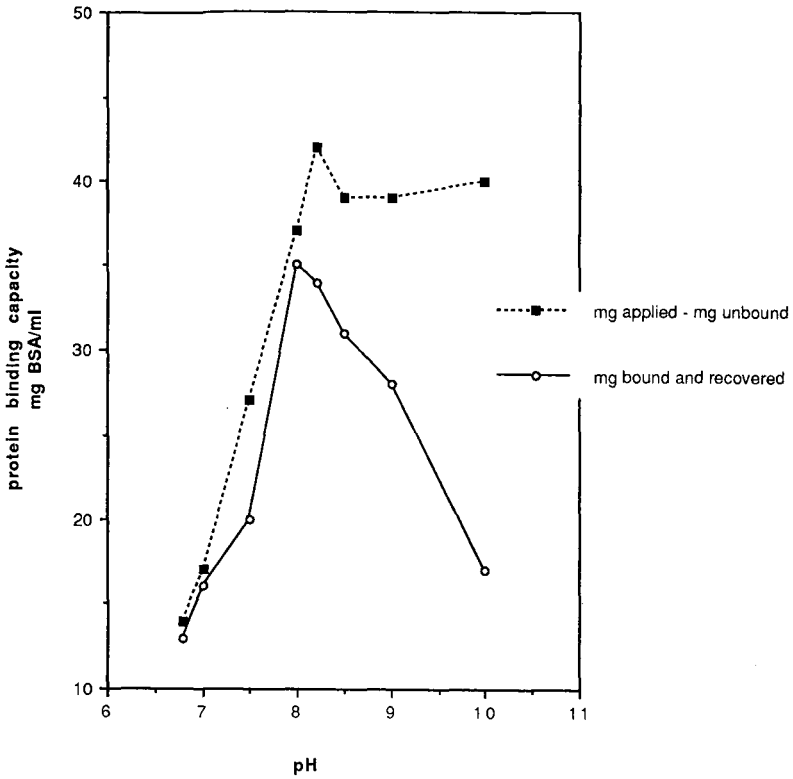

Fig. 9. Protein-binding capacity as a function of pH on Protein-Pak DEAE 8HR. Eluent A (for pH 6.8–9.0): 20 m*M* Tris–HCl; eluent B (for pH 6.8–9.0): eluent A + 1 *M* sodium chloride; eluent A (for pH 10.0): 20 m*M* CHES; eluent B (for pH 10.0): eluent A + 1 *M* sodium chloride; flow-rate: 1 ml/min; detector: 280 nm; sample: bovine serum albumin in eluent A.

ionic capacity) are 100 to 500 μmol/ml of packing [11]. The average degree of substitution of the Protein-Pak HR series is 250 μmol/ml. For Mono Q and Mono S the corresponding figure is 300 μmol/ml. The available capacity or protein-binding capacity of an ion-exchange packing is defined as the amount of protein that can be bound. Only part of the ionic groups are available to bind proteins. The capacity depends on both the operating conditions and the given protein.

The capacity for bovine serum albumin (BSA) was studied as a function of pH on the DEAE 8HR packing with BSA. Fig. 9 shows that there was an increase in capacity as the pH was increased. A plateau was seen after pH 8.0 when the capacity was measured by the amount retained (measured as the difference between total mg BSA applied and mg BSA unbound). However, a decrease in capacity was noticed if the protein binding capacity was only from the amount of bound BSA that was recovered. In all cases the mg bound relative to the amount recovered was used to measure percent recovery of BSA.

The above results may be interpreted from a conclusion reached by Gooding and Schmuck [12]. They noted an increase in protein-binding capacity when they compared

TABLE IV

STUDY OF PROTEIN-BINDING CAPACITY *VERSUS* pH ON THE PROTEIN-PAK DEAE 8HR

Conditions: eluent A: 20 m*M* Tris–HCl (pH 6.8–9.0); eluent B: eluent A + 1 *M* sodium chloride; eluent A: 20 m*M* CHES (pH 10.0); eluent B: eluent A + 1 *M* sodium chloride. Sample: bovine serum albumin in eluent A.

pH	Capacity $\left(\frac{\text{mg applied} - \text{mg bound}}{\text{column volume}}\right)$	Capacity $\left(\frac{\text{mg bound and recovered}}{\text{column volume}}\right)$	Recovery (%)
6.8	14	13	94
7.0	17	16	97
7.5	27	20	86
8.0	37	35	95
8.2	42	34	88
8.5	39	31	80
9.0	39	28	72
10.0	40	17	44

weak and strong anion exchangers. In addition, they noted that the backbone of the polymeric resin became more hydrophobic as the pH increased. Therefore, they concluded that the capacity measured was a combination of both ionic and hydrophobic interactions. The recovery data for the Protein-Pak DEAE HR packing supports their observation since when the pH was increased to 10.0, the protein-binding capacity measured by the amount retained remained on a plateau of 40 mg BSA/ml, but the recovery of BSA dropped to 44%; data are shown in Table IV. The BSA bound by hydrophobic interactions did not elute, therefore the capacity measured by the amount of protein recovered in high salt instead of the amount retained, dropped to only 17 mg BSA/ml at pH 10.0 from the 34 mg/ml at pH 8.2. From these data, the best pH range to determine protein-binding capacity for the DEAE packings was pH 8.0 to 8.5.

The Protein-Pak DEAE 8HR had an average capacity of 45 mg BSA/ml while the DEAE 15HR and 40HR had capacities of 40 mg BSA/ml. The DEAE-5PW had a protein-binding capacity of 68 mg/ml of BSA. When these values were compared on a per column basis, the DEAE-HR (API glass column 100 × 10 mm) columns had more capacity than the DEAE-5PW (75 × 8 mm); 8HR, 15HR and 40HR had capacities of 310–350 mg BSA/column and DEAE-5PW was 262 mg BSA/column, as shown in Table V. For reference, a Pharmacia Mono Q 5/5 HR (1 ml volume) column has a capacity of 100 mg BSA, as measured by the same protein-binding capacity procedure. Since the capacity is extremely sensitive to the availability of charged groups and thus to pore size, differences in capacity are expected for the various ion exchangers, even those with similar degrees of substitution [11].

A pH *versus* protein-binding capacity curve was also examined for the Protein-Pak SP 8HR packing. The capacity was highest at pH 5, 30 mg cytochrome *c*/ml, dropped to 13.6 mg cytochrome *c* at pH 6.5 and remained relatively constant between pH 6.5 to 7.5. The capacity at pH 5.0 was higher in 25 m*M* MES buffer (pK_a 6.15), 39 mg cytochrome *c*/ml, than in 20 m*M* sodium acetate buffer, 30 mg cytochrome *c*.

TABLE V

PROTEIN-BINDING CAPACITY OF THE PROTEIN-PAK HR SERIES AND THE PROTEIN-PAK 5PW PACKINGS

Conditions: *DEAE*: eluent A: 20 m*M* Tris–HCl, pH 8.2; eluent B: eluent A + 1 *M* sodium chloride; sample: bovine serum albumin in eluent A. *SP*: eluent A: 25 m*M* MES, pH 5.0; eluent B: eluent A + 1 *M* sodium chloride; sample: cytochrome *c* in eluent A. *Column HR series*: API (100 mm × 10 mm) = 7.85 ml. *Column 5PW*: (75 mm × 8 mm) = 3.80 ml.

	mg BSA/ml	mg BSA/column	mg cyto-chrome *c*/ml	mg cyto-chrome *c*/column
Anion exchangers				
Protein-Pak DEAE 8HR	45	353		
Protein-Pak DEAE 15HR	40	314		
Protein-Pak DEAE 40HR	40	314		
Protein-Pak DEAE-5PW	69	262		
Cation exchangers				
Protein-Pak SP 8HR			40	314
Protein-Pak SP 15HR			40	314
Protein-Pak SP 40HR			22	173
Protein-Pak SP-5PW			50	190

The average protein-binding capacities of the SP 8HR and 15HR were greater than that of the SP 40HR, 40 mg/ml *versus* 22 mg cytochrome *c*/ml. The SP-5PW column had a protein-binding capacity of 50 mg/ml of cytochrome *c*. When these values were compared on a per column basis, the SP 8HR and 15HR (AP 100 × 10 mm) glass columns have more capacity than the SP-5PW (75 × 8 mm) column: the values for SP 8HR and 15HR were 314 mg cytochrome *c*/column and SP-5PW was 190 mg cytochrome *c*/column, as given in Table V. The corresponding value for a Pharmacia Mono S 5/5 HR column (1 ml volume) was 60 mg cytochrome *c* as measured by the outlined procedure.

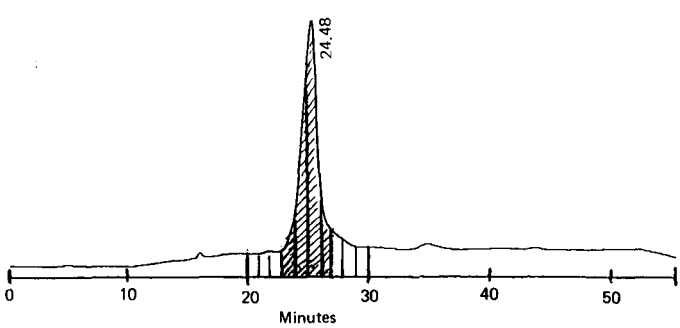

Fig. 10. Recovery of mass and biological activity on Protein-Pak DEAE 15HR. Column: API (100 mm × 10 mm) glass column; eluent A: 20 m*M* Tris–acetate at pH 8; eluent B: eluent A + 0.5 *M* sodium acetate; flow-rate: 1.25 ml/min; detector: 280 nm; gradient: 0 to 100% eluent B over 44 min; sample: glucose-6-phosphate dehydrogenase from yeast (1 mg/ml); injection volume: 100 μl (100 μg).

TABLE VI

RECOVERY OF MASS AND BIOLOGICAL ACTIVITY

Conditions: *Protein-Pak DEAE 15HR*: eluent A: 20 m*M* Tris–acetate, pH 8.0; eluent B: eluent A + 0.5 *M* sodium acetate; sample: glucose-6-phosphate dehydrogenase from yeast (1 mg/ml); reference: Fig. 11. *Protein-Pak SP 8HR*: eluent A: 20 m*M* sodium phosphate, pH 7.0; eluent B: eluent A + 1 *M* sodium chloride; sample: hen egg whites (25 mg/ml); reference: Fig. 12.

	DEAE 15HR	SP 8HR
Mass applied	100 μg	50 mg
Mass recovered	115 μg	44.9 mg
Mass recovery (%)	115	90
Units activity applied	18.5	94 400
Units activity recovered	16.8	76 673
Units activity recovery (%)	91	81
Initial specific activity (units/mg)	185	1888
Specific activity over 4 fractions (units/mg)	183 (fractions 23–27)	44 838 (fractions 41–45)
Purification factor	0.99	24

Biological activity

Glucose-6-phosphate dehydrogenase from yeast was assayed for recovery of biological activity and protein mass on the Protein-Pak DEAE 15HR material; the data are given in Fig. 10 and Table VI. The specific activity of the pooled four main fractions was 183 units/mg, which shows that the protein was not denatured or altered on the column because the specific activity prior to chromatography was the same, 185 units/mg. There was a 91% recovery of biological activity units and a 115% recovery of total protein.

The Protein-Pak SP 8HR material was used in a purification of lysozyme from chicken egg white; data are given in Table VI and chromatography is in Fig. 11. The majority of the components in egg white are acidic, with p*I* values between 3.9 and 6.6;

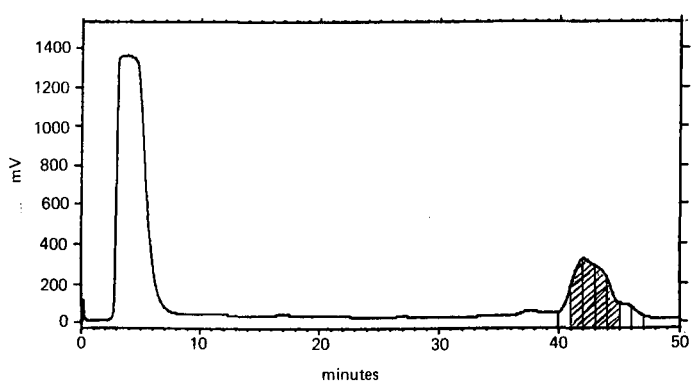

Fig. 11. Purification of lysozyme from egg white on Protein-Pak SP 8HR. Column: API (100 mm × 10 mm) glass column; eluent A: 20 m*M* sodium phosphate at pH 7.0; eluent B: eluent A + 1 *M* sodium chloride; flow-rate: 1.56 ml/min; detector: 280 nm; gradient: 0 to 50% eluent B over 84 min; sample: egg white from hen (25 mg/ml); injection volume: 50 mg.

only lysozyme (p*I* 10.5–11.0) and avidin (p*I* 9.5–10.0) are on the basic side [13]. The initial specific activity of lysozyme, before chromatography, was 1888 units/mg. The specific activity of the pooled four main fractions was 44 838 units/mg which shows a 24-fold purification factor of the lysozyme. There was a 90% recovery of total protein and an 81% recovery of biological activity units.

APPLICATIONS

Scale-up studies

The goal of the scale-up was to demonstrate scalability between the AP1 and AP5 glass columns utilizing 5–10% of the total dynamic capacity of the column. The protein mixture was baseline resolved at the 0.5 mg protein load on the Protein-Pak DEAE 8HR glass column, as previously shown in Fig. 1. The chromatography was repeated without the adenosine, the unretained marker, in the mixture (Fig. 12). When the sample load on this column was scaled-up from 0.5 mg to 22 mg (from 0.2% to 6.2% of total column dynamic capacity), the proteins were still well resolved. The retention times of the peaks were within 5% of each other, as shown in Fig. 13. To demonstrate the scalability of the Advanced Purification columns, an AP5 (100 × 50 mm) glass column was packed with the DEAE-8HR material. The AP5 column was loaded with the protein mix at 6% of total column capacity or 550 mg in 110 ml, the same % column capacity as shown on the AP1 column but a twenty-five times greater amount of protein. The equations that were used to scale-up the separation are given in Appendix 1. The separation on the AP5 column demonstrates the ability to scale to larger diameter columns with the same particle size packing and obtain equivalent separations, as shown in Figs. 13 and 14.

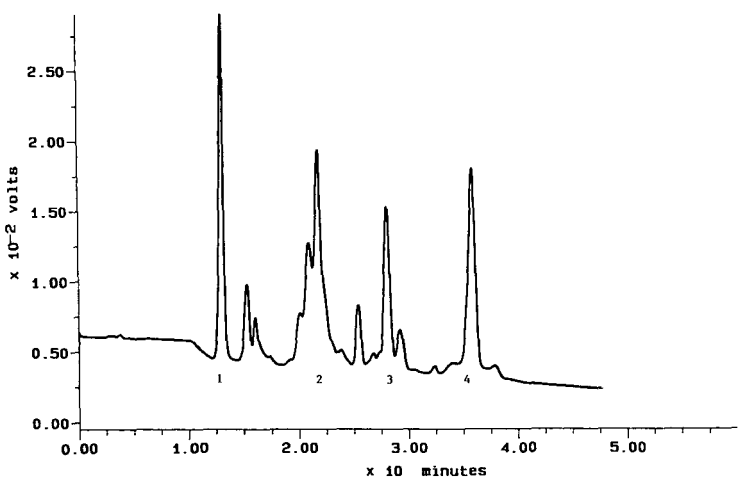

Fig. 12. Scale-up study: 0.5 mg protein mixture load on AP1 glass column. Column: AP1 (100 mm × 10 mm) glass column; eluent A: 20 m*M* Tris–HCl at pH 8.2; eluent B: eluent A + 1 *M* sodium chloride; flow-rate: 1.56 ml/min; detector: 280 nm; gradient: 0 to 25% eluent B over 38 min; sample load: 0.5 mg protein in 100 μl eluent A (0.2% of dynamic column capacity). Peaks: 1 = carbonic anhydrase; 2 = human transferrin; 3 = ovalbumin; 4 = soybean trypsin inhibitor.

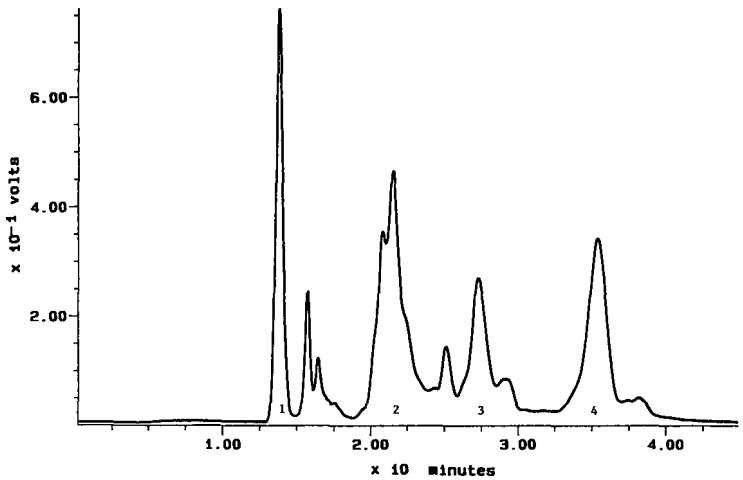

Fig. 13. Scale-up study: 22 mg protein mixture load on AP1 glass column. Column: AP1 (100 mm × 10 mm) glass column; eluent A: 20 m*M* Tris–HCl at pH 8.2; eluent B: eluent A + 1 *M* sodium chloride; flow-rate: 1.56 ml/min; detector: 280 nm; gradient: 0 to 25% eluent B over 38 min; sample load: 22 mg protein in 4.4 ml eluent A (6.2% of dynamic column capacity). Peaks: 1 = carbonic anhydrase; 2 = human transferrin; 3 = ovalbumin; 4 = soybean trypsin inhibitor.

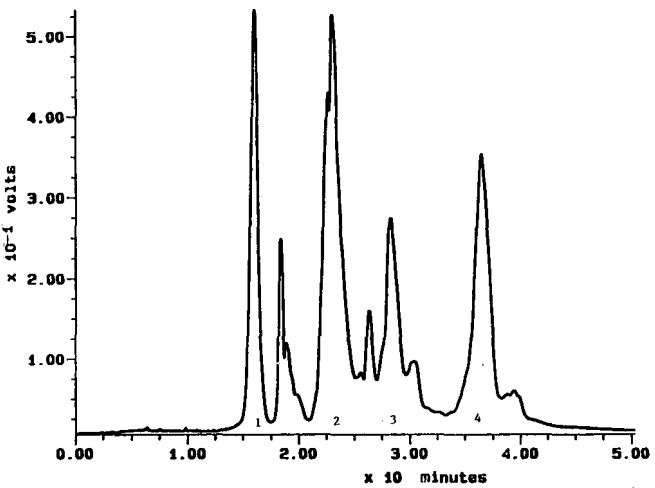

Fig. 14. Scale-up study: 550 mg protein mixture load on AP5 glass column. Column: AP5 (100 mm × 50 mm) glass column; eluent A: 20 m*M* Tris–HCl at pH 8.2; eluent B: eluent A + 1 *M* sodium chloride; flow-rate: 39 ml/min; detector: 280 nm; gradient: 0 to 25% eluent B over 38 min; sample load: 550 mg protein in 110 ml eluent A (6% of dynamic column capacity). Peaks: 1 = carbonic anhydrase; 2 = human transferrin; 3 = ovalbumin; 4 = soybean trypsin inhibitor.

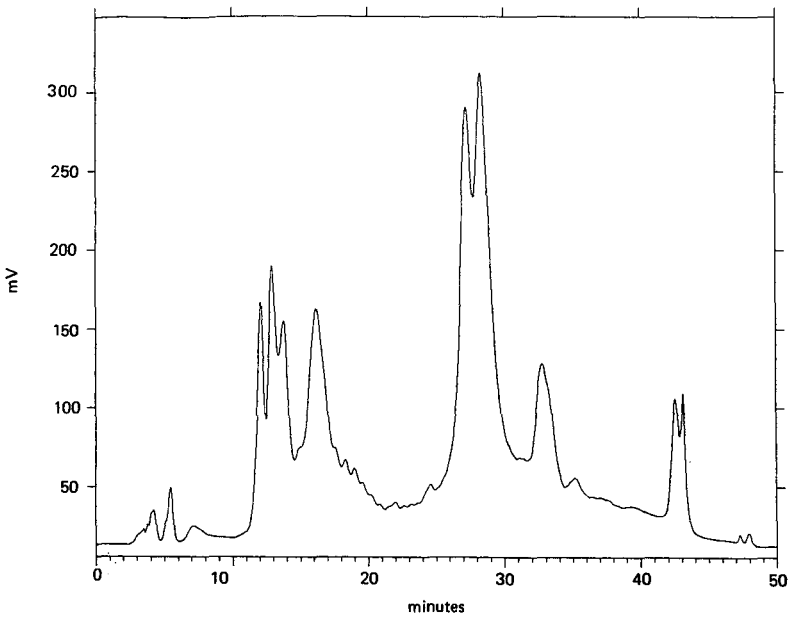

Fig. 15. Resolution of mouse serum proteins on Protein-Pak DEAE 15HR anion-exchange column. Column: AP1 (100 mm × 10 mm) glass column; eluent A: 20 m*M* Tris–HCl at pH 8.2; eluent B: eluent A + 1 *M* sodium chloride; flow-rate: 1.56 ml/min; detector: 280 nm; gradient: 0 to 25% eluent B over 38 min; sample load: 75 μl (4 mg).

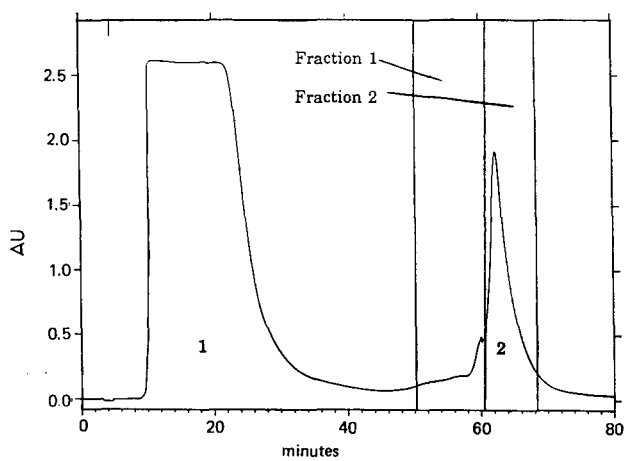

Fig. 16. Plasmid separation on Protein-Pak DEAE 8HR anion-exchange column. Column: AP1 (100 mm × 10 mm) glass column; eluent A: 25 m*M* Tris–HCl with 1 m*M* EDTA at pH 8; eluent B: eluent A + 1 *M* sodium chloride; flow-rate: 1.5 ml/min; detector: 280 nm; gradient: isocratic at 40% eluent B for 40 min and then increased linearly to 60% eluent B over 40 min; sample load: 20.8 mg of a partially purified preparation containing pRSVcat plasmid. Peaks: 1 = unretained peak; 2 = plasmid.

Mouse serum

Mouse serum contains polyclonal immunoglobulin G, transferrin and serum albumin as major proteins. Mouse ascites fluid for monoclonal antibody production has a similar protein composition. The identity of the peaks were not determined, but the overall resolution of the serum proteins was noted. The DEAE 8HR and 15HR resolved the mouse serum proteins into 14 and 12 peaks. The performance of DEAE 8HR is similar to that of the DEAE-5PW which resolved the mouse serum into 16 peaks. The chromatogram for mouse serum on the DEAE 15HR is shown in Fig. 15.

Plasmid purification

Traditionally, purification of plasmid DNA from crude cell lysates containing proteins, RNA and chromosomal DNA was performed using cesium chloride density gradient ultracentrifugation in the presence of ethidium bromide. This technique is time-consuming and does not yield a totally pure plasmid fraction. The isolation of the pRSVcat plasmid on the Protein-Pak DEAE 8HR material gave a high purity fraction; the chromatography is in Fig. 16. The isolation of the plasmid was complete in less than 60 min and the purified fraction possessed excellent biological activity.

CONCLUSION

The Protein-Pak HR series of resin-based, high-performance ion-exchange packings provide high resolution, excellent recovery and high capacity. The Protein-Pak HR series performed comparable and in some cases better than the Protein-Pak 5PW columns. The range of particle sizes and column configurations facilitates full scalability from mg to gram quantities for chromatographic separations of biomolecules such as proteins and nucleic acids. The scale-up strategy shown here demonstrates that the new Protein-Pak HR series successfully employs the same particle size and chemistry to optimize the separation and loading at the analytical scale and to obtain the same resolution at the preparative scale after adjusting the load and linear velocity for column diameter.

APPENDIX 1

Scale-up equations

Sample load. Scale the sample load according to the internal volumes of the columns, as follows:

$$m_1 = m_2 \cdot \frac{d_1^2 l_1}{d_2^2 l_2}$$

where m = sample mass (mg), d = internal diameter of the AP column (cm), l = length of the AP column (cm); in all equations, subscripts 1 and 2 refer to the preparative and analytical columns, respectively.

Flow-rate. Scale-up the flow-rate (F) to maintain the same linear velocity in the preparative column as in the previously developed analytical separation, as follows:

$$F_1 = F_2 \cdot \frac{d_1^2}{d_2^2}$$

Gradient duration. Scale-up the duration of the gradient so the preparative gradient occurs over the same number of column volumes as the analytical gradient, as follows:

$$t_{g_1} = \frac{V_1 t_{g_2} F_2}{V_2 F_1}$$

where V = void volume of the AP column (ml) and t_g = gradient duration (min).

ACKNOWLEDGEMENT

Holly L. Hodgdon contributed toward this research during her internship at Waters Chromatography, Division of Millipore, from Worcester Polytechnic Institute in Worcester, MA, U.S.A.

REFERENCES

1 M. T. W. Hearn, A. N. Hodder and M. I. Aguilar, *J. Chromatogr.*, 458 (1988) 45.
2 F. E. Regnier, *Science (Washington, D.C.)*, 222 (1983) 243.
3 H. A. Sober and E. A. Peterson, *J. Am. Chem. Soc.*, 78 (1956) 751.
4 J. Porath, J. C. Janson and T. Låås, *J. Chromatogr.*, 60 (1971) 167.
5 Y. Kato, K. Nakamura and T. Hashimoto, *J. Chromatogr.*, 245 (1982) 193.
6 S. H. Chang, K. M. Gooding and F. E. Regnier, *J. Chromatogr.*, 120 (1976) 321.
7 Y. Kato, K. Nakamura and T. Hashimoto, *J. Chromatogr.*, 266 (1983) 385.
8 C. C. Worthington (Editor), *Worthington Enzyme Manual*, Worthington Biochemical, Freehold, NJ, 1988, p. 219.
9 D. Shugar, *Biochim. Biophys. Acta*, 8 (1952) 302.
10 W. Kopaciewicz, M. A. Rounds, J. Fausnaugh and F. E. Regnier, *J. Chromatogr.*, 266 (1983) 3.
11 J. Janson and L. Ryden, *Protein Purification, Principles, High Resolution Methods and Applications*, VCH, New York, 1989, p. 117.
12 K. M. Gooding and M. N. Schmuck, *J. Chromatogr.*, 50 (1985) 139.
13 G. D. Fasman (Editor), *CRC Handbook of Biochemistry and Molecular Biology*, CRC Press, Boca Raton, FL, 3rd ed., 1982, p. 1293.

Journal of Chromatography, 535 (1990) 147–161
Elsevier Science Publishers B.V., Amsterdam

CHROMSYMP. 2014

Monosized stationary phases for chromatography

TURID ELLINGSEN* and ODDVAR AUNE
SINTEF Applied Chemistry, Trondheim (Norway)
JOHN UGELSTAD
University of Trondheim, Trondheim (Norway)
and
STEINAR HAGEN
Dyno Particles AS, Lillestrøm (Norway)

ABSTRACT

Polymer particles with a highly monodisperse particle size distribution were produced by a two-step microsuspension method. This process is based on the activation of monosized polymer seed particles by the introduction of a low-molecular-weight material, which leads to a large increase in the monomer swelling capacity of the seed particles. The versatility of the process allows the preparation of polymer monosized compact or macroporous particles of predetermined particle size in the range 1–100 μm and with application of a wide selection of polymeric materials. Underivatized, rigid, porous particles were developed for size-exclusion chromatography in organic solvents. The uniform packing that may be achieved with monosized particles has resulted in chromatographic columns with unusual efficiency and separation capacity. By coating the particle surface with a hydrophilic cross-linked polymer, supports for aqueous phase ion-exchange and size-exclusion chromatography may be produced.

INTRODUCTION

The conventional method of preparing polymeric packing materials is by suspension polymerization processes. Such methods involve the addition of monomer or monomer mixtures and a monomer-soluble initiator to a stirred reactor containing water with a small amount of steric stabilizer. Polymerization is effected by heating the reaction mixture, and the product particle size distribution is determined by parameters such as speed of stirring, polymerization temperature and type and amount of stabilizer. A broad particle-size distribution is a typical result of this method.

Monodisperse, small latex particles of diameter 0.5 μm may be produced by well known emulsion polymerization methods if the reaction conditions and the purity of the reagents are carefully controlled. The preparation of larger monosized beads has been a challenge to polymer chemists for many years. A method of successive seeding was published by Kim *et al.* [1]. This method involves equilibrium swelling of the seed particles with monomer before polymerization is carried out. In order to obtain a substantial increase in particle size, the sequence of swelling and polymer-

0021-9673/90/$03.50

ization must be repeated several times, *e.g.*, five times to go from 1 to 10 μm. This is so because polymer particles in aqueous dispersion are capable of absorbing only a limited amount of monomer, *i.e.*, of the order of 2–5 times by volume [2]. The low swelling ratio implies that during most of the successive seeding process the particles are in "sticky-state" conditions with a high risk of particle coagulation. Moreover, the low swelling ratio means that the seed constitutes a substantial part by volume of the swollen particles. This may cause phase separation and particle deformation by the subsequent polymerization if the monomer applied in the final polymerization is different from that in the seed.

In a series of papers, Ugelstad and co-workers [3–6] described new processes by which highly monodisperse polymer particles may be prepared by a two-step activated swelling technique. These processes resulted from developments of methods by which the capacity of polymer particles to absorb the monomer is greatly enhanced.

THE ACTIVATED SWELLING METHOD

The main feature of the new processes is that one initially activates polymer seed particles so that in aqueous dispersion they are capable of absorbing monomer in an amount which far exceeds that of pure polymer particles. The activation of the seed particles results from the presence in the particles of a highly water-insoluble, relatively low-molecular-weight compound (Y), which is introduced under conditions that allow it to be transported through the aqueous phase to become absorbed in the seed.

For comparison of the swelling capacity of such activated particles with that of pure polymer particles the following equations should be considered:

(i) swelling of pure polymer particles with monomer (Morton equation [2]):

$$\ln \varphi_M + \varphi_P + \varphi_P^2 \chi_{MP} + 2\bar{V}_M \gamma / rRT = 0 \tag{1}$$

(ii) swelling of polymer particles containing compound Y:

$$\ln \varphi_M + (1 - J_M/J_Y)\varphi_Y + \varphi_P + \varphi_Y^2 \chi_{MY} + \varphi_P^2 \chi_{MP} + \varphi_Y \varphi_P (\chi_{MY} + \chi_{MP} - \chi_{YP} J_M/J_Y) + 2\bar{V}_M \gamma / rRT = 0 \tag{2}$$

where φ_i is the volume fraction of compound i, χ_{ij} is the interaction energy per mole of compound i, J_M/J_Y is the ratio of number of segments in the monomer, M, and the oligomer, Y, $\bar{V}_M$ is the partial molar volume of the monomer, γ is the interfacial tension and r is the radius of the particles at equilibrium.

The increase in swelling capacity when part of the polymer in the particles is replaced with an oligomer, Y, is illustrated in Fig. 1, which shows the relationship between the logarithm of the volume of monomer V_M absorbed by the total volume of the activated particles $V_Y + V_P$ and log γ/r_0, where r_o is the radius of the polymer/oligomer particles at the start. The volume $V_Y + V_P$ is set equal to 1. Graphical curves are given for various compositions, *i.e.*, from pure polymer particles, $V_Y = 0$, $V_P = 1$, to pure oligomer, $V_Y = 1$, $V_P = 0$. The value of J_M/J_Y is set equal to 0.2, $\chi_{MY} = \chi_{MP} = 0.5$ and $\chi_{YP} = 0$.

As shown in Fig. 1, the swelling capacity at a given value of γ/r_0 increases with

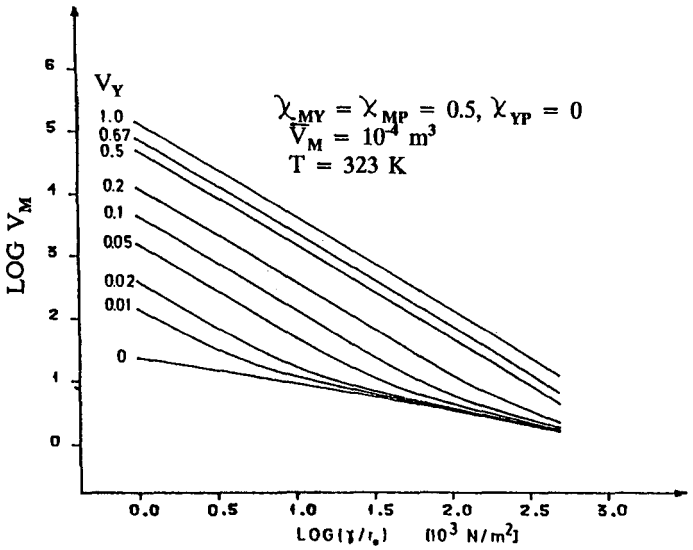

Fig. 1. Volume of monomer, V_M, which may be absorbed per unit volume of seed particles as a function of γ/r_0 at different values of V_Y. r_0 = radius of the polymer/oligomer particles prior to swelling. $V_Y + V_P = 1$.

increasing ratio of compound Y to polymer in the seed particles. Fig. 1 also shows that the swelling increases towards lower values of γ/r_0, *i.e.*, as the particle radius increases and the interfacial tension decreases.

As an example, with an interfacial tension of 10 mN/m and seed particles of 1-μm radius, containing 50% of compound Y, one would expect a swelling capacity of the seed particles which is 200 times higher than that of pure polymer.

Three methods have been applied to introduce oligomeric (Y) material into the particles in the first step of the process:

(1) Polymer seed particles are swollen with monomer containing a chain-transfer agent, followed by polymerization.

(2) Polymer seed particles are swollen with an oil-soluble initiator and monomers of types and in such a ratio that the subsequent polymerization leads to the formation of oligomeric material.

(3) Polymer seed particles are swollen with a relatively low-molecular-weight, highly water-insoluble compound (Y). To facilitate the diffusion process by which Y is transported through the water phase to the particles, compound Y may be added in the form of a finely divided aqueous dispersion.

In method 3, the swelling of the particles with Y in the first step then takes the form

$$\ln \varphi_Y + \varphi_P + \varphi_P^2 \chi_{YP} + 2\bar{V}_Y \gamma / rRT = 2\bar{V}_Y \gamma / r_Y RT \qquad (3)$$

where r_Y is the radius of the droplets of Y. An oil-soluble initiator may be used as compound Y, which then acts boths as an initiator for the polymerization and as an activator for monomer absorption. Also, the second-step swelling (eqn. 2) may be

facilitated by addition of the monomers in the form of an aqueous emulsion [4].

Starting with monosized seed particles, these swelling processes, when properly performed, secure an equal swelling of each particle, maintaining the monodispersity during the process. By combination of methods 1 and 2 with method 3, one may obtain monodisperse product particles which are more than 1000 times larger by volume than the original seed particles.

A characteristic feature of this process is that, when the polymerization of the monomer or monomer mixture is started, all necessary ingredients are present in the highly swollen seed particles. This implies that the activated swelling method is especially suitable for the preparation of cross-linked polymer particles. Moreover, this method is equally suitable for the preparation of porous macroreticular particles, in which case the second-step swelling is carried out by applying inert diluents in addition to monomers, including cross-linkers.

MONOSIZED POLYMER PARTICLES

Examples of monomers which have been applied to prepare monosized polymer particles by the activated swelling process are styrene and styrene derivatives, vinylbenzyl chloride, vinylpyridine, divinylbenzene (DVB) and alkyl acrylates and methacrylates such as hydroxyethyl acrylate and methacrylate (HEMA), glycidyl methacrylate (GMA), ethylene glycol dimethacrylate (EDMA) and trimethylolpropane trimethacrylate (TRIM). In addition, we have synthesized monomers with special functionalities for application in this process.

A wide range of applications for monosized polymer particles in various sizes and materials have been developed during the last few years. Some of these applications are illustrated in Fig. 2.

Fig. 3 shows an example of a scanning electron micrograph of 10-μm compact and cross-linked polystyrene (PS)–DVB particles. These particles were prepared directly from a 1-μm oligomeric seed latex. The high swelling ratio, 1000 times by volume, ensures a spherical shape and a smooth surface. The high degree of monodispersity causes the particles to arrange themselves in an ordered array on the microscope slide.

Fig. 4 shows a histogram of the size distribution of the 10-μm particles in Fig. 3, measured with a high-precision Coulter instrument. A relative standard deviation of the diameter of $< 1\%$ was obtained. The ordinary Coulter technique with an electrical sensing zone may not always be suitable for the characterization of the size distribution of highly monosized spheres, as an additional peak may appear in the histograms, in addition to the normal peak [7].

By an extension of the process, the preparation of monosized beads containing magnetic material is achieved [8]. For this purpose, porous particles are produced which in a subsequent step are made magnetizable by *in situ* deposition of magnetic iron oxides in the particle pores. Examples of applications of magnetic beads are selective cell separation processes and magnetic DNA technology [9,10].

PREPARATION OF POROUS MATRICES

Porous matrices are obtained when polymerization and cross-linking take place

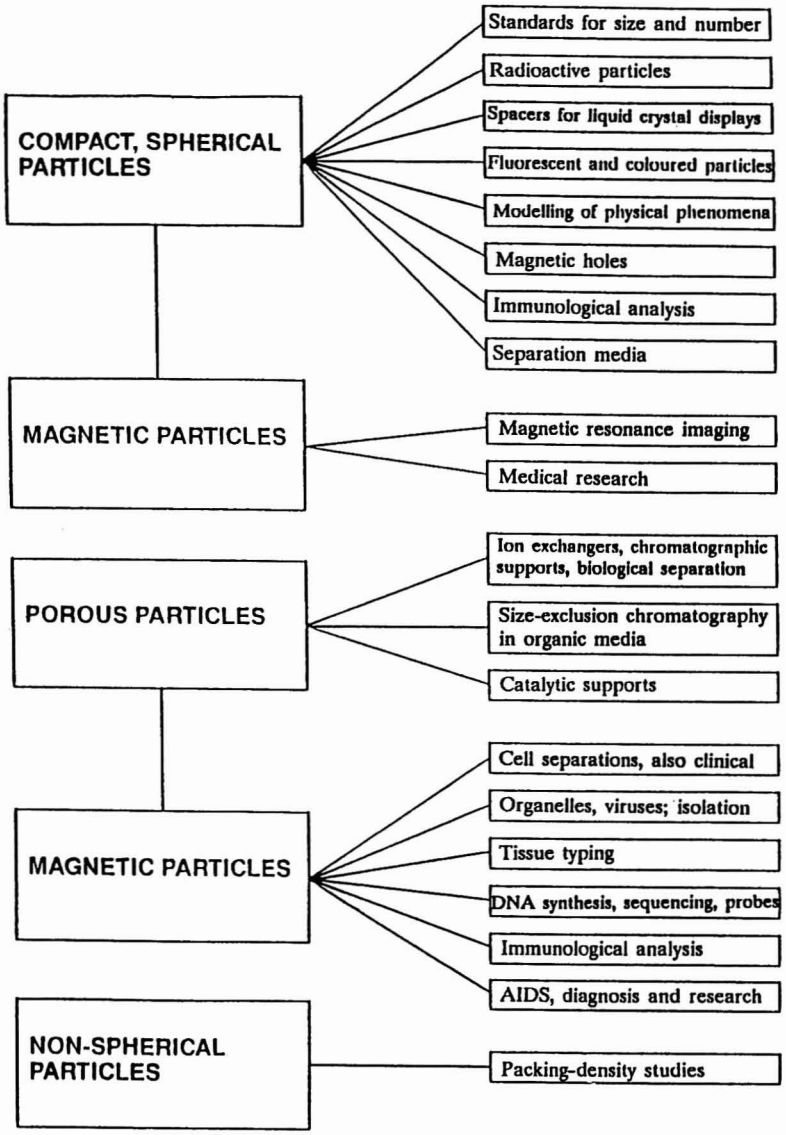

Fig. 2. Schematic illustration of various applications of compact and porous monosized polymer particles.

in the presence of inert diluents, which lead to the formation of permanent pores in the material after removal of the diluent. The most important parameters for the construction of special pore sizes are monomer type and reactivity, degree of cross-linking, amount of diluent and diluent solvency for the polymer (solvent–non-solvent).

By increasing the amount of polyfunctional monomer (cross-linker) in the reaction mixture, micropores (< 50 Å) are formed in the material, while larger pores may

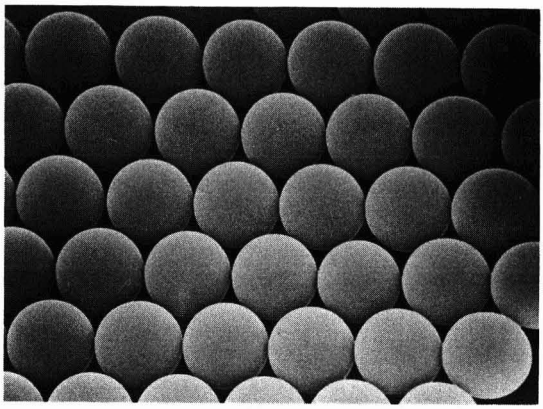

Fig. 3. SEM of 10-μm compact and cross-linked PS–DVB particles.

be obtained by increasing the amount of diluent and/or reducing the diluent solvency. Solvent–non-solvent mixtures are frequently applied to design tailor-made pore-size distributions for special applications, such as supports for liquid chromatography.

Cross-linked and porous PS–DVB materials have been described in the literature for over 25 years [11,12] and are still a focus of attention of both scientists and producers. PS–DVB matrices may be developed into highly rigid and mechanically and chemically stable chromatographic packing materials which are able to operate over a wide pH range. Acrylic porous particles have been less widely described [13,14]. Although acrylates contain ester linkages that are somewhat labile, methyl-substituted acrylates are far more stable than the unsubstituted derivatives towards hydrolysis. Methacrylic macroporous polymers can be used in many applications where prolonged exposure to high pH is not required.

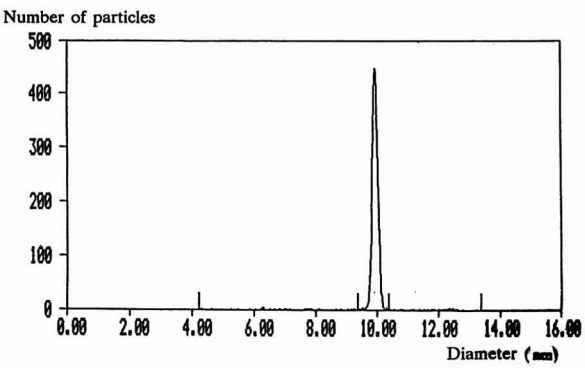

Fig. 4. Histogram of the size distribution of 10-μm PS–DVB particles.

PORE-SIZE CHARACTERIZATION

For applications in the chromatographic field it is important to have a good knowledge of the porous particle characteristics, the specific surface area, the total pore volume and the pore-size distribution. The nitrogen adsorption–desorption method, which covers the pore radius range 10–250 Å, is commonly used to characterize fine- and medium-pore-sized materials, whereas mercury porosimetry is to be preferred when the materials contain medium and large pores, 100 Å–1 μm. A complete pore-size distribution curve will in most instances require characterization by both methods.

The BET method and the mercury intrusion method both require drying of the porous materials. With nitrogen adsorption the measurements are performed at very low temperatures. Drying and lowering of the temperature may cause shrinkage of porous materials that are not completely rigid. A newly described characterization method which does not require drying is thermoporometry [15]. Inverse gel permeation chromatography (GPC) is a chromatographic pore-size determination method [16] in which narrow-molecular-weight polymer standards are applied to determine the pore-size distributions and the exclusion limit of chromatographic supports. For porous matrices of high rigidity we have found a good correlation between pore-size measurements by the mercury intrusion method and inverse GPC.

Fig. 5. shows the cumulative pore volume curves for 5-μm monosized porous PS–DVB particles with 50, 60 and 70% porosity. The curves were drawn by over-

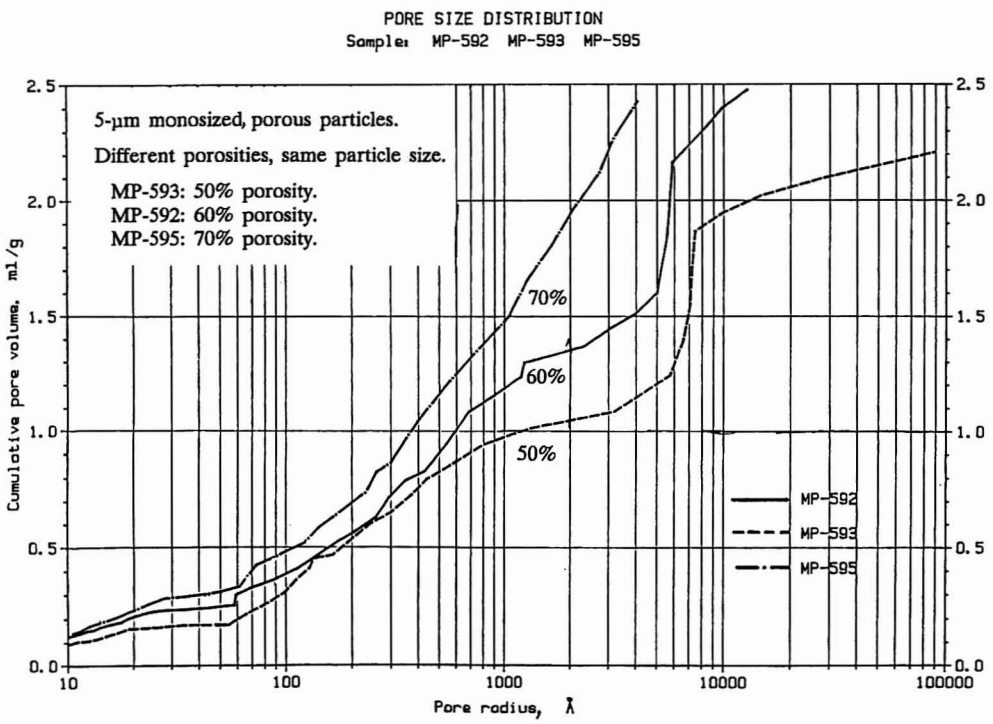

Fig. 5. Cumulative pore volume curves of 5-μm monosized porous particles.

lapping measurements from nitrogen adsorption–desorption and mercury intrusion. These polymer matrices were prepared by increasing the amount of inert diluent in the monomer mixture. As is evident from the curves, this leads to higher total pore volume and more of the larger pores in the particle matrix. When mercury is forced into a sample of porous spherical material, the inter-particle void volume will be measured in addition to the particle pore volume. The steep rise of the curves in the range 5000–7000 Å is specific for 5-μm particles and is due to registration of the void volume between the monosized spheres. For larger particle sizes this rise will move to higher inter-particle size ranges. The particle porosities and surface areas were measured using a Carlo Erba Sorptomatic 1800 and a Carlo Erba Model 1500 porosimeter.

Excellent additional information about the particle morphology, sphericity and particle size distribution may be obtained from scanning electron microscopy (SEM). A scanning electron micrograph of the 5-μm monosized particles with 50% porosity is shown in Fig. 6.

Scanning electron micrographs of two high-porosity 15-μm monosized materials are shown in Fig. 7. The pore-size distributions of these materials are presented in Table I. Material A is a matrix of high surface area and broad pore-size distribution with 70% porosity. When applied in chromatography, this material will combine a high load capacity with easy accessibility to the pores. Material B is a typical wide-pore matrix with 73% porosity.

RIGIDITY OF POROUS MATRICES

Investigation of the rigidity of a porous matrix is easily performed with monosized particles. Especially for chromatographic applications in organic solvents there is a high demand for packing materials that are non-compressible and able to withstand high pressures. Compressibility is closely related to the swelling of the porous matrix. The volume swelling of a monosized porous material may be observed and

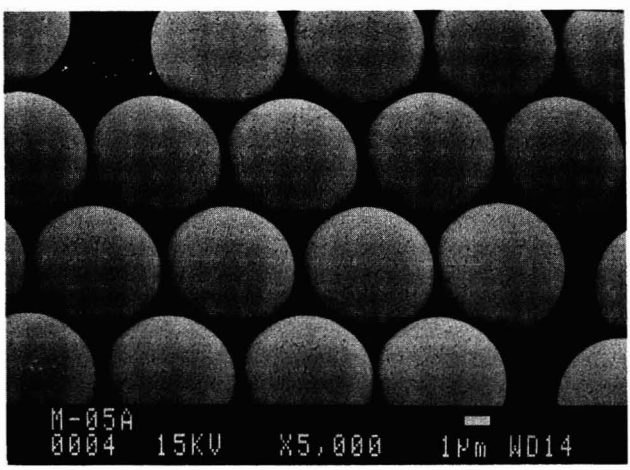

Fig. 6. SEM of 5-μm porous particles of 50% porosity.

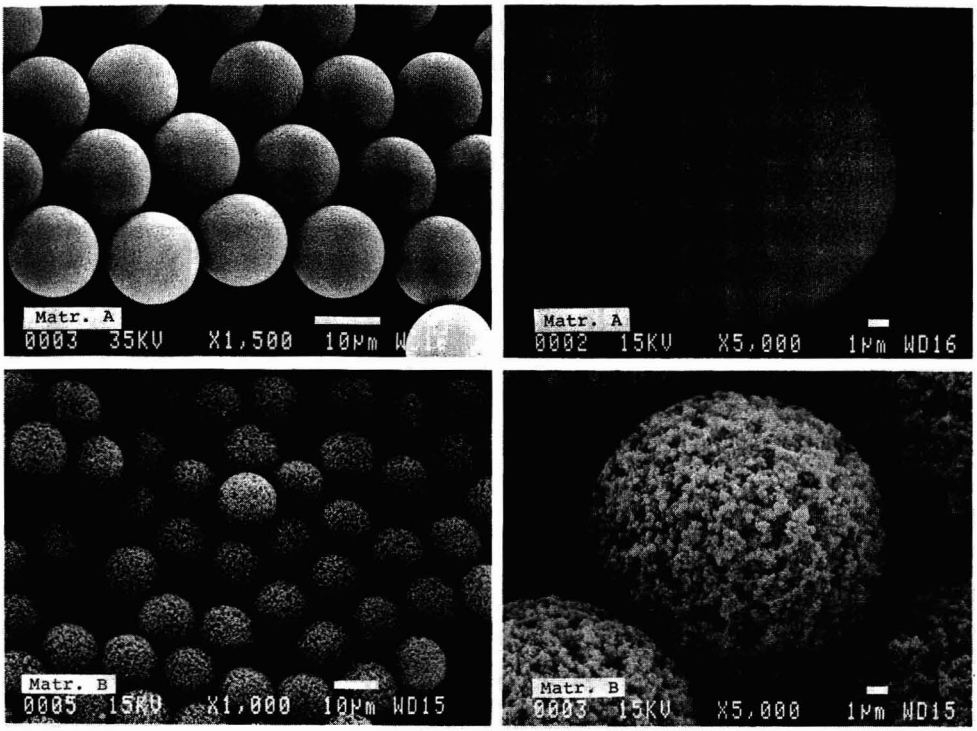

Fig. 7. Morphology studies by SEM of highly porous materials. (A) Monosized porous particles of high surface area and broad pore-size distribution. (B) Monosized porous particles with mainly large pores.

calculated from optical micrographs of dry and swollen particles. Table II shows the results from measurements of swelling of 15-μm highly porous, monosized PS–DVB particles in methanol, tetrahydrofuran (THF) and toluene. It is evident that the degree of cross-linking (% DVB) is a highly important factor. High-percentage DVB monomers have been prepared in our laboratory by purification of a commercial 63% technical-grade DVB [17]. Other parameters that influence the swelling of porous matrices are particle diameter (smaller particles swell more than larger particles), matrix porosity (higher porosity leads to increased swelling) and diluent solvency (reduced solvency gives less swellable matrices) [18].

TABLE I

PORE-SIZE DISTRIBUTIONS OF THE POROUS MATERIALS SHOWN IN FIG. 7

Sample	Surface area (BET) (m^2/g)	Pore volume (ml/g)	Pore-size distribution (radius) (ml/g)					
			< 50 Å	50–100 Å	100–300 Å	300–500 Å	500–2000 Å	2000–5000 Å
A	660	2.22	0.32	0.18	0.36	0.26	0.68	0.42
B	387	2.55	0.18	0.08	0.22	0.19	1.26	0.62

TABLE II

CHARACTERISTICS OF 15-μm, HIGHLY POROUS PS–DVB PARTICLES: EFFECT OF CROSS-LINKING ON TOTAL SURFACE AREA, PORE VOLUME AND SWELLING IN ORGANIC SOLVENTS.

DVB (%)	Surface area (BET) (m^2/g)	Pore volume (ml/g)	Swelling in organic solvents (%, v/v)[a]		
			Methanol	THF	Toluene
40	269	2.35	49	49	49
50	431	2.55	26	26	21
60	463	2.63	14	10	14
80	644	2.80	3	3	3
97	674	3.00	*ca.* 0	*ca.* 0	*ca.* 0

[a] % (v/v) swelling = $(V_{sp} - V_p)/V_p \cdot 100$, where V_{sp} = volume of swollen particle and V_p = volume of dry particle.

SIZE DISTRIBUTION OF PACKING MATERIALS

It is generally known that in chromatography the large particles in a packing material with a broad particle-size distribution will limit the resolution whereas the presence of fines will reduce the column permeability and necessitate high pressure to produce reasonable flow-rates. Particle segregation may occur during packing, and this will produce variations in the packing density. Variable resistance to flow across the column will be the result. The optimum size distribution, considering both back-pressure and resolution, should therefore be monodisperse.

Dawkins *et al.* [19] demonstrated the superiority of a narrow particle-size distribution in size-exclusion chromatography by using mechanically sieved fractions of a material obtained by suspension polymerization. Their results showed that the height equivalent to a theoretical plate (HETP) was proportional to the particle diameter (d_p) according to the relationship HETP $\approx d_P^{1.95}$. It has been deduced theoretically that HETP should be proportional to the square of the particle diameter [20].

Packing of spheres of identical size in a hexagonal close packing gives a packing density of 0.7405, regardless of the size of the spheres. This implies that a void volume as low as 26% is theoretically attainable. It is our experience that in practice a well packed chromatographic column of monosized beads will have a void volume of about 35%.

MONOSIZED STATIONARY PHASES

The advantages of monosized chromatographic supports are a uniform column packing, uniform flow velocity profile, no fines, low back-pressure, high resolution and high speed of separation compared with materials of broad size-distribution. For porous supports, the monodisperse technology ensures equal bead-to-bead morphology.

Optical micrographs of 20-μm monosized macroporous particles and a commercial liquid chromatographic material of size 12–28 μm are shown in Fig. 8. There

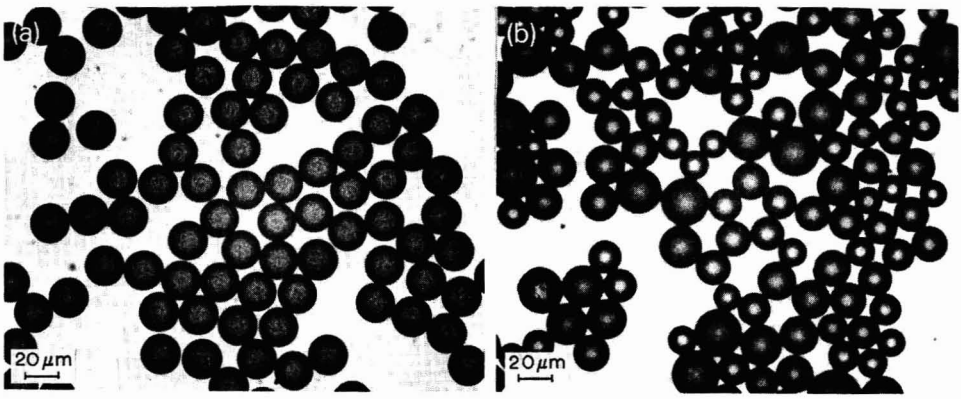

Fig. 8. Optical micrograph of macroporous chromatographic column materials. (a) Monosized particles of 20 μm. (b) Commercial column filling of 12–28 μm.

is a clear difference in size distribution between the monodisperse particles and a traditional column material.

Special types of 10-μm monosized porous particles, prepared by our activated swelling method, were the basis for the widely used Fast Protein Liquid Chromatographic (FPLC) system, introduced by Pharmacia in 1982 [21,22]. The MonoBeads made rapid and high-efficiency chromatography of labile biomolecules possible.

For chromatographic purposes we have prepared macroporous, spherical, monosized particles with a wide range of particle sizes and pore-size distributions. Underivatized porous particles, applied in size-exclusion chromatography (SEC) in organic solvents, have resulted in columns with unusual efficiency and separation capacity. By coating the particles with hydrophilic polymer, monosized chromatographic supports for aqueous phase ion-exchange and size-exclusion chromatography were developed. Examples of applications are given below.

Non-aqueous SEC

Monosized porous PS–DVB particles of three different particle sizes, 20, 10 and 5 μm, were tested by SEC in toluene [23]. Chromatographic calibration was performed with polystyrene standards with narrow molecular-weight distributions in the range 450–$2.7 \cdot 10^6$ dalton.

Results from the SEC calibrations are presented in Table III. The plate counts are averages from several chromatograms with each particle-size material. A considerable increase in plate count with decreasing particle diameter was obtained, giving more than 50 000 plates per foot for the 5-μm monosized particles. In this instance, the HETP was almost as small as the particle diameter (HETP = 0.006 mm). The results in Table III lead to the proportionality HETP $\approx d_p^{2.06}$.

The three batches of 50% porosity particles had nearly identical pore-size distributions. This resulted in calibration graphs which were similar for all three particle sizes and linear in the range 20 000–350 000 dalton. In a forthcoming study, we shall introduce wider pore sizes into the monosized SEC materials in order to extend the linear calibration range to higher molecular weights.

TABLE III

SIZE-EXCLUSION CHROMATOGRAPHY IN TOLUENE: PERFORMANCE OF 20-, 10- AND 5-μm COLUMNS IN THE SEPARATION OF POLYSTYRENE STANDARDS

Column, 300 × 7.8 mm I.D.; flow-rate, 1 ml/min.

Particle diameter (μm)	Plate count (plates/ft.)	Resolution factor, R_{sp}[a]
20.6	3000	2.4
10.5	13 000	2.8
5.3	> 50 000	4.4

[a] $R_{sp} = 0.58/\sigma D_2$, where σ = peak standard deviation and D_2 = slope of calibration graph.

Fig. 9 shows the SEC results with application of 10- and 5-μm monosized particles. The pore-size distribution of the 5-μm material is the 50% porosity curve in Fig. 5.

Protein recovery studies

Underivatized PS–DVB particles are extremely hydrophobic and cannot be used in aqueous media. Acrylic polymers, such as copolymers of HEMA and EDMA,

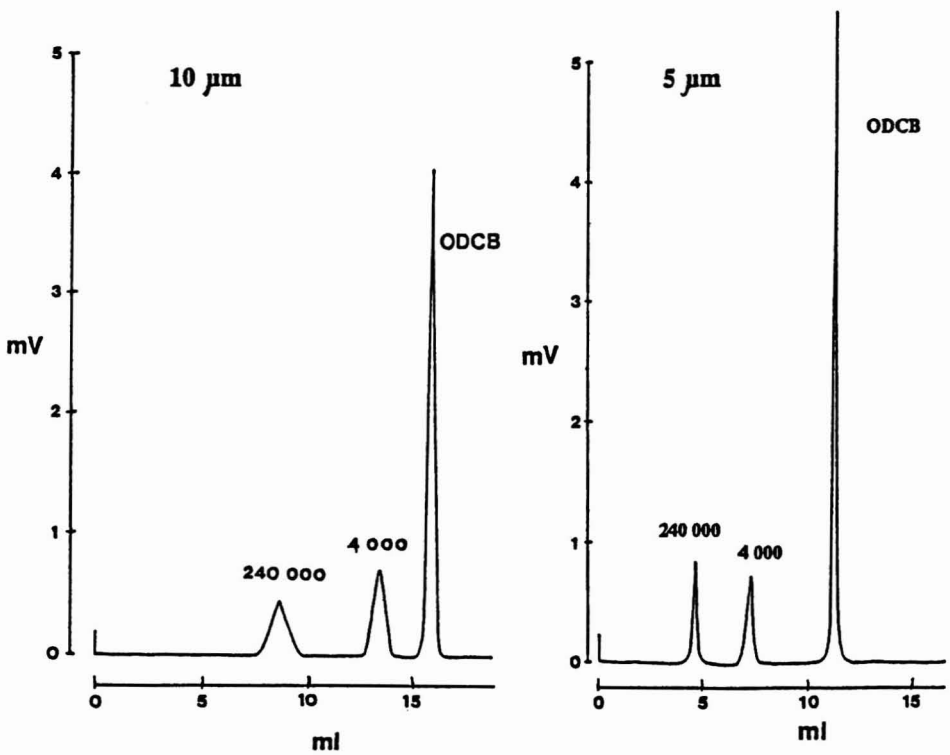

Fig. 9. Separation of polystyrene standards of molecular weight 240 000 and 4000 and *o*-dichlorobenzene by 10- and 5-μm monosized porous PS–DVB column materials.

are considerably more hydrophilic, but exhibit some hydrophobic character that leads to non-specific protein adsorption.

Hydrophilization of PS–DVB and acrylic polymers may be obtained by coating the particle surfaces with a hydrophilic polymer. A surface hydrophilic layer which is covalently bonded to the matrix is preferable to a physically adsorbed layer. A thin, uniform coating which does not permit any protein adsorption would be ideal.

By grafting of a hydrophilic polymer to residual double bonds in the cross-linked polymer matrix, we hydrophilized 20-μm monosized acrylic particles for the aqueous phase SEC of proteins. This acrylic matrix was HEMA–EDMA copolymer, possessing a hydrophobic character and a specific surface area of 141 m^2/g. Underivatized particles exhibited total non-specific adsorption of all proteins. Grafting of a linear hydrophilic polymer to this matrix reduced the surface area to 71 m^2/g, closed the matrix micropores and resulted in a considerable increase in the yield of proteins. In a last step the hydrophilic polymer layer was cross-linked with epichlorohydrin. After this treatment, the protein recovery was high for all proteins, including the smallest protein molecules. These results are presented in Table IV.

An example of the performance of a well hydrophilized, 15-μm monosized, porous PS–DVB matrix is shown in Table V. In this case cross-linking of the hydrophilic layer again led to an increased yield of the smallest molecules, *i.e.*, the peptides.

ION-EXCHANGE CHROMATOGRAPHY

Column materials for ion exchange in aqueous media were prepared by introduction of charged groups to the hydrophilized surface layer of the porous matrices. These new ion-exchange sorbents are based on monosized polymer particles having a uniform, rigid and chemically stable structure. The chromatograms in Fig. 10 illustrate the separation of standard protein mixtures on 15-μm monosized anion and cation exchangers. The charged group of the anion exchanger (AQ) is a quaternary

TABLE IV

PERFORMANCE OF 20-μm ACRYLIC MONOSIZED PARTICLES IN AQUEOUS GPC: RECOVERY OF STANDARD PROTEINS

Column, 5 cm × 5 mm I.D.; mobile phase, 0.1 *M* phosphate buffer (pH 7.1); flow-rate, 0.2 ml/min.

Protein	Mol. wt.	Protein recovery (%)		
		Uncoated particles	Linear polymer coating	Cross-linked coating
Ferritin	440 000	0	100	82
Aldolase	158 000	0	6	74
Bovine serum albumin	67 000	0	68	89
Ovalbumin	43 000	0	63	92
Chymotrypsinogen	25 000	0	100	91
Ribonuclease	13 700	0	100	92
Cytochrome *c*	13 000	0	0	85
Lysozyme	14 600	0	1	90

TABLE V

PERFORMANCE OF MONOSIZED 15-μm HYDROPHILIZED PS–DVB PARTICLES: RECOVERY OF PROTEINS AND PEPTIDES

Column, 5 cm × 5 mm I.D.; mobile phase, 20 m*M* phosphate buffer (pH 7.0); flow-rate, 0.2 ml/min; load, 1 mg/ml.

Protein/peptide	Mol. wt.	Recovery (%)	
		Linear polymer coating	Cross-linked coating
Thyroglobulin	669 000	85	76
Ferritin	440 000	65	59
Immunoglobulin G	160 000	97	100
Bovine serum albumin	67 000	100	100
Ovalbumin	43 000	94	76
Ribonuclease	13 700	89	100
Cytochrome *c*	13 000	100	96
Angiotensin I	1290	0	100
Angiotensin II	1050	58	90

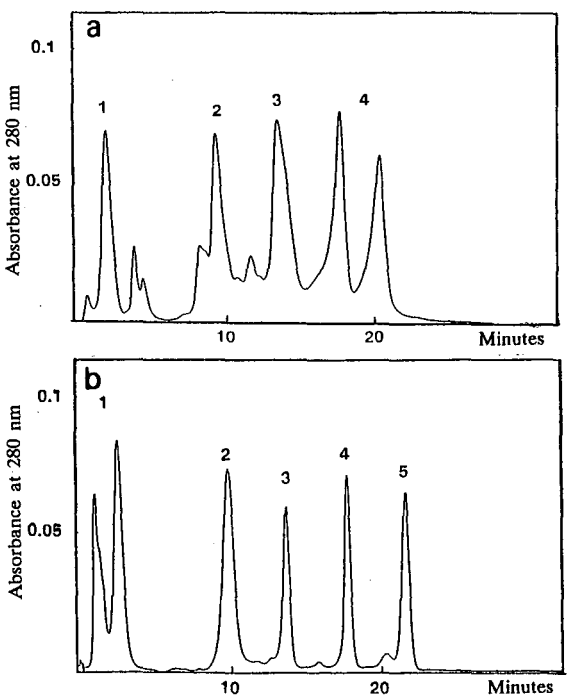

Fig. 10. Separation of protein mixtures by ion-exchange chromatography. Column, 5 cm × 5 mm I.D.; flow-rate, 5 cm/min (1 ml/min); gradient, 20 column volumes (20 ml); sample volume, 100 μl. (a) 15-μm monosized anion-exchange particles. Protein mixture (all from Sigma): 1 = carbonic anhydrase, 0.75 mg/ml (C-7500); 2 = ovalbumin, 3.00 mg/ml (A-7638); 3 = bovine serum albumin, 3.00 mg/ml (A-7638); 4 = β-lactoglobulin (A + B), 3.00 mg/ml (L-4756). Buffer: (A) 20 m*M* Tris–HCl (pH 8.0); (B) A + 0.5 *M* sodium acetate (pH 8.0). (b) 15-μm monosized cation-exchange particles. Protein mixture (all from Sigma): 1 = myoglobin, 0.5 mg/ml (M-1882); 2 = aldolase, 1.0 mg/ml (A-1893); 3 = chymotrypsinogen, 0.2 mg/ml (C-4879); 4 = cytochrome *c*, 0.2 mg/ml (C-7752); 5 = lysozyme, 0.2 mg/ml (L-6870). Buffer: (A) 20 m*M* N-(2-acetamido)iminodiacetic acid (ADA) (pH 6.3); (B) A + 0.5 *M* NaCl.

amine with ligand density of 0.18–0.22 mmol/ml gel. The charged group of the cation exchanger (CS) is sulphopropyl with ligand density of 0.16–0.20 mmol/ml gel.

CONCLUSION

New methods for the preparation of highly monodisperse particles have made available a number of different polymeric supports for chromatography. The monodisperse porous packing materials have proved to be very suitable in various liquid chromatographic applications. High-performance chromatographic materials were developed by careful control of important parameters, such as particle size, particle-size distribution, pore-size distribution and surface chemistry.

ACKNOWLEDGEMENTS

The authors thank Dyno Particles AS for permission to publish these results. The authors are also indebted to Mr. Ø. Sødahl, SINTEF Metallurgy Division, for the scanning electron micrographs and Dr. O. Tronstad, Norwegian Institute of Technology, for the surface-area and pore-size characterizations.

REFERENCES

1 J. H. Kim, E. D. Sudol, M. S. El-Aasser, J. W. Vanderhoff and D. M. Kornfeld, *Chem. Eng. Sci.*, 43 (1988) 2025.
2 M. Morton, S. Kaizerman and M. W. Altier, *J. Colloid Sci.*, 9 (1954) 300.
3 J. Ugelstad, P. C. Mørk, K. H. Kaggerud, T. Ellingsen and A. Berge, *Adv. Colloid Interface Sci.*, 13 (1980) 101.
4 J. Ugelstad, P. C. Mørk, A. Berge, T. Ellingsen and A. A. Khan, in I. Piirma (Editor), *Emulsion Polymerization*, Academic Press, New York, 1982 p. 383.
5 J. Ugelstad, H. M. Mfutakamba, P. C. Mørk, T. Ellingsen, A. Berge, R. Schmid, L. Holm, A. Jørgedal, F. K. Hansen and K. Nustad, *J. Polym. Sci., Polym. Symp.*, 72 (1985) 225.
6 J. Ugelstad, A. Berge, T. Ellingsen, O. Aune, L. Kilaas, T. N. Nilsen, R. Schmid, P. Stenstad, S. Funderud, G. Kvalheim, K. Nustad, T. Lea and F. Fartdal, *Makromol. Chem., Makromol. Symp.*, 17 (1988) 177.
7 C. M. L. Atkinson and R. Wilson, *Powder Technol.*, 34 (1983) 275.
8 J. Ugelstad, T. Ellingsen, A. Berge and B. Helgee, *U.S. Pat.*, 4 654 267, 1987.
9 J. G. Treleaven, F. M. Gibson, J. Ugelstad, A. Rembaum and J. Kemshead, *Magn. Sep. News*, 1 (1984) 103.
10 M. Uhlen, *Nature (London)*, 340 (1989) 733.
11 J. C. Moore, *J. Polym. Sci., Part A2*, (1964) 835.
12 J. Seidl, J. Malinski, K. Dusek and W. Heitz, *Adv. Polym. Sci.*, 5 (1967) 113.
13 F. Švec, J. Hradil, J. Čoupek and J. Kálal, *Angew. Makromol. Chem.*, 48 (1975) 135.
14 O. Mikeš, P. Štrop and J. Čoupek, *J. Chromatogr.*, 153 (1978) 23.
15 A. Guyot and M. Bartholin, *Prog. Polym. Sci.*, 8 (1982) 277.
16 I. Halacz, and K. Martin, *Angew. Chem.*, 90 (1978) 954.
17 G. Popov and G. Schwachula, *Chem. Tech.*, 30 (1978) 144.
18 T. Ellingsen, SINTEF, unpublished results.
19 J. V. Dawkins, T. Stone and G. Yeadon, *Polymer*, 18 (1977) 1179.
20 W. W. Yau, J. J. Kirkland and D. D. Bly, *Modern Size Exclusion Liquid Chromatography*, Wiley, New York 1979.
21 *FPLC™ Ion Exchange Chromatography and Chromatofocusing. Information Booklet*, Pharmacia Laboratory Separation Division, Uppsala, 1982.
22 J. Ugelstad, L. Søderberg, A. Berge and J. Bergstrøm, *Nature (London)*, 303 (1983) 95.
23 L. I. Kulin, P. Flodin, T. Ellingsen and J. Ugelstad, *J. Chromatogr.*, 514 (1990) 1.

Journal of Chromatography, 535 (1990) 163–172
Elsevier Science Publishers B.V., Amsterdam

CHROMSYMP. 2005

Synthesis of mixed-functional-phase silica supports for liquid chromatography and their applications to assays of drugs in serum

JUN HAGINAKA*, JUNKO WAKAI and HIROYUKI YASUDA
Faculty of Pharmaceutical Sciences, Mukogawa Women's University, 11–68, Koshien Kyuban-cho, Nishinomiya 663 (Japan)

ABSTRACT

Mixed-functional-phase (MFP) silica supports were designed for the direct injection determination of drugs in serum. The MFP silicas were synthesized from porous silica materials in three or four steps: introduction of 3-glycidoxypropyl phases, introduction of phenyl, butyl or octyl phases and hydrolysis of the oxirane ring to diol phases, or these three steps plus further introduction of glycerylpropyl (*i.e.*, diol) phases. Although the further introduction of glycerylpropyl phases resulted in a reduction in the column efficiency, serum proteins were completely recovered in the first injection of serum samples. The prepared MFP packing materials can be used for the direct injection determination of hydrophobic and hydrophilic drugs in serum.

INTRODUCTION

Since the introduction of internal surface reversed-phase (ISRP) silica supports [1], various new stationary phases have been developed for direct injection assays of drugs and/or their metabolites in biological samples. The ISRP silica column, which is commercially available, designed by Hagestam and Pinkerton [1], involves binding glycyl-L-phenylalanyl-L- phenylalanine tripeptide and glycine residues bonded on glycerylpropyl-bonded porous silica particles as internal and external surfaces, respectively. These negatively charged and less hydrophobic phases resulted in low recoveries of serum proteins at eluent pH values below 6.0 and almost no retention of hydrophilic drugs such as amphoteric drugs [2]. We prepared a neutral ISRP silica support having N-octanoylaminopropyl and N-(2,3-dihydroxypropyl)aminopropyl phases as internal and external surfaces, respectively [2,3]. The neutral ISRP packing materials can be used for direct injection assays of hydrophilic or hydrophobic drugs in serum over the eluent pH range 3–7. However, the above ISRP packing materials were prepared by enzymatic cleavage of external hydrophobic phases or the enzymatic cleavage and attachment of diol phases. Hence, it was difficult to obtain batch-to-

0021-9673/90/$03.50

batch reproducibility of the support properties, because enzymatic reactions were included in the preparation processes.

Kimata *et al.* [4] reported a new method for the preparation of ISRP packing materials, including partial decomposition of alkylsilylated silica stationary phases with aqueous acid followed by introduction of diol phases. Gisch *et al.* [5] prepared a shielded hydrophobic phase silica support which consists of a polymeric bonded phase containing a hydrophobic phenyl group in a hydrophilic polyoxyethylene network. Recently, Williams and Kabra [6] reported novel dual-zone material adsorbents having perfluorobutylethylenedimethylsilyl and octadecylsilyl groups on external and internal zones, respectively.

We have prepared and evaluated a novel chromatographic support, termed mixed-functional-phase (MFP) packings, for direct serum injection assays of achiral and chiral drugs [7,8]. The MFP supports have the properties that the pores are small enough to restrict the access of macromolecules such as serum proteins to the pores and the mixed functionality of hydrophilic and hydrophobic phases is introduced for avoiding the destructive accumulation of proteins and retaining small molecules such as drugs. Two MFP packing materials having phenyl–diol [7] and β-cyclodextrin–diol [8] phases have been developed for determinations of achiral and chiral drugs, respectively.

In this paper, we report the synthesis and characterization of MFP silica supports having phenyl, butyl or octyl groups as hydrophobic phases and diol groups as hydrophilic phases, and their applications to the direct injection determination of hydrophobic and hydrophilic drugs in serum.

EXPERIMENTAL

Reagents and materials

Theobromine was purchased from Nacalai Tesque (Kyoto, Japan), acetonitrile of HPLC grade from Kanto Chemical (Tokyo, Japan), 3-glycidoxypropyltrimethoxysilane, phenyltrimethoxysilane, butyltrimethoxysilane and octyltriethoxysilane from Petrach Systems (Bristol, PA, U.S.A.) and N,N-diisopropylethylamine from Aldrich (Milwaukee, WI, U.S.A.). The other reagents, of analytical-reagent grade, and control human serum (Control Serum I) were purchased from Wako (Osaka, Japan). Phenobarbital, phenytoin, caffeine, carbamazepine, theophylline, cefotaxime, cefmenoxime and cefamandole were kindly donated by Sankyo (Tokyo, Japan), Nippon Ciba-Geigy (Takarazuka, Japn), Eisai (Tokyo, Japan), Hoechst Japan (Tokyo, Japan), Takeda Chemical Industry (Osaka, Japan) and Shionogi (Osaka, Japan). Develosil silica [particle diameter 5 μm; nominal pore size 55 Å (specified by the manufacturer); specific surface area 525 m^2/g] was obtained from Nomura Chemicals (Seto, Aichi, Japan).

Water prepared with a Nanopure II unit (Barnstead, Boston, MA, U.S.A.) was used for the preparation of the eluent and the sample solution.

Preparation of the MFP silica

Preparation of 3-glycidoxypropylsilica. Develosil silica gel (2 g) was dried *in vacuo* over P_2O_5 at 150°C for 6 h and the dry silica gel was added to 120 ml of dry toluene. The mixture was heated to reflux until all the water had been removed as an

azeotrope into a Dean–Stark-type trap. Next, 3.8 ml of 3-glycidoxypropyltrimethoxysilane, which is equivalent to 16 μmol per square metre of surface area, were added to the mixture, which was then reacted at 95°C for 3 h. The reaction mixture was cooled to room temperature, filtered and washed with toluene and methanol. The isolated silica gel was then dried *in vacuo* over P_2O_5 at 60°C for 2 h. The silica support thus obtained is abbreviated to 16G, derived from the number of micromoles of 3-glycidoxypropyltrimethoxysilane per square metre of surface area used for the reaction.

Preparation of phenyl-, butyl- or octylsilica. 3-Glycidoxypropylsilica (3 g) was added to 80 ml of dry toluene and stirred. To the mixture, 2.0, 2.0 or 3.3 ml of phenyl- or butyltrimethoxysilane or octyltriethoxysilane and 6.0 ml of N,N-diisopropylethylamine as a basic catalyst were added under a nitrogen atmosphere and the mixture was refluxed for 9 h. The reaction mixture was cooled to room temperature, filtered and washed with toluene and methanol. The isolated silica gel was dried *in vacuo* over P_2O_5 at 60°C for 2 h.

Hydrolysis of the oxirane ring to diol phases. To 2 g of the phenyl-, butyl- or octylsilica, 80 ml of perchloric acid (pH 3.0) were added and the mixture was refluxed for 4 h. The mixture was filtered and washed with water and methanol. The isolated silica was dried *in vacuo* over P_2O_5 at 60°C for 2 h. The MFP silica supports thus obtained are abbreviated to 16G-Ph, 16G-Bu and 16G-Oc, respectively, derived from the organosilanes used for the reaction.

Further introduction of diol phases. To 2 g of 16G-Ph silicas, 30 ml of aqueous solution containing 2.3 ml of 3-glycidoxypropyltrimethoxysilane, whose pH was adjusted to 3.5 by addition of perchloric acid, were added and the mixture was reacted at 90°C for 4 h. The mixture was filtered and washed with water and methanol. The isolated silica was dried *in vacuo* over P_2O_5 at 60°C for 2 h. The MFP silica support thus obtained is abbreviated to 16G-Ph-10G.

Intrumentation

The amounts of 3-glycidoxypropyl-, phenyl- or butyltrimethoxysilane or octyltriethoxysilane reacted were determined by elemental analysis using Type MT-3 CHN analyser (Yanagimoto, Kyoto, Japan).

The prepared MFP silica support was packed into a 50 × 4.6 mm I.D. or 100 × 4.6 mm I.D. stainless-steel tube by conventional high-pressure slurry-packing procedures [9].

The chromatographic system consisted of a Model 880 pump (Japan Spectroscopic, Tokyo, Japan) equipped with a a Model 875-UV variable-wavelength detector (Japan Spectroscopic). The eluents used are specified in the captions of tables and figures. Detection was performed at 254 or 275 nm. The precolumn (50 × 4.6 mm I.D.) packed with LC-sorb Sp-A-ODS (particle size 25–40 μm; Chemco Scientific, Osaka, Japan) was inserted between the pump and injector to protect the analytical column from microparticles in the eluent. Samples were injected with a Sil-9A Auto Injector (Shimadzu, Kyoto, Japan). The chromatograms were recorded and integrated using a Chromatopac CR-6A (Shimadzu). All separations were carried out at ambient temperature.

Preparation of human serum samples

Drugs were dissolved in human serum at a known concentration and an

appropriate volume of the serum sample was applied to the MFP silica support after filtration through a 0.22-μm membrane filter (Nippon Millipore, Tokyo, Japan).

Recovery of serum proteins from the MFP silica

The recovery of serum proteins from the MFP silicas was measured as described previously [2].

RESULTS AND DISCUSSION

Characterization of the MFP silica support

Previously [7], we reported a method for the preparation of an MFP silica support having phenyl and diol phases. The MFP silica support could be used for the direct injection determination of hydrophilic and hydrophobic drugs in serum. The MFP packing material was prepared by three steps: introduction of 3-glycidoxypropyl phases, introduction of phenyl phases and hydrolysis of the oxirane ring to diol phases. In this study, we tried to introduce phenyl, butyl or octyl groups as hydrophobic phases into silica matrices and to compare the three MFP silicas with respect to physical and chromatographic properties.

The introduction of diol phases was kept constant by reaction with 16 μmol/m^2 of 3-glycidoxypropyltrimethoxysilane without the addition of a basic catalyst. The introduction of phenyl, butyl or octyl phases was intended to the maximum by adding N,N-diisopropylethylamine as a basic catalyst. Table I gives the carbon contents and surface coverages of the MFP packing materials. The ligand density of octyl phases introduced was lower than that of phenyl or butyl phases, as steric hindrance impedes diffusion of octyltriethoxysilane into the pores during silanization, because the reactivity of ethoxysilane (used for the introduction of octyl phases) is almost comparable to that of methoxysilane (used for the introduction of phenyl or butyl phases) [10].

Table II gives the retention properties of anticonvulsant drugs, methylxanthine derivatives and cephalosporins on the MFP silicas. The solutes tested were well retained on the 16G-Ph silica compared with the 16G-Bu and 16G-Oc silicas. This might be due to the low ligand density of the 16G-Oc silica and the low hydrophobicity of the 16G-Bu silica. Anticonvulsant drugs were well separated on the three MFP silicas, as shown in Table II. Methylxanthine derivatives, theophylline and theo-

TABLE I

CARBON CONTENTS AND SURFACE COVERAGES OF THE MFP PACKING MATERIALS

Silica	Carbon content (%)	Surface coverage (μmol/m^2)	
		Diol phase	Hydrophobic phase
16G	3.69	0.75	–
16G-Ph	8.40	0.75	1.94
16G-BU	5.50	0.75	1.42
16G-Oc	4.57	0.75	0.45
16G-Ph-10G	12.60	–	1.94

TABLE II

RETENTION PROPERTIES OF VARIOUS COMPOUNDS ON THE MFP PACKING MATERIALS (100 × 4.6 mm I.D. COLUMN)

Compound	Capacity factor (k')			
	16G-Ph	16G-Bu	16G-Oc	16G-Ph-10G
Anticonvulsant drugs[a]				
Phenobarbital	2.24	1.10	0.61	3.16
Phenytoin	9.56	4.21	2.85	16.59
Carbamazepine	12.86	5.98	4.21	13.34
Methylxanthine derivatives[b]				
Theophylline	5.06	1.10	0.73	2.28
Theobromine	7.39	1.16	0.74	2.69
Caffeine	15.15	1.97	1.97	5.55
Cephalosporins[c]				
Cefotaxime	1.42	2.12	1.64	1.00
Cefmenoxime	3.30	4.01	3.26	1.86
Cefamandole	3.31	4.06	4.71	2.23

[a] Capacity factors were measured under the following chromatographic conditions: eluent, 50 m*M* NaH_2PO_4 + 50 m*M* Na_2HPO_4–CH_3CN (9:1, v/v); flow-rate, 0.8 ml/min.

[b] Capacity factors were measured under the following chromatographic conditions: eluent, 50 m*M* NaH_2PO_4 + 50 m*M* Na_2HPO_4–CH_3CN (23:1, v/v); flow-rate, 0.8 ml/min.

[c] Capacity factors were measured under the following chromatographic conditions: eluent, 90 m*M* NaH_2PO_4 + 10 m*M* Na_2HPO_4–CH_3CN (12:1, v/v) for the 16G-Ph and 16G-Ph-10G silicas and 90 m*M* NaH_2PO_4 + 10 m*M* Na_2HPO_4–CH_3CN (100:1, v/v) for 16G-Bu and 16G-Oc silicas; flow-rate, 0.8 ml/min.

bromine were not separated on the 16G-Bu and 16G-Oc silicas but were separated on the 16G-Ph silica. The separation of cephalosporins, cefmenoxime and cefamandole was not achieved on the 16G-Ph and 16G-Bu silicas with a short run time, but was successful on the 16G-Oc silica. These results indicate that the introduction of different functionalities could be useful for selective separations of various solutes. Almost the same column efficiency was obtained in spite of differences in hydrophobic phases introduced; the number of theoretical plates (N) was 2600, 2400 and 2200 for carbamazepine for the 16G-Ph, 16G-Bu and 16G-Oc silicas, respectively, packed into a 100 × 4.0 mm I.D. column.

The average pore diameters of the prepared MFP supports were 50, 51 and 58 Å for 16G-Ph, 16G-Bu and 16G-Oc silicas, respectively, when measured by the inverse size-exclusion chromatographic method reported by Cook and Pinkerton [11]. The recovery of serum proteins for the first injection increased in the sequence 16G-Oc < 16G-Ph < 16G-Bu by 30, 50 and 80%, respectively. The serum proteins were completely recovered with the second injection of a 20-μl human serum sample for the 16G-Bu silica or with the third injection for the 16G-Ph and 16G-Oc silicas, when MFP silicas packed into a 50 × 4.6 mm I.D. stainless-steel column were used. It has been reported that the recovery of ovalbumin on a reversed-phase column decreased with increasing alkyl chain length [12] and proteins were less completely recovered from silica-bonded alkyl silanes with low surface coverage [13]. Hence it is plausible that the

16G-Oc silica gives the lowest recovery of serum proteins in the first injection. These results reveal that the 16G-Bu and 16G-Oc silicas in addition to the 16G-Ph silica [7] can be used for direct serum injection assays of drugs.

Further introduction of diol phases to the 16G-Ph silica

In order to recover serum proteins completely from the MFP silica with the first injection, we tried to introduce further hydrophilic phases (*i.e.*, diol phases) into the 16G-Ph silica. The further introduction of diol phases to the 16G-Ph silica was achieved by reaction with 3-glycidoxypropyltrimethoxysilane in aqueous media [14]. The serum proteins were completely recovered from the obtained MFP silica, 16G-Ph-10G, which has an average pore diameter of 39 Å. However, the column efficiency of the 16G-Ph-10G silica was decreased to about half of that of the 16G-Ph

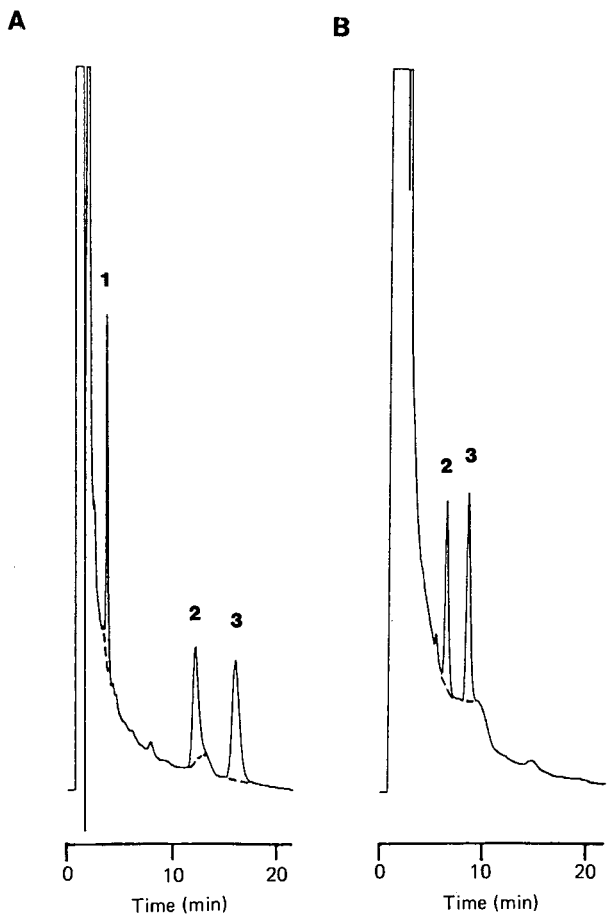

Fig. 1. Chromatograms of control serum spiked with (1) phenobarbital (20 μg/ml), (2) phenytoin (40 μg/ml) and (3) carbamazepine (8 μg/ml) on (A) 16G-Ph and (B) 16G-Bu silica. Chromatographic conditions: column, MFP silicas packed into a 100 × 4.0 mm I.D. column; eluent, 50 m*M* NaH_2PO_4 + 50 m*M* Na_2HPO_4–CH_3CN (9:1, v/v); flow-rate, 0.8 ml/min; detection, 254 nm; sensitivity, 0.032 a.u.f.s.; injection volume, 10 μl. Dashed lines indicate serum blank.

silica. The 16G-Ph-10G silica showed excellent chromatographic selectivity, that is, separations of cefmenoxime and cefamandole and also theophylline and theobromine were achieved, as shown in Table II. Also, it should be noted that the elution order of phenytoin and carbamazepine should be reversed on the 16G-Ph and 16G-Ph-10G silicas.

Direct injection determination of drugs in serum

Fig. 1A and B show chromatograms of the direct injection determination of anticonvulsant drugs, phenobarbital, phenytoin and carbamazepine, in human serum on the 16G-Ph and 16G-Bu silicas, respectively. Under these conditions, phenobarital was not separated from the background components of serum on the 16G-Bu silica. Fig. 2 shows a chromatogram of the direct injection determination of theophylline, theobromine and caffeine in serum on the 16G-Ph silica. Fig. 3 shows separation of cefmenoxime and cefamandole by direct serum injection on the 16G-Oc silica. Fig.

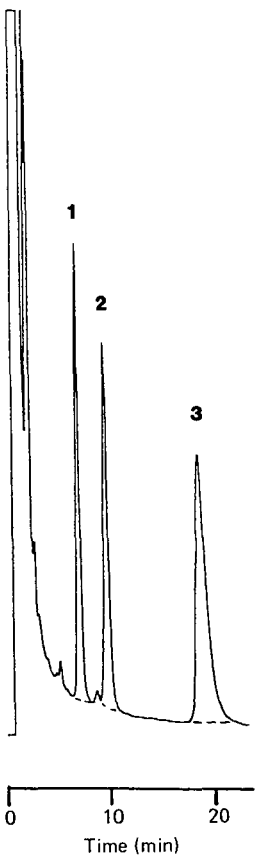

Fig. 2. Chromatogram of control serum spiked with (1) theophylline (10 μg/ml), (2) theobromine (10 μg/ml) and (3) caffeine (20 μg/ml). Chromatographic conditions: column, 16G-Ph silica packed into a 100 × 4.0 mm I.D. column; eluent, 50 m*M* NaH_2PO_4 + 50 m*M* Na_2HPO_4–CH_3CN (23:1, v/v); fow-rate, 0.8 ml/min; detection, 275 nm; sensitivity, 0.032 a.u.f.s.; injection volume, 10 μl. Dashed line indicates serum blank.

4 shows a chromatogram of anticonvulsant drugs in serum on the 16G-Ph-10G silica.

As shown in Figs. 1–4, these hydrophobic or hydrophilic drugs were eluted following the elution of serum proteins in the void volume, and were well separated from the background components of serum.

Durability of the MFP silicas

In a previous paper [7], we reported that the 16G-Ph silica could tolerate up to about 500 repetitive injections of a 10-μl serum sample (total serum sample of 5 ml) with no change in the column efficiency and back-pressure. However, previously [7] the column was washed with the stronger eluent after about 100–150 injections of a 10-μl serum sample. In this study, repetitive injections of serum samples onto the

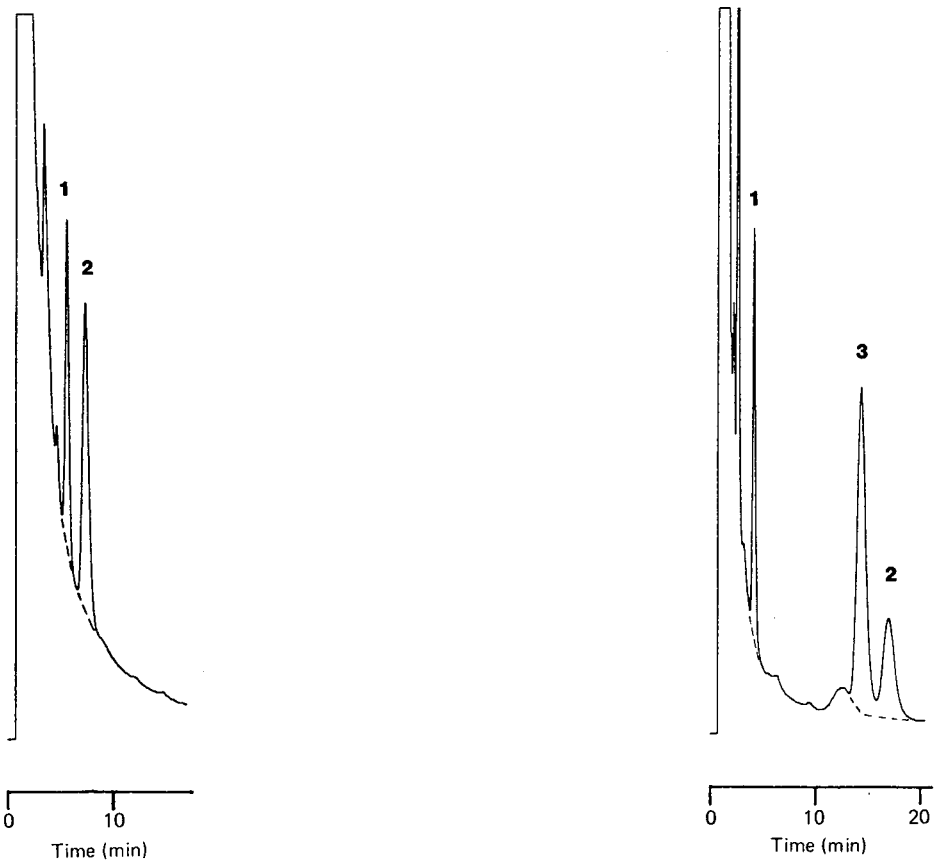

Fig. 3. Chromatogram of control serum spiked with (1) cefmenoxime (20 μg/ml) and (2) cefamandole (40 μg/ml). Chromatographic conditions: column, 16G-Oc silica packed into a 100 × 4.0 mm I.D. column; eluent, 90 m*M* NaH_2PO_4 + 10 m*M* Na_2HPO_4–CH_3CN (100:1, v/v); flow-rate, 0.8 ml/min; detection, 254 nm; sensitivity, 0.032 a.u.f.s.; injection volume, 10 μl. Dashed line indicates serum blank.

Fig. 4. Chromatogram of control serum spiked with (1) phenobarbital (20 μg/ml), (2) phenytoin (40 μg/ml) and (3) carbamazepine (20 μg/ml) on the 16G-Ph-10G silica. Chromatographic conditions as in Fig. 1 except sensitivity, 0.016 a.u.f.s. Dashed line indicates serum blank.

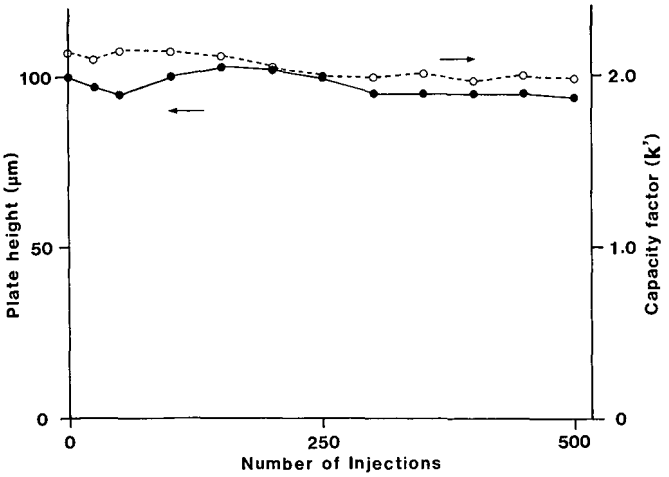

Fig. 5. Dependence of the plate height and capacity factor measured for phenobarbital on the number of injections of a 20-μl serum sample. Chromatographic conditions as in Fig. 1.

16G-Ph-10G support were tried without washing the column and without using the in-line filter and the guard column. As shown in Fig. 5, no changes in the column efficiency and capacity factor for phenobarbital were observed after about 500 repetitive injections of a 20-μl serum sample (total serum sample of 10 ml) without an increase in back-pressure. The more hydrophilic MFP silica 16G-Ph-10G, could be more suitable than the 16G-Ph silica for direct serum injection assays of drugs.

MFP silica supports having hydrophobic (phenyl, butyl or octyl) and diol phases were prepared for direct serum injecton assays of drugs. These supports could be used for the assays of drugs in serum either alone or in combination with conventional reversed-phase supports such as C_{18} or C_8. The preparation method can be applied to the preparation of MFP packing materials having various functionalities for a wider range of applications.

ACKNOWLEDGEMENTS

This work was supported in part by Grant-in-Aids from the Research Foundation for Pharmaceutical Sciences and Inoue Foundation for Science.

REFERENCES

1 I. H. Hagestam and T. C. Pinkerton, *Anal. Chem.*, 57 (1985) 1757.
2 J. Haginaka, N. Yasuda, J. Wakai, H. Matsunaga, H. Yasuda and Y. Kimura, *Anal. Chem.*, 61 (1989) 2445.
3 J. Haginaka, J. Wakai, N. Yasuda, H. Yasuda and Y. Kimura, *J. Chromatogr.*, 515 (1990) 59.
4 K. Kimata, R. Tsuboi, K. Hosoya, N. Tanaka and T. Araki, *J. Chromatogr.*, 515 (1990) 73.
5 D. J. Gisch, B. T. Hunter and B. Feibush, *J. Chromatogr.*, 433 (1988) 264.
6 D. E. Williams and P. M. Kabra, *Anal. Chem.*, 62 (1990) 807.
7 J. Haginaka and J. Wakai, *Chromatographia*, 29 (1990) 223.
8 J. Haginaka and J. Wakai, *Anal. Chem.*, 62 (1990) 997.

9 L. R. Snyder and J. J. Kirkland, *An Introduction to Modern Liquid Chromatography*, Wiley-Interscience, New York, 2nd ed., 1979, Ch. 5.
10 K. D. Lork, K. K. Unger and J. N. Kinkel, *J. Chromatogr.*, 352 (1986) 199.
11 S. E. Cook and T. C. Pinkerton, *J. Chromatogr.*, 368 (1986) 233.
12 E. C. Nice, M. W. Capp, N. Cooke and M. J. O'Hare, *J. Chromatogr.*, 218 (1981) 569.
13 N. H. C. Cooke, B. G. Archer, M. J. O'Hare, E. C. Nice and M. Capp, *J. Chromatogr.*, 255 (1983) 115.
14 F. E. Regnier and R. Noel, *J. Chromatogr. Sci.*, 14 (1976) 316.

Journal of Chromatography, 535 (1990) 173–180
Elsevier Science Publishers B.V., Amsterdam

CHROMSYMP. 2038

Effect of composition of polyacrylamide gels on exclusion limits

KIICHI SUZUKI* and KEN'ICHI NAKAZATO
School of Hygienic Science, Kitasato University, 1–15–1, Kitasato, Sagamiharashi, Kanagawaken, 228 (Japan)

ABSTRACT

An aqueous ethanol solution of acrylamide, N,N'-methylenebisacrylamide as cross-linked agent, and a third monomer was dispersed in an *n*-alkane and the three monomers were copolymerized to spherical porous gels. The effect of the composition of the third monomer in the feed on the exclusion limits of the gels was investigated. As the third monomers, acrylonitrile, methacrylamide, N,N-dimethylacrylamide, N,N-dimethylaminopropylacrylamide hydrochloride and N,N-dimethylaminopropylmethacrylamide hydrochloride were used. The logarithm of the exclusion limits of the polyacrylamide terpolymer gels bears a linear relationship to the difference between the values of the solubility parameter of the solvent and gels.

INTRODUCTION

Among the packing materials used for the separation and purification of various compounds by size exclusion, the advantage of polyacrylamide (PAAm) gels is the lower content of ionic groups and the lower adsorption capacity for samples other than gels. For the Bio-Gel P type (Bio-Rad Labs., Richmond, CA, U.S.A.), used for this purpose, an increase in exclusion limits is accompanied by a narrowing of the fractionation ranges and an increase in gel softness.

Dawkins and co-workers [1,2] carried out more rapid separations (flow-rate 1 ml/min) of water-soluble materials with spherical PAAm gels; these were prepared by inverse suspension polymerization. This gel has an exclusion limit of *ca.* $1 \cdot 10^5$ and a wider fractionation range than the Bio-Gel P types. The gel particles are porous, rigid and of the macroreticular (MR) type, and have a swelling coefficient of *ca.* 1.15. With a view to obtaining gels that have macropores and a wide fractionation range, we studied the preparation of terpolymer gels, composed acrylamide of (AAm), N,N'-methylenebisacrylamide (MBAA) and a third monomer by inverse suspension polymerization and characterized the MR type for these terpolymer gels by testing them as packing materials [3,4].

When using acrylonitrile (AN) or methacrylamide (MAAm) as the third monomer, having a lower solubility parameter (δ) than AAm, the exclusion limits of the gel (AN–AAm–MBAA or MAAm–AAm–MBAA) increased as the molar ratio of AN or

0021-9673/90/$03.50

MAAm to AAm increased [5]. When using N,N-dimethylacrylamide (DMAAm), having about the same δ value as AAm, the exclusion limits of the gel (DMAAm–AAm–MBAA) have the same value, independent of an increase in the molar ratio of DMAAm to AAm.

When using N,N-dimethylaminopropylacrylamide hydrochloride (DMAPAA · HCl) or N,N-dimethylaminopropylmethacrylamide hydrochloride (DMAPMA · HCl) as the third monomer, having higher δ values than AAm, the exclusion limits of the gel (DMAPAA · HCl–AAm–MBAA or DMPMA · HCl–AAm–MBAA) decreased as the molar ratio of DMAPAA · HCl or DMAPMA · HCl to AAm increased [6].

EXPERIMENTAL

The terpolymer gels used have been reported previously, together with their characteristics when used as packing materials [3,4]. Macroporus gel particles were produced in an inverse suspension process by polymerizing AAm, MBAA and the third monomer. The inverse suspension polymerizations of terpolymers were carried out under nitrogen in a 1-l cylindical flask, fitted with a turbine-type stirrer and gas inlet and outlet tubes. The reaction was performed by dispersing an aqueous ethanol solution (11.4 vol.%) of three monomers in an *n*-alkane (Solvent M; Nichibeikoyu, Tokyo, Japan) (d_4^{30}= 0.749;b.p. = 220–245°C), containing a nonionic surfactant (sorbitan monostearate), with stirring. Ammonium peroxydisulphate as an initiator was introduced as an aqueous ethanol solution after mixing the two phases, and the reaction flask was kept at 55 ± 2°C for 2 h.

The particles were filtered, washed with toluene, extracted with acetone to remove water and dried in a stream of warm air at 50 ± 2°C. Monomers were purified in the usual way, and other materials were used without further prufication. The gel particles were swollen in water and were sieved to obtain a 100–200-mesh (74–148 μm) sieve fraction. The sieved gel particles were packed into a glass column (500 × 8 mm I.D.) at atmospheric pressure.

The chromatographic apparatus consisted of a Model 396-31 pump (Milton Roy, Boca Raton, FL, U.S.A.), and a Shodex RI SE-11 differential refractometer (Showa Denko, Tokyo, Japan). Degassed, deionized water and 0.001 mol/l sodium chloride solution were used as eluents. The chromatographic behaviour was studied by elution of the water-soluble compounds, oligo (ethylene oxide)s and poly(ethylene oxide)s, at a pressure of 0–2 kg/cm^2 and flow- rate 82 cm/h (0.69 ml/min) as shown in Table I.

Tables II and III show the compositions and properties of the terpolymer gels used.

The solubility parameter (δ) of the gels was determined by a swelling method [7]. Dry gel particles were placed in a graduated cylinder and their weight (g/ml) was measured. They were then swollen at 25 ± 1°C in various liquids [8] and their volumes on swelling equilibrium were measured. Other swelling agents used were mixtures of two liquids. The value of δ for liquid mixtures may be calculated as follows [9]:

$$\delta_{mix} = (x_1 v_1 \delta_1 + x_2 v_2 \delta_2)/(x_1 v_1 + x_2 v_2)$$

TABLE I

SAMPLE MATERIALS

Sample	MW	Concentration of aqueous solution (%, w/w)
Polystyrene latex[a]		0.2
BD[b]	$2.00 \cdot 10^6$	0.2
PEO-SE 150[c]	$1.20 \cdot 10^6$	0.5
PEO-SE 70[c]	$6.61 \cdot 10^5$	0.5
PEO-SE 30[c]	$2.78 \cdot 10^5$	0.5
PEO-SE 15[c]	$1.48 \cdot 10^5$	0.5
PEO-SE 8[c]	$7.3 \cdot 10^4$	0.5
PEO-SE 5[c]	$4.0 \cdot 10^4$	0.5
PEO-SE 2[c]	$2.5 \cdot 10^4$	0.5
PEG 6000[d]	7900	1.0
PEG 4000[d]	3300	1.0
PEG 2000[d]	2100	1.0
PEG 600[d]	650	1.0
PEG 200[d]	230	1.0
Ethylene glycol	62	1.0
Acetone	58	5.0
Methanol	32	1.0

[a] Dow Chemical (Midland, MI, U.S.A.) (particle diameter 0.109 μm).
[b] Pharmacia (Uppsala Sweden)
[c] Poly(ethylene oxide) standard sample (Toyo Soda, Tokyo, Japan).
[d] Poly(ethylene glycol) (Wako, Osaka, Japan).

where x is the molar fraction and v is the molar volume of components 1 and 2 at 25°C. The degree of swelling (Q) was defined as the ratio of the wet bed volume (ml) in a liquid per unit weight (g) of the gel. The values of Q for various liquids were plotted against the δ values of the liquids used.

The values of δ for the gel were obtained as the maximum value obtained on the curve. Further, the values obtained for the gels were confirmed according to the method of Mangaraj [10] and Mangaray *et al.* [11].

TABLE II

COMPOSITION AND EXCLUSION LIMITS OF GELS

Gel No.	AAm (g)	MBAA (g)	Third monomer		MBAA in monomer feed (mol %)	Molar ratio of third monomer to AAm	Exclusion limits (molecular weight)
			Compound	Amount (g)			
1	30	10.0	None		13.3	0	$1.6 \cdot 10^4$
2	27.5	10.0	NA	2.5	13.0	0.120	$2.5 \cdot 10^4$
3	25.0	10.0	AN	5.0	12.7	0.270	$6.9 \cdot 10^4$
4	20.0	10.0	AN	10.0	12.2	0.670	$2.6 \cdot 10^5$
5	15.5	10.0	AN	15.0	11.6	1.34	$1.4 \cdot 10^6$
6	27.5	10.0	MAAm	2.5	13.5	0.075	$4.5 \cdot 10^4$
7	25.0	10.0	MAAm	5.0	13.6	0.168	$7.2 \cdot 10^4$
8	20.0	10.0	MAAm	10.0	14.0	0.416	$2.0 \cdot 10^5$
9	15.0	10.0	MAAm	15.0	14.4	0.834	$4.4 \cdot 10^5$

TABLE III

COMPOSITION AND EXCLUSION LIMITS OF GELS

Gel No.	AAm (g)	MBAA (g)	Third monomer		MBAA in monomer feed (mol %)	Molar ratio of third monomer to AAm	Exclusion limits (molecular weight)
			Compound	Amount (g)			
10	29.7	10.0	DMAAm	0.42	13.3	0.010	$1.3 \cdot 10^4$
11	29.1	10.0	DMAAm	1.29	13.3	0.032	$1.1 \cdot 10^4$
12	28.5	10.0	DMAAm	2.09	13.3	0.052	$1.1 \cdot 10^4$
13	27.1	10.0	DMAAm	4.16	13.3	0.110	$1.0 \cdot 10^4$
14	24.0	10.0	DMAAm	8.37	13.3	0.249	$1.1 \cdot 10^4$
15	29.7	10.0	DMAPMA · HCl	0.72	13.3	0.10	$5.5 \cdot 10^4$
16	29.1	10.0	DMAPMA · HCl	2.21	13.3	0.032	$1.6 \cdot 10^4$
17	28.5	10.0	DMAPMA · HCl	3.59	13.3	0.052	$7.9 \cdot 10^3$
18	27.1	10.0	DMAPMA · HCl	7.15	13.3	0.110	$7.9 \cdot 10^3$
19	24.0	10.0	DMAPMA · HCl	14.37	13.3	0.249	$4.7 \cdot 10^3$
20	29.7	10.0	DMAPAA · HCl	0.66	13.3	0.010	$1.4 \cdot 10^4$
21	29.1	10.0	DMAPAA · HCl	2.03	13.3	0.32	$3.9 \cdot 10^3$
22	28.5	10.0	DMAPAA · HCl	3.30	13.3	0.52	$3.8 \cdot 10^3$
23	27.1	10.0	DMAPAA · HCl	6.56	13.3	0.110	$8.7 \cdot 10^2$

RESULTS AND DISCUSSION

Table II shows the compositions and properties of the terpolymer gels prepared. The results have been reported previously [3,4]. As shown in Table II, when AN was used as the third monomer, at a fixed amount (10.0 g) of MBAA in the monomer feed, the exclusion limits of the resulting gels (AN–AAm–MBAA) increased from $1.6 \cdot 10^4$ to $1.4 \cdot 10^6$ with an increase in the molar ratio of AN to AAm from 0 to 1.34. Similary, when MAAm was used as the third monomer at a fixed amount (10.0 g) of MBAA in the monomer feed, the exclusion limits of the gels obtained (MAAm–AAm–MBAA) increased from $1.6 \cdot 10^4$ to $4.4 \cdot 10^5$ with an increase in the molar ratio of MAAm to AAM from 0 to 0.834.

In general, aggregation and growth of microgels occur in the process of gel formation. Therefore, the increase in the exclusion limit on addition of AN and MAAm is assumed to occure as follows. Addition of the third monomer decreases the solubility of the polymers that constitute the microgels as shown in Fig. 1. Consequently, it promotes aggregation of the microgels rather than growth of polymerization; in other words, phase separation is accelarated. As shown in Fig. 2, the δ values for AN–AAm–MBAA gels decreased from 17.60 to 17.24 with an increase in the molar ratio of AN to AAm from 0 to 1.34. Also, the δ values for MAAm–AAm–MBAA gels decreased from 17.60 to 17.35 with increasing molar ratio of MAAm to AAm.

As shown in Table III, when DMAAm was used as the third monomer with a fixed amount (10.0 g) of MBAA in the monomer feed, the exclusion limits of the gels obtained (DMAAm–AAm–MBAA) were in the range $1.0 \cdot 10^4 - 1.6 \cdot 10^4$, unlike the results for the other terpolymer gels whose exclusion limits were influenced by the molar ratio of the third monomer to AAm.

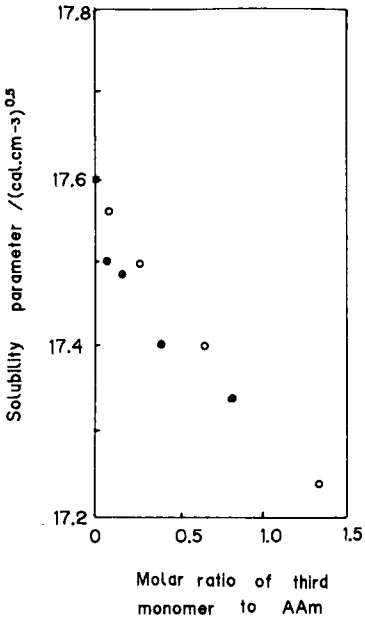

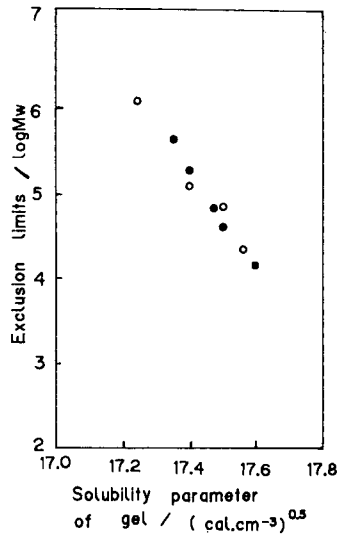

Fig. 1. Correlation of solubility parameters of the gels with molar ratio of the third monomer to AAm. ■ = AAm–MBAA gel; ○ = AN–AAm–MBAA gel; ● = MAAm–AAm–MBAA gel.

Fig. 2. Correlation of exclusion limits with the solubility parameters of the gels. ■ = AAm–MBAA gel; ○ = AN–AAm–MBAA gel; ● = MAAm–AAm–MBAA gel. Mw = Molecular weight

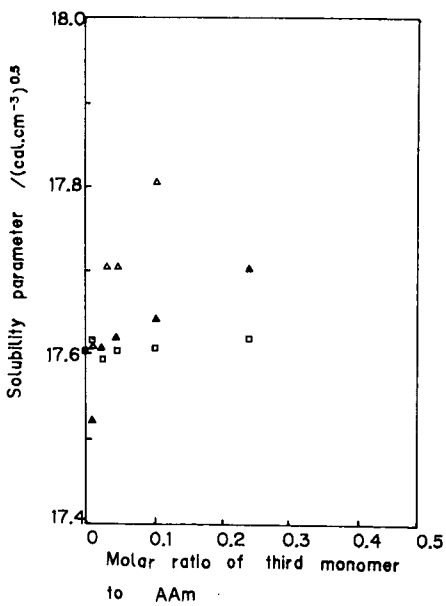

Fig. 3. Correlation of solubility parameters of the gels with molar ratio of third monomer to AAm. ■ = AAm–MBAA gel; ▲ = DMAPMA · HCl–AAm–MBAA gel; △ = DMAPAA · HCl–AAm–MBAA gel; □ = DMAAm–AAm–MBAA gel.

When DMAPAA · HCl was used as the third monomer with a fixed amount (10.0 g) of MBAA in the monomer feed, the exclusion limits of the gels obtained (DMAPAA · HCl–AAm–MBAA) decreased from $1.6 \cdot 10^4$ to $8.7 \cdot 10^2$ as the molar ratio of DMAPAA · HCl to AAm increased from 0 to 0.110.

When DMAPMA · HCl was used as the third monomer with a fixed amount (10.0 g) of MBAA in the monomer feed, the exclusion limits of the gels obtained (DMAPMA · HCl–AAm–MBAA) decreased from $5.5 \cdot 10^4$ to $4.7 \cdot 10^3$ as the molar ratio of DMAPAA · HCl to AAm increased from 0.01 to 0.249, but increased from $1.6 \cdot 10^4$ to $5.5 \cdot 10^4$ as the molar ratio of DMAPMA · HCl to AAm increased from 0 to 0.010.

Fig. 3 shows that ths δ values for DMAAm–AAm–MBAA gels ranged from 17.58 to 17.65 and were independent of increase in the molar ratio of DMAAm to AAM. The δ values for DMAPAA · HCl–AAm–MBAA gels increased from 17.60 to 17.80 as the molar ratio of DMAPAA · HCl to AAm increased from 0 to 0.110. The δ values of DMAPMA · HCl–AAm–MBAA gels increased from 17.60 to 17.70 as the molar ratio of DMAPMA · HCl to AAm increased from 0.01 to 0.249, but decreased from 17.60 to 17.50 as the molar ratio of DMAPMA · HCl to AAm increased from 0 to 0.010.

These results with respect to DMAPMA · HCl–AAm–MBAA gels were contrary to the assumption that as the molar ratio increases, the exclusion limits and the δ values of the gels increase, as was found to be true with DMAPAA · HCl–AAm–MBAA gels. We consider that this difference results from the presence of the α-methyl group in DMAPMA. This was supported by the finding of acceleration of phase separation by the α-methyl group in the MAAm–AAm–MBAA gels. Based on the relationship between exlusion limits and molar ratio for DMAPMA · HCl–AAM–MBAA gels, we hypothesize that there are factors which depress phase separation,

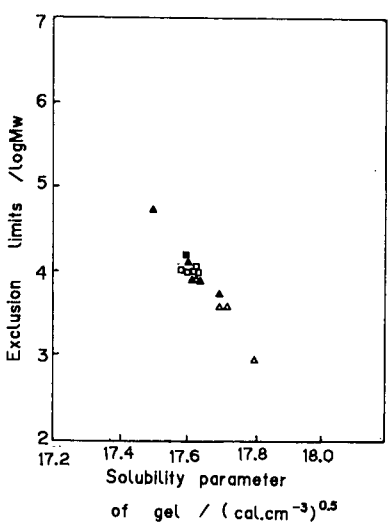

Fig. 4. Correlation of exclusion limits with the solubility parameters of the gels. ■ = AAM–MBAA gel; ▲ = DMAPMA · HCl–AAm–MBAA gel; △ = DMAPAA · HCl–AAm–MBAA gel; □ = DMAAm–AAm–MBAA gel.

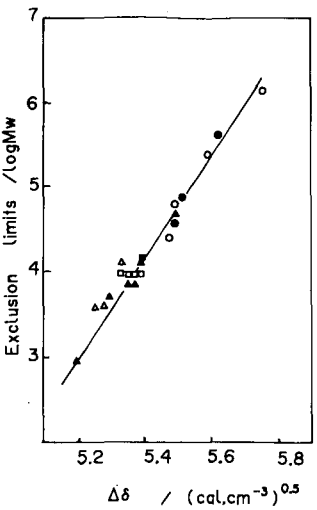

Fig. 5. Correlation of exclusion limits with with the difference in the solubility parameters between the polymerization solvent and the gels, $\Delta\delta$. ■ = AAM–MBAA gel; ○ = AN–AAm–MBAA gel; ● = MAAm–AAm–MBAA gel; □ = DMAA–AAm–MBAA gel; ▲ = DMAPMA · HCl–AAm–MBAA gel; △ = DMAPAA · HCl–AAm–MBAA gel.

e.g., electrostatic repulsion between the dimethylaminopropyl groups and the hydrophilic nature of the pedant group, and factors that accelerate phase separation, *e.g.*, hydrophobic interaction between α-methyl groups. With a molar ratio of 0–0.010, the factors accelerating phase separation are stronger than the opposing factors.

Fig. 4 shows the correlation between the values for the terpolymer gels and exclusion limits. The exclusion limits of DMAPAA · HCl–AAm–MBAA and DMAPMA · HCl–AAm–MBAA gels correlated with the δ values of the gels.

Fig. 5 also clearly shows that an approximately linear relationship exists between the logarithm of the exclusion limits of the gels and the difference in the solubility parameters between the polymerization solvent and gels ($\Delta\delta$). This relationship applied in the three instances in which the third monomer component of the terpolymer gels has a lower δ value than AAm, a δ value about the same as that of AAm and a higher δ value than AAm. The straight line obeyed the equation.

$$\log (\text{mol.wt.})_{\text{lim}} = 5.58\Delta\delta - 25.94 \quad (r = 0.990)$$

CONCLUSION

The logarithm of the exclusion limits of the polyacrylamide terpolymer gels bears a linear relationship to the difference between the value of the solubility parameter of the polymerization solvent and the gels, and the magnitude of δ for the polymer chains of the PAAm terpolymer gels governs the aggregation and growth of microgels in the process of gel formation.

ACKNOWLEDGEMENTS

We thank Professor Yasuji Ohtsuka and Haruma Kawaguchi of Keio University for helpful discussions.

REFERENCES

1 J. V. Dawkins and N. P. Gabbott, *Polymer*, (1981) 291.
2 J. V. Dawkins, N. P. Gabbott and M. C. J. Montenegro, *J. Chromatogr.*, 371 (1986) 283.
3 K. Suzuki, K. Nakazato and T. Takasaki, *Nippon Kagaku Kaishi*, (1979) 1327.
4 K. Nakazato and K. Suzuki, *Nippon Kagaku Kaishi*, (1984) 1919.
5 K. Nakazato and K. Suzuki, *Macromolecules*, 22 (1989) 1497.
6 K. Nakazato and K. Suzuki, *Macromolecules*, 23 (1990) 1800.
7 T. A. Orobino, H. B. Hopfenberg and V. Sanett, *J. Macromol. Sci. Phys.*, B3 (1963) 717, 777.
8 C. M. Hansen, *J. Paint Technol*, (1967) 39, 104.
9 H. Burrell, *Encyclopedia of Polymer Science and Technology*, Vol. 12, Interscience, New York, 1971, p. 618.
10 D. Mangaraj, *Makromol. Chem.*, 65 (1963) 29.
11 D. Mangaraj, S. Patra and S. Rashid, *Markomol. Chem.*, 65 (1963) 39.

Journal of Chromatography, 535 (1990) 181–187
Elsevier Science Publishers B.V., Amsterdam

CHROMSYMP. 2054

Retention prediction based on the electrostatic model of reversed-phase ion-pair high-performance liquid chromatography: effect of pairing ion concentration

ÁKOS BARTHA
Institute for Analytical Chemistry, Veszprem University, POB 158, H-8201 Veszprem (Hungary)
and
JAN STÅHLBERG*
Quality Control, ASTRA Pharmaceutical Production AB, S-151 85 Södertälje (Sweden)

ABSTRACT

Based on the electrostatic model of reversed-phase ion-pair chromatography, a practical equation was developed to describe the relationship between the capacity factor of ionic solutes and the eluent concentration of the amphiphilic pairing ion. At constant ionic strength and organic modifier concentration, the logarithm of solute capacity factor can be approximated as a linear function of the logarithm of the pairing ion concentration. The slope of this relationship is determined by the sign and number of charges of the solute ion and the pairing ion. The limitations and the practical use of the proposed model are discussed in detail.

INTRODUCTION

Reversed-phase ion-pair liquid chromatography (RP-IPC) is a well established method for the separation of ionic organic compounds. One of the main chromatographic variables for controlling the retention of ionic solutes is the mobile phase concentration of the amphiphilic ion-pairing reagent. When the pairing ion concentration increases, the retention of the ionic solutes decreases for charges of identical sign and increases for charges of opposite sign.

In a number of studies [1–7], when the capacity factor of the solute ion (k'_{cB}) was plotted against the mobile phase concentration of the pairing ion (c_A) on a logarithmic scale, an approximately linear relationship was obtained. The linearity of this relationship allowed Billiet and co-workers [5,6] to apply an efficient iterative optimization strategy to the selectivity optimization of ion-pair liquid chromatographic separations.

In fact, a linear $\log k'_{cB}$ *vs.* $\log c_A$ relationship can be derived from some of the retention models suggested for ion-pair chromatography. However, these models disagree on the slope of this log–log relationship.

0021-9673/90/$03.50

Schoenmakers [8] has shown that in an ideal case the ion-pair partition model predicts a slope of unity. Van de Venne *et al.* [3] assumed a Freundlich-type adsorption isotherm for the pairing ion together with a dynamic ion-exchange mechanism. According to their retention equation [3], the slope of the log k'_{cB} *vs.* log c_A relationship is identical with the slope of the Freundlich isotherm of the pairing ion at constant ionic strength.

The analysis of experimental IPC data from different studies indicated that the slope of the log k'_{cB} *vs.* log c_A relationship is usually less than unity [3,5,7], is less sensitive to variations in the adsorption properties of the pairing ions [9,10] and is more sensitive to the sign and number of charges carried by the respective solute ions [4]. Ståhlberg [11] developed an electrostatic retention model for RP-IPC. Since its introduction, the electrostatic theory has been thoroughly tested [12,13] and extended to account for the eluent concentration of the electrolyte [14,15] and the organic modifiers [15,16].

In this paper, we discuss the relationship between ionic solute retention and pairing ion concentration on the basis of the electrostatic retention model. A general retention equation is derived to approximate the retention of ionic solutes when they have either single or multiple charges with similar or opposite sign as compared with that of a monocharged pairing ion. Theoretical predictions are compared with experimental retention data for differently charged analytes measured in the presence of either positively (tetrabutylammonium) or negatively charged (octylsulphate) pairing ions.

THEORY

The basic assumption of the electrostatic theory [11–13] is that the adsorbed amphiphilic pairing ions and the counter ions of the buffer form an electrical double layer at the interface between the stationary and mobile phase, creating an electrostatic surface potential. This surface potential will influence both the adsorption isotherm of the pairing ion and the retention of the ionic solutes. Owing to this complicated interrelationship [13] (adsorption–surface potential–retention), it is not possible to develop a closed-form expression describing the solute capacity factor (k'_{cB}) as a function of the eluent concentration of the pairing ion (c_A).

However, an approximate expression can be obtained by combining the surface potential-modified Langmuir adsorption isotherm of the pairing ion [13–15] and the linear form of the Gouy–Chapman equation [13]. Assuming non-zero pairing ion concentrations ($c_A > 0$) and using a series expansion, separate expressions can be obtained for the oppositely and for the similarly charged ionic solutes [16]. When there is a unit charge of opposite sign on both the solute ion and the pairing ion,

$$\log k'_{cB} = \log k'_{oB} + 1/2 \log c_A + K_1 - K_0 \quad (1)$$

and when there is a unit charge of identical sign on both the solute ion and the pairing ion,

$$\log k'_{cB} = \log k'_{oB} - 1/2 \log c_A - K_1 - K_0 \quad (2)$$

where k'_{cB} is the capacity factor of solute ion B in the presence of the pairing ion, k'_{oB} is

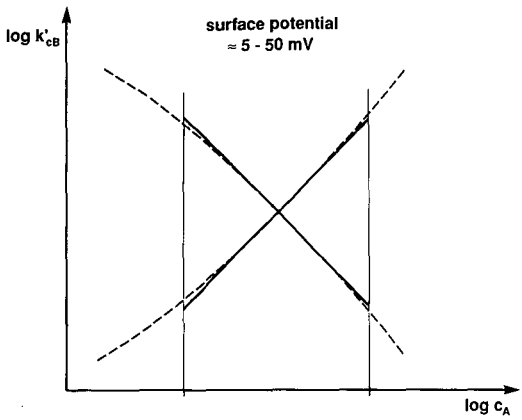

Fig. 1. Schematic illustration of log k'_{cB} as a function of log c_A obtained from the complete electrostatic theory (dashed lines) and from the approximate theory, eqn. 3 (solid lines).

the capacity factor of solute ion B in the absence of the pairing ion and c_A is the mobile phase concentration of pairing ion A. According to the electrostatic retention model, K_0 and K_1 are independent of the solute. The value of K_1 decreases when the ionic strength increases [13], and the value of K_0 decreases when less hydrophobic pairing ions and higher organic modifier concentrations [16] are used.

Eqns. 1 and 2 can be combined into a more general form which holds for any value and sign of the charge of the solute ions and for monocharged pairing ions:

$$\log k'_{cB} = K_2 - \tfrac{1}{2} z_B/z_A \log c_A \quad (3)$$

where $z_B = \pm 1,2,\ldots$ is the charge of solute ion B, $z_A = \pm 1$ is the charge of pairing ion A and K_2 is a constant, depending on the solute, pairing ion, organic modifier concentration and ionic strength. According to this simplified equation, log k'_{cB} is a linear function of log c_A with a slope of $\tfrac{1}{2} z_B$ for opposite-signed charges and $-\tfrac{1}{2} z_B$ for similar-signed charges of the solute ion and the pairing ion.

Eqn. 3 is approximately valid when the surface potential-modified Langmuir adsorption isotherm is linear and when the surface potential lies between 5 and 50 mV [15]. Practical chromatographic work is often performed under such conditions. Therefore, reasonably wide applicability can be foreseen for eqn. 3. Above and below the imposed limits, *i.e.*, at high and low eluent concentrations of the pairing ion, non-linear retention behaviour is theoretically expected. This is illustrated schematically in Fig. 1, where log k'_{cB} is plotted as a function of log c_A for the complete electrostatic theory and compared with the approximate theory, *i.e.*, eqn. 3.

EXPERIMENTAL

Analytical-reagent grade benzenesulphonic acid, naphthalene-2-sulphonic acid, anthraquinone-2-sulphonate, 1,5-naphthalenedisulphonate, tetrabutylammonium bromide and Orange G were purchased from Fluka (Buchs, Switzerland) and

benzyltrimethylammonium bromide, benzyltriethylammonium bromide, sodium octylsulphate and sodium octylsulphonate from Merck (Darmstadt, F.R.G.). Pharmacopeial-grade bupivacaine and etidocaine were supplied by Astra Pharmaceutical Production AB (Södertälje, Sweden).

A Model LC 5000 liquid chromatograph (Varian Aerograph, Walnut Creek, CA, U.S.A.), equipped with a UV detector (254 nm) and with Model 7010 and 7126 injection valves (Rheodyne, Cotati, CA, U.S.A.), was used. The analytical columns were packed with μBondapak C_{18} (150 mm × 3.9 mm I.D.) (Waters Assoc., Milford, MA, U.S.A.) and ODS-Hypersil (200 mm × 4.6 mm I.D.) (Shandon, Runcom, U.K.). The eluents were prepared with 25 m*M* phosphoric acid and 25 m*M* sodium dihydrogenphosphate (pH 2.1), and various concentrations of acetonitrile and ion-pairing reagents. Eluents for the experiments with octylsulphonate also contained sodium bromide (I = 0.15 *M*).

RESULTS AND DISCUSSION

Retention behaviour of monocharged solute ions

In Figs. 2 and 3, the capacity factors (log k'_{cB}) of positively and negatively charged analytes are plotted against the mobile phase concentration (log c_A) of positively charged (tetrabutylammonium) and negatively charged (octylsulphonate and octylsulphate) pairing ions, respectively. Full lines show the theoretical retention behaviour with a slope of ± 1/2 as predicted by eqn. 3. The theoretical lines were placed

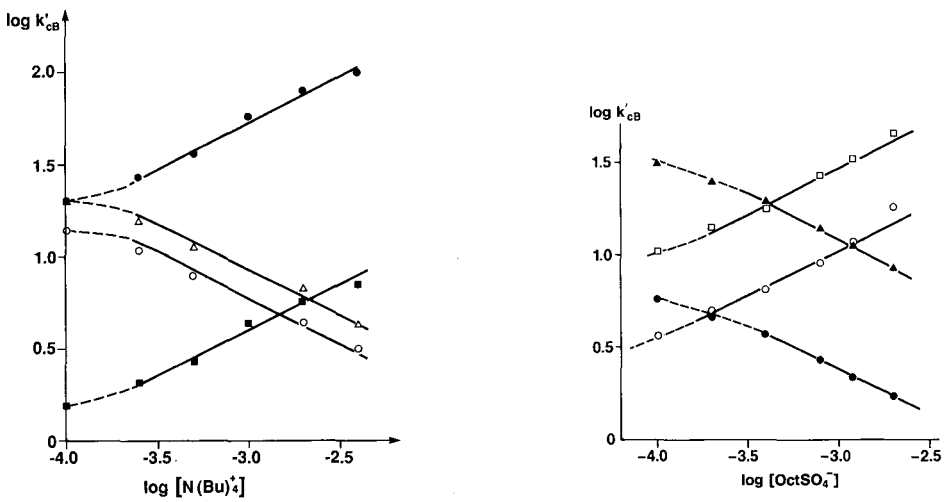

Fig. 2. Log k'_{cB} *vs.* log c_A relationships for positively and negatively charged analytes and positively charged tetrabutylammonium bromide [$N(Bu)_4^+$] as pairing ion. Solutes: (■) benzenesulphonate, (●) naphthalene-2-sulphonate, (△) bupivacaine and (○) etidocaine. Solid lines indicate the theoretically predicted behaviour. Column, μBondapak C_{18}; eluent, 10% acetonitrile in 0.10 *M* phosphate buffer (pH 2.1); temperature, 27°C.

Fig. 3. Log k'_{cB} *vs.* log c_A relationships for positively and negatively charged analytes and negatively charged octylsulphate ($OctSO_4^-$) as pairing ion. Solutes: (▲) anthraquinone-2-sulphonate, (●) naphthalene-2-sulphonate, (○) benzyltrimethylammonium and (□) benzyltriethylammonium. Solid lines indicate the theoretically predicted behaviour. Other conditions as in Fig. 2.

as close to the experimental points as possible (*i.e.*, with arbitrary intercept values along the ordinate), using the theoretical slope values.

In accordance with the electrostatic model of ion-pair chromatography [11], solute ions with opposite and similar charges show symmetrical behaviour. The experimental log k'_{cB} values agree well with the predictions made from eqn. 13 for all solute ion–pairing ion combinations. At low c_A values some deviation can be observed from the linear model. Obviously, these deviations between the complete and approximate equation do not allow the accurate description of ionic solute retention over a broad range of pairing ion concentrations. However, the simplified model can be still used in practice to estimate the magnitude of retention changes for ionic solutes in RP-IPC.

An important area of such applications is the determination of initial mobile phase compositions, which lead to chromatograms with reasonable analysis times, prior to systematic selectivity optimization [17,18]. In this early stage of optimization parameter selection, predictions must be made from limited number of chromatographic experiments while larger errors in the predicted retention times are still acceptable.

When the charge type (z_B) and the retention (log k'_{cB}) of the solute are known at a single eluent concentration (log c_A) of the pairing ion (z_A), eqn. 3 can be used to calculate K_2 and estimate the solute capacity factors at other pairing ion concentrations.

Retention behaviour of doubly-charged solute ions

Another important test of eqn. 3 is the comparison of the retentions of singly- and multiply-charged solute ions under typical ion-pair chromatographic conditions. In Figs. 4 and 5, the retention (log k'_{cB}) of singly-charged (benzenesulphonate, naphthalene-2-sulphonate) and doubly-charged (1,5-naphthalenedisulphonate, Orange G) negative solute ions is plotted against the eluent concentration (log c_A) of a positively (tetrabutylammonium) and a negatively charged (octylsulphonate) pairing ion, respectively.

The experimental data closely follow the theoretically predicted behaviour (solid lines), for both increasing (Fig. 4) and decreasing (Fig. 5) solute retention. The slopes doubled (from $\pm 1/2$ to ± 1) with doubling the charge of the solute ions. Again, slight deviations from linearity indicate some of the limitations of this simplified model, as discussed above.

However, the physically consistent and unambiguous difference in the values for the two slopes for the singly- and doubly-charged solutes allows other practical applications of eqn. 3. For example, by simply measuring the retention of a (unknown) solute at two different pairing ion concentrations and calculating the slope, information can be obtained not only about the charge type (positive, negative, zero) of the analyte but also about the number of charges carried.

It should be noted that the data in Figs. 4 and 5 were measured on different columns, which gives further support to the generality of the model described.

It must be emphasized that the application of eqn. 3 requires a constant ionic strength and organic modifier concentration in the mobile phase, otherwise K_2 (and K_1) will not be constant. When the pairing ion and the organic modifier concentration are varied simultaneously, the extended form of eqns. 1 and 2 must be used [16].

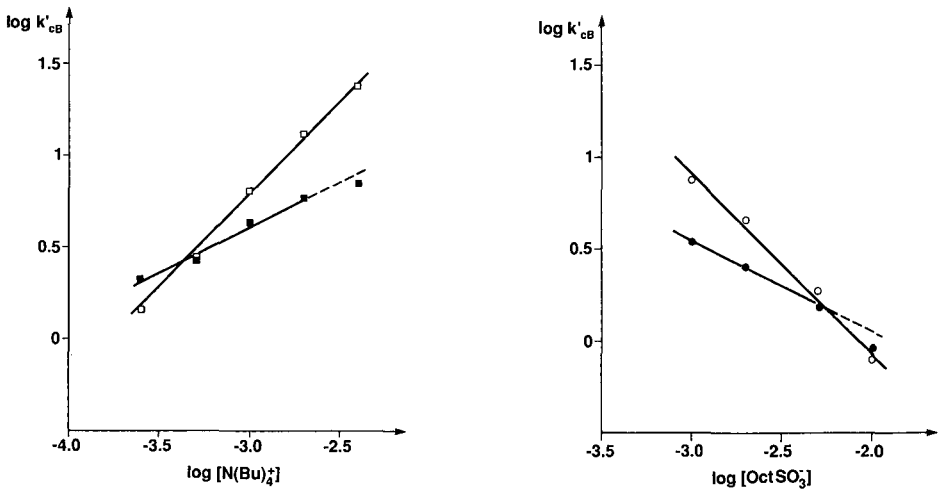

Fig. 4. Log k'_{cB} *vs.* log c_A relationships for singly- and doubly-charged negative solute ions and positively charged tetrabutylammonium bromide [$N(Bu)_4^+$] as pairing ion. Solutes: (■) benzenesulphonate and (□) 1,5-napthalenedisulphonate. Solid lines indicate the theoretically predicted behaviour. Other conditions as in Fig. 2.

Fig. 5. Log k'_{cB} *vs.* log c_A relationships for singly- and doubly-charged negative solute ions and negatively charged octylsulphonate ($OctSO_3^-$) as pairing ion. Solutes: (●) naphthalene-2-sulphonate and (○) Orange G. Solid lines indicate the theoretically predicted behaviour. Column, ODS-Hypersil; eluent, 6% acetonitrile in 50 m*M* phosphate buffer (pH 2.1); temperature, 25°C.

CONCLUSIONS

The electrostatic theory of ion-pair chromatography has been used to derive simple equations to approximate the retention of ionic solutes as a function of the eluent concentration of the pairing ion. At constant ionic strength and organic modifier concentration, a linear relationship is predicted between the logarithm of the capacity factor of the ionic solute and the logarithm of the eluent concentration of the amphiphilic pairing ion.

According to the electrostatic theory, the slope of this relationship depends only on the sign and number of charges of the solute ion and the pairing ion. For singly-charged pairing ions, the slope is $+ \frac{1}{2}z_B$ for oppositly and $- \frac{1}{2}z_B$ for similarly (singly- and multiplȳ) charged solute ions, where z_B is the charge of the analyte.

Predictions of the retention model agreed well with experimental data for all solute ion–pairing ion combinations. When the eluent concentration of the pairing ions varied over a broad range, the log(retention) *vs.* log(pairing ion concentration) relationship may become non-linear. Such deviations from the theoretical behaviour limit the practical use of the simplified retention model to the approximation rather than the precise description of the retention of ionic solutes.

In conclusion, the electrostatic retention model gives a physically consistent description of the retention effect of the sign and number of charges of the ionic solutes (in ion-pair chromatography) and allows the rationalization of experimental data.

REFERENCES

1 K. G. Wahlund, *J. Chromatogr.*, 115 (1975) 411.
2 C. P. Terweij-Groen, S. Heemstra and J. C. Kraak, *J. Chromatogr.*, 161 (1978) 69.
3 J. L. M. Van de Venne, J. L. H. M. Hendrikx and R. S. Deelder, *J. Chromatogr.*, 167 (1978) 1.
4 P. Jandera and J. Churacek, *Gradient Elution in Column Liquid Chromatography*, Elsevier, Amsterdam, 1985, p. 34.
5 H. A. H. Billiet, A. C. J. H. Drouen and L. de Galan, *J. Chromatogr.*, 316 (1984) 231.
6 H. A. H. Billiet, J. Vuik, J. K. Strasters and L. de Galan, *J. Chromatogr.*, 384 (1987) 153.
7 A. Zein and M. Baerns, *J. Chromatogr. Sci.*, 27 (1989) 249.
8 P. J. Schoenmakers, *Optimization of Chromatographic Selectivity —A Guide to Method Development* (*Journal of Chromatography Library*, Vol. 35), Elsevier, Amsterdam, 1986, pp. 93–98.
9 A. Bartha, Gy. Vigh, H. A. H. Billiet and L. de Galan, *J. Chromatogr.*, 303 (1984) 29.
10 A. Bartha, Gy. Vigh, H. A. H. Billiet and L. de Galan, *Chromatographia*, 20 (1985) 587.
11 J. Ståhlberg, *J. Chromatogr.*, 356 (1986) 231.
12 J. Ståhlberg and A. Furängen, *Chromatographia*, 24 (1987) 783.
13 J. Ståhlberg, *Chromatographia*, 24 (1987) 820.
14 J. Ståhlberg and I. Hägglund, *Anal. Chem.*, 60 (1988) 1958.
15 J. Ståhlberg and A. Bartha, *J. Chromatogr.*, 456 (1988) 253.
16 A. Bartha, Gy. Vigh and J. Ståhlberg, *J. Chromatogr.*, 506 (1990) 85.
17 P. J. Schoenmakers and M. Mulholland, *Chromatographia*, 25 (1988) 737.
18 A. Bartha, H. A. H. Billiet and L. de Galan, *J. Chromatogr.*, 464 (1989) 225.

Journal of Chromatography, 535 (1990) 189–198
Elsevier Science Publishers B.V., Amsterdam

CHROMSYMP. 2006

Nature of the eddy dispersion in packed beds

A. L. BERDICHEVSKY and U. D. NEUE*
Waters Chromatography Division of Millipore Corp., Milford, MA 01757 (U.S.A.)

ABSTRACT

Relationships describing the dependence of the height equivalent to a theoretical plate (HETP) on the linear velocity u contain a term that is traditionally called the eddy dispersion term. In some theories, this term is independent of velocity, in others it results in a curved relationship with velocity. Both have been observed experimentally. In this paper, we advocate a theory which is capable of explaining both. This theory is based on the mass-transfer between sections of the mobile phase that move at different velocities. The equation obtained is formally identical to the equation derived by Giddings. However, the meaning of the coefficients in both theories is different. In our approach, the coefficients are related to structural parameters of the packed bed and can be assessed quantitatively. This is helpful in the interpretation of eddy dispersion terms obtained in column packing experiments.

The mathematical approach used here allows the calculation of all moments of the peak and therefore a prediction of the peak-shape. Although a relationship exists between structural parameters of the packed bed and the experimental observations of peak width and peak symmetry, this relationship can only be expressed in the form of the product of velocity difference with a characteristic distance. This term cannot be deconvoluted further. Thus, large velocity differences over small distances result in the same peak-width and -shape as small velocity differences over large distances.

INTRODUCTION

Klinkenberg and Sjenitzer [1] and Van Deemter *et al.* [2] first introduced an equation for the relationship between band-spreading and linear velocity, which contains a term which was called eddy dispersion. In their theory, this term is independent of velocity. Subsequent treatments adopted this term and related it to the non-uniformity of the packed bed. Giddings [3] postulated, that some of the terms related to flow-path non-uniformities couple with mass-transfer terms originating in the same type of non-uniformities. These coupled terms result in a curved relationship with velocity. Kennedy and Knox [4] approximated the Giddings equation with a term containing the third root of the velocity.

It has been argued [5], that the origin of the coupling postulated by Giddings lies in the relaxation of radial concentration gradients by the combined effect of diffusion and eddy dispersion. This is precisely the model which is used in the quantitative theoretical treatment which follows.

BACKGROUND

The propagation of a solute in a liquid flowing through a capillary was first

0021-9673/90/$03.50

considered in the famous works of Aris [6] and Taylor [7]. They found that the band width depends on the diffusion coefficient of the solute, the flow profile and the flow-rate. The result is the diffusion equation (1), which describes the change of the average concentration, C, of a species as a function of the longitudinal coordinate x and the time t. Averaging was done over the cross-section of the capillary.

$$\frac{\partial}{\partial t}C + v\frac{\partial}{\partial x}C = D\frac{\partial^2}{\partial x^2}C \tag{1}$$

Here, v is the average linear velocity of the liquid and D is an analogue of the diffusion coefficient. This coefficient is often called the effective diffusion coefficient and sometimes the dispersion coefficient.

In laminar flow regimes the expression for this coefficient is as follows

$$D = D_{\text{mol}} + c\frac{r_c^2 v^2}{D_{\text{mol}}} \tag{2}$$

Here, D_{mol} is the molecular diffusion coefficient, r_c is the radius of the capillary and c is a constant which depends on the flow profile. For laminar flow in a circular capillary the value of the constant c is 1/48. This effective diffusion coefficient is closely related to h, the reduced plate height, which is the parameter commonly used in chromatography.

$$h = \frac{D}{rv}$$

It is important to note, that the deduction of the eqns. 1 and 2 assumes that the time of peak propagation is sufficiently large. The result of this "long" peak propagation is that the shape of the peak becomes completely symmetrical. Such peaks are called Gaussian peaks.

Golay [8] has generalized the deduction of Aris and Taylor to the case in which the surface layer of the capillary has retentive properties. In this case, sample molecules spend some time in the boundary layer thus causing a delay of the peak in the capillary and some additional band spreading. In general, the form of the equation which describes the evolution of the concentration profile remains the same as in the case of no retention. In other words, chromatography in long capillaries always yields symmetrical peaks. The work of Golay is a cornerstone of the theory of chromatography, which has been refined since by a large number of researchers [9,10].

The phenomena observed in a capillary are also encountered in a packed bed. However additional complications arise from the structural properties of the packed bed. These structural properties give rise to additional terms in the relationship of band-broadening and flow velocity. They can also be the cause of peak asymmetry. In the theory developed below, both effects are explained on the basis of the propagation of the sample band under equilibrium conditions in a packed bed with non-uniformities on the micro-scale. In this context the prefix "micro" means that the scale is in the range of a few particle diameters.

It is proper to point out, that the results of this work are applicable not only to packed beds, but also to any other porous media, since no assumption is made on the particular inner geometry of the medium. Nevertheless, for the sake of consistency we will refer to the medium as a packed bed.

STATEMENT OF THE MODEL

Let us suppose, for simplicity, that our packed bed consists of two component phases in which the migration velocity of the peak is different. Segments with different interstitial porosities or particles with different particle porosities or surface chemistry could cause this effect. The parameters of these phases are denoted by the indices 1 and 2. Each of them will be considered as a continuum. Let v_β and D_β be respectively the average linear velocity and coefficient of effective diffusion of a solute in the segments with the index β (β can take the values 1 or 2). Also suppose, that these phases are evenly mixed. A clear and simple example of such a mixture might be a structure, where flat layers of these phases alternate and the column axis is parallel to these layers. Let δ_β be the thickness of these layers.

It is important to remember, that v_β and D_β are not just flow velocities and molecular diffusion coefficients, but are rather the peak propagation velocities and effective dispersion coefficients (which are, generally speaking, a function of the velocities v_β). The tensor nature of the diffusion coefficients is apparent from the difference between the components of these tensors in the direction of the respective velocities and the components in the directions orthogonal to the velocities. Denote C_α the concentration of the sample in each phase and λ the mass transfer coefficient between these phases. The system of equations describing the band propagation in such a medium may be written as follows

$$\frac{\partial}{\partial t}C_1 + v_1\frac{\partial}{\partial x}C_1 = D_1\frac{\partial^2}{\partial x^2}C_1 + \kappa_1(C_2 - C_1) \tag{3}$$

$$\frac{\partial}{\partial t}C_2 + v_2\frac{\partial}{\partial x}C_2 = D_2\frac{\partial^2}{\partial x^2}C_2 + \kappa_2(C_1 - C_2) \tag{4}$$

If the volume fractions of the phases are α_1 and α_2 then

$$\alpha_1 + \alpha_2 = 1 \tag{5}$$

$$\kappa_1 = \frac{\lambda}{\alpha_1} \qquad \kappa_2 = \frac{\lambda}{\alpha_2} \tag{6}$$

Eqns. 3 and 4 are one-dimensional and have the same nature as eqn. 1. The coefficients D_1 and D_2 are just the longitudinal components of the corresponding effective diffusion tensors. Cross-sectional mixing is taken into account by adding the mass-transfer terms to the system of equations. The mass-transfer coefficient λ can be derived from the effective diffusion coefficients in the direction across the column (which generally speaking are different for the two components because they are functions of the velocities v_1 and v_2).

MASS-TRANSFER COEFFICIENT

Let C^* be the concentration of the sample at the interface between these two phases. The mass flux of the sample from the first phase to the second is

$$F = D_{\mathrm{rad}_1}\frac{S}{\delta_1}(C_1 - C^*) \tag{7}$$

Here, D_{rad_1} is the effective diffusion coefficient in the first phase in the radial direction and S is the interface area per unit of column volume.

On the other hand

$$F = D_{\mathrm{rad}_2}\frac{S}{\partial_2}(C^* - C_2) \tag{8}$$

and

$$F = \lambda(C_1 - C_2) \tag{9}$$

Eliminating F and C^* from the eqns. 7, 8 and 9 one obtains the expression for the mass-transfer coefficient λ

$$\lambda = \frac{SD_{\mathrm{rad}_1}D_{\mathrm{rad}_2}}{\delta_2\delta_1\left(\frac{D_{\mathrm{rad}_2}}{\delta_2} + \frac{D_{\mathrm{rad}_1}}{\delta_1}\right)} \tag{10}$$

To estimate the mass-transfer coefficient λ one must first derive the effective coefficients of the radial diffusion. In a packed bed, this type of diffusion is a sum of essentially two terms. One is related to molecular diffusion and the second is caused by the branching of the flow-paths on the micro-scale. From the dimensional analysis the expression is of the following form

$$D_{\mathrm{rad}} = \frac{1}{1 + k''}(BD_{\mathrm{mol}} + 2Arw)$$

In this expression the interstitial velocity of the flow w is usually used instead of the peak propagation velocity v. The ratio of these velocities is $w/v = 1 + k''$. k'' is called the zone capacity factor [9]. k'' is equal to zero for samples which do not penetrate the particles and are not retained on the surface of the particles.

The dimensionless constant B contains the obstruction factors for molecular diffusion in the packed bed and in the particle combined with a factor for the ratio of the pore volume to the interstitial volume.

The dimensionless quantity A may also be a function of the dimensionless velocity rw/D_{mol} (at least the dimensional analysis creates no obstacle for such a dependence). In the literature [11,12] a constant value has been accepted for this term.

For further estimations we simplify the expression 10 via the following two hypotheses:

$$D_{\mathrm{rad}_1} = D_{\mathrm{rad}_2} \qquad S = \frac{a}{(\delta_2 + \delta_1)}$$

The second expression might be obtained for specific structures, when the phases are stretched along the column and evenly distributed over the cross section. A chess board structure (in the cross section of the column) might be a good example here. The constant a is a dimensionless constant, which is proportional to the number of interphase surfaces passing through the unit area of the cross section of the column. In this case one can get the following expression for λ

$$\lambda = \frac{a}{(\delta_2 + \delta_1)^2} D_{\mathrm{rad}} = \frac{a(BD_{\mathrm{mol}} + 2Arw)}{(\delta_2 + \delta_1)^2(1 + k'')} \tag{10a}$$

EQUATION FOR THE AVERAGE CONCENTRATION

In practice, the only measurable quantity is the average concentration C.

$$C \equiv C_1\alpha_1 + C_2\alpha_2$$

Hence, it is suitable to transform the eqns. 3 and 4 into the form where C is one of the dependent variables. As a coupled variable, the difference Δ between concentrations C_1 and C_2 might be chosen

$$\Delta \equiv C_2 - C_1$$

At equilibrium, this number becomes much smaller than the average concentration C and in the limit approaches zero. In this way, the value of Δ is the indicator of the closeness to the state of equilibrium.

It is easy to see that

$$C_1 = C - \Delta\alpha_2 \qquad C_2 = C + \Delta\alpha_1 \tag{11}$$

To derive the equation for C one can multiply the eqns. 3 and 4 by α_1 and α_2, respectively, add the results, and substitute then C_1 and C_2 by the expressions 11.

$$\frac{\partial}{\partial t}C + v\frac{\partial}{\partial x}C = D\frac{\partial^2}{\partial x^2}C - (v_2 - v_1)\frac{\partial}{\partial x}\Delta + (D_2 - D_1)\frac{\partial^2}{\partial x^2}\Delta \tag{12}$$

Here, v is the average velocity

$$v = v_1\alpha_1 + v_2\alpha_2$$

and D is the average effective longitudinal diffusion coefficient

$$D = D_1\alpha_1 + D_2\alpha_2$$

Subtracting eqns. 4 and 3 and substituting the expressions 11 and 12 one can get the equation for Δ

$$\frac{\partial}{\partial t}\Delta + (v_2\alpha_1 + v_1\alpha_2)\frac{\partial}{\partial x}\Delta - (D_2\alpha_1 + D_1\alpha_2)\frac{\partial^2}{\partial x^2}\Delta + \Delta(\kappa_2 + \kappa_1) =$$

$$= -(v_2 - v_1)\frac{\partial}{\partial x}C + (D_2 - D_1)\frac{\partial^2}{\partial x^2}C \qquad (13)$$

EQUATIONS FOR THE MOMENTS

Further analysis of the system of eqns. 12 and 13, is facilitated by rewriting this system in the frame moving along the axis x with the velocity v. If v is the peak migration velocity, then all the moments of C in this coordinate system will automatically be central.

The corresponding equations are as follows

$$\frac{\partial}{\partial t}C - D\frac{\partial^2}{\partial x^2}C = -(v_2 - v_1)\frac{\partial}{\partial x}\Delta + (D_2 - D_1)\frac{\partial^2}{\partial x^2}\Delta \qquad (14)$$

$$\frac{\partial}{\partial t}\Delta + (v_2 - v_1)(\alpha_1 - \alpha_2)\frac{\partial}{\partial x}\Delta - (D_2\alpha_1 + D_1\alpha_2)\frac{\partial^2}{\partial x^2}\Delta + \Delta(\kappa_2 + \kappa_1) =$$

$$= -(v_2 - v_1)\frac{\partial}{\partial x}C + (D_2 - D_1)\frac{\partial^2}{\partial x^2}C \qquad (15)$$

By definition, the nth moment of functions $C(t,x)$ and $\Delta(t,x)$ are

$$M_n(t) = \int_{-\infty}^{+\infty} x^n C(t,x)\mathrm{d}x \qquad N_n(t) = \int_{-\infty}^{+\infty} x^n \Delta(t,x)\mathrm{d}x$$

Let at the initial time $C(0,x) = \delta(x)$ and $\Delta(0,x) = 0$.

Multiplying the eqns. 14 and 15 by x^n and integrating them (by parts, where it is necessary) one can get

$$\frac{\mathrm{d}}{\mathrm{d}t}M_n = Dn(n-1)M_{n-2} + (v_2 - v_1)nN_{n-1} + (D_2 - D_1)n(n-1)N_{n-2}$$

$$\frac{\mathrm{d}}{\mathrm{d}t}N_n = (v_2 - v_1)(\alpha_1 - \alpha_2)nN_{n-1} + (D_2\alpha_1 + D_1\alpha_2)n(n-1)N_{n-2} \qquad (16)$$

$$- N_n(\kappa_2 + \kappa_1) + (v_2 - v_1)nM_{n-1} + (D_2 - D_1)n(n-1)M_{n-2}$$

It was taken into account that $N_{-2} = N_{-1} = M_{-2} = M_{-1} = 0$ and the limits of the expressions like $x^n C(t,x)$ and $x^n(t,x)$ are equal to zero in the limit $x \to \infty$.

We can now proceed to calculate step by step the moments of the peak. The second moment is a measure of the peak-width, and the third moment is a measure of the asymmetry of the peak.

The procedure for the solution of this system of equations is merely a recursion. Asymptotically for $t \to \infty$ one can get the solution for the first four moments of the average concentration (the most important from a practical standpoint). How fast these values are reached (or in other words how quickly the equilibrium state is reached) depends only on the constant $\lambda/\alpha_1\alpha_2$. The larger this constant is, the faster this system reaches the state of equilibrium.

The zeroth moment has the meaning of the total sample mass in the system. For normalization it is set to $M_0 = 1$.

The first moment M_1 is the coordinate of the center of gravity of the peak. It is easy to show that $M_1 = 0$. This means that the velocity of the band (in the moving coordinate system) is zero. Hence, v is indeed the peak migration velocity.

The second moment

$$M_2 = 2\left[D + \frac{\alpha_1\alpha_2}{\lambda}(v_2 - v_1)^2\right]t$$

may be interpreted as the action of some effective diffusion, equal to

$$D_{\text{eff}} = D + \frac{\alpha_1\alpha_2(v_2 - v_1)^2}{\lambda}$$

As soon as the velocity difference is not zero, the new effective diffusion D_{eff} differs from D. The consequences of such a difference are discussed later.

The last moment to be considered here is M_3. This moment serves as a measure of the asymmetry of the peak.

$$M_3 = 6\left[(\alpha_1 - \alpha_2)\left(\frac{\alpha_1\alpha_2}{\lambda}\right)^2(v_2 - v_1)^3 + \frac{\alpha_1\alpha_2}{\lambda}(D_2 - D_1)(v_2 - v_1)\right]t$$

It is clear now, that the magnitude and the sign of the third moment (and consequently the degree of tailing or fronting of the peak) is not automatically zero. The skewness α is a dimensionless measure of asymmetry and is defined as $M_3/M_2^{3/2}$. The skewness is approaching zero with $1/\sqrt{t}$. Hence, after a sufficiently long time the peak always becomes symmetrical. The significance of the asymmetry effect is determined solely by the relation between the second and the third moments, which in turn is a function of time.

NUMERICAL ESTIMATIONS

For comparison with other equations commonly used in chromatography, the model presented here should be translated into the nomenclature of chromatography.

As it was mentioned in the introduction, $h = D_{\text{eff}}/rv$. Substituting the expressions for the effective diffusion coefficient and the mass-transfer coefficient λ one obtains

$$h = \frac{D}{rv} + \frac{4\alpha_1\alpha_2\omega^2\delta^2 wr}{a(BD_{\text{mol}} + 2Arw)} \tag{17}$$

Here the following abbreviations have been used:

$$\delta^2 = \frac{(\delta_2 + \delta_1)^2}{4r^2} \qquad \omega^2 = \frac{\alpha_1\alpha_2(v_2 - v_1)^2}{v^2}$$

δ is the characteristic size of the non-uniformity (in non-dimensional form) and ω is a measure of the velocity variation. With the Peclet number $Pe = 2wr/D_{\text{mol}}$ the eqn. 17 can be expressed in non-dimensional form

$$h = \frac{B^*}{Pe} + C^*Pe + \frac{EPe}{\left(\frac{B}{A} + Pe\right)} \tag{18}$$

The first and second terms in eqn. 18 are nothing but the effect of molecular diffusion and mass-transfer in the two phases considered. The form of this equation is identical to the coupling equation derived by Giddings [3]. The coefficient E is defined as

$$E = \frac{2\omega^2\delta^2}{aA}$$

This coefficient contains all assumed non-uniformities, *i.e.* the velocity ratio in the two phases, the characteristic size of the phases, their volume fractions and their characteristic contact area.

When Pe is large compared to the ratio B/A in the denominator of the last term of eqn. 18 then this term becomes constant. Therefore it is interesting to estimate the order of the ratio B/A. If one accepts the value of 0.75 as a typical obstruction factor for molecular diffusion, then $B \approx 0.75$ for a bed prepared from non-porous particles and $B \approx 1.5$ for a bed packed with fully porous particles. In the literature [9], the factor A is given as $A = 0.278(1-\varepsilon)^{1/2}$, where ε is the interstitial porosity. For a typical column $\varepsilon \approx 0.4$ and consequently $A \approx 0.215$. The ratio B/A then becomes about 3.5 for non-porous particles and 7 for porous particles.

Typical coefficients B^* *and* C^* for a column packed with a well-designed fully porous chromatographic adsorbent are $B^* \approx 3$ and $C^* \approx 1/12$. Therefore the point at which the terms in Pe and $1/Pe$ of eqn. 18 are equal is at $Pe \approx 6$. Consequently the curvature of these two terms intermingles with the curvature of the term derived in this paper and the minimum of the $h(Pe)$ relationship becomes a function of the term E.

There are two equations commonly used in the chromatographic literature to describe the observed relationship between dispersion and velocity. The older one was first derived by van Deemter *et al.* [2] and is given here in dimensionless form:

$$h(Pe) = A^* + \frac{B^*}{Pe} + C^*Pe$$

The second one was first given by Knox and Parcher [13]:

$$h(Pe) = A^* Pe^{\frac{1}{3}} + \frac{B^*}{Pe} + C^* Pe$$

In both equations the A^* term is an empirical descriptor of the quality of the packed bed (eddy diffusion). As above, the B^* term describes molecular diffusion in the direction of flow and the C^* term incorporates all mass-transfer phenomena. It can be shown, that the model 18 yields curves which are indistinguishable from both equations and thus serves as an explanation of the empirical terms with A^*, and our constant E corresponds to the constant A^*.

This constant can be obtained experimentally and can be used to estimate the magnitude of the velocity fluctuations ω over the size of the non-uniformities δ.

$$\omega\delta \leqslant \sqrt{\frac{1}{2}EaA} \tag{19}$$

This relationship is obviously indeterminate, *i.e.* within the context of the model it is impossible to tell whether a particular value of E determined by experiment is caused by large velocity fluctuations over a small distance or by small velocity fluctuations over a large distance. It can only be said that at the averaging scale δ the average fluctuation ω of the velocity does not exceed a value given by the square-root in eqn. 19. This "uncertainty principle" should be considered in attempts to understand the internal structure of a packed bed based on experimental data of dispersion as a function of velocity.

SYMBOLS

C	average concentration of the solute
w	average linear velocity of the liquid
v	peak migration velocity
D_{mol}	molecular diffusion coefficient
r_c	radius of the capillary
h	reduced plate height
v_β	average linear velocity of a solute in the continua with the index β (β can take the values 1 or 2)
D_β	coefficient of effective diffusion of a solute in the continua with the index β
δ_β	characteristic size of the continua with the index β
α_β	volume fraction of the continua with the index β
λ	mass transfer coefficient between these phases
D_{rad}	effective diffusion coefficient in the radial direction
S	interface area per unit of column volume
k''	zone capacity factor
Δ	difference between concentrations C_1 and C_2
D	average coefficient of the effective longitudinal diffusion
M_n	nth central moment of a function $C(t,x)$

N_n nth central moment of a function $D(t,x)$
D_{eff} effective diffusion coefficient
δ non-dimensional characteristic size of the non-uniformity
ω non-dimensional measure of the velocity variation
Pe Peclet number

REFERENCES

1 A. Klinkenberg and F. Sjenitzer, *Chem. Eng. Sci.*, 5 (1956) 258.
2 J. J. van Deemter, F. J. Zuiderweg and A. Klinkenberg, *Chem. Eng. Sci.*, 5 (1956) 271.
3 J. C. Giddings, *Dynamics of Chromatography*, Part 1, Marcel Dekker, New York, 1965, Ch. 2.10.
4 G. J. Kennedy and J. H. Knox, *J. Chromatogr. Sci.*, 13 (1975) 25.
5 C. L. de Ligny, *J. Chromatogr.*, 49 (1970) 393.
6 R. Aris, *Proc. R. Soc. (London)*, A235 (1956) 67.
7 G. I. Taylor, *Proc. R. Soc. (London)*, A219 (1953) 196.
8 M. J. E. Golay, *J. Chromatogr.*, 186 (1979) 341.
9 S. G. Weber and P. W. Carr, *High Performance Liquid Chromatography*, Wiley, New York, 1989.
10 S. Yamamoto, K. Nakanishi and R. Matsuno, *Ion-Exchange Chromatography of Proteins*, Marcel Dekker, New York, 1988.
11 M. A. Aerov, O. M. Todes and D. A. Narinski, *Apparatus with Packed Beds*, Chemistry, Moscow, 1979.
12 D. L. Koch and J. F. Brady, *J. Fluid Mech.*, 154 (1985) 399.
13 J. H. Knox and J. F. Parcher, *Anal. Chem.*, 41 (1969) 1599.

Journal of Chromatography, 535 (1990) 199–205
Elsevier Science Publishers B.V., Amsterdam

CHROMSYMP. 2013

Computer assisted internal standard selection for reversed-phase liquid chromatography

N. E. SKELLY, S. W. BARR* and A. P. ZELINKO
The Dow Chemical Company, Midland, MI 48667 (U.S.A.)

ABSTRACT

A convenient method to place an internal standard in a reversed-phase liquid chromatogram has always been a challenge to the analytical chemist. Generally, this has been accomplished by trial and error or the use of a homologous series of compounds. With a database of 90 potential internal standards arranged in a retention time order, and the use of a marker solution, this selection process can be greatly simplified. The marker solution and the sample for which an internal standard is desired are injected into the liquid chromatograph and chromatographed under the same gradient conditions as those used for the database. The retention times of the marker solution for a given column are entered into the computer to rearrange the database. The sample chromatogram is examined for "open windows" and the computer is requested to suggest internal standards. This approach applies to aqueous acetonitrile eluents but is essentially column-manufacturer independent. Because of changes in selectivity with aqueous methanol or aqueous tetrahydrofuran eluents, the approach may not apply as described. However, the database should make the internal standard selection for these mobile phases much easier.

INTRODUCTION

The placement of an internal standard in a reversed-phase liquid chromatogram has always been a time-consuming operation for the analytical chemist. Methods that make use of a homologous series of compounds [1] are generally used. From a database of 90 potential internal standards, arranged in retention time order, and the use of a marker solution, this selection process can be greatly simplified. This approach applies to aqueous acetonitrile eluents but is essentially column-manufacturer independent. Because of changes in selectivity with aqueous methanol or aqueous tetrahydrofuran eluents, the approach may not apply as described. However, the database should make the internal standard selection for these mobile phases much easier. A list of criteria that an internal standard should possess is described elsewhere [2].

EXPERIMENTAL

Materials

A Hewlett-Packard Model 1090A liquid chromatograph with photodiode-array

0021-9673/90/$03.50

detector and the following reversed-phase liquid chromatography columns were used in the study: Nova-Pak C_{18}, 150 × 3.9 mm I.D. (Millipore, Waters Chromatography Division, Milford, MA, U.S.A.); Partisil 5 ODS-3, 100 × 4.6 mm I.D. (Whatman, Clifton, NJ, U.S.A.); Spherisorb ODS-1, 3 μm, 100 × 4.6 mm I.D. (Phase Separations, Deeside, U.K.); Zorbax ODS, 150 × 4.5 mm I.D. (MAC-MOD, Chadds Ford, PA, U.S.A.). The chemicals were purchased from various chemical supply houses and were used without further purification. Stock solutions of each were prepared by dissolving 10 to 15 mg of each in 10 ml of acetonitrile. These solutions were used without further dilution to obtain retention times and spectra. Because publication of the spectra in this report would require too much space, they are not included. However, copies are available upon request from the authors.

Methods

The potential internal standards were separated by gradient elution. The "A" reservoir contained 0.005 *M* aqueous sulfuric acid and the "B" reservoir contained acetonitrile. A linear gradient from 20 to 100% B in 15 min was employed. For those compounds not eluted in this time interval, elution was continued at 100% B. A 3-min reequilibration was used. The flow-rate was 1 ml/min and the injection volume 2 μl. The chromatograms were monitored at 254 nm and a full-scale absorbance setting of 0.064 a.u. was used.

The marker solution retention times will be identical, whether water or 0.005 *M* (aq.) H_2SO_4 is used in the "A" reservoir. The use of the dilute acid is only required if acidic components are present in the sample under study.

Samples of 50 mg of acetanilide, benzophenone, α-tetralone, and 30 mg of trans-stilbene were dissolved in 50 ml of acetonitrile. A chromatogram of the marker solution is shown in Fig. 1.

The 90 potential internal standards were injected on the Nova Pak C-18 column and chromatographed as described previously. They were arranged in retention time order and entered into a terminal-format file to be ready for the BASIC program.

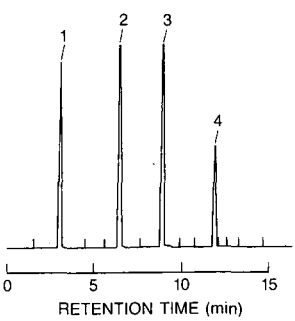

Fig. 1. Liquid chromatogram of marker solution. The marker solution containing components: 1 = acetanilide, 2 = α-tetralone, 3 = benzophenone and 4 = *trans*-stilbene as chromatographed on Nova-Pak C_{18} 150 × 3.9 mm I.D., with a linear gradient from 20 to 100% B in 15 min, where A = 0.005 *M* aq. H_2SO_4 and B = acetonitrile. The flow-rate was 1 ml/min with detection at 254 nm for an injection volume of 2 μl. Signal range was 0.064 a.u.f.s.

The BASIC program

The program, Window, was written in VAX BASIC (version 3.3) and compiled to run on VAX/VMS, version 5.0 (Digital Equipment Corp.). Each standard material required two lines in the data file: chemical name, followed by retention time. Since the BASIC program uses Linput statements when reading the data file, chemical names can include punctuations and spaces. A terminal-format file was chosen to facilitate editing of the standard data. Window only accesses the data file for input, and cannot alter reference data.

The 15-min span of standard retention times is divided into four segments with one marker compound acting as a relative retention standard for each segment. The segment boundaries (start and end times) and the associated standard for that segment are identified in Data statements in the BASIC program. The relative retention times for each standard are calculated by finding the ratio of actual marker retention time to the stored marker retention time. The retention time for each component in a segment is then multiplied by the corresponding ratio for that segment. A copy of the full program is available from the authors.

When the possible internal standards in the user-specified retention Window are displayed, their adjusted retention times are also shown. Other database files could be created and used with Window, including databases for different solvents gradients or isocratic conditions.

Internal standard selection

An aliquot of 2 μl of the marker solution is injected and chromatographed as described above and 2 μl of an appropriate concentration of the sample for which an internal standard is desired are alo injected. The concentration should be sufficient to show the impurities. The use of a sample enriched in impurities might be helpful. A larger injection volume and the use of a more sensitive monitoring wavelength (210 nm) could be used. The four-marker compound retention times are entered into the Window program, which adjusts retention times in the database to the particular column being used.

The sample chromatogram is examined for potential internal standard locations. Because gradient elution will tend to give a more compressed chromatogram than isocratic elution, this must be taken into account when the internal standard is being selected for an isocratic application. The retention window of interest is entered into Window (when prompted) for the window "start" and "end" times. The program will display a sorted list of possible internal standards. Window will ask if the user wants to specify another window or quit.

An example for the internal standard selection method is given in Fig. 2. The marker solution is injected in the analyst's column, Partisil 5 ODS-3, and chromatographed under the prescribed conditions (Fig. 2A). The marker solution retention times are entered into the computer to rearrange the database. Then, an impure insecticide is injected and examined under the same conditions except the separation was monitored at 210 nm to accentuate the presence of the impurities (Fig. 2B). Following examination of the insecticide chromatogram for possible "open windows", the computer was requested to suggest internal standards for these retention time intervals. The computer suggested hexamethylenebenzene (13.4 min) and 1,4-dibromonaphthalene (13.6 min). The latter was selected because of its better spectral

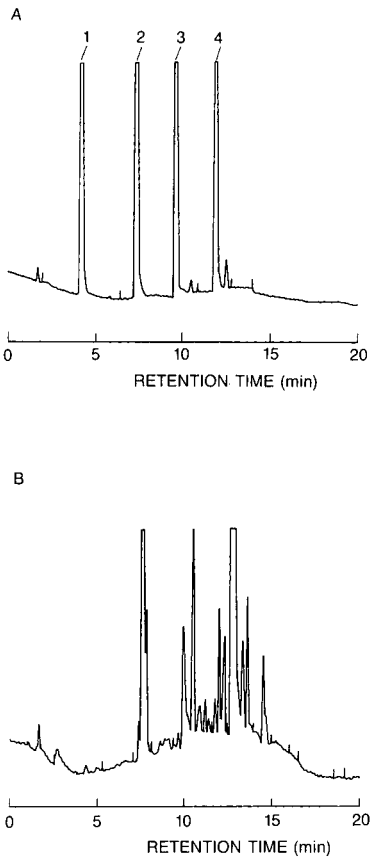

Fig. 2. Liquid chromatograms of marker solution and impure insecticide. (A) marker solution containing components: 1 = acetanilide, 2 = α-tetralone, 3 = benzophenone and 4 = *trans*-stilbene as chromatographed on Partisil 5 ODS-3, 150 mm × 4.6 mm I.D., with a linear gradient from 20 to 100% B in 15 min, where A = 0.005 *M* aq. H_2SO_4 and B = acetonitrile. The flow-rate was 1 ml/min with detection at 254 nm for an injection volume of 2 μl. Signal range was 0.064 a.u.f.s. (B) An impure insecticide chromatographed under the same conditions, except detection was at 210 nm.

compatibility. Spectra for the individual internal standards are available for examination to assess their suitability for absorption at a certain wavelength. These spectra are available from the authors.

DISCUSSION

Aqueous acetonitrile eluents are generally preferred over aqueous tetrahydrofuran and aqueous methanol for reversed-phase chromatography, because they are more UV-transparent and produce less backpressure. Therefore, our internal standard selection approach was centered on aqueous acetonitrile. There are differences in selectivity when the retention time for the latter two mobile phases are compared with

TABLE I

REVERSED-PHASE LIQUID CHROMATOGRAPHIC RETENTION TIMES BY GRADIENT ELUTION WITH THE RESPECTIVE SOLVENTS IN THE "B" RESERVOIR

Compound	Retention time (min)		
	Acetonitrile	Methanol	Tetrahydrofuran
Acetic acid amide (N-4-hydroxyphenyl)	1.40	2.23	1.51
Acetaminophen	1.40	2.24	1.51
Saccharin	1.59	2.48	1.70
2,6-Dimethyl-4-pyrone	1.94	3.72	1.11
Benzamide	1.96	3.42	1.69
2-Acetamodiphenol	2.20	3.55	2.51
Phenylurea	2.20	3.77	2.31
Benzoic acid, 2-methylamino	2.32	4.09	1.91
Salicylamide	2.79	4.63	3.33
4-Hydroxyacetophenone	2.79	4.88	3.22
Phthalimide	2.84	4.87	2.92
Phthalic acid diamide	2.84	4.87	2.95
Acetanilide	2.99	4.91	2.74
4-Methoxyphenol	3.21	4.70	3.73
2-Methoxybenzoic acid	3.27	5.68	2.78
Benzoic acid	3.86	6.88	4.58
4-Methoxybenzoic acid	4.64	7.34	4.18
4,4'-Biphenol	4.50	7.05	5.50
Coumarin	4.53	6.58	3.45
1,1-Diphenylurea	4.87	8.30	3.28
o-Toluic acid	4.88	8.36	5.52
m-Toluic acid	5.04	8.70	5.42
Tri(4-hydroxyphenyl)methane	5.23	8.11	5.33
Acetophenone	5.14	7.16	4.12
Methane bis(4-hydroxyphenyl)	5.33	8.61	5.11
Acetamide 2,4-dichlorophenoxy	5.80	9.55	5.28
3,5-Dimethylphenol	5.95	8.80	3.46
4-Bromophenol	6.02	8.84	6.22
4-Ethylphenol	6.14	8.91	6.27
Benzamide: 3-methyl-N,N-diethyl	6.48	9.74	3.86
α-Tetralone	6.40	9.02	4.05
4-Hydroxybenzoic acid, methyl ester	6.52	9.83	6.38
Bisphenol A	6.58	10.03	5.87
trans-4-Phenylcyclohexanol	6.72	10.74	6.87
2,4-Dichlorophenoxyacetic acid	6.76	10.11	6.87
4-Methoxybenzoic acid	6.79	9.61	5.43
4-Methoxypropiophenone	6.86	9.44	4.64
Propiophenone	6.88	9.06	5.68
1,3-Diphenylurea	6.93	9.47	6.82
4-Chloroacetophenone	7.09	9.54	5.96
2,4-Dihydroxybenzophenone	7.16	10.41	6.96
Diphenylsulfone	7.20	8.61	5.37
n-Butoxyphenol	7.38	10.32	6.13
4-Phenylphenol	7.55	10.73	6.11

(Continued on p. 204)

TABLE I *(continued)*

Compound	Retention time (min)		
	Acetonitrile	Methanol	Tetrahydrofuran
Benzoic acid 2-hydroxyamino-4-phenyl	7.82	10.21	6.10
4-*tert.*-Butylphenol	7.94	11.05	7.02
2-Phenylphenol	7.90	10.67	7.16
4-Benzylphenol	8.04	11.17	7.20
n-Butyrophenone	8.30	10.53	6.07
Benzophenone	8.85	11.19	6.84
9-Fluorenone	8.92	11.61	5.81
4-Phenylacetophenone	9.29	12.14	6.67
1,3-Diphenyl-2-propanone	9.22	11.31	7.42
Benzil	9.18	11.27	7.07
Diphenyl carbonate	9.31	11.62	5.41
2,4,6-Tribromophenol	9.45	12.73	8.25
Valerophenone	9.54	11.03	7.61
4-Cyclohexylphenol	9.64	12.76	7.95
Naphthalene	9.64	12.27	7.63
2-Hydroxybenzoic acid, phenyl ester	10.07	12.83	5.95
Triphenylmethanol	10.27	12.86	6.92
Chlorotriphenylmethane	10.28	12.86	6.85
Diphenyl oxide	10.59	13.03	7.98
Biphenyl	10.73	13.38	8.20
Hexanophenone	10.76	12.92	8.25
Dibenzofuran	10.80	13.58	7.94
2-Methylnaphthalene	10.90	13.50	8.19
Fluorene	11.20	13.99	8.29
Dibenzo-*p*-dioxin	11.30	14.06	
2-Bromonaphthalene	11.48	13.84	8.34
1-Bromonaphthalene	11.53	13.90	8.16
Benzylbutylphthalate	11.54	13.53	8.42
trans-Stilbene	11.75	14.33	8.34
4-Phenyltoluene	11.78	14.34	8.70
2-Ethylnaphthalene	11.83	14.21	8.69
Dibutylphthalate	11.86	13.62	8.48
1,2-Diphenylethane	11.90	14.38	8.01
Butylbenzene	weak	weak	weak
4,4′-Ditolylether	12.52	14.68	9.03
m-Diphenoxybenzene	12.86	14.85	9.04
Triphenylmethane	12.77	14.83	
Octanophenone	12.92	14.50	9.21
m-Diphenoxybenzene	12.87	14.85	9.04
2,6-Di-*tert.*-butyl-4-methylphenol	13.43	14.87	9.88
Hexamethylenebenzene	13.55	15.77	9.72
1,4-Dibromonaphthalene	13.77	15.38	8.93
Tetraphenylethylene	14.51	15.70	9.52
Decanophenone	14.78	15.57	9.91
Heptylbenzene	15.14	16.04	8.37
Laurophenone	16.14	16.35	10.51
Dioctylphthalate	16.74	16.50	10.70
Myristylphenone	17.36	17.07	10.98

aqueous acetonitrile, as shown in Table I. The general approach should still be applicable, but there would be less certainty in the selection process.

The 90 potential internal standards, together with the marker solution, were chromatographed by 0.005 *M* sulfuric acid–acetonitrile gradient elution on three additional reversed-phased octadecyl columns. Using the marker solution retention times from the Spherisorb, Partisil and Zorbax columns and the database from the Nova-Pak column, the retention times for the 90 potential internal standards were obtained from the computer for the three columns. When compared with the actual retention times measured for these columns, the average difference was 0.02 min with an average standard deviation of 0.34 min.

The use of multicomponents in the marker solution was expected to provide a more satisfactory correction of retention times, should a manufacturer's column show more variability towards polar and/or non-polar compounds. Also, this would tend to average out retention time corrections, should there be some column selectivity towards a particular class of compounds.

CONCLUSIONS

A four-component marker solution and the sample for which an internal standard is desired is injected into any reversed-phase column of the analyst's choice and developed under prescribed gradient conditions. After entering the retention times for the marker solution, the sample chromatogram is examined for "open windows". The computer is then requested to suggest internal standards for these time windows.

REFERENCES

1 M. Verzele, L. Use and M. Van Kerrebroeck, *J. Chromatogr.*, 289 (1984) 333–337.
2 L. R. Snyder and J. J. Kirkland, *Introduction to Modern Liquid Chromatography*, 2nd ed., Wiley, New York, 1979, p. 554.

Journal of Chromatography, 535 (1990) 207–212
Elsevier Science Publishers B.V., Amsterdam

CHROMSYMP. 2061

Measurement of limiting ionic equivalent conductance by single-column ion chromatography

Z. L. SHAN
Gansu Institute of Environmental Protection, Lanzhou (China)
and
H. XIAO and P. L. ZHU*
Department of Chemistry, Lanzhou University, Lanzhou (China)

ABSTRACT

A new approach to the measurement of the limiting ionic equivalent conductance, λ, by single-column ion chromatography is proposed. When the eluent counter ion is replaced with an equivalent concentration of sample ion, a change in conductance, *i.e.*, a detector response, will be observed. By adjusting the pH of the eluent to change its degree of electrolytic dissociation, a pH might be found at which the response of sample ions is restrained. For a given eluent, λ is a function only of pH. The calibration graph of λ *versus* eluent pH to restrain the sample response can be obtained by eluting ions of known λ at different pH values and assessing the eluent pH where no detector response is given. From the calibration graph, λ values of other ions can be measured.

INTRODUCTION

An important aspect of non-analytical applications of chromatography, including gas and liquid chromatography, is in physico-chemical measurements [1,2]. The advantages of chromatography lie in its accuracy, convenience, specificity, versatility, speed and requirement for only small amounts of sample [2]. In this paper, a new approach for measuring limiting ionic equivalent conductance by single-column ion chromatography is proposed.

Ion chromatography (IC) can be subdivided into two types: that which uses a suppressor (dual-column IC) and that which does not (single-column IC) [3,4]. More commonly in single-column IC, the effluent from the ion-exchange column is sent to a conductivity detector, the response of which depends on the conductance of sample ions, counter ions and co-existing ions. Hence it is possible for single-column IC to be used for the measurement of limiting ionic equivalent conductance with some characteristics that the usual method does not possess.

THEORY

When the eluent anion is replaced with an equivalent concentration of a sample

0021-9673/90/$03.50

anion in single-column IC, the resulting change in conductance, *i.e.*, the detector response, is given by

$$\Delta G = \frac{(\lambda_{E^+} + \lambda_{S^-})I_S - (\lambda_{E^+} + \lambda_{E^-})I_E I_S}{10^{-3}K} \cdot C_S \quad (1)$$

where ΔG is the detector response, K the cell constant, λ the limiting equivalent conductance of cation or anion, C the normality and I the degree of electrolytic dissociation, and E^+, E^-, E, S^- and S represent the eluent cation, eluent anion, eluent, sample anion, and sample, respectively [5]. A similar equation can be obtained for the cation-exchange process. If it is assumed that $\Delta G = 0$, then

$$(\lambda_{E^+} + \lambda_{S^-}) - (\lambda_{E^+} + \lambda_{E^-})I_E = 0$$

or

$$\lambda_{S^-} = (\lambda_{E^+} + \lambda_{E^-})I_E - \lambda_{E^+} \quad (2)$$

As λ_{E^+} and λ_{E^-} are constant for a given eluent and I_E depends on the ionization constant of the corresponding acid and the eluent pH, λ_{S^-} is a function only of the eluent pH at which the sample peak is restrained. The calibration graph of λ *versus* the eluent pH to restrain the sample peak can be obtained by eluting the ions with known λ at different pH values and assessing the eluent pH where no detector response is given. From the calibration graph, limiting equivalent conductances of other ions could be measured.

EXPERIMENTAL

Reagents and instrumentation

The chemicals used were obtained from a variety of suppliers. Doubly distilled water was used for the preparations of aqueous solutions.

Chromatographic experiments were performed on a Model HLC-601 ion chromatograph (Toyo Soda, Japan) equipped with a conductivity detector. The injection valve had a 100-μl loop. A TSK 3066 flat-bed pen recorder was connected to the 1-V output of the detector.

Chromatographic system

An IC-Anion-SW anion-exchange column (Toyo Soda) was used. The mobile phase was 1 or 2 m*M* oxalic acid solution adjusted to the desired pH with 5% sodium hydroxide solution. All measurements were carried out at 25°C.

RESULTS AND DISCUSSION

Selection of counter ion

The requirements which must be met by the counter ion in IC for the measurement of the limiting ionic equivalent conductance are the following. First, when an anion-exchange process is considered, the degree of electrolytic dissociation

of the acid corresponding to the counter ion should vary with a certain variable, such as the pH of the mobile phase, in order to establish the conditions satisfying eqn. 2 for different sample ions through changing the variable. Hence, it is necessary to select a weak acid as the electrolyte of the mobile phase. The dissociation constant, K_a, of the acid should be small enough to give a reasonable pH range in which I_E can be adjusted to meet $G = 0$, but not too small to achieve complete dissociation even in alkaline medium. Second, the limiting ionic equivalent conductance of the counter ion should be as large as possible. The measurement should be carried out only for sample ions with values of λ lower than that of the counter ion, otherwise, the contribution of sample ions to conductance can never be compensated for completely by that of the counter ions.

In this work, oxalic acid, which is a dibasic acid with $pK_1 = 1.27$ and $pK_2 = 4.27$, was selected. The fractions of oxalic acid present in solution in various forms are a function of pH. Oxalic acid in the form $H_2C_2O_4$ is gradually converted into $HC_2O_4^-$ and finally $C_2O_4^{2-}$ as the pH increases from 0 to about 6. The limiting ionic equivalent conductance of $C_2O_4^{2-}$, 74.2 S cm^2 equiv.$^{-1}$ (25°C), is larger than those of most inorganic anion and many organic anions. On the other hand, the reducing property of oxalic acid limits its application to the measurement of oxidizing anions.

Restraint of conductance

Using 1 m*M* oxalic acid at different pH values as the mobile phase, samples containing SCN^- were injected and the variation of peak height with pH was observed; the results are shown in Figs. 1 and 2. At low pH, the ionization of oxalic acid is restrained and the contribution of SCN^- to the conductance is larger than that of the replaced oxalate anion, so that a positive peak will be obtained. At high pH, because oxalic acid is ionized almost completely and the SCN^- anion has a smaller equivalent conductance than the oxalate anion, a negative peak is obtained. There will be a pH between the two extreme situations where the ion-exchange process is not accompanied by the corresponding conductance response. The key step in the measurement of limiting ionic equivalent conductance by IC is to seek the pH that restrains the conductance. Sometimes the peak of the sample ion does not disappear completely, but has the shape of a sine curve near the pH where conductance is restrained. If so, fitting can be used to obtain the pH at which $\Delta G = 0$.

The degree of electrolytic dissociation of a given weak acid depends on the hydrogen ion concentration, not on its analytical concentration, when the effect of activity coefficient is ignored. Therefore, the pH at which $\Delta G = 0$ is not influenced significantly by the oxalic acid concentration. For example, with 1 and 2 m*M* oxalic acid solutions as mobile phases, the pH values evaluated by the approach described previously are 4.63 and 4.42, respectively. The slight difference between the two might result from ignoring the effect of activity coefficient.

Effect of sample ion concentration on measurement

The sample ion concentration is not involved in eqn. 2 and so does not influence the measurement of the pH at which $G = 0$. However, the detector response, ΔG, is proportional to the concentration of sample ion, C_S, when $\Delta G \neq 0$. The plots of peak height *versus* pH of the mobile phase for samples with different concentrations are shown in Fig. 2 and indicate that the restraining points coincide with each other, although the peak height increases with increasing sample ion concentration.

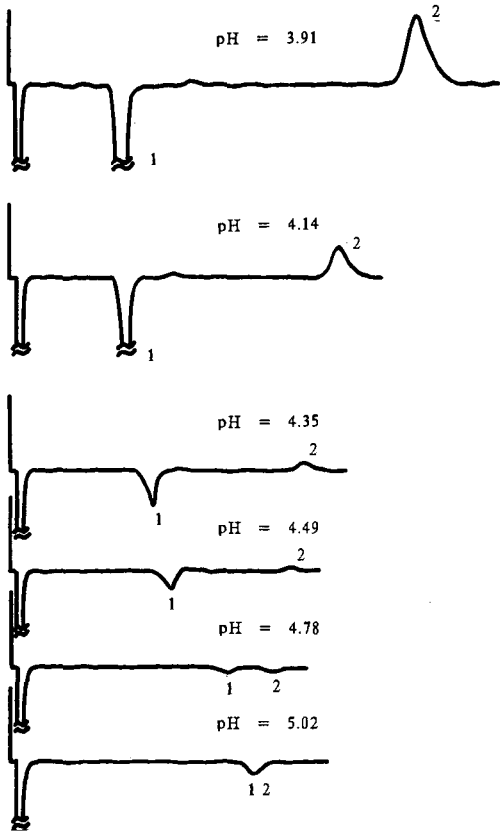

Fig. 1. Chromatograms of 40 ppm of SCN^- at different pH values. 1 = System peak; 2 = SCN^-.

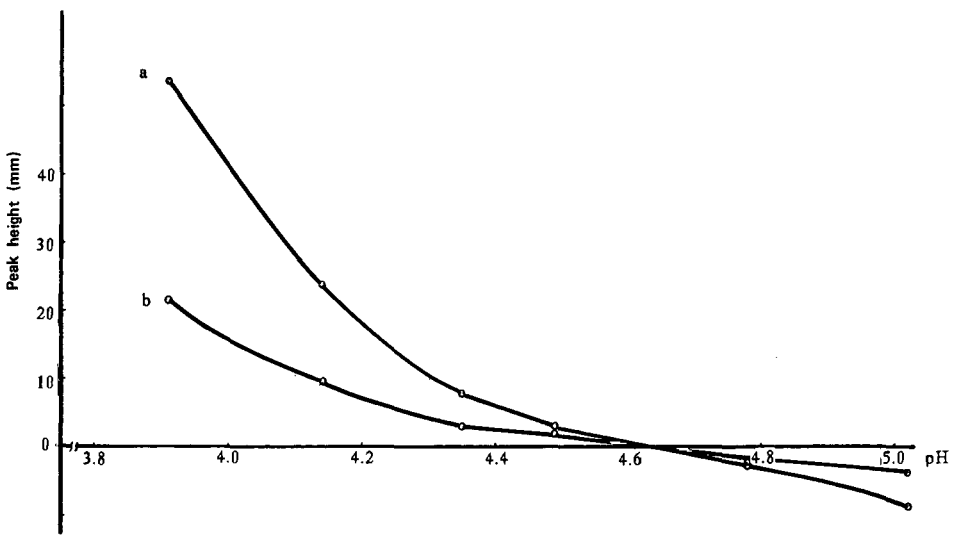

Fig. 2. Peak height *versus* pH. Concentration of SCN^- in sample: (a) 100 ppm; (b) 40 ppm.

TABLE I

LIMITING IONIC EQUIVALENT CONDUCTANCES AND pH VALUES AT WHICH $\Delta G = 0$ FOR DIFFERENT ANIONS

Anion	λ_S- at 25°C (S cm^2 equiv.$^{-1}$)[a]	pH ($\Delta G = 0$)
CH_3COO^-	40.9	3.86
$HCOO^-$	54.6	4.05
ClO_3^-	64.6	4.24
SCN^-	66.0	4.42
ClO_4^-	67.9	4.65
$C_2O_4^{2-}$	74.2	

[a] Data taken from ref. 6.

Effect of co-existing ions

The common practice in measuring limiting ionic equivalent conductance is to subtract the limiting equivalent conductance of co-existing ions from that of the electrolyte. In IC, the sample ion is carried along the column, independently of the others, toward the outlet. Hence the measurement by the proposed method is characterized as "absolute".

Strength of acids corresponding to sample ions

As in the discussion of the effect of sample ion concentration, the strength of the acids corresponding to sample anions influences the detector response, as I_S is involved in eqn. 1. However, I_S does not appear in eqn. 2 when $\Delta G = 0$, so the proposed method is suitable for the measurement of both strong and weak acid anions. This differs from the common practice of measuring limiting equivalent conductance.

Calibration graph

The pH values when $\Delta G = 0$ and the limiting ionic equivalent conductances for some anions are listed in Table I. The existence of a correlation between them indicates

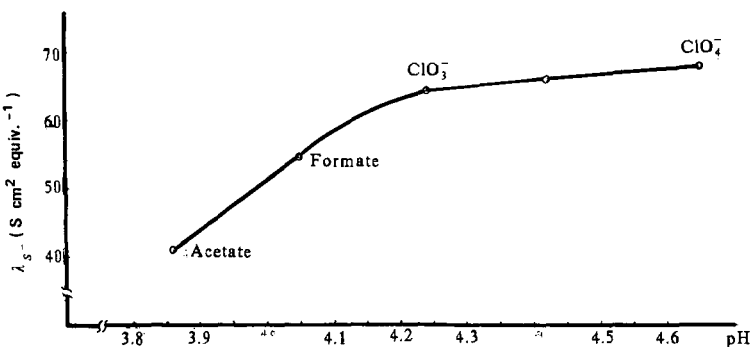

Fig. 3. Calibration graph of λ_S- *versus* the pH value to restrain the detector response.

that measurement by IC is feasible. A calibration graph of λ_S- *versus* pH is given in Fig. 3 from the data in Table I. The shape of the plot depends on the nature of the counter ion. With oxalic acid, a 2-m*M* solution has a pH of 2.75 and the degree of electrolytic dissociation changes with pH up to about pH 6. The slope of the graph decreases with increasing pH.

CONCLUSION

The principle of measuring limiting ionic equivalent conductance by IC has been introduced. In addition to oxalic acid, other counter ions might be selected for setting up systems for the measurement of anions. Based on the same principle, a system for cationic measurement might be established. For instance, ethylenediamine as the counter ion for cation exchange might be used for this purpose. The proposed method has the advantages that it is suitable for both strong and weak electrolytes, co-existing ions are not involved in the measurement and the concentration of the sample ions does not influence the measurement.

ACKNOWLEDGEMENT

The work was supported by the National Science Foundation of China.

REFERENCES

1 M. A. Kaiser, in R. L. Grob (Editor), *Modern Practice of Gas Chromatography*, Wiley, New York, 1977, Ch. 11, p. 553.
2 Cs. Horváth, in C. F. Simpson (Editor), *Techniques in Liquid Chromatography*, Wiley, New York, 1982, Ch. 10, p. 229.
3 J. S. Fritz, D. T. Gjerde and C. Pohlandt, *Ion Chromatography*, Hüthig, New York, 1982, p. 84.
4 D. T. Gjerde, J. S. Fritz and G. Schmuchler, *J. Chromatogr.*, 186 (1979) 509.
5 D. T. Gjerde and J. S. Fritz, *Anal. Chem.*, 53 (1981) 2324.
6 J. A. Dean (Editor), *Lange's Handbook of Chemistry*, McGraw-Hill, New York, 11th ed., 1973.

Journal of Chromatography, 535 (1990) 213–227
Elsevier Science Publishers B.V., Amsterdam

CHROMSYMP. 2040

Elution orders in the separation of enantiomers by high-performance liquid chromatography with some chiral stationary phases

NAOBUMI ÔI*, HAJIMU KITAHARA and REIKO KIRA
Sumika Chemical Analysis Service, Ltd., 3–1–135 Kasugade-naka, Konohana-ku, Osaka 554 (Japan)

ABSTRACT

Enantioselectivity and elution order in the separation of various racemic compounds by high-performance liquid chromatography with some urea derivatives containing two asymmetric carbon atoms attached to two nitrogen atoms of the urea group derived from (*S*)- or (*R*)-valine (Val) and (*S*)- or (*R*)-1-(α-naphthyl)ethylamine (NEA) as chiral stationary phases (CSPs) were investigated in order to explain the mechanism of enantiomer separation. The chromatographic results showed that two kinds of diastereometric interactions are produced and each of the two chiral centres may contribute to the chiral recognition. In the separation of racemic amino acid methyl esters, the Val component may control the chiral recognition for N-acetyl derivatives and the NEA component for N-3,5-dinitrobenzoyl derivatives. In the direct separation of various racemic alcohols and esters, the Val component may control mainly the chiral recognition. The NEA component may efficiently increase the enantioselectivity as shown in allethrolone, etc., but it may also decrease the enantioselectivity as shown in terallethrin, etc. We can assume that the overall enantioselectivity and elution order on these CSPs are determined by the combination of the structure effects and the chiral recognition mechanisms on two chiral components.

INTRODUCTION

In previous papers [1,2] we reported some urea derivatives of chiral amino acid and amines, such as N-(*tert.*-butylaminocarbonyl)-L-valylaminopropylsilica gel and (*R*)-1-(α-naphthyl)ethylaminocarbonylaminopropylsilica gel, were efficient for the separation of derivatives of racemic amino acid esters and amines. It was found that it is sufficient for a chiral stationary phase (CSP) to contain one asymmetric carbon atom attached to the nitrogen atom of the urea group in order to display enantioselectivity in its interaction with amide enantiomers.

During the course of our research to examine the effect of the structure of urea derivatives on enantioselectivity, we have found [3] that two novel CSPs derived from (*S*)- and (*R*)-1-(α-naphthyl)ethylamine (NEA) with (*S*)-valine (Val), which contain two asymmetric carbon atoms attached to two nitrogen atoms of the urea group, showed excellent enantioselectivity for the separation of various racemic compounds. The second chiral constituent improved the enantioselectivity of the urea derivatives, but the mechanism of separation with these phases had not been investigated.

In this study, we examined the enantioselectivity and elution order in separations by high-performance liquid chromatography (HPLC) with CSPs containing two asymmetric carbon atoms attached to the urea group in order to determine the relative contributions to the overall enantiomer separation of each of the two chiral centres in the urea derivatives.

EXPERIMENTAL

Chiral stationary phases

The structures of the CSPs used in this study are shown in Fig. 1. General procedures for the synthesis of CSPs derived from (*S*)- or (*R*)-Val and (*S*)- or (*R*)-NEA were given in previous papers [1–3]. The CSPs were obtained starting from γ-aminopropylsilica gel [Develosil-NH_2, 5 μm (Nomura Chemical, Seto, Japan) and LiChrosorb-NH_2, 5 μm (E. Merck, Darmstadt, F.R.G.)]. Grafting rates were calculated according to the C and N elemental analysis for each CSP: **1a** (0.50 mmol/g), **1b** (0.48 mmol/g), **2a** (0.53 mmol/g), **2b** (0.50 mmol/g), **3a** (0.37 mmol/g), **3b** (0.37 mmol/g), **4a** (0.41 mmol/g), **4b** (0.40 mmol/g).

Liquid chromatography

The experiments were carried out using a Waters Assoc. 510 high-performance liquid chromatograph equipped with a variable-wavelength UV detector operated at 230 and 254 nm. Stainless-steel columns (250 × 4 mm I.D.) were slurry packed using a conventional technique. The chromatographic conditions are given in Tables I–IV. Elution orders were determined by successive injection of racemic and enriched mixtures (in the *S* or *R* isomer) of test solutes.

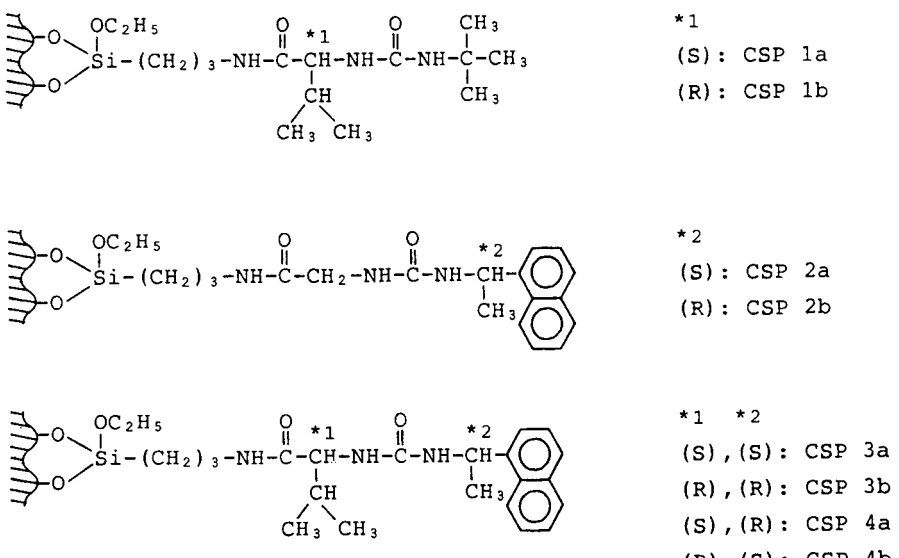

Fig. 1. Structures of the CSPs.

Mobile phase

n-Hexane, 1,2-dichloroethane, ethanol and acetic acid of analytical-reagent grade were purchased from Wako (Osaka, Japan).

RESULTS AND DISCUSSION

The structures of the N-acetyl-(AC) and N-3,5-dinitrobenzoyl-(DNB) amino acid methyl esters, DNB-amines, O-3,5-dinitrophenylurethane (DNPU) derivatives of hydroxy acid methyl esters and DNPU derivatives of alcohols used are shown in Fig. 2. These derivatives were prepared in our laboratory [4,5]. The structures of various racemic compounds used for the direct separation are shown in Fig. 3. These compounds were kindly provided by Sumitomo Chemical (Osaka, Japan). HPLC results are summarized in Tables I–IV and typical chromatograms are shown in Figs. 4–7. The separation factor of the enantiomers, α, is the ratio of their capacity factors and k'_1 is the capacity factor for the initially eluted enantiomer.

As the configuration of CSPs **1b–4b** is opposite stereochemically to that of CSPs **1a–4a**, the results that inversion of elution orders and nearly identical magnitudes of the separation factors are observed between these CSPs are reasonable. As shown in Table I, in the separation of racemic AC-amino acid methyl esters the retention of *S* isomers was longer than that of *R* isomers on CSP **1a**, which contains (*S*)-Val as the chiral component, showing that the association between the *S* isomer and CSP **1a** was the more stable. It is natural that the retention of *R* isomers was longer on CSP **1b**, which contains (*R*)-Val. These separations may depend entirely on hydrogen bonding association and involve no other stronger complexations [2]. Racemic AC-amino acid methyl esters were hardly separated on CSPs **2a** and **2b**, indicating that the NEA component is insufficient for the separation of these enantiomers depending on the diastereomeric hydrogen bonding association.

The results that the retention of *S* isomers was longer than that of *R* isomers on CSPs **3a** and **4a** derived from (*S*)-Val with (*S*)- and (*R*)-NEA and the opposite elution order was obtained on CSPs **3b** and **4b** derived from (*R*)-Val with (*R*)- and (*S*)-NEA suggest that the chiral recognition may be controlled by the Val component in these separations.

DNB-amino acid methyl esters were resolved not only with CSPs **1a** and **1b** but also with **2a** and **2b**, as shown in Table II. The elution orders of DNB- and AC-amino acid methyl esters on CSPs **1a** and **1b** are the same, but the separation factors of the DNB derivatives are smaller than those of the AC derivatives. This result suggests that AC derivatives are convenient stereochemically for the association with CSPs **1a** and **1b** by hydrogen bonding. On the other hand, DNB derivatives may easily associate with CSPs **2a** and **2b** by the combination of the π–π donor–acceptor interaction and hydrogen bonding. It was noted that the elution orders of AC- and DNB-amino acid methyl esters were clearly different on CSPs containing two asymmetric carbon atoms. Inversion of the elution orders was found in DNB derivatives on CSPs **3a** and **4a**, and also on CSPs **3b** and **4b**. The results that the retention of *S* isomers was longer than that of *R* isomers on CSPs **3a** and **4b** derived from (*S*)-NEA with (*S*)- and (*R*)-Val and the opposite elution order was obtained on CSPs **3b** and **4a** derived from (*R*)-NEA with (*S*)- and (*R*)-Val suggest that the NEA component mainly contributes to the chiral recognition in these separations.

(1) 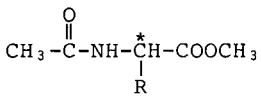

R=-CH_3 : (1a), (2a)

R=-$CH<^{CH_3}_{CH_3}$: (1b), (2b)

R=-CH_2-$CH<^{CH_3}_{CH_3}$: (1c), (2c)

(2) 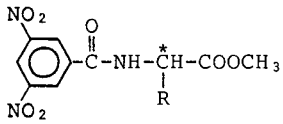

R=-CH_2-CH_2-S-CH_3 : (1d), (2d)

R=  : (1e), (2e)

R=-CH_2-  : (1f), (2f)

(3) 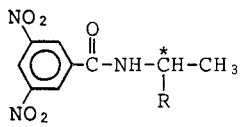

R=  : (3a)

R= 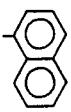 : (3b)

(4) 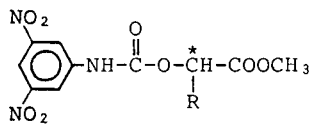

R=-CH_3 : (4a)

R=-CH_2-$COOCH_3$: (4b)

R=  : (4c)

(5) 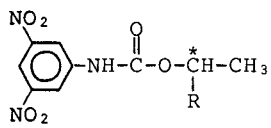

R=-$(CH_2)_5$-CH_3 : (5a)

R=  : (5b)

Fig. 2. Structures of N-acetyl-(AC) amino acid methyl esters (**1**), N-3,5-dinitrobenzoyl-(DNB) amino acid methyl esters (**2**), N-DNB-amines (**3**), O-3,5-dinitrophenylurethane (DNPU) derivatives of hydroxy acid methyl esters (**4**) and O-DNPU derivatives of alcohols (**5**).

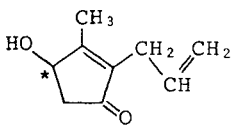

(a)

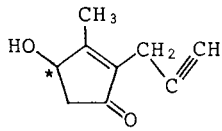

(b)

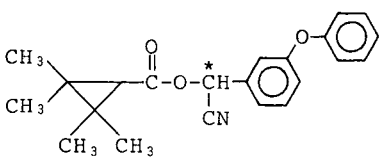

(c)

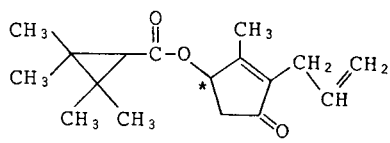

(d)

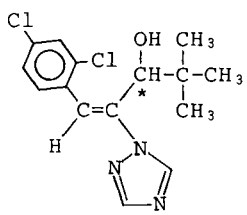

(e)

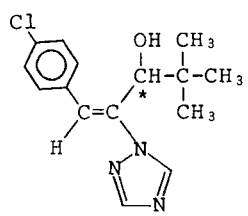

(f)

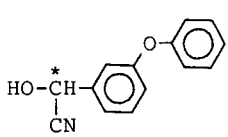

(g)

Fig. 3. Structures of various racemic compounds: allethrolone (**a**), propargyllone (**b**), fenpropathrin (**c**), terallethrin (**d**), diniconazole (**e**) uniconazole (**f**) and α-cyano-3-phenoxybenzyl alcohol (**g**).

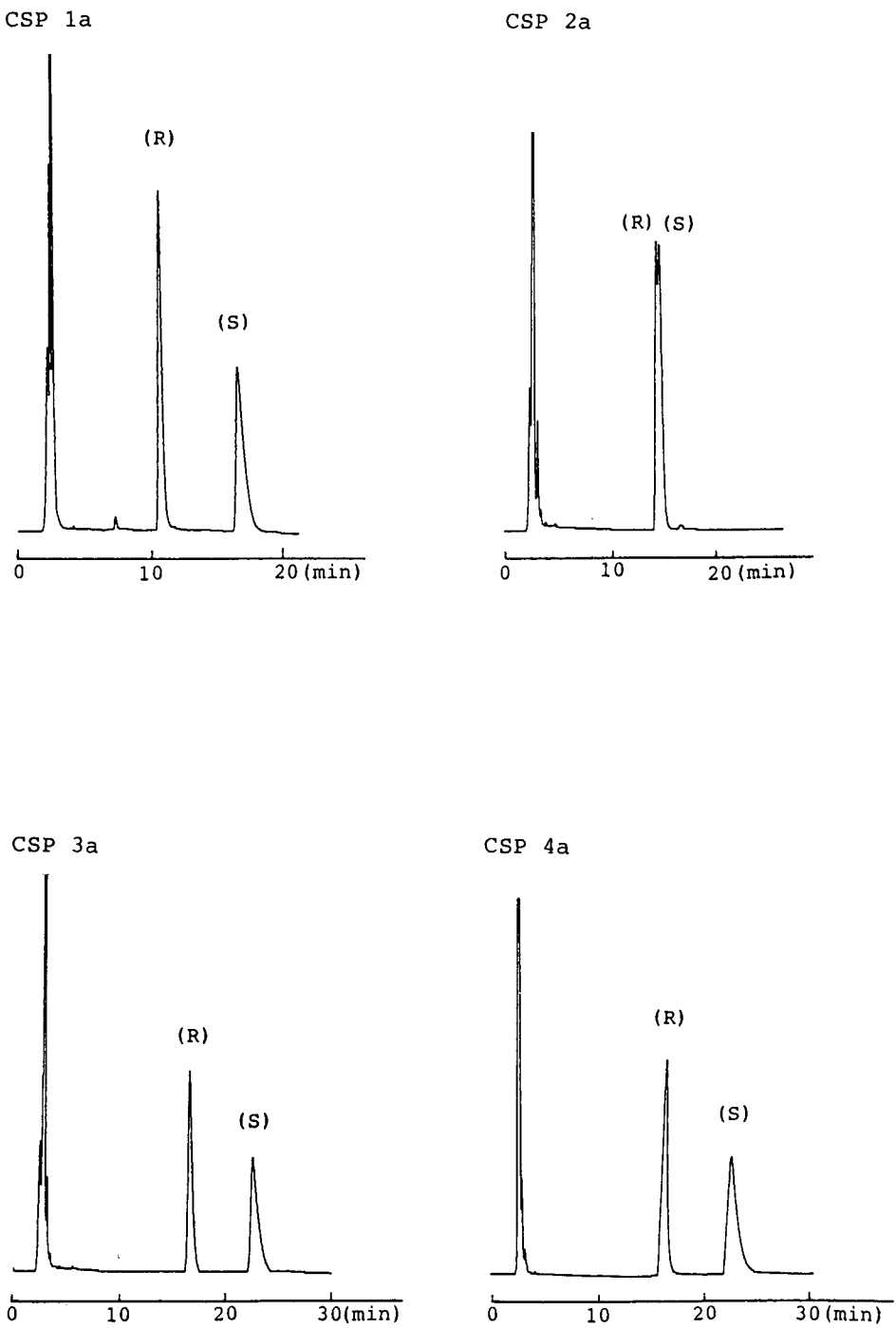

Fig. 4. Enantiomer separation of racemic N-acetylvaline methyl esters. Chromatographic conditions as in Table I.

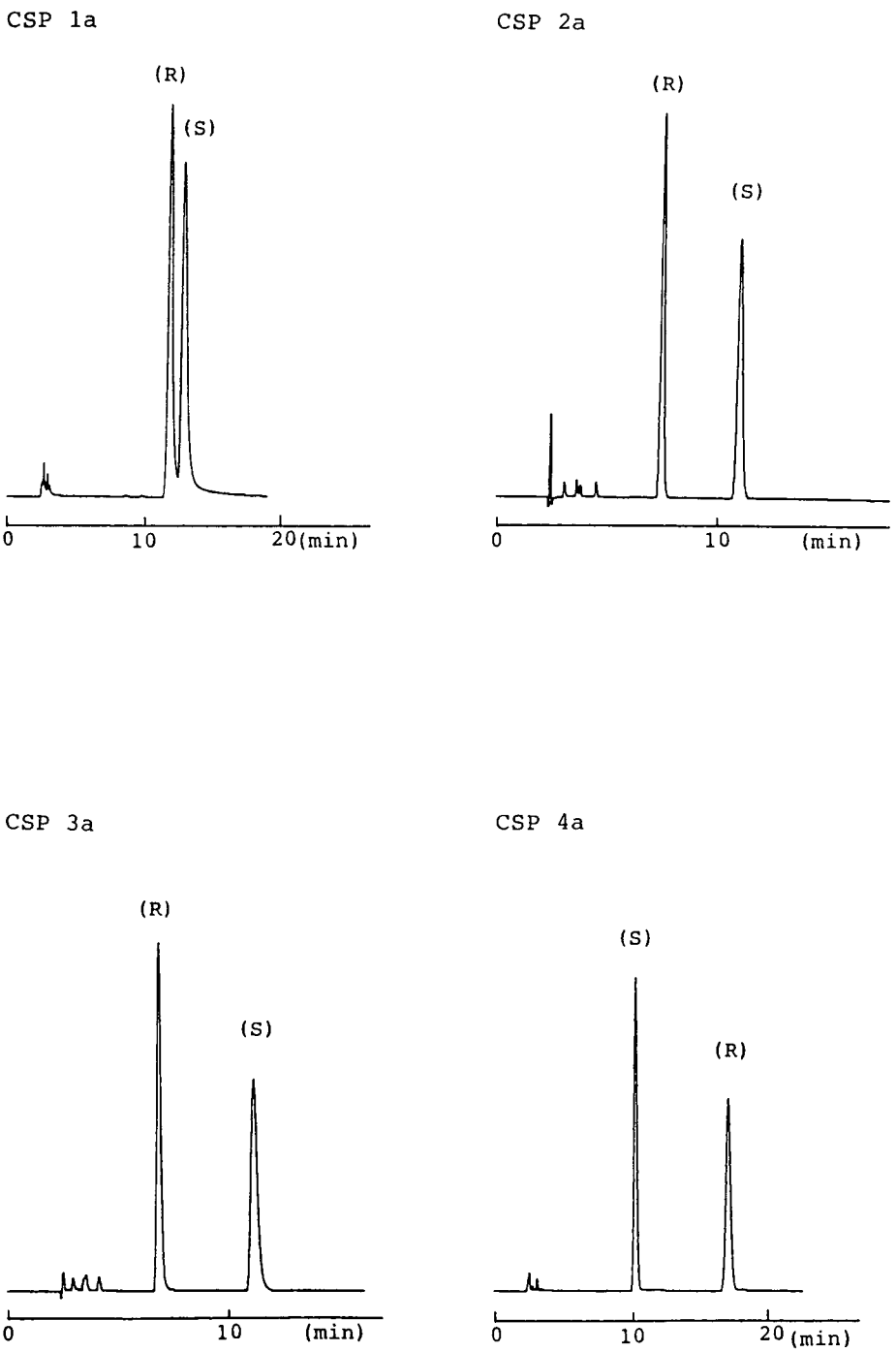

Fig. 5. Enantiomer separation of racemic N-3,5-dinitrobenzoylvaline methyl esters. Chromatographic conditions as in Table II.

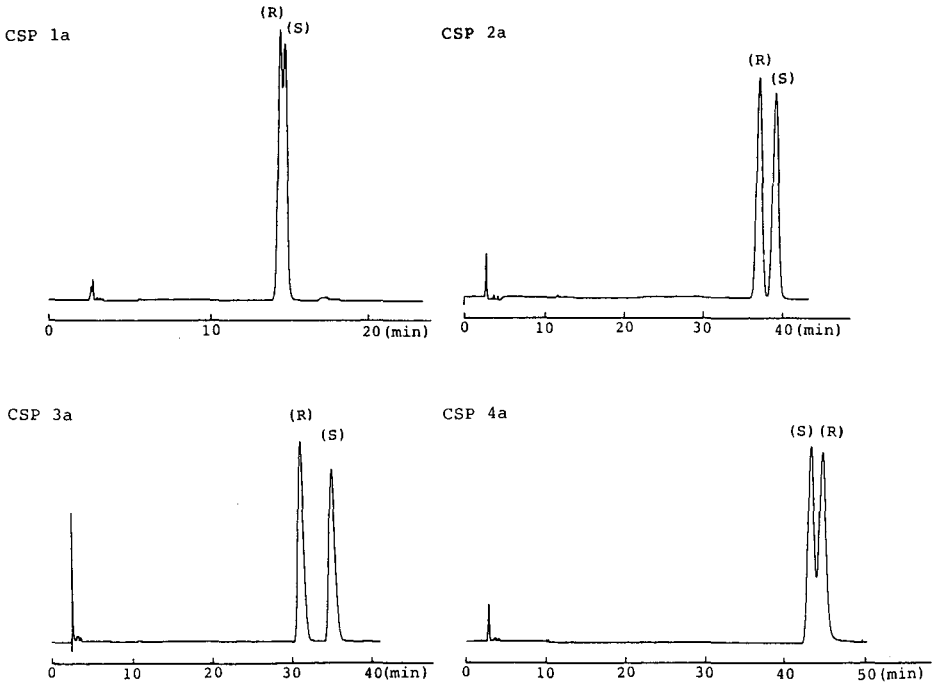

Fig. 6. Enantiomer separation of O-3,5-dinitrophenylurethane derivatives of racemic 2-octanol. Chromatographic conditions as in Table III.

In Table II the abnormal behaviour of DNB-phenylglycine methyl ester and DNB-phenylalanine methyl ester remains unclear, but it is assumed that the structure effect of the phenyl group may be introduced into the chiral recognition mechanism.

Similar elution orders were observed in the enantiomer separation of DNB-amines, DNPU-hydroxy acid methyl esters and DNPU alcohols, as shown in Table III. As these derivatives contain the 3,5-dinitrophenyl group, which can act as a π-acid, the π–π interaction may play an important role in the formation of the diastereomeric association complexes. The NEA component, which can act as a π-base in CSPs **3a**, **3b**, **4a** and **4b** may contribute to the chiral recognition in the separation of these derivatives and in the enantiomer separation of DNB-amino acid methyl esters.

In Table IV, it is emphasized that racemic allethrolone and propargyllone are well resolved directly with CSPs **3a**, **3b**, **4a** and **4b**, although these compounds were hardly resolved with CSPs **1a**, **1b**, **2a** and **2b**. These results show that the second chiral constituent in CSPs, which contain two chiral centres, may efficiently improve the enantioselectivity. Judging from the fact that the same elution order (*S,R*) is obtained on CSPs **3a** and **4a**, and *R,S* on CSP **3b** and **4b**, and also in the separation of AC-amino acid methyl ester enantiomers, the chiral recognition may be controlled by the Val component, and the NEA component may contribute to improve the enantioselectivity. The small difference between separation factors on CSPs **3a** and **3b** and those on CSPs **4a** and **4b** may depend on the combination of the configuration on two chiral components.

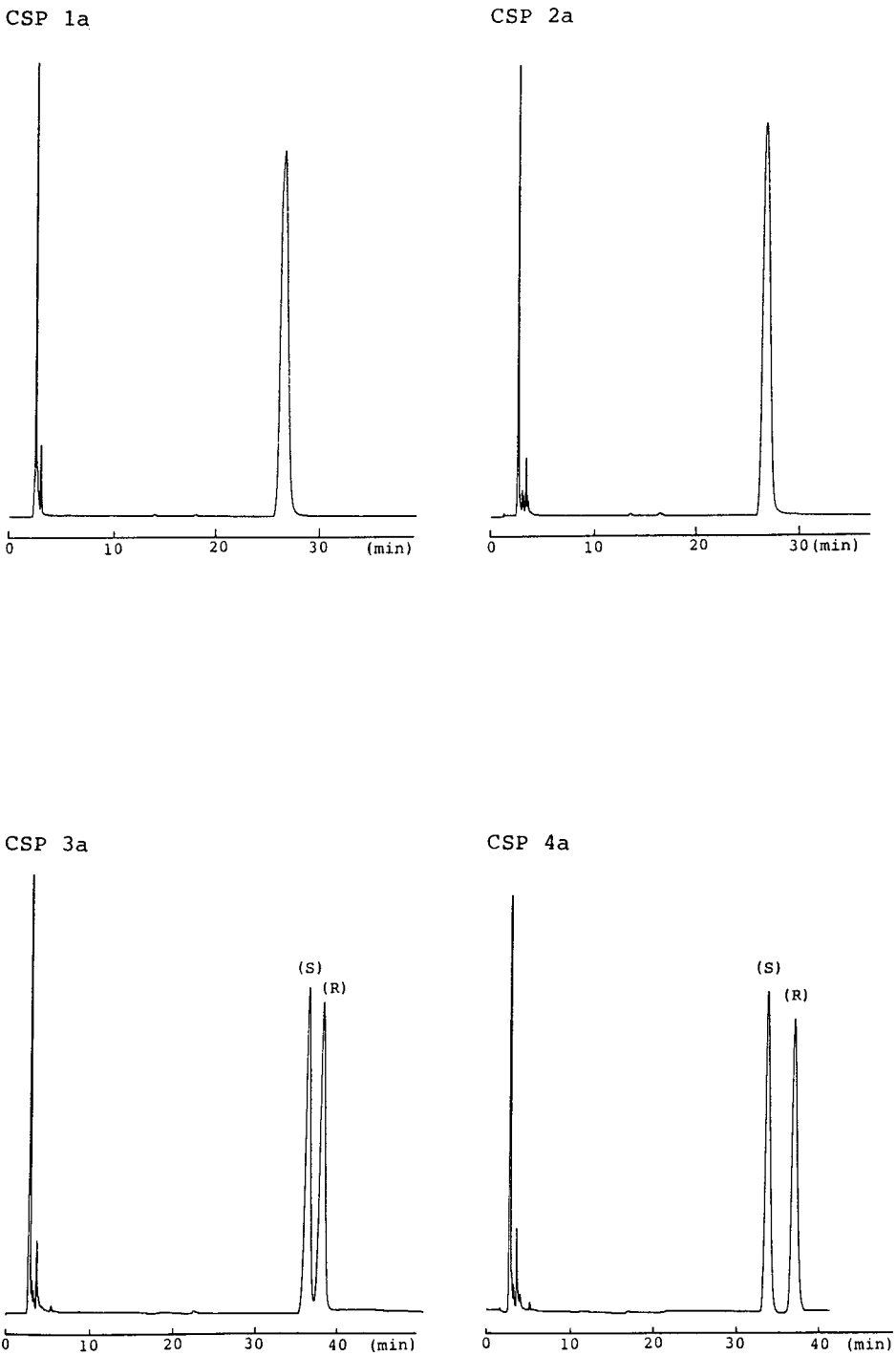

Fig. 7. Enantiomer separation of racemic allethrolone. Chromatographic conditions as in Table IV.

TABLE I

ENANTIOSELECTIVITIES AND ELUTION ORDERS OF N-ACETYLAMINO ACID METHYL ESTERS

Mobile phase (M): (A) *n*-hexane–1,2-dichloroethane–ethanol (40:10:1); (B) *n*-hexane–1,2-dichloroethane–ethanol (100:20:1). A flow-rate of 1.0 ml/min was used with a 250 × 4 mm I.D. column at room temperature.

N-AC-amino acid methyl ester[a]		CSP **1a**				CSP **1b**				CSP **2a**				CSP **2b**			
		k'_1	α	Elution order	M	k'_1	α	Elution order	M	k'_1	α	Elution order	M	k'_1	α	Elution order	M
1a	Alanine	2.72	1.24	*R,S*	A	2.82	1.27	*S,R*	A	3.20	1.00		A	3.94	1.00		A
1b	Valine	3.19	1.73	*R,S*	B	3.76	1.73	*S,R*	B	4.82	1.02	*R,S*	B	5.80	1.04	*S,R*	B
1c	Leucine	4.65	1.99	*R,S*	B	4.03	1.89	*S,R*	B	4.86	1.00		B	6.36	1.00		B
1d	Methionine	1.91	1.48	*R,S*	A	2.03	1.57	*S,R*	A	2.76	1.00		A	3.63	1.00		A
1e	Phenylglycine	3.71	1.39	*R,S*	B	3.99	1.39	*S,R*	B	4.92	1.00		B	6.98	1.00		B
1f	Phenylalanine	3.01	1.66	*R,S*	B	3.50	1.74	*S,R*	B	4.43	1.00		B	6.55	1.00		B
		CSP **3a**				CSP **3b**				CSP **4a**				CSP **4b**			
		k'_1	α	Elution order	M	k'_1	α	Elution order	M	k'_1	α	Elution order	M	k'_1	α	Elution order	M
1a	Alanine	3.67	1.17	*R,S*	A	3.90	1.21	*S,R*	A	3.87	1.16	*R,S*	A	3.35	1.17	*S,R*	A
1b	Valine	5.74	1.43	*R,S*	B	5.53	1.42	*S,R*	B	5.70	1.47	*R,S*	B	4.49	1.41	*S,R*	B
1c	Leucine	6.59	1.46	*R,S*	B	6.24	1.43	*S,R*	B	5.17	1.74	*R,S*	B	4.16	1.71	*S,R*	B
1d	Methionine	2.85	1.30	*R,S*	A	3.20	1.26	*S,R*	A	2.86	1.44	*R,S*	A	2.55	1.35	*S,R*	A
1e	Phenylglycine	5.87	1.20	*R,S*	B	5.96	1.20	*S,R*	B	4.95	1.30	*R,S*	B	4.84	1.28	*S,R*	B
1f	Phenylalanine	5.52	1.33	*R,S*	B	5.49	1.31	*S,R*	B	5.07	1.56	*R,S*	B	4.26	1.53	*S,R*	B

[a] See Fig. 2.

TABLE II

ENANTIOSELECTIVITIES AND ELUTION ORDERS OF N-3,5-DINITROBENZOYLAMINO ACID METHYL ESTERS

Mobile phase (M): (A) *n*-hexane–1,2-dichloroethane–ethanol (200:20:1); (B) *n*-hexane–1,2-dichloroethane–ethanol (40:10:1). A flow-rate of 1.0 ml/min was used with a 250 × 4 mm I.D. column at room temperature.

N-DNB-amino acid methyl ester[a]		CSP **1a**				CSP **1b**				CSP **2a**				CSP **2b**			
		k'_1	α	Elution order	M	k'_1	α	Elution order	M	k'_1	α	Elution order	M	k'_1	α	Elution order	M
2a	Alanine	12.66	1.11	*R,S*	A	11.91	1.09	*S,R*	A	5.27	1.69	*R,S*	B	7.25	1.71	*S,R*	B
2b	Valine	3.34	1.11	*R,S*	A	4.01	1.07	*S,R*	A	2.04	1.79	*R,S*	B	3.23	1.85	*S,R*	B
2c	Leucine	0.69	1.16	*R,S*	B	0.53	1.19	*S,R*	B	2.96	1.45	*R,S*	B	4.14	1.48	*S,R*	B
2d	Methionine	0.86	1.06	*R,S*	B	0.75	1.09	*S,R*	B	4.68	1.68	*R,S*	B	7.12	1.74	*S,R*	B
2e	Phenylglycine	4.63	1.00		A	4.38	1.00		A	4.85	1.11	*S,R*	B	6.82	1.09	*R,S*	B
2f	Phenylalanine	0.52	1.08	*R,S*	B	0.56	1.07	*S,R*	B	4.34	1.25	*R,S*	B	6.89	1.27	*S,R*	B
		CSP **3a**				CSP **3b**				CSP **4a**				CSP **4b**			
		k'_1	α	Elution order	M	k'_1	α	Elution order	M	k'_1	α	Elution order	M	k'_1	α	Elution order	M
2a	Alanine	4.50	2.19	*R,S*	B	5.57	2.07	*S,R*	B	6.22	1.73	*S,R*	B	6.14	1.81	*R,S*	B
2b	Valine	1.74	1.98	*R,S*	B	2.06	1.99	*S,R*	B	3.04	1.87	*S,R*	B	2.64	1.92	*R,S*	B
2c	Leucine	2.04	1.54	*R,S*	B	2.28	1.56	*S,R*	B	4.78	1.26	*S,R*	B	4.20	1.28	*R,S*	B
2d	Methionine	4.20	2.04	*R,S*	B	4.72	2.13	*S,R*	B	7.35	1.63	*S,R*	B	6.54	1.61	*R,S*	B
2e	Phenylglycine	3.44	1.29	*S,R*	B	4.02	1.30	*R,S*	B	6.04	1.30	*R,S*	B	5.66	1.25	*S,R*	B
2f	Phenylalanine	3.63	1.33	*R,S*	B	4.26	1.35	*S,R*	B	7.82	1.03	*R,S*	B	6.76	1.04	*S,R*	B

[a] See Fig. 2.

TABLE III

ENANTIOSELECTIVITIES AND ELUTION ORDERS OF DERIVATIVES OF AMINES, HYDROXY ACIDS AND ALCOHOLS

Mobile phase (M): (A) *n*-hexane–1,2-dichloroethane–ethanol (200:20:1); (B) *n*-hexane–1,2-dichloroethane–ethanol (80:20:3). (C) *n*-hexane–1,2-dichloroethane–ethanol (50:15:1); (D) *n*-hexane–1,2-dichloroethane–ethanol (100:20:1). A flow-rate of 1.0 ml/min was used with a 250 × 4 mm I.D. column at room temperature.

Solute[a]		CSP **1a**				CSP **1b**				CSP **2a**				CSP **2b**			
		k'_1	α	Elution order	M	k'_1	α	Elution order	M	k'_1	α	Elution order	M	k'_1	α	Elution order	M
3a	1-Phenylethylamine[b]	10.92	1.05	*R,S*	A	11.22	1.04	*S,R*	A	3.72	1.93	*R,S*	B	7.00	1.91	*S,R*	B
3b	1-(α-Naphthyl)-ethylamine[b]	10.45	1.10	*R,S*	A	9.33	1.11	*S,R*	A	3.89	2.85	*R,S*	B	6.57	3.07	*S,R*	B
4a	Lactic acid[c]	1.36	1.80	*R,S*	C	1.84	2.01	*S,R*	C	4.09	1.29	*R,S*	C	9.34	1.34	*S,R*	C
4b	Malic acid[c]	1.51	1.32	*R,S*	C	2.14	1.38	*S,R*	C	6.76	1.09	*R,S*	C	16.73	1.12	*S,R*	C
4c	Mandelic acid[c]	0.89	1.48	*R,S*	C	1.25	1.51	*S,R*	C	3.96	1.22	*R,S*	C	9.99	1.30	*S,R*	C
5a	2-Octanol[d]	4.06	1.02	*R,S*	A	4.66	1.05	*S,R*	A	12.19	1.06	*R,S*	A	28.99	1.06	*S,R*	A
5b	1-Phenylethanol[d]	2.75	1.03	*R,S*	D	2.96	1.05	*S,R*	D	10.16	1.16	*R,S*	D	22.35	1.22	*S,R*	D
		CSP **3a**				CSP **3b**				CSP **4a**				CSP **4b**			
		k'_1	α	Elution order	M	k'_1	α	Elution order	M	k'_1	α	Elution order	M	k'_1	α	Elution order	M
3a	1-Phenylethylamine[b]	2.28	1.96	*R,S*	B	3.29	2.02	*S,R*	B	3.37	2.50	*S,R*	B	4.23	2.41	*R,S*	B
3b	1-(α-Naphthyl)-ethylamine[b]	1.92	3.64	*R,S*	B	2.66	4.06	*S,R*	B	3.29	4.20	*S,R*	B	3.75	4.12	*R,S*	B
4a	Lactic acid[c]	3.41	1.83	*R,S*	C	4.47	1.87	*S,R*	C	4.58	1.07	*S,R*	C	7.84	1.08	*R,S*	C
4b	Malic acid[c]	4.99	1.23	*R,S*	C	8.44	1.27	*S,R*	C	5.32	1.06	*S,R*	C	9.53	1.08	*R,S*	C
4c	Mandelic acid[c]	3.27	1.50	*R,S*	C	4.46	1.60	*S,R*	C	3.90	1.34	*S,R*	C	6.31	1.36	*R,S*	C
5a	2-Octanol[d]	11.88	1.14	*R,S*	A	15.42	1.13	*S,R*	A	14.67	1.04	*S,R*	A	18.96	1.04	*R,S*	A
5b	1-Phenylethanol[d]	9.60	1.49	*R,S*	D	11.01	1.49	*S,R*	D	9.27	1.29	*S,R*	D	13.02	1.30	*R,S*	D

[a] See Fig. 2.
[b] Resolved as N-3,5-dinitrobenzoyl derivatives.
[c] Resolved as O-3,5-dinitrophenylurethane O-methyl ester derivatives.
[d] Resolved as O-3,5-dinitrophenylurethane derivatives.

TABLE IV

ENANTIOSELECTIVITIES AND ELUTION ORDERS OF VARIOUS RACEMIC COMPOUNDS

Mobile phase (M): (A) *n*-hexane–1,2-dichloroethane–ethanol (100:20:1); (B) *n*-hexane–1,2-dichloroethane–ethanol (500:10:0.05). (C) *n*-hexane–1,2-dichloroethane–ethanol (500:30:0.15); (D) *n*-hexane–1,2-dichloroethane–ethanol–acetic acid (500:150:5:0.6). A flow-rate of 1.0 ml/min was used with a 250 × 4 mm I.D. column at room temperature.

Solute[a]		CSP **1a**				CSP **1b**				CSP **2a**				CSP **2b**			
		k'_1	α	Elution order	M	k'_1	α	Elution order	M	k'_1	α	Elution order	M	k'_1	α	Elution order	M
a	Allethrolone	10.44	1.00		A	11.23	1.00		A	8.57	1.00		A	14.21	1.03	*S,R*	A
b	Propargyllone	14.00	1.00		A	15.93	1.00		A	12.31	1.00		A	23.00	1.03	*S,R*	A
c	Fenpropathrin	1.28	1.14	*R,S*	B	1.40	1.19	*S,R*	B	4.07	1.00		B	4.14	1.00		B
d	Terallethrin	2.41	1.17	*S,R*	C	1.88	1.22	*R,S*	C	7.20	1.00		C	3.26	1.04	*R,S*	C
e	Diniconazole	3.04	1.02	*R,S*	A	2.81	1.04	*S,R*	A	3.19	1.02	*S,R*	A	6.63	1.04	*R,S*	A
f	Uniconazole	4.45	1.05	*R,S*	A	3.96	1.08	*S,R*	A	4.21	1.00		A	8.58	1.00		A
g	α-Cyano-3-phenoxy-benzyl alcohol	2.93	1.03	*R,S*	D	3.67	1.02	*S,R*	D	4.11	1.04	*S,R*	D	8.90	1.04	*R,S*	D
		CSP **3a**				CSP **3b**				CSP **4a**				CSP **4b**			
		k'_1	α	Elution order	M	k'_1	α	Elution order	M	k'_1	α	Elution order	M	k'_1	α	Elution order	M
a	Allethrolone	12.21	1.05	*S,R*	A	12.89	1.05	*R,S*	A	11.86	1.10	*S,R*	A	13.58	1.11	*R,S*	A
b	Propargyllone	15.69	1.04	*S,R*	A	19.44	1.04	*R,S*	A	17.19	1.09	*S,R*	A	20.34	1.09	*R,S*	A
c	Fenpropathrin	4.22	1.11	*R,S*	B	3.88	1.10	*S,R*	B	3.03	1.04	*R,S*	B	1.66	1.05	*S,R*	B
d	Terrallethrin	5.32	1.16	*S,R*	C	6.11	1.16	*R,S*	C	3.22	1.00		C	3.06	1.00		C
e	Diniconazole	3.99	1.22	*R,S*	A	4.73	1.17	*S,R*	A	3.32	1.27	*R,S*	A	3.22	1.26	*S,R*	A
f	Uniconazole	5.45	1.15	*R,S*	A	6.11	1.12	*S,R*	A	5.04	1.18	*R,S*	A	4.49	1.17	*S,R*	A
g	α-Cyano-3-phenoxy-benzyl alcohol	4.80	1.00		D	6.26	1.00		D	4.46	1.08	*R,S*	D	5.80	1.08	*S,R*	D

[a] See Fig. 3.

Racemic fenpropathrin and terallethrin were well resolved on CSPs **1a** and **1b**, but hardly resolved on CSPs **2a** and **2b**, in addition to racemic AC-amino acid methyl esters. Moreover, the same elution orders were obtained on CSPs **1a**, **3a** and **4a**, containing an (*S*)-Val component, and on CSPs **1b**, **3b** and **4b**, containing an (*R*)-Val component. These results show the Val component may control the chiral recognition in the separation of these compounds. The separation factors of fenpropathrin were very small on CSPs **4a** and **4b** and terallethrin was not resolved on CSPs **4a** and **4b**. Moreover, the separation factors of these compounds on CSPs **3a** and **3b** were smaller than those on CSPs **1a** and **1b**. These results suggest that the NEA component may decrease the enantioselectivity, and its structure effect may depend on the combination of the configuration.

In the separation of racemic diniconazole and uniconazole, the same elution order (*R, S*) was found on CSPs **1a**, **3a** and **4a**, and *S, R* on CSPs **1b**, **3b** and **4b**. Again, it is suggested the Val component may control the chiral recognition. However, it was noticed in the separation of these compounds that larger separation factors were obtained on CSPs **4a** and **4b** than on **3a** and **3b**, in contrast to the results with racemic fenpropathrin and terallethrin. In order to rationalize these results, the elution orders of racemic diniconazole on CSPs containing one chiral centre, *R, S* on CSP **1a**, *S, R* on CSP **1b**, *S, R* on CSP **2a** and *R, S* on CSP **2b**, offer helpful suggestions. We can assume that the enantioselectivity may be increased by the combinations of two chiral recognition mechanisms working in same stereochemical senses on two chiral components, and decreased by the combination of two mechanisms working in opposite stereochemical senses. For the enantiomer separation of diniconazole, the *S–S* or *R–R* configuration of the CSP may decrease the enantioselectivity and the *S–R* or *R–S* configuration of the CSP may increase the enantioselectivity.

In the separation of racemic α-cyano-3-phenoxybenzyl alcohol, very different enantioselectivity was found. A good separation was achieved on CSP **4a** or **4b**, but surprisingly no separation on CSP **3a** or **3b**. This result can also be rationalized by the above assumption. As the elution orders for this compound are *R, S* on CSP **1a**, *S, R* on CSP **1b**, *S, R* on CSP **2a** and *R, S* on CSP **2b**, the enantioselectivity may be increased in CSP **4a** and **4b** (*S–R* and *R–S* configuration) and decreased in CSP **3a** and **3b** (*S–S* and *R–R* configuration).

It was difficult to determine k' values from these results, as we prepared the chiral stationary phases using different aminopropylsilanized silica gels. However, both the retention mechanism and the chiral recognition mechanism are very important and interesting, and we intend to make further investigations of these mechanisms.

CONCLUSION

The enantioselectivity and the elution order in the HPLC separation of various racemic compounds with urea derivatives containing two asymmetric carbon atoms as CSPs were investigated, and it was demonstrated that the elution order and the magnitude of the separation factors can offer helpful suggestions for rationalizing the mechanism of enantiomer separation.

The chromatographic results indicate that two kinds of diastereomeric interactions are produced and each of the two chiral centres may contribute to the chiral

recognition. We can assume that the overall enantioselectivity and elution order on these CSPs are determined by a combination of the structure effects and the chiral recognition mechanisms on two chiral components.

ACKNOWLEDGEMENTS

The authors thank Sumitomo Chemical for providing various racemic compounds.

REFERENCES

1 N. Ôi, H. Kitahara, T. Doi and S. Yamamoto, *Bunseki Kagaku*, 32 (1983) 345.
2 N. Ôi and H. Kitahara, *J. Chromatogr.*, 285 (1984) 198.
3 N. Ôi and K. Kitahara, *J. Liq. Chromatogr.*, 9 (2&3), (1986) 511.
4 N. Ôi and H. Kitahara, *J. Chromatogr.*, 265 (1983) 117.
5 N. Ôi, M. Nagase and T. Doi, *J. Chromatogr.*, 257 (1983) 111.

Journal of Chromatography, 535 (1990) 229–238
Elsevier Science Publishers B.V., Amsterdam

CHROMSYMP. 2034

Resolution of enantiomeric lorazepam and its acyl and O-methyl derivatives and racemization kinetics of lorazepam enantiomers

XIANG-LIN LU and SHEN K. YANG*

Department of Pharmacology, F. Edward Hébert School of Medicine, Uniformed Services University of the Health Sciences, Bethesda, MD 20889-4799 (U.S.A.)

ABSTRACT

Enantiomeric pairs of lorazepam (LZ) and its 3-O-acyl, 1-N-acyl-3-O-acyl, and 3-O-methyl ether derivatives were resolved on high-performance liquid chromatography columns packed with six different chiral stationary phases (CSPs). Resolution was achieved, with several mobile phases of different solvent compositions and with varying chromatograhic resolutions, on at least five of the six CSPs tested. Resolved enantiomers of LZ underwent racemization, whereas enantiomers of 3-O-acyl and 3-O-methyl derivatives were stable. Racemization half-lives of LZ enantiomers were determined by monitoring changes in ellipticity as a function of time. Stability of LZ enantiomers vary substantially depending on the solvents used.

INTRODUCTION

Lorazepam (LZ) is used clinically for the treatment of anxiety and insomnia and has a hydroxyl group at the asymmetric C-3 carbon (see structure in Fig. 1). 3-O-acyl and 3-O-methyl derivatives of LZ are also pharmacologically active in several animals tests [1]. (+)3*S*-Enantiomers of several 1,4-benzodiazepines containing asymmetric carbons at C-3 have been found to possess higher potency in displacing [^{3}H]diazepam (or [^{3}H]flunitrazepam) binding than the respective (−)3*R* enantiomer in synaptosomal preparations from rat cerebral cortex [2–4].

Pirkle and Tsipouras [5] reported the resolution of LZ enantiomers on a column [(*R*)-DNBPG-C] with covalently bonded (*R*)-N-(3,5-dinitrobenzoyl)phenylglycine selectivity, $\alpha = 1.21$); the (+)3*S*-enantiomer was retained more strongly. However,

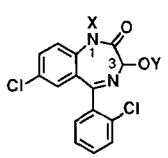

LZ, X = Y = H
LZA, X = H, Y = $COCH_3$
LZAA, X = Y = $COCH_3$
LZM, X = H, Y = CH_3

Fig. 1. Structures of LZ, LZA, LZAA and LZM.

0021-9673/90/$03.50

LZ enantiomers were not resolved on a column [(S)-DNBL-C] with covalently bonded (*S*)-N-(3,5-dinitrobenzoyl)leucine [5]. Bertucci *et al.* [6] reported that LZ enantiomers can be resolved ($\alpha = 1.59$, the 3*S*-enantiomer was retained more strongly) on a chiral stationary phase (CSP) prepared by anchoring N-methylquininium iodide to γ-mercaptopropylsilanized silica gel.

This paper reports CSP-high-performance liquid chromatographic (HPLC) resolution of enantiomeric pairs of LZ, 3-O-acyl-LZ (LZA), 1-N-acyl-3-O-acyl-LZ (LZAA), and 3-O-methyl-LZ (LZM) (see structures in Fig. 1) with mobile phases of different solvent compositions on six different CSP columns. CSP columns employed were: (1) two covalently bonded (*R*)-DNBPG columns manufactured by different processes, (2) a covalently bonded (*S*)-DNBL-C column, (3) a cellulose triphenylcarbamate ("Chiralcel OC") column, (4) a covalently bonded poly-N-acryloyl-(*S*)-phenylalanine ethyl ester ("Chiraspher") column, and (5) a covalently bonded N-3,5-dinitrophenylaminocarbonyl-(*S*)-valine ("Sumipax OA-3100") column. Half-lives of racemization of LZ enantiomers in a variety of solvents were determined.

EXPERIMENTAL

Materials

LZ[7-chloro-1,3-dihydro-3-hydroxy-5-(*o*-chlorophenyl)-2H-1,4-benzodiazepin-2-one] was generously provided by Dr. Yvon Lefebvre of Wyeth-Ayerst Research (Princeton, NJ, U.S.A.). Molar extinction coefficient of LZ (in methanol) was determined to be 34970 cm^{-1} M^{-1} at 230 nm. LZA and LZAA were prepared by reaction of LZ with acetic anhydride in pyridine overnight at room temperature, followed by normal-phase HPLC separation (see below). LZM was converted from LZA in methanol containing 3.4 *M* HCl at 50°C for 40 min, followed by normal-phase HPLC purification. Molar extinction coefficients of LZM, LZA and LZAA, which have UV absorption spectra closely similar to that of LZ, are assumed to be the same as that of LZ.

High-performance liquid chromatography

HPLC was performed using a Waters Assoc. (Milford, MA, U.S.A.) liquid chromatograph consisting of a Model 6000A solvent system, a Model M45 solvent delivery system, a Model 660 solvent programmer and a Kratos (Ramsey, NJ, U.S.A.) Model Spectraflow 757 UV–VIS variable-wavelength detector. Samples were injected via a Valco (Houston, TX, U.S.A.) Model N60 loop injector. Retention time and area under chromatographic peaks were determined with a Hewlett-Packard Model 3390A integrator.

Normal-phase HPLC

LZA and LZAA were isolated by normal-phase HPLC on a Zorbax SIL column (25 cm × 6.2 mm I.D., DuPont). The mobile phase was 10% of ethanol–acetonitrile (2:1, v/v) in hexane at a flow-rate of 2 ml/min. Purified LZA and LZAA (racemic as well as enantiomeric) are more stable when the solvents are evaporated and stored at 4°C.

Chiral stationary phase HPLC

Enantiomeric resolutions of LZ, LZA, LZAA and LZM were carried out on six

different CSP columns. These CSP columns are: (1) (*R*)-N-(3,5-dinitrobenzoyl)phenylglycine covalently bonded to spherical particles of 5 μm diameter of γ-aminopropylsilanized silica ["Hi-Chrom Pirkle covalent phenylglycine", abbreviated as (*R*)-DNBPG-C1, 25 cm × 4.6 mm I.D., Regis, Morton Grove, IL, U.S.A.], (2) (*R*)-N-(3,5-dinitrobenzoyl)phenylglycine covalently bonded to spherical particles of 5 μm diameter of γ-aminopropylsilanized silica ("Rexchrom Pirkle covalent D-phenylglycine", abbreviated as (*R*)-DNBPG-C2, 25 cm × 4.6 mm I.D., Regis), (3) (*S*)-N-(3,5-dinitrobenzoyl)leucine covalently bonded to spherical particles of 5 μm diameter of γ-aminopropylsilanized silica [abbreviated as (*S*)-DNBL-C, 25 cm × 4.6 mm I.D., Regis], (4) a column packed with cellulose coated with trisphenylcarbamate (abbreviated as "Chiralcel OC", 25 cm × 4.6 mm I.D., Daicel, Los Angeles, CA, U.S.A.), (5) a column packed with poly-N-acryloyl-(*S*)-phenylalanine ethyl ester covalently bonded to silica gel (abbreviated as "Chiraspher", 25 cm × 4.6 mm I.D., Bodman Chemicals, Stone Mountain, CA, U.S.A.), and (6) a column packed with N-3,5-dinitrophenylaminocarbonyl-(*S*)-valine bonded covalently to silica gel (15 cm × 4.6 mm I.D., abbreviated as "Sumipax OA-3100", Regis). The difference(s) in the manufacturing (*R*)-DNBPG-C1 and (*R*)-DNBPG-C2 columns was not disclosed by Regis. Mobile phases (2 ml/min) were: EA7 and EA8.5 [7% and 8.5% of ethanol–acetonitrile (2:1, v/v) in hexane, respectively]; DC20P*x*[20% dichloroethane, *x*% 2-propanol, and (100 − 20 − x)% hexane]; DC20E*x*[20% dichloroethane, *x*% ethanol, and (100 − 20 − x)% hexane].

Kinetics of racemization

Within 30 s of separation by CSP-HPLC, changes of ellipticity ($\Delta\Phi$) of an enantiomeric LZ(0.6 to 1.5 A_{230} per ml of HPLC elution solvent) were recorded at 255 or 260 nm (at or near the peak of a Cotton effect) as a function of time in a thermostated quartz cuvette [7,8]. Because LZ does not absorb above 360 nm and for the purpose of reducing the monitoring time, ellipticity at 370 nm was used as the baseline for a completely racemized sample. The half-life of racemization ($t_{1/2}$) was determined by plotting log ($\Delta\Phi$) versus time. Racemization of enantiomeric LZ in all solvents tested follows first-order kinetics. Organic solvents for determining $t_{1/2}$ are the mobile phases used in CSP-HPLC. For the determination of racemization $t_{1/2}$ in aqueous solutions and protic organic solvents such as methanol, ethanol and 2-propanol, LZ enantiomers were resolved using solvent DC20P5 (solvent mixtures are described in the section above) on the Chiralcel OC column. Solvent was evaporated by a stream of nitrogen and the LZ enantiomer was redissolved in either an aqueous solution or an alcohol just prior to monitoring changes in ellipticity as described above.

Spectral analysis

Mass spectral analysis was performed on a Finnigan 4000 gas chromatograph–mass spectrometer with a Technivent 1050 data system. Samples were introduced by a Vacumetrics DCI desorption probe with a 150°C ionizer temperature in either the electron impact (EI) mode at 70 eV or chemical ionization (CI, NH_3) mode. UV–VIS absorption spectra of samples (in methanol) were determined using a 1-cm path length quartz cuvette with a Cary 118C (Varian, Palo Alto, CA, U.S.A.) spectrophotometer. Circular dichroism (CD) spectra of samples (in acetonitrile) in a quartz cell of 1 cm

path length were measured at ambient temperature with a Jasco 500A spectropolarimeter equipped with a Model DP500 data processor. The concentration of the sample is indicated by $A_{\lambda 2}$/ml (absorbance units at wavelength $\lambda 2$ per ml of solvent). CD spectra are expressed by ellipticity ($\Phi_{\lambda 1}/A_{\lambda 2}$, in millidegrees) for solutions that have an absorbance of $A_{\lambda 2}$ unit per ml of solvent at wavelength $\lambda 2$ (usually the wavelength of maximal absorption). Under conditions of measurements indicated above, the molar ellipticity ($[\theta]_{\lambda 1}$, in degrees cm^2 dmole^{-1}) and ellipticity ($\Phi_{\lambda 1}/A_{\lambda 2}$, in millidegrees) are related to the extinction coefficient ($\varepsilon_{\lambda 2}$, in cm^{-1} M^{-1}) as follows:

$$[\theta]_{\lambda 1} = 0.1\,\varepsilon_{\lambda 2}(\Phi_{\lambda 1}/A_{\lambda 2})$$

RESULTS AND DISCUSSION

Preparation of LZ derivatives

Acetylation of LZ in pyridine with acetic anhydride produced a monoacetate LZA (M^+ at m/z 362/364 with fragment ions at m/z 320/322, 291/293 and 275/277; EI) and a diacetate LZAA ($M^+ + 1$ at m/z 404/406 with fragment ions at m/z 363/365, 337/339, 320/322, 305/307 and 295/297; CI, NH_3). A minor unknown product was eluted immediately after LZAA (Fig. 2). The 3-O-methyl product LZM (M^+ at m/z 355; EI) was converted from LZA in HCl–methanol and purified by normal-phase HPLC (retention time 18.5 min in Fig. 2). LZA slowly underwent spontaneous hydrolysis in solution to form LZ. LZAA was slowly hydrolyzed in solution to form

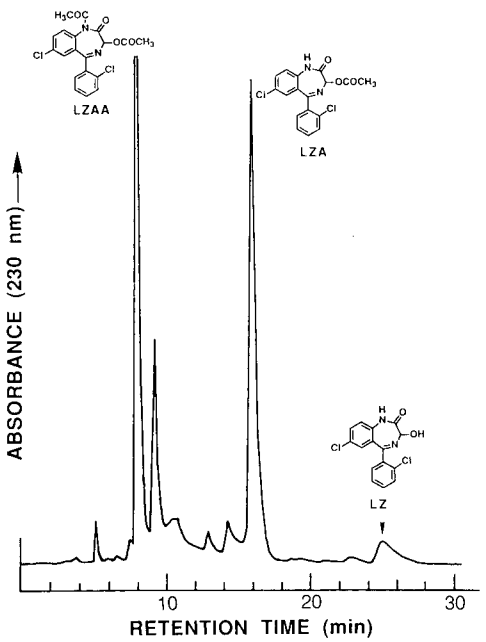

Fig. 2. Normal-phase HPLC separation of LZAA, LZA and LZ. Column, Zorbax SIL (250 mm × 6.2 mm I.D.); mobile phase, 10% ethanol–acetonitrile (2:1) in hexane; flow-rate, 2 ml/min. Under the same chromatographic conditions, LZM has a retention time of 18.5 min.

LZA and LZ. Both LZA and LZAA were more stable at 4°C following removal of solvent.

CSP-HPLC resolution and absolute configuration of enantiomers

The enantiomeric pairs of LZ, LZA, LZAA and LZM were separated on six different CSPs, with varying chromatographic resolutions (Table I). Several mobile phases containing various proportions of the following solvents were used: 2-propanol–hexane, ethanol–acetonitrile–hexane, dichloroethane–2-propanol–hexane, dichloroethane–ethanol–hexane. Consistent with an earlier report on the enantiomeric resolution of oxazepam and its derivatives [7], replacing 10% of 2-propanol in hexane with 7–10% of ethanol–acetonitrile (2:1, v/v) in hexane reduced the retention times of enantiomers and improved the efficiency of enantiomeric separation. The elution order of enantiomeric pairs was established by CD spectral analysis. It is known that the enantiomers of oxazepam, LZ and other 3-substituted 1,4-benzodiazepines that are more strongly retained on the (*R*)-DNBPG-C1 column have positive signs of optical rotations at 589 nm [5]. Furthermore, the (+)-oxazepam has the 3*S* absolute stereochemistry [5]. The 3*R*-enantiomers of many 3-substituted 1,4-benzodiazepines including oxazepam and LZ all have negative signs of CD Cotton effects at *ca.* 255 nm [6–11]. Based on the available information [5–11], the relationship between elution order on CSP-HPLC, sign of optical rotation at 589 nm, CD spectrum, and absolute configuration of LZ enantiomers is therefore established. The CD spectrum of the 3*R*-LZ less strongly retained on (*R*)-DNBPG-C1 is shown in Fig. 3. The enantiomers of LZA, LZAA and LZM that have CD spectra similar to that of 3*R*-LZ are assigned to have the 3*R* absolute stereochemistry (Fig. 3).

The major observations of the enantiomeric resolution of LZ, LZA, LZAA and LZM (Table I) are summarized below:

(1) The enantiomers of LZ were separated on both (*R*)-DNBPG-C1 and (*R*)-DNBPG-C2, but were not separated on (*S*)-DNBL-C. These results are consistent with those reported by Pirkle and Tsipouras [5], who used 10% of 2-propanol in hexane as the mobile phase.

(2) According to Regis, (*R*)-DNBPG-C1 and (*R*)-DNBPG-C2 are prepared by different processes. Retention times of enantiomers on (*R*)-DNBPG-C2 were longer than on (*R*)-DNBPG-C1. However, the enantiomeric pairs were resolved with comparable resolution values.

(3) The enantiomeric pairs of LZA, LZAA, and LZM were efficiently resolved on (*S*)-DNBL-C, while LZ enantiomers could only be resolved with resolution value $\leqslant 0.1$ (Table I). Pirkle and Tsipouras [5] have proposed that the hydrogen at the N1 amide nitrogen of 3-substituted 1,4-benzodiazepines is important for the chiral recognition responsible for the resolution of enantiomers. Since the enantiomers of LZ were not resolved on the (*S*)-DNBL-C, it appears that LZ is an exception to the chiral recognition mechanism proposed [5]. Both LZA and LZM have a free hydrogen at the N1 amide nitrogen. Unlike those of LZ, the enantiomeric pairs of LZA and LZM were efficiently resolved. Substitution of the N1 amide hydrogen of LZA with an acyl group did not reduce the separability of LZAA enantiomers. Thus the chiral recognition mechanism proposed for the (*R*)-DNBPG-C in the enantiomeric resolution of 3-substituted 1,4-benzodiazepines [5] is not applicable for the (*S*)-DNBL-C. It is also interesting to note that, substitution of the N1 amide hydrogen of LZA with an acyl group did not reduce the separability of LZAA enantiomers on (*R*)-DNBPG-C.

TABLE I

CSP-HPLC RESOLUTION OF ENANTIOMERIC LZ, LZA, LZAA and LZM

See text for the assignment of absolute configurations of resolved enantiomers. Enantiomers are designated by E_1 and E_2 according to their elution order. CSPs are described in the Experimental section. Eluents EA7 and EA8.5 are 7% and 8.5% of ethanol–acetonitrile (2:1, v/v) in hexane, respectively. Eluent P10 is 2-propanol–hexane (9:1, v/v). Eluents DC20P*x* are 20% dichloroethane, *x*% 2-propanol and (100 − 20 − x)% hexane. Eluents DC20E*x* are 20% dichloroethane, *x*% ethanol and (100 − 20 − *x*)% hexane. The flow-rate of eluent was 2 ml/min. α and R_s are selectivity and resolution, respectively.

Chemical	CSP	Eluent	Retention Time (min)		α	R_s
			E_1	E_2		
LZ	(*R*)-DNBPG-C1	EA7	30.4 (*R*)	32.5 (*S*)	1.1	1.0
		EA8.5	21.8 (*R*)	23.3 (*S*)	1.1	1.1
		DC20P5	22.5 (*R*)	26.2 (*S*)	1.2	1.5
		P10	40.4 (*R*)	47.3 (*S*)	1.2	0.9
	(*R*)-DNBPG-C2	EA8.5	35.9 (*R*)	39.0 (*S*)	1.1	1.3
		DC20P5	66.2 (*R*)	71.1 (*S*)	1.2	0.8
	(*S*)-DNBL-C	EA8.5	21.0 (*R*)	21.2 (*S*)	1.0	*ca.* 0.1[a]
		DC20P6	25.5	25.5	1.0	0
	Chiralcel OC	DC20P5	21.0 (*R*)	37.4 (*S*)	1.9	4.7
		DC20P8	13.5 (*R*)	23.3 (*S*)	1.9	3.9
	Chiraspher	EA7	40.0 (*S*)	41.7 (*R*)	1.1	0.7
		DC20P6	31.6 (*S*)	35.5 (*R*)	1.1	1.7
	Sumipax OA-3100	DC20E7	21.1 (*S*)	24.3 (*R*)	1.2	1.0
		DC20P10	21.3 (*S*)	24.6 (*R*)	1.2	0.9
LZA	(*R*)-DNBPG-C1	EA7	15.8 (*R*)	17.2 (*S*)	1.1	1.6
		EA8.5	14.4 (*R*)	15.8 (*S*)	1.1	1.8
		DC20P4	10.9 (*R*)	13.4 (*S*)	1.3	2.0
	(*R*)-DNBPG-C2	EA8.5	17.1 (*R*)	19.0 (*S*)	1.1	1.8
		DC20P4	13.5 (*R*)	17.1 (*S*)	1.3	1.8
	Chiralcel OC	DC20P5	10.0	10.0	1.0	0
	(*S*)-DNBL-C	EA7	15.9 (*S*)	17.6 (*R*)	1.1	1.9
		EA8.5	10.2 (*S*)	10.7 (*R*)	1.1	0.8
		DC20P3	18.0 (*S*)	22.3 (*R*)	1.3	2.2
	Chiraspher	DC20P5	12.5 (*S*)	14.0 (*R*)	1.1	1.4
	Sumipax OA-3100	DC20E5	7.3 (*R*)	8.6 (*S*)	1.3	1.3
LZAA	(*R*)-DNBPG-C1	EA5	22.3 (*R*)	24.6 (*S*)	1.1	1.5
		EA8.5	14.2 (*R*)	15.6 (*S*)	1.1	1.8
		DC20P4	11.4 (*R*)	13.8 (*S*)	1.3	1.8
	(*R*)-DNBPG-C2	EA8.5	16.8 (*R*)	18.6 (*S*)	1.1	1.8
		DC20P4	13.0 (*R*)	16.4 (*S*)	1.3	2.2
	(*S*)-DNBL-C	EA7	16.1 (*S*)	17.9 (*R*)	1.1	1.6
		EA8.5	11.2 (*S*)	12.1 (*R*)	1.1	0.8
		DC20P3	17.8 (*S*)	22.1 (*R*)	1.3	2.0
	Chiralcel OC	DC20P3	17.8	17.8	1.0	0
	Chiraspher	DC20P5	12.6 (*S*)	14.1 (*R*)	1.1	1.4
	Sumipax OA-3100	DC20E3	12.8 (*R*)	14.3 (*S*)	1.2	0.8
LZM	(*R*)-DNBPG-C1	EA7	26.2 (*R*)	28.3 (*S*)	1.1	1.3
		EA8.5	21.0 (*R*)	23.2 (*S*)	1.1	2.1
		DC20P4	27.9 (*R*)	33.3 (*S*)	1.2	1.7
	(*R*)-DNBPG-C2	EA8.5	30.4 (*R*)	33.1 (*S*)	1.1	1.9
		DC20P4	38.0 (*R*)	57.5 (*S*)	1.6	1.5
	(*S*)-DNBL-C	EA7	25.3 (*S*)	27.3 (*R*)	1.1	1.4
		DC20P3	49.9 (*S*)	55.9 (*R*)	1.1	1.0
	Chiralcel OC	DC20P5	12.4 (*S*)	14.4 (*R*)	1.2	1.0
	Chiraspher	DC20P6	13.9 (*S*)	19.6 (*R*)	1.5	4.2
	Sumipax OA-3100	DC20E8	17.5 (*R*)	18.4 (*S*)	1.1	0.3

[a] Elution order of enantiomers was established by CD spectral measurement of the front one-third and back one-third of the chromatographic peak.

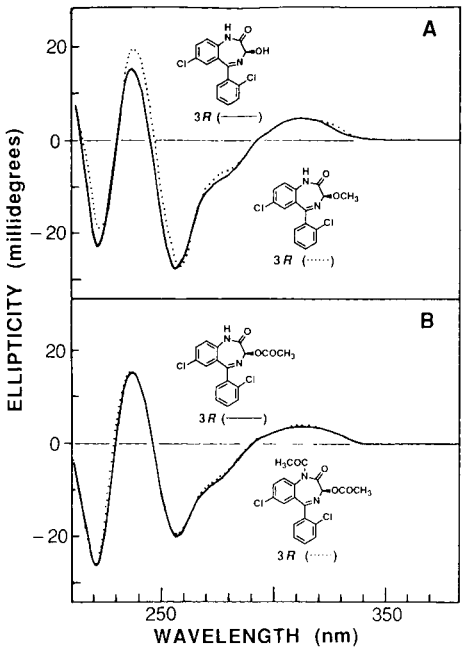

Fig. 3. CD spectra of the 3*R*-enantiomers of LZ(A), LZM(A), LZA(B) and LZAA(B) in acetonitrile. Enantiomers of LZ were separated on Chiralcel OC with eluent DC20P5 (this eluent minimizes the racemization following enantiomeric separation; see racemization $t_{1/2}$ in Table II). The characteristic CD Cotton effects are: 3*R*-LZ (enantiomeric excess, ee $\geqslant$ 95%), $\Phi_{255}/A_{227} = -27.8$ millidegrees; 3*R*-LZM (*ca.* 99% ee), $\Phi_{257}/A_{229} = -27.3$ millidegrees; 3R-LZA (*ca.* 99% ee), $\Phi_{257}/A_{229} = -20.2$ millidegrees; 3*R*-LZAA, 3*R*-LZM (*ca.* 96% ee), $\Phi_{257}/A_{229} = -19.6$ millidegrees.

(4) The most efficient separation of LZ enantiomers ($R_s \geqslant 3.9$) was achieved with the Chiralcel OC column. The Chiralcel OC column also afforded the separation of LZM enantiomers ($R_s = 1.0$), but not the enantiomeric pairs of LZA and LZAA ($R_s = 0$).

(5) Enantiomeric pairs of LZ, LZA, LZAA and LZM were all resolved on the Chiraspher and Sumipax OA-3100 columns, with R_s ranging from 0.3 to 4.2.

(6) Elution orders of enantiomeric pairs on various CSPs are indicated in Table I. On the covalently bonded (*R*)-DNBPG columns, the *S*-enantiomers of LZ, LZA, LZAA and LZM were all more strongly retained. On the (*S*)-DNBL-C, the *S*-enantiomer of LZ was more strongly retained, while the *S*-enantiomers of LZA, LZAA and LZM were less strongly retained. The CSP of Chiraspher contained (*S*)-phenylalanine. The *R* enantiomers of LZ, LZA, LZAA and LZM were all more strongly retained on Chiraspher. In comparison, the CSP of Sumipax OA-3100 contains (*S*)-valine. However, the *R* enantiomers of LZ was more strongly retained, while the *R* enantiomers of LZA, LZAA and LZM were all less strongly retained on Sumipax OA-3100. On the Chiralcel OC column, enantiomeric pairs of LZ and LZM were resolved with different elution order; enantiomeric pairs of LZA and LZAA were not resolved.

(7) Enantiomeric pairs of LZ and LZA can be separated by a single

chromatographic run on either (*R*)-DNBPG-C1 or (*R*)-DNBPG-C2. This observation has been applied successfully as a simple and sensitive analytical method in the analysis of hydrolysis products of racemic LZA by esterases (unpublished data). In two earlier reports [7,12], an (*S*)-DNBL-C column was used successfully to analyze samples resulting from enantioselective hydrolysis of racemic 3-O-acyloxazepam by esterases prepared from the livers and brains of rats and from human livers.

Kinetics of racemization of LZ enantiomers

Enantiomers of LZ readily undergo racemization in a variety of solvents. We have recently developed a method to determine racemization half-lives of enantiomers of several 3-hydroxylated 1,4-benzodiazepines [7,8,11]. Kinetics of racemization of LZ enantiomers in various solvents were determined (Table II). The solvents were mostly the mobile phases used in CSP-HPLC separation of enantiomers. Enantiomeric LZ have a fairly long racemization $t_{1/2}$ (88 min, Table II) in solvent DC20P5. Hence, for determining racemization $t_{1/2}$ in aqueous solutions and protic organic solvents, LZ enantiomers were obtained using solvent DC20P5 on Chiralcel OC column. Evaporation of solvent DC20P5 did not cause significant racemization of LZ enantiomers.

As shown in Table II, increase of the percentages of 2-propanol in solvents DC20P*x* (x = 5 to 10% of 2-propanol) results in the decrease of racemization $t_{1/2}$. Thus the rate of racemization is progressively faster in solvents of increasing polarity. Replacing 2-propanol with ethanol (or a mixture of ethanol and acetonitrile) in solvents DC20P*x* (x = 5 to 10% of 2-propanol) significantly reduces racemization $t_{1/2}$. Racemization $t_{1/2}$ (min) in several pure organic solvents are: methanol (9.2), ethanol (14.3), 2-propanol (33.0), dichloroethane (>5000) and acetonitrile (>5000). These results suggest that LZ enantiomers are more stable (against racemization) in an

TABLE II

RACEMIZATION HALF-LIVES OF ENANTIOMERIC LZ IN VARIOUS SOLVENTS

3*R*-LZ and 3*S*-LZ have identical racemization $t_{1/2}$. Solvents EA7 and EA8.5 are 7% and 8.5% of ethanol–acetonitrile (2:1, v/v) in hexane, respectively. Solvents DC20P*x* are 20% dichloroethane, x% 2-propanol and (100−20−x)% hexane. Solvents DC20E*x* are 20% dichloroethane, x% ethanol and (100−20−x)% hexane. $t_{1/2}$ determined as previously described [7,8,11].

Solvent	Temperature (°C)	$t_{1/2}$ (min)
0.1 *M* Tris–HCl, pH 7.5	37	1.3
0.1 *M* Tris–HCl, pH 7.5	23	5.0
Methanol	23	9.2
Ethanol	23	14.3
2-Propanol	23	33.0
EA7	23	26.2
EA8.5	23	23.0
DC20E7	23	27.5
DC20P10	23	55.0
DC20P8	23	75.5
DC20P6	23	81.0
DC20P5	23	88.0
Dichloroethane	23	>5000[a]
Acetonitrile	23	>5000[a]

[a] No detectable change in ellipticity for 3–6 hours of monitoring.

aprotic environment. Decrease in temperature also stabilizes the LZ enantiomers. These results are consistent with those of an earlier study on the stability of oxazepam enantiomers [7]. Enantiomers of LZA, LZAA and LZM did not undergo racemization in the solvents studied. Enantiomers of other 3-hydroxy-1,4-benzodiazepines such as temazepam, lormetazepam, 3-hydroxyprazepam and 3-hydroxyhalazepam also undergo racemization with various racemization $t_{1/2}$ [7,8,11].

Racemization of oxazepam enantiomers was proposed to be due to equilibrium with a tautomer with an open aldehyde form [13,14]. Similar mechanism of racemization probably also operates in the racemization of enantiomeric LZ and other 3-hydroxy-1,4-benzodiazepines. It appears that the open aldehyde tautomers of 3-hydroxy-1,4-benzodiazepine enantiomers form more easily as the polarity of solvent increases. Enantiomers of 3-hydroxyprazepam (with a cyclopropylmethyl group at N1 of oxazepam) and 3-hydroxyhalazepam (with a trifluoroethyl group at N1 of oxazepam) undergo racemization in 0.1 *M* Tris–HCl (pH 7.5) at 37°C with racemization half-lives of *ca.* 90 and *ca.* 150 min, respectively [8,11]. The racemization half-lives (min) of several other enantiomeric 3-hydroxy-1,4-benzodiazepines in 0.1 *M* Tris–HCl (pH 7.5) at 37°C are: oxazepam (*ca.* 3.0) [8], temazepam (*ca.* 3.4) [8], LZ (*ca.* 1.3) (ref. 8 and Table II), and lormetazepam (*ca.* 0.7) [8]. Thus the enantiomers of 3-hydroxyprazepam and 3-hydroxyhalazepam are considerably more stable than the enantiomeric oxazepam, temazepam, LZ and lormetazepam. These results suggest that it may be possible to substantially stabilize enantiomers of 3-hydroxy-1,4-benzodiazepines such as oxazepam and LZ by substituting either a strong electron-donating group or a strong electron-withdrawing group at N1 position. Substitution at aromatic ring positions and introduction of steric factors into the molecule may also influence the stability of enantiomers.

CONCLUSIONS

Enantiomers of LZ, LZA, LZAA and LZM can be separated with various chromatographic resolution values by HPLC using several different types of CSP columns with a variety of mobile phases. LZ enantiomers undergo facile racemization and the rates of racemization in organic and aqueous solvents can be determined by monitoring changes in ellipticity as a function of time with a spectropolarimeter. LZ enantiomers can be stabilized in aprotic solvents and other media of low polarity.

ACKNOWLEDGEMENTS

We thank Henri Weems for mass spectral analysis. This work was supported by Uniformed Services University of the Health Sciences Protocol RO7502. The opinions or assertions contained herein are the private ones of the authors and are not to be construed as official or reflecting the views of the Department of Defense or the Uniformed Services University of the Health Sciences.

REFERENCES

1 S. C. Bell, R. J. McCaully, C. Gochman, S. J. Childress and M. I. Gluckman, *J. Med. Chem.*, 11 (1968) 457.
2 H. Möhler and T. Okada, *Science (Washington, D.C.)*, 198 (1977) 849.

3 J. L. Waddington and F. Owen, *Neuropharmacol*, 17 (1978) 215.
4 V. G. Blaschke, H. Kley and W. E. Müller, *Arzneim.-Forsch. (Drug Res.)*, 36 (1986) 893.
5 W. H. Pirkle and A. Tsipouras, *J. Chromatogr.*, 291 (1984) 291.
6 C. Bertucci, C. Rosini, D. Pini and P. Salvadori, *J. Pharm. Biomed. Anal.*, 5 (1987) 171.
7 S. K. Yang and X. L. Lu, *J. Pharm. Sci.*, 78 (1989) 789.
8 X. L. Lu and S. K. Yang, *Mol. Pharmacol.*, 36 (1989) 932.
9 A. Corbella, P. Gariboldi, G. Jommi, A. Forgione, F. Marcucci, P. Martelli, E. Missini and F. Mauri, *J. Chem. Soc., Chem. Commun.*, (1973) 721.
10 I. Kavács, G. Maksay, Zs. Tegyey, J. Visy, I. Fitos, M. Kajtár, M. Simonyi and L. Ötovös, *Stud. Org. Chem. (Bio-Organic Heterocycles)*, 18 (1984) 239.
11 X. L. Lu and S. K. Yang, *Chirality*, 2 (1990) 1.
12 S. K. Yang, K. Liu and F. P. Guengerich, *Chirality*, 2 (1990) 150–155.
13 M. Stromar, V. Sunjic, T. Kovac, L. Klasinc and F. Kajfez, *Croat. Chem. Acta*, 46 (1974) 265.
14 G. Lhoest and A. Frigerio, in A. Frigerio (Editor), *Advances in Mass Spectrometry in Biochemistry and Medicine*, Spectrum, London, 1976, pp. 339–349.

Journal of Chromatography, 535 (1990) 239–253
Elsevier Science Publishers B.V., Amsterdam

CHROMSYMP. 2019

Resolution of enantiomeric triols, triol-hydroxyethylthioethers, and methoxy-triols derived from three benzo[*a*]pyrene diol-epoxides by chiral stationary phase high-performance liquid chromatography

HENRI B. WEEMS and SHEN K. YANG*

Department of Pharmacology, F. Edward Hébert School of Medicine, Uniformed Services University of the Health Sciences, Bethesda, MD 20889-4799 (U.S.A.)

ABSTRACT

Benzo[*a*]pyrene 7,8-diol-*anti*-9,10-epoxide, 7,8-diol-*syn*-9,10-epoxide, and 9,10-diol-*anti*-7,8-epoxide were converted to triol, triol-hydroxyethylthioether, and methoxy-triol derivatives. Enantiomeric pairs of these derivatives were resolved by high-performance liquid chromatography with Pirkle's π-electron acceptor chiral stationary phases. Resolution of enantiomers was confirmed by ultraviolet-visible absorption, circular dichroism, and mass spectral analyses. Relative to those of tetrols, these derivatives are less polar and have shorter retention times and improved enantiomeric resolution on chiral stationary phases. Absolute stereochemistries of most enantiomeric derivatives were deduced by comparing their circular dichroism spectra to those of similar compounds derived from enantiomeric diol-epoxides of known absolute stereochemistry.

INTRODUCTION

Benzo[*a*]pyrene (BP) 7,8-diol-*anti*-9,10-epoxide (see structures and abbreviations in Fig. 1) is the predominant ultimate carcinogenic metabolite of BP [1,2]. The metabolically formed BP 7,8-diol-*anti*-9,10-epoxide is enriched in the (7*R*,8*S*,9*S*,10*R*)-enantiomer and reacts covalently with cellular macromolecules [1,2]. BP 7,8-diol-*anti*-9,10-epoxide is hydrolyzed to form 7,8,9,10-tetrahydroxy-7,8,9,10-tetrahydro derivatives (tetrols) and reduced by NADPH (or NADH) to 7,8,9-trihydroxy-7,8,9,10-tetrahydro derivatives (triols) [2–4].

Since the BP 7,8-diol-*anti*-9,10-epoxide is formed by three stereoselective enzymatic reactions in the metabolism of BP [1,2], the hydrolysis products (tetrols) and reduction products (triols) are also highly enriched in one enantiomer. We have recently reported the resolution of the enantiomeric pairs of BP 7,8-diol-9,10-epoxides (*anti* and *syn* isomers), BP 9,10-diol-*anti*-7,8-epoxide, and their hydrolysis products (tetrols) by chiral stationary phase (CSP) high-performance liquid chromatography (HPLC) and have established their absolute configurations [5]. In this paper, we report the resolution of enantiomeric pairs of triols, triol-hydroxyethylthioethers, and

0021-9673/90/$03.50

methoxy-triols derived from BP 7,8-diol-9,10-epoxides (*anti* and *syn* isomers) and BP 9,10-diol-*anti*-7,8-epoxide by HPLC using covalently bonded Pirkle's π-electron acceptor CSPs. Reduction of diol-epoxides with $NaBH_4$ yields triols. Reactions of diol-epoxides with 2-mercaptoethanol (β-ME) in an alkaline aqueous solution or methanolic sodium methylate produce triol-hydroxyethylthioethers or methoxy-triols, respectively. Relative to tetrols, conversion of diol-epoxides to the triolic derivatives reduces the polarity and improves the enantiomeric resolution of enantiomers.

EXPERIMENTAL

Materials

Racemic BP 7,8-diol-*anti*-9,10-epoxide, BP 7,8-diol-*syn*-9,10-epoxide, and BP 9,10-diol-*anti*-7,8-epoxide were obtained from the Chemical Repository of the National Cancer Institute. BP (7,10/8)-triol was a gift from Dr. Peter Fu of the National Center for Toxicological Research, Jefferson, AR, U.S.A. Sodium borohydride ($NaBH_4$) and sodium methylate ($NaOCH_3$) were obtained from Fisher Scientific (Fair Lawn, NJ, U.S.A.). Lithium aluminium hydride ($LiAlH_4$) was purchased from Aldrich (Milwaukee, WI, U.S.A.). 2-Mercaptoethanol (β-ME) was purchased from Sigma (St. Louis, MO, U.S.A.). Solvents were HPLC grade (methanol, Baker, Phillipsburg, NJ, U.S.A.); hexane, tetrahydrofuran (THF), diethyl ether, acetonitrile, Mallinkrodt, Paris, KY, U.S.A.; ethanol, Midwest Grain, Perkin, IL, U.S.A.; dioxane, Aldrich).

Preparation of tetrols

Approximately 0.1 mg of either a racemic or an enantiomeric diol-epoxide was dissolved in 0.4 ml of THF, diluted with 4 ml of 0.1 *M* HCl and stored at ambient temperature overnight (16 h). The hydrolysis products were extracted twice with an equal volume of ethyl acetate, transferred to a new tube, and evaporated to dryness under nitrogen at 50°C. Tetrols were dissolved in methanol and isolated by gradient reversed-phase HPLC.

Preparation of triols

Approximately 0.1 mg of an enantiomeric or racemic diol-epoxide was dissolved in 4 ml of ethanol. Since the presence of water will hydrolyze the diol-epoxide, the ethanol was dried with $NaBH_4$ prior to use. An excess amount of $NaBH_4$ ($\approx$ 5 mg) was added, mixed, and stored at 50°C overnight (16 h). Reduction products were partitioned and extracted twice with ethyl acetate and water. The organic phase was transferred to a new tube and evaporated to dryness under nitrogen at 50°C. Triols (yield $\approx$ 93%) were dissolved in methanol and isolated by gradient reversed-phase HPLC.

Preparation of triol-hydroxyethylthioethers

Approximately 0.1 mg of an enantiomeric or racemic diol-epoxide was dissolved in 0.5 ml of a 2 *M* aqueous β-ME solution (containing 0.4 *M* NaOH) and allowed to react for 15 min at ambient temperature. Reaction products were extracted twice with an equal volume of ethyl acetate, transferred to a new tube, and dried under nitrogen at 50°C. The resulting triol-hydroxyethylthioethers (yield $\approx$ 90%) were dissolved in methanol and isolated by gradient reversed-phase HPLC.

Preparation of methoxy-triols

Approximately 0.1 mg of an enantiomeric or racemic diol-epoxide was dissolved in 1 ml of methanol containing 2% (w/v) of $NaOCH_3$ and allowed to react overnight (16 h) at ambient temperature. Products were partitioned and extracted with equal volumes of ethyl acetate and water. The organic phase was transferred to a new tube and dried under nitrogen at 50°C. Methoxy-triols (yield $\approx$ 80%) were dissolved in methanol and isolated by gradient reversed-phase HPLC.

High-performance liquid chromatography

HPLC was performed using a Waters Assoc. (Milford, MA, U.S.A.) Model 510 solvent delivery system, an Autochrom (Milford, MA, U.S.A.) Model OPG/S gradient system, a Kratos (Ramsey, NJ, U.S.A.) Model 757 variable absorbance detector, a Valco (Houston, TX, U.S.A.) Model N60 loop injector, and a Hewlett-Packard (Palo Alto, CA, U.S.A.) Model 3390A integrator.

Reversed-phase HPLC

Derivatives of diol-epoxides were separated on a Zorbax ODS column (80 × 6.2 mm I.D., 3-μm particle, MAC-MOD, Chadds Ford, PA, U.S.A.). Compounds were eluted with 30 min linear gradient from methanol–water (1:1, v/v) to methanol at a flow-rate of 1 ml/min and monitored at 247 nm. For the purpose of comparing retention times to those of tetrols, the column was eluted isocratically at ambient temperature with premixed methanol–water (1:1, v/v) at a flow-rate of 1 ml/min.

Chiral stationary phase HPLC

Resolution of enantiomeric diol-epoxides or triolic derivatives of diol-epoxides was carried out on CSP columns, 250 × 4.6 mm I.D., Regis Chemical (Morton Grove, IL, U.S.A.) packed with spherical particles of 5 μm diameter of γ-aminopropylsilanized silica to which either (*S*)-N-(3,5-dinitrobenzoyl)leucine [(*S*)-DNBL] or (*R*)-N-(3,5-dinitrobenzoyl)phenylglycine [(*R*)-DNBPG] was bonded ionically (I) or covalently (C). The (*R*)-DNBPG-C column used in this study was labeled as "Hi-Chrom Pirkle covalent phenylglycine" by Regis Chemical. This is different from the more recent "Rexchrom Pirkle covalent D-phenylglycine" column marketed by Regis Chemical. BP diol-epoxides and derivatives were resolved on CSP columns using from 10 to 30% of solvent A (ethanol–acetonitrile, 2:1, v/v) in hexane at a flow-rate of 2 ml/min. Since leaching of stationary phases occurs with ionically bonded columns with mobile phases of high polarity, solvents containing greater than 15% of solvent A in hexane were avoided when using ionic bonded CSPs [6]. For this reason, separations which required 20–30% of solvent A were restricted to covalently bonded CSPs. Elution order of enantiomeric pairs on different CSPs was established by chromatographing a sample containing unequal amounts of two enantiomers.

Absolute configuration of enantiomeric triolic derivatives

Racemic and enantiomeric BP diol-epoxides were converted to triols, triol-hydroxyethylthioethers, or methoxy-triols as described above and resolution of each enantiomeric pair of the triolic derivatives was tested by CSP-HPLC. Triolic derivatives were purified by reversed-phase HPLC prior to CSP-HPLC separation. Circular dichroism (CD) spectra of triolic derivatives enriched in one enantiomer were

obtained. Since the absolute configuration of enantiomeric BP 7,8-diol-*anti*-9,10-epoxides has been established [5], the absolute stereochemistry of their enantiomeric triol derivatives can be readily deduced. CD spectra of some enantiomeric triolic derivatives resolved by CSP-HPLC were compared to those of similar derivatives from enantiomeric BP diol-epoxides. However, all reduction reactions of resolved BP 7,8-diol-*syn*-9,10-epoxide enantiomers did not give identifiable products. The CSP-HPLC and CD spectral analyses have enabled us to establish the elution order-absolute configuration-CD spectrum relationship of most of the enantiomeric triolic derivatives described in this report.

Spectral analysis

Mass spectral analysis was performed on a Finnigan 4000 gas chromatograph–mass spectrometer with a Technivent 1050 data system. Samples were introduced by a solid probe in the electron impact mode at 70 eV with a 250°C ionizer temperature or by a Vacumetrics DCI desorption probe with a 150°C ionizer temperature. Ultraviolet-visible absorption spectra of samples (in methanol) were determined using 1 cm path length quartz cuvette with either a Cary 118C (Varian, Palo Alto, CA, U.S.A.) spectrophotometer or a DW2000 UV/VIS scanning spectrophotometer (slit 2 nm and scan rate 2 nm/sec; SLM Instruments, Urbana, IL, U.S.A.). Circular dichroism (CD) spectra of samples (in methanol) in a quartz cell of 1 cm path length were measured at ambient temperature with a Jasco 500A spectropolarimeter equipped with a Model DP500 data processor. The concentration of the sample is indicated by $A_{\lambda 2}$/ml (absorbance units at wavelength $\lambda 2$ per ml of solvent). CD spectra are expressed by ellipticity ($\Phi_{\lambda 1}/A_{\lambda 2}$, in millidegrees) for solutions that have an absorbance of $A_{\lambda 2}$ unit per ml of solvent at wavelength $\lambda 2$ (usually the wavelength of maximal absorption). Under conditions of measurements indicated above, the molar ellipticity ($[\Theta]_{\lambda 1}$, in deg cm^2 dmole^{-1}) and ellipticity ($\Phi_{\lambda 1}/A_{\lambda 2}$, in millidegrees) are related to the extinction coefficient ($\varepsilon_{\lambda 2}$, in cm^{-1} M^{-1}) as follows:

$$[\theta]_{\lambda 1} = 0.1\ \varepsilon_{\lambda 2}\ (\Phi_{\lambda 1}/A_{\lambda 2})$$

RESULTS

Triols

The structures of triols derived by reduction of each of the three BP diol-epoxides with $NaBH_4$ are shown in Fig. 1. Reduction of BP 7,8-diol-*anti*-9,10-epoxide produced only one triol, whereas reduction of either BP 7,8-diol-*syn*-9,10-epoxide or BP 9,10-diol-*anti*-7,8-epoxide gave two stereoisomeric triols. The elution order and retention time (in min) of BP tetrols and triols on reversed-phase HPLC using a Zorbax ODS column (80 × 6.2 mm I.D.) and methanol–water (1:1, v/v) at a flow-rate of 1 ml/min are: (7,10/8,9)-tetrol, 10.9; (7,8,9/10)-tetrol, 12.7; (7,9/8,10)-tetrol, 13.6; (7/8,9,10)-tetrol, 15.1; (8,9/10)-triol, 18.9; (7,9/8)-triol, 20.2; (7,9,10/8)-tetrol, 22.6; (7/8,9)-triol, 22.8; (7,9/10)-triol, 35.3; (7,10/8)-triol, 45.4. All triols exhibited M^+ at m/z 304 with fragment ions at m/z 286 (loss of H_2O), and 268 (loss of two H_2O) by mass spectral analysis.

The retention times and resolution values of some enantiomeric triol derivatives by HPLC using (*R*)-DNBPG-C and (*S*)-DNBL-C columns are listed in Table I.

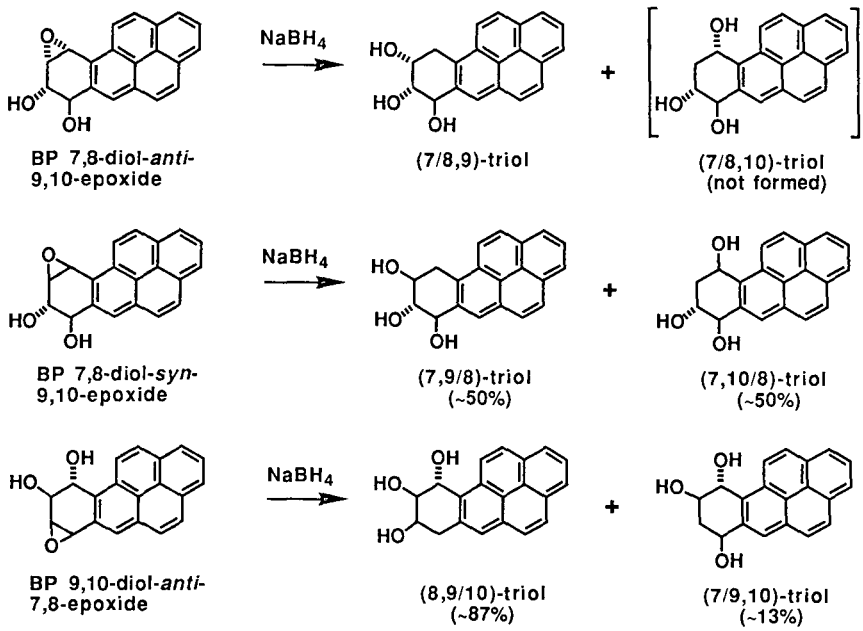

Fig. 1. Structures, abbreviations, and relative configurations of stereoisomeric BP diol-epoxides and their reduction triol products.

Absolute configurations of resolved enantiomers, whenever established, are also indicated in Table I. Each of the resolved enantiomeric triols was confirmed by UV-VIS absorption, CD, and mass spectral analyses.

BP 7,8-diol-*anti*-9,10-epoxide was reduced with $NABH_4$ to produce a (7/8,9)-triol. The second possible reduction product [(7/8,10)-triol, Fig. 1], which may be formed by reduction at the non-benzylic C9 position, was not detected. The (7/8,9)-triol was identical to the (7/8,9)-triol formed by reduction of BP 7,8-diol-*anti*-9,10-epoxide with either NADPH or NADH reported earlier [3,4]. Elution order of (7/8,9)-triol enantiomers is the same on both (*R*)-DNBPG-C and (*S*)-DNBL-C columns (Table I). A BP 7,8-diol-*anti*-9,10-epoxide enriched in the (7*R*,8*S*,9*S*,10*R*)-enantiomer was obtained by CSP-HPLC on a (*R*)-DNBPG-C column [5] and was reduced to a (7/8,9)-triol enriched in the (7*R*,8*R*,9*R*)-enantiomer. The UV absorption and CD spectra of this (7*R*,8*R*,9*R*)-triol is shown in Fig. 2A. This (7*R*,8*R*,9*R*)-triol enantiomer is more strongly retained on both (*R*)-DNBPG-C and (*S*)-DNBL-C columns (Table I). The CD spectrum of the (7/8,9)-triol enantiomer more strongly retained on the (*S*)-DNBL-C column was identical to that of (7*R*,8*R*,9*R*)-triol shown in Fig. 2A. The CD spectrum of (7*R*,8*R*,9*R*)-triol is similar to that of BP 7,8,9,10-tetrahydro-(7*R*,8*R*)-diol [6]. Hence the elution order of (7/8,9)-triol enantiomers on the CSP columns was established (Table I).

BP 7,8-diol-*syn*-9,10-epoxide was reduced with $NaBH_4$ in ethanol at ambient temperature to form two triols. Either dioxane or diethyl ether may be used to replace ethanol in the reduction reaction. Reduction with $LiA1H_4$ in fresh THF at ambient

TABLE I

CSP-HPLC RESOLUTION OF BP TRIOLS

Chemical[a]	CSP[b]	%A[c]	Retention time (min)		*RV*[e]
			Enantiomer 1[d]	Enantiomer 2[d]	
From BP 7,8-diol-anti-9,10-epoxide:					
BP (7/8,9)-triol	(*R*)-DNBPG-C	30	16.5 (7*S*,8*S*,9*S*)	16.9 (7*R*,8*R*,9*R*)	0.2
		20	28.7 (7*S*,8*S*,9*S*)	29.4 (7*R*,8*R*,9*R*)	0.3
	(*S*)-DNBL-C	30	12.5 (7*S*,8*S*,9*S*)	13.5 (7*R*,8*R*,9*R*)	0.6
		20	22.6 (7*S*,8*S*,9*S*)	24.5 (7*R*,8*R*,9*R*)	0.7
From BP 7,8-diol-syn-9,10-epoxide:					
BP (7,9/8)-triol	(*R*)-DNBPG-C	30	7.9 (7*S*,8*S*,9*R*)	8.4 (7*R*,8*R*,9*S*)	0.8
		20	18.3 (7*S*,8*S*,9*R*)	19.5 (7*R*,8*R*,9*S*)	1.2
	(*S*)-DNBL-C	30	5.3 (7*S*,8*S*,9*R*)	5.6 (7*R*,8*R*,9*S*)	0.8
		20	11.2 (7*S*,8*S*,9*R*)	12.0 (7*R*,8*R*,9*S*)	1.6
BP (7,10/8)-triol	(*R*)-DNBPG-C	30	13.3	13.3	0
		20	26.2	26.2	0
		15	43.1	43.1	0
	(*S*)-DNBL-C	30	7.2	7.2	0
		20	13.5	13.7	~0.1
		15	23.0	23.0	0
From BP 9,10-diol-anti-7,8-epoxide:					
BP (8,9/10)-triol	(*R*)-DNBPG-C	30	16.5	16.5	0
		20	41.4	41.4	0
	(*S*)-DNBL-C	30	7.3 (8*S*,9*S*,10*S*)	7.7 (8*R*,9*R*,10*R*)	0.9
		20	16.8 (8*S*,9*S*,10*S*)	17.8 (8*R*,9*R*,10*R*)	1.2
BP (7,9/10)-triol	(*R*)-DNBPG-C	30	7.2 (A)[f]	7.4 (B)[f]	0.4
		20	14.1 (A)	14.7 (B)	0.6
	(*S*)-DNBL-C	30	5.1 (B)	5.3 (A)	0.7
		20	9.4 (B)	9.8 (A)	1.0

[a] Relative configuration for stereoisomers is designated as described in Fig. 1.

[b] CSPs are described in Experimental section.

[c] Percent of solvent A [ethanol–acetonitrile, 2:1 (v/v)] in hexane at a flow-rate of 2 ml/min and a void volume of 2.4 ml.

[d] Enantiomers are designated 1 and 2 according to elution order.

[e] RV = resolution value = $2\,(V_2 - V_1)/(W_2 + W_1)$, where V is retention volume and W is peak width at base.

[f] A and B indicate two enantiomers whose absolute configurations have not been established.

temperature gave identical results. Two triols ($\approx$ 1:1) were separated by reversed-phase HPLC. The late eluting triol had the same retention time as that of an authentic standard (7,10/8)-triol on both reversed-phase HPLC and CSP-HPLC. The enantiomers of (7,10/8)-triol were not resolved by CSP-HPLC (Table I). The earlier eluting triol had the 7,9/8 relative stereochemistry (Fig. 1) and its enantiomers were resolved by CSP-HPLC (Table I). Elution order of (7,9/8)-triol enantiomers is the same on both (*R*)-DNBPG-C and (*S*)-DNBL-C columns (Table I). The CD spectrum of the less strongly retained (7,9/8)-triol enantiomer (Fig. 2B) is similar to the major (7*S*,8*R*,9*R*,10*R*)-tetrol derived from BP 7*S*,8*R*-diol-*syn*-9*S*,10*S*-epoxide [5]. Because the benzylic hydroxyl group is responsible for CSP recognition [7] and the BP 7,8,9,10-tetrahydro-(7*R*,8*R*)-diol is more strongly retained on the (*R*)-DNBPG-C [8],

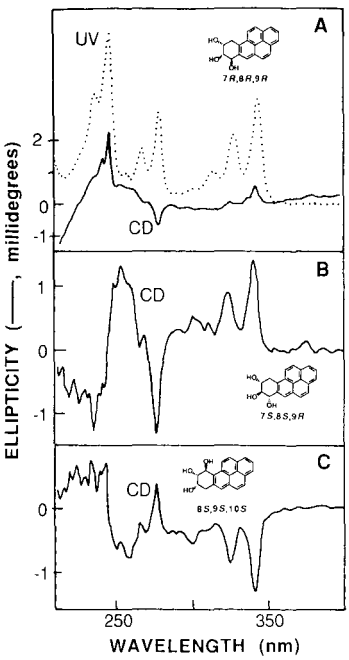

Fig. 2. CD spectra of (A) (7*R*,8*R*,9*R*)-triol, (B) (7*S*,8*S*,9*R*)-triol, and (C) (8*S*,9*S*,10*S*)-triol. The (7*R*,8*R*,9*R*)-triol [concn. 1.0 A_{246}/ml methanol; Φ_{342} = + 0.47 mdeg, ≈90% enantiomer excess (ee)] in A was derived from BP 7*R*,8*S*-diol-*anti*-9*S*,10*R*-epoxide. The (7*S*,8*S*,9*R*)-triol (concn. 1.0 A_{246}/ml methanol; Φ_{340} = + 1.4 mdeg, ≈99% ee) in B was the (7,9/8)-triol enantiomer less strongly retained on the (*S*)-DNBL-C. The (8*S*,9*S*,10*S*)-triol (concn. 1.0 A_{245}/ml methanol; Φ_{341} = − 1.30 mdeg, ≈91% ee) in C was derived from BP 9*R*,10*S*-diol-*anti*-7*S*,8*R*-epoxide.

the (7,9/8)-triol enantiomer more strongly retained on the CSP is therefore assigned to have the 7*R*,8*R*,9*S* absolute stereochemistry.

BP 9,10-diol-*anti*-7,8-epoxide was reduced with $NaBH_4$ in ethanol at ambient temperature to form two triols (Fig. 1). Two triols were separated by reversed-phase HPLC and the areas under chromatographic peaks indicated that the two triols were formed in a ratio of ≈7:1, with the major triol eluting earlier. The result on the reduction of 7,8-diol-*anti*-9,10-epoxide by $NaBH_4$ indicated that the benzylic C10 position is the predominant site of reduction (see Fig. 1 and description above). Hence the major site of reduction of 9,10-diol-*anti*-7,8-epoxide is also expected to be at the benzylic C7 position, resulting in the formation of (8,9/10)-triol as the major product. The minor reduction product was therefore assigned to be the (7,9/10)-triol. The enantiomers of the major (8,9/10)-triol were resolved on (*S*)-DNBL-C, but not on (*R*)-DNBPG-C (Table I). A BP 9,10-diol-*anti*-7,8-epoxide enriched in the (7*R*,8*S*,9*S*,10*R*)-enantiomer was obtained by CSP-HPLC on a (*R*)-DNBPG-C column [5] and was reduced with $NaBH_4$ to form two triols. The CD spectrum of the major (8,9/10)-triol, enriched in the (8*S*,9*S*,10*S*)-enantiomer, is shown in Fig. 2C. The CD spectrum of the less strongly retained enantiomer of the (8,9/10)-triol on the (*S*)-DNBL-C was identical to that shown in Fig. 2C. Hence the (8,9/10)-triol enantiomer with a CD spectrum shown in Fig. 2C is deduced to have the 8*S*,9*S*,10*S*

absolute stereochemistry. The CD spectrum of (8*S*,9*S*,10*S*)-triol is also similar to that of BP 7,8,9,10-tetrahydro-(9*S*,10*S*)-diol [6,9]. The enantiomers of the minor (7,9/10)-triol were resolved on both the (*R*)-DNBPG-C and (*S*)-DNBL-C columns (Table I). However, the absolute configurations of the (7,9/10)-triol enantiomers have not been established.

Triol-hydroxyethylthioethers

The structures of triol-hydroxyethylthioethers derived by reaction of each of the three BP diol-epoxides with β-ME in an alkaline aqueous solution are shown in Fig. 3. Only one triol-hydroxyethylthioether was formed by *trans*-addition of the thiol group at the benzylic position of each BP diol-epoxide. It is known that compounds such as *tert.*-butyl mercaptan [10] and β-ME [11] react with BP 7,8-diol-*anti*-9,10-epoxide by *trans*-addition at the benzylic C10 position. Since hydrolysis of BP 9,10-diol-*anti*-7,8-epoxide occurs predominantly by *trans*-addition at the benzylic C7 position [5], it is reasonable to assume that reaction of BP 9,10-diol-*anti*-7,8-epoxide with β-ME in an alkaline aqueous solution also occurs by *trans*-addition at the benzylic C7 position, resulting in the formation of 8,9,10-triol-7-hydroxyethylthioether with a 7,10/8,9 relative stereochemistry (Fig. 3). In comparison, hydrolysis of BP 7,8-diol-*syn*-9,10-epoxide occurs predominantly by *cis*-addition at C10 position [4]. Hence we assume that the reaction of BP 7,8-diol-*syn*-9,10-epoxide with β-ME in an alkaline aqueous solution also occurs by *cis*-addition at the benzylic C10 position, resulting in the formation of 7,8,9-triol-10-hydroxyethylthioether with a 7,9,10/8 relative stereochemistry (Fig. 3).

Each triol-hydroxyethylthioether was purified by reversed-phase HPLC prior to CSP-HPLC separation of enantiomers. The retention times and resolution values of enantiomeric triol-hydroxyethylthioethers by HPLC on either (*R*)-DNBPG-C or (*S*)-DNBL-C are listed in Table II. Absolute configurations of resolved enantiomers, whenever established, are also indicated in Table II. Each triol-hydroxyethylthioether was confirmed by UV-VIS absorption, CD, and mass spectral analyses. All triol-hydroxyethylthioethers exhibited M^+ at *m/z* 380 by mass spectral analysis.

A racemic BP 7,8-diol-*anti*-9,10-epoxide was reacted with β-ME in an alkaline aqueous solution to form a 7,8,9-triol-10-hydroxyethylthioether with a 7,10/8,9 relative stereochemistry (Fig. 3). Consistent with an earlier report [12], this 7,8,9-triol-10-hydroxyethylthioether has a characteristic absorption band with a maximum at 348 nm (Fig. 4). In comparison, BP triols and tetrols have absorption maxima at ≈344 nm in the same wavelength region [3,5]. The enantiomers of this triol-hydroxyethylthioether were resolved on both (*R*)-DNBPG-C and (*S*)-DNBL-C columns (Fig. 5 and Table II). The less strongly retained enantiomer on the (*S*)-DNBL-C column had a CD spectrum as shown in Fig. 4A. A 7,8-diol-*anti*-9,10-epoxide enantiomer enriched in the (7*S*,8*R*,9*R*,10*S*)-enantiomer was obtained by CSP-HPLC on a (*R*)-DNBPG-C column [5] and was reacted with β-ME in an alkaline aqueous solution to form a 7,8,9-triol-10-hydroxyethylthioether enriched in the (7*S*,8*R*,9*R*,10*R*)-enantiomer. This enantiomeric 7,8,9-triol-10-hydroxyethylthioether had a CD spectrum identical to that shown in Fig. 4A. Hence the elution order-CD spectrum-absolute configuration relationship of the enantiomeric 7,8,9-triol-10-hydroxyethylthioethers derived from BP 7,8-diol-*anti*-9,10-epoxide was established (Fig. 4A and Table II).

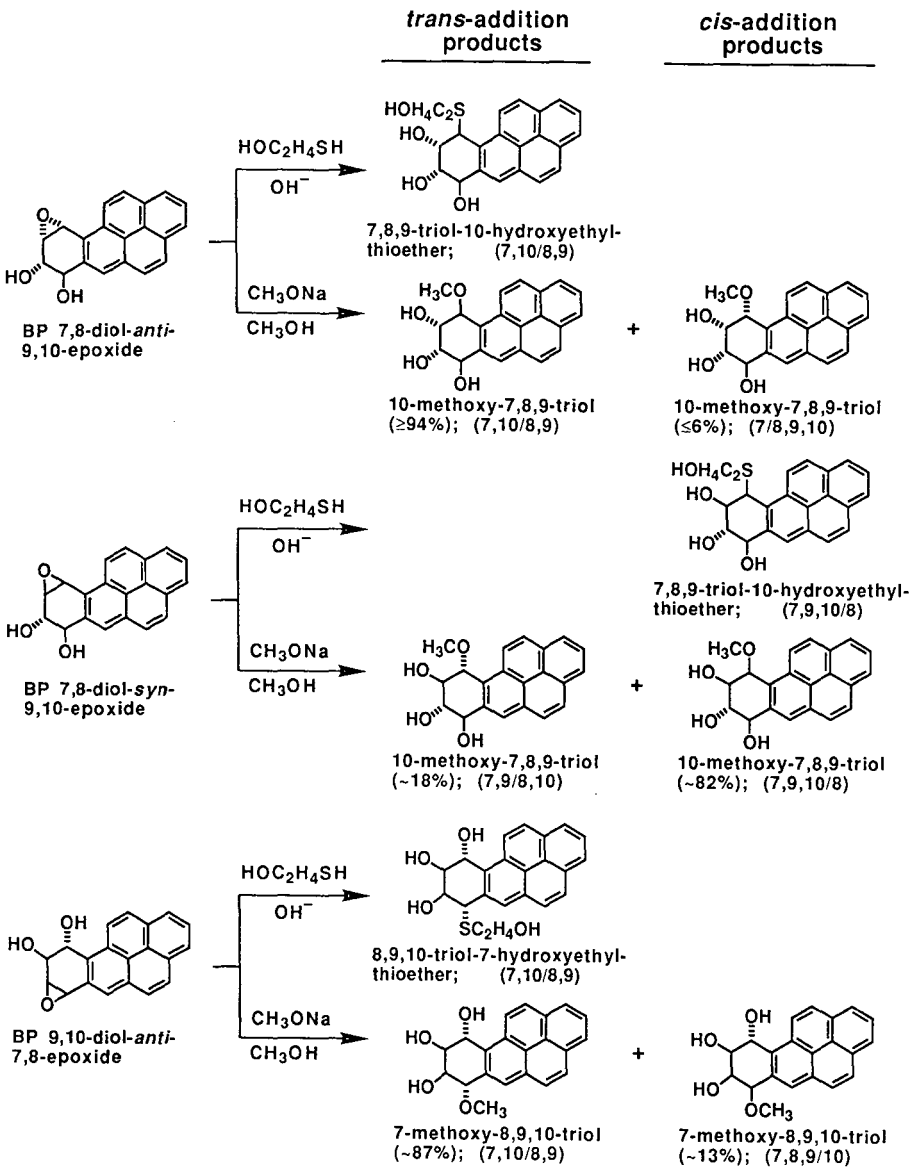

Fig. 3. Structures, abbreviations, and relative configurations of stereoisomeric BP diol-epoxides and their methoxylation and hydroxyethylthiolation products.

A racemic BP 7,8-diol-*syn*-9,10-epoxide was reacted with β-ME in an alkaline aqueous solution to produce a 7,8,9-triol-10-hydroxyethylthioether with a 7,9,10/8 relative stereochemistry (Fig. 3). This triol-hydroxyethylthioether has an absorption maximum identical to the 7,8,9-triol-10-hydroxyethylthioether derived from BP 7,8-diol-*anti*-9,10-epoxide (Fig. 4A). The enantiomers of this 7,8,9-triol-10-hydroxyethylthioether were resolved on both the (*R*)-DNBPG-C and (*S*)-DNBL-C columns

TABLE II

CSP-HPLC RESOLUTION OF BP TRIOL-HYDROXYETHYLTHIOETHERS

Chemical[a]	CSP[b]	%A[c]	Retention time (min)		*RV*[e]
			Enantiomer 1[d]	Enantiomer 2[d]	
From BP 7,8-diol-anti-9,10-epoxide:					
BP 10-SE-7,8,9-triol (7,10/8,9)	(*R*)-DNBPG-C	30	12.1 (7*R*,8*S*,9*S*,10*S*)	13.3 (7*S*,8*R*,9*R*,10*R*)	0.8
		20	32.2 (7*R*,8*S*,9*S*,10*S*)	35.5 (7*S*,8*R*,9*R*,10*R*)	1.2
	(*S*)-DNBL-C	30	6.2 (7*S*,8*R*,9*R*,10*R*)	7.2 (7*R*,8*S*,9*S*,10*S*)	2.1
		25	8.2 (7*S*,8*R*,9*R*,10*R*)	9.7 (7*R*,8*S*,9*S*,10*S*)	2.5
		20	14.5 (7*S*,8*R*,9*R*,10*R*)	18.0 (7*R*,8*S*,9*S*,10*S*)	2.7
From BP 7,8-diol-syn-9,10-epoxide:					
BP 10-SE-7,8,9-triol (7,9,10/8)	(*R*)-DNBPG-C	30	9.3 (7*R*,8*S*,9*R*,10*S*)	9.6 (7*S*,8*R*,9*S*,10*R*)	0.4
		20	25.5 (7*R*,8*S*,9*R*,10*S*)	26.6 (7*S*,8*R*,9*S*,10*R*)	0.5
	(*S*)-DNBL-C	30	5.2 (7*S*,8*R*,9*S*,10*R*)	5.5 (7*R*,8*S*,9*R*,10*S*)	0.8
		20	12.8 (7*S*,8*R*,9*S*,10*R*)	13.7 (7*R*,8*S*,9*R*,10*S*)	1.3
		15	22.5 (7*S*,8*R*,9*S*,10*R*)	24.3 (7*R*,8*S*,9*R*,10*S*)	1.5
From BP 9,10-diol-anti-7,8-epoxide:					
BP 7-SE-8,9,10-triol (7,10/8,9)	(*R*)-DNBPG-C	30	12.1 (7*S*,8*S*,9*S*,10*R*)	12.9 (7*R*,8*R*,9*R*,10*S*)	0.7
		20	27.1 (7*S*,8*S*,9*S*,10*R*)	28.9 (7*R*,8*R*,9*R*,10*S*)	0.8
	(*S*)-DNBL-C	30	7.5	7.5	0
		20	15.7	15.7	0

[a] Relative configuration for stereoisomers is designated as described in Fig. 3. SE abbreviates for the $HOCH_2CH_2S$ group.

[b] CSPs are described in Experimental section.

[c] Percent of solvent A [ethanol–acetonitrile, 2:1 (v/v)] in hexane at a flow-rate of 2 ml/min and a void volume of 2.4 ml.

[d] Enantiomers are designated 1 and 2 according to elution order.

[e] RV = resolution value = $2(V_2 - V_1)/(W_2 + W_1)$, where V is retention volume and W is peak width at base.

(Table II). The CD spectrum of the less strongly retained enantiomer on the (*S*)-DNBL-C column is identical to that of the major (7*S*,8*R*,9*R*,10*R*)-tetrol derived by hydrolysis of BP 7*S*,8*R*-*syn*-9*S*,10*R*-epoxide [5]. Hence the elution order-CD spectrum-absolute configuration relationship of the enantiomeric 7,8,9-triol-10-hydroxyethylthioethers derived from BP 7,8-diol-*syn*-9,10-epoxide was established (Fig. 4B and Table II).

A racemic BP 9,10-diol-*anti*-7,8-epoxide was reacted with β-ME in an alkaline aqueous solution to produce a 8,9,10-triol-7-hydroxyethylthioether with a 7,10/8,9 relative stereochemistry (Fig. 3). This triol-hydroxyethylthioether has an absorption maximum at ≈344 nm (Fig. 4C). In contrast, the 10-hydroxyethylthioethers derived from BP 7,8-diol-*anti*-9,10-epoxide and 7,8-diol-*syn*-9,10-epoxide have an absorption maximum at 348 nm in the same wavelength region (Fig. 4A). Thus the absorption maximum at 348 nm is a unique property of 7,8,9-triol-10-hydroxyethylthioethers in which the 10-hydroxyethylthiol group is in the sterically crowded bay region. The CD spectrum of the more strongly retained enantiomer on (*R*)-DNBPG-C (Fig. 4C) is identical to that of the 8,9,10-triol-7-hydroxyethylthioether derived by reaction of β-ME with BP 9*R*,10*S*-diol-*anti*-7*S*,8*R*-epoxide. The latter was obtained from the

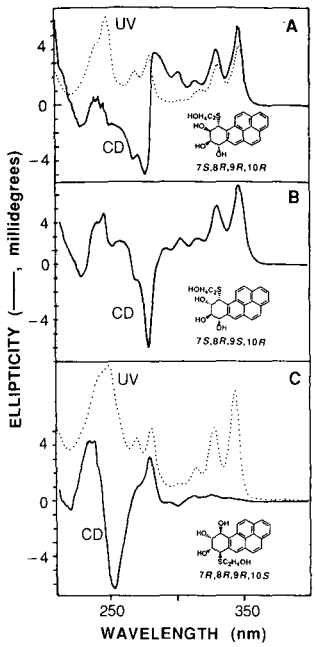

Fig. 4. CD spectra of (A) 7*S*,8*R*,9*R*-triol-10*R*-hydroxyethylthioether, (B) 7*S*,8*R*,9*S*-triol-10*R*-hydroxyethylthioether, and (C) 7*R*-hydroxyethylthioether-8*R*,9*R*,10*S*-triol. The 7*S*,8*R*,9*R*-triol-10*R*-hydroxyethylthioether (concn. 1.0 A_{248}/ml methanol; Φ_{347} = + 5.6 mdeg, ≈86% ee) in A was derived from BP 7*S*,8*R*-diol-*anti*-9*R*,10*S*-epoxide. The (7*S*,8*R*,9*S*)-triol-10*R*-hydroxyethylthioether (concn. 1.0 A_{247}/ml methanol; Φ_{346} = + 5.6 mdeg, ≈84% ee) in B was the less strongly retained enantiomer on the (*S*)-DNBL-C (Table II). The 7*R*-hydroxyethylthioether-8*R*,9*R*,10*S*-triol (concn. 1.0 A_{248}/ml methanol Φ_{254} = − 6.4 mdeg, ≈58% ee) in C was derived from BP 9*R*,10*S*-diol-*anti*-7*S*,8*R*-epoxide.

racemic compound by CSP-HPLC resolution on a (*R*)-DNBPG-C column [5]. The elution order-CD spectrum-absolute configuration relationship of the enantiomeric 8,9,10-triol-7-hydroxyethylthioethers derived from BP 9,10-diol-*anti*-7,8-epoxide was therefore established (Fig. 4C and Table II).

Methoxy-triols

The structures of methoxy-triols derived by reaction of each of the three BP diol-epoxides with CH_3ONa in methanol are shown in Fig. 3. Similar to the formation of tetrols [4], methoxylation of each of the three BP diol-epoxides occurs by *trans*- and *cis*-addition at the benzylic position, forming two methoxy-triols (Fig. 3). The relative amount of the major and the minor methoxy-triols formed (Fig. 3) were similar to that of the tetrols formed [4]. The methoxy-triols were purified by reversed-phase HPLC prior to CSP-HPLC separation of enantiomers. The retention times and resolution values of enantiomeric methoxy-triols by HPLC using (*R*)-DNBPG-C and (*S*)-DNBL-C columns are listed in Table III. Absolute configurations of resolved enantiomers were established by comparing their CD spectra with those of tetrols of similar structure and known absolute stereochemistry [5]. Each of the resolved enantiomeric methoxy-triols was confirmed by UV-VIS absorption, CD, and mass spectral analyses. Unlike the enantiomers of triol-hydroxyethylthioethers, the CD

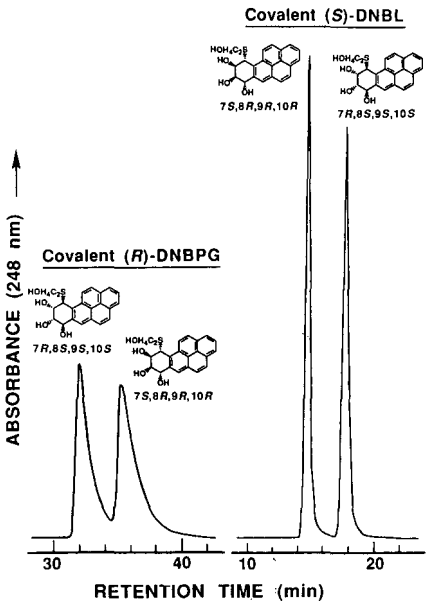

Fig. 5. CSP-HPLC resolution of enantiomeric BP 7,8,9-triol-10-hydroxyethylthioether (7,10/8,9 relative stereochemistry) on DNBPG-C (left chromatogram) and DNBL-C (right chromatogram). Both chromatograms were obtained using 20% of ethanol–acetonitrile (2:1, v/v) in hexane at a flow-rate of 2 ml/min. Column: 250 × 4.6 mm I.D.

spectra of enantiomeric methoxy-triols are closely similar to the corresponding tetrol enantiomers. All methoxy-triols exhibited M^+ at *m/z* 334 with fragment ions at *m/z* 316 (loss of H_2O), and 284 (loss of H_2O and CH_3OH) by mass spectral analysis. The retention times of each pair of methoxy-triols on the reversed-phase HPLC are: 12.8 min (major, $\geq 94\%$) and 17.3 min (minor, $\leqslant 6\%$) derived from BP 7,8-diol-*anti*-9,10-epoxide; 14,3 min (minor, $\approx 18\%$) and 16.0 min (major, $\approx 82\%$) derived from BP 7,8-diol-*syn*-9,10-epoxide; 13.3 min (major, $\approx 87\%$) and 15.3 min (minor, $\approx 13\%$) derived from BP 9,10-diol-*anti*-7,8-epoxide.

DISCUSSION

We have previously studied the enantiomeric separation of oxygenated polycyclic aromatic hydrocarbon (PAH) derivatives ranging from relatively less polar compounds containing one oxygen atom (epoxides and cyclic alcohols) to very polar compounds containing four oxygen atoms (tetrols) [9]. The recommended mobile phases for CSP-HPLC are a mixture of 2-propanol and hexane, which cannot be used to separate enantiomeric pairs of compounds with high polarity. For the purpose of resolving enantiomers of diol derivatives of PAH's, we developed a mobile phase {various percentages of solvent A [ethanol–acetonitrile (2:1, v/v) in hexane]} with relatively high polarity [6] and this solvent mixture has been used succesfully in resolving various kinds of PAH derivatives [9]. However, due to possible leaching of CSPs, mixtures containing greater than 15% of solvent A in hexane cannot be used

TABLE III

CSP-HPLC RESOLUTION OF BP METHOXY-TRIOLS AND TETROLS

Chemical[a]	CSP[b]	%A[c]	Retention time (min)		*RV*[e]
			Enantiomer 1[d]	Enantiomer 2[d]	
From BP 7,8-diol-anti-9,10-epoxide:					
BP 10-MeO-7,8,9-triol	(*R*)-DNBPG-C	30	12.6	12.6	0
(7,10/8,9), major		20	24.8	24.8	0
	(*S*)-DNBL-C	30	6.8 (7*S*,8*R*,9*R*,10*R*)	7.3 (7*R*,8*S*,9*S*,10*S*)	1.5
		20	12.7 (7*S*,8*R*,9*R*,10*R*)	13.7 (7*R*,8*S*,9*S*,10*S*)	1.7
		15	21.6 (7*S*,8*R*,9*R*,10*R*)	23.5 (7*R*,8*S*,9*S*,10*S*)	1.9
BP (7,10/8,9)-tetrol[f]	(*R*)-DNBPG-C	30	20.9 (7*S*,8*R*,9*S*,10*R*)	22.1 (7*R*,8*S*,9*R*,10*S*)	0.4
	(*S*)-DNBL-C	30	20.7 (7*S*,8*R*,9*S*,10*R*)	23.2 (7*R*,8*S*,9*R*,10*S*)	0.7
BP 10-MeO,7,8,9-triol	(*R*)-DNBPG-C	30	10.8 (7*S*,8*R*,9*R*,10*S*)	11.1 (7*R*,8*S*,9*S*,10*R*)	0.3
(7/8,9,10), minor		20	20.4 (7*S*,8*R*,9*R*,10*S*)	21.1 (7*R*,8*S*,9*S*,10*R*)	0.5
	(*S*)-DNBL-C	30	9.7 (7*S*,8*R*,9*R*,10*S*)	9.9 (7*R*,8*S*,9*S*,10*R*)	0.2
		20	17.7 (7*S*,8*R*,9*R*,10*S*)	18.2 (7*R*,8*S*,9*S*,10*R*)	0.3
BP (7/8,9,10)-tetrol[f]	(*R*)-DNBPG-C	30	17.4 (7*S*,8*R*,9*S*,10*S*)	17.9 (7*R*,8*S*,9*R*,10*R*)	0.3
	(*S*)-DNBL-C	30	17.5	17.5	0
From BP 7,8-diol-syn-9,10-epoxide:					
BP 10-MeO-7,8,9-triol	(*R*)-DNBPG-C	30	9.8	9.8	0
(7,9,10/8), major		20	17.9	17.9	0
	(*S*)-DNBL-C	30	5.7	5.7	0
		20	9.8 (7*S*,8*R*,9*S*,10*R*)	10.0 (7*R*,8*S*,9*R*,10*S*)	0.2
		15	14.9 (7*S*,8*R*,9*S*,10*R*)	15.2 (7*R*,8*S*,9*R*,10*S*)	0.4
		10	27.5 (7*S*,8*R*,9*S*,10*R*)	28.3 (7*R*,8*S*,9*R*,10*S*)	0.7
BP (7,9,10/8)-tetrol[f]	(*R*)-DNBPG-C	30	29.4 (7*R*,8*S*,9*S*,10*S*)	34.2 (7*S*,8*R*,9*R*,10*R*)	1.0
	(*S*)-DNBL-C	30	32.9 (7*R*,8*S*,9*S*,10*S*)	35.4 (7*S*,8*R*,9*R*,10*R*)	0.3
BP 10-MeO-7,8,9,-triol	(*R*)-DNBPG-C	30	27.3 (7*S*,8*R*,9*S*,10*S*)	29.7 (7*R*,8*S*,9*R*,10*R*)	0.6
(7,9/8,10), minor	(*S*)-DNBL-C	30	9.6 (7*R*,8*S*,9*R*,10*R*)	10.0 (7*S*,8*R*,9*S*,10*S*)	0.6
		20	17.7 (7*R*,8*S*,9*R*,10*R*)	18.5 (7*S*,8*R*,9*S*,10*S*)	0.7
BP (7,9/8,10)-tetrol[f]	(*R*)-DNBPG-C	30	20.6 (7*S*,8*R*,9*R*,10*S*)	22.4 (7*R*,8*S*,9*S*,10*R*)	0.7
	(*S*)-DNBL-C	30	28.6	28.6	0
From BP 9,10-diol-anti-7,8-epoxide:					
BP 7-MeO-8,9,10-triol	(*R*)-DNBPG-C	30	10.8	10.8	0
(7,10/8,9), major		20	21.0	21.0	0
	(*S*)-DNBL-C	30	6.2 (7*S*,8*S*,9*S*,10*R*)	6.5 (7*R*,8*R*,9*R*,10*S*)	0.6
		20	11.7 (7*S*,8*S*,9*S*,10*R*)	12.2 (7*R*,8*R*,9*R*,10*S*)	0.9
		15	20.8 (7*S*,8*S*,9*S*,10*R*)	21.9 (7*R*,8*R*,9*R*,10*S*)	1.3
BP 7-MeO-8,9,10-triol	(*R*)-DNBPG-C	30	10.2 (7*S*,8*R*,9*R*,10*S*)	10.7 (7*R*,8*S*,9*S*,10*R*)	0.5
(7,8,9/10), minor		20	19.9 (7*S*,8*R*,9*R*,10*S*)	21.0 (7*R*,8*S*,9*S*,10*R*)	0.8
	(*S*)-DNBL-C	30	6.0	6.0	0
		20	11.4	11.4	0
		15	18.5	18.5	0

[a] Relative configuration for stereoisomers is designated as described in Fig. 3. MeO abbreviates for the methoxy group.

[b] CSPs are described in Experimental section.

[c] Percent of solvent A [ethanol–acetonitrile, 2:1 (v/v)] in hexane at a flow-rate of 2 ml/min and a void volume of 2.4 ml.

[d] Enantiomers are designated 1 and 2 according to elution order.

[e] RV = resolution value = $2\,(V_2 - V_1)/(W_2 + W_1)$, where V is retention volume and W is peak width at base.

[f] Data taken from ref. 5 for ready comparison.

when ionically bonded CSPs are used. Mobile phase of high polarity can be used with covalently bonded CSPs.

An approach to improve enantiomeric separation is to reduce the polarity of analytes by blocking polar groups via derivatization, thereby reducing the polarity of mobile phase and possibly increasing the efficiency of resolution. Derivatization of dihydrodiol derivatives of PAH's to O-methyl ethers, for example, has been shown to improve enantiomeric separation [13,14]. In this report, we compared the enantiomeric separation of highly polar derivatives of PAHs including tetrols, triols, triol-hydroxyethylthioethers, and methoxy-triols. All of these compounds were derived from BP diol-epoxides either by reduction with $NaBH_4$ or by reaction with nucleophiles such as water, CH_3O^-, and $HOC_2H_4S^-$.

Enantiomeric pairs of all triolic derivatives were separated with varying efficiency (resolution values 0–2.7) by one or both of the two covalent CSPs utilized (Tables I–III). Elution order of an enantiomeric pair, when resolved, may either be the same or different, depending on the compound. There is no apparent rule for predicting the elution order of enantiomers on any particular CSP column. Overall, the (*S*)-DNBL-C provided better resolution than the (*R*)-DNBPG-C. For example (Fig. 5), with identical mobile phase, the enantiomers of 7,8,9-triol-10-hydroxyethylthioether with a 7,10/8,9 relative stereochemistry are more efficiently separated on the (*S*)-DNBL-C than on the (*R*)-DNBPG-C.

The effects of substituents at C10 position of the triolic derivatives under study on the retention and enantiomeric resolution can be seen by the results obtained with derivatives (with a 7,10/8,9 relative stereochemistry) obtained from BP 7,8-diol-*anti*-9,10-epoxide (Fig. 6). The results were obtained by using 30% solvent A in hexane at a flow-rate of 2 ml/min on a (*S*)-DNBL-C column. The relative retention time of the more strongly retained enantiomer decreases depending on the structure of the C10 substituent: OH (23.2 min) >> H (13.5 min) >> OCH_3 (7.3 min) > SC_2H_4OH (7.2 min) (Fig. 6). This decrease in retention time (hence a decrease in polarity) is accompanied with an increased efficiency in the resolution of enantiomers

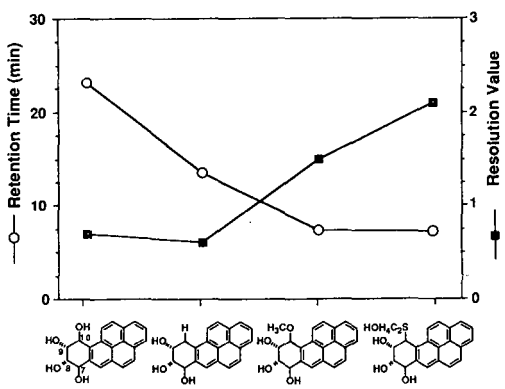

Fig. 6. Effects of substituent at C10 position of BP triolic derivatives on the retention and enantiomeric resolution on (*S*)-DNBL-C column. Samples were obtained as derivatives of BP 7,8-diol-*anti*-9,10-epoxide, isolated by reversed-phase HPLC, and resolved on (*S*)-DNBL-C using 30% of ethanol–acetonitrile (2:1, v/v) in hexane at a flow-rate of 2 ml/min. Data are taken from Tables I–III.

(Fig. 6). The C10 position is in the sterically crowded bay region. Any substituent at C10 adopts a quasiaxial conformation. It appears that the larger the quasiaxial substituent at C10 the better is the resolution of enantiomers on the (*S*)-DNBL-C column. Compared to tetrols, methoxy-triols are lower in polarity and the enantiomeric pairs are more efficiently resolved (Table III).

In conclusion, blocking one of the hydroxyl groups in BP 7,8,9,10-tetrols decreases retention time and increases enantiomeric resolution when compared to tetrol derivatives on Pirkle's covalently bonded CSPs. Changes in the retention and resolution are related to size and polarity of the substituent with the greatest changes noted in the bay region. The use of enantiomeric diol-epoxide enantiomers prior to derivatization has allowed elucidation of the absolute configurations of most of the triolic enantiomers.

ACKNOWLEDGEMENTS

This work was supported by Uniformed Services University of the Health Sciences Protocol RO7502 and U.S. Public Health Service grant CA29133. The opinions or assertions contained herein are the private ones of the authors and are not to be construed as official or reflecting the views of the Department of Defense or the Uniformed Services University of the Health Sciences.

REFERENCES

1 A. H. Conney, *Cancer Res.*, 42 (1982) 4875.
2 S. K. Yang, D. W. McCourt, J. C. Leutz and H. V. Gelboin, *Science (Washington, D.C.)*, 196 (1977) 1199.
3 S. K. Yang and H. V. Gelboin, *Cancer Res.*, 36 (1976) 4185.
4 S. K. Yang, D. W. McCourt, H. V. Gelboin, R. Miller and P. P. Roller, *J. Am. Chem. Soc.*, 99 (1977) 5124.
5 H. B. Weems and S. K. Yang, *Chirality*, 1 (1989) 276.
6 H. B. Weems and S. K. Yang, *Anal. Biochem.*, 125 (1982) 156.
7 W. H. Pirkle, J. M. Finn, B. C. Hamper, J. Screiner and J. R. Pribish, in E. L. Iliel and S. Otsuka (Editors), *Asymmetric Reactions and Processes in Chemistry*, (*ACS Symposium Series*, No. 185), American Chemical Society, Washington, DC, 1982, pp. 245–260.
8 S. K. Yang, H. B. Weems, M. Mushtaq and P. P. Fu, *J. Chromatogr.*, 316 (1984) 569.
9 S. K. Yang, H. B. Weems and M. Mushtaq, in B. Holmstedt, H. Frank, B. Testa (Editors), *Chirality and Biological Activity*, Alan Liss, New York, 1990, pp. 81–109; and references cited therein.
10 F. A. Beland and R. G. Harvey, *J. Chem. Soc., Chem. Commun.*, (1976) 84.
11 D. P. Michaud, S. C. Gupta, D. L. Whalen, J. M. Sayer and D. M. Jerina, *Chem. Biol. Interact.*, 44 (1983) 41.
12 M. C. MacLeod and L. Lew, *Carcinogenesis*, 9 (1988) 2133.
13 H. B. Weems, M. Mushtaq and S. K. Yang, *Anal. Chem.*, 59 (1987) 2679.
14 S. K. Yang, M. Mushtaq, Z. Bao, H. B. Weems, M. Shou and X-L. Lu, *J. Chromatogr.*, 461 (1989) 377.

Journal of Chromatography, 535 (1990) 255–261
Elsevier Science Publishers B.V., Amsterdam

CHROMSYMP. 2035

Assay of hydroxyfarrerol in biological fluids

A. MARZO*, E. ARRIGONI MARTELLI and G. BRUNO
Drug Metabolism and Pharmacokinetic Department, Sigma-Tau SpA, Via Pontina, km. 30.400, 00040 Pomezia, Rome (Italy)
and
E. M. MARTINELLI and G. PIFFERI
Research and Development Laboratories, Inverni della Beffa, Via Ripamonti 99, 22100 Milan (Italy)

ABSTRACT

A high-performance liquid chromatographic method for the determination of hydroxyfarrerol (IdB 1031) in biological samples was developed. IdB 1031 was first extracted by liquid–solid partition and the extracts were evaporated and analysed on a reversed-phase column under isocratic conditions, using either an electrochemical or a UV detector. The detection limit was *ca.* 5 ng/ml. Preliminary pharmacokinetic data showed that rats treated orally with 500 mg/kg had an average peak plasma concentration (C_{max}) of 497 ng/ml after 2 h.

INTRODUCTION

In previous pharmacological investigations, (±)-3-hydroxyfarrerol (IdB 1031) was found to possess interesting mucokinetic properties [1]. For pharmacokinetic studies of IdB 1031, a high-performance liquid chromatographic (HPLC) method was developed and validated for quantitative assays in biological fluids.

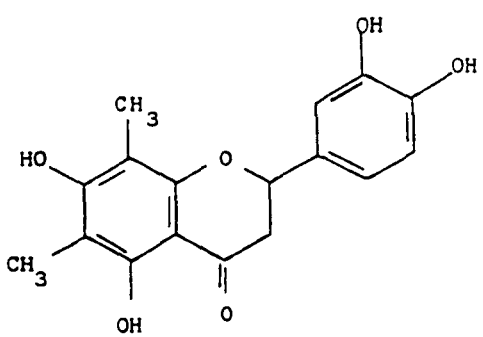

IdB 1031

0021-9673/90/$03.50

Like other structurally related flavonoids, IdB 1031 can be easily extracted from plasma by liquid–solid partition, using methanol as extraction solvent, and determined by reversed-phase HPLC with eluents buffered to pH 2–3 with phosphoric acid [2–4]. The presence and the amounts of acetonitrile, methanol and 2-propanol in the eluent markedly influence the shape of the peak, the retention time and the selectivity for this kind of compound.

EXPERIMENTAL

Materials

IdB 1031 Lot 1/30 (Inverni della Beffa, Milan, Italy) was used as a reference product. Eriodictyol from Extrasynthèse (Genay, France) and naringenin from Aldrich (Steinheim, F.R.G.) respectively were used as internal standards, for electrochemical (ED) and UV detection. HPLC-grade solvents used for the preparation of samples and chromatographic eluents (methanol, acetonitrile, water, 2-propanol) were purchased from Merck (Bracco, Milan, Italy).

The liquid chromatograph consisted of a Millipore–Waters (Milford, MA, U.S.A.) Model 510 pump controlled by a Model 680 programmer equipped with an additional pulse damper, a Rheodyne (Calabasas, CA, U.S.A.) Model 7125 injector, an ESA Model 5100A two-cell electrochemical detector (Environmental Sciences, Bedford, MA, U.S.A.), a Varian (Sunnyvale, CA, U.S.A.) Model 2050 variable-wavelength UV detector and an HP 3390 integrator–recorder (Hewlett-Packard, Avondale, PA, U.S.A.). Data were analysed with an Apple II plus personal computer (Apple Computer, Cupertino, CA, U.S.A.).

The solid-phase extraction was carried out with Sep-Pak C_{18} (Waters Assoc., Milford, MA, U.S.A.).

Preparation of reference solutions

A stock solution (0.25 mg/ml) of internal standard was prepared by dissolving eriodictyol or naringenin in methanol containing phosphoric acid (0.5%, v/v). The solutions for the assay of IdB 1031 were prepared as follows: IdB 1031 (25 mg) was dissolved in methanol (100 ml) containing phosphoric acid (0.5%, v/v) (solution A). Solution A (1 ml) was diluted to 50 ml with the same solvent (solution B). Solution A (1 ml) and internal standard stock solution (1 ml) were diluted to 50 ml with the HPLC eluent. Thus, a solution containing 5 μg/ml of IdB 1031 and 5 μg/ml of internal standard was obtained. Solution B (5 ml) and internal standard stock solution (1 ml) were diluted to 50 ml with the HPLC eluent. Thus, a solution containing 0.5 μg/ml of IdB 1031 was obtained. The internal standard solution used for sample preparation was obtained by diluting the stock solution (1 ml) to 20 ml with water.

Sample preparation

The extraction of plasma was carried out as follows. Internal standard (40 μl, corresponding to 0.5 μg of product) and water (1 ml), containing phosphoric acid (0.5%, v/v), were added to 0.5 ml of plasma. After mixing on a vortex mixer, this suspension was loaded onto a Sep-Pak C_{18} cartridge, previously equilibrated with methanol (2 ml), water (5 ml) and water containing 0.5% (v/v) phosphoric acid (0.5 ml). After elution of the plasma suspension, the cartridge was washed with 1 ml of

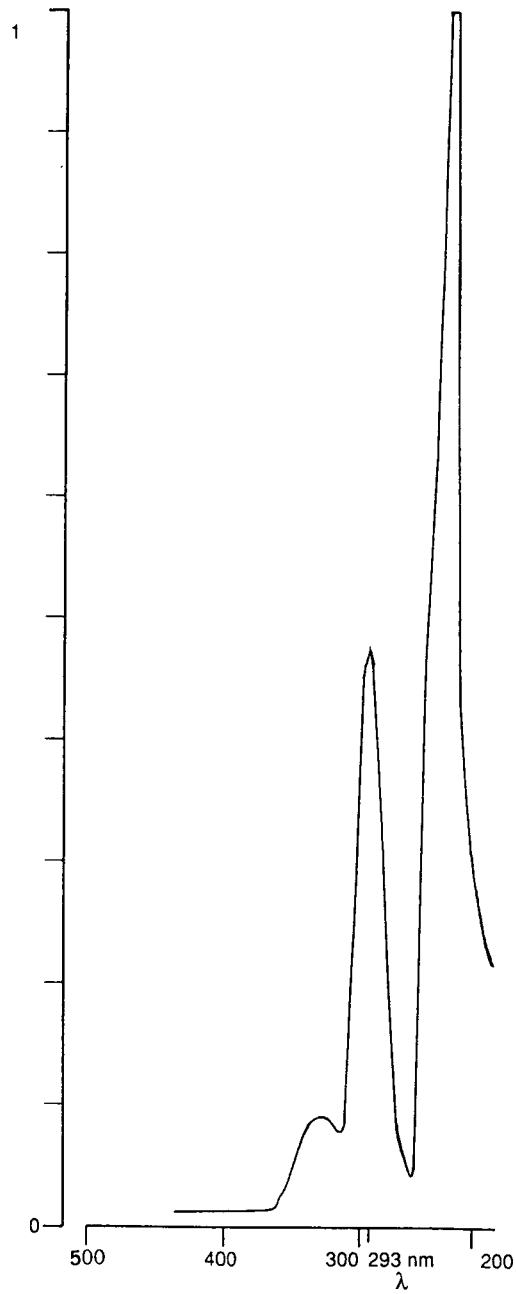

Fig. 1. UV spectrum of IdB 1031. Scan, 500–190 nm; scan rate, 100 nm/min; chart speed, 2 cm/min; λ_{max}, 293 nm; absorbance, 0.494; $E^{1\%}_{1\ cm}$, 617; ε, 19 500 l/mol · cm.

water, containing 0.5% (v/v) phosphoric acid, and then with 0.5 ml of methanol in order to remove the water absorbed by the stationary phase. The eluates were discarded and the cartridge was washed with 0.5-ml portions of methanol twice. The eluates were collected and concentrated to a small volume at 40°C under a gentle stream of nitrogen. The residue was resuspended in 100 μl of the HPLC eluent and filtered through filters of 0.45-μm porosity.

Chromatographic conditions

The UV spectrum of IdB 1031 in methanol showed λ_{max} = 293 nm with ε = 19 500 l/mol · cm (Fig. 1). The presence of a catechol moiety makes the molecule electrochemically active and oxidizable at a low potential (0.3 V *vs.* H_2/H^+), so both ED and UV detection can be performed on this molecule.

The eluent was prepared by mixing 30 volumes of acetonitrile, 8 volumes of 2-propanol and 62 volumes of water. Phosphoric acid (2 ml/l) was added and the pH was adjusted to 2.5 with a few drops of 1 *M* sodium hydroxide solution. The column (250 mm × 4.6 mm I.D.) was packed with Nucleosil C_8 (5 μm) (Macherey, Nagel & Co., Düren, F.R.G.). The flow-rate was 0.6 ml/min. The electrochemical detector was set to a potential of +0.01 V in the first cell (used as background noise filter) and to 0.30 V in the second cell. The UV detector was set at 293 nm. The retention times of eriodictyol, naringerin and IdB 1031 were 7, 8.5 and 10 min, respectively.

Treatment schedule

IdB 1031 was administered by gastric gavage to rats fasted for 18 h at 500 mg/kg.

TABLE I

LIQUID–SOLID EXTRACTION RECOVERY OF IdB 1031 FROM RAT PLASMA

UV detection was used, although ED detection gave identical results.

IdB 1031 added (= x)[a] (ng/ml)	IdB 1031 recovered (= y)[a] (ng/ml)	Recovery (%)
10	10.343	103.4
	9.328	93.3
25	17.781	71.3
	18.317	73.3
50	47.222	94.4
	47.175	94.3
100	80.682	80.7
	87.944	94.4
300	243.815	81.3
	259.872	86.6
500	441.269	88.2
	430.118	86.0
Mean:		87.3
S.D.:		9.44
R.S.D. (%):		10.81

[a] Linear correlation gave the relationship $y = -0.880 + 0.865x$ ($r^2 = 0.9986$).

Animals, divided into eight per group, were killed before and 0.25, 0.5, 1, 2, 4, 6, 8, 24 and 48 h after treatment; heparinized blood was collected and the resulting plasma was immediately separated and processed as described above.

RESULTS AND DISCUSSION

The results obtained led to the conclusion that IdB 1031 can be evaluated by HPLC by using both ED and UV detection with standards enabling the assay to be performed in biological samples.

Owing to its structure (it is a weakly acidic compound), IdB 1031 can be extracted from previously acidified plasma by liquid–solid partition, with a mean recovery of about 87% (Table I). HPLC can be carried out on reversed-phase columns with a mobile phase buffered to pH 2.5 with phosphoric acid (Fig. 2). Good results are obtained if IdB 1031 is dissolved in aqueous–alcoholic solutions, acidified to pH 2–3 in which it is fairly stable. The extraction recovery was linear in the range 10–500 ng/ml in plasma with both ED and UV detection. The reproducibility, expressed as relative standard deviation (R.S.D.), was 6.05% with ED and 10.81% with UV detection. The lowest detectable concentration was 5 ng/ml with both detection methods. Both methods seem to be equivalent for pharmacokinetic purposes, even though ED allows a better signal-to-noise ratio to be achieved.

Data for IdB 1031 plasma levels in rats after a single oral dose (500 mg/kg) indicate rapid absorption (t_{max} = 2 h), followed first by a fast and then by a slower elimination phase. The peak concentration (C_{max}) was, on average, 497 ng/ml (Fig. 3). HPLC recordings also revealed the presence of two unknown peaks, possibly corresponding to two metabolites (M_1, M_2) (Fig. 4).

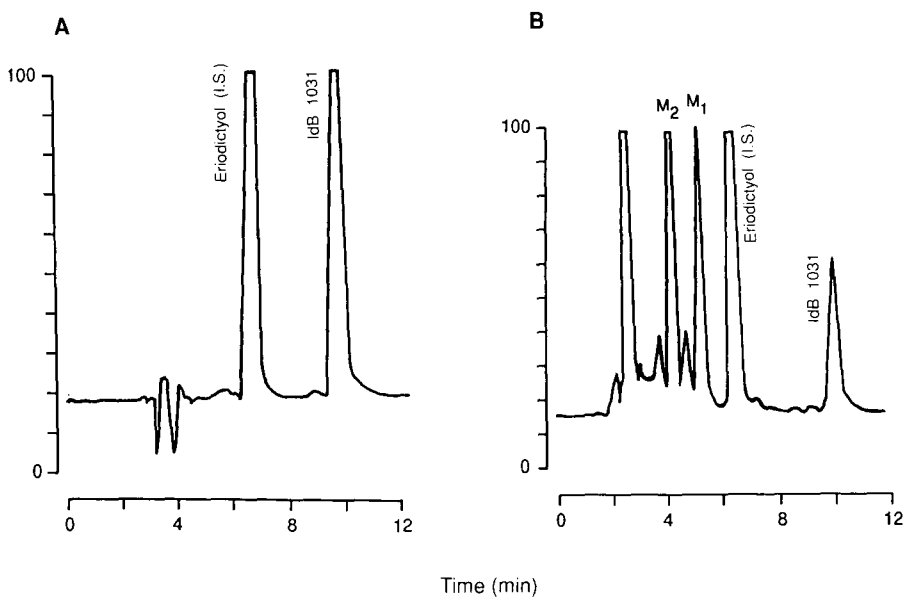

Fig. 2. Typical HPLC recordings obtained with ED. (A) IdB 1031 and eriodictyol as authentic standards. (B) Rat plasma 2 h after oral administration of IdB 1031 (500 mg/kg).

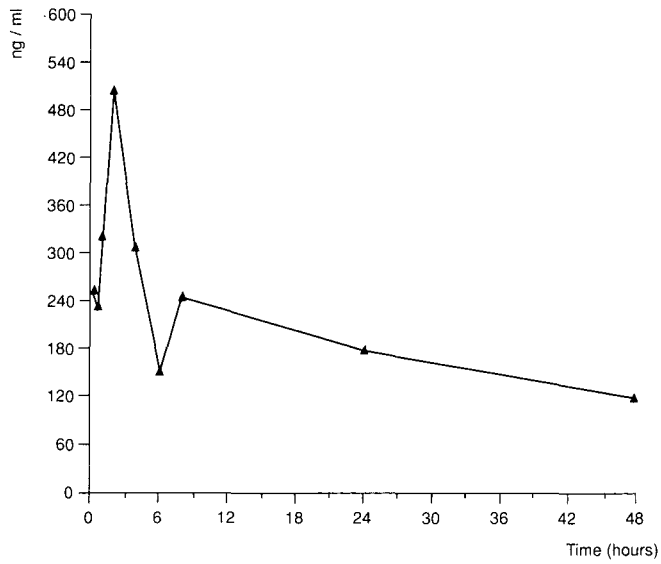

Fig. 3. Mean plasma levels (n = 8) of IdB 1031 in rats after oral administration (500 mg/kg) of IdB 1031. The standard deviations were on average 66% of the mean value, ranging from 50 to 80%.

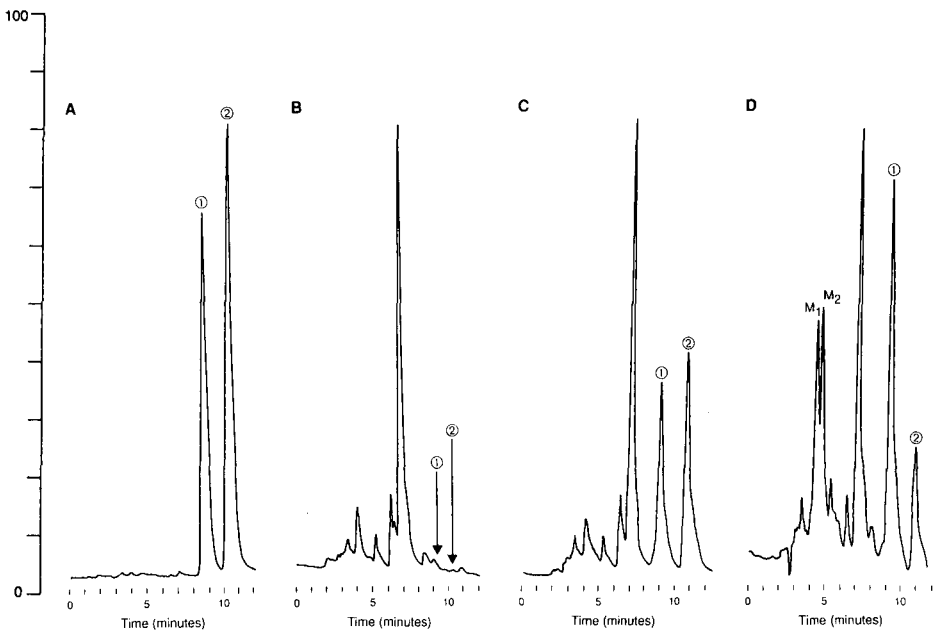

Fig. 4. Chromatograms showing the separation between IdB 1031 and naringenin. (A) Standard solution; (B) blank plasma; (C) plasma spiked with IdB 1031 and naringenin; (D) plasma sample after oral administration of IdB 1031 (500 mg/kg) to rats. UV detection, 293 nm. Peaks: 1 = naringenin; 2 = IdB 1031; M_1, M_2 = unknown metabolites.

REFERENCES

1 M. Conti and M. J. Magistretti, *Pharmacol. Res.*, 22 (1990) 122 (Suppl. 2); *Eur. Pat.*, 0 122 053 (1989).
2 D. J. Daigle and E. J. Conkerton, *J. Chromatogr.*, 240 (1982) 202.
3 K. V. Casteele, H. Geiger and C. F. Van Sumere, *J. Chromatogr.*, 240 (1982) 81.
4 D. J. Daigle and E. J. Conkerton, *J. Liq. Chromatogr.*, 6 (1983) 105.

Journal of Chromatography, 535 (1990) 263–269
Elsevier Science Publishers B.V., Amsterdam

CHROMSYMP. 2051

Determination of saterinone enantiomers in plasma samples with an internal standard using a Chiralcel OD column, fractionation and reversed-phase chromatography

MARTIN RUDOLPH*, DAGMAR VOLK and GERHARD SCHMIEDEL
Pharmaceutical Development, Beiersdorf AG, Unnastrasse 48, D-2000 Hamburg 20 (F.R.G.)

ABSTRACT

A specific and validated high-performance liquid chromatographic method was developed for the determination of the *S*-(−) and *R*-(+) enantiomers of saterinone, 1-[(4-cyano-1,2-dihydro-6-methyl-2-oxopyridin-5-yl)phenoxyl]-3-[4-(2-methoxyphenyl)piperazin-1-yl]propan-2-ol, in plasma at the low ng/ml level. The enantiomers of saterinone and an internal standard, 1-[(4-cyano-1,2-dihydro-6-methyl-2-oxopyridin-5-yl)phenoxy]-3-[4-(2-ethoxyphenyl)piperazin-1-yl]propan-2-ol, were chromatographed on a chiral Chiralcel OD stationary phase. However, the *S*-(−) enantiomers of saterinone and the internal standard were unresolved, as were the *R*-(+) enantiomers of both substances. Therefore, the two fractions were collected and each was separately resolved on an achiral Polyencap A reversed-phase column and quantified. The detection limit was 0.5 ng/ml of enantiomer, allowing the determination of plasma levels up to 36 h after oral administration of 90, 150 and 180 mg of saterinone to twelve subjects.

INTRODUCTION

Saterinone, 1-[(4-cyano-1,2-dihydro-6-methyl-2-oxopyridin-5-yl)phenoxy]-3-[4-(2-methoxyphenyl)piperazin-1-yl]propan-2-ol (A, Fig. 1), is a drug for the treatment of chronic cardiac insufficiency and is administered as the racemate in clinical studies.

To investigate the equivalence of the saterinone enantiomers *in vivo*, a sensitive method is needed to determine plasma levels of the two enantiomers down to the low

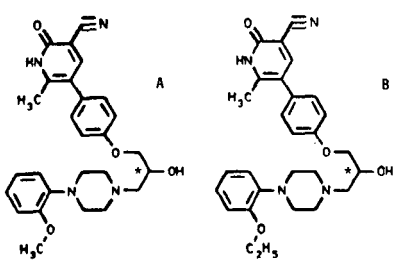

Fig. 1. Structures of (A) saterinone and (B) the internal standard.

0021-9673/90/$03.50

ng/ml level. The determination of racemic saterinone in biological fluids and its direct chromatographic resolution for the determination of the enantiomeric purity of synthesized bulk drugs have been accomplished recently in our laboratory [1,2].

In this paper, a high-performance liquid chromatographic (HPLC) method for the determination of the *S*-(−) (**I**) and *R*-(+) (**II**) enantiomers of saterinone in plasma samples after oral administration of the racemate is described and validated. The pharmacokinetic parameters of the results are presented.

EXPERIMENTAL

Plasma samples

Twelve healthy male subjects, aged 18–40 years, received single oral dose of 90, 150 and 180 mg (3, 5 or 6 tablets, respectively, each containing 30 mg) of saterinone. The medication was administered to the subjects 1 h after breakfast. Plasma samples were collected 0 (prior to administration), 0.25, 0.5, 0.75, 1, 1.5, 2, 3, 4, 6, 8, 10, 12, 14, 24 and 36 h after administration. All samples were stored in a refrigerator at −85°C until analysed.

Reagents

Perchloric acid (70%), 1 *M* sodium hydroxide solution and methanol of analytical-reagent grade (E. Merck, Darmstadt, F.R.G.) and water purified on a Bion exchanger (Pierce, Rodgau, F.R.G.) were used. *S*-(−)-Saterinone (BDF 9147, CH 1564), *R*-(+)-saterinone (BDF 9144, CH 1516), racemic saterinone (BDF 8634, G 884.2) and the internal standard, 1-[(4-cyano-1,2-dihydro-6-methyl-2-oxopyridin-5-yl)phenoxy]-3-[4-(2-methoxyphenyl)piperazin-1-yl]propan-2-ol (BDF 8803 · H_2O · HCl, Roe 956), were synthesized in our Chemical Department.

Equipment

Screw-capped glass vessels (12 ml) with PTFE gaskets from Schott (Mainz, F.R.G.), a vortex Reax-2000 mixer from Heidolph (Kelheim, F.R.G.), a vortex evaporator from Haake–Buchler (Saddle River, NJ, U.S.A.) and an F3 circulation thermostat from Haake Mess-Technik (Karlsruhe, F.R.G.) were used.

Apparatus and HPLC conditions

The HPLC system for the enantiomeric separation consisted of a Model L-6000 pump, a Model F-1000 fluorimeter and a Model D-2500 integrator, all from Merck–Hitachi (E. Merck). The samples were injected with a WISP autosampler (Waters Assoc., Eschborn, F.R.G.) and collected with a Model 202 fraction collector (Abimed, Langenfeld, F.R.G.). A Chiralcel OD (10 μm) column (250 × 4.6 mm I.D.) (Daicel, Tokyo, Japan) with a 0.5-μm eluent filter was used. The column temperature was set to 26 ± 1°C. The eluent was methanol at a flow-rate of 0.5 ml/min. The injection volume was 75 μl.

The fluorimeter was set at an excitation wavelength of 345 nm and an emission wavelength of 435 nm.

Quantification was carried out by using the HPLC system described previously [1]. A Polyencap A (5 μm) column (125 × 4 mm I.D.) (Bischoff Analysentechnik, Leonberg, F.R.G.) with a 20-mm Spherisorb ODS II (5 μm) precolumn was used. The

mobile phase consisted of 1.92 g of sodium 1-pentanesulphonate, 500 ml of water, 300 ml of 0.01 *M* perchloric acid, 300 ml of acetonitrile and 50 ml of tetrahydrofuran. The solution was mixed and filtered through a 0.2-μm PTFE membrane before use. The flow-rate was 0.75 ml/min, the injection volume was 50 μl and the retention times were 3.1 min for **I** and 4.4 min for **II**.

Analytical procedure

To 1 ml of plasma in a screw-capped glass vessel, 50 μl of 1 *M* sodium hydroxide solution were added and extracted with 3 ml of dichloromethane for 15 min. The mixture was centrifuged (2850 *g* for 10 min) and the lower organic phase was transferred to another screw-capped glass vessel and evaporated to dryness. The residue was dissolved in 100 μl of methanol, transferred to an autosampler vial and 75 μl were injected into the HPLC system for fractionation. The two fractions were collected and evaporated to dryness. The residue was dissolved in 75 μl of mobile phase and 50 μl were transferred to an autosampler vial and injected automatically for quantification.

RESULTS AND DISCUSSION

Reproducibility

The day-to-day reproducibility was verified by preparing four calibration graphs. Two analyses were performed for each concentration. No significant difference between the slopes of the four graphs from **I** and **II** was obtained (confidence interval 99% [3]). The results are presented in Table I and show that the method is reproducible.

Linearity

A concentration range of 1.5–50 ng/ml was chosen for the spiked plasma samples, with individual concentrations of 1.5, 2.5, 5, 12.5, 25 and 50 ng/ml each of **I** and **II**. Each analysis was performed four times. The parameters for the resulting

TABLE I

REPRODUCIBILITY OF THE DETERMINATION OF SATERINONE ENANTIOMERS IN PLASMA

Each result is the mean of two determinations.

Enantiomer	Date	Slope	Intercept on ordinate	Correlation coefficient
I	08/08/89	19.06	0.40	0.999
	09/08/89	19.16	0.64	0.998
	30/08/89	20.06	0.02	0.998
	31/08/89	19.58	0.40	0.999
II	08/08/89	19.39	0.77	0.999
	09/08/89	20.22	0.36	0.997
	30/08/89	20.05	0.31	0.999
	31/08/89	19.00	0.99	0.998

TABLE II

ACCURACY AND LINEARITY OF THE DETERMINATION OF SATERINONE ENANTIOMERS IN PLASMA

Each result is the mean of four determinations.

Concentration added (ng/ml)	Concentration found (ng/ml)		Deviation from amount added (%)	
	I	II	I	II
1.5	1.70	1.77	+13.3	+18.1
2.5	2.22	2.60	−11.2	+4.0
5.0	4.54	4.21	−9.2	−15.8
12.5	13.18	12.90	+5.4	+3.2
25.0	15.50	26.01	+2.0	+4.0
50.0	49.56	49.36	−0.9	−1.3
		x_{median}	+0.6	+3.6

Parameter	I	II
Intercept on ordinate	0.32	0.48
Slope	19.48	19.71
Correlation coefficient	0.999	0.999

calibration graphs are given in Table II. The calibration graphs were linear for the chosen concentration range.

Accuracy

The data for accuracy were calculated following the requirements given previously [1] and are given in Table II. Four analyses were performed for each concentration. The deviations of the two lowest concentrations were relatively high compared with the others. Minor contaminations in the low concentration range caused higher absolute deviations than those at higher concentrations. However, small matrix effects seemed to be responsible for the higher deviations.

The calculated slopes were 1.003 (**I**) and 1.005 (**II**) and the deviations, x_{median}, were 0.6% (**I**) and 3.6% (**II**). The accuracy of the method was therefore confirmed.

Detection and determination limits

The above limits were calculated as described previously [1]. The detection limit of 0.5 ng/ml and the determination limit of 1.5 ng/ml are identical for both **I** and **II**.

Analytical procedure

An established method for the separation of the enantiomers in bulk drugs [2] proved to be insufficient for the sensitive determination of **I** and **II** in plasma.

To achieve higher sensitivities, the fractions of **I** and **II** were collected and concentrated, after separation on the Chiralcel OD column (Fig. 2a). By using pure methanol, there were no interferences from additives, *e.g.*, buffers or solvents with high boiling points, after gentle evaporation of the eluent. The residues were dissolved and analysed using a second HPLC unit with a reversed-phase column (Fig. 2b), following

the method for the determination of saterinone racemate in biological fluids [1]. The short retention times and sharp peaks obtained resulted in a detection limit down to 0.5 ng/ml of enantiomer in plasma.

To check the work-up procedure, a saterinone analogue with structure and physico-chemical properties both similar to those of saterinone, was chosen as internal standard (B, Fig. 1). The elution profile on the chiral phase was similar to that of saterinone. Both *S*-(−) enantiomers co-eluted and were collected in one fraction, as were the *R*-(+) enantiomers. Quantification was achieved by calculating the ratio of **I** to *S*-(−)-internal standard and of **II** to *R*-(+)-internal standard.

In contrast to preliminary studies, the column temperature was set at 26 ± 1°C in order to obtain shorter retention times with sufficient resolution. The back-pressure of the column increased after analyses of more than 900 samples. Therefore, the column was regenerated by rinsing it in the opposite direction with solvents of different polarity: methanol, methanol–propan-2-ol, propan-2-ol, propan-2-ol–*n*-hexane and *n*-hexane. After this procedure, the back-pressure and the selectivity of the column were the same as those at the beginning of the studies. To check the reproducibility

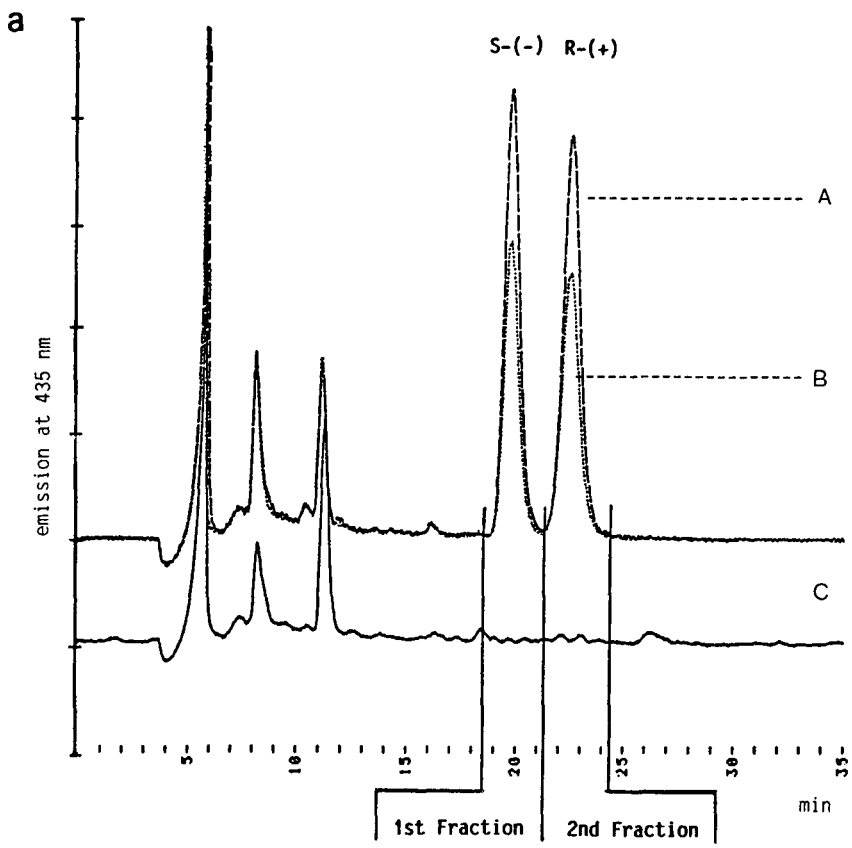

Fig. 2.

(Continued on p. 268)

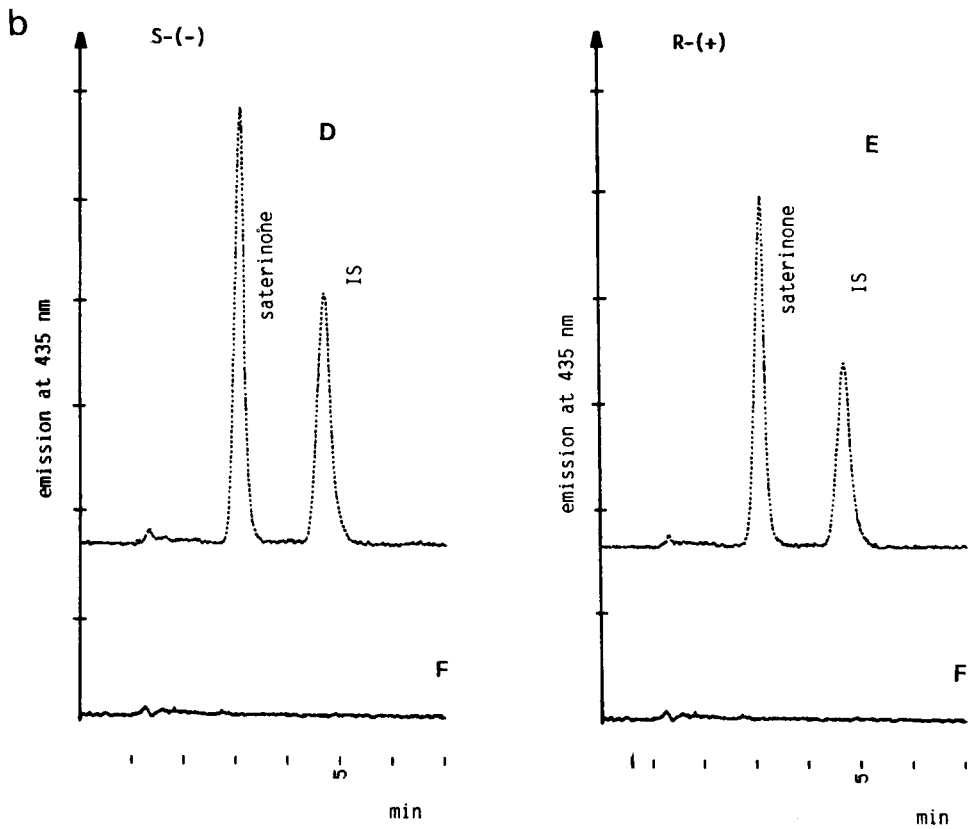

Fig. 2. (a) Chromatograms obtained by injecting 75 μl of (A) plasma sample spiked with 50 ng/ml of saterinone racemate and 50 ng/ml of internal standard, (B) plasma sample spiked with 25 ng/ml of *S*-(−) and 25 ng/ml of *R*-(+) enantiomers of the internal standard and (C) blank. Conditions: 250 mm × 4.6 mm I.D. Chiralcel OD column; eluent, methanol; flow-rate, 0.5 ml/min; temperature, 26°C. (b) Chromatograms obtained by injecting 50 μl of (D) fraction 1, 25 ng/ml of **I** and 25 ng/ml of *S*-(−) enantiomer of the internal standard [see (a)], (E) fraction 2, 25 ng/ml of **II** and 25 ng/ml of *R*-(+) enantiomer of the internal standard [see (a)] and (F) blank. Conditions: 125 mm × 4 mm I.D. reversed-phase Polyencap A column with 20 mm ODS II precolumn; flow-rate, 0.75 ml/min; eluent, 1.92 g of sodium 1-pentanesulphonate salt, 500 ml of water, 300 ml of 0.01 *M* perchloric acid, 300 ml of acetonitrile and 50 ml of tetrahydroforan.

from column to column, a second Chiralcel OD column from a different lot was used. The separation of the enantiomers was well reproduced, showing that the enantiomeric separation was reproducible.

Pharmacokinetic results

The bioequivalence of the enantiomers was studied in twelve volunteers after administration of three different oral doses (90, 150 and 180 mg of saterinone racemate). The elimination half-lives were determined according to the residual technique and the areas under the curves (AUC) were determined by using the trapezoidal rule. The pharmacokinetic results are presented in Table III.

No significant differences for the AUC (0–36 h), AUC (0–∞) and C_{max}

TABLE III

DETERMINATION OF SATERINONE ENANTIOMERS IN PLASMA: MEAN RESULT OF TWELVE DETERMINATIONS

Amount administered (mg)	Parameter	I	II	Ratio (I/II)
90	$t_{1/2}$ (h)	7.5 ± 1.8	9.2 ± 2.5	
	C_{max} (ng/ml)	65.9 ± 24.9	63.6 ± 24.7	1.04 ± 0.05
	AUC (0–t)	208.6 ± 101.8	213.3 ± 93.3	0.98 ± 0.11
	AUC (0–∞)	216.5 ± 106.9	229.8 ± 103.0	0.94 ± 0.10
150	$t_{1/2}$ (h)	7.8 ± 1.6	8.0 ± 1.7	
	C_{max} (ng/ml)	107.2 ± 38.8	106.4 ± 43.3	1.01 ± 0.04
	AUC (0–t)	505.0 ± 178.2	527.8 ± 177.8	0.96 ± 0.08
	AUC (0–∞)	526.5 ± 190.0	552.4 ± 188.6	0.95 ± 0.10
180	$t_{1/2}$ (h)	7.1 ± 1.7	7.9 ± 1.7	
	C_{max} (ng/ml)	115.8 ± 56.0	116.3 ± 54.8	1.00 ± 0.03
	AUC (0–t)	530.5 ± 162.1	573.3 ± 143.0	0.93 ± 0.13
	AUC (0–∞)	545.6 ± 165.4	600.1 ± 159.1	0.91 ± 0.15

parameters between **I** and **II** at the three dose levels were found. These results show that the *S*-(−) and *R*-(+) enantiomers of saterinone are bioequivalent after oral administration of the racemate.

CONCLUSIONS

An HPLC method for the determination of the enantiomeric purity in bulk drugs [2] was improved to determine **I** and **II** in plasma down to the low ng/ml level. The analysis were carried out by using an internal standard with similar structure and chromatographic behaviour for the enantiomeric separation to those of saterinone. The fractionation and quantification were carried out automatically to analyse approximately 40 samples per day.

Because of the low detection limit of 0.5 ng/ml, the plasma samples could be analysed up to 36 h after application. At all three dose levels the pharmacokinetic parameters (AUC 0–∞, AUC 0–t and C_{max}) of **I** and **II** were calculated and tested for their bioequivalence. The statistical evaluation [4] showed no significant differences for the parameters between **I** and **II**.

REFERENCES

1 M. Rudolph, *J. Chromatogr.*, 497 (1989) 342.
2 M. Rudolph, *J. Chromatogr.*, 525 (1990) 161.
3 K. Doerffel, *Statistik in der analytischen Chemie*, VCH, Weinheim, 4th ed., 1987.
4 R. Rettig-Zinke, *GENERICA, Software for Testing Bioequivalence, V2.2*, Coesfeld, 1990.

Journal of Chromatography, 535 (1990) 271–277
Elsevier Science Publishers B.V., Amsterdam

CHROMSYMP. 2023

Simultaneous separation and determination (in serum) of phenytoin and carbamazepine and their deuterated analogues by high-performance liquid chromatography–ultraviolet detection for tracer studies

GEORGE K. SZABO* and RICHARD J. PYLILO

Neuropharmacology Laboratory, Department of Neurology, Boston University School of Medicine, 80 E. Concord Street, Boston, MA 02118 (U.S.A.); and Neurology Service, Veterans Administration Medical Center, 150 South Huntington Avenue, Boston, MA 02130 (U.S.A.)

ROBERT J. PERCHALSKI

Research Service, Veterans Administration Medical Center, Gainesville, FL (U.S.A.)

and

THOMAS R. BROWNE

Neuropharmacology Laboratory, Department of Neurology, Boston University, School of Medicine, 80 E. Concord Street, Boston, MA 02118 (U.S.A.); and Neurology Service, Veterans Administration Medical Center, 150 South Huntington Avenue, Boston, MA 02130 (U.S.A.)

ABSTRACT

The use of stable isotope-labeled tracer compounds is the safest and most effective method to perform many steady state pharmacokinetic and drug interaction studies. We describe a method by which the heavily deuterated $^{2}H_{10}$ analogues of carbamazepine ($^{2}H_{10}$ CBZ) and phenytoin ($^{2}H_{10}$ PHT) can be chromatographically separated by high-performance liquid chromatography from unlabeled CBZ and PHT. All compounds are quantitated against an internal standard (IS) (10,11-dihydrocarbamazepine) and measured using conventional UV detection rather than mass spectrometry. Baseline resolution of extracted serum containing $^{2}H_{10}$ CBZ, CBZ, $^{2}H_{10}$ PHT, PHT and IS is achieved on a heated (55°C) 25 cm × 4.6 mm BioAnalytical Systems Phase II 5 μm ODS column with an isocratic mobile phase consisting of water–acetonitrile–tetrahydrofuran (80:16:4, v/v/v) at 1.2 ml/min. Eluting compounds were monitored at a UV wavelength of 214 nm. Calculated resolution of $^{2}H_{10}$ CBZ from CBZ and of $^{2}H_{10}$ PHT from PHT were 1.3. Serum standard curves were linear ($R \geq 0.999$) over a range of 0.5–14 μg/ml for $^{2}H_{10}$ CBZ, 0.5–20 μg/ml for CBZ, 0.5–20 μg/ml for $^{2}H_{10}$ PHT, and 0.5–30 μg/ml for PHT. Within-day percent relative standard deviations (precision) were less than 6% in all cases.

INTRODUCTION

Stable isotope-labeled (SIL) tracer methods have many demonstrated advantages over alternative methods in human pharmacokinetic and drug interaction studies [1,2]. Nevertheless, SIL tracer methods are not widely used [3], largely because of the cost and scarcity of gas chromatographic–mass spectrometry (GC–MS) equipment. Separation of a drug and its heavily deuterated analogue by capillary GC

0021-9673/90/$03.50

[4,5] and also by high-performance liquid chromatography (HPLC) [6] has been described; however, the potential of this technique has not been exploited in human tracer studies. We report a method for quantitating the concentration of unlabeled and SIL carbamazepine (CBZ) and phenytoin (PHT) in serum suitable for tracer studies using only a simple isocratic HPLC system with conventional ultraviolet (UV) detection.

EXPERIMENTAL

Instrumentation

This study employed a Waters Model 6000A solvent pump and a Model 710B WISP autosampler (Waters Assoc., Milford, MA, U.S.A.). Eluents were monitored using a Spectroflow Model SF770S variable-wavelength detector (Applied Biosystems, Ramsey, NJ, U.S.A.). Column temperature was maintained by a Model LC22A column heater (BioAnalytical Systems, West Lafayette, IN, U.S.A.). Chromatograms were recorded on a Model DB111 flatbed recorder (Kipp and Zonen, Delft, The Netherlands) and also on a Packard Bell PBVX88 computer for peak integration and quantitation using GrayMatter™ software (Binary Systems, Newton, MA, U.S.A.).

Standards and reagents

The internal standard, 10,11-dihydrocarbamazepine and 5,5-diphenylhydantoin (phenytoin) were obtained from Aldrich (Milwaukee, WI, U.S.A.). The 5H-dibenz[*b*,*f*]azepine-5-carboxamide (carbamazepine) was supplied by Sigma (St. Louis,

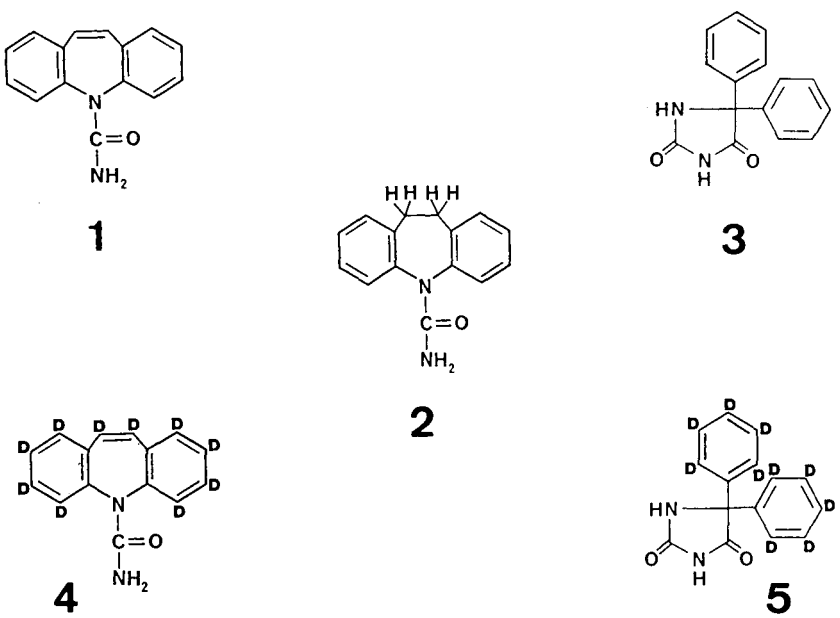

Fig. 1. Chemical structures and isotopic labeling of standards. 1 = CBZ; 2 = 10,11-dihydro-CBZ (internal standard); 3 = PHT; 4 = [$^2H_{10}$]CBZ; 5 = [$^2H_{10}$]PHT; D = deuterium.

MO, U.S.A.) and the [$^2H_{10}$]CBZ was from MSD Isotopes (Montreal, Canada). The [$^2H_{10}$]PHT was obtained from Tracer Technologies (Somerville, MA, U.S.A.). Chemical structures and isotopic labeling sites are shown in Fig. 1. HPLC-grade ethyl acetate, methylene chloride, acetonitrile, tetrahydrofuran (THF), and methanol were obtained from Fisher Scientific (Pittsburgh, PA, U.S.A.). Monobasic and dibasic potassium phosphate were obtained from Mallinckrodt (Paris, KY, U.S.A.).

Phosphate buffer (pH 6.0 $\pm$ 0.05) solution was prepared by addition of dibasic potassium phosphate (0.067 mol/l) to 750 ml of monobasic potassium phosphate (0.067 mol/l) with stirring while monitoring the pH potentiometrically. Stock analytical and internal standard solutions for CBZ, [$^2H_{10}$]CBZ, PHT, [$^2H_{10}$]PHT and 10,11-dihydro-CBZ were prepared by dissolving 10 mg of each compound in methanol and diluting to 10 ml. Methanolic working standards containing all analytes at varying concentrations for calibration and controls were prepared by dilution of stock solutions. Working internal standard solution was prepared in methanol–distilled water (1:1) at a concentration of 50 μg/ml.

Chromatographic conditions

The mobile phase consisted of HPLC-grade water–acetonitrile–THF (80:16:4, v/v/v). The separation was achieved isocratically on a BioAnalytical Systems Phase II ODS 5-μm (25 cm $\times$ 4.6 mm I.D.) stainless-steel column that was maintained at 55°C. The flow-rate was 1.2 ml/min and eluent was monitored at 214 nm with a sensitivity of 0.05 a.u.f.s.

Sample preparation

Calibrants and control samples were prepared by evaporating 1.0 ml of the various working standard solutions in 125 mm $\times$ 16 mm disposable glass culture tubes and adding 1.0 ml of drug free serum. To 1.0 ml of control or patient serum 1.0 ml of phosphate buffer (pH 6.0) and 100 μl of working internal standard were added. The tubes were swirled briefly and then extracted by adding 8.0 ml ethyl acetate and 1.0 ml methylene chloride. Samples were capped with polyethylene Tainer Tops (Fisher Scientific) and set on a horizontal shaker (Eberbach Corp., Ann Arbor, MI, U.S.A.) for 10 min at 180 cycles/min, then centrifuged at room temperature long enough to break any emulsion that may have formed. The samples were then immersed in a methanol–dry ice bath for 15 min to freeze the aqueous (lower) layer. A subsequent brief (30–45 s) centrifugation (2000 rpm) at -10°C settled any remaining frozen aqueous crystals suspended in the organic layer. Then the organic layer was decanted into a clean tube for concentration and placed on a Meyer N-VAP evaporator (Organomation, Berlin, MA, U.S.A.). After evaporation of the organic fraction under a gentle stream of air at 45°C, the residue was reconstituted with 200 μl of methanol, vortexed, and transferred to WISP autosampler vials. At this point, 15–30 μl of sample was injected on the HPLC.

RESULTS

Precision and accuracy

Each working methanolic standard had combined in it CBZ (0.5–20.0 μg/ml), [$^2H_{10}$]CBZ (0.5–14.0 μg/ml), PHT (0.5–30.0 μg/ml), and [$^2H_{10}$]PHT (0.5–20.0 μg/ml).

Three 13-point calibration curves were prepared from methanolic standard solutions and drug-free serum for determination of linearity, and within-day accuracy and precision. All samples were prepared according to the described method. Unweighted linear least squares regression analysis of peak height ratio *versus* analyte concentration was performed, and residuals were calculated. Correlation coefficients (linearity) for all four analytes were equal to or greater than 0.999. Percent relative standard deviations (precision) were less than 6% in all cases. Fig. 2 shows the calibration plots with residuals (accuracy) calculated using the method of Johnson *et al.* [7] shown as percentages for all analytes. Residuals were within 8% for CBZ and [$^2H_{10}$]CBZ, and within 4% for all concentrations greater than 1 μg/ml. The lowest concentrations of PHT and [$^2H_{10}$]PHT contributed to high negative residuals; however, all concentrations above 0.5 μg/ml had residuals less than 8%. A weighted regression analysis would probably decrease the residuals at low concentrations.

Fig. 3 shows typical chromatograms obtained under the specified experimental conditions.

DISCUSSION

Sample preparation

The freezing out extraction technique employed in this method was a modifica-

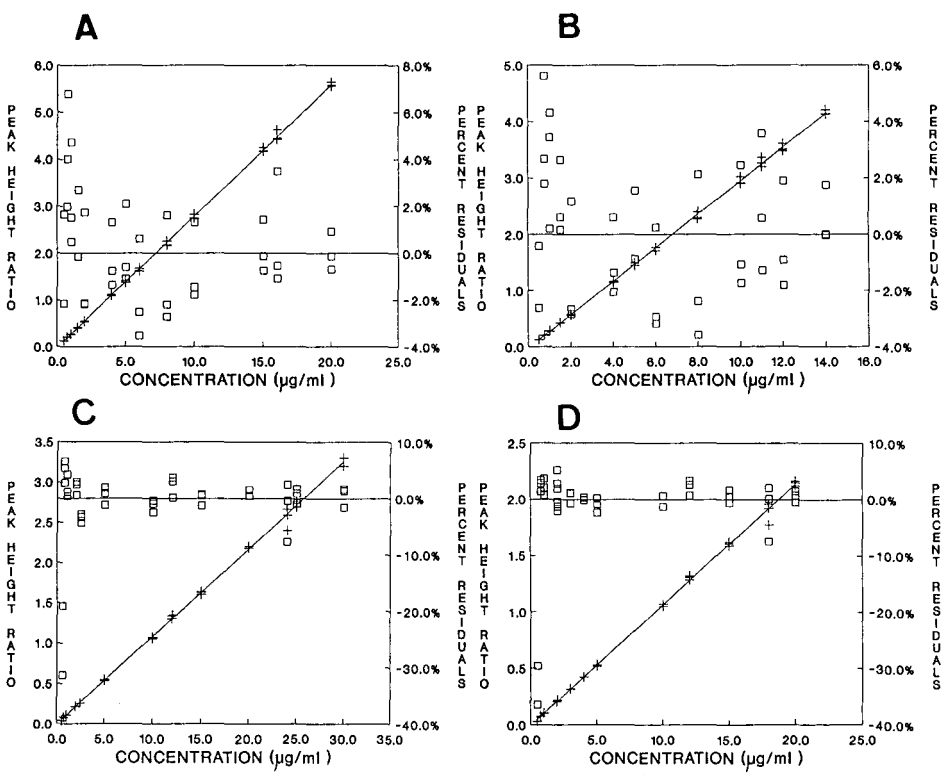

Fig. 2. Calibration plot with residuals (%) for CBZ (A), [$^2H_{10}$]CBZ (B), PHT (C) and [$^2H_{10}$]PHT (D). + = Peak height ratio; □ = residuals; ——— = regression.

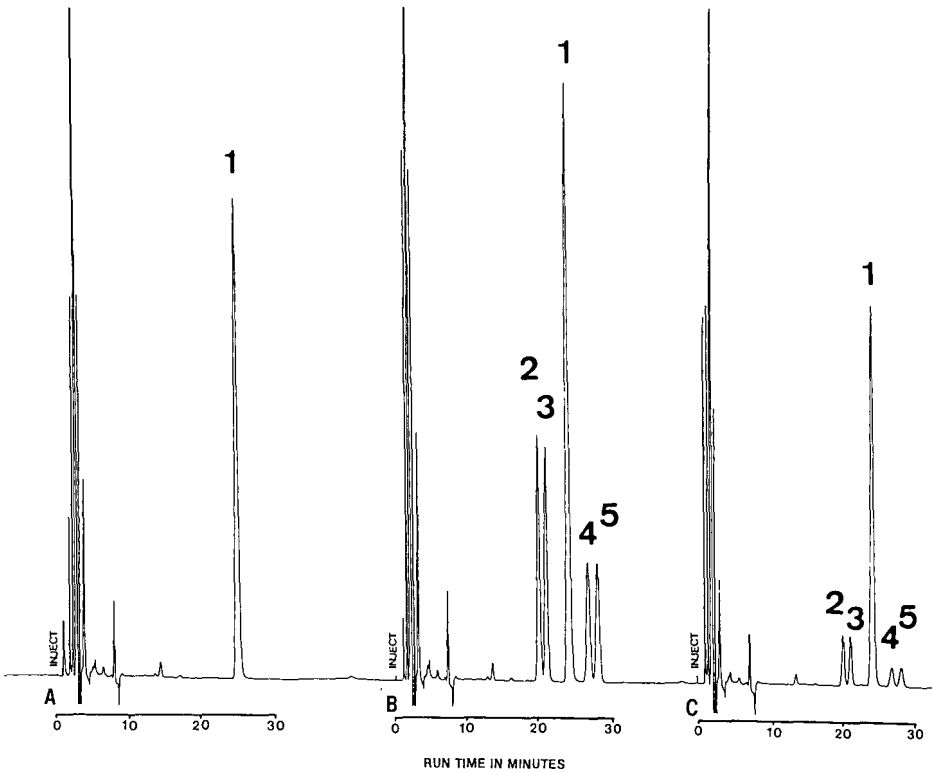

Fig. 3. Chromatograms of 15-μl injections of: blank serum containing 10,11-dihydro-CBZ (internal standard) 5.0 μg/ml (A); serum control containing [$^2H_{10}$]CBZ, CBZ 1.5 μg/ml and [$^2H_{10}$]PHT, PHT 2.0 μg/ml (B); serum calibrant containing [$^2H_{10}$]CBZ, CBZ, [$^2H_{10}$]PHT and PHT 0.5 μg/ml (C). Peaks: 1 = 10,11-di-hydro-CBZ; 2 = [$^2H_{10}$]CBZ; 3 = CBZ; 4 = [$^2H_{10}$]PHT; 5 = PHT.

tion of a procedure described by Schmidt *et al.* [8]. Their method was a multiple step hexane extraction, back extraction and re-extraction performed in a batch mode with time to freeze samples between steps in a −20°C freezer. A freezer is also applicable with this procedure; however, flash freezing in the dry ice bath is faster. The quick −10°C centrifugation step was necessary because, unlike hexane, ethyl acetate absorbs water which freezes out of solution and becomes ice crystals suspended in the organic layer. After centrifugation the dried organic fraction was quickly and easily poured off into the evaporation tube. Besides the ease and speed of not having to transfer the aqueous layer by pipetting, fast evaporation was facilitated by the removal of absorbed water.

Chromatography

On most C_{18} reversed-phase columns used for the separation of CBZ and PHT, a binary mobile phase of acetonitrile and water gives an elution order in which CBZ follows PHT. The addition of a small percentage of THF reversed the elution order since THF has a much greater effect on the retention of CBZ, and seems also to facilitate the separation of drug from its isotopomer (Fig. 3). The use of a heated

column is necessary to prevent run times from becoming too lengthy for practical applications. Total run times under the conditions described here varied from 28 to 32 min. Even though these run times seem long compared to conventional clinical HPLC assays, the ease of sample preparation (without derivatization, etc.) and use of automation makes this method a viable alternative to GC–MS procedures. Chromatographic resolution (R_s) between drugs and their isotopomers in serum controls was 1.3. Resolution [9] was defined as:

$$R_s = \frac{t_2 - t_1}{0.5(w_1 + w_2)}$$

where t_1 and t_2 are retention times of adjacent components ($t_2 > t_1$), and w_1 and w_2 are base widths of the peaks in time units.

Deuterium is the most cost-effective stable isotope to use for SIL labeling in terms of synthesis and market availability. Depending on placement of the deuterons in the drug molecule, *in vivo* or *in vitro* "isotope effects" can be negligible or profound [10–14]. Tanaka and Thornton [15] first described a mechanism for liquid chromatographic separation of labeled and unlabeled compounds based on hydrophobic interactions. It was also shown that isotope effect changes proportionately with the number of deuterons used [16]. Another way to characterize the isotope effect is as a reduction of lipophilicity [17]. As an index of lipophilicity, strong correlations have been shown between changes in partition coefficients and chromatographic retention of heavily deuterated aromatic compounds [17–19] and drugs with aromatic rings in their structures [19,20]. Absence of isotope effects of [$^2H_{10}$]PHT to PHT has been demonstrated in human pharmacokinetic studies [18–20].

CONCLUSIONS

The use of SIL compounds in pharmaceutical research has not gained universal acceptance, in part because of the cost and technical complexities associated with analytical MS. This paper describes an assay procedure for the simultaneous separation and quantitation of the two most commonly used antiepileptic drugs and their decadeuterated analogues [$^2H_{10}$]CBZ, [$^2H_{10}$]PHT) for SIL dilution studies. The freeze extraction procedure described allows for simple, rapid sample preparation and offers both a time and a cost effective alternative to mass spectrometry. Tremendous advances have been made in particle and surface chemistries yielding highly selective and efficient HPLC columns that could be used for assay of a variety of heavily deuterated pharmaceuticals. Assuming no pharmacokinetically deleterious *in vivo* isotope effect for a heavily deuterated compound is demonstrated, SIL tracer studies for pharmaceutical development, drug interaction studies and pharmacokinetic research could be conducted using HPLC without MS detection. A study of possible pharmacokinetic isotope effects of [$^2H_{10}$]CBZ and CBZ is underway. This paper is a preliminary study demonstrating the capabilities of this assay. Additional validation studies are in progress to fully characterize this method (between-day precision, absolute recovery, and limits of minimum detection).

ACKNOWLEDGEMENTS

Supported in part by the United States Veterans Administration.

REFERENCES

1 T. R. Browne, *Clin. Pharm.*, 18 (1990) 423.
2 T. R. Browne, D. J. Greenblatt, G. E. Schumacher, G. K. Szabo, J. E. Evans, B. A. Evans, R. J. Perchalski and R. J. Pylilo, in W. H. Pitlick, H. J. Kupferberg, R. H. Levy, R. J. Porter and R. H. Mattson (Editors), *Antiepileptic Drug Interactions*, Demos, New York, 1972, p. 3.
3 R. L. Wolen, in T. A. Baillie and J. R. Jones (Editors), *Synthesis and Applications of Isotopically Labeled Compounds, Proc. 3rd Int. Symp., Innsbruck, July 17–21, 1988*, Elsevier, Amsterdam, 1989, pp. 147–156.
4 D. J. Hoffman and W. R. Porter, *J. Chromatogr.*, 276 (1983) 301.
5 W. A. Van Hook, *J. Chromatogr.*, 338 (1985) 333.
6 T. K. Gerding, B. F. H. Drenth and R. A. de Zeeuw, *Anal. Biochem.*, 171 (1988) 382.
7 E. L. Johnson, D. L. Reynolds, D. S. Wright and L. A. Pachla, *J. Chromatogr. Sci.*, 26 (1988) 372.
8 J. Schmid and F.-W. Koss, *J. Chromatogr.*, 227 (1982) 71.
9 L. R. Snyder and J. J. Kirkland, *Introduction to Modern Liquid Chromatography*, Wiley, New York, 2nd ed., 1979.
10 M. I. Blake, H. L. Crespi and J. J. Katz, *J. Pharm. Sci.*, 64 (1975) 367.
11 A. Van Langenhove, *J. Clin. Pharm.*, 26 (1986) 383.
12 S. Ottoboni, P. Caldera, A. Trevor and N. Castagnoli, Jr., *J. Biol. Chem.*, 264 (1989) 13684.
13 J. P. Thenot, T. I. Ruo, G. P. Stec and A. J. Atkinson, in A. Frigerio and M. McCamish (Editors), *Recent Developments in Biochemistry and Medicine, 6*, Elsevier, Amsterdam, 1980, p. 373.
14 Y. Cherrah, J. B. Falconnet, M. Desage, J. L. Brazier, R. Zini and J. P. Tillement, *Biomed. Env. Mass Spectrom.*, 14 (1987) 653.
15 N. Tanaka and E. R. Thornton, *J. Am. Chem. Soc.*, 98 (1976) 1617.
16 N. Tanaka and E. R. Thornton, *J. Am. Chem. Soc.*, 99 (1977) 7300.
17 N. El Tayar, H. van de Waterbeemd, M. Gryllaki, B. Testa and W. F. Trager, *Int. J. Pharm.*, 19 (1984) 271.
18 I. M. Kovach and D. M. Quinn, *J. Am. Chem. Soc.*, 105 (1983) 1947.
19 G. P. Cartoni and I. Ferreti, *J. Chromatogr.*, 122 (1976) 287.
20 J. B. Falconnet, N. El Tayar, A. Bechalany, Y. Cherrah, V. Benchekroun, P. A. Carrupt, B. Testa and J. L. Brazier, in T. A. Baillie and J. R. Jones (Editors), *Synthesis and Applications of Isotopically Labeled Compounds, Proc. 3rd Int. Symp. Innsbruck, July 17–21, 1988*, Elsevier, Amsterdam, 1989, pp. 355–360.
21 Y. Kasuya, K. Mamada, S. Baba and M. Matsukura, *J. Pharm. Sci.*, 74 (1985) 503.
22 K. Kamada, Y. Kasuya and S. Baba, *Drug Met. Disp.*, 14 (1986) 509.
23 M. Claesen, M. Moustafa, J. Adline, D. Vandervorst and J. Poupaert, *Drug Met. Disp.*, 10 (1982) 667.

Journal of Chromatography, 535 (1990) 279–285
Elsevier Science Publishers B.V., Amsterdam

CHROMSYMP. 2062

Simultaneous determination of *p*-hydroxylated and dihydrodiol metabolites of phenytoin in urine by high-performance liquid chromatography

GEORGE K. SZABO*, RICHARD J. PYLILO, HAMID DAVOUDI and THOMAS R. BROWNE
Neuropharmacology Laboratory, Boston University School of Medicine and Neurology Service, Veterans Administration Medical Center, Boston, MA (U.S.A.)

ABSTRACT

Accurate urinary measurements of the two major metabolites of phenytoin, 5-(*p*-hydroxyphenyl)-5-phenylhydantoin (*p*-HPPH) and 5-(3,4-dihydroxy-cyclohexa-1,5-dienyl)-5-phenylhydantoin (dihydrodiol, DHD), are necessary for pharmacokinetic and drug-interaction studies of this commonly used antiepileptic drug. We describe a simple, rapid, acid hydrolysis, with liquid–liquid extraction and simultaneous isocratic reversed-phase high-performance liquid chromatography of *p*-HPPH and 5-(*m*-hydroxyphenyl)-5-phenylhydantoin (*m*-HPPH) (hydrolytic end product of DHD). *p*-HPPH and *m*-HPPH were quantitated against their separate respective internal standards of alphenal and tolylbarb. The mobile phase consisted of water–dioxane–tetrahydrofuran (80:15:5, v/v/v) at 2 ml/min and at 50°C, with detection at 225 nm. Baseline separation was achieved by use of a 16 cm × 3.9 mm Nova-Pak C_{18} column and total analysis time of 12 min. *p*-HPPH and *m*-HPPH concentrations ranged from 10 to 200 and from 2 to 30 μg/ml, respectively, with between-day coefficients of variation of 3.3–4.5% and 2.2–5.1% for controls. All standard curves were linear with *r* values > 0.993. The DHD concentration was determined by multiplying *m*-HPPH concentrations by 2.3.

INTRODUCTION

Phenytoin (PHT) is one of the most widely used and extensively studied drugs for the treatment of epilepsy. It is well established that PHT has non-linear "dose-dependent" pharmacokinetic properties. Therefore, relatively minor variations in the daily dose of the drug can significantly affect steady-state plasma concentrations, metabolism and elimination of PHT. Drug absorption can vary with drug formulation [1].

In a study in which the bioavailability of a generic extended-release form of Na PHT was compared with the brand name Na PHT (Dilantin) it was necessary to make accurate and precise measurements of PHT and its major metabolites in plasma and urine. Steady-state plasma PHT concentrations (for area under the curve (AUC) values) and clearance were measured by our method described elsewhere [2]. The major hydroxylated metabolite of phenytoin in urine (*p*-HPPH) occurs in unconjugated and conjugated (glucuronide) form. For quantitation of total urinary

0021-9673/90/$03.50

p-HPPH it was necessary to convert conjugated *p*-HPPH to its unconjugated form. This can be accomplished by either enzymatic [3,5–14] or acid hydrolysis [4,5,13,15–21] of the glycosidic bond in the glucuronide. Enzymatic hydrolysis is time consuming, and was considered unreliable by the sponsors of the clinical study. Acid hydrolysis was fast and reproducible; however, it was known [4,5,13,22] to complicate *p*-HPPH measurements with the dehydration of the dihydrodiol PHT metabolite (DHD) to produce derived *p*-HPPH and derived *m*-HPPH (Fig. 1). The problem was that existing high-performance liquid chromatographic (HPLC) procedures [7,14,17–21] could not resolve the *m* and *p* forms of HPPH and so could not accurately quantitate the metabolites. We developed a HPLC method that separates and measures against an internal standard total *p*-HPPH and derived *m*-HPPH. Accurate quantitation of urinary *p*-HPPH and DHD concentration can be accomplished with a few simple calculations (eqns. 1–4).

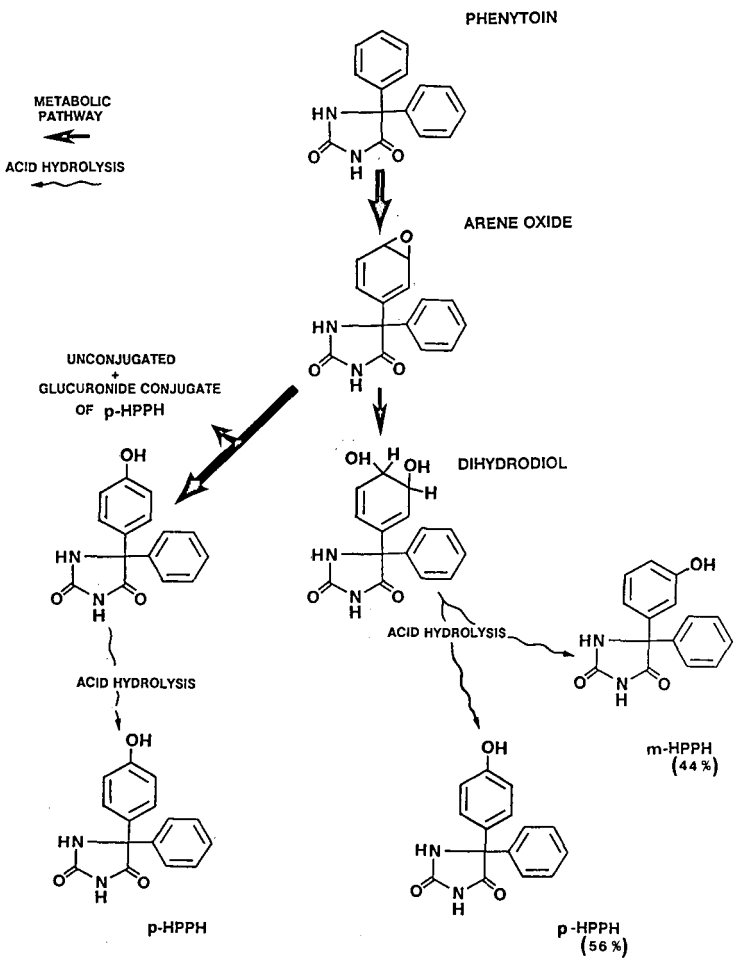

Fig. 1. Metabolic fate of phenytoin and its principal analytes after acid hydrolysis.

$$\text{Corrected total } p\text{-HPPH} = (\text{24-h urine volume} \times \text{measured } p\text{-HPPH}) - \left[\text{total measured } m\text{-HPPH} \times \left(\frac{56\%\ \text{derived } p\text{-HPPH}}{44\%\ \text{derived } m\text{-HPPH}}\right)\right] \quad (1)$$

or

$$\text{Corrected total } p\text{-HPPH} = \text{total measured } p\text{-HPPH} - (\text{total measured } m\text{-HPPH} \times 1.3) \quad (2)$$

$$\text{Corrected total DHD} = (\text{24-h urine volume} \times \text{measured } m\text{-HPPH}) \times \left(\frac{100\%\ \text{DHD}}{24\%\ \text{derived } m\text{-HPPH}}\right) \times \left[\frac{\text{mol.wt. DHD (286)}}{\text{mol.wt. } m\text{-HPPH (268)}}\right] \quad (3)$$

or

$$\text{Corrected total DHD} = \text{total measured } m\text{-HPPH} \times 2.3 \times 1.07 \quad (4)$$

EXPERIMENTAL

Instrumentation

The HPLC system consisted of a Model 2350 solvent pump and Model V4 variable-wavelength UV detector, both from ISCO (Lincoln, NE, U.S.A.) with an autosampler WISP Model 710B from Waters Assoc. (Milford, MA, U.S.A.). Chromatography was performed on a Nova-Pak C_{18} (4 μm particle size, 15 cm × 3.9 mm I.D.) stainless-steel column from Waters Assoc., heated with a water circulator pump, Model FE, Haake Instruments (Saddlebrook, NJ, U.S.A.). Detector output was monitored by a Recordall Series 5000 strip-chart recorder, Fisher Scientific (Pittsburgh, PA, U.S.A.) and peak quantitation was performed on a Canon AS-100 computer from Binary Systems (Newton, MA, U.S.A.), with an analog-to-digital converter from Quasitronics (Houston, PA, U.S.A.) and software designed by Binary Systems.

Standards and reagents

The analytical standards, D,L-5-(4-hydroxyphenyl)-5-phenylhydantoin (*p*-HPPH), 5-(3-hydroxyphenyl)-5-phenylhydantoin (*m*-HPPH) (Fig. 1) and internal standard 5-ethyl-5-(*p*-methylphenyl)-barbituric acid (tolylbarb) were obtained from Aldrich (Milwaukee, WI, U.S.A.). The other internal standard, 5-allyl-5-phenylbarbituric acid (alphenal) was obtained from Applied Science Labs. (State College, PA, U.S.A.). Disodium hydrogenphosphate, potassium dihydrogenphosphate, disodium hydrogenphosphate heptahydrate, hydrochloric acid, HPLC-grade diethyl ether, 1,4-dioxane, tetrahydrofuran (THF) and methanol reagents and solvents were obtained from Fisher Scientific. Stock analytical and internal standard solutions for *p*-HPPH, *m*-HPPH, alphenal and tolylbarb were prepared by dissolving 10 mg of each

compound in 10 ml of methanol. Methanolic working standards at varying concentrations were prepared from stock solutions for construction of standard curves and urine controls. Working internal standard solutions were prepared in methanol–distilled water (1:1) at concentrations of 500 μg/ml and 50 μg/ml for alphenal and tolylbarb, respectively.

Chromatographic conditions

The isocratic mobile phase consisted of a ternary mixture of HPLC-grade water–dioxane–THF (80:15:5, v/v/v). The flow-rate was 2 ml/min, and column temperature was stabilized at 55°C. Eluents were UV monitored at a wavelength of 225 nm with the detector set at 0.05 absorbance units full scale (a.u.f.s.).

Sample preparation

Patient urine samples collected for this study consisted of pre-study blank urine and a specimen 24 h after the last dose from each phase of the cross-over design. Urines were kept frozen at −20°C until assayed. The hydrolysis and extraction of conjugated and unconjugated urinary metabolites of phenytoin were previously described by Sawchuk and Cartier [19], with only slight modifications.

A 500-μl volume of methanolic standard solution was added to 125 × 16 mm disposable glass culture tubes (for standard curve samples only) and evaporated to dryness. To this tube, 0.5 ml of drug-free urine were then added.

In similar fashion, 0.5 ml of control or patient urine was added to clean tubes. Next, to all tubes 0.5 ml of concentrated (12 *M*) hydrochloric acid were added. Tubes were gently mixed and placed in a preheated oven for 1.5 hours at 100°C. Solutions were allowed to cool and 100 μl of working internal standard solutions were added, followed by 5.0 ml of diethyl ether. For extraction, tubes were capped with polyethylene Tainer Tops (Fisher Scientific) and horizontally shaken on a mechanical shaker (Eberbach, Ann Arbor, MI, U.S.A.) for 10 min at 180 cycles per min. Next, tubes were centrifuged for 5 min at 650 *g*. The ether layer was then transferred to a clean 125 × 16 mm culture tube that contained 1.0 ml of phosphate buffer pH 11.2. Back extraction was then performed. Tubes were recapped, shaken and centrifuged as before, then the ether layer was aspirated off. To the remaining aqueous fraction 1.0 ml of phosphate buffer pH 6.8 was added. The resulting solution was mixed, 5 ml of ether was added and re-extracted as in the previous steps. The ether layer was then transferred to a clean culture tube. The ether fraction was evaporated under a gentle stream of dry air at 40°C in the Organomation Meyer N-VAP (Berlin, MA, U.S.A.). In the final step the dried residue was reconstituted with 200 μl of methanol. The tube is then vortexed (15 s) and the solution is transferred to a WISP vial for 15 μl injection on LC system.

RESULTS

Precision and accuracy

Separate stock standards and working standards of *p*-HPPH and *m*-HPPH were prepared for each of the three days of the precision study. A fourth set of stock standards was used to prepare the controls in blank human urine. Three separate replications of a six-point standard curve and three sets of quality-control urine at low,

mid and high concentrations were assayed on each day of the precision study. The control samples had between-day coefficients of variation (C.V.) of 2.2–5.1% (Table I). Accuracy of the standard-curve points was evaluated by a comparison of the experimentally measured values (back-calculated from regression analysis) to the expected concentrations. The ratio of observed to expected concentrations was expressed as a relative percent of the expected concentrations. The percents for both compounds ranged from mean values of 96 to 106% at standard-curve concentrations for *p*-HPPH 10.0–200.0 μg/ml and *m*-HPPH 2.0–30.0 μg/ml (Table 1).

CALCULATIONS

PHT-metabolite concentration values were calculated from peak-height ratios of *p*-HPPH to alphenal and *m*-HPPH to tolylbarb *versus* standard values by least-square linear regression analysis. All curves were linear with r values > 0.993. Patient urine *p*-HPPH and DHD concentrations required corrections from derived *p*-HPPH and derived *m*-HPPH produced from the acid hydrolysis. As described by Maguire *et al.* [4], and reproduced in our laboratory, pure DHD reproduces 56% derived *p*-HPPH and 44% derived *m*-HPPH upon treatment with acid and heat. In a patient's urine sample, the corrected total *p*-HPPH concentration is equal to the ratio of derived *p*-HPPH percent (56%) to derived *m*-HPPH percent (44%) multiplied by the measured *m*-HPPH concentration and subtracted from the measured *p*-HPPH (eqns. 1 and 2). In a patient's urine sample the total corrected DHD concentration is equal to the ratio of DHD percent (100%) to derived *m*-HPPH percent (44%) multiplied by measured *m*-HPPH times the molecular-weight ratio of DHD (286) to *m*-HPPH (268) (eqns. 3 and 4).

TABLE I

ACCURACY OF STANDARDS AND PRECISION OF CONTROLS

	Standards			Controls		
	Expected concentration (μg/ml)	Mean measured concentration[a] (μg/ml) (n = 9)	Mean relative (%) measured/expected[a] (n = 9)	Expected concentration (μg/ml)	Mean measured concentration (μg/ml) (n = 9)	C.V.
p-HPPH	10.0	10.6	106			
	20.0	19.9	100	30.0	30.7	4.5
	50.0	49.8	100			
	100.0	99.8	100	90.0	86.2	4.1
	150.0	150.2	100			
	200.0	199.2	100	180.0	178.1	3.3
m-HPPH	2.0	2.1	106			
	5.0	4.8	96	6.0	5.9	5.1
	10.0	10.1	101			
	15.0	14.9	99	12.0	11.6	2.2
	20.0	20.2	101			
	30.0	29.9	100	18.0	17.9	3.8

[a] See text for definition.

DISCUSSION

Sample preparation

The modified sample procedures of Sawchuk and Cartier [19], gave good recoveries of all compounds. We tried eliminating the back-extraction into pH 11.2 buffer; however, endogenous interfering peaks from some (but not all) acid-hydrolyzed urines necessitated the use of the clean-up step.

Chromatography

After experimenting with different combinations of organic solvent concentrations in the mobile phase, optimal resolution of *m*-HPPH from *p*-HPPH was obtained. Since between 50–75% of total phenytoin dose is recovered as *p*-HPPH [4], large amounts of *p*-HPPH could be expected in 24-h urine samples. This was especially critical in samples with low total-urine-volume output. In our procedure *m*-HPPH is well resolved from *p*-HPPH even as the concentration of *p*-HPPH rises (Fig. 2). This phenomenon of extreme concentration variation also necessitated the use of separate internal standards for each measured compound. The use of a heated column allowed for a relatively short run time under isocratic conditions and helped to reduce band spreading.

CONCLUSIONS

The method we describe for quantitation of urinary PHT metabolites has a simple, fast and reproducible sampling procedure, with demonstrated accuracy and

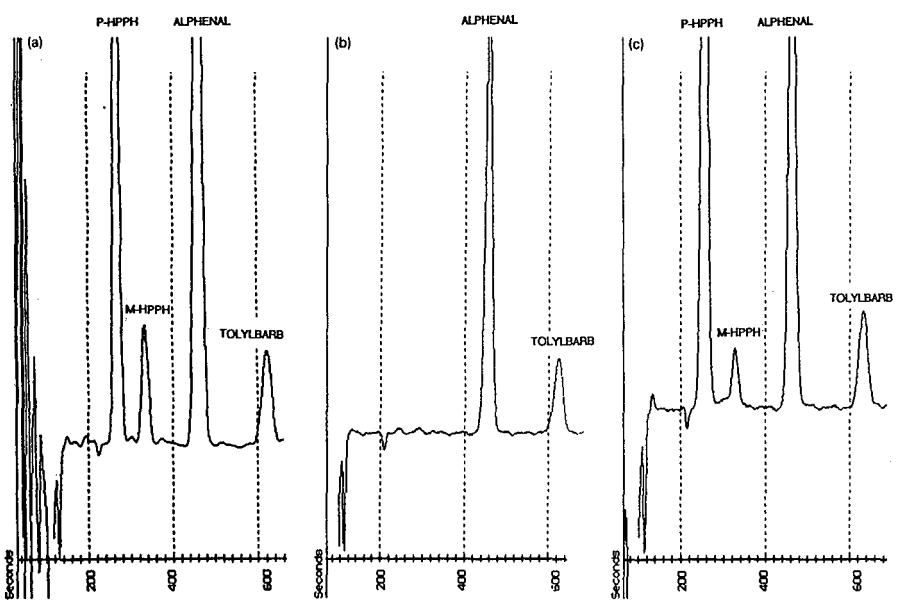

Fig. 2. Chromatograms of extracted urine samples. (a) Standard urine containing *p*-HPPH (50 μg/ml) and *m*-HPPH (10 μg/ml); (b) patient pre-study 24-h urine (blank) with internal standards; (c) patient 24-h urine containing *p*-HPPH (130.2 μg/ml) and *m*-HPPH (6.4 μg/ml).

precision over a representative concentration range. This method has proven suitable for bioequivalency studies. With minor alterations in the dynamic range, this method would also have use in pharmacokinetic and drug interaction studies where the measurement of alternative metabolic pathways is important.

ACKNOWLEDGEMENTS

Supported in part by the United States Veterans Administration and Warner-Lambert/Parke-Davis Pharmaceuticals.

REFERENCES

1 R. H. Levy, F. E. Deifus, R. H. Mattson, B. S. Meldrum and J. Kiffin Penry (Editors), *Absorption Distribution and Excretion*, Raven Press, 3rd ed., 1989, Ch. 11.
2 G. K. Szabo and T. R. Browne, *Clin. Chem.*, 28 (1982) 100.
3 T. C. Butler, K. H. Dudley, D. Johnson and S. B. Roberts, *J. Pharmacol. Exper. Ther.*, 199 (1976) 82.
4 J. H. Maguire, B. L. Kraus, T. C. Butler and K. H. Dudley, *Ther. Drug Monit.*, 1 (1979) 359.
5 K. M. Witkin, D. L. Bius, B. L. Teague, L. S. Wiese, L. W. Boyles and K. H. Dudly, *Ther. Drug Monit.*, 1 (1979) 11.
6 S. A. Chow, D. M. Charkowski and L. J. Fischer, *Life Sci.*, 27 (1980) 2476.
7 M. Claesen, M. A. A. Mustafa, J. Adline, D. Vandervorst and J. H. Poupaert, *Drug Metab. Dispos.*, 10 (1982) 667.
8 W. R. Bartle, S. E. Walker and T. Shapero, *Clin. Pharmacol. Ther.*, 33 (1983) 649.
9 R. G. Dickinson, W. D. Hooper, M. Patterson, M. J. Eadie and B. Maguire, *Ther. Drug Monit.*, 7 (1985) 283.
10 J. T. Lum, N. A. Vassanji and P. G. Wells, *J. Chromatogr.*, 338 (1985) 242.
11 J. H. Maguire and D. C. Wilson, *J. Chromatogr.*, 342 (1985) 323.
12 J. S. McClanahan and J. H. Maguire, *J. Chromatogr.*, 381 (1986) 438.
13 M. A. A. Moustafa, F. Beial and A. A. El-Emam, *J. Pharm. Belg.*, 42 (1987) 53.
14 D. Roy and W. R. Snodgrass, *Ther. Drug Monit.*, 11 (1989) 57.
15 J. Hermansson and B. Karlen, *J. Chromatogr.*, 130 (1977) 422.
16 C. Hoppel, M. Garle and M. Elander, *J. Chromatogr.*, 116 (1976) 53.
17 P. M. Kabra and L. J. Marton, *Clin. Chem.*, 22 (1976) 1672.
18 R. W. Dykeman and D. J. Ecobichon, *J. Chromatogr.*, 162 (1979) 104.
19 R. J. Sawchuk and L. L. Cartier, *Clin. Chem.*, 26 (1980) 835.
20 U. Jurgens, *J. Chromatogr.*, 275 (1983) 335.
21 K. Shimada, Y. Izumo and T. Sakaguchi, *J. Chromatogr.*, 275 (1983) 97.
22 J. H. Poupaert, A. Garzon, M. Mustafa, M. Claesen and P. Dumoni, *J. Pharm. Belg.*, 35 (1980) 320.

Journal of Chromatography, 535 (1990) 287–292
Elsevier Science Publishers B.V., Amsterdam

CHROMSYMP. 2046

Automated liquid chromatographic determination of ranitidine in microliter samples of rat plasma

A. B. SEGELMAN[a,*]

Department of Chemical Biology and Pharmacognosy, College of Pharmacy, Rutgers-The State University, Piscataway, NJ 08854 (U.S.A.)

and

V. E. ADUSUMALLI and F. H. SEGELMAN

Wallace Laboratories, Division of Carter-Wallace, Inc., Half Acre Road, Cranbury, NJ 08512 (U.S.A.)

ABSTRACT

An improved high-performance liquid chromatographic method with UV detection at 313 nm has been developed for quantitation of ranitidine in 100 μl of rat plasma over the range 25 to 1000 ng/ml. To each sample were added the internal standard (metiamide) and 2 *M* NaOH. After dichloromethane extraction, the nitrogen-dried extracts were reconstituted in the mobile phase of 0.01 *M* phosphate buffer–triethylamine–methanol–water (530:5:390:75, v/v). Chromatography on μBondapak C_{18} with quantitation by peak height ratios showed an analyte recovery of 97%; a limit of detection of 10 ng/ml; a precision of 1–10% and an accuracy of 1–5%. About 90 samples can be processed in 24 h.

INTRODUCTION

Ranitidine {N-[2-[[[5-[(dimethylamino)methyl]-2-furanyl]-methyl]thio]ethyl]-N^1-methyl-2-nitro-1,1-ethenediamine} is a H_2-receptor antagonist, effective in inhibiting histamine- and pentagastrin-induced secretion of gastric acid [1,2]. The drug is widely used for the management of peptic ulcer disease [3].

Several high-performance liquid chromatographic (HPLC) methods for measuring ranitidine in biological fluids have been reported [4–10]. Some of these methods require *ca.* 1 ml of plasma [4–7] to achieve a detection limit of 10–20 ng/ml. Varughese and Lee [8] reported a method for determining ranitidine by direct injection of the supernatant from protein precipitiation of plasma with acetonitrile. However, with this method we observed a relatively high limit of detection (50 ng/ml), endogenous interferences, and the need for a rigorous column clean-up schedule to maintain acceptable results. Vandenberghe *et al.* [9], using a variable-wavelength detector, described a method for ranitidine assay in 200 μl of human plasma with a detection limit of 10 ng/ml. However, this method would not be suitable for serial blood sampling typical of rat pharmacokinetic studies, since it would require at least 400 μl of

[a] Present address: Nature's Sunshine Products, Spanish Fork, UT 84660, U.S.A.

0021-9673/90/$03.50

whole blood to be withdrawn *ca.* 15 times over a period of 12 hours, thus compromising homeostasis of this small animal.

We describe here a sensitive HPLC method for the determination of ranitidine with UV detection at 313 nm in 100 μl of rat plasma obtained from *ca.* 225 μl of blood. Pursuant to our studies on tannin-drug interactions, we have routinely employed this procedure to analyze large numbers of rat plasma samples from single animals over 24 h without compromising the animal or the sensitivity of ranitidine quantitation.

EXPERIMENTAL

Chemicals

Ranitidine hydrochloride (Zantac® injectable, 25 mg of ranitidine/ml) was purchased from Glaxo (Research Triangle Park, NC, U.S.A.). The internal standard (I.S.), metiamide, was supplied by Smith, Kline & French Labs. (Philadelphia, PA, U.S.A.). All chemicals were purchased from the vendors indicated: sodium hydroxide, potassium phosphate monobasic, sodium phosphate dibasic (Fisher Scientific, Fair Lawn, NJ, U.S.A.); HPLC-grade methanol, acetonitrile, dichloromethane and 2-propanol (Burdick & Jackson, purchased through Baxter Healthcare, McGaw Park, IL, US.A.); triethylamine (Pierce, Paris, KY, U.S.A.); HPLC-grade water was obtained using a Milli-Q® water system (Millipore, Bedford, MA, U.S.A.). Blank rat plasma (heparinized) was obtained from normal, untreated male Sprague-Dawley rats.

Instrumentation

HPLC was performed on a Waters Assoc. (Milford, MA, U.S.A.) component system, equipped with a Model M4 pump, Model 710B WISP autoinjector, and a Model 441 fixed-wavelength detector (313 nm), which was interfaced with the HP3357 Laboratory Automation System (LAS) (Hewlett-Packard, Avondale, PA, U.S.A.). Using a 313-nm filter compared to those at 214 and 280 nm, there was no interference by plasma endogenates and excellent sensitivity of detection was achieved. The maximum absorptivity of ranitidine in the mobile phase occurred at 315 nm.

Chromatographic conditions

The mobile phase consisted of 0.01 *M* phosphate buffer [11] (pH 7.5)–triethylamine–methanol–acetonitrile (530:5:390:75, v/v). After the addition of triethylamine to the phosphate buffer, the pH was readjusted to 7.5 with phosphoric acid (85%, v/v), and the final solution was mixed with the organic components. Chromatography was performed at ambient temperature (22 ± 1°C) on a 300 × 3.9 mm I.D. Waters μBondapak C_{18} column, 10-μm particle size, protected with a Waters C_{18} Corasil Bondapak guard column. The flow-rate was 1.0 ml/min, and the eluent was monitored at 313 nm with the attenuation set at 0.01 a.u.f.s. Peak heights for ranitidine and the I.S. were measured using the HP3357 LAS. These data were used to generate peak height ratios (ranitidine/I.S.) for establishing standard curves. Retention times of I.S. (metiamide) and ranitidine were approximately 4.7 ± 0.5 and 6.6 ± 0.3 min, respectively. After about 90 analyses, the column was washed consecutively with 100 ml of each, water, acetonitrile and methanol before re-equilibration with mobile phase.

Standard solutions

Three ranitidine stock solutions (0.1 mg/ml) were prepared from individual vials of commercially available ranitidine injectable solution (25 mg/ml). Working standards in water and plasma containing 25, 50, 100, 250, 500 and 1000 ng/ml of ranitidine were prepared from each stock solution. HPLC analysis of the water samples as well as the plasma standards after extraction, was performed immediately to determine recovery of the drug from plasma and intra-day variability of the assay. Standards were kept frozen at −15°C until used for the determination of inter-day assay variability as well as drug stability in rat plasma. The metiamide I.S. solution (20 mg/ml) was freshly prepared in 50% aqueous 2-propanol, since it has been reported to be unstable in aqueous solution [9].

Extraction procedure

To 100 μl of each fortified blank plasma sample in a 75 × 12 mm glass tube was added 100 μl of 2 *M* sodium hydroxide, 0.5 ml of the I.S. solution and 2.0 ml of dichloromethane. The sample was extracted by vortex mixing for 30 s and then centrifuged for 5 min at 600 *g* to give well-separated phases. The upper organic phase was aspirated off, and the lower organic phase (*ca.* 1.7 ml) was transferred to a clean 75 × 12 mm glass tube for evaporation under nitrogen at room temperature. The dried residue was reconstituted in 100 μl of mobile phase by vortex mixing, and 80 μl was injected for HPLC analysis.

RESULTS AND DISCUSSION

Fig. 1 shows the chromatogram, (A) without and (B) with triethylamine in the

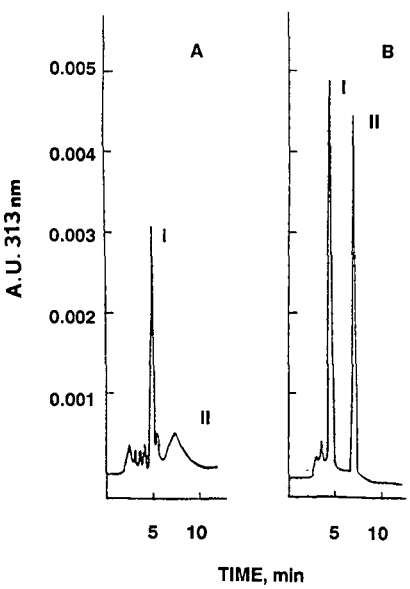

Fig. 1. Chromatography of rat plasma extracts from plasma containing 200 μg/ml metiamide I.S. (I) and 500 ng/ml ranitidine (II) with a mobile phase (A) containing no triethylamine and (B) containing triethylamine.

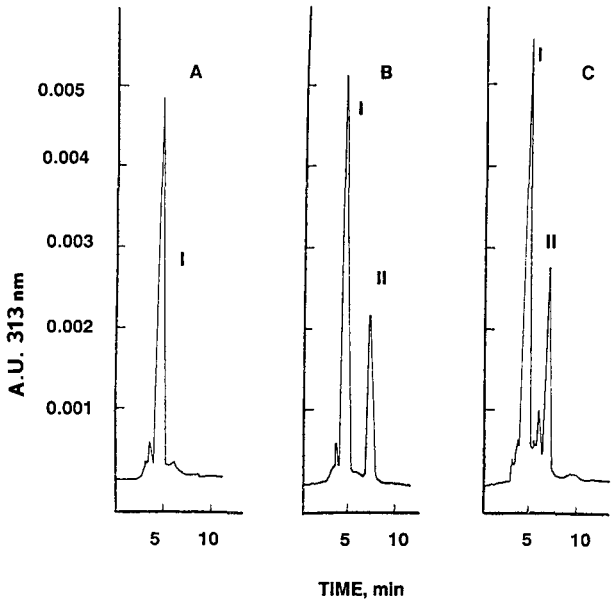

Fig 2. Typical chromatograms, representing extracts of: (A) blank rat plasma with 200 μg/ml I.S. (I), (B) plasma standard with 250 ng/ml ranitidine (II) and (C) plasma from a rat, 2 h after an oral dose of 10 mg/kg ranitidine.

mobile phase. Unique to our ranitidine assay method, with the triethylamine added, the ranitidine peak sharpness improved markedly and thereby increased the assay sensitivity by peak height measurements. Typical chromatograms are shown in Fig. 2, representative of a plasma blank, standard, and test sample.

Linearity of detector response for ranitidine in rat plasma standards was achieved over the concentration range 25 to 1000 ng/ml, as evidenced by the correlation coefficient ($r^2 > 0.999$). The assay precision, measured by the coefficient of variation (C.V.), and the assay accuracy, measured by the relative mean error (R.M.E.) were calculated from the with-in day sets of plasma standards, prepared from three separate ranitidine stock solutions (Table I). The precision of the method ranged from 1 to 10% and the accuracy from 1 to 5%. The average absolute recoveries of the drug and the I.S. were 97 and 87%, respectively. This was determined by comparison of the peak heights obtained from fortified plasma standards with those from directly injected standard solutions at each concentration level. The inter-day reproducibility of the assay was determined periodically over 52 days (Table I). The limit of detection (D) was found to be 10 ng/ml, as calculated from the formula $D = xb + fs$, where xb represents the mean determined values for a series of blank plasma samples, s is the standard deviation for these blank determinations, and f is a factor associated with the number of replicates [12].

Storage of the drug plasma standards at −15°C did not alter the amount of ranitidine recovered at days 4, 17, 30 and 52 *versus* day 0 as tested by two-way ANOVA calculation, $F_{0.05}$ (4,5) < 5.19.

Application of the method was demonstrated by measuring plasma levels of

TABLE I

PRECISION AND ACCURACY OF ASSAY FOR RANITIDINE IN RAT PLASMA

Ranitidine added (ng/ml)	Mean ranitidine determined (ng/ml)	Coefficient of variation (%)	Relative mean error (%)	Absolute recovery (%)
Intra-day (n = 3)				
25	24	9.6	−5.2	118
50	50	2.6	0.1	104
100	99	2.1	−0.6	98
250	256	0.5	2.4	96
500	491	1.0	−1.8	89
1000	1008	1.3	0.8	89
Inter-day (n = 5)				
25	25	13.2	−0.8	
50	52	7.2	3.8	
100	97	3.9	−2.7	
250	253	3.0	1.1	
500	495	2.3	−1.1	
1000	1005	0.9	0.5	

ranitidine in rats ($n = 8$) after oral administration of 10 mg/kg of drug (Fig. 3). In order to facilitate the analyses, a fully automated and computerized HPLC method was developed. The HPLC analysis time per sample was *ca.* 10 min. About 90 samples could be extracted and analyzed in a 24-h period. At least 1500 samples have been assayed per column with proper column care.

As previously stated, other reported methods for ranitidine quantitiation, were

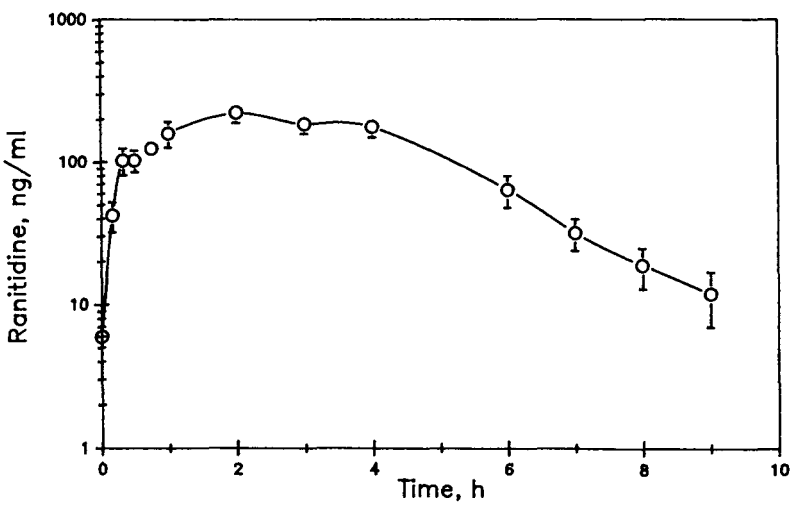

Fig. 3. Plasma concentrations of ranitidine following a 10 mg/kg oral administration of the drug to rats ($n = 8$).

not suitable for pharmacokinetic studies in rats, since relatively large amounts of blood would have to be taken at each of many serial blood samplings, and the total of which would compromise the animal. Although one reported method [7] used smaller amounts of sample, it was found to have two major disadvantages, namely, low sensitivity and a tedious column clean-up procedure. The facile and efficient extraction and HPLC procedure reported here permits the rapid, accurate and sensitive quantitation of ranitidine in 100 μl of rat plasma.

REFERENCES

1 J. Bradshaw, R. T. Brittain, J. W. Clitterous, M. J. Daly, B. J. Price and R. Stables, *Br. J. Pharmacol.*, 66 (1979) 464.
2 N. R. Penden, J. H. B. Saunders and J. C. Emmet, *Lancet,* 1 (1979) 690.
3 M. Gibaldi, *Persp. Clin. Pharmacol.*, 3 (1985) 19.
4 P. F. Carey and L. E. Martin, *J. Liq. Chromatogr.*, 2 (1979) 690.
5 P. F. Carey, L. E. Martin and P. E. Owen, *J. Chromatogr.*, 225 (1981) 161.
6 G. W. Mihaly, O. H. Drummer, A. Marshall, R. A. Smallwood and W. J. Louis, *J. Pharm. Sci.*, 69 (1980) 1155.
7 J. Boutagy, D. G. More, I. A. Munro and G. M. Shenfield, *J. Liq. Chromatogr.*, 1 (1984) 1651.
8 A. Varughese and C. S. Lee, *Drugs Exp. Clin. Res.*, 9 (1983) 837.
9 H. M. Vandenberghe, S. M. MacLeod, N. A. Mahon, P. A. Lebert and S. J. Soldin, *Ther. Drug Monit.*, 2 (1980) 379.
10 P. F. Carey and L. E. Martin, *Automatographia*, 19 (1985) 200.
11 G. Monoli, *Proc. Soc. Exptl. Biol. Med.*, 68 (1948) 354.
12 D. L. Massart, L. Kaufman and A. Dijkstra, *Evaluation and Optimization of Laboratory Methods and Analytical Procedures,* Elsevier, Amsterdam, 1978, p. 150.

Journal of Chromatography, 535 (1990) 293–304
Elsevier Science Publishers B.V., Amsterdam

CHROMSYMP. 2053

Analysis of carbamazepine in serum by liquid chromatography with direct sample injection and surfactant-containing eluents

DETLEF BENTROP, F. VINCENT WARREN, Jr., STEFAN SCHMITZ and BRIAN A. BIDLINGMEYER*
Waters Chromatography Division of Millipore Corporation, 34 Maple Street, Milford, MA 01757 (U.S.A.)

ABSTRACT

Surfactant-containing eluents are evaluated for the analysis of carbamazepine in serum with conventional reversed-phase columns. Bovine serum was quantitatively eluted at the column void volume using surfactant concentrations in conventional reversed-phase eluents. The effect of pH, guard columns and column switching was evaluated with respect to separating and detecting clinical levels of the drug and its primary metabolite. Column lifetime was also investigated.

INTRODUCTION

Because the requirement for sample preparation adds to the labor and cost associated with liquid chromatographic (LC) methods for drug analysis, a number of alternatives for minimizing sample preparation have been investigated [1,2]. Some of these approaches allow the direct injection of serum into the LC system. One such approach is the use of specially designed column packings which do not promote the adsorption or precipitation of proteins. The internal-surface reversed-phase (ISRP) [3] and shielded hydrophobic phase [4] packings are the best known commercial implementations of this strategy. A related strategy is the coating of conventional column packings with surfactants [5] or serum proteins [6,7], in order to permit their use with direct serum injection. One disadvantage of all special packings is the relatively small number of available phases. For example, Haginaka *et al.* [8] could not adequately retain hydrophilic drugs on the commercial ISRP phase and found it necessary to synthesize a new ISRP phase with a more hydrophobic ligand. Another consideration in the use of coated columns is the need to restrict the use of certain eluent components (*e.g.*, organic solvents) capable of removing or deactivating the column coating [5], possibly leading to a change in retentivity toward drug solutes.

Another approach to direct serum injection is the use of conventional column packings in combination with eluents capable of solubilizing serum components. In micellar LC, eluents are used which contain surfactants at concentrations above the critical micelle concentration (CMC), and these eluents have been shown to permit

0021-9673/90/$03.50

direct serum injection [9–11]. Properly designed eluents bring about the elution of serum proteins at or near the column void volume.

We have recently demonstrated [12] that the constraints which micellar LC imposes upon eluent composition can be relaxed considerably without compromising the ability to perform direct serum injection. Specifically, much lower surfactant concentrations (*i.e.* sub-CMC) and much higher organic solvent compositions (*e.g.*, 40% methanol) can be used in eluents for direct serum injection. The broader allowable ranges for these eluents permit direct serum injection methods to be developed similarly to paired-ion chromatographic methods [13], with the use of columns, eluents and rules of thumb familiar to chromatographers.

In the previous study [12], a sample consisting of 50 mg/ml bovine serum albumin (BSA) was used in the testing and development of eluents. This paper extends those efforts, substituting a more realistic sample matrix for the model serum and focusing on practical issues. Column lifetime was studied both with and without a guard column, and the stability of retention time and peak area were evaluated. The conditions used for the analysis of carbamazepine and its 10,11-epoxide metabolite have permitted hundreds of analyses via direct injection of spiked serum samples.

EXPERIMENTAL

Instrumentation

The modular liquid chromatograph from Waters Chromatography Division of Millipore (Milford, MA, U.S.A.) consisted of a Model 510 solvent delivery module(s), a Model 712 WISP autoinjector with cooling unit, and a Model 441Z absorbance detector or a Model 440 absorbance detector, equipped with an extended-wavelength module. A detection wavelength of 214 nm was used for all of the work reported here. Instrument control was provided by a Model 840 chromatography control station, analog data being monitored with a Model SE120 dual-pen recorder. Digital data were auto-archived to a Model 860 networking chromatography station for processing and storage. An eluent stabilization system (Waters) was pressurized with helium and used in the blanket mode to provide a steady supply of eluent to the solvent delivery modules. A flow-rate of 2.0 ml/min was used, unless otherwise noted.

For the column switching methods, a column switching valve (Waters) was controlled by the 840 chromatography control station. Connections to the six valve ports (see Fig. 1) were: (1) guard column inlet, (2) injector outlet, (3) waste, (4) guard column outlet, (5) analysis pump outlet and (6) analysis column inlet. The column switching method required two pumps, a loading pump for the aqueous 5 m*M* sodium dodecyl sulfate (SDS) loading eluent and an analysis pump for the methanol–water –SDS analysis eluent. The injector was positioned between the loading pump and port 2 of the column switching valve.

Columns, eluents and reagents

A fresh μBondapak Phenyl steel column (15 × 0.39 cm I.D.) (Waters) was used for each of the lifetime studies or examples discussed. When used, the guard column was either a μBondapak Phenyl Guard Pak cartridge, housed in a Guard Pak holder (Waters), or a Guard Column kit, dry-packed with Corasil Phenyl bulk packing (Waters). The particle size of the pellicular Corasil Phenyl packing is 37–53 μm. An

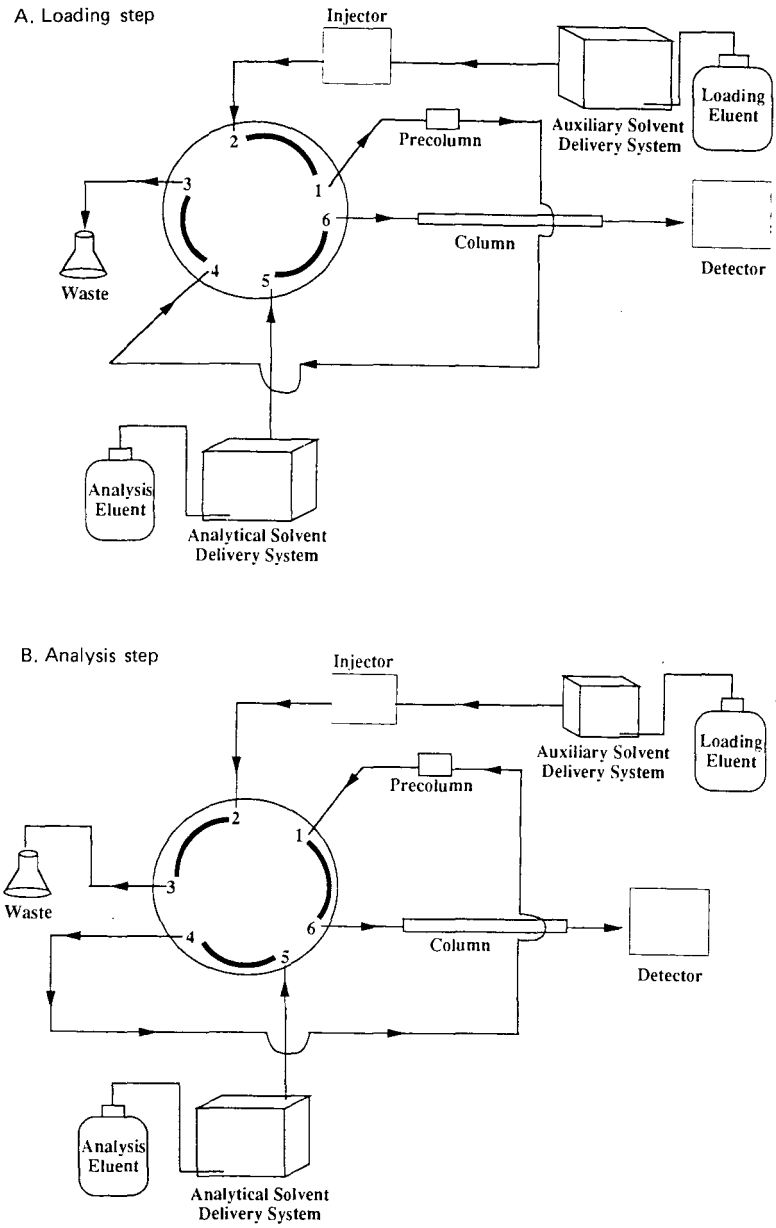

Fig. 1. Valve port and system diagram used with the column switching option.

in-line precolumn filter kit, containing a 2-μm filter assembly, was used throughout this work, with the filter assembly changed regularly as noted in the text. For the separation in Fig. 2, a Pinkerton ISRP GFF column (15 × 0.46 cm I.D.) was obtained from Regis (Morton Grove, IL, U.S.A.) and used according to the manufacturer's recommendations.

Purified, filtered water was obtained with a Milli-Q water purification system (Millipore Corporation, Bedford, MA, U.S.A.). HPLC-grade methanol was purchased from J. T. Baker (Phillipsburg, NJ, U.S.A.), and SDS was obtained in puriss. quality from Fluka (Ronkonkoma, NY, U.S.A.). The SDS-containing eluents were prepared by dissolving the required quantity of SDS in a water–methanol blend of the desired composition. When foaming was not severe, eluents were degassed by filtration under vacuum through a 0.45-μm cellulose acetate filter, housed in a solvent clarification kit (Waters) or equivalent. Otherwise, ultrasonication under vacuum was used for degassing.

The sample matrix was adult bovine serum (triple filtered through a 0.1-μm filter by the manufacturer) from HyClone Labs. (Logan, UT, U.S.A.). When received, the adult bovine serum was divided into 10-ml aliquots and stored frozen until needed. Spiked bovine serum samples were prepared by adding small volumes of 1 mg/ml methanolic solutions of carbamazepine (Sigma, St. Louis, MO, U.S.A.) and carbamazepine-10,11-epoxide (Alltech-Applied Science, State College, PA, U.S.A.) to aliquots of adult bovine serum. Unless otherwise specified in the text, all spiked serum samples contained 2.0 μg carbamazepine-10,11-epoxide (CBE) and 4.8 μg carbamazepine (CBZ) per ml of bovine serum.

RESULTS AND DISCUSSION

CBZ analysis was selected as the example of a drug analysis problem for this work. Serum levels of this anticonvulsant must be monitored regularly in patients taking the drug, due to its narrow therapeutic range (4–10 μg/ml serum) as well as the poor correlation of dosage to serum concentration. *In vivo*, CBZ is metabolized to the pharmacologically active CBE, which has little ultraviolet absorbance at 254 nm. LC is frequently used for CBZ analysis, especially when the epoxide metabolite must be monitored, since currently available immunoassay approaches do not respond selectively to the metabolite [14].

Our previous report [12] suggested that both methanol and surfactant concentration could be varied over a broader-than-expected range for direct serum injection methods with complete elution of the protein. However, the "model serum" used in that work, a 50 mg/ml aqueous solution of BSA, provided a relatively simple matrix. Adult bovine serum was used as a more realistic sample matrix in the studies described here. Additional testing and confirmation with human serum samples [15] indicated that the results obtained for bovine serum will also be obtainable for human serum samples.

The choice of CBZ analysis as an analytical problem imposes a detection challenge not usually discussed in reports on direct serum injection methods, since the analysis of CBE requires UV monitoring at a low wavelength (*e.g.*, 214 nm). Serum proteins respond strongly at this detection wavelength, and excessive tailing of the early-eluted serum peak can potentially interfere with quantitation of the less-retained analytes.

Effect of eluent variables on serum-related peaks

Serum peak tailing is a problem in all direct serum injection methods and is not specific to surfactantcontaining eluents. For example, Fig. 2 shows the separation of

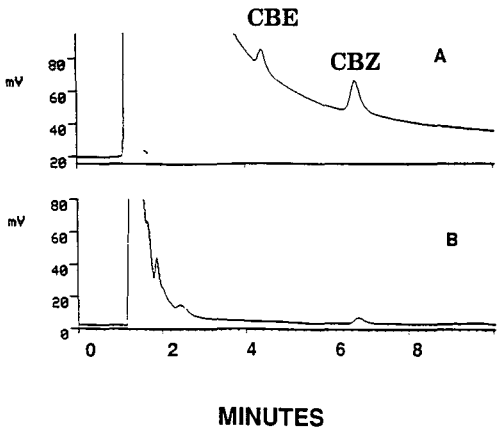

Fig. 2. Effect of detection wavelength on chromatograms of CBE and CBZ in spiked bovine serum with UV detection at (A) 214 nm and (B) 254 nm. Column, Regis 5-μm ISRP GFF (15 × 0.46 cm); eluent, 0.1 *M* KH_2PO_4 (pH 6.8)–acetonitrile (80:20, v/v), flow-rate, 1.0 ml/min. Ordinate scale: 0.08 a.u.f.s.

clinical levels of CBZ and CBE added to bovine serum on a Regis ISRP column with the eluent for carbamazepine analysis suggested by the manufacturer. At 254 nm (Fig. 2B), the serum peak is relatively small and the peak of CBZ is eluted on a flat baseline. However, clinical levels of CBE cannot be detected at 254 nm. Detection at 214 nm (Fig. 2A) reveals a peak for CBE, but the serum peak tail is increased so dramatically that even CBZ occurs as a rider peak. Thus, the control of serum peak tailing becomes a part of the methods development process for carbamazepine analysis because of the requirement for monitoring at low UV wavelengths.

As a transition between our previous work [12] with model serum (50 mg BSA/ml) and the use of bovine serum in the work reported here, we considered the effect of methanol and surfactant concentration on the elution of serum proteins from these matrices. Fig. 3 compares the peak profiles obtained with eluents containing 1 or 50 m*M* sodium dodecylsulfate (SDS) for 10-μl injections of the model serum and bovine serum. Confirming our previous findings, there is little discernible difference between the model serum chromatograms with either an aqueous eluent (Fig. 3A) or in the presence of 30% methanol (Fig. 3B). However, bovine serum presents a substantially more complex peak profile. Tailing is significant at either surfactant concentration, and actually appears much worse in the 100% aqueous eluent (Fig. 3C) than in the methanol-containing eluent (Fig. 3D). In addition, a number of small peaks follow the main serum peak, suggesting the possibility of interference problems with early-eluted sample components.

It was not clear initially whether the small peaks obtained in Fig. 3C and D were due to the elution of distinct proteins present in serum or whether they represent an artifact related to column overload. To better understand this, we collected two fractions of the serum peak tail for subsequent reinjection. (Fraction 1 was the volume collected between 0.6 and 2.0 min and fraction 2 was between 2.0 and 3.1 min.) When portions of the collected fractions were reinjected, sharp peaks were observed at the column void volume. Apparently, the severe tailing and multiple peak production

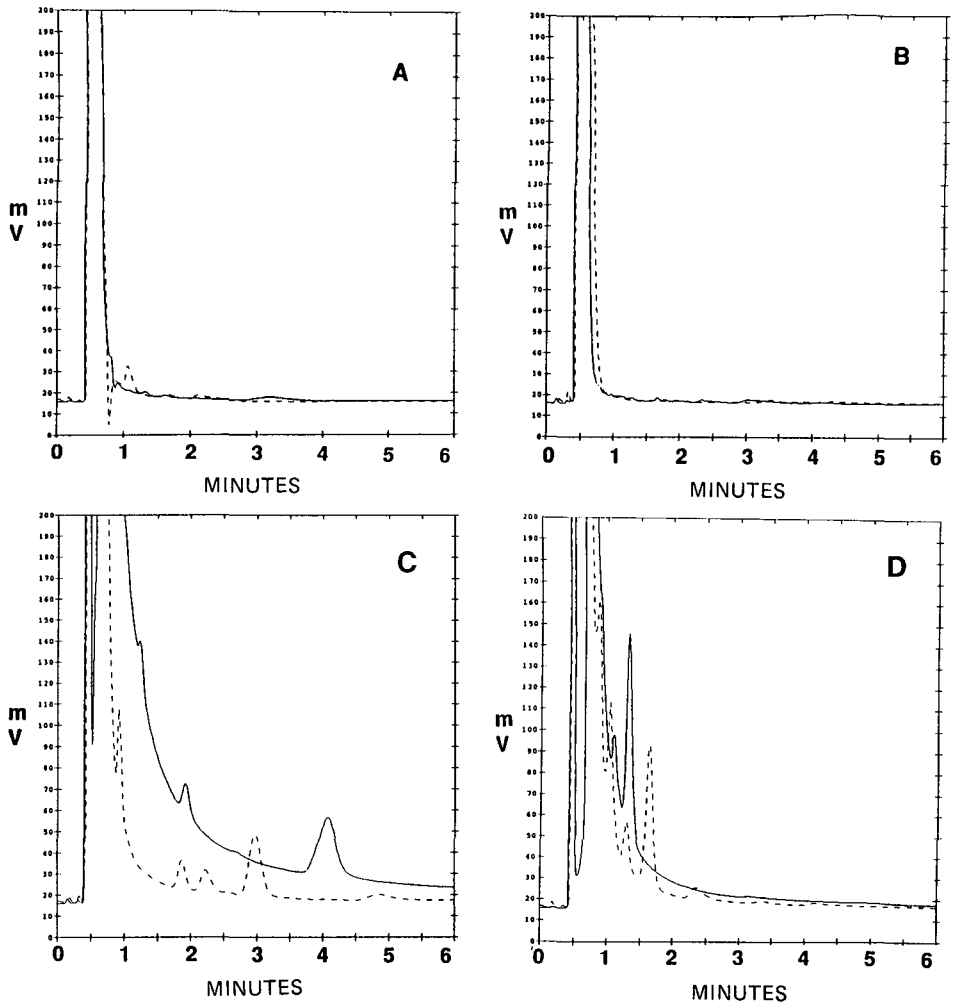

Fig. 3. Effect of methanol and SDS concentration on peaks observed for 10-μl injections of model serum (A, B), and bovine serum (C,D) at two levels of SDS concentration (solid line is 1 m*M* and dashed line is 50 m*M*). Methanol concentration of 0% (v/v) in A and C, or 30% in B and D. Column μBondapak Phenyl (15 × 0.39 cm); flow-rate 2 ml/min; 214 nm. Ordinate scale: 0.20 a.u.f.s.

associated with the injection of bovine serum is the result of overload. Fortunately, most of the eluents used in this study contain enough methanol and SDS to produce the relatively early elution of the serum peak seen in Fig. 3D.

Although pH is not a key variable for controlling the elution of CBZ and CBE, we were interested in the influence of this variable on the serum peak profile. A series of 10 m*M* phosphate buffers at pH 2.8, 5.0 and 7.5 were prepared. Eluents containing 50 m*M* SDS, 30% methanol and 70% of these buffers were compared with an unbuffered but otherwise identical eluent for the elution of 10-μl injections of bovine serum. Fig. 4 summarizes the results of the pH study. The greatest amount of tailing is observed for

the pH 5.0 eluent, possibly reflecting the reduced solubility of serum albumin near its pI value. The pH 2.8 eluent produces the greatest number of small peaks following the main serum peak, with the last of these eluted at *ca.* 7 min. The possibility of interference with analyte peaks is significant for this low pH eluent.

The best results in Fig. 4 are obtained with the pH 7.5 eluent, which produces a serum peak profile nearly identical with that of the unbuffered eluent. While unbuffered eluents are used in all of the work reported here, it appears that a buffered eluent at a neutral or slightly basic pH would also be appropriate. Interestingly, Fig. 4 shows that the solubilization of serum proteins by SDS is not sufficient to completely eliminate the influence of eluent pH on the elution of serum components, at least in eluents containing 30% methanol and 10 m*M* buffer strength. However, the situation is greatly improved compared to the use of eluents containing no surfactant. When ISRP columns are applied to direct serum injection, Pinkerton *et al.* [3] recommend the use of eluents at pH 6.8 as the best compromise in order to avoid problems of protein precipitation and to maintain column life.

While methanol-containing eluents are mentioned throughout this report, we briefly considered the influence of other organic modifiers upon serum-related peaks. As Fig. 5 shows, eluents containing acetonitrile or 2-propanol produce a serum chromatogram similar to that with a methanol-containing eluent when all three are adjusted to give a comparable retention of carbamazepine (7–8 min). Based on our past experience with methanol, we continued working with this modifier. However, recent efforts in our laboratory have produced excellent results for direct serum injection methods with 2-propanol-containing eluents.

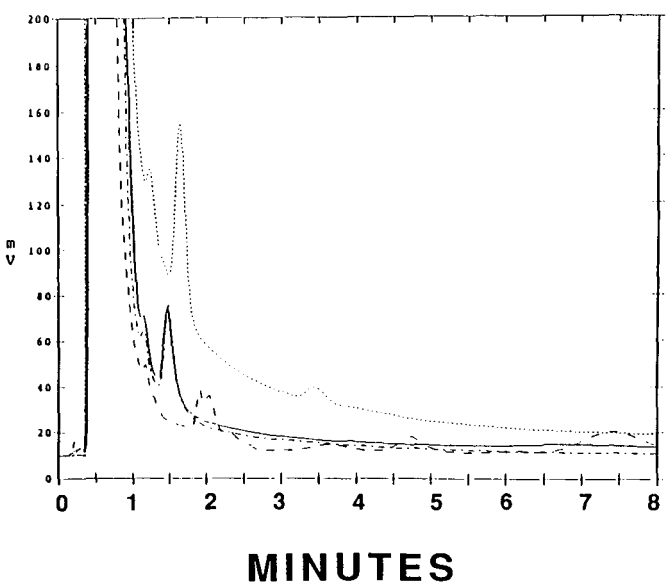

Fig. 4. Effect of pH on the chromatogram observed for 10-μl bovine serum. Eluent, 50 m*M* SDS in methanol–aqueous 10 m*M* sodium phosphate (30:70, v/v) at pH 2.8 (– – –), pH 5.0 (·····) or pH 7.5 (– · – · –). For comparison, the solid line chromatogram is methanol–water (30:70) using no buffer. Other conditions as in Fig 3.

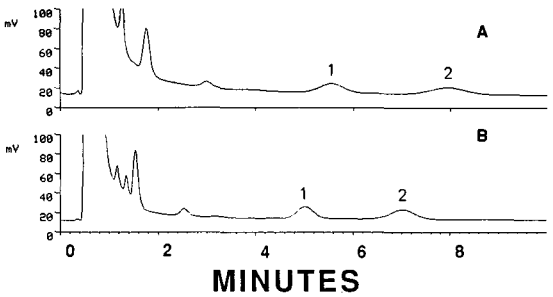

Fig. 5. Effect of organic modifier on the serum chromatogram under conditions which produce a retention time of 7 to 8 min for CBZ. Eluent, 50 m*M* SDS in water and (A) 10% 2-propanol or (B) 15% acetonitrile. Other conditions as in Fig. 3. Injection volume, 10-μl containing 2.0 μg/ml of CBE (peak 1) and 4.8 μg/ml of CBZ (peak 2).

Effect of eluent variables on retention of CBE and CBZ

The selection of a suitable eluent for direct serum injection involves a trade-off between analysis time, column efficiency and serum peak tailing. The most significant variables for retention adjustment are methanol and SDS composition in the present system. An increase in either of these variables will result in earlier elution of CBE and CBZ, as Table I shows. However, increasing the SDS concentration from 10 to 100 m*M* causes at least a two-fold reduction in plate count. An increase in methanol, on the other hand, alters the serum peak profile significantly (Fig. 3). As a compromise, we selected an eluent consisting of methanol–water (30:70) with an overall SDS concentration of 50 m*M*. This eluent provides an analysis time under 10 min without excessive loss of column efficiency, while eluting the majority of the serum-related peaks in less than 4 min.

Column lifetime studies

Having selected a suitable eluent (30% methanol, 50 m*M* SDS), it was possible

TABLE I

EFFECT OF SDS CONCENTRATION ON RETENTION AND EFFICIENCY

t_R = Retention time, min; N = plate number.

Methanol (%, v/v)	Parameter	[SDS] (m*M*)					
		10		50		100	
		CBE	CBZ	CBE	CBZ	CBE	CBZ
15	t_R	39.79	74.59	8.63	11.53	4.70	5.98
	N	1417	2081	838	840	580	580
22	t_R	20.98	40.97	8.06	10.70	4.23	5.31
	N	1333	1989	810	789	721	708
30	t_R	14.55	19.19	4.98	7.15	3.48	4.44
	N	1381	1687	1008	1121	807	635

to consider the effect of a large number of serum samples on chromatographic resolution, system pressure and the stability of retention time, peak height and peak area for CBZ and CBE. A series of three lifetime studies were conducted, with the lessons learned in each applied to improve performance in the next.

Experiments conducted prior to the first lifetime study showed that spiked bovine serum samples could not be left in the autoinjector at room temperature for more than a few hours without the formation of precipitates and consequent pressure problems. This was avoided either by using a refrigerated autoinjector or by keeping serum samples at room temperature for less than 4 h. As an additional precaution, the analytical column was protected by an in-line filter, containing a 2-μm stainless-steel frit. A new filter frit was installed daily (after each 50–100 injections), although a much less frequent change would probably have provided acceptable results.

Using these precautions, a 15-cm μBondapak Phenyl steel column was able to provide stable retention times (relative standard deviation, R.S.D. = 3.0–3.5%) for CBZ and CBE over the course of 738 injections (10-μl) of spiked bovine serum. In the course of these injections, two observed trends were of some concern. First, the serum peak increased in width throughout the study (see Fig. 6). Second, the CBZ and CBE peaks broadened steadily, despite the stability of their retention times. While neither of these phenomena prevented quantitation of the drugs, we were interested in minimizing both types of peak broadening in subsequent lifetime studies.

Use of guard columns

The changes in the size of the serum peak which were observed during the first lifetime study might arise from the accumulation of serum components at the head of the analytical column. While SDS is known to be an effective solubilizing agent for

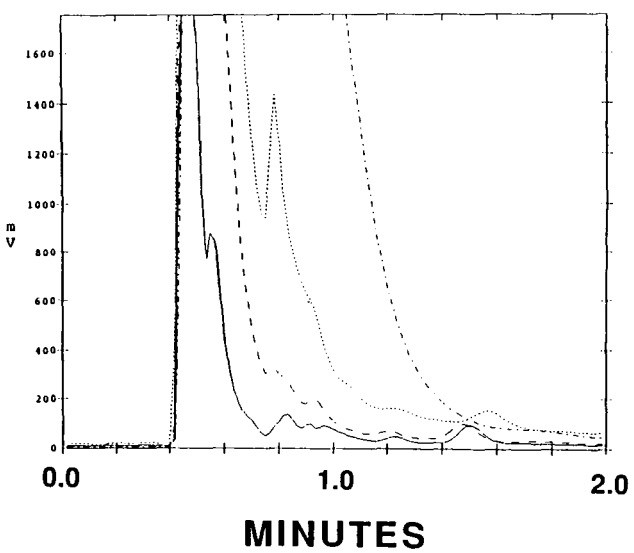

Fig. 6. Change in the serum chromatogram of 10-μl of spiked bovine serum during the first lifetime study (no guard column). Injection number 1 (———), 30 (– – –), 200 (·····) and 490 (– · – · –) are shown. Eluent, 50 m*M* SDS in methanol–water (30:70). Ordinate scale: 1.75 a.u.f.s. Other conditions as in Fig. 3.

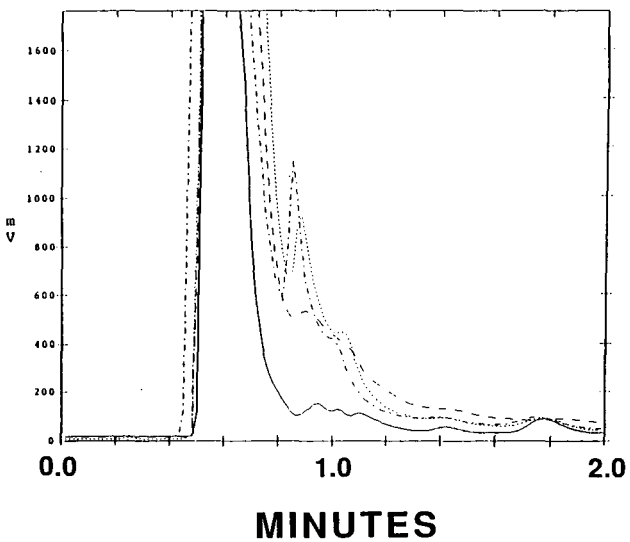

Fig. 7. Change in serum chromatogram of 10 μl of spiked bovine serum during the second lifetime study (with μBondapak Phenyl Guard Pak cartridge). Injections number 1 (———), 30 (– – – –), 200 (·····) and 863 (– · – · –) are shown. Conditions as in Fig. 6.

serum albumin, other serum components (*e.g.* lipids or proteins other than serum albumin) might be strongly retained. In other direct serum injection studies, backpressure problems observed with the use of aqueous–organic eluents have been attributed to buildup of serum lipids and related compounds [16], and guard columns have been used successfully to improve performance. Thus, Pinkerton *et al.* [3] were able to substantially extend the lifetime of the analytical column in their direct serum injection studies when a guard column was included in the system.

The system used in the first lifetime study was modified to include a μBondapak Phenyl Guard Pak cartridge between the in-line filter and analytical column. The serum samples were handled identically, and a second lifetime study was begun with a fresh μBondapak Phenyl analytical column. The Guard Pak cartridge was replaced with a fresh cartridge after each 50–100 injections, although the cartridges could perhaps have been used much longer.

The effect of the Guard Pak cartridge in controlling the width of the serum peak is clear in the chromatograms presented in Fig. 7. Some broadening was observed during the first few injections, but beyond about the 30th injection the serum peak profile changed relatively little until the termination of the study at 880 injections. Retention time precision improved to 2.1–2.4% R.S.D. for the drug peaks, and the width of those peaks was considerably more stable than in the first lifetime study. After about 830 injections, system backpressure problems began to appear, and efforts to prolong the study were ineffective. Changes of the column inlet and outlet frits and reversal of the direction of flow provided only short-term improvements. Nonetheless, we were encouraged by the ability to perform over 800 injections of serum without significant loss in chromatographic performance for CBZ and CBE.

In the first two lifetime studies, CBZ and CBE were present in the spiked bovine

serum at relatively high levels to simplify detection and to maintain a focus on column longevity. Building upon the results of these two studies, a lifetime study was then conducted using bovine serum spiked with clinical levels of CBZ and CBE. All other conditions were as in the second study. As was noted above, the use of 214 nm as a detection wavelength is required for the quantitation of CBE but leads to a chromatogram which is dominated by the serum peak tail. Nonetheless, peak areas can be easily obtained with the integration software, which permits tangent skimming on a sloped linear baseline. We were able to perform 900 injections (10-μl) of spiked bovine serum before it was necessary to terminate the study due to backpressure problems and excessive analyte peak broadening.

For the retention time, relative standard deviations of 2.0% (CBE) and 2.9% (CBZ) were obtained. This is comparable with the results of the second lifetime study. More importantly, peak area precisions were disappointing at 10.0% (CBE) and 8.0% (CBZ), although there was no overall trend in either the retention or peak area data. While the reason for the relatively high R.S.D. values for peak area is unknown, one possibility is difficulty of reproducible integration due to the large serum peak tail. To allow the analysis of CBZ and CBE peaks on a flat baseline, we investigated column switching strategies which would permit the majority of the serum peak to be sent to waste prior to the analysis.

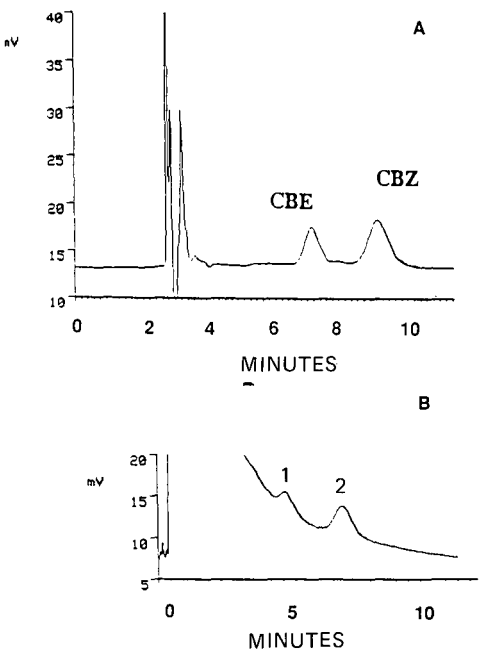

Fig. 8. Comparison of column switching method to non-column switching method. Chromatogram A was of a 10-μl sample of spiked bovine serum obtained with the column switching method. Valve position for the six-port valve was changed at 2.0 min. Loading eluent: 5 m*M* SDS in water. Guard column: μBondapak Phenyl Guard Pak cartridge. Analysis eluent and column as in Fig. 6. Flow-rate: 2 ml/min. Ordinate scale: 0.03 a.u.f.s. Chromatogram B represents injection 379 of the third lifetime study with direct sample injection and no column switching. Ordinate scale: 0.015 a.u.f.s. Other conditions as in Fig. 6. Injection volume, 10 μl containing 2.0 μg/ml of CBE (peak 1) and 4.8 μg/ml of CBZ (peak 2).

Column switching

Because the serum peak is eluted near the column void volume with the SDS-containing eluents discussed here, it is a relatively simple matter to design a sample cleanup strategy which will remove the majority of the serum peak from the chromatogram. The column switching cleanup strategy consists of two steps (see Fig. 1). In the loading step, the sample is injected into a μBondapak Phenyl Guard Pak cartridge, using an aqueous SDS-containing loading eluent. Most of the serum peak is eluted to waste in this step, while the drugs are strongly bound. In the analysis step, the Guard Pak cartridge is backflushed with the analysis eluent (in this case, the same eluent was used in the lifetime studies). The methanol-containing analysis eluent elutes the drugs from the Guard Pak cartridge into the analysis column, leading to the chromatogram shown in Fig. 8A. This is contrasted to the typical chromatogram obtained with direct injection using no column switching shown in Fig. 8B.

As desired, the baseline in Fig. 8A is flat in the region where the drug peaks are eluted, and the serum peak appears to be almost completely removed. Note that the 5 m*M* SDS loading eluent for this analysis contains surfactant at a concentration below the CMC, in keeping with our previous findings that micelles are not a requirement for direct serum injection. Given the absence of serum-related peaks in the analytical chromatogram (Fig. 8A), it may be possible to reduce or even eliminate the SDS component of the analysis eluent as well. This would improve column efficiency, according to Table I. The use of other organic modifiers to modify selectivity should also be possible.

In a preliminary column switching lifetime study with 200 injections, the same chromatographic performance as shown in Fig. 8A was maintained. Work is currently underway in our laboratory to select the best combination of guard column and analysis column, and to determine the column lifetime and stability of retention time and peak area that can be expected for an optimized column-switching strategy.

REFERENCES

1 D. Westerlund, *Chromatographia,* 24 (1987) 155.
2 Z. K. Shihabi, *J. Liq. Chromatogr.*, 11 (1988) 1579.
3 T. C. Pinkerton, T. D. Miller, S. E. Cook, J. A. Perry, J. D. Rateike and T. J. Szczerba, *Biochromatogr.*, 1 (1986) 96.
4 D. J. Gisch, B. T. Hunter and B. Feibush, *J. Chromatogr.*, 433 (1988) 264.
5 C. Desilets and F. E. Regnier, presented at the *12th International Symposium on Column Liquid Chromatography, Washington, DC, June 19–24, 1988,* poster WP 326.
6 H. Yoshida, K. Takano, I. Morita, T. Masujima and H. Imai, *Jpn. J. Clin. Chem.*, 12 (1983) 312.
7 J. A. Adamovics, *J. Pharm. Biomed. Anal.*, 5 (1987) 267.
8 J. Haginaka, N. Yasuda, J. Wakai, H. Matsunaga, H. Yasuda and Y. Kimura, *Anal. Chem.*, 61 (1989) .2445.
9 L. J. Cline Love, S. Zibas, J. Noroski and M. Arunyanart, *J. Pharm. Biomed. Anal.*, 3 (1985) 511.
10 L. J. Cline Love and M. Arunyanart, *J. Chromatogr.*, 342 (1985) 293.
11 K. B. Sentell, J. F. Clos and J. G. Dorsey, *Biochromatogr.*, 4 (1989) 35.
12 R. A. Grohs, F. V. Warren, Jr. and B. A. Bidlingmeyer, *Anal. Chem.*, in press.
13 B. A. Bidlingmeyer, *J. Chromatogr. Sci.*, 18 (1980) 525.
14 R. Hartley, M. Lucock, W. I. Forsythe and R. W. Smithells, *J. Liq. Chromatogr.*, 10 (1987) 2393.
15 L. Bowers, University of Minnesota at Minneapolis, personal communication.
16 T. Arvidsson, K. G. Wahlund and N. Daoud, *J. Chromatogr.*, 317 (1984) 213.

Journal of Chromatography, 535 (1990) 305–309
Elsevier Science Publishers B.V., Amsterdam

CHROMSYMP. 2058

Micro-scale liquid chromatographic method for the determination of bamifylline and its major metabolite in human plasma

FLAVIO BELLIARDO*
Dipartimento di Scienza e Tecnologia del Farmaco, Facoltà di Farmacia, Università di Turin, Via P. Giuria 9, 10125 Turin (Italy)
and
CLAUDIO LUCARELLI
Istituto Superiore di Sanità, Viale Regina Elena 229, 00161 Rome (Italy)

ABSTRACT

A sensitive micro-scale method based on isocratic elution reversed-phase ion-pair chromatography for the determination of bamifylline and its major metabolite (AC 119) in human plasma is described. The method is based on a liquid–liquid extraction clean-up followed by analysis on an LC-Packings Fusica (Delta Pak, RP-18, 5 μm, 300 Å) column (15 cm × 330 μm, I.D.) with 0.03 *M* heptanesulphonate (pH 3.5)–acetonitrile (7:3, v/v) as the mobile phase. Data with respect to recovery, reproducibility and limits of detection are reported and discussed.

INTRODUCTION

Bamifylline (Fig. 1a), a 7,8-disubstituted derivative of theophylline with bronchodilatator properties, is used in the treatment of asthma and reversible airway

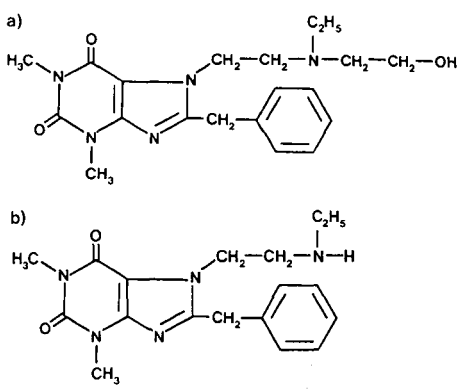

Fig. 1. Structures of (a) bamifylline and (b) metabolite AC-119.

0021-9673/90/$03.50

obstructions. The drug exhibits distinct metabolic and pharmacokinetic charcteristics, which differ markedly from those of theophylline. In earlier investigations on the pharmacokinetic behaviour of bamifylline, only a sophisticated mass fragmentographic technique was able to determine the very low plasma concentrations in the terminal range of the elimination curve.

The aim of this study was to develop a sensitive micro-scale method based on isocratic elution reversed-phase ion-pair chromatography to detect, in the nanomole range, bamifylline and its major metabolite (AC 119) (Fig. 1b) in human plasma.

EXPERIMENTAL

Samples

Four young, healthy volunteers (two men and two women) with a mean age of 27.3 ± 2.5 years, mean weight 65.4 ± 10.4 kg and mean height 170.4 ± 6.4 cm took part in the study. All the subjects received 300 mg of bamyfylline twice a day for 6 days (a total of 12 doses of 600 mg). Blood specimens for drug monitoring were obtained 1, 2, 4, 8 and 10 h after the first and at the last dose and the end of each dosing period (12th hour).

Sample preparation

A simple liquid–liquid extraction technique was used for both clean-up and extraction [1]. To a 1-ml sample of plasma in a 10-ml Teflon-lined screw-capped glass tube were added 0.2 ml of 2 *M* HCl and 4 ml of dichloromethane–diethyl ether (4.7, v/v). After vortex mixing and centrifugation (10 min, 1000 *g*), the upper layer was discarded and 0.1 ml of 5 *M* sodium hydroxide solution and 5 ml of dichloromethane–diethyl ether (4:7, v/v) were added to the aqueous layer. The tubes were shaken and then centrifuged at 1000 *g* for 10 min. The upper phase was carefully transferred into a 10-ml conical vial and the organic solvent was evaporated to a volume of *ca.* 0.5 ml under a stream of nitrogen at 35°C. The residue was then transferred into a 0.5-ml conical vial and evaporated to dryness. The dry residue was reconstituted in 100 μl of methanol.

Extraction efficiency

Spiked plasma samples ($n=4$) containing 60, 90, 120 and 150 ng/ml of bamifylline were extracted according to the procedure described under *Sample preparation*. The peak areas in these samples were then compared with those obtained from unextracted bamifylline standard solutions with comparable concentrations.

Standard solutions

Bamifylline and AC 119 (metabolite of bamifylline) standards were provided by Alfa Farmaceutici (Bologna, Italy) and were used without further purification. Stock solutions of bamifylline and AC 119 (150 μg/ml) were prepared by dissolving 215 mg of each standard, exactly weighed on a Cahn Model G2 electrobalance, in water purified using a Water I system (Gelman Ann Arbor, MI, U.S.A.) and diluted to volume in a 100-ml volumetric flask.

Apparatus

The liquid chromatographic (LC) system consisted of the following components: a Carlo Erba (Milan, Italy) Phoenix 20 CU micro-pump, a Kontron (Zurich, Switzerland) Model 433 UV capillary detector, equipped with an ultrasensitive UV flow cell (total volume 90 nl, optical path length 20 mm), a Valco (Houston, TX, U.S.A.) Model C14W injector with a 200-nl internal loop and an HP 9000 Series 300 work-station (Hewlett-Packard, Avondale, PA, U.S.A.) equipped with an HP 7440A plotter.

Chromatographic conditions

A Fusica (Delta Pak, RP-18,5 μm, 300 Å) column (15 cm × 330 μm I.D.) (LC-Packings international, Amsterdam, The Netherlands) was used. The column was connected directly to the injector, and the column outlet capillary was connected directly to the flow cell via a small piece of Teflon tubing (Teflon tubing kit, TF-K1, LC-Packings International).

The separations reported were achieved under the following conditions: mobile phase, 0.03 *M* heptanesulphonate (pH 3.5)–acetonitrile (70:30, v/v); flow-rate, 8 μl/min; chart speed, 0.5 cm/min; temperature, 20°C; and detection wavelength, 210 nm.

The amounts of bamifylline and AC119 were calculated by applying the external standard method.

RESULTS AND DISCUSSION

Mobile phase selection was crucial for achieving the desired sensitivity and resolution. In preliminary experiments various C_5–C_8 alkanesulphonates were investigated as ion-pair reagents. The relationship between the chain length of the alkanesulphonate and the retention of bamifylline and AC 119 was studied. For a given mobile phase, as the chain length of the pairing reagent increased, so did the capacity factor (k'). In agreement with reported data [1], the influence of counter-ion

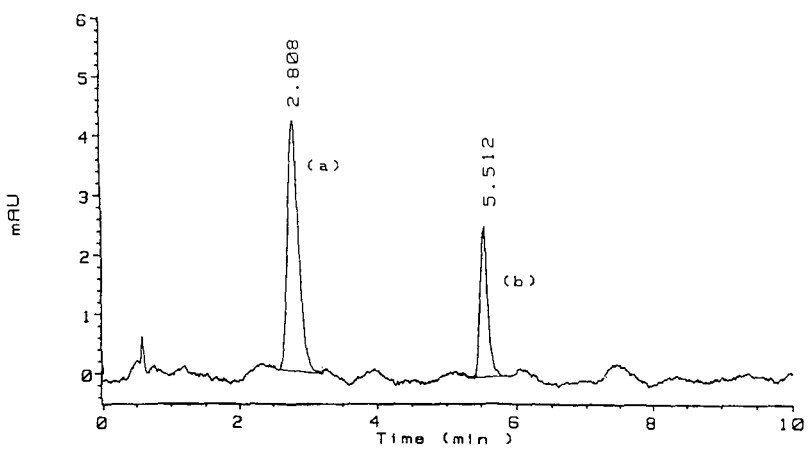

Fig. 2. Chromatograms of (a) bamifylline (20 ng) and (b) AC 119 (15 ng) standards. For conditions, see text.

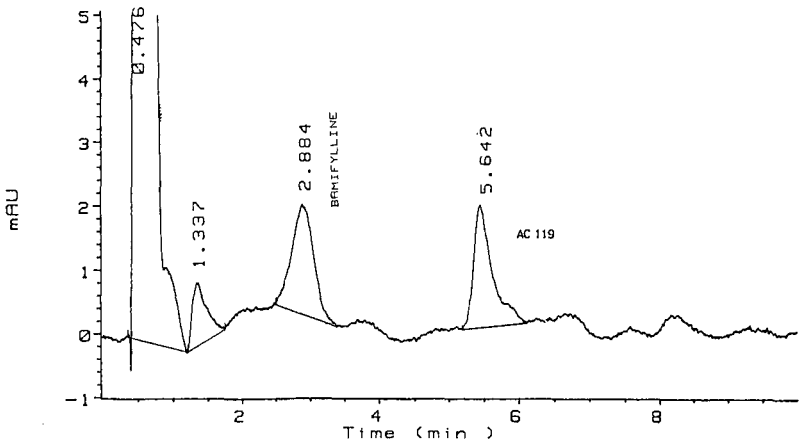

Fig. 3. Chromatogram of bamifylline and AC119 in plasma, 12 h after the oral administration of a 600-mg dose of bamifylline. For conditions, see text.

size on the selectivity factor (α) for bamifylline and AC119 showed a relative improvement with an increase in the chain length of the pairing reagent. Based on the selectivity and the total analysis time, heptanesulphonate was selected as the ion-pair reagent in the mobile phase. Preliminary experiments did not reveal that the presence of salts (potassium clhoride or sodium sulphate) in the mobile phase resulted in better resolution and peak asymmetry.

Example of chromatograms resulting from the LC assay of bamifylline and AC119 in plasma are shown in Figs. 2 and 3. With the solvent system used, the Fusica column was found to give sharp, symmetrical peaks and good selectivity. No interference with the retention times of the analyte peaks due to endogenous components was observed. In agreement with published data [2,3], the highest plasma levels of bamifylline were always reached about 1 h after dosing; 18 h after the last dose, the plasma concentrations of bamifylline and AC119 showed variations in each subject; the lowest value detected was 12 ng/ml.

The overall precision of the retention time was studied with respect to run-to-run and day-to-day variations. The run-to-run precision [relative standard deviation (R.S.D.)] for 20 runs within a single day averaged 1.66% and the day-to-day precision over a 3-week period with the same column was slightly higher, *ca.* 2.75%.

Calibration graphs were obtained by analysing spiked plasma samples over bamifylline and AC 119 concentration ranges of 30–900 and 40–1000 ng/ml, respectively. The least-squares regression fit showed good linearity (correlation coefficient = 0.998) for both bamifylline and AC 119. The intra- and inter-assay recoveries of bamifylline from spiked plasma sample were 90.3% with an R.S.D. of 2.8% and 92.1% with an R.S.D. of 3.4% (both 250 ng/ml, $n = 10$), respectively. The detection limits, with a signal-to-noise ratio of 3, were 12 ng for bamifylline and 9 ng for AC 119.

A storage stability study showed a slow decrease in bamifylline concentrations in both refrigerated and frozen plasma samples. The refrigerated sample showed little

loss after 4 weeks, but by week 8 the concentration of bamifylline in these samples had decreased by 11–15%. The same trend was observed with frozen plasma, but a significant decrease in bamifylline was found later (week 10).

In conclusion, the proposed method offers high selectivity and sensitivity for the determination of bamifylline and its major metabolite AC 119 in human plasma. This LC method, with a simple clean-up step, is suitable for pharmacokinetic studies.

ACKNOWLEDGEMENT

The authors are grateful to Alfa Farmaceutici (Bologna, Italy) for providing pure standards of bamifylline and AC 119.

REFERENCES

1 G. Nicot, G. Lachatre, C. Gonnet, J. L. Rocca, J. P. Valette, L. Merle and Y. Nouaille, *J. Chromatogr.*, 277 (1983) 239.
2 L. Dodion, Ph. Dusart, P. Temmerman, *Arzneim.-Forsch.*, 19 (1969) 785.
3 J. B. Fourtillan, M. A. Lefebvre, I. Ingrand, F. Patte, F. Boita and M. M. Ouechni, *Thérapie*, 38 (1983) 647.

Journal of Chromatography, 535 (1990) 311–316
Elsevier Science Publishers B.V., Amsterdam

CHROMSYMP. 2057

Determination of phenol, *m*-, *o*- and *p*-cresol, *p*-aminophenol and *p*-nitrophenol in urine by high-performance liquid chromatography

AUGUSTA BREGA
Laboratorio Biomed, Via delle Camerate 11, Concesio (BS) (Italy)
PAOLO PRANDINI* and CARLO AMAGLIO
SPE Sistemi e Progetti Elettronici, Via Gualla 48, Brescia (Italy)
and
EMILIO PAFUMI
Laboratoria Biomed, Via delle Camerate 11, Concesio (BS) (Italy)

ABSTRACT

A method for the biological monitoring of human exposure to aromatic hydrocarbons, nitrocompounds, amines and phenols has been developed. Phenol, cresols, *p*-aminophenol, *p*-nitrophenol and their glucorono- or sulpho-conjugates, were quantified by HPLC; 4-chlorphenol was added as internal standard. After enzymatic hydrolysis, the free compounds were extracted with an organic solvent and analyzed by an isocratic HPLC Perkin Elmer system at ambient temperature and at a flow-rate of 1 ml/min. The column was a reversed-phase Pecosphere 3 × 3 C_{18} Perkin Elmer; the mobile phase was a 30:70:0.1 (v/v/v) methanol–water–orthophosphoric acid mixture and the chromatogram was monitored at 215 nm. Identification was based on retention time and quantification was performed by automatic peak height determination, corrected for the internal standard.

The recovery was *ca.* 95% for phenol and cresols; 90% for *p*-nitrophenol; 85% for *p*-aminophenol; the coefficients of variance were $<6\%$ within analysis ($n=20$) and $<10\%$ between analysis ($n=20$). The detection limits, at a signal/noise ratio of 2, were 0.5 mg/l for phenol and cresols and 1 mg/l for *p*-aminophenol and *p*-nitrophenol.

INTRODUCTION

Urinary phenol, cresols, *p*-nitrophenol and *p*-aminophenol are biological indicators of human exposure to aromatic hydrocarbons, nitro compounds, amines and phenols. Phenol, cresols and their glucurono or sulpho conjugates are excreted in urine by workers exposed to phenol and cresols. About 30% of retained benzene also gives rise to phenol *in vivo*. Therefore, the measurement of excreted urinary phenol has applications in the evaluation of exposure [1].

The determination of urinary cresols (particularly *o*-cresol) has been proposed [2,3] as a biological monitoring method for toluene. However, only a small fraction of the inhaled vapour is oxidized at the aromatic ring with the production of cresols. The

0021-9673/90/$03.50

urinary concentration of *p*-nitrophenol has been proposed for assessing the exposure to nitrobenzene [4], which is used in many industrial processes, mainly handled in solution, the skin being the principal route of exposure [5]. *p*-Aminophenol excretion in urine is a biological indicator of exposure to aniline [6], which is readily absorbed through the skin as either a liquid or vapour.

Several methods have been developed for the determination of free and conjugated phenolic biological indicators, especially spectrophotometry and gas chromatography [7,8]. Gas chromatographic methods are specific and precise when used with an internal standard [9]. Many workers have developed gas chromatographic methods for the determination of urinary phenol, cresols, *p*-nitrophenol and *p*-aminophenol [10–18]. However, published gas chromatographic methods suffer from a number of problems.

Pretreatment of samples is necessary to hydrolyse the conjugated compounds and then extract the compounds of interest. Better results can be obtained by distillation of the specimen after acidification and direct analysis of the aqueous distillate by gas chromatography [19] high-performance liquid chromatography (HPLC), but this is time consuming and laborious. Enzymatic hydrolysis seems to be the method of choice, taking into consideration the relative volatility of phenols, but the addition of a protein matrix introduces the need for another extraction.

The purpose of this study was to determine urinary phenol, cresols, *p*-nitrophenol and *p*-aminophenol by using a reversed-phase HPLC system with an isocratic mobile phase. Enzymatic hydrolysis and extraction of the compounds of interest with an organic solvent are followed by return to the alkaline aqueous phase and HPLC.

EXPERIMENTAL

Materials

The following standard solutions were used: 4-aminophenol, *o*-cresol, *p*-cresol, *m*-cresol, 4-methoxyphenol and phenol from Merck (Darmstadt, F.R.G.), 4-nitrophenol from BDH (Poole, U.K.) and *p*-chlorophenol from Fluka (Buchs, Switzerland). Acetic acid, ethyl acetate, hydrochloric acid, orthophosphoric acid, sodium hydroxide pellets, dichloromethane, methyl ethyl ketone from Merck, HPLC-grade methanol from Fluka and β-glucuronidase–arylsulphatase (*Helix pomatia*) from Boehringer (Mannheim, F.R.G.) were used. The urine control Lyphochek level 1 was obtained from Bio-Rad Labs. (Anaheim, CA, U.S.A.).

Apparatus

Chromatographic separation and peak detection of urinary phenol, cresols, *p*-nitrophenol and *p*-aminophenol were carried out on a Pecosphere 3 × 3 C_{18} reversed-phase column, 3 μm packing, 3.3 cm × 4.6 mm (Perkin-Elmer, Norwalk, CT, U.S.A.) with a Perkin-Elmer HPLC system with a Series 10 LC pump and an LC 90 UV ultraviolet spectrophotometric detector coupled to an integrator developed by SPE Sistemi e Progetti Elettronici (Brescia, Italy). The mobile phase was methanol–water–orthophosphoric acid (30:70:0.1, v/v/v) at flow-rate of 1.0 ml/min.

Methods

The urine specimens were obtained from healthy men and from workers exposed

in a workshop and were kept in dark, well closed containers. Stock standard solutions were prepared by dissolving known amounts of phenol and cresols in methanol, *p*-nitrophenol and *p*-aminophenol in water to obtain a 1 g/l concentration and kept in dark, well stoppered glass bottles. Whereas the stock solutions of phenol and cresols remain stable for 30 day at 4°C, those of *p*-aminophenol and *p*-nitrophenol were prepared immediately before use. Working standard solutions were prepared by diluting the stock standard solutions with water.

The enzymatic hydrolysis of each sample or standard (2 ml in test-tubes with screw caps at pH 5 in 1 *M* acetate buffer) was carried out with β-glucuronidase–arylsulphatase for 12 h at 37°C. The internal standard, *p*-chlorophenol, was added to all samples at a final concentration of 50 mg/l. After hydrolysis, phenol, cresols and *p*-nitrophenol were extracted by vortex mixing the samples (acidified to pH 2 with hydrochloric acid) with 4 ml of dichloromethane, and *p*-aminophenol at pH 5 with 4 ml of methyl ethyl ketone.

After centrifugation at 2400 *g* for 15 min, 2.5 ml of each organic extract was transferred into another test-tube, 0.5 ml of 0.2 *M* sodium hydroxide solution were added and, by vortex mixing, the compounds returned to the aqueous phase. An aliquot (0.3 ml) of the alkaline phase was transferred to the final test-tube and brought to pH 7.0 with hydrochloric acid; 10 µl of this solution were injected at room temperature into the HPLC system; the mobile phase was methanol–water–orthophosphoric acid (30:70:0.1, v/v/v) and the chromatogram was monitored at 215 nm. Identification was based on retention times, and quantification was performed by automatic peak-height determination, corrected for the internal standard.

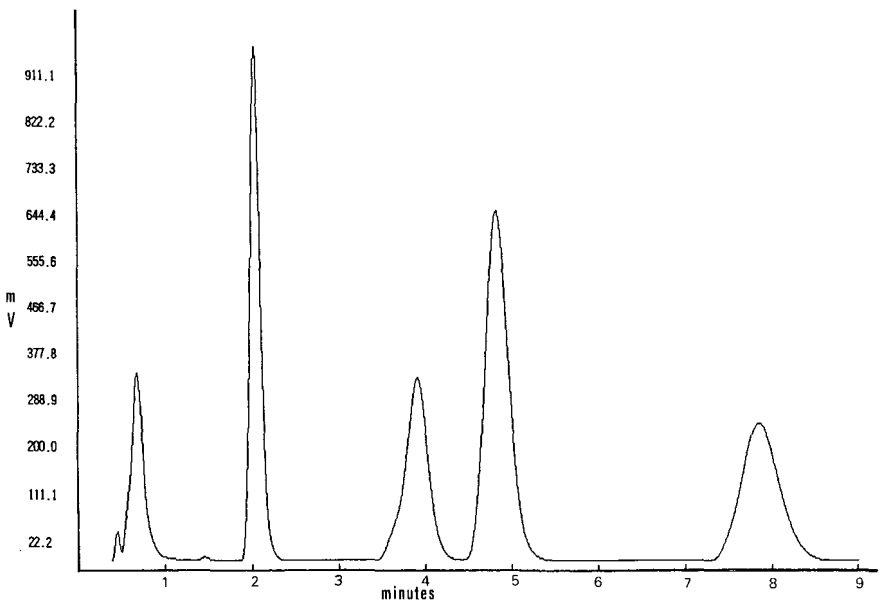

Fig. 1. Chromatographic elution (from left to right) of *p*-aminophenol, phenol, *p*-nitrophenol, cresols and internal standard (*p*-chlorophenol). Column, Pecosphere 3 × 3 C_{18} reversed-phase column (Perkin-Elmer); mobile phase, methanol–water–orthophosphoric acid (30:70:0.1, v/v/v); room temperature; injection volume, 10 µl; detection at 210 nm.

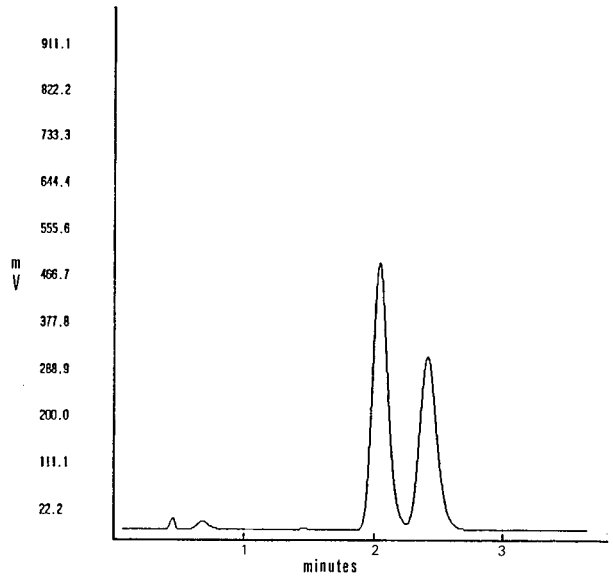

Fig. 2. Chromatographic elution of phenol and *p*-methoxyphenol, with retention times of 2.02 and 2.39 min respectively. Detector signals, 509.3 and 330.1 mV.

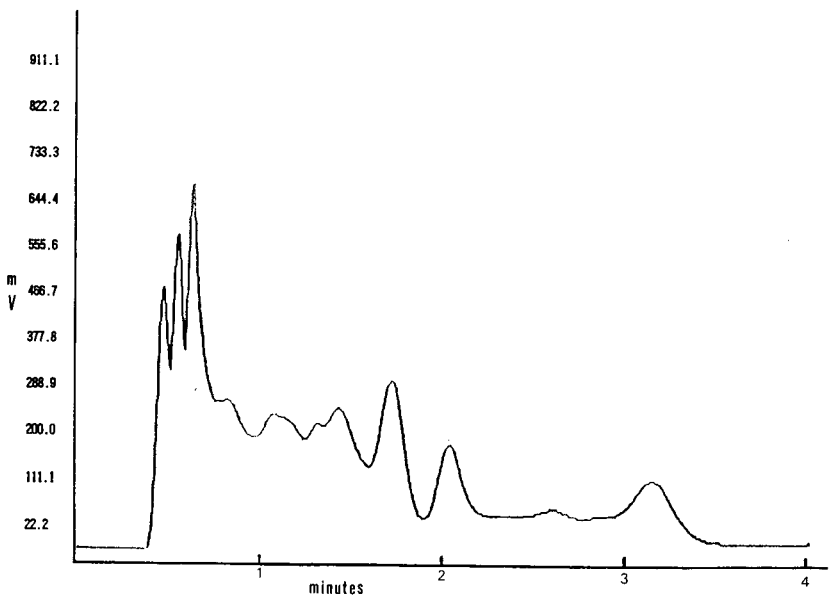

Fig. 3. Determination of phenol in urine control Lyphochek level 1. The retention time is 2.02 min; detector signal, 193.8 mV.

RESULTS AND DISCUSSION

The retention times of *p*-aminophenol, phenol, *p*-nitrophenol and cresols were 0.40, 2.02, 3.54, 4.49 and 7.40 min, respectively (Fig. 1). *p*-Methoxyphenol, used in pharmaceutical preparations, does not interfere with phenol (Fig. 2). *o*-Cresol, *m*-cresol and *p*-cresol have identical retention times.

Background absorptions in urine specimens obtained from healthy, unexposed men contained negligible amounts of *p*-amino and *p*-nitrophenol. However, for phenol, we obtained concentration values < 10 mg/l (40 samples), in good agreement with the data from gas chromatographic methods [9,11].

The calibration graphs for phenol, cresols, *p*-nitrophenol and *p*-aminophenol in water were linear up to at least 50 mg/l. The precision of the method was satisfactory, with relative standard deviations of $< 6\%$ within analyses ($n = 20$) and $< 10\%$ between analyses ($n = 20$). The recovery was *ca.* 95% for phenol and cresols, 90% for *p*-nitrophenol and 85% for *p*-aminophenol. Solutions of phenol, cresols, *p*-nitrophenol and *p*-aminophenol were diluted to give concentrations of 0.5 mg/l in water (phenol and cresols) and 1 mg/l in normal urine samples (*p*-amino- and *p*-nitrophenol), hydrolysed and extracted as usual. We calculated the detection limits, at a signal-to-noise ratio of 2, to be 0.5 mg/l for phenol and cresols and 1 mg/l for *p*-amino and a*p*-nitrophenol.

We examined urine samples from workers exposed to phenol and benzene; the results obtained in at least 500 samples examined were less than biological limits of exposure adopted by ACGHI 1987/88 [20].

Urine control Lyphochek level 1 (Fig. 3) is used in assessing the accuracy and precision of assay procedures; the experimental concentrations obtained for phenol ($n = 230$) were in the range 10.8–17.2 mg/l, which compared well with the target values for phenol by HPLC of 10.4–17.4 mg/l.

ACKNOWLEDGEMENTS

The authors thank Dr. C. Lucarelli, Istituto Superiore di Sanità, Rome, and Professor B. D. Prandini, Spedali Civili, Brescia, for helpful suggestions.

REFERENCES

1 E. De Rosa and G. B. Bartolucci, presented at *Società Italiana di Medicina del Lavoro e Igiene Industriale 48° Congresso Nazionale, Pavia, September 18–21, 1985*, Monduzzi Editore SPA, Bologna, 1985, p. 473.
2 J. Angerer, *Int. Arch. Occup. Environ. Health*, 43 (1979) 63.
3 W. Woiwode and K. Drysch, *Br. J. Ind. Med.*, 38 (1981) 194.
4 R. J. Levine, M. J. Turner, Y. S. Crume, M. E. Dale, T. B. Starr and D. E. Rickert, *J. Occup. Med.*, 27 (1985) 627.
5 R. L. Bronaugh and H. I. Maiback, *J. Invest. Dermatol.*, 84 (1985) 180.
6 *Early Detection of Occupational Diseases*, WHO, Geneva, 1986.
7 H. Buckwald, *Ann. Occup. Hyg.*, 9 (1966) 7.
8 J. J. Docter and R. L. Zielhuis, *Ann. Occup. Hyg.*, 10 (1967) 317.
9 J. P. Buchet, R. Lauwerys and M. Cambier, *J. Eur. Toxicol.*, 1 (1972) 27.
10 O. M. Bakke and R. R. Sheline, *Anal. Biochem.*, 27 (1969) 451.
11 S. M. Dirmikis and A. Darbre, *J. Chromatogr.*, 94 (1974) 169.
12 J. Lebbe, J. P. Lafarge and R. A. Menard, *Arch. Mal. Prof. Hyg. Toxicol. Ind.*, 27 (1966) 565.
13 A. B. Van Haaften and S. T. Sie, *Am. Ind. Hyg. Assoc. J.*, 26 (1965) 52.

14 R. Lauwerys, in L. Alessio, A. Berlin, M. Boni, R. Roi (Editors) *Biological Indicators for the Assessment of Human Exposure to Industrial Chemicals,* Commission of the European Communities (C. E. C.), Luxembourg, 1988, p. 3.
15 J. Angerer and K. Behling, *Int. Arch. Occup. Environ. Health.*, 48 (1981) 137.
16 G. Bouley, A. Dubreuil and J. Godin, *Ann. Occup. Hyg.*, 19 (1976) 27.
17 J. Piotrowski, *Br. J. Ind. Med.*, 24 (1967) 60.
18 P. Apostoli, F. Brugnone, L. Perbellini, V. Cocheo, M. L. Bellomo and R. Silvestri, *Int. Arch. Occup. Environ. Health*, 50 (1982) 153.
19 P. B. Van Roosmalen, J. Purdham and I. Drummond, *Clin. Chem.*, 26 (1980) 1059.
20 V. F. Thomas, P. O. Droz, L. K. Lowry, J. T. Pierce, J. Rosenberg and J. W. Yager, *Threshold Limit Values for Chemical Substances in the Work Environment,* ACGIH (American Conference of Governmental Industrial Hygienists), Cincinnati, OH, 1987, p. 53.

Journal of Chromatography, 535 (1990) 317–323
Elsevier Science Publishers B.V., Amsterdam

CHROMSYMP. 2045

Rapid and sensitive detection of citrinin production during fungal fermentation using high-performance liquid chromatography

ROBERT B. VAIL and MICHAEL J. HOMANN*
Department of Microbiological and Cell Culture Development, Schering-Plough Corporation, 1011 Morris Avenue, Union, NJ 07083 (U.S.A.)

ABSTRACT

A rapid and sensitive assay was developed for the detection of the mycotoxin citrinin by reversed-phase chromatography. Citrinin was eluted from a radial-compression C_{18} column with a retention time of 3.86 min (flow-rate of 2.5 ml/min) with acetonitrile–water–acetic acid (40:59:1) containing tetrabutylammonium phosphate (0.025 *M*). Comparative analysis revealed fluorescence detection to be 100 times more sensitive than detection by conventional ultraviolet absorbance. The fluorescence excitation and emission maxima of citrinin were 330 and 500 nm, respectively. The assay was linear over the concentration range between 0.01–100 μg/ml. Recovery experiments conducted by addition of citrinin to fermentation samples, revealed the assay quantitation efficiency to be 91–102%. Assay utility was demonstrated by using an *Aspergillus niveus* culture, propagated in complex liquid medium. Citrinin production was detected as early as 20 h following inoculation and increased dramatically when the culture entered the stationary phase of growth, analogous to other secondary metabolites. Unlike previously reported methods, this procedure has the advantage of enabling the direct quantitative analysis of citrinin in crude microbial fermentations without sample extraction.

INTRODUCTION

Citrinin is a mycotoxin, produced by several species of the genera *Aspergillus* and *Penicillium* [1,2]. This secondary metabolite has been characterized as a pentaketide, synthesized from acetyl- and malonyl-coenzyme A [3,4]. Although acetyl- and malonyl-coenzyme A are commonly associated with fatty acid synthesis, these primary metabolic precursors can be utilized in a polycondensation reaction to form polyketide rings which are modified to yield a variety of secondary metabolites [3,4]. Early investigations with citrinin revealed that this compound is toxic to bacteria, fungi and protozoa [3–8]. Despite the apparent broad antimicrobial activity, therapeutic applications involving citrinin are not possibile, since citrinin has been shown to cause acute tubular necrosis in kidney [9] and impaired liver function [10].

The formation of citrinin by various fungi that contaminate feed grains has been implicated as a causative agent in renal disease and death of swine, poultry, and possibly humans [2]. An additional potential hazard may also involve therapeutics

0021-9673/90/$03.50

derived from fungal fermantations. Propagation of fungi in various complex liquid media has been reported to elicit citrinin synthesis [11,12]. Consequently, citrinin analysis of fungal fermentations, utilized for the synthesis of therapeutic drugs, is imperative and requires the development of sensitive assay methodology. This paper describes a rapid reversed-phase high-performance liquid chromatography (HPLC) assay. This assay allows the highly sensitive fluorescence detection of citrinin in crude microbial fermentation samples without the need for sample extraction.

EXPERIMENTAL

Materials

Acetonitrile and methanol (HPLC grade) and reagent-grade acetic acid were purchased from Fisher Scientific (Springfield, NJ, U.S.A.); tetrabutylammonium phosphate was from Waters (Milford, MA, U.S.A.); citrinin, $MgSO_4 \cdot 7H_2O$, $ZnSO_4 \cdot 7H_2O$, KH_2PO_4, L-lysine and glycerol were from Sigma (St. Louis, MO, U.S.A.); cerelose (90% D-glucose, 10% H_2O) was from Corn Products (Englewood Cliffs, NJ, U.S.A.); tastone-154 (yeast extract) from Universal Food Corp. (Milwaukee, WI, U.S.A.); and Bacto-agar from Difco Labs. (Detroit, MI, U.S.A.).

Culture growth conditions

Aspergillus niveus strain ATCC 56745 was obtained form the American Type Culture Collection (Rockville, MD, U.S.A.). *A. niveus*, a known producer of citrinin [13], was propagated by inoculating conidia onto agar slants of complex medium, containing 2.0% cerelose, 1% tastone-154, 0.25% KH_2PO_4, 0.1% L-lysine, 0.025% $MgSO_4 \cdot 7H_2O$, 0.005% $ZnSO_4 \cdot 7H_2O$, 0.5% glycerol and 2% agar. The pH of the medium was adjusted to 5.2 with 1 *M* HCl prior to heat sterilization. Culture slants for the generation of conidia were incubated at 34°C. Liquid fermentation cultures were grown by inoculating 100 ml (300-ml erlenmeyer flask) of complex medium with conidia ($1 \cdot 10^6$/ml), harvested from 7–10-day-old culture slants. Cultures were grown at 30°C with an agitation rate of 250 rpm (G-52 shaker, New Brunswick Scientific, Edison, NJ, U.S.A.).

HPLC assay

HPLC analysis of citrinin was performed utilizing the following Waters HPLC equipment: Model 600E pump, Model 710B WISP, Model 481 ultraviolet detector, Model 990 photodiode-array detector, Model 470 scanning fluorescence detector (16-μl flow-cell), and a Model 745 integrator. Isolation of citrinin was achieved on a Waters Radial-Pak 4-μm C_{18} analytical column (diameter, 8 mm), with a C_{18} μBondapak precolumn, inserted in-line upstream of the column. The injection volume was 10 μl for all experiments. Only deionized distilled water was used for the preparation of mobile phase solutions. The mobile phase contained acetonitrile–water–acetic acid (40:59:1) and tetrabutylammonium phosphate (0.025 *M*), which was filtered through a 0.45-μm hydrophobic membrane (Millipore, Milford, MA, U.S.A.) prior to use. The eluent was degassed during chromatography by constant sparging with helium (5 ml/min). The flow-rate was 2.5 ml/min.

An ultraviolet absorbance scan of citrinin was obtained with the photodiode-array detector at 0.08 absorbance units full scale (a.u.f.s.). Analysis by ultraviolet

absorbance was performed at 330 nm at 0.001 a.u.f.s. Fluorescence scanning of both the excitation and emission spectra of citrinin was performed at medium detector sensitivity. Analysis by fluorescence detection was performed at full detector sensitivity (emission band width, 18 nm) with an excitation wavelength of 330 nm and an emission wavelength of 500 nm.

Sample preparation

Citrinin standards were prepared in methanol and stored at −20°C. Fermentation samples were diluted in methanol (1:1), mixed vigorously, followed by centrifugation at 2400 *g* for 10 min. Supernatant was removed for subsequent citrinin analysis by HPLC. Assay recovery efficiency was subsequently determined by measuring fermentation samples with known levels of exogenously added citrinin.

Dry cell weight determination

Fermentation samples (10 ml) were filtered through Whatman (Maidstone, U.K.) GF/A filter paper and washed with deionized distilled water (30 ml). The filtered mycelium was allowed to dry at room temperature for 16 h. Mycelium dry cell weight was determined using an automated volatility computer (CEM Corp., Indian Trail, NC, U.S.A.).

RESULTS AND DISCUSSION

Fermentation samples often contain a complex array of compounds of small and large molecular weight, making the accurate quantitation of of specific metabolic products difficult. Although detection of citrinin in complex samples can be enhanced by employing various extraction procedures [14–18] this approach is time-consuming, and losses may adversely influence accurate quantitation. Direct sample quantitation would require that an assay method possess a significant degree of chromatographic resolution in combination with sensitive differential detection. In this study, reversed-phase chromatography was utilized to establish an accurate and efficient assay for the direct quantitation of citrinin from fermentation samples.

Citrinin was eluted from a C_{18} (4-μm particle) radial-compression column at a flow-rate of 2.5 ml/min with a mobile phase composed of acetonitrile–water–acetic acid (40:59:1) at pH 3.8, containing the ion-pairing agent tetrabutylammonium phosphate (0.025 *M*). Tailing of the citrinin peak due to ionization was prevented by lowering the eluent pH with acetic acid. A guard column (C_{18} μBondapak), employed as a precolumn filter, significantly increased the analytical column life and did not adversely influence the retention time for citrinin elution.

The detection sensitivity for citrinin by ultraviolet absorbance and fluorescence spectroscopy was investigated. Fig. 1 illustrates the ultraviolet absorbance spectrum of citrinin. The ultraviolet absorbance maximum for citrinin was 330 nm. The assay was linear over the concentration range of 1–100 μg/ml. This represents a detection sensitivity similar to that previously reported by Phillips *et al.* [19]. Alternatively, various investigators have employed fluorescence detection for the analysis of citrinin [17,18,20]. Using a scanning fluorescence detector the excitation and emission spectra of citrinin were determined. As depicted in Fig. 2, the emission maximum of citrinin was 500 nm, whereas the excitation maximum was 330 nm for an emission wave-

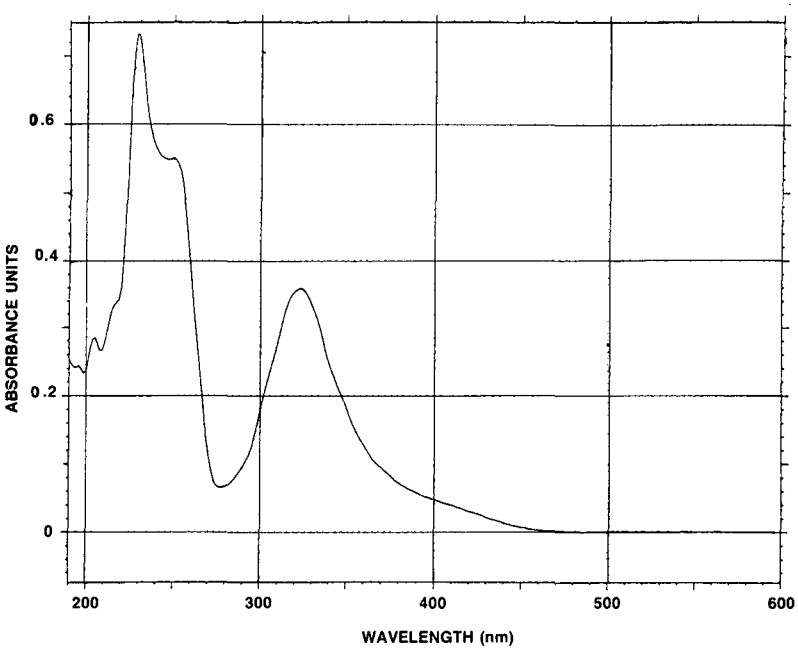

Fig. 1. UV absorbance of citrinin standard in methanol (500 μg/ml).

length of 500 nm. The assay was linear over the concentration range 0.01–100 μg/ml. As little as 0.1 ng of citrinin in a 10-μl injection volume could be accurately measured by fluorescence detection. Only 10 ng of citrinin (10-μl injection volume) could be accurately measured by ultraviolet absorbance detection. This indicates that fluorescence detection is approximately 100 times more sensitive than ultraviolet absorbance. Levels of citrinin in fermentation samples that were undetectable by ultraviolet absorbance, were accurately quantified using fluorescence detection (Fig. 3).

Assay reproducibility with fluorescence detection was evaluated by 30 succes-

TABLE I

ANALYSIS OF ASSAY REPRODUCIBILITY FOR CITRININ BY HPLC WITH FLUORESCENCE DETECTION

Thirty successive 10-μl injections, each of 2.5 or 100 ng per injection, of citrinin were performed. The peak height and area reported have been normalized to 1 ng per injection. The separation of citrinin was carried out at full detector sensitivity, as described in Experimental.

	Peak area (μV · s)	Peak height (μV)	Retention time (s)
Range (× 1000)	320–351	9.9–11.1	228.0–233.4
Mean (× 1000)	335	10.4	231.6
Standard deviation (× 1000)	9.0	0.25	1.6
Coefficient of variation (%)	2.7	2.4	0.7
Sensitivity (× 1000)	335	10.4	

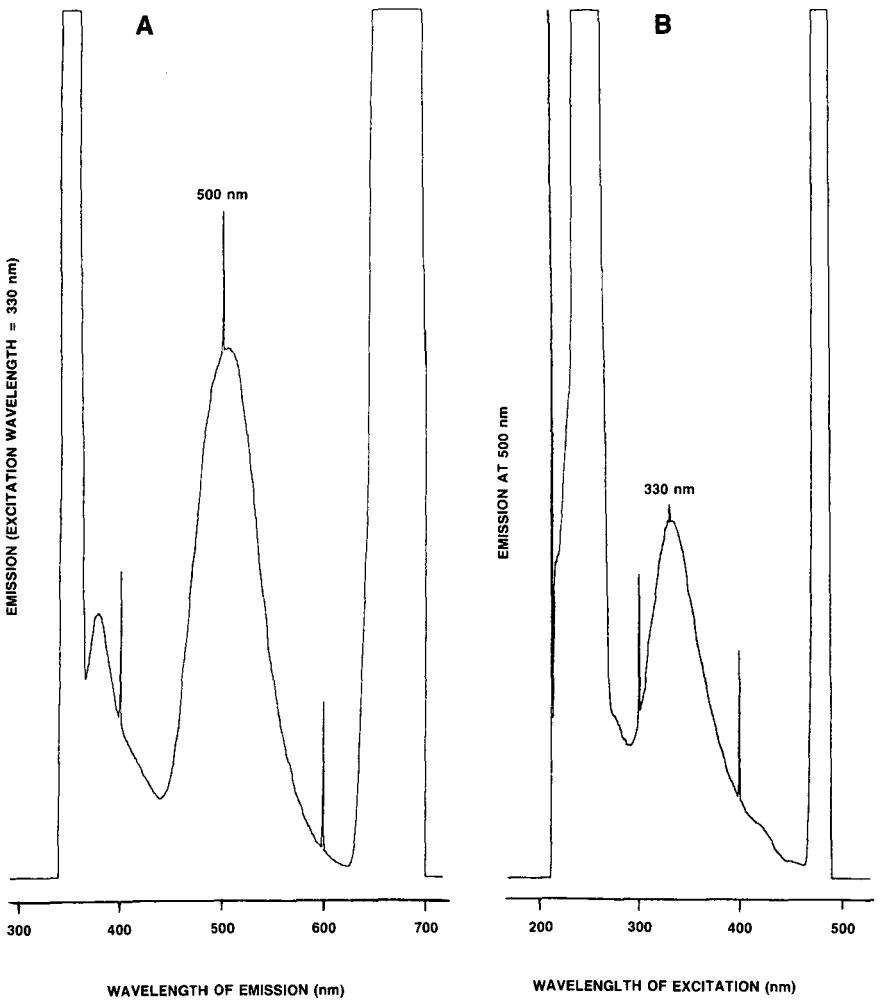

Fig. 2. Fluorescence scan of the emission and excitation spectra of citrinin. (A) Emission scan of citrinin in methanol (10 μg/ml), at the UV absorbance maximum of 330 nm as the excitation wavelength. (B) Excitation scan of citrinin in methanol (10 μg/ml) at the emission maximum of 500 nm observed in (A).

TABLE II

RECOVERY OF CITRININ FROM FERMENTATION SAMPLES

Known amounts of citrinin were added to a 20-h culture of *A. niveus* (ATCC 56745), grown in complex medium, and subsquently analyzed for citrinin by fluorescence detection, as described in Experimental. Values represent an average of two duplicate samples, each assayed in triplicate.

Citrinin added (μg/ml)	Amount detected (μg/ml)	Recovery (%)	Standard deviation
0.0	0.00	–	–
0.1	0.10	102	5.3
2.0	1.82	91	0.7
5.0	4.88	97	3.8
10.0	10.00	100	2.0

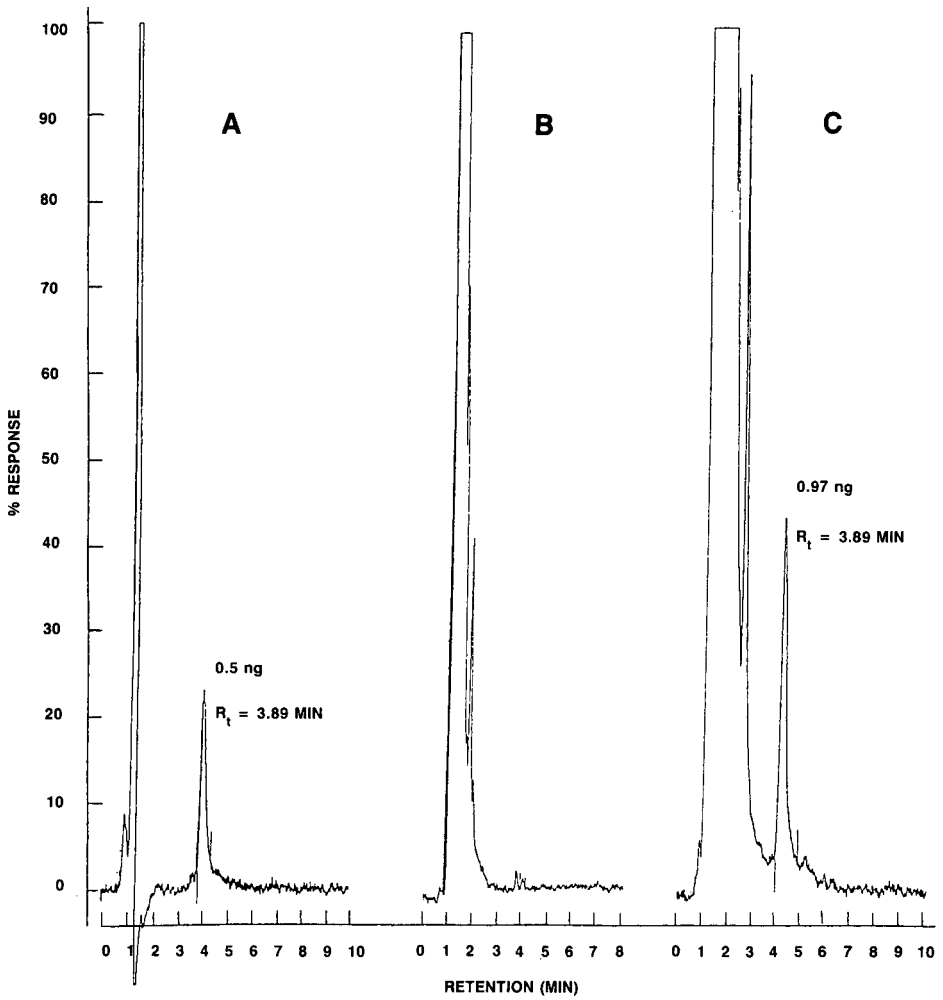

Fig. 3. Chromatograms of *A. niveus* fermentation sample. (A) Citrinin standard in methanol (50 ng/ml) using fluorescence detection. (B) UV detection of a 20-h *A. niveus* fermentation sample. (C) Fluorescence detection of the identical fermentation sample depicted in (B). R_t = Retention time.

sive injections (10 μl) each of 2.5 ng or 100 ng of citrinin standard. Table I lists the data obtained for the measurement of peak height, peak area and retention time. Citrinin quantitation was evaluated by adding known amounts of citrinin to fermentation samples prior to analysis. Quantitation efficiency of citrinin in fermentation samples was 91–102% (Table II). Similar efficiencies for the analysis of citrinin from plasma, urine and bile samples were previously reported by Phillips *et al.* [19]. For ultraviolet absorbance, the detection sensitivity limit of this method was only 10–30 ng. Accurate quantitation of citrinin was achieved without extensive sample extraction protocols or pre-column concentration [17,20].

This methodology was applied to a study of citrinin production by an *Aspergil-*

lus niveus culture (ATCC 56745), propagated in complex liquid medium. Trace levels of citrinin production were detected as early as 20 h following inoculation. Citrinin synthesis increased dramatically when the culture entered the stationary phase of growth, yielding a concentration of 270 μg/ml following a 72 h fermentation. This result is in agreement with earlier studies indicating that citrinin biosynthesis by *A. niveus* is associated with secondary metabolism [3,4]. Characterization of the factors involved in the regulation of citrinin synthesis will require further investigation.

ACKNOWLEDGEMENTS

We are grateful to William Brian and Ellen S. Baron for their helpful suggestions during the preparation of this manuscript.

REFERENCES

1 B. Hald and P. Krogh, *J. Assoc. Off. Anal. Chem.*, 56 (1973) 1440–1443.
2 V. Betina, in V. Betina (Editor), *Mycotoxins–Production, Isolation, Separation and Purification*, Elsevier, Amsterdam 1983, Ch. 10, pp. 217–236.
3 A. J. Birch, P. Fitton, E. Pride, A. J. Ryan, H. Smith and W. P. Whalley, *J. Chem. Soc.*, (1958) 4576–4581.
4 E. Schwenk, G. L. Alexander, A. M. Gold and D. F. Stevens, *J. Biol. Chem.*, 233 (1958) 1211–1213.
5 H. Raistrick, and G. Smith, *Chem. Ind. (London)*, 6 (1941) 828–830.
6 P. M. Robinson and D. Park, *Nature (London)*, 211 (1966) 883–884.
7 H. Barathova, V. Beting and P. Nemec, *Folia Microbiol.*, 14 (1969) 475–483.
8 V. Betina and E. Ruckoua, *Biologia (Bratislava)*, 26 (1971) 463–468.
9 R. D. Phillips, W. O. Berndt and A. W. Hayes, *Toxicology*, 12 (1979) 285–298.
10 C. S. Ramadoss and E. R. B. Shanmugasundaram, *Ind. J. Biochem. Biophys.*, 10 (1973) 296–297.
11 R. F. Curtis, C. H. Hassall and M. Nazar, *J. Chem. Soc. C.*, (1968) 85–93.
12 C. Damodaran, C. S. Ramadoss and E. R. B. Shanmugasundarm, *Anal. Biochem.*, 52 (1973) 482–488.
13 K. B. Raper and C. Thom, *A Manual of the Pencillia*, Williams & Wilkins, Baltimore, MO, 1949; *Microbiol.*, 29 (1975) 118–120.
14 N. D. Davis, D. K. Dalby, U. L. Diener and G. A. Sansing, *Appl. Microbiol.*, 29 (1975) 118–120.
15 A. C. Hetherington and H. Raistrick, *Phil. Trans. R. Soc. London, Ser. B*, 220 (1931) 269–295.
16 A. Ciegler, R. F. Vesonder and L. K. Jackson, *Appl. Environ. Microbiol.*, 33 (1977) 1004–1006.
17 L. R. Marti, D. M. Wilson and B. D. Evans, *J. Assoc. Off. Anal. Chem.*, 61 (1978) 1353–1358.
18 P. Lepom, *J. Chromatogr.*, 355 (1986) 335–339.
19 R. D. Phillips, A. W. Hayes and W. O. Berndt, *J. Chromatogr.*, 190 (1980) 419–427.
20 D. L. Orti, R. H. Hill, Jr., J. A. Liddle and L. L. Needham, *J. Anal. Toxicol.*, 10 (1986) 41–45.

PUBLICATION SCHEDULE FOR 1991

Journal of Chromatography and Journal of Chromatography, Biomedical Applications

MONTH	D 1990	J	F	M	
Journal of Chromatography	535/1 + 2	536/1 + 2 537/1 + 2 538/1	538/2 539/1 539/2	The publication schedule for further issues will be published later	
Cumulative Indexes, Vols. 501–550					
Bibliography Section					
Biomedical Applications		562/1 + 2 563/1	563/2	564/1	

INFORMATION FOR AUTHORS

(Detailed *Instructions to Authors* were published in Vol. 522, pp. 351–354. A free reprint can be obtained by application to the publisher, Elsevier Science Publishers B.V., P.O. Box 330, 1000 AH Amsterdam, The Netherlands.)

Types of Contributions. The following types of papers are published in the *Journal of Chromatography* and the section on *Biomedical Applications:* Regular research papers (Full-length papers), Review articles and Short Communications. Short Communications are usually descriptions of short investigations, or they can report minor technical improvements of previously published procedures; they reflect the same quality of research as Full-length papers, but should preferably not exceed six printed pages. For Review articles, see inside front cover under Submission of Papers.

Submission. Every paper must be accompanied by a letter from the senior author, stating that he/she is submitting the paper for publication in the *Journal of Chromatography*.

Manuscripts. Manuscripts should be typed in double spacing on consecutively numbered pages of uniform size. The manuscript should be preceded by a sheet of manuscript paper carrying the title of the paper and the name and full postal address of the person to whom the proofs are to be sent. As a rule, papers should be divided into sections, headed by a caption (*e.g.*, Abstract, Introduction, Experimental, Results, Discussion, etc.). All illustrations, photographs, tables, etc., should be on separate sheets.

Introduction. Every paper must have a concise introduction mentioning what has been done before on the topic described, and stating clearly what is new in the paper now submitted.

Abstract. All articles should have an abstract of 50–100 words which clearly and briefly indicates what is new, different and significant.

Illustrations. The figures should be submitted in a form suitable for reproduction, drawn in Indian ink on drawing or tracing paper. Each illustration should have a legend, all the *legends* being typed (with double spacing) together on a *separate sheet.* If structures are given in the text, the original drawings should be supplied. Coloured illustrations are reproduced at the author's expense, the cost being determined by the number of pages and by the number of colours needed. The written permission of the author and publisher must be obtained for the use of any figure already published. Its source must be indicated in the legend.

References. References should be numbered in the order in which they are cited in the text, and listed in numerical sequence on a separate sheet at the end of the article. Please check a recent issue for the layout of the reference list. Abbreviations for the titles of journals should follow the system used by *Chemical Abstracts.* Articles not yet published should be given as "in press" (journal should be specified), "submitted for publication" (journal should be specified), "in preparation" or "personal communication".

Dispatch. Before sending the manuscript to the Editor please check that the envelope contains four copies of the paper complete with references, legends and figures. One of the sets of figures must be the originals suitable for direct reproduction. Please also ensure that permission to publish has been obtained from your institute.

Proofs. One set of proofs will be sent to the author to be carefully checked for printer's errors. Corrections must be restricted to instances in which the proof is at variance with the manuscript. "Extra corrections" will be inserted at the author's expense.

Reprints. Fifty reprints of Full-length papers and Short Communications will be supplied free of charge. Additional reprints can be ordered by the authors. An order form containing price quotations will be sent to the authors together with the proofs of their article.

Advertisements. Advertisement rates are available from the publisher on request. The Editors of the journal accept no responsibility for the contents of the advertisements.

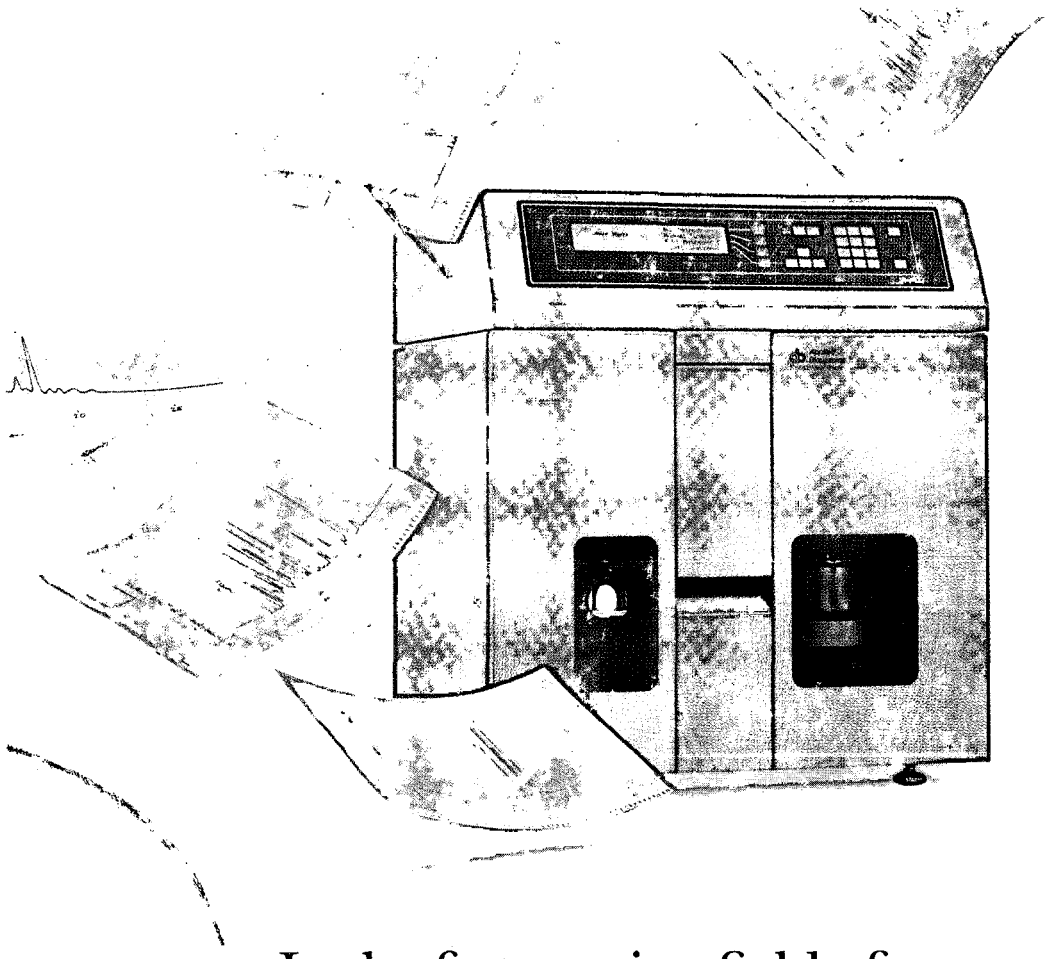

In the fast-moving field of capillary electrophoresis, only the Model 270A puts you in the lead.

Harness the power of capillary electrophoresis (CE) with high performance instrumentation. For meaningful quantitation and reliable analysis, CE's inherent selectivity and resolution must be complemented with accuracy and precision.

The Model 270A Analytical Capillary Electrophoresis System is the first fully integrated system designed to meet the stringent demands of quantitative CE. The system you need when every minute, every result, counts.

The human serum albumin digest was provided courtesy of Delta Biotechnology Ltd., Nottingham, U.K.

True quantitation begins with precision and accuracy in both sample injection and column temperature control. The Applied Biosystems Model 270A combines automation with a unique injector design, a thermostatted capillary compartment and proven detector technology to achieve unsurpassed reproducibility of peak areas and electrophoretic mobility.

Count on your first results within minutes after installing the Model 270A. Select a preprogrammed separation protocol, or create and store your own methods using the interactive display and keypad. The Model 270A is designed for both the novice and the seasoned user of analytical instrumentation.

Contact Applied Biosystems today, and join the leaders in advancing capillary electrophoresis from theory to application.

Applied Biosystems

U.S.A. 850 Lincoln Centre Drive, Foster City, CA 94404. Tel: (415) 570-6667, (800) 874-9868, in California (800) 831-3582. Telex: 470052 APBIO UI. Fax: (415) 572-2743.
Mississauga, Canada. Tel: (416) 821-8183. Fax: (416) 821-8246.
Warrington, U.K. Tel: 0925-825650. Telex: 629611 APBIO G. Fax: 0925-828196.
Weiterstadt, West Germany. Tel: 06151-87940. Telex: 4197318 Z ABI D. Fax: 06151-84899.
Paris, France. Tel: (1) 48 63 24 44. Telex: 230458 ABIF. Fax: (1) 48 63 22 82.
Milan, Italy. Tel: 02-835 4920. Fax: 02-832 1655.
Rotterdam, The Netherlands. Tel: (0) 10 452 35 11. Telex: 26249. Fax: (0) 10 452 91 57.
Burwood, Australia. Tel: (03) 288-7777. Fax: (03) 887-1469.
Tokyo, Japan. Tel: (03) 699-0700. Fax: (03) 699-0733.